OPTIMIZATION OF POWER SYSTEM OPERATION

Jizhong Zhu

OPTIMIZATION OF POWER SYSTEM OPERATION

OPTIMIZATION OF POWER SYSTEM OPERATION

Jizhong Zhu, Ph.D

Principal Engineer, AREVA T&D Inc. Redmond, WA, USA
Advisory Professor, Chongqing University, Chongqing, China

IEEE
PRESS
SERIES
ON POWER
ENGINEERING

Mohamed E. El-Hawary, *Series Editor*

IEEE

Celebrating 125 Years
of Engineering the Future

WILEY

A JOHN WILEY & SONS, INC., PUBLICATION

To My Wife and Son

TABLE OF CONTENTS

PREFACE

I have been undertaking the research and practical applications of power system optimization since the early 1980s. In the early stage of my career, I worked in universities such as Chongqing University (China), Brunel University (UK), National University of Singapore, and Howard University (USA). Since 2000 I have been working for AREVA T&D Inc (USA). When I was a full-time professor at Chongqing University, I wrote a tutorial on power system optimal operation, which I used to teach my senior undergraduate students and postgraduate students in power engineering until 1996. The topics of the tutorial included advanced mathematical and operations research methods and their practical applications in power engineering problems. Some of these were refined to become part of this book.

This book comprehensively applies all kinds of optimization methods to solve power system operation problems. Some contents are analyzed and discussed for the first time in detail in one book, although they have appeared in international journals and conferences. These can be found in Chapter 9 "Steady-State Security Regions", Chapter 11 "Optimal Load Shedding", Chapter 12 "Optimal Reconfiguration of Electric Distribution Network", and Chapter 13 "Uncertainty Analysis in Power Systems."

This book covers not only traditional methods and implementation in power system operation such as Lagrange multipliers, equal incremental principle, linear programming, network flow programming, quadratic programming, nonlinear programming, and dynamic programming to solve the economic dispatch, unit commitment, reactive power optimization, load shedding, steady-state security region, and optimal power flow problems, but also new technologies and their implementation in power system operation in the last decade. The new technologies include improved interior point method, analytic hierarchical process, neural network, fuzzy set theory, genetic algorithm, evolutionary programming, and particle swarm optimization. Some new topics (wheeling model, multiarea wheeling, the total transfer capability computation in multiareas, reactive power pricing calculation, congestion management) addressed in recent years in power system operation are also dealt with and put in appropriate chapters.

In addition to having the rich analysis and implementation of all kinds of approaches, this book contains much hand-on experience for solving power system operation problems. I personally wrote my own code and tested the presented algorithms and power system applications. Many materials presented in the book are derived from my research accomplishments and publications when I worked at Chongqing University, Brunel University, National University of Singapore, and Howard University, as well as currently with AREVA T&D Inc. I appreciate these organizations for providing me such good working environments. Some IEEE papers have been used as primary sources and are cited wherever appropriate. The related publications for each topic are also listed as references, so that those interested may easily obtain overall information.

I wish to express my gratitude to IEEE book series editor Professor Mohammed El-Hawary of Dalhousie University, Canada, Acquisitions Editor Steve Welch, Project Editor Jeanne Audino, and the reviewers of the book for their keen interest in the development of this book, especially Professor Kit Po Wong of the Hong Kong Polytechnic University, Professor Loi Lei Lai of City University, UK, Professor Ruben Romero of Universidad Estadual Paulista, Brazil, and Dr. Ali Chowdhury of California Independent System Operator, who offered valuable comments and suggestions for the book during the preparation stage.

Finally, I wish to thank Professor Guoyu Xu, who was my PhD advisor twenty years ago at Chongqing University, for his high standards and strict requirements for me ever since I was his graduate student. Thanks to everyone, including my family, who has shown support during the time-consuming process of writing this book.

<div align="right">Jizhong Zhu</div>

1

INTRODUCTION

The electric power industry is being relentlessly pressured by governments, politicians, large industries, and investors to privatize, restructure, and deregulate. Before deregulation, most elements of the power industry, such as power generation, bulk power sales, capital expenditures, and investment decisions, were heavily regulated. Some of these regulations were at the state level, and some at the national level. Thus new deregulation in the power industry meant new challenges and huge changes. However, despite changes in different structures, market rules, and uncertainties, the underlying requirements for power system operations to be secure, economical, and reliable remain the same.

This book attempts to cover all areas of power systems operation. It also introduces some new topics and new applications of the latest new technologies that have appeared in recent years. This includes the analysis and discussion of new techniques for solving the old problems and the new problems that are arising from deregulation.

According to the different characteristics and types of the problems as well as their complexity, power systems operation is divided into the following aspects that are addressed in the book:

- Power flow analysis (Chapter 2)
- Sensitivity analysis (Chapter 3)
- Classical economic dispatch (Chapter 4)
- Security-constrained economic dispatch (Chapter 5)
- Multiarea systems economic dispatch (Chapter 6)

- Unit commitment (Chapter 7)
- Optimal power flow (Chapter 8)
- Steady-state security regions (Chapter 9)
- Reactive power optimization (Chapter 10)
- Optimal load shedding (Chapter 11)
- Optimal reconfiguration of electric distribution network (Chapter 12)
- Uncertainty analysis in power system (Chapter 13)

From the view of optimization, the various techniques including traditional and modern optimization methods, which have been developed to solve these power system operation problems, are classified into three groups [1–13]:

(1) Conventional optimization methods including
   - Unconstrained optimization approaches
   - Nonlinear programming (NLP)
   - Linear programming (LP)
   - Quadratic programming (QP)
   - Generalized reduced gradient method
   - Newton method
   - Network flow programming (NFP)
   - Mixed-integer programming (MIP)
   - Interior point (IP) methods
(2) Intelligence search methods such as
   - Neural network (NN)
   - Evolutionary algorithms (EAs)
   - Tabu search (TS)
   - Particle swarm optimization (PSO)
(3) Nonquantity approaches to address uncertainties in objectives and constraints
   - Probabilistic optimization
   - Fuzzy set applications
   - Analytic hierarchical process (AHP)

1.1   CONVENTIONAL METHODS

1.1.1   Unconstrained Optimization Approaches

Unconstrained optimization approaches are the basis of the constrained optimization algorithms. In particular, most of the constrained optimization problems in power system operation can be converted into unconstrained

optimization problems. The major unconstrained optimization approaches that are used in power system operation are gradient method, line search, Lagrange multiplier method, Newton–Raphson optimization, trust-region optimization, quasi–Newton method, double dogleg optimization, and conjugate gradient optimization, etc. Some of these approaches are used in Chapter 2, Chapter 3, Chapter 4, Chapter 7, and Chapter 9.

1.1.2   Linear Programming

The linear programming (LP)-based technique is used to linearize the nonlinear power system optimization problem, so that objective function and constraints of power system optimization have linear forms. The simplex method is known to be quite effective for solving LP problems. The LP approach has several advantages. First, it is reliable, especially regarding convergence properties. Second, it can quickly identify infeasibility. Third, it accommodates a large variety of power system operating limits, including the very important contingency constraints. The disadvantages of LP-based techniques are inaccurate evaluation of system losses and insufficient ability to find an exact solution compared with an accurate nonlinear power system model. However, a great deal of practical applications show that LP-based solutions generally meet the requirements of engineering precision. Thus LP is widely used to solve power system operation problems such as security-constrained economic dispatch, optimal power flow, steady-state security regions, reactive power optimization, etc.

1.1.3   Nonlinear Programming

Power system operation problems are nonlinear. Thus nonlinear programming (NLP) based techniques can easily handle power system operation problems such as the OPF problems with nonlinear objective and constraint functions. To solve a nonlinear programming problem, the first step in this method is to choose a search direction in the iterative procedure, which is determined by the first partial derivatives of the equations (the reduced gradient). Therefore, these methods are referred to as first-order methods, such as the generalized reduced gradient (GRG) method. NLP-based methods have higher accuracy than LP-based approaches, and also have global convergence, which means that the convergence can be guaranteed independent of the starting point, but a slow convergent rate may occur because of zigzagging in the search direction. NLP methods are used in this book from Chapter 5 to Chapter 10.

1.1.4   Quadratic Programming

Quadratic programming (QP) is a special form of nonlinear programming. The objective function of QP optimization model is quadratic, and the constraints are in linear form. Quadratic programming has higher accuracy than LP-based

approaches. Especially, the most often-used objective function in power system optimization is the generator cost function, which generally is a quadratic. Thus there is no simplification for such objective function for a power system optimization problem solved by QP. QP is used in Chapters 5 and 8.

1.1.5 Newton's Method

Newton's method requires the computation of the second-order partial derivatives of the power flow equations and other constraints (the Hessian) and is therefore called a second-order method. The necessary conditions of optimality commonly are the Kuhn–Tucker conditions. Newton's method is favored for its quadratic convergence properties, and is used in Chapters 2, 4, and 8.

1.1.6 Interior Point Methods

The interior point (IP) method is originally used to solve linear programming. It is faster and perhaps better than the conventional simplex algorithm in linear programming. IP methods were first applied to solve OPF problems in the 1990s, and recently, the IP method has been extended and improved to solve OPF with QP and NLP forms. The analysis and implement of IP methods are discussed in Chapters 8 and 10.

1.1.7 Mixed-Integer Programming

The power system problem can also be formulated as a mixed-integer programming (MIP) optimization problem with integer variables such as transformer tap ratio, phase shifter angle, and unit on or off status. MIP is extremely demanding of computer resources, and the number of discrete variables is an important indicator of how difficult an MIP will be to solve. MIP methods that are used to solve OPF problems are the recursive mixed-integer programming technique using an approximation method and the branch and bound (B&B) method, which is a typical method for integer programming. A decomposition technique is generally adopted to decompose the MIP problem into a continuous problem and an integer problem. Decomposition methods such as Benders' decomposition method (BDM) can greatly improve efficiency in solving a large-scale network by reducing the dimensions of the individual subproblems. The results show a significant reduction of the number of iterations, required computation time, and memory space. Also, decomposition allows the application of a separate method for the solution of each subproblem, which makes the approach very attractive. Mixed-integer programming can be used to solve the unit commitment, OPF, as well as the optimal reconfiguration of electric distribution network.

1.1.8   Network Flow Programming

Network flow programming (NFP) is special linear programming. NFP was first applied to solve optimization problems in power systems in 1980s. The early applications of NFP were mainly on a linear model. Recently, nonlinear convex network flow programming has been used in power systems' optimization problems. NFP-based algorithms have the features of fast speed and simple calculation. These methods are efficient for solving simplified OPF problems such as security-constrained economic dispatch, multiarea systems economic dispatch, and optimal reconfiguration of an electric distribution network.

1.2   INTELLIGENT SEARCH METHODS

1.2.1   Optimization Neural Network

Optimization neural network (ONN) was first used to solve linear programming problems in 1986. Recently, ONN was extended to solve nonlinear programming problems. ONN is completely different from traditional optimization methods. It changes the solution of an optimization problem into an equilibrium point (or equilibrium state) of nonlinear dynamic system, and changes the optimal criterion into energy functions for dynamic systems. Because of its parallel computational structure and the evolution of dynamics, the ONN approach appears superior to traditional optimization methods. The ONN approach is applied to solve the classic economic dispatch, multiarea systems economic dispatch, and reactive power optimization in this book.

1.2.2   Evolutionary Algorithms

Natural evolution is a population-based optimization process. The evolutionary algorithms (EAs) are different from the conventional optimization methods, and they do not need to differentiate cost function and constraints. Theoretically, like simulated annealing, EAs converge to the global optimum solution. EAs, including evolutionary programming (EP), evolutionary strategy (ES), and GA are artificial intelligence methods for optimization based on the mechanics of natural selection, such as mutation, recombination, reproduction, crossover, selection, etc. Since EAs require all information to be included in the fitness function, it is very difficult to consider all OPF constraints. Thus EAs are generally used to solve a simplified OPF problem such as the classic economic dispatch, security-constrained economic power dispatch, and reactive optimization problem, as well as optimal reconfiguration of an electric distribution network.

1.2.3   Tabu Search

The tabu search (TS) algorithm is mainly used for solving combinatorial optimization problems. It is an iterative search algorithm, characterized by the use of a flexible memory. It is able to eliminate local minima and to search areas beyond a local minimum. The TS method is also mainly used to solve simplified OPF problems such as unit commitment and reactive optimization problems.

1.2.4   Particle Swarm Optimization

Particle swarm optimization (PSO) is a swarm intelligence algorithm, inspired by social dynamics and an emergent behavior that arises in socially organized colonies. The PSO algorithm exploits a population of individuals to probe promising regions of search space. In this context, the population is called a swarm and the individuals are called particles or agents. In recent years, various PSO algorithms have been successfully applied in many power engineering problems including OPF. These are analyzed in Chapters 7, 8 and 10.

1.3   APPLICATION OF FUZZY SET THEORY

The data and parameters used in power system operation are usually derived from many sources, with a wide variance in their accuracy. For example, although the average load is typically applied in power system operation problems, the actual load should follow some uncertain variations. In addition, generator fuel cost, VAR compensators, and peak power savings may be subject to uncertainty to some degree. Therefore, uncertainties due to insufficient information may generate an uncertain region of decisions. Consequently, the validity of the results from average values cannot represent the uncertainty level. To account for the uncertainties in information and goals related to multiple and usually conflicting objectives in power system optimization, the use of probability theory, fuzzy set theory, and analytic hierarchical process may play a significant role in decision-making.

The probabilistic methods and their application in power systems operation with uncertainty are discussed in Chapter 13. The fuzzy sets may be assigned not only to objective functions, but also to constraints, especially the nonprobabilistic uncertainty associated with the reactive power demand in constraints. Generally speaking, the satisfaction parameters (fuzzy sets) for objectives and constraints represent the degree of closeness to the optimum and the degree of enforcement of constraints, respectively. With the maximization of these satisfaction parameters, the goal of optimization is achieved and simultaneously the uncertainties are considered. The application of fuzzy set theory to the OPF problem is also presented in Chapter 13. The analytic hierarchical process (AHP) is a simple and convenient method to analyze a complicated

problem (or complex problem). It is especially suitable for problems that are very difficult to analyze wholly quantitatively, such as OPF with competitive objectives, or uncertain factors. The details of the AHP algorithm are given in Chapter 7. AHP is employed to solve unit commitment, multiarea economic dispatch, OPF, VAR optimization, optimal load shedding, and uncertainty analysis in the power system.

REFERENCES

[1] L.K. Kirchamayer, *Economic Operation of Power Systems*, New York: John Wiley & Sons, 1958.

[2] M.E. El-Hawary and G.S. Christensen, *Optimal Economic Operation of Electric Power Systems, Academic*, New York, 1979.

[3] C. Gross, *Power System Analysis*, New York: John Wiley & Sons, 1986.

[4] A.J. Wood and B. Wollenberg, *Power Generation Operation and Control*, 2nd ed. New York: John Wiley & Sons, 1996.

[5] G.T. Heydt, *Computer Analysis Methods for Power Systems*, Stars in a circle publications, AR. 1996.

[6] T.H. Lee, D.H. Thorne, and E.F. Hill, "A transportation method for economic dispatching—Application and comparison", *IEEE Trans. on Power System*", 1980, Vol. 99, pp. 2372–2385.

[7] J.Z. Zhu and J.A. Momoh, "Optimal VAR pricing and VAR placement using analytic hierarchy process," *Electric Power Systems Research*, 1998, Vol. 48, No.1, pp. 11–17.

[8] W.J. Zhang, F.X. Li, and L.M. Tolbert, "Review of reactive power planning: objectives, constraints, and algorithms," *IEEE Trans. Power Syst.*, vol. 22, no. 4, 2007, pp. 2177–2186.

[9] J.Z. Zhu, D. Hwang, and A. Sadjadpour "Real Time Congestion Monitoring and Management of Power Systems," IEEE/PES T&D 2005 Asia Pacific, Dalian, August 14–18, 2005.

[10] J. Nocedal and S. J. Wright, *Numerical Optimization*. Springer, 1999.

[11] D.G. Luenberger, *Introduction to linear and nonlinear programming*, Addison-Wesley Publishing Company, Inc. USA, 1973.

[12] J. Kennedy and R. Eberhart, "Particle swarm optimization," in *Proc. IEEE Int. Conf. Neural Networks*, Perth, Australia, 1995, vol. 4, pp. 1942–1948.

[13] J.I. Hopfield, "Neural Networks and Physical Systems with Emergent Collective Computational Abilities," *Proc Natl Acad Sci*, *USA*, Vol.79, 1982, pp. 2554–2558.

2

POWER FLOW ANALYSIS

This chapter deals with the power flow problem. The power flow algorithms include the Newton–Raphson method in both polar and rectangle forms, the Gauss–Seidel method, the DC power flow method, and all kinds of decoupled power flow methods such as fast decoupled power flow, simplified BX and XB methods, as well as decoupled power flow without major approximation.

2.1   MATHEMATICAL MODEL OF POWER FLOW

Power flow is well known as "load flow." This is the name given to a network solution that shows currents, voltages, and real and reactive power flows at every bus in the system. Since the parameters of the elements such as lines and transformers are constant, the power system network is a linear network. However, in the power flow problem, the relationship between voltage and current at each bus is nonlinear, and the same holds for the relationship between the real and reactive power consumption at a bus or the generated real power and scheduled voltage magnitude at a generator bus. Thus power flow calculation involves the solution of nonlinear equations. It gives us the electrical response of the transmission system to a particular set of loads and generator power outputs. Power flows are an important part of power system operation and planning.

Generally, for a network with n independent buses, we can write the following n equations.

$$\left.\begin{array}{l} Y_{11}\dot{V}_1 + Y_{12}\dot{V}_2 +, \ldots, +Y_{1n}\dot{V}_n = \dot{I}_1 \\ Y_{21}\dot{V}_1 + Y_{22}\dot{V}_2 +, \ldots, +Y_{2n}\dot{V}_n = \dot{I}_2 \\ \qquad \ldots\ldots \\ Y_{n1}\dot{V}_1 + Y_{n2}\dot{V}_2 +, \ldots, +Y_{nn}\dot{V}_n = \dot{I}_n \end{array}\right\} \tag{2.1}$$

The matrix form is

$$\begin{bmatrix} Y_{11} & Y_{12} & \ldots & Y_{1n} \\ Y_{21} & Y_{22} & \ldots & Y_{2n} \\ \vdots & \vdots & & \vdots \\ Y_{n1} & Y_{n2} & \ldots & Y_{nn} \end{bmatrix} \begin{bmatrix} \dot{V}_1 \\ \dot{V}_2 \\ \vdots \\ \dot{V}_n \end{bmatrix} = \begin{bmatrix} \dot{I}_1 \\ \dot{I}_2 \\ \vdots \\ \dot{I}_n \end{bmatrix} \tag{2.2}$$

or

$$[Y][V] = I \tag{2.3}$$

where I is the bus current injection vector, V is the bus voltage vector, and Y is called the bus admittance matrix. Its diagonal element Y_{ii} is called the self-admittance of bus i, which equals the sum of all branch admittances connecting to bus i. The off-diagonal element of the bus admittance matrix Y_{ij} is the negative of branch admittance between buses i and j. If there is no line between buses i and j, this term is zero. Obviously, the bus admittance matrix is a sparse matrix.

In addition, the bus current can be represented by bus voltage and power, that is,

$$\dot{I}_i = \frac{\hat{S}_i}{\hat{V}_i} = \frac{\hat{S}_{\mathrm{G}i} - \hat{S}_{\mathrm{D}i}}{\hat{V}_i} = \frac{(P_{\mathrm{G}i} - P_{\mathrm{D}i}) - j(Q_{\mathrm{G}i} - Q_{\mathrm{D}i})}{\hat{V}_i} \tag{2.4}$$

where

S: The complex power injection vector
$P_{\mathrm{G}i}$: The real power output of the generator connecting to bus i
$Q_{\mathrm{G}i}$: The reactive power output of the generator connecting to bus i
$P_{\mathrm{D}i}$: The real power load connecting to bus i
$Q_{\mathrm{D}i}$: The reactive power load connecting to bus i

Substituting equation (2.4) into equation (2.1), we have

$$\frac{(P_{\mathrm{G}i} - P_{\mathrm{D}i}) - j(Q_{\mathrm{G}i} - Q_{\mathrm{D}i})}{\hat{V}_i} = Y_{i1}\dot{V}_1 + Y_{i2}\dot{V}_2 +, \ldots, +Y_{in}\dot{V}_n, \quad i = 1, 2, \ldots, n \tag{2.5}$$

In the power flow problem, the load demands are known variables. We define the following bus power injections as

$$P_i = P_{Gi} - P_{Di} \qquad (2.6)$$

$$Q_i = Q_{Gi} - Q_{Di} \qquad (2.7)$$

Substituting equations (2.6) and (2.7) into equation (2.5), we can get the general form of power flow equation as

$$\frac{P_i - jQ_i}{\hat{V}_i} = \sum_{j=1}^{n} Y_{ij} \dot{V}_j, \quad i = 1, 2, \ldots, n \qquad (2.8)$$

or

$$P_i + jQ_i = \dot{V}_i \sum_{j=1}^{n} \hat{Y}_{ij} \hat{V}_j, \quad i = 1, 2, \ldots, n \qquad (2.9)$$

If we divide equation (2.9) into real and imaginary parts, we can get two equations for each bus with four variables, that is, bus real power P, reactive power Q, voltage V, and angle θ. To solve the power flow equations, two of these should be known for each bus. According to the practical conditions of the power system operation, as well as known variables of the bus, we can have three bus types as follows:

(1) PV bus: For this type of bus, the bus real power P and the magnitude of voltage V are known and the bus reactive power Q and the angle of voltage θ are unknown. Generally the bus connected to the generator is a PV bus.

(2) PQ bus: For this type of bus, the bus real power P and reactive power Q are known and the magnitude and the angle of voltage (V, θ) are unknown. Generally the bus connected to load is a PQ bus. However, the power output of some generators is constant or cannot be adjusted under the particular operation conditions. The corresponding bus will also be a PQ bus.

(3) Slack bus: The slack bus is also called the swing bus, or the reference bus. Since power loss of the network is unknown during the power flow calculation, at least one bus power cannot be given, which will balance the system power. In addition, it is necessary to have a bus with a zero voltage angle as reference for the calculation of the other voltage angles. Generally, the slack bus is a generator-related bus, whose magnitude and the angle of voltage (V, θ) are unknown. The bus real power P and reactive power Q are unknown variables. Traditionally, there is only one slack bus in the power flow calculation. In the practical application, distributed slack buses are used, so all buses that connect the

adjustable generators can be selected as slack buses and used to balance the power mismatch through some rules. One of these rules is that the system power mismatch is balanced by all slacks based on the unit participation factors.

Since the voltage of the slack bus is given, only $n - 1$ bus voltages need to be calculated. Thus the number of power flow equations is $2(n - 1)$.

2.2   NEWTON–RAPHSON METHOD

2.2.1   Principle of Newton–Raphson Method

A nonlinear equation with single variable can be expressed as

$$f(x) = 0 \tag{2.10}$$

For solving this equation, select an initial value x^0. The difference between the initial value and the final solution will be Δx^0. Then $x = x^0 + \Delta x^0$ is the solution of nonlinear equation (2.10), that is,

$$f(x^0 + \Delta x^0) = 0 \tag{2.11}$$

Expanding the above equation with the Taylor series, we get

$$f(x^0 + \Delta x^0) = f(x^0) + f'(x^0)\Delta x^0 + f''(x^0)\frac{(\Delta x^0)^2}{2!} + , \dots ,$$

$$+ f^{(n)}(x^0)\frac{(\Delta x^0)^n}{n!} + , \dots = 0 \tag{2.12}$$

where $f'(x^0)$, ..., $f^{(n)}(x^0)$ are the derivatives of the function $f(x)$.

If the difference Δx^0 is very small (meaning that the initial value x^0 is close to the solution of the function), the terms of the second and higher derivatives can be neglected. Thus equation (2.12) becomes a linear equation as below:

$$f(x^0 + \Delta x^0) = f(x^0) + f'(x^0)\Delta x^0 = 0 \tag{2.13}$$

Then we can get

$$\Delta x^0 = -\frac{f(x^0)}{f'(x^0)} \tag{2.14}$$

The new solution will be

$$x^1 = x^0 + \Delta x^0 = x^0 - \frac{f(x^0)}{f'(x^0)} \tag{2.15}$$

Since equation (2.13) is an approximate equation, the value of Δx^0 is also an approximation. Thus the solution x is not a real solution. Further iterations are needed. The iteration equation is

$$x^{k+1} = x^k + \Delta x^{k+1} = x^k - \frac{f(x^k)}{f'(x^k)} \qquad (2.16)$$

The iteration can be stopped if one of the following conditions is met:

$$\begin{aligned} & |\Delta x^k| < \varepsilon_1 \\ or \quad & |f(x^k)| < \varepsilon_2 \end{aligned} \qquad (2.17)$$

where ε_1, ε_2, which are the permitted convergence precision, are small positive numbers.

The Newton method can also be expanded to a nonlinear equation with n variables.

$$\left.\begin{aligned} f_1(x_1, x_2, \ldots, x_n) &= 0 \\ f_2(x_1, x_2, \ldots, x_n) &= 0 \\ &\cdots \\ f_n(x_1, x_2, \ldots, x_n) &= 0 \end{aligned}\right\} \qquad (2.18)$$

For a given set of initial values $x_1^0, x_2^0, \ldots, x_n^0$, we have the corrected values Δx_1^0, $\Delta x_2^0, \ldots, \Delta x_n^0$. Then equation (2.18) becomes

$$\left.\begin{aligned} f_1(x_1^0 + \Delta x_1^0, x_2^0 + \Delta x_2^0, \ldots, x_n^0 + \Delta x_n^0) &= 0 \\ f_2(x_1^0 + \Delta x_1^0, x_2^0 + \Delta x_2^0, \ldots, x_n^0 + \Delta x_n^0) &= 0 \\ &\cdots \\ f_n(x_1^0 + \Delta x_1^0, x_2^0 + \Delta x_2^0, \ldots, x_n^0 + \Delta x_n^0) &= 0 \end{aligned}\right\} \qquad (2.19)$$

Similarly, expanding equation (2.19) and neglecting the terms of second and higher derivatives, we get

$$\left.\begin{aligned} f_1(x_1^0, x_2^0, \ldots, x_n^0) + \frac{\partial f_1}{\partial x_1}\bigg|_{x_1^0} \Delta x_1^0 + \frac{\partial f_1}{\partial x_2}\bigg|_{x_2^0} \Delta x_2^0 + \cdots + \frac{\partial f_1}{\partial x_n}\bigg|_{x_n^0} \Delta x_n^0 &= 0 \\ f_2(x_1^0, x_2^0, \ldots, x_n^0) + \frac{\partial f_2}{\partial x_1}\bigg|_{x_1^0} \Delta x_1^0 + \frac{\partial f_2}{\partial x_2}\bigg|_{x_2^0} \Delta x_2^0 + \cdots + \frac{\partial f_2}{\partial x_n}\bigg|_{x_n^0} \Delta x_n^0 &= 0 \\ &\cdots \\ f_n(x_1^0, x_2^0, \ldots, x_n^0) + \frac{\partial f_n}{\partial x_1}\bigg|_{x_1^0} \Delta x_1^0 + \frac{\partial f_n}{\partial x_2}\bigg|_{x_2^0} \Delta x_2^0 + \cdots + \frac{\partial f_n}{\partial x_n}\bigg|_{x_n^0} \Delta x_n^0 &= 0 \end{aligned}\right\} \qquad (2.20)$$

Equation (2.20) can also be written in matrix form

$$\begin{bmatrix} f_1(x_1^0, x_2^0, \ldots, x_n^0) \\ f_2(x_1^0, x_2^0, \ldots, x_n^0) \\ \ldots \\ f_n(x_1^0, x_2^0, \ldots, x_n^0) \end{bmatrix} = - \begin{bmatrix} \left.\dfrac{\partial f_1}{\partial x_1}\right|_{x_1^0} & \left.\dfrac{\partial f_1}{\partial x_2}\right|_{x_2^0} & \cdots & \left.\dfrac{\partial f_1}{\partial x_n}\right|_{x_n^0} \\ \left.\dfrac{\partial f_2}{\partial x_1}\right|_{x_1^0} & \left.\dfrac{\partial f_2}{\partial x_2}\right|_{x_2^0} & \cdots & \left.\dfrac{\partial f_2}{\partial x_n}\right|_{x_n^0} \\ \vdots & \vdots & & \vdots \\ \left.\dfrac{\partial f_n}{\partial x_1}\right|_{x_1^0} & \left.\dfrac{\partial f_n}{\partial x_2}\right|_{x_2^0} & \cdots & \left.\dfrac{\partial f_n}{\partial x_n}\right|_{x_n^0} \end{bmatrix} \begin{bmatrix} \Delta x_1^0 \\ \Delta x_2^0 \\ \vdots \\ \Delta x_n^0 \end{bmatrix} \tag{2.21}$$

From equation (2.21) we can get $\Delta x_1^0, \Delta x_2^0, \ldots, \Delta x_n^0$. Then the new solution can be obtained. The iteration equation can be written as follows:

$$\begin{bmatrix} f_1(x_1^k, x_2^k, \ldots, x_n^k) \\ f_2(x_1^k, x_2^k, \ldots, x_n^k) \\ \ldots \\ f_n(x_1^k, x_2^k, \ldots, x_n^k) \end{bmatrix} = - \begin{bmatrix} \left.\dfrac{\partial f_1}{\partial x_1}\right|_{x_1^k} & \left.\dfrac{\partial f_1}{\partial x_2}\right|_{x_2^k} & \cdots & \left.\dfrac{\partial f_1}{\partial x_n}\right|_{x_n^k} \\ \left.\dfrac{\partial f_2}{\partial x_1}\right|_{x_1^k} & \left.\dfrac{\partial f_2}{\partial x_2}\right|_{x_2^k} & \cdots & \left.\dfrac{\partial f_2}{\partial x_n}\right|_{x_n^k} \\ \vdots & \vdots & & \vdots \\ \left.\dfrac{\partial f_n}{\partial x_1}\right|_{x_1^k} & \left.\dfrac{\partial f_n}{\partial x_2}\right|_{x_2^k} & \cdots & \left.\dfrac{\partial f_n}{\partial x_n}\right|_{x_n^k} \end{bmatrix} \begin{bmatrix} \Delta x_1^k \\ \Delta x_2^k \\ \vdots \\ \Delta x_n^k \end{bmatrix} \tag{2.22}$$

$$x_i^{k+1} = x_i^k + \Delta x_i^k \quad i = 1, 2, \ldots, n \tag{2.23}$$

Equations (2.22) and (2.23) can be expressed as

$$F(X^k) = -J^k \Delta X^k \tag{2.24}$$

$$X^{k+1} = X^k + \Delta X^k \tag{2.25}$$

where J is an $n \times n$ matrix and called a Jacobian matrix.

2.2.2 Power Flow Solution with Polar Coordinate System

If the bus voltage in equation (2.9) is expressed with a polar coordinate system, the complex voltage and real and reactive powers can be written as

$$\dot{V}_i = V_i(\cos\theta_i + j\sin\theta_i) \tag{2.26}$$

$$P_i = V_i \sum_{j=1}^{n} V_j(G_{ij}\cos\theta_{ij} + B_{ij}\sin\theta_{ij}) \tag{2.27}$$

$$Q_i = V_i \sum_{j=1}^{n} V_j(G_{ij}\sin\theta_{ij} - B_{ij}\cos\theta_{ij}) \tag{2.28}$$

where $\theta_{ij} = \theta_i - \theta_j$, which is the angle difference between bus i and bus j.

Assuming that buses $1 \sim m$ are PQ buses, buses $m + 1 \sim n - 1$ are PV buses and the nth bus is the slack bus. The V_n, θ_n are given, and the magnitude of the PV bus $V_{m+1} \sim V_{n-1}$ are also given. Then, $n - 1$ bus voltage angles are unknown, and m magnitudes of voltage are unknown. For each PV or PQ bus we have the following real power mismatch equation:

$$\Delta P_i = P_{is} - P_i = P_{is} - V_i \sum_{j=1}^{n} V_j (G_{ij} \cos \theta_{ij} + B_{ij} \sin \theta_{ij}) = 0 \qquad (2.29)$$

For each PQ bus, we also have the following reactive power equation:

$$\Delta Q_{is} = Q_{is} - Q_i = Q_{is} - V_i \sum_{j=1}^{n} V_j (G_{ij} \sin \theta_{ij} - B_{ij} \cos \theta_{ij}) = 0 \qquad (2.30)$$

where P_{is}, Q_{is} are the calculated bus real and reactive power injection, respectively.

According to the Newton method, the power flow equations (2.29) and (2.30) can be expanded into Taylor series and the following first-order approximation can be obtained

$$\begin{bmatrix} \Delta P \\ \Delta Q \end{bmatrix} = -J \begin{bmatrix} \Delta \theta \\ \Delta V / V \end{bmatrix}$$

$$or \quad \begin{bmatrix} \Delta P \\ \Delta Q \end{bmatrix} = -\begin{bmatrix} H & N \\ K & L \end{bmatrix} \begin{bmatrix} \Delta \theta \\ V_D^{-1} \Delta V \end{bmatrix} \qquad (2.31)$$

where

$$\Delta P = \begin{bmatrix} \Delta P_1 \\ \Delta P_2 \\ \vdots \\ \Delta P_{n-1} \end{bmatrix} \qquad (2.32)$$

$$\Delta Q = \begin{bmatrix} \Delta Q_1 \\ \Delta Q_2 \\ \vdots \\ \Delta Q_m \end{bmatrix} \qquad (2.33)$$

$$\Delta \theta = \begin{bmatrix} \Delta \theta_1 \\ \Delta \theta_2 \\ \vdots \\ \Delta \theta_{n-1} \end{bmatrix} \qquad (2.34)$$

$$\Delta V = \begin{bmatrix} \Delta V_1 \\ \Delta V_2 \\ \vdots \\ \Delta V_m \end{bmatrix} \qquad (2.35)$$

$$V_D = \begin{bmatrix} V_1 & & & \\ & V_2 & & \\ & & \ddots & \\ & & & V_m \end{bmatrix} \tag{2.36}$$

H is a $(n-1) \times (n-1)$ matrix, and its element is $H_{ij} = \dfrac{\partial \Delta P_i}{\partial \theta_j}$.

N is a $(n-1) \times m$ matrix, and its element is $N_{ij} = V_j \dfrac{\partial \Delta P_i}{\partial V_j}$.

K is a $m \times (n-1)$ matrix, and its element is $K_{ij} = \dfrac{\partial \Delta Q_i}{\partial \theta_j}$.

L is a $m \times m$ matrix, and its element is $L_{ij} = V_j \dfrac{\partial \Delta Q_i}{\partial V_j}$.

If $i \neq j$, the expressions of the elements in Jacobian matrix are as follows:

$$H_{ij} = -V_i V_j \left(G_{ij} \sin \theta_{ij} - B_{ij} \cos \theta_{ij} \right) \tag{2.37}$$

$$N_{ij} = -V_i V_j \left(G_{ij} \cos \theta_{ij} - B_{ij} \sin \theta_{ij} \right) \tag{2.38}$$

$$N_{ij} = V_i V_j \left(G_{ij} \cos \theta_{ij} - B_{ij} \sin \theta_{ij} \right) \tag{2.39}$$

$$L_{ij} = -V_i V_j \left(G_{ij} \sin \theta_{ij} - B_{ij} \cos \theta_{ij} \right) \tag{2.40}$$

If $i = j$, the expressions of the elements in Jacobian matrix are as follows:

$$H_{ii} = V_i^2 B_{ii} + Q_i \tag{2.41}$$

$$N_{ii} = -V_i^2 G_{ii} - P_i \tag{2.42}$$

$$K_{ii} = V_i^2 G_{ii} - P_i \tag{2.43}$$

$$L_{ii} = V_i^2 B_{ii} - Q_i \tag{2.44}$$

The calculation steps of the Newton power flow solution are as follows [1,2]:

Step (1): Given input data.

Step (2): Form bus admittance matrix.

Step (3): Assume the initial values of bus voltage.

Step (4): Compute the power mismatch according to equations (2.29) and (2.30). Check whether the convergence conditions are satisfied.

$$\max |\Delta P_i^k| < \varepsilon_1 \tag{2.45}$$

$$\max |\Delta Q_i^k| < \varepsilon_2 \tag{2.46}$$

If equations (2.45) and (2.46) are met, stop the iteration, and calculate the line flows and real and reactive power of the slack bus. If not, go to next step.
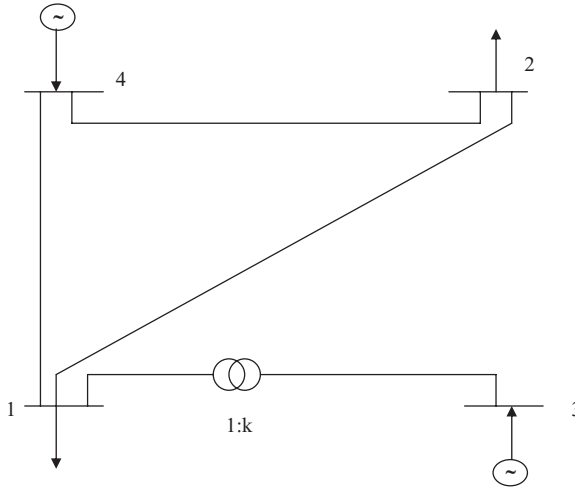
FIGURE 2.1   Four-bus power system

Step (5): Compute the elements in Jacobian matrix (2.37)–(2.44).

Step (6): Compute the corrected values of bus voltage, using equation (2.31).
Then compute the bus voltage:

$$V_i^{k+1} = V_i^k + \Delta V_i^k \tag{2.47}$$

$$\theta_i^{k+1} = \theta_i^k + \Delta \theta_i^k \tag{2.48}$$

Step (7): Return to Step (4) with new values of bus voltage.

Example 2.1

The test example for power flow calculation, which is shown in Figure 2.1, is taken from reference [2].

The parameters of the branches are as follows:

$z_{12} = 0.10 + j0.40$
$y_{120} = y_{210} = j0.01528$
$z_{13} = j0.30, k = 1.1$
$z_{14} = 0.12 + j0.50$
$y_{140} = y_{410} = j0.01920$
$z_{24} = 0.08 + j0.40$
$y_{240} = y_{420} = j0.01413$

Buses 1 and 2 are PQ buses, bus 3 is a PV bus, and bus 4 is a slack bus. The given data are:

$P_1 + jQ_1 = -0.3 - j0.18$
$P_2 + jQ_2 = -0.55 - j0.13$
$P_3 = 0.5; V_3 = 1.1;$
$V_4 = 1.05; \theta_4 = 0$

First, we form the bus admittance matrix as follows:

$$Y = \begin{bmatrix} 1.0421 - j8.2429 & -0.5882 + j2.3529 & j3.6666 & -0.4539 + j1.8911 \\ -0.5882 + j2.3529 & 1.0690 - j4.7274 & 0 & -0.4808 + j2.4038 \\ j3.6666 & 0 & -j3.3333 & 0 \\ -0.4539 + j1.8911 & -0.4808 + j2.4038 & 0 & 0.9346 - j4.2616 \end{bmatrix}$$

given the initial bus voltage as

$$\dot{V}_1^0 = \dot{V}_2^0 = 1.0\angle 0^0, \quad \dot{V}_3^0 = 1.1\angle 0^0$$

Computing the bus power mismatch with equations (2.29) and (2.30), we get

$$\Delta P_1^0 = P_{1s} - P_1^0 = -0.30 - (-0.02269) = -0.27731$$

$$\Delta P_2^0 = P_{2s} - P_2^0 = -0.55 - (-0.02404) = -0.52596$$

$$\Delta P_3^0 = P_{3s} - P_3^0 = 0.5$$

$$\Delta Q_1^0 = Q_{1s} - Q_1^0 = -0.18 - (-0.12903) = -0.05097$$

$$\Delta Q_2^0 = Q_{2s} - Q_2^0 = -0.13 - (-0.14960) = 0.0196$$

Then compute the bus voltage correction, using equation (2.31)

$$\Delta\theta_1^0 = -0.505922^0, \quad \Delta\theta_2^0 = -6.177633^0, \quad \Delta\theta_3^0 = 6.597038^0$$

$$\Delta V_1^0 = -0.00649, \quad \Delta V_2^0 = -0.02366$$

The new bus voltage will be

$$\theta_1^1 = \theta_1^0 + \Delta\theta_1^0 = -0.505922^0$$

$$\theta_2^1 = \theta_2^0 + \Delta\theta_2^0 = -6.177633^0$$

$$\theta_3^1 = \theta_3^0 + \Delta\theta_3^0 = 6.597038^0$$

$$V_1^1 = V_1^0 + \Delta V_1^0 = 0.99351$$

$$V_2^1 = V_2^0 + \Delta V_2^0 = 0.97634$$

Conduct the second iteration, using new voltage values. If the convergence tolerance is $\varepsilon = 10^{-5}$, the power flow will be converged after three iterations, which are shown in Tables 2.1 and 2.2.

Table 2.1   Bus power mismatch change

Iteration k	ΔP_1	ΔP_2	ΔP_3	ΔQ_1	ΔQ_2
0	−0.27731	−0.52596	0.5	−0.05097	0.01960
1	-4.0×10^{-3}	-2.047×10^{-2}	4.51×10^{-3}	-4.380×10^{-2}	-2.454×10^{-2}
2	1.0×10^{-4}	-4.2×10^{-4}	8.0×10^{-5}	-4.5×10^{-4}	-3.2×10^{-4}
3	$<10^{-5}$	$<10^{-5}$	$<10^{-5}$	$<10^{-5}$	$<10^{-5}$

Table 2.2   Bus voltage change

Iteration k	θ_1	θ_2	θ_3	V_1	V_2
1	-0.505922^0	-6.177633^0	6.597038^0	0.99351	0.97634
2	-0.500765^0	-6.445204^0	6.729964^0	0.98477	0.96495
3	-0.500192^0	-6.450361^0	6.732257^0	0.98467	0.96480

Finally, we compute the power of the slack bus and the power flows for all branches:

For slack bus:

$$P_4 + jQ_4 = 0.3678824 + j0.2647003$$

For branches

$$P_{12} + jQ_{12} = 0.2462439 - j0.0146505$$

$$P_{13} + jQ_{13} = -0.5000002 - j0.0292640$$

$$P_{14} + jQ_{14} = -0.0462439 - j0.1360884$$

$$P_{21} + jQ_{21} = -0.2399902 + j0.0106270$$

$$P_{24} + jQ_{24} = -0.3100099 - j0.1406267$$

$$P_{31} + jQ_{31} = 0.4999998 + j0.0934093$$

$$P_{41} + jQ_{41} = 0.0482163 + j0.1045228$$

$$P_{42} + jQ_{42} = 0.3196662 + j0.1601774$$

2.2.3   Power Flow Solution with Rectangular Coordinate System

2.2.3.1   Newton Method   If the bus voltage in equation (2.9) is expressed with a rectangular coordinate system, the complex voltage and real and reactive powers can be written as

$$\dot{V}_i = e_i + jf_i \tag{2.49}$$

$$P_i = e_i \sum_{j=1}^{n} (G_{ij}e_j - B_{ij}f_j) + f_i \sum_{j=1}^{n} (G_{ij}f_j + B_{ij}e_j) \tag{2.50}$$

$$Q_i = f_i \sum_{j=1}^{n} (G_{ij}e_j - B_{ij}f_j) - e_i \sum_{j=1}^{n} (G_{ij}f_j + B_{ij}e_j) \tag{2.51}$$

For each PQ bus, we have the following power mismatch equations:

$$\Delta P_i = P_{is} - P_i = P_{is} - e_i \sum_{j=1}^{n} (G_{ij}e_j - B_{ij}f_j) - f_i \sum_{j=1}^{n} (G_{ij}f_j + B_{ij}e_j) = 0 \tag{2.52}$$

$$\Delta Q_i = Q_{si} - Q_i = Q_{si} - f_i \sum_{j=1}^{n} (G_{ij}e_j - B_{ij}f_j) + e_i \sum_{j=1}^{n} (G_{ij}f_j + B_{ij}e_j) = 0 \tag{2.53}$$

For each PV bus, we have the following equations:

$$\Delta P_i = P_{is} - P_i = P_{is} - e_i \sum_{j=1}^{n} (G_{ij}e_j - B_{ij}f_j) - f_i \sum_{j=1}^{n} (G_{ij}f_j + B_{ij}e_j) = 0 \tag{2.54}$$

$$\Delta V_i^2 = V_{is}^2 + V_i^2 = V_{is}^2 - (e_i^2 + f_i^2) = 0 \tag{2.55}$$

There are $2(n - 1)$ equations in equations (2.52)–(2.55). According to the Newton method, we have the following correction equation:

$$\Delta F = -J\Delta V \tag{2.56}$$

where

$$\Delta F = \begin{bmatrix} \Delta P_1 \\ \Delta Q_1 \\ \vdots \\ \Delta P_m \\ \Delta Q_m \\ \Delta P_{m+1} \\ \Delta V_{m+1}^2 \\ \vdots \\ \Delta P_{n-1} \\ \Delta V_{n-1}^2 \end{bmatrix} \tag{2.57}$$

$$\Delta V = \begin{bmatrix} \Delta e_1 \\ \Delta f_1 \\ \vdots \\ \Delta e_m \\ \Delta f_m \\ \Delta e_{m+1} \\ \Delta f_{m+1} \\ \vdots \\ \Delta e_{n-1} \\ \Delta f_{n-1} \end{bmatrix} \tag{2.58}$$

$$J = \begin{bmatrix} \dfrac{\partial \Delta P_1}{\partial e_1} & \dfrac{\partial \Delta P_1}{\partial f_1} & \cdots & \dfrac{\partial \Delta P_1}{\partial e_m} & \dfrac{\partial \Delta P_1}{\partial f_m} & \dfrac{\partial \Delta P_1}{\partial e_{m+1}} & \dfrac{\partial \Delta P_1}{\partial f_{m+1}} & \cdots & \dfrac{\partial \Delta P_1}{\partial e_{n-1}} & \dfrac{\partial \Delta P_1}{\partial f_{n-1}} \\[2mm] \dfrac{\partial \Delta Q_1}{\partial e_1} & \dfrac{\partial \Delta Q_1}{\partial f_1} & \cdots & \dfrac{\partial \Delta Q_1}{\partial e_m} & \dfrac{\partial \Delta Q_1}{\partial f_m} & \dfrac{\partial \Delta Q_1}{\partial e_{m+1}} & \dfrac{\partial \Delta Q_1}{\partial f_{m+1}} & \cdots & \dfrac{\partial \Delta Q_1}{\partial e_{n-1}} & \dfrac{\partial \Delta Q_1}{\partial f_{n-1}} \\[2mm] \vdots & \vdots & & \vdots & \vdots & \vdots & \vdots & & \vdots & \vdots \\[2mm] \dfrac{\partial \Delta P_m}{\partial e_1} & \dfrac{\partial \Delta P_m}{\partial f_1} & \cdots & \dfrac{\partial \Delta P_m}{\partial e_m} & \dfrac{\partial \Delta P_m}{\partial f_m} & \dfrac{\partial \Delta P_m}{\partial e_{m+1}} & \dfrac{\partial \Delta P_m}{\partial f_{m+1}} & \cdots & \dfrac{\partial \Delta P_m}{\partial e_{n-1}} & \dfrac{\partial \Delta P_m}{\partial f_{n-1}} \\[2mm] \dfrac{\partial \Delta Q_m}{\partial e_1} & \dfrac{\partial \Delta Q_m}{\partial f_1} & \cdots & \dfrac{\partial \Delta Q_m}{\partial e_m} & \dfrac{\partial \Delta Q_m}{\partial f_m} & \dfrac{\partial \Delta Q_m}{\partial e_{m+1}} & \dfrac{\partial \Delta Q_m}{\partial f_{m+1}} & \cdots & \dfrac{\partial \Delta Q_m}{\partial e_{n-1}} & \dfrac{\partial \Delta Q_m}{\partial f_{n-1}} \\[2mm] \dfrac{\partial \Delta P_{m+1}}{\partial e_1} & \dfrac{\partial \Delta P_{m+1}}{\partial f_1} & \cdots & \dfrac{\partial \Delta P_{m+1}}{\partial e_m} & \dfrac{\partial \Delta P_{m+1}}{\partial f_m} & \dfrac{\partial \Delta P_{m+1}}{\partial e_{m+1}} & \dfrac{\partial \Delta P_{m+1}}{\partial f_{m+1}} & \cdots & \dfrac{\partial \Delta P_{m+1}}{\partial e_{n-1}} & \dfrac{\partial \Delta P_{m+1}}{\partial f_{n-1}} \\[2mm] \dfrac{\partial \Delta V_{m+1}^2}{\partial e_1} & \dfrac{\partial \Delta V_{m+1}^2}{\partial f_1} & \cdots & \dfrac{\partial \Delta V_{m+1}^2}{\partial e_m} & \dfrac{\partial \Delta V_{m+1}^2}{\partial f_m} & \dfrac{\partial \Delta V_{m+1}^2}{\partial e_{m+1}} & \dfrac{\partial \Delta V_{m+1}^2}{\partial f_{m+1}} & \cdots & \dfrac{\partial \Delta V_{m+1}^2}{\partial e_{n-1}} & \dfrac{\partial \Delta V_{m+1}^2}{\partial f_{n-1}} \\[2mm] \vdots & \vdots & & \vdots & \vdots & \vdots & \vdots & & \vdots & \vdots \\[2mm] \dfrac{\partial \Delta P_{n-1}}{\partial e_1} & \dfrac{\partial \Delta P_{n-1}}{\partial f_1} & \cdots & \dfrac{\partial \Delta P_{n-1}}{\partial e_m} & \dfrac{\partial \Delta P_{n-1}}{\partial f_m} & \dfrac{\partial \Delta P_{n-1}}{\partial e_{m+1}} & \dfrac{\partial \Delta P_{n-1}}{\partial f_{m+1}} & \cdots & \dfrac{\partial \Delta P_{n-1}}{\partial e_{n-1}} & \dfrac{\partial \Delta P_{n-1}}{\partial f_{n-1}} \\[2mm] \dfrac{\partial \Delta V_{n-1}^2}{\partial e_1} & \dfrac{\partial \Delta V_{n-1}^2}{\partial f_1} & \cdots & \dfrac{\partial \Delta V_{n-1}^2}{\partial e_m} & \dfrac{\partial \Delta V_{n-1}^2}{\partial f_m} & \dfrac{\partial \Delta V_{n-1}^2}{\partial e_{m+1}} & \dfrac{\partial \Delta V_{n-1}^2}{\partial f_{m+1}} & \cdots & \dfrac{\partial \Delta V_{n-1}^2}{\partial e_{n-1}} & \dfrac{\partial \Delta V_{n-1}^2}{\partial f_{n-1}} \end{bmatrix} \tag{2.59}$$

If $i \neq j$, the expressions of the elements in the Jacobian matrix are as follows:

$$\frac{\partial \Delta P_i}{\partial e_i} = -\frac{\partial \Delta Q_i}{\partial f_i} = -(G_{ij}e_i + B_{ij}f_i) \tag{2.60}$$

$$\frac{\partial \Delta P_i}{\partial f_i} = -\frac{\partial \Delta Q_i}{\partial e_i} = -(G_{ij}f_i - B_{ij}e_i) \tag{2.61}$$

$$\frac{\partial \Delta V_i^2}{\partial e_i} = -\frac{\partial \Delta V_i^2}{\partial f_i} = 0 \tag{2.62}$$

If $i = j$, the expressions of the elements in the Jacobian matrix are as follows:

$$\frac{\partial \Delta P_i}{\partial e_i} = -\sum_{j=1}^{n}(G_{ij}e_j - B_{ij}f_j) - G_{ii}e_i - B_{ii}f_i \tag{2.63}$$

$$\frac{\partial \Delta P_i}{\partial f_i} = -\sum_{j=1}^{n}(G_{ij}f_j + B_{ij}e_j) - G_{ii}f_i + B_{ii}e_i \tag{2.64}$$

$$\frac{\partial \Delta Q_i}{\partial e_i} = \sum_{j=1}^{n}(G_{ij}f_j + B_{ij}e_j) - G_{ii}f_i + B_{ii}e_i \tag{2.65}$$

$$\frac{\partial \Delta Q_i}{\partial f_i} = -\sum_{j=1}^{n}(G_{ij}e_j - B_{ij}f_j) + G_{ii}e_i + B_{ii}f_i \tag{2.66}$$

$$\frac{\partial \Delta V_i^2}{\partial e_i} = -2e_i \tag{2.67}$$

$$\frac{\partial \Delta V_i^2}{\partial f_i} = -2f_i \tag{2.68}$$

Equation (2.56) can be written in matrix form:

$$\begin{bmatrix} \Delta F_1 \\ \Delta F_2 \\ \cdots \\ \Delta F_{n-1} \end{bmatrix} = -\begin{bmatrix} J_{11} & J_{12} & \cdots & J_{1,n-1} \\ J_{21} & J_{22} & \cdots & J_{2,n-1} \\ \vdots & \vdots & & \vdots \\ J_{n-1,1} & J_{n-1,2} & \cdots & J_{n-1,n-1} \end{bmatrix} \begin{bmatrix} \Delta V_1 \\ \Delta V_2 \\ \vdots \\ \Delta V_{n-1} \end{bmatrix} \tag{2.69}$$

where ΔF_i *and* ΔV_i are two-dimensional vectors. J_{ij} is a 2×2 matrix.

$$\Delta V_i = \begin{bmatrix} \Delta e_i \\ \Delta f_i \end{bmatrix} \tag{2.70}$$

For a PQ bus, we have

$$\Delta F_i = \begin{bmatrix} \Delta P_i \\ \Delta Q_i \end{bmatrix} \tag{2.71}$$

$$J_{ij} = \begin{bmatrix} \dfrac{\partial \Delta P_i}{\partial e_j} & \dfrac{\partial \Delta P_i}{\partial f_j} \\ \dfrac{\partial \Delta Q_i}{\partial e_j} & \dfrac{\partial \Delta Q_i}{\partial f_j} \end{bmatrix} \tag{2.72}$$

For a PV bus, we have

$$\Delta F_i = \begin{bmatrix} \Delta P_i \\ \Delta V_i^2 \end{bmatrix} \tag{2.73}$$

$$J_{ij} = \begin{bmatrix} \dfrac{\partial \Delta P_i}{\partial e_j} & \dfrac{\partial \Delta P_i}{\partial f_j} \\ \dfrac{\partial \Delta V_i^2}{\partial e_j} & \dfrac{\partial \Delta V_i^2}{\partial f_j} \end{bmatrix} \tag{2.74}$$

It can be observed from equations (2.60)–(2.68) that the elements of the Jacobian matrix are the function of bus voltage, which will be updated through iterations. The element of the submatrix J_{ij} of the Jacobian matrix in equation (2.69) is related to the corresponding element in bus admittance matrix Y_{ij}. If $Y_{ij} = 0$, then $J_{ij} = 0$. Therefore, the Jacobian matrix in equation (2.69) is also a sparse matrix that is the same as the bus admittance matrix.

The steps of rectangular coordination-based Newton power flow solution are similar to those in the polar coordination-based algorithm, which was described in Section 2.2.2.

Example 2.2

For the same system as in Example 2.1, the Newton method with the rectangle coordinate system is used to solve power flow.

The bus admittance matrix is the same as in Example 2.1. Given the initial values of bus voltages:

$$e_1^0 = e_2^0 = e_3^0 = 1.0,$$

$$f_1^0 = f_2^0 = f_3^0 = 0.0,$$

$$e_4^0 = 1.05, \quad f_4^0 = 0.0$$

Computing the bus power mismatch and ΔV_i^2 with equations (2.52) and (2.55), we get

$$\Delta P_1^0 = P_{1s} - P_1^0 = -0.30 - (-0.02269) = -0.27731$$

$$\Delta P_2^0 = P_{2s} - P_2^0 = -0.55 - (-0.02404) = -0.52596$$

$$\Delta P_3^0 = P_{3s} - P_3^0 = 0.5$$

$$\Delta Q_1^0 = Q_{1s} - Q_1^0 = -0.18 - 0.23767 = -0.41763$$

$$\Delta Q_2^0 = Q_{2s} - Q_2^0 = -0.13 - (-0.14960) = 0.0196$$

$$\Delta V_3^{2(0)} = |V_{3s}|^2 - |V_3^0|^2 = 0.21$$

Computing the elements of the Jacobian matrix with equations (2.60) and (2.68), we get the following correction equation:

$$-\begin{bmatrix} -1.01936 & -8.00523 & 0.58823 & 2.35294 & 0.00000 & 3.66666 \\ -8.48049 & 1.06478 & 2.35294 & -0.58823 & 3.66666 & 0.00000 \\ 0.58823 & 2.35294 & -1.04496 & -4.87698 & 0.00000 & 0.00000 \\ 2.35294 & -0.58823 & -4.57777 & 1.09304 & 0.00000 & 0.00000 \\ 0.00000 & 3.66666 & 0.00000 & 0.00000 & 0.00000 & -3.66666 \\ 0.00000 & 0.00000 & 0.00000 & 0.00000 & -2.00000 & 0.00000 \end{bmatrix} \begin{bmatrix} \Delta e_1^0 \\ \Delta f_1^0 \\ \Delta e_2^0 \\ \Delta f_2^0 \\ \Delta e_3^0 \\ \Delta f_3^0 \end{bmatrix} = \begin{bmatrix} \Delta P_1^0 \\ \Delta Q_1^0 \\ \Delta P_2^0 \\ \Delta Q_2^0 \\ \Delta P_3^0 \\ \Delta Q_3^0 \end{bmatrix}$$

It can be observed from the above equation that most of the elements in the Jacobian matrix that have the maximal absolute values are not on the diagonals, which easily cause a calculation error. To avoid this, we switch rows 1 and 2, rows 3 and 4, rows 5 and 6; then we get:

$$-\begin{bmatrix} -8.48049 & 1.06478 & 2.35294 & -0.58823 & 3.66666 & 0.00000 \\ -1.01936 & -8.00523 & 0.58823 & 2.35294 & 0.00000 & 3.66666 \\ 2.35294 & -0.58823 & -4.57777 & 1.09304 & 0.00000 & 0.00000 \\ 0.58823 & 2.35294 & -1.04496 & -4.87698 & 0.00000 & 0.00000 \\ 0.00000 & 0.00000 & 0.00000 & 0.00000 & -2.00000 & 0.00000 \\ 0.00000 & 3.66666 & 0.00000 & 0.00000 & 0.00000 & -3.66666 \end{bmatrix} \begin{bmatrix} \Delta e_1^0 \\ \Delta f_1^0 \\ \Delta e_2^0 \\ \Delta f_2^0 \\ \Delta e_3^0 \\ \Delta f_3^0 \end{bmatrix} = \begin{bmatrix} \Delta Q_1^0 \\ \Delta P_1^0 \\ \Delta Q_2^0 \\ \Delta P_2^0 \\ \Delta Q_3^0 \\ \Delta P_3^0 \end{bmatrix}$$

Solving the above correction equation, we get

$$\begin{bmatrix} \Delta e_1^0 \\ \Delta f_1^0 \\ \Delta e_2^0 \\ \Delta f_2^0 \\ \Delta e_3^0 \\ \Delta f_3^0 \end{bmatrix} = \begin{bmatrix} -0.00369632 \\ -0.00943011 \\ -0.02220685 \\ -0.10808215 \\ 0.10500000 \\ 0.12693353 \end{bmatrix}$$

The new bus voltage will be

$$e_1^1 = e_1^0 + \Delta e_1^0 = 0.99630368$$

$$f_1^1 = f_1^0 + \Delta f_1^0 = -0.00943011$$

$$e_2^1 = e_2^0 + \Delta e_2^0 = 0.97779365$$

$$f_2^1 = f_2^0 + \Delta f_2^0 = -0.10808215$$

$$e_3^1 = e_3^0 + \Delta e_3^0 = 1.10500000$$

$$f_3^1 = f_3^0 + \Delta f_3^0 = 0.12693353$$

We then conduct the second iteration, using new voltage values. If the convergence tolerance is $\varepsilon = 10^{-5}$, the power flow will be converged after three iterations, which are shown in Tables 2.3 and 2.4.

Table 2.3   Change of bus mismatches

Iteration k	ΔP_1	ΔQ_1	ΔP_2	ΔQ_2	ΔP_3	ΔV_3^2
0	−0.2773	−0.4176	−0.5260	0.0196	0.500	0.210
1	2.90×10^{-3}	-4.18×10^{-3}	-1.28×10^{-2}	-5.50×10^{-2}	-1.91×10^{-3}	-2.71×10^{-2}
2	-1.29×10^{-5}	-6.74×10^{-5}	-2.86×10^{-4}	-1.07×10^{-3}	4.58×10^{-5}	-1.60×10^{-4}
3	$<10^{-5}$	$<10^{-5}$	$<10^{-5}$	$<10^{-5}$	$<10^{-5}$	$<10^{-5}$

Table 2.4   Change of bus voltages

Iteration k	$e_1 + jf_1$	$e_2 + jf_2$	$e_3 + jf_3$
1	0.9963 − j0.0094	0.9778 − j0.1081	1.1050 + j0.1269
2	0.9848 − j0.0086	0.9590 − j0.1084	1.0925 + 0.1289
3	0.9846 − j0.0086	0.9587 − j0.1084	1.0924 + j0.1290

The final bus voltages are expressed in the polar coordinate system as

$$\dot{V}_1 = 0.9847\angle - 0.500^0$$

$$\dot{V}_2 = 0.9648\angle - 6.450^0$$

$$\dot{V}_3 = 1.1\angle 6.732^0$$

Finally, we compute the power of the slack bus as

$$P_4 + jQ_4 = 0.36788 + j0.26469$$

Compared with Example 2.1, the same power flow solution is obtained.

2.2.3.2   Second-Order Power Flow Method   It is noted that equations (2.50) and (2.51) are a second-order equation on voltage. They can be expanded into Taylor series without approximation [3]. That is,

$$P_{i\mathrm{SP}} = P_{is} + \frac{\partial P_i}{\partial e^{\mathrm{T}}}\Delta e + \frac{\partial P_i}{\partial f^{\mathrm{T}}}\Delta f +$$

$$\frac{1}{2}\left[\Delta e^{\mathrm{T}}\frac{\partial^2 P_i}{\partial e \partial e^{\mathrm{T}}}\Delta e + \Delta e^{\mathrm{T}}\frac{\partial^2 P_i}{\partial e \partial f^{\mathrm{T}}}\Delta f + \Delta f^{\mathrm{T}}\frac{\partial^2 P_i}{\partial f \partial e^{\mathrm{T}}}\Delta e + \Delta f^{\mathrm{T}}\frac{\partial^2 P_i}{\partial f \partial f^{\mathrm{T}}}\Delta f\right] \quad (2.75)$$

$$Q_{i\mathrm{SP}} = Q_{is} + \frac{\partial Q_i}{\partial e^{\mathrm{T}}}\Delta e + \frac{\partial Q_i}{\partial f^{\mathrm{T}}}\Delta f +$$

$$\frac{1}{2}\left[\Delta e^{\mathrm{T}}\frac{\partial^2 Q_i}{\partial e \partial e^{\mathrm{T}}}\Delta e + \Delta e^{\mathrm{T}}\frac{\partial^2 Q_i}{\partial e \partial f^{\mathrm{T}}}\Delta f + \Delta f^{\mathrm{T}}\frac{\partial^2 Q_i}{\partial f \partial e^{\mathrm{T}}}\Delta e + \Delta f^{\mathrm{T}}\frac{\partial^2 Q_i}{\partial f \partial f^{\mathrm{T}}}\Delta f\right] \quad (2.76)$$

The matrix form is

$$\begin{bmatrix} \Delta P \\ \Delta Q \end{bmatrix} = J \begin{bmatrix} \Delta e \\ \Delta f \end{bmatrix} + \begin{bmatrix} SP \\ SQ \end{bmatrix} \tag{2.77}$$

Where J is the Jacobian matrix

$$J = \begin{bmatrix} \dfrac{\partial P_i}{\partial e^{\mathrm{T}}} & \dfrac{\partial P_i}{\partial f^{\mathrm{T}}} \\ \dfrac{\partial Q_i}{\partial e^{\mathrm{T}}} & \dfrac{\partial Q_i}{\partial f^{\mathrm{T}}} \end{bmatrix} \tag{2.78}$$

SP and SQ are the second-order term vectors and can be simplified as [3]

$$SP = P_{is}(\Delta e, \Delta f) \tag{2.79}$$

$$SQ = Q_{is}(\Delta e, \Delta f) \tag{2.80}$$

There are no third- or higher-order terms in equation (2.77). If we ignore the second-order term, it will be similar to the Newton algorithm we just discussed in this section. Here, we keep the second-order term, and estimate their values based on the previous iteration values of voltage components. Thus equation (2.77) can be written as

$$\begin{bmatrix} \Delta P - SP \\ \Delta Q - SQ \end{bmatrix} = J \begin{bmatrix} \Delta e \\ \Delta f \end{bmatrix} \tag{2.81}$$

From the above, we obtain increment voltage components:

$$\begin{bmatrix} \Delta e \\ \Delta f \end{bmatrix} = J^{-1} \begin{bmatrix} \Delta P - SP \\ \Delta Q - SQ \end{bmatrix} \tag{2.82}$$

For a PV bus, the voltage magnitude is fixed; thus the increment voltage components must satisfy the following equation:

$$e_i \Delta e_i + f_i \Delta f_i = V_i \Delta V_i \tag{2.83}$$

Therefore, the reactive power equation in (2.77) for a PV bus will be replaced by the above equation.

The second-order power flow algorithm is summarized below.

(1) Given the input data, initialize all the arrays.
(2) Set SP and SQ vectors equal to zero.

(3) Compute the P_{is}, Q_{is} vectors.

(4) Compute the power mismatches ΔP *and* ΔQ. Check whether the convergence conditions are satisfied.

$$\max|\Delta P_i^k| < \varepsilon_1 \tag{2.84}$$

$$\max|\Delta Q_i^k| < \varepsilon_2 \tag{2.85}$$

If equations (2.84) and (2.85) are met, stop the iteration, and calculate the line flows and real and reactive power of the slack bus. If not, go to next step.

(5) Compute the Jacobian matrix.

(6) Compute Δe, Δf, using equation (2.82).

(7) Update the voltages

$$e^{k+1} = e^k + \Delta e \tag{2.86}$$

$$f^{k+1} = f^k + \Delta f \tag{2.87}$$

(8) Compute the second-order terms SP and SQ, using Δe, Δf. Then go back to step (3).

2.3 GAUSS–SEIDEL METHOD

For a nonlinear equation with *n* variables (2.18), we can get the solutions as

$$\left. \begin{array}{l} x_1 = g_1(x_1, x_2, \ldots, x_n) \\ x_2 = g_2(x_1, x_2, \ldots, x_n) \\ \qquad \cdots \\ x_n = g_n(x_1, x_2, \ldots, x_n) \end{array} \right\} \tag{2.88}$$

If the values of the variables at the *k*th iteration are obtained, substituting them into the right side of the above equation we can get the new values of these variables as below:

$$\left. \begin{array}{l} x_1^{k+1} = g_1(x_1^k, x_2^k, \ldots, x_n^k) \\ x_2^{k+1} = g_2(x_1^k, x_2^k, \ldots, x_n^k) \\ \qquad \cdots \\ x_n^{k+1} = g_n(x_1^k, x_2^k, \ldots, x_n^k) \end{array} \right\} \tag{2.89}$$

or

$$x_i^{k+1} = g_i\left(x_1^k, x_2^k, \ldots, x_n^k\right), \quad i = 1, 2, \ldots, n \tag{2.90}$$

The iteration will be stopped if the following convergence conditions are satisfied for all variables:

$$\left|x_i^{k+1} - x_i^k\right| < \varepsilon \tag{2.91}$$

The Newton method that is described in Section 2.2 is based on this iteration calculation. To speed up the convergence, the formula of the iteration calculation is modified as below:

$$\left.\begin{aligned}
x_1^{k+1} &= g_1\left(x_1^k, x_2^k, \ldots, x_n^k\right) \\
x_2^{k+1} &= g_2\left(x_1^{k+1}, x_2^k, \ldots, x_n^k\right) \\
&\cdots \\
x_n^{k+1} &= g_n\left(x_1^{k+1}, x_2^{k+1}, \ldots, x_{n-1}^{k+1}, x_n^k\right)
\end{aligned}\right\} \tag{2.92}$$

or

$$x_i^{k+1} = g_i\left(x_1^{k+1}, x_2^{k+1}, \ldots, x_{i-1}^{k+1}, x_n^k\right), \quad i = 1, 2, \ldots, n \tag{2.93}$$

The main idea of the approach is to substitute the new values of variables in the calculation of the next variable immediately, rather than waiting until the next iteration. This iteration method is called the Gauss–Seidel method. It can be also used to solve the power flow equations.

Assuming the system consists of n buses. buses $1 \sim m$ are PQ buses, buses $m + 1 \sim n - 1$ are PV buses, and the nth bus is the slack bus. The iteration calculation does not include the slack bus.

From equation (2.8), we get

$$\dot{V}_i = \frac{1}{Y_{ii}}\left[\frac{P_i - jQ_i}{\hat{V}_i} - \sum_{\substack{j=1 \\ j \neq i}}^{n} Y_{ij}\dot{V}_j\right] \tag{2.94}$$

According to the Gauss–Seidel method, the iteration formula of equation (2.94) can be written as:

$$\dot{V}_i^{k+1} = \frac{1}{Y_{ii}}\left[\frac{P_i - jQ_i}{\hat{V}_i^k} - \sum_{j=1}^{i-1} Y_{ij}\dot{V}_j^{k+1} - \sum_{j=i+1}^{n} Y_{ij}\dot{V}_j^k\right] \tag{2.95}$$

For the PQ bus, the real and reactive powers are known. Thus, if the initial bus voltage $\dot{V}_i^0$ is given, we can use equation (2.95) to perform the iteration calculation.

For the PV bus, the bus real power and the magnitude of the voltage are known. It is necessary to give the initial value for bus reactive power. The bus reactive power will then be computed by iteration calculation. That is,

$$Q_i^k = \text{Im}\left[\dot{V}_i^k \, \hat{I}_i^k \right] = \text{Im}\left[\dot{V}_i^k \left(\sum_{j=1}^{i-1} \hat{Y}_{ij} \hat{V}_j^{k+1} + \sum_{j=i}^{n} \hat{Y}_{ij} \hat{V}_j^k \right) \right] \qquad (2.96)$$

After the iteration is over, all bus real and reactive powers, as well as the voltages, are obtained. The power of the slack bus can be obtained by solving the following equation:

$$P_n + jQ_n = \dot{V}_n \sum_{j=1}^{n} \hat{Y}_{nj} \hat{V}_j \qquad (2.97)$$

The line power flow can also be obtained as below:

$$S_{ij} = P_{ij} + jQ_{ij} = \dot{V}_i \hat{I}_{ij} = \dot{V}_i^2 y_{i0} + \dot{V}_i(\hat{V}_i - \hat{V}_j)\hat{y}_{ij} \qquad (2.98)$$

where y_{ij} is the admittance of the branch ij and y_{i0} is the admittance of the ground branch at the end i.

2.4 P-Q DECOUPLING METHOD

2.4.1 Fast Decoupled Power Flow

According to Section 2.2.2, the updated equation in the Newton power flow method is as below:

$$\begin{bmatrix} \Delta P \\ \Delta Q \end{bmatrix} = -\begin{bmatrix} H & N \\ K & L \end{bmatrix}\begin{bmatrix} \Delta\theta \\ V_D^{-1}\Delta V \end{bmatrix} \qquad (2.99)$$

The Newton power flow is a robust power flow algorithm. It is also called full AC power flow since there is no simplification in the calculation. However, the disadvantage of the Newton power flow is that the terms in the Jacobian matrix must be recalculated in each iteration. Actually, the reactance of the branch is generally far greater than the resistance of the branch in a practical power system. Thus there exists a strong relationship between the real power and the voltage angle, but weak coupling between the real power and the magnitude of voltage. That means the real power is little influenced by changes in voltage magnitude; that is,

$$\frac{\partial \Delta P_i}{\partial V_j} \approx 0 \qquad (2.100)$$

while the reactive power and the magnitude of voltage have a strong coupling relationship and weak coupling for the reactive power and voltage angle. It means that the reactive power is little influenced by changes in voltage angle; that is,

$$\frac{\partial \Delta Q_i}{\partial \theta_j} \approx 0 \tag{2.101}$$

Therefore, the values of the elements in submatrix N and K in equation (2.99) are very small; that is,

$$N_{ij} = V_j \frac{\partial \Delta P_i}{\partial V_j} \approx 0 \tag{2.102}$$

$$K_{ij} = \frac{\partial \Delta Q_i}{\partial \theta_j} \approx 0 \tag{2.103}$$

Equation (2.99) becomes

$$\begin{bmatrix} \Delta P \\ \Delta Q \end{bmatrix} = - \begin{bmatrix} H & 0 \\ 0 & L \end{bmatrix} \begin{bmatrix} \Delta\theta \\ V_D^{-1}\Delta V \end{bmatrix} \tag{2.104}$$

or

$$\Delta P = -H\Delta\theta \tag{2.105}$$

$$\Delta Q = -LV_D^{-1}\Delta V = -L(\Delta V/V) \tag{2.106}$$

The simplified equations (2.105) and (2.106) make power flow iteration very easy. The bus real power mismatch is only used to revise the voltage angle, and the bus reactive power mismatch is only used to revise the voltage magnitude. These two equations are iteratively calculated, respectively, until the convergence conditions are satisfied. This method is called the real and reactive power decoupling method.

Actually, equations (2.105) and (2.106) can be further simplified. Since the difference of the voltage angles of two ends in the line ij is small (generally less than $10^0 - 20^0$), $\sin(\theta_i - \theta_j)$ is also small. Thus we have

$$\cos\theta_{ij} = \cos(\theta_i - \theta_j) \cong 1$$

$$G_{ij}\sin\theta_{ij} \ll B_{ij}$$

Assuming that

$$Q_i \ll V_i^2 B_{ii}$$

then the elements of the matrices H and L can be expressed as

$$H_{ij} = V_i V_j B_{ij} \quad i, j = 1, 2, \ldots, n-1 \tag{2.107}$$

$$L_{ij} = V_i V_j B_{ij} \quad i, j = 1, 2, \ldots, m \tag{2.108}$$

or we have the following derivatives:

$$\frac{\partial P_i}{\partial \theta_j} = -V_i V_j B_{ij} \quad i, j = 1, 2, \ldots, n-1 \tag{2.109}$$

$$\frac{\partial Q_i}{\left(\dfrac{\partial V_j}{V_j}\right)} = -V_i V_j B_{ij} \quad i, j = 1, 2, \ldots, m \tag{2.110}$$

Therefore, the matrices H and L can be written as

$$
H = \begin{bmatrix}
V_1 B_{11} V_1 & V_1 B_{12} V_2 & \cdots & V_1 B_{1,n-1} V_{n-1} \\
V_2 B_{21} V_1 & V_2 B_{22} V_2 & \cdots & V_2 B_{2,n-1} V_{n-1} \\
\vdots & \vdots & & \vdots \\
V_{n-1} B_{n-1,1} V_1 & V_{n-1} B_{n-1,1} V_2 & \cdots & V_{n-1} B_{n-1,n-1} V_{n-1}
\end{bmatrix}
$$

$$
= \begin{bmatrix}
V_1 & & & \\
& V_2 & & \\
& & \ddots & \\
& & & V_{n-1}
\end{bmatrix}
\begin{bmatrix}
B_{11} & B_{12} & \cdots & B_{1,n-1} \\
B_{21} & B_{22} & \cdots & B_{2,n-1} \\
\vdots & \vdots & & \vdots \\
B_{n-1,1} & B_{n-1,2} & \cdots & B_{n-1,n-1}
\end{bmatrix}
\times
\begin{bmatrix}
V_1 & & & \\
& V_2 & & \\
& & \ddots & \\
& & & V_{n-1}
\end{bmatrix}
= VB'V \tag{2.111}
$$

$$
L = \begin{bmatrix}
V_1 B_{11} V_1 & V_1 B_{12} V_2 & \cdots & V_1 B_{1m} V_m \\
V_2 B_{21} V_1 & V_2 B_{22} V_2 & \cdots & V_2 B_{2m} V_m \\
\vdots & \vdots & & \vdots \\
V_m B_{m1} V_1 & V_m B_{m2} V_2 & \cdots & V_m B_{mm} V_m
\end{bmatrix}
$$

$$
= \begin{bmatrix}
V_1 & & & \\
& V_2 & & \\
& & \ddots & \\
& & & V_m
\end{bmatrix}
\begin{bmatrix}
B_{11} & B_{12} & \cdots & B_{1m} \\
B_{21} & B_{22} & \cdots & B_{2m} \\
\vdots & \vdots & & \vdots \\
B_{m1} & B_{m2} & \cdots & B_{mm}
\end{bmatrix}
\times
\begin{bmatrix}
V_1 & & & \\
& V_2 & & \\
& & \ddots & \\
& & & V_m
\end{bmatrix}
= VB''V \tag{2.112}
$$

Substituting equations (2.111) and (2.112) into equations (2.105) and (2.106), we have

$$\Delta P = VB'V \Delta\theta \tag{2.113}$$

$$\Delta Q = VB''\Delta V \tag{2.114}$$

We rewrite equations (2.113) and (2.114) as below:

$$\frac{\Delta P}{V} = B'V\Delta\theta \tag{2.115}$$

$$\frac{\Delta Q}{V} = B''\Delta V \tag{2.116}$$

where

$$B' = -\begin{bmatrix} B_{11} & B_{12} & \ldots & B_{1,n-1} \\ B_{21} & B_{22} & \ldots & B_{2,n-1} \\ \vdots & \vdots & & \vdots \\ B_{n-1,1} & B_{n-1,2} & \ldots & B_{n-1,n-1} \end{bmatrix} = \begin{bmatrix} -B_{11} & -B_{12} & \ldots & -B_{1,n-1} \\ -B_{21} & -B_{22} & \ldots & -B_{2,n-1} \\ \vdots & \vdots & & \vdots \\ -B_{n-1,1} & -B_{n-1,2} & \ldots & -B_{n-1,n-1} \end{bmatrix}$$

$$B'' = -\begin{bmatrix} B_{11} & B_{12} & \ldots & B_{1m} \\ B_{21} & B_{22} & \ldots & B_{2m} \\ \vdots & \vdots & & \vdots \\ B_{m1} & B_{m2} & \ldots & B_{mm} \end{bmatrix} = \begin{bmatrix} -B_{11} & -B_{12} & \ldots & -B_{1m} \\ -B_{21} & -B_{22} & \ldots & -B_{2m} \\ \vdots & \vdots & & \vdots \\ -B_{m1} & -B_{m2} & \ldots & -B_{mm} \end{bmatrix}$$

Equations (2.113) and (2.114) are the simplified power flow adjustment equations, which can be written in matrix forms:

$$\begin{bmatrix} \dfrac{\Delta P_1}{V_1} \\[2mm] \dfrac{\Delta P_2}{V_2} \\[1mm] \vdots \\[1mm] \dfrac{\Delta P_{n-1}}{V_{n-1}} \end{bmatrix} = \begin{bmatrix} -B_{11} & -B_{12} & \ldots & -B_{1,n-1} \\ -B_{21} & -B_{22} & \ldots & -B_{2,n-1} \\ \vdots & \vdots & & \vdots \\ -B_{n-1,1} & -B_{n-1,2} & \ldots & -B_{n-1,n-1} \end{bmatrix} \begin{bmatrix} V_1\Delta\theta_1 \\ V_2\Delta\theta_2 \\ \vdots \\ V_{n-1}\Delta\theta_{n-1} \end{bmatrix} \tag{2.117}$$

$$\begin{bmatrix} \dfrac{\Delta Q_1}{V_1} \\[2mm] \dfrac{\Delta Q_2}{V_2} \\[1mm] \vdots \\[1mm] \dfrac{\Delta Q_m}{V_m} \end{bmatrix} = \begin{bmatrix} -B_{11} & -B_{12} & \ldots & -B_{1m} \\ -B_{21} & -B_{22} & \ldots & -B_{2m} \\ \vdots & \vdots & & \vdots \\ -B_{m1} & -B_{m2} & \ldots & -B_{mm} \end{bmatrix} \begin{bmatrix} \Delta V_1 \\ \Delta V_2 \\ \vdots \\ \Delta V_m \end{bmatrix} \tag{2.118}$$

In equations (2.117) and (2.118), matrices B' and B" only contain the imagination part of bus admittance matrix. Thus they are constant symmetrical matrices and need to be triangularized once only at the beginning of the analysis.

Thus equations (2.117) and (2.118) are called the "fast decoupled power flow model" [4–6].

In practical application, the voltage magnitudes of the right side in equations (2.115) and (2.117) are assumed to be 1.0. In this way, the real power adjustment equation in the fast decoupled power flow model can be further simplified as

$$\frac{\Delta P}{V} = B' \Delta \theta \qquad (2.119)$$

$$
\begin{bmatrix}
\dfrac{\Delta P_1}{V_1} \\
\dfrac{\Delta P_2}{V_2} \\
\vdots \\
\dfrac{\Delta P_{n-1}}{V_{n-1}}
\end{bmatrix}
=
\begin{bmatrix}
-B_{11} & -B_{12} & \cdots & -B_{1,n-1} \\
-B_{21} & -B_{22} & \cdots & -B_{2,n-1} \\
\vdots & \vdots & & \vdots \\
-B_{n-1,1} & -B_{n-1,2} & \cdots & -B_{n-1,n-1}
\end{bmatrix}
\begin{bmatrix}
\Delta \theta_1 \\
\Delta \theta_2 \\
\vdots \\
\Delta \theta_{n-1}
\end{bmatrix}
\qquad (2.120)
$$

In addition, there are two fast decoupled power flow versions according to the different handling of the constant matrices B', B''. These are the BX and XB versions.

For the XB version, the resistance is ignored during the calculation of B'. The elements of B', B'' are computed as

$$B'_{ij} = B_{ij} \qquad (2.121)$$

$$B'_{ii} = -\sum_{j \neq i} B'_{ij} \qquad (2.122)$$

$$B''_{ij} = \frac{B_{ij}^2 + G_{ij}^2}{B_{ij}} \qquad (2.123)$$

$$B''_{ii} = -2B_{i0} - \sum_{j \neq i} B''_{ij} \qquad (2.124)$$

where B_{i0} is the shunt reactance to ground.

In the practical calculation, the following assumptions are also adopted in the XB version fast decoupled power flow model.

- Assume $r_{ij} \ll x_{ij}$, which leads to $B_{ij} = -\dfrac{1}{x_{ij}}$
- Eliminate all shunt reactance to ground.
- Omit all effects from phase shift transformers

The **XB** version fast decoupled power flow model can then be expressed as

$$B'_{ij} = -\frac{1}{x_{ij}} \tag{2.125}$$

$$B'_{ii} = \sum_{j \neq i} \frac{1}{x_{ij}} \tag{2.126}$$

$$B''_{ij} = -\frac{x_{ij}}{r_{ij}^2 + x_{ij}^2} \tag{2.127}$$

$$B''_{ii} = -\sum_{j \neq i} B''_{ij} \tag{2.128}$$

where r_{ij}, x_{ij} are the resistance and reactance of branch ij, respectively.

For the BX version, the resistance is ignored during the calculation of B''. The elements of B', B'' are computed as

$$B'_{ij} = \frac{B_{ij}^2 + G_{ij}^2}{B_{ij}} \tag{2.129}$$

$$B'_{ii} = -\sum_{j \neq i} B'_{ij} \tag{2.130}$$

$$B''_{ij} = B_{ij} \tag{2.131}$$

$$B''_{ij} = -2B_{i0} - \sum_{j \neq i} B''_{ij} \tag{2.132}$$

Similarly, the BX version of the fast decoupled power flow model can also be simplified as

$$B'_{ij} = -\frac{x_{ij}}{r_{ij}^2 + x_{ij}^2} \tag{2.133}$$

$$B'_{ii} = \sum_{j \neq i} \frac{x_{ij}}{r_{ij}^2 + x_{ij}^2} \tag{2.134}$$

$$B''_{ij} = -\frac{1}{x_{ij}} \tag{2.135}$$

$$B''_{ii} = -\sum_{j \neq i} B''_{ij} \tag{2.136}$$

It is noted that the fast decoupled power flow algorithm may fail to converge when some of the major assumptions such as $r_{ij} \ll x_{ij}$ do not hold. In this situation, Newton power flow or decoupled power flow without major approximation is recommended.

Example 2.3

In this example we solve the system in Example 2.1 with the decoupled PQ method.

First form the B', B'' matrices as below:

$$B' = \begin{bmatrix} -8.2429 & 2.3529 & 3.6666 \\ 2.3529 & -4.7274 & 0.0000 \\ 3.6666 & 0.0000 & -3.3333 \end{bmatrix}$$

$$B'' = \begin{bmatrix} -8.2429 & 2.3529 \\ 2.3539 & -4.7274 \end{bmatrix}$$

Conducting triangular decomposition to B', B'', respectively, we get Tables 2.5 and 2.6.

Given the initial bus voltage as

$$\dot{V}_1^0 = \dot{V}_2^0 = 1.0\angle 0^0, \quad \dot{V}_3^0 = 1.1\angle 0^0, \quad \dot{V}_4^0 = 1.05\angle 0^0$$

Computing the bus real power mismatch with equation (2.29), we get

$$\Delta P_1^0 = P_{1s} - P_1^0 = -0.30 - (-0.02269) = -0.27731$$

$$\Delta P_2^0 = P_{2s} - P_2^0 = -0.55 - (-0.02404) = -0.52596$$

$$\Delta P_3^0 = P_{3s}s - P_3^0 = 0.5$$

$$\frac{\Delta P_1^0}{V_1^0} = -0.277308$$

$$\frac{\Delta P_2^0}{V_2^0} = -0.525961$$

$$\frac{\Delta P_3^0}{V_3^0} = 0.454545$$

Computing the voltage angle by solving correction equation (2.117):

$$\Delta\theta_1^0 = -0.737161^0, \quad \Delta\theta_2^0 = -6.7415620^0, \quad \Delta\theta_3^0 = 6.3656065^0$$

$$\theta_1^1 = \theta_1^0 + \Delta\theta_1^0 = -0.7371761^0$$

$$\theta_2^1 = \theta_2^0 + \Delta\theta_2^0 = -6.7415620^0$$

$$\theta_3^1 = \theta_3^0 + \Delta\theta_3^0 = 6.3656065^0$$

Table 2.5   Result of triangular decomposition to B'

−0.121317	−0.285452	−0.444829
	−0.246565	−0.258069
		−0.698234

Table 2.6   Result of triangular decomposition to B''

−0.121317	−0.285452
	−0.246565

Then perform the reactive power iteration. Computing the bus real power mismatch with equation (2.30), we get

$$\Delta Q_1^0 = Q_{1s} - Q_1^0 = -0.18 - (-0.1404097) = -0.0395903$$

$$\Delta Q_2^0 = Q_{2s} - Q_2^0 = -0.13 - (-0.0015500) = -0.1315500$$

$$\frac{\Delta Q_1^0}{V_1^0} = -0.0395904$$

$$\frac{\Delta Q_2^0}{V_2^0} = -0.1315500$$

Compute voltage magnitude by solving correction equation (2.118):

$$\Delta V_1^0 = -0.01486806, \quad \Delta V_2^0 = -0.035223$$

$$V_1^1 = V_1^0 + \Delta V_1^0 = 0.985139$$

$$V_2^1 = V_2^0 + \Delta V_2^0 = 0.964777$$

Conduct the second iteration, using new voltage values. If the convergence tolerance is $\varepsilon = 10^{-5}$, the power flow will be converged after five iterations, which are shown in Tables 2.7 and 2.8.

Compared with the Newton method, the decoupled PQ method obtained almost the same results.

Table 2.7 Bus power mismatch change

Iteration k	ΔP_1	ΔP_2	ΔP_3	ΔQ_1	ΔQ_2
0	−0.27731	−0.52596	0.5	-3.95903×10^{-2}	−0.13155
1	4.051×10^{-3}	1.444×10^{-2}	8.691×10^{-3}	-2.037×10^{-3}	1.568×10^{-3}
2	-6.603×10^{-3}	-3.488×10^{-3}	6.826×10^{-4}	-1.537×10^{-3}	-1.123×10^{-3}
3	-1.227×10^{-3}	2.148×10^{-3}	-4.967×10^{-5}	-2.694×10^{-4}	7.3477×10^{-4}
4	9.798×10^{-5}	-1.552×10^{-4}	-1.140×10^{-5}	2.513×10^{-5}	-3.277×10^{-5}
5	$<10^{-5}$	$<10^{-5}$	$<10^{-5}$	$<10^{-5}$	$<10^{-5}$

Table 2.8 Bus voltage change

Iteration k	θ_1	θ_2	θ_3	V_1	V_2
1	-0.737^0	-6.742^0	6.366^0	0.9851	0.9648
2	-0.349^0	-6.356^0	6.871^0	0.9850	0.9650
3	-0.497^0	-6.475^0	6.737^0	0.9847	0.9646
4	-0.500^0	-6.448^0	6.732^0	0.9847	0.9648
5	-0.500^0	-6.450^0	6.732^0	0.9847	0.9648

2.4.2   Decoupled Power Flow Without Major Approximation

Assuming the voltage magnitude in the Newton power flow model (2.99) to be 1.0, we have

$$\begin{bmatrix} \Delta P \\ \Delta Q \end{bmatrix} = - \begin{bmatrix} H & N \\ K & L \end{bmatrix} \begin{bmatrix} \Delta\theta \\ \Delta V \end{bmatrix} \qquad (2.137)$$

Premultiplying the ΔP equations by KH^{-1} and adding the resulting equations to the ΔQ equations leads to the system of equations

$$\begin{bmatrix} \Delta P \\ \Delta Q - KH^{-1}\Delta P \end{bmatrix} = - \begin{bmatrix} H & N \\ 0 & L - KH^{-1}N \end{bmatrix} \begin{bmatrix} \Delta\theta \\ \Delta V \end{bmatrix} \qquad (2.138)$$

Premultiplying the ΔQ equations by NL^{-1} and adding the resulting equations to the ΔP equations leads to the system of equations

$$\begin{bmatrix} \Delta P - NL^{-1}\Delta Q \\ \Delta Q \end{bmatrix} = - \begin{bmatrix} H - NL^{-1}K & 0 \\ K & L \end{bmatrix} \begin{bmatrix} \Delta\theta \\ \Delta V \end{bmatrix} \qquad (2.139)$$

By combining the operations performed to obtain equations (2.138) and (2.139), we get

$$\begin{bmatrix} \Delta P - NL^{-1}\Delta Q \\ \Delta Q - KH^{-1}\Delta P \end{bmatrix} = - \begin{bmatrix} H - NL^{-1}K & 0 \\ 0 & L - KH^{-1}N \end{bmatrix} \begin{bmatrix} \Delta\theta \\ \Delta V \end{bmatrix} \qquad (2.140)$$

or

$$\begin{bmatrix} \Delta P - NL^{-1}\Delta Q \\ \Delta Q - KH^{-1}\Delta P \end{bmatrix} = - \begin{bmatrix} H_{eq} & 0 \\ 0 & L_{eq} \end{bmatrix} \begin{bmatrix} \Delta\theta \\ \Delta V \end{bmatrix} \qquad (2.141)$$

where the equivalent matrices H_{eq} and L_{eq} are defined as

$$H_{eq} = H - NL^{-1}K \qquad (2.142)$$

$$L_{eq} = L - KH^{-1}N \qquad (2.143)$$

It can be observed that equation (2.140) or (2.141) is equivalent to the original system (2.137) but has the decoupled solution structure in which $\Delta\theta$ and ΔV are calculated separately. This decoupled procedure is not approximation way by ignoring the off-diagonal submatrices N and K, which was adopted in fast decoupled power flow in Section 2.4.1. Thus the solution will be close to the Newton power flow solution. However, the solution procedures are different from the Newton method, where the different $\Delta\theta$ and ΔV are not computed simultaneously but separately.

The following decoupled algorithm can be used to solve equation (2.138) for $\Delta\theta$ and ΔV [6]:

Step (1): Compute temporary angle corrections

$$\Delta\theta_H = -H^{-1}\Delta P(V, \theta) \tag{2.144}$$

Step (2): Compute voltage corrections

$$\Delta V = -L_{eq}^{-1}\Delta Q(V, \theta + \Delta\theta_H) \tag{2.145}$$

Step (3): Compute additional angle corrections

$$\Delta\theta_N = -H^{-1}N\Delta V \tag{2.146}$$

It can be verified that ΔV and $\Delta\theta = \Delta\theta_H + \Delta\theta_N$ are the solution vectors of equation (2.138). This algorithm considers the coupling effect represented by K.

For equation (2.139), we have the dual algorithm:

Step (1): Compute temporary voltage corrections

$$\Delta V_L = -L^{-1}\Delta Q(V, \theta) \tag{2.147}$$

Step (2): Compute angle corrections

$$\Delta\theta = -H_{eq}^{-1}\Delta P(V + \Delta V_L, \theta) \tag{2.148}$$

Step (3): Compute additional voltage corrections

$$\Delta V_K = -L^{-1}K\Delta\theta \tag{2.149}$$

where $\Delta V = \Delta V_L + \Delta V_K$

Although the above iteration algorithms (2.144)–(2.146) and (2.147)–(2.149) yield the correct solutions for the power flow model (2.137), they are not suited for practical implementation [6]. The reasons are:

- In the first algorithm angle corrections $\Delta\theta$ are computed in two steps ($\Delta\theta_H$ and $\Delta\theta_N$), while in the second algorithm voltage magnitude corrections ΔV are computed in two steps (ΔV_L and ΔV_K).
- The matrices H_{eq} and L_{eq} may be full.

The following iteration algorithm is suggested because of the above two difficulties. For solving equations (2.144)–(2.146), the iteration steps for the suggested algorithm are described below:

$$\Delta\theta_H^k = -H^{-1}\Delta P(V^k, \theta^k) \tag{2.150}$$

$$\Delta\theta_{\text{temp}}^{k+1} = \theta^k + \Delta\theta_H^k \tag{2.151}$$

$$\Delta V^k = -L_{\text{eq}}^{-1}\Delta Q(V^k, \theta_{\text{temp}}^{k+1}) \tag{2.152}$$

$$\Delta V^{k+1} = V^k + \Delta V^k \tag{2.153}$$

$$\Delta\theta_N^k = -H^{-1}N\Delta V^k \tag{2.154}$$

$$\theta^{k+1} = \Delta\theta_{\text{temp}}^{k+1} + \Delta\theta_N^k \tag{2.155}$$

Then compute the temporary angle vector of the next iteration:

$$\Delta\theta_H^{k+1} = -H^{-1}\Delta P(V^{k+1}, \theta^{k+1}) \tag{2.156}$$

$$\Delta\theta_{\text{temp}}^{k+2} = \theta^{k+1} + \Delta\theta_H^{k+1} \tag{2.157}$$

By adding the two successive angle corrections, we get

$$\begin{aligned}
\Delta\theta_N^k + \Delta\theta_H^{k+1} &= -H^{-1}\left[\Delta P(V^{k+1}, \theta^{k+1}) - N\Delta V^k\right]\\
&\approx -H^{-1}\left[\Delta P(V^{k+1}, \theta_{\text{temp}}^{k+1}) - H\Delta\theta_N^k - N\Delta V^k\right]\\
&\approx -H^{-1}\Delta P(V^{k+1}, \theta_{\text{temp}}^{k+1})
\end{aligned} \tag{2.158}$$

The above combined angle correction can be obtained by a single forward/backward solution using the active mismatches computed at V^{k+1} and $\theta_{\text{temp}}^{k+1}$. Similar iteration steps can be obtained for the algorithm (2.147)–(2.149).

2.5   DC POWER FLOW

AC power flow algorithms have high calculation precision but do not have fast speed. In real power dispatch or power market analysis, the requirement of calculation precision is not very high, but the requirement of calculation speed is of most concern, especially for a large-scale power system. More simplification power flow algorithms than fast decoupled power flow algorithms are used. One algorithm is called "MW Only." In this method, the Q-V equation in the fast decoupled power flow model is completely dropped. Only the following $P - \theta$ equation is used to correct the angle according to the real power mismatch.

$$\begin{bmatrix} \dfrac{\Delta P_1}{V_1} \\[2mm] \dfrac{\Delta P_2}{V_2} \\[1mm] \vdots \\[1mm] \dfrac{\Delta P_{n-1}}{V_{n-1}} \end{bmatrix} = \begin{bmatrix} -B_{11} & -B_{12} & \cdots & -B_{1,n-1} \\ -B_{21} & -B_{22} & \cdots & -B_{2,n-1} \\ \vdots & \vdots & & \vdots \\ -B_{n-1,1} & -B_{n-1,2} & \cdots & -B_{n-1,n-1} \end{bmatrix} \begin{bmatrix} \Delta\theta_1 \\ \Delta\theta_2 \\ \vdots \\ \Delta\theta_{n-1} \end{bmatrix} \tag{2.159}$$

In the MW-only power flow calculation, the voltage magnitude can be handled either as constant or as 1.0 during each $P - \theta$ iteration. For the convergence, only real power mismatch is checked no matter what the reactive power mismatch is.

Another most simplified power flow algorithm is DC power flow. It is also an MW-only method but has the following assumptions:

(1) All the voltage magnitudes are equal to 1.0.
(2) Ignore the resistance of the branch; i.e., the susceptance of the branch is

$$B_{ij} = -\frac{1}{x_{ij}} \tag{2.160}$$

(3) The angle difference on the two ends of the branch is very small, so that we have

$$\sin\theta_{ij} = \theta_i - \theta_j \tag{2.161}$$

$$\cos\theta_{ij} = 1 \tag{2.162}$$

(4) Ignore all ground branches; that is,

$$B_{i0} = B_{j0} = 0 \tag{2.163}$$

Therefore, the DC power flow model will be

$$\begin{bmatrix} \Delta P_1 \\ \Delta P_2 \\ \vdots \\ \Delta P_{n-1} \end{bmatrix} = [B'] \begin{bmatrix} \Delta\theta_1 \\ \Delta\theta_2 \\ \vdots \\ \Delta\theta_{n-1} \end{bmatrix} \tag{2.164}$$

or

$$[\Delta P] = [B'][\Delta\theta] \tag{2.165}$$

where the elements of the matrix B' are the same as those in the **XB** version of fast decoupled power flow but we ignore the matrix B''. That is,

$$B'_{ij} = -\frac{1}{x_{ij}} \tag{2.166}$$

$$B'_{ii} = -\sum_{j \neq i} B'_{ij} \tag{2.167}$$

The DC power flow is a purely linear equation, so only one iteration calculation is needed to obtain the power flow solution. However, it is only good for calculating real power flows on transmission lines and transformers. The power flowing on each line using the DC power flow is then

$$P_{ij} = -B_{ij}(\theta_i - \theta_j) = \frac{\theta_i - \theta_j}{x_{ij}} \tag{2.168}$$

REFERENCES

[1] J.Z. Zhu, "Power System Optimal Operation," Tutorial of Chongqing University, 1990.

[2] Y. He, Z.Y. Wen, F.Y. Wang, and Q.H. Zhou, *Power Systems Analysis*, Huazhong Polytechnic University Press, 1985.

[3] A. Keyhani, A. Abur, and S. Hao, "Evaluation of Power Flow Techniques for Personal Computers," *IEEE Trans. on Power System*, Vol. 4, No. 2, 1989, pp. 817–826.

[4] O. Alsac and B. Sttot, "Fast Decoupled power flow," *IEEE Trans. on Power System*, Vol. 93, 1974, pp. 859–869.

[5] R.A.M. Van Amerongen, "A General Purpose Version of the Fast Decoupled power flow," IEEE Summer Meeting, 1988.

[6] A. Monticelli, A. Garcia, and O.R. Saavedra, "Decoupled power flow,: Hypothesis, Derivations, and Testing," *IEEE Trans. on Power System*, Vol. 5, No. 4, 1990, pp. 1425–1431.

3

SENSITIVITY CALCULATION

Currently, sensitivity analysis is becoming more and more important in practical power system operations including in power market operations. This chapter analyzes and discusses all kinds of sensitivity factors such as loss sensitivity factor, generator shift factor, pricing node shift factor, constraint shift factor, line outage distribution factor (LODF), outage transfer distribution factor (OTDF), response factor for the transfer path, and voltage sensitivity factor. It also addresses the practical application of these sensitivity factors including a practical method to convert the sensitivities with different references.

3.1 INTRODUCTION

This chapter focuses on the analysis and implementation details of the calculations of several sensitivities such as loss sensitivity, voltage sensitivity, generator constraint shift factor, and area-based constraint shift factor in the practical transmission network and energy markets. The power operator uses these to study and monitor market and system behavior and detect possible problems in the operation. These sensitivity calculations are also used to determine whether the online capacity as indicated in the resource plan is located in the right place in the network to serve the forecasted demand. If congestion or violation exists, the generation scheduling based on the sensitivity calculations can determine whether or not a different allocation of the available resources could resolve the congestion or violation problem.

In the early energy market, transmission losses were neglected for computational simplicity reasons, but they are addressed in the standard market design (SMD) [1–4]. Loss calculation is considered for the dispatch functions of SMD such as location-based marginal prices (LMP). Loss allocation does not affect generation levels or power flows; however, it does modify the value of LMP [5]. The early and classic loss calculation approach is the loss formula–B coefficient method [6], which has been replaced by the more accurate inverse Jacobian transpose method [7]. Numerous loss calculation methods have been proposed in the literature and can be categorized into pro rata [8], incremental [9], proportional sharing [10], and Z-bus loss allocation [11].

Calculation of loss sensitivity is based on the distributed slack buses in the energy control center [6, 11–13]. In real-time energy markets, LMP or economic dispatch is implemented based on market-based reference, which is an arbitrary slack bus, instead of the distributed slack buses in the traditional energy management system. Meanwhile, the existing loss calculation methods in traditional EMS systems are generally based on the generator slacks or references. Since the units with automatic generation control (AGC) are selected as the distributed slacks, and the patterns or status of AGC units are variable for different time periods in the real-time energy market, the sensitivity values will keep changing, which complicates the issue. This chapter presents a fast and useful formula to calculate loss sensitivity for any slack bus [14, 15].

The simultaneous feasibility test (SFT) performs the network sensitivity analysis in the base case and in contingency cases in the power system. The base case and postcontingency MW flows are compared against their respective limits to generate the set of critical constraints. For each critical constraint, SFT calculates constraint coefficients (shift factors) that represent linearized sensitivity factors between the constrained quantity (e.g., MW branch flow) and MW injections at network buses. The B-matrix used to calculate the shift factors is constructed to reflect proper network topology [16–18].

The objective of SFT is to identify whether or not network operation is feasible for a real power injection scenario. If operational limits are violated, generic constraints are generated that can be used to prevent the violation if presented with the same network conditions [16].

In the energy market systems, the trade is often considered between the source and the sink (i.e., the point of delivery, POD and point of receipt, POR). The source and the sink may be an area or any bus group. Therefore, the area-based sensitivities are needed, which can be computed through the constraint shift factors within the area.

Another type of sensitivity that is frequently used is related to voltage stability, especially static voltage stability, which investigates the stability of an operating point and applies a linearized model. Static voltage instability is mainly associated with reactive power imbalance. This imbalance mainly occurs on a local network or a specified bus in a system, which is called the weak bus. Therefore, the reactive power supports have to be locally adequate.

   Voltage sensitivity analysis can detect the weak buses/nodes in the power system where the voltage is low. It can be used to select the optimal locations of VAR support service [19–25]. According to the sensitivity values voltage benefit factor (VBF) and loss benefit factor (LBF), a ranking of VAR support sites can also be obtained.

3.2 LOSS SENSITIVITY CALCULATION

This section presents a fast and useful formula to calculate loss sensitivity for any slack bus. The formula is based on the loss sensitivity results from the distributed slacks without computing a new set of sensitivity factors through the traditional power flow calculation. In particular, the loads are selected as the distributed slacks rather than the usual generator slacks. The loss sensitivity values will be unchanged for the same network topology no matter how the status of the AGC units changes.

   In the energy market, the formulation of the optimum economic dispatch can be represented as follows:

$$Min\ F = \sum_j C_j P_j \quad j \in NG \tag{3.1}$$

Such that

$$s.t. \sum P_D + P_L = \sum_j P_{Gj} \quad j \in NG \tag{3.2}$$

$$\sum_j S_{ij} P_j \le P_{i\max} \quad j \in NG, i \in K_{\max} \tag{3.3}$$

$$P_{Gj\min} \le P_{Gj} \le P_{Gj\max} \quad j \in NG \tag{3.4}$$

where

   P_D: The real power load
   P_{imax}: The maximum requirement of power supply at the active constraint i
   P_{Gj}: The real power output at generator bus j
   P_{Gjmin}: The minimal real power output at generator j
   P_{Gjmax}: The maximal real power output at generator j
   P_L: The network losses
   S_{ij}: The sensitivity (shift factor) for resource or unit j and active constraint i with respect to the market-based reference
   C_j: The real-time price for the resource (or unit) j
   K_{max}: The maximum number of active constraints
   NG: The number of units

The Lagrangian function is obtained from equations (3.1) and (3.2).

$$F_L = \sum_i f_i(P_{Di}) + \lambda \left(\sum_i P_{Di} + P_L - \sum_j P_{Gj} \right) \tag{3.5}$$

Traditionally, generation reference (single or distributed slack) is used in the calculation of loss allocation. This works, but it may be inconvenient or confusing for the users who frequently use the loss factors. The reason is that the AGC status or patterns of units are variable in the real-time EMS or energy markets. The loss sensitivity values based on the distributed unit references will keep changing because of the change of unit AGC status. Thus the distributed load slack or reference is used here.

The optimality criteria of the Lagrange function (3.5) are written as follows:

$$\frac{\partial F_L}{\partial P_{Di}} = \frac{df_i}{dP_{Di}} + \lambda \left(1 + \frac{\partial P_L}{\partial P_{Di}} \right) = 0 \quad i \in ND \tag{3.6}$$

$$\frac{\partial F_L}{\partial P_{Gj}} = \frac{df_i}{dP_{Gj}} + \lambda \left(\frac{\partial P_L}{\partial P_{Gj}} - 1 \right) = 0 \quad j \in NG \tag{3.7}$$

$$\frac{df_i}{dP_{Di}} L_{Di} = \lambda \quad i \in ND \tag{3.8}$$

$$L_{Di} = -\frac{1}{1 + \dfrac{\partial P_L}{\partial P_{Di}}} \quad i \in ND \tag{3.9}$$

$$\frac{df_i}{dP_{Gj}} L_{Gj} = \lambda \quad j \in NG \tag{3.10}$$

$$L_{Gj} = \frac{1}{1 - \dfrac{\partial P_L}{\partial P_{Gj}}} \quad j \in NG \tag{3.11}$$

where

λ: The Lagrangian multiplier

$\dfrac{\partial P_L}{\partial P_{Di}}$: The loss sensitivity with respect to load at bus i

$\dfrac{\partial P_L}{\partial P_{Gj}}$: The loss sensitivity with respect to unit at bus j

We use $\dfrac{\partial P_L}{\partial P_i}$, which is the loss sensitivity with respect to an injection at bus i, to stand for both $\dfrac{\partial P_L}{\partial P_{Di}}$ and $\dfrac{\partial P_L}{\partial P_{Gj}}$. Since the distributed slack buses are used here, all loss sensitivity factors are nonzero.

If an arbitrary slack bus, k, is selected, then P_k is the function of the other injections, i.e.,

$$P_k = f(P_i) \quad i \in n, i \neq k \tag{3.12}$$

where n is the total number of buses in the system and P_i is the power injection at bus i, which includes the load P_{Di} and generation P_{Gj}. Actually, the load can be treated as a negative generation. Then equations (3.9) and (3.11) can be changed to equation (3.13), and equations (3.8) and (3.10) can be changed to equation (3.14).

$$L_i = \frac{1}{1 - \dfrac{\partial P_L}{\partial P_i}} \quad i \in n \tag{3.13}$$

$$\frac{df_i}{dP_i} L_i = \lambda \quad i \in n \tag{3.14}$$

Equation (3.2) will be rewritten as

$$P_L = P_k + \sum_{i \neq k} P_i \quad i \in n \tag{3.15}$$

The new Lagrangian function can be obtained from equations (3.1) and (3.15).

$$F_L^* = \sum_i f_i(P_i) + \lambda \left(P_L - P_k - \sum_{i \neq n} P_i \right) \tag{3.16}$$

The optimality criteria can be obtained from the Lagrangian function (3.16).

$$\frac{\partial F_L^*}{\partial P_i} = \frac{df_i}{dP_i} + \frac{df_k}{dP_k} \frac{\partial P_k}{\partial P_i} + \lambda \left(\frac{\partial P_L}{\partial P_i} - \frac{\partial P_k}{\partial P_i} - 1 \right) = 0 \quad i \in n, i \neq k \tag{3.17}$$

From equation (3.15), we get

$$\frac{\partial P_L}{\partial P_i} = 1 + \frac{\partial P_k}{\partial P_i} \tag{3.18}$$

From equations (3.17) and (3.18), we get

$$\frac{df_i}{dP_i} L_i^* = \frac{df_k}{dP_k} \tag{3.19}$$

$$L_i^* = \frac{1}{1 - \dfrac{\partial P_L}{\partial P_i}} \quad i \in n, i \neq k \tag{3.20}$$

It is noted that L_i and L_i^* are similar, but they have different meanings [14]. The former is based on the distributed slack buses, and the latter is based on an arbitrary slack bus k. Similarly, the loss sensitivity in L_i is based on the distributed slack, i.e., $\left.\dfrac{\partial P_L}{\partial P_i}\right|_{DS}$ (the subscript DS means the distributed slack); the loss sensitivity in L_i^* is based on an arbitrary single slack bus k, i.e., $\left.\dfrac{\partial P_L}{\partial P_i}\right|_k$. Note that the kth loss sensitivity, with bus k as the slack bus, is zero.

From equations (3.14) and (3.19), we have the following equation:

$$L_i^* = \frac{L_i}{L_k}, \quad L_k^* = 1 \tag{3.21}$$

From equations (3.13), (3.20), and (3.21), we get

$$\frac{1}{1 - \left.\dfrac{\partial P_L}{\partial P_i}\right|_k} = \frac{1 - \left.\dfrac{\partial P_L}{\partial P_k}\right|_{DS}}{1 - \left.\dfrac{\partial P_L}{\partial P_i}\right|_{DS}} \tag{3.22}$$

$$1 - \left.\frac{\partial P_L}{\partial P_i}\right|_k = \frac{1 - \left.\dfrac{\partial P_L}{\partial P_i}\right|_{DS}}{1 - \left.\dfrac{\partial P_L}{\partial P_k}\right|_{DS}} \tag{3.23}$$

Hence, with one set of incremental transmission loss coefficients for the distributed slack buses, the loss sensitivity for an arbitrary slack bus can be calculated from the following formula:

$$\left.\frac{\partial P_L}{\partial P_i}\right|_k = \frac{\left.\dfrac{\partial P_L}{\partial P_i}\right|_{DS} - \left.\dfrac{\partial P_L}{\partial P_k}\right|_{DS}}{1 - \left.\dfrac{\partial P_L}{\partial P_k}\right|_{DS}} \tag{3.24}$$

The formula of loss sensitivity calculation is very simple, but it is accurate and efficient for real-time energy markets. It will avoid computing a new set of loss sensitivity factors whenever the slack bus k changes. Consequently, it means a huge time savings. In addition, the loss factors based on the distributed load reference will not be changed no matter how the AGC statuses of units vary, as long as the network topology is the same as before.

3.3 CALCULATION OF CONSTRAINED SHIFT SENSITIVITY FACTORS

3.3.1 Definition of Constraint Shift Factors

The objective of SFT is to identify whether or not network operation is feasible for a real power injection scenario. If operational limits are violated, generic constraints and corresponding sensitivities (the shift factors) are generated, which can be used to prevent the violation if presented with the same network conditions. Meanwhile, the shift factors can also be used in the generation scheduling or economic dispatch to alleviate the overload of transmission lines.

The SFT calculations include the contingency analysis (CA), in which the decoupled power flow (DPF) or DC power flow is used. The set of component changes that can be analyzed include transmission line, transformer, circuit breaker, load demand, and generator outages. SFT informs the users about the contingencies that could cause conditions violating operating limits. These limits include branch overloads, abnormal voltages, and voltage angle differences across specified parts of the network. SFT reports the sensitivity (shift factor) of the constraint with respect to the controls. These controls include unit MW control, phase shifter, and load MW control.

3.3.1.1 Unit MW Control The unit MW control is the most efficient and cheapest control among the available controls. The formulation of sensitivity for a unit can be written as follows:

$$S_{kj} = \frac{\partial P_k}{\partial P_{Gj}} \quad k = 1, \ldots\ldots, K_{\max}, \quad j = 1, \ldots\ldots PG_{\max} \qquad (3.25)$$

where

S_{kj}: The sensitivity of the power change on constraint k with respect to power change on the unit MW control j

P_k: The MW power on the constraint k

P_{Gj}: The MW power on generating unit control j

K_{max}: The maximum number of constraints

PG_{max}: The maximum number of generator unit MW controls

According to KCL law, it is impossible that power change on the branch constraint will be greater than one MW if the generator control has only one MW power change. Thus the maximum value of the sensitivity of the branch constraint with respect to the unit MW control is 1.0 (generally, less than 1.0).

3.3.1.2 Phase Shifter Control The phase shifter is another efficient control among the available controls. There are some assumptions for the phase shifter in the SFT design. The phase shifter control variable is tap number (e.g., phase shifter angle). Normally tap number is an integer, but it can be handled as a real number in the practical SFT calculation. In addition, all opened phase shifters will be skipped over, that is, the sensitivity for the phase shifter that is open at any end will not be calculated.

The step on the tap-type is the sensitivity of angle with respect to tap number. Thus the sensitivity of the constraint to the phase shifter is about the power change on the constraint to the angle change of the phase shifter. The angle unit may be degree or radiant. Since the value of sensitivity may be very small if the angle unit is degree, radiant is adopted in the practical calculation. The formulation of sensitivity for phase shifter can be written as follows:

$$S_{kjp} = \frac{\partial P_k}{\partial \phi_{jp}^{ps}} \quad k = 1, \ldots \ldots, K_{\max}, \quad jp = 1, \ldots \ldots PS_{\max} \tag{3.26}$$

where

S_{kjp}: The sensitivity of the constraint k to the phase shifter control jp

ϕ_{jp}^{ps}: The phase shifter angle of the phase shifter control jp

K_{max}: The maximum number of constraints

PS_{max}: The maximum number of phase shifter controls

It is noted that there is a special "branch in constraint" logic that must be implemented when the phase shifter branch itself is in the constraint. Basically the artificial flow through transformer branch must be subtracted from constraint flow.

In addition, the sensitivity of the constraint to the phase shifter control is different from the sensitivity of the constraint to the generator control or other bus injection type control. The value of the latter cannot be greater than 1.0, but the former does not have this constraint.

3.3.1.3 Load MW Control The load MW control should be the last control when other controls are not available. The formulation of sensitivity for load MW control can be written as follows:

$$S_{kjd} = -\frac{\partial P_k}{\partial P_{jd}} \quad k = 1, \ldots \ldots, K_{\max}, \quad jd = 1, \ldots \ldots LD_{\max} \tag{3.27}$$

where

S_{kjd}: The sensitivity of the constraint k to the load MW control jd

P_{jd}: The MW power on load control jd

K_{max}: The maximum number of constraints

LD_{max}: The maximum number of load MW controls in the whole system

It is noted that the sensitivity sign for load MW control is negative. The reason is that increasing load will cause more serious constraint violation rather than reducing the constraint violation. According to the sensitivity relationship between the constraint and the load MW control, it is needed to reduce/shed load for alleviating or deleting the constraint violation.

In the market application, the sensitivity of the pricing node is interested. The pricing node does not have the generator or load connected to it. Thus the above sensitivity calculation of unit/load control can be expanded to any bus injection, that is,

$$S_{kbs} = -\frac{\partial P_k}{\partial P_{bs}} \qquad k = 1, \ldots\ldots, K_{\max}, \quad bs = 1, \ldots\ldots NB_{\max}$$

where

S_{kbs}: The sensitivity of the constraint k to the bus injection on bus bs

P_{bs}: The MW power injection on bus bs

NB_{max}: The maximum number of buses in the whole system

3.3.1.4 Constraint Value For each constraint, the constraint value (DC value) is computed from the control values multiplied by sensitivities. The formulation can be written as follows:

$$\text{DCVAL}_k = \sum_{j=1}^{U\max} \text{VAL\_}U_j * S_{kj} \tag{3.28}$$

where

$DCVAL_k$: The constraint value for constraint k

VAL_U_j: The value of control j. Here, the controls include unit MW control, phase shifter, and load MW control.

S_{kj}: The sensitivity or shift factor of constraint k to control j

U_{max}: The maximum number of controls

3.3.2 Computation of Constraint Shift Factors

3.3.2.1 Constraint Shift Factors Without Line Outage The constraint shift factors without line outage are also called as the generation shift factor.

From DC power flow algorithm, we have the following equation:

$$\begin{bmatrix} \Delta P_1 \\ \Delta P_2 \\ \vdots \\ \Delta P_n \end{bmatrix} = [B'] \begin{bmatrix} \Delta\theta_1 \\ \Delta\theta_2 \\ \vdots \\ \Delta\theta_n \end{bmatrix} \tag{3.29}$$

Then the standard matrix calculation of the DC power flow can be written as below:

$$\boldsymbol{\theta} = [X]\mathbf{P} \tag{3.30}$$

Since the DC power flow model is a linear model, we may calculate perturbations about a given set of system conditions by use of the same model. Thus we can compute the changes in bus phase angles $\Delta\theta$ for a given set of changes in the bus power injections ΔP:

$$\Delta\boldsymbol{\theta} = [X]\Delta\mathbf{P} \tag{3.31}$$

where the net perturbation of the reference bus equals the sum of the perturbations on all the other buses.

Now we compute the generation shift factors for the generator on bus i. To do this, we will set the perturbation on bus i to $+1$ pu and the perturbation on all the other buses to zero. Then we can solve for the change in bus phase angles with the following matrix calculation:

$$\Delta\boldsymbol{\theta} = [X]\begin{bmatrix} +1 \\ -1 \end{bmatrix} \begin{matrix} \leftarrow \ row\ i \\ \leftarrow ref\ row \end{matrix} \tag{3.32}$$

The vector of bus power injection perturbations in equation represents the situation when a 1-pu power increase is made at bus i and is compensated by a 1-pu decrease in power at the reference bus. The $\Delta\theta$ values in equation are thus equal to the derivative of the bus angles with respect to a change in power injection at bus i.

Thus the constraint shift factors S_{ki} without considering the line outage can be derived as follows.

Let p and q be the two ends of constraint k; the power flowing on the constraint line k using DC power flow is:

$$P_k = \frac{1}{x_k}(\theta_p - \theta_q) \tag{3.33}$$

The generation shift factors are defined as

$$\begin{aligned} S_{ki} &= \frac{\mathrm{d}P_k}{\mathrm{d}P_i} = \frac{\mathrm{d}}{\mathrm{d}P_i}\left[\frac{1}{x_k}(\theta_p - \theta_q)\right] \\ &= \frac{1}{x_k}\left(\frac{\mathrm{d}\theta_p}{\mathrm{d}P_i} - \frac{\mathrm{d}\theta_q}{\mathrm{d}P_i}\right) = \frac{1}{x_k}(X_{pi} - X_{qi}) \end{aligned} \tag{3.34}$$

In the practical application, the generation shift factors of the network can be directly obtained from $[B']$ through forward and back calculation.

Suppose a branch k that is from p to q with the reactance x_k. From $[B'][\theta] = [P]$, we get

$$[B'][\theta] = \begin{bmatrix} 0 \\ \vdots \\ 0 \\ +\dfrac{1}{x_k} \\ 0 \\ \vdots \\ 0 \\ -\dfrac{1}{x_k} \\ 0 \\ \vdots \\ 0 \end{bmatrix} \begin{matrix} \\ \\ \\ \leftarrow \text{row } p \\ \\ \\ \\ \leftarrow \text{row } q \\ \\ \\ \end{matrix} \tag{3.35}$$

Through implying forward and back calculation to the above equation, the solution will be the generation shift factors for all bus with respect to the constraint line k. If a constraint consists of multiple lines (branches), the superposition theory can be applied. For example, a constraint contains two lines k (from p to q) and t (from i to j) with reactance x_k and x_t, respectively. We get the following relationship:

$$[B'][\theta] = \begin{bmatrix} 0 \\ \vdots \\ 0 \\ +\dfrac{1}{x_k} \\ 0 \\ \vdots \\ 0 \\ -\dfrac{1}{x_k} \\ 0 \\ \vdots \\ 0 \\ +\dfrac{1}{x_t} \\ 0 \\ \vdots \\ 0 \\ -\dfrac{1}{x_t} \\ 0 \\ \vdots \\ 0 \end{bmatrix} \begin{matrix} \\ \\ \\ \leftarrow \text{row } p \\ \\ \\ \\ \leftarrow \text{row } q \\ \\ \\ \\ \leftarrow \text{row } i \\ \\ \\ \\ \leftarrow \text{row } j \\ \\ \\ \end{matrix}$$

   Through implying forward and back calculation to the above equation, the
solution will be the generation shift factors for all buses with respect to lines
k and t.

3.3.2.2 Line Outage Distribution Factors [17] The simulation of line
outage is shown in Figure 3.1. Figure 3.1(a) is a network without line outage.
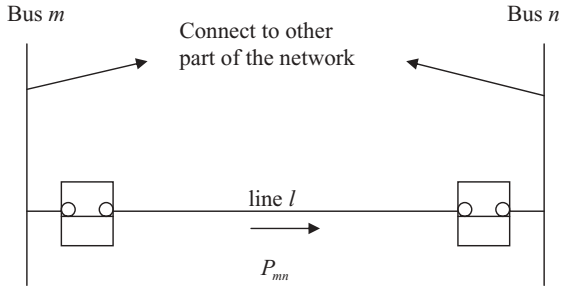
(a) Network before line *l* outage
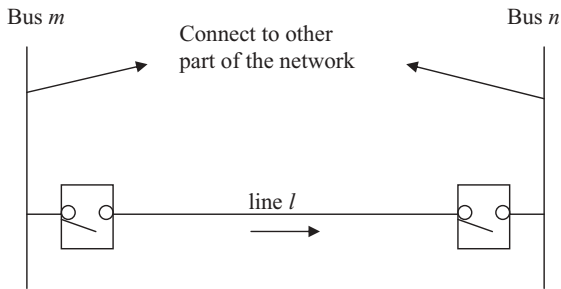
(b) Network after line *l* outage
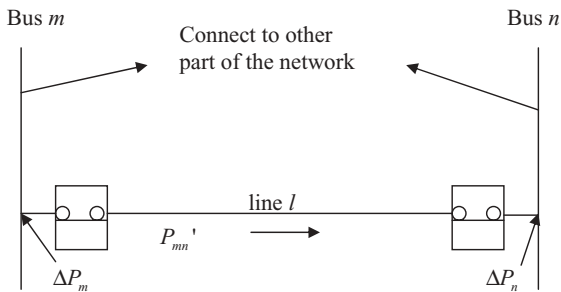
(c) Modeling line *l* outage using injections

FIGURE 3.1   Network for simulating line outage

Suppose line l from bus m to bus n were opened by circuit breakers as shown in Figure 3.1(b). A line outage may be modeled by adding two power injections to a system, one at each end of the line to be dropped, which is shown in Figure 3.1(c). The line is actually left in the system, and the effects of its being dropped are modeled by injections. Note that when the circuit breakers are opened, no current flows through them and the line is completely isolated from the remainder of the network. In Figure 3.1, the breakers are still closed but injections ΔP_m and ΔP_n have been added to bus m and bus n, respectively. If $\Delta P_m = P_{mn}$, and $\Delta P_n = -P_{mn}$, where P_{mn} is equal to the power flowing over the line, we will still have no current flowing through the circuit breakers even though they are closed. As far as the remainder of the network is concerned, the line is disconnected.

Using the equation relating to $\Delta \boldsymbol{\theta}$ and $\Delta \mathbf{P}$,

$$\Delta \boldsymbol{\theta} = [X] \Delta \mathbf{P} \tag{3.36}$$

Since only power injections at buses m and n have been changed after line outage by adding two power injections to a system, then

$$\Delta \mathbf{P} = \begin{bmatrix} 0 \\ \vdots \\ 0 \\ \Delta P_m \\ 0 \\ \vdots \\ 0 \\ \Delta P_n \\ 0 \\ \vdots \\ 0 \end{bmatrix} \tag{3.37}$$

Thus we can get the incremental changes of the phase angle at buses m and n of the line l from the outage

$$\Delta \theta_m = X_{mn} \Delta P_n + X_{mm} \Delta P_m \tag{3.38}$$

$$\Delta \theta_n = X_{nn} \Delta P_n + X_{nm} \Delta P_m \tag{3.39}$$

where

θ_m: The phase angle at bus m of line l before the outage
θ_n: The phase angle at bus n of line l before the outage
P_{mn}: The power flow on line l from bus m to bus n before the outage
$\Delta \theta_m$: The incremental changes of the phase angle at bus m of line l from the outage

$\Delta\theta_n$: The incremental changes of the phase angle at bus n of line l from the outage

ΔP_{mn}: The incremental changes of the power flow on line l of line l from the outage

θ'_m: The phase angle at bus m of line l after the outage

θ'_n: The phase angle at bus n of line l after the outage

P'_{mn}: The power flow on line l from bus m to bus n after the outage

The outage modeling criterion requires that the incremental injections ΔP_n and ΔP_m equal the power flowing over the outaged line *after* the injections are imposed. Then, if we let the line reactance be x_l

$$P'_{mn} = \Delta P_m = -\Delta P_n \tag{3.40}$$

$$\Delta P_{mn} = \frac{1}{x_l}(\Delta\theta_m - \Delta\theta_n) \tag{3.41}$$

Since $\Delta P_n = -\Delta P_m$, equations (38) and (39) can be written as

$$\Delta\theta_m = X_{mn}\Delta P_n + X_{mm}\Delta P_m = X_{mn}(-\Delta P_m) + X_{mm}\Delta P_m$$
$$= (X_{mm} - X_{mn})\Delta P_m \tag{3.42}$$

$$\Delta\theta_n = X_{nn}\Delta P_n + X_{nm}\Delta P_m = X_{nn}(-\Delta P_m) + X_{nm}\Delta P_m$$
$$= (X_{nm} - X_{nn})\Delta P_m \tag{3.43}$$

where

$$X_{mn} = X_{nm} \tag{3.44}$$

Thus

$$\Delta P_{mn} = \frac{1}{x_l}(\Delta\theta_m - \Delta\theta_n)$$

$$= \frac{1}{x_l}[(X_{mm} - X_{mn})\Delta P_m - (X_{nm} - X_{nn})\Delta P_m]$$

$$= \frac{1}{x_l}(X_{mm} + X_{nn} - 2X_{mn})\Delta P_m \tag{3.45}$$

The power flow on line l from bus m to bus n after the outage P'_{mn} is computed as follows:

$$P'_{mn} = P_{mn} + \Delta P_{mn}$$

$$= P_{mn} + \frac{1}{x_l}(X_{mm} + X_{nn} - 2X_{mn})\Delta P_m \tag{3.46}$$

From equations (3.40) and (3.46), we get

$$\Delta P_m = P_{mn} + \frac{1}{x_l}(X_{mm} + X_{nn} - 2X_{mn})\Delta P_m \tag{3.47}$$

that is,

$$\Delta P_m = \frac{P_{mn}}{1 - \frac{1}{x_l}(X_{mm} + X_{nn} - 2X_{mn})} \tag{3.48}$$

Since there are only two nonzero elements at buses m and n in the power injection vector, the incremental change of phase angle at any bus i can be computed as follows:

$$
\begin{aligned}
\Delta \theta_i &= X_{in}\Delta P_n + X_{im}\Delta P_m \\
&= (X_{im} - X_{in})\Delta P_m \\
&= (X_{im} - X_{in}) \times \frac{P_{mn}}{1 - \frac{1}{x_l}(X_{mm} + X_{nn} - 2X_{mn})} \\
&= \frac{x_l(X_{im} - X_{in})P_{mn}}{x_l - (X_{mm} + X_{nn} - 2X_{mn})} = S_{i,l}P_{mn} \tag{3.49}
\end{aligned}
$$

where

$$S_{i,l} = \frac{\Delta \theta_i}{\Delta P_l} = \frac{x_l(X_{im} - X_{in})}{x_l - (X_{mm} + X_{nn} - 2X_{mn})} \tag{3.50}$$

which is the sensitivity factor of the change in phase angle of bus i with respect to power flow on line l before the outage.

For computing the effect of line l outage on the other line k, the line outage distribution factor is defined as below:

$$
\begin{aligned}
LODF_{k,l} = \frac{\Delta P_k}{\Delta P_l} &= \frac{\frac{1}{x_k}(\Delta \theta_p - \Delta \theta_q)}{\Delta P_l} \\
&= \frac{1}{x_k}\left(\frac{\Delta \theta_p}{\Delta P_l} - \frac{\Delta \theta_q}{\Delta P_l}\right) \\
&= \frac{1}{x_k}(S_{p,l} - S_{q,l}) \tag{3.51}
\end{aligned}
$$

From equation (3.50), $S_{p,l}$, $S_{q,l}$ can be written as

$$S_{p,l} = \frac{\Delta\theta_p}{\Delta P_l} = \frac{x_l\left(X_{pm} - X_{pn}\right)}{x_l - \left(X_{mm} + X_{nn} - 2X_{mn}\right)} \tag{3.52}$$

$$S_{q,l} = \frac{\Delta\theta_q}{\Delta P_l} = \frac{x_l\left(X_{qm} - X_{qn}\right)}{x_l - \left(X_{mm} + X_{nn} - 2X_{mn}\right)} \tag{3.53}$$

Thus

$$
\begin{aligned}
LODF_{k,l} &= \frac{1}{x_k}(S_{p,l} - S_{q,l}) \\
&= \frac{1}{x_k}\left(\frac{x_l\left(X_{pm} - X_{pn}\right)}{x_l - \left(X_{mm} + X_{nn} - 2X_{mn}\right)} - \frac{x_l\left(X_{qm} - X_{qn}\right)}{x_l - \left(X_{mm} + X_{nn} - 2X_{mn}\right)}\right) \\
&= \frac{1}{x_k}\left(\frac{x_l\left(X_{pm} - X_{pn}\right) - x_l\left(X_{qm} - X_{qn}\right)}{x_l - \left(X_{mm} + X_{nn} - 2X_{mn}\right)}\right) \\
&= \frac{1}{x_k}\left(\frac{x_l\left(X_{pm} - X_{qm} - X_{pn} + X_{qn}\right)}{x_l - \left(X_{mm} + X_{nn} - 2X_{mn}\right)}\right) \\
&= \frac{\dfrac{x_l}{x_k}\left(X_{pm} - X_{qm} - X_{pn} + X_{qn}\right)}{x_l - \left(X_{mm} + X_{nn} - 2X_{mn}\right)}
\end{aligned}
\tag{3.54}
$$

3.3.2.3 *Outage Transfer Distribution Factors*   Because we know that the generation shift factors and line outage distribution factors are linear models, we can use superposition to extend them to compute the network constraint sensitivity factors after a branch has been lost. They are also called the outage transfer distribution factors (OTDF). Let us compute the sensitivity factor OTDF between line k and generator bus j when line l is opened. This is calculated by first assuming that the change in generation on bus j, ΔP_j, has a direct effect on line k and an indirect effect through its influence on the power flowing on line l, which, in turn, influences line k when line l is in outage. Then

$$
\begin{aligned}
\Delta P_k &= S_{kj}\Delta P_j + LODF_{k,l}\Delta P_l \\
&= S_{kj}\Delta P_j + LODF_{k,l}(S_{lj}\Delta P_j) \\
&= (S_{kj} + LODF_{k,l}S_{lj})\Delta P_j
\end{aligned}
\tag{3.55}
$$

Therefore, the sensitivity OTDF after line l outage can be defined as

$$\text{OTDF}_{k,j} = \frac{\Delta P_k}{\Delta P_j} = (S_{kj} + LODF_{k,l}S_{lj}) \tag{3.56}$$

where

$OTDF_{kj}$: The sensitivity factor between line k and generator bus j when line l is opened

3.3.3 Constraint Shift Factors with Different References

The shift factor computed in SFT is based on the reference bus in EMS topology, but it can be easily converted to any market-based reference.

Let y be market-based reference unit, and the shift factor of the constraint k with respect to any unit j that is obtained based on the EMS reference bus is S_{kj}. For unit y, the shift factor of the constraint k is S_{ky}. Then, the shift factors after converting to market-based reference unit k can be computed as follows:

$$S'_{ky} = 0 \quad k = 1, \ldots\ldots, K_{\max} \tag{3.57}$$

$$S'_{kj} = S_{kj} - S_{ky} \quad k = 1, \ldots\ldots, K_{\max}, \quad j \neq y \tag{3.58}$$

where

S_{kj}: The shift factor of constraint k with respect to unit j that is based on the EMS reference

S_{ky}: The shift factor of constraint k with respect to unit y that is based on the EMS reference

S'_{kj}: The shift factor of constraint k with respect to unit j that is based on the market-based reference y

S'_{ky}: The shift factor of constraint k with respect to unit y that is based on the market-based reference y

We know that the shift factor of the constraint is related to the selected reference, i.e., the value of shift factor will be different if the reference is different even if the system topology and conditions are the same. Sometimes system operators would like to have the stable shift factor values without caring about the selection of reference bus/unit. Thus the distributed load reference will be used to get the unique constraint shift factors if the system topology and conditions are unchanged.

Let S_{kldref} be the sensitivity of load distribution reference for the constraint k, and the shift factor of the constraint k with respect to any control j that is obtained based on the EMS reference bus is S_{kj}. Then the shift factors based on the load distribution reference LDREF can be computed as follows:

$$S'_{kj} = S_{kj} - S_{kldref} \quad k = 1, \ldots\ldots, K_{\max} \tag{3.59}$$

where

S_{kldref}: The sensitivity of load distribution reference for constraint k, that is,

$$S_{kldaref} = \frac{\sum\limits_{jd=1}^{LD_{\max}} (S_{kjd} * LD_{jd})}{\sum\limits_{jd=1}^{LD_{\max}} LD_{jd}} \quad k = 1, \ldots\ldots, K_{\max} \tag{3.60}$$

where

S_{kjd}: The sensitivity of load jd with respect to constraint k

LD_{jd}: The load demand at load bus jd

In the practical energy markets such as the independent system operator (ISO), the system consists of many areas, but one major area in the ISO system is called the internal area and others are called external areas. If the internal area is a major concern during the price calculation for this market system, the load distribution reference can be selected based on the internal area only. Similarly, Let LDA_{max} be the total number of load controls in the internal area of the ISO system, which is less than the total number of load controls in the whole ISO system, LD_{max}. The shift factors based on the area load distribution reference LDAREF can be computed as follows:

$$S'_{kj} = S_{kj} - S_{kldaref} \quad k = 1, \ldots\ldots, K_{max} \tag{3.61}$$

where

$S_{kldaref}$: The sensitivity of load distribution reference in area A for the constraint k, that is,

$$S_{kldaref} = \frac{\sum_{jd=1}^{LDA_{max}} (S_{kjd} * LD_{jd})}{\sum_{jd=1}^{LDA_{max}} LD_{jd}} \quad k = 1, \ldots\ldots, K_{max}$$

$$LDA_{max} \in LD_{max} \tag{3.62}$$

where

LDA_{max}: The maximum number of load MW controls in area A

3.3.4   Sensitivities for the Transfer Path

A transfer path is an energy transfer channel between a point of delivery (POD) and a point of receipt (POR). The POD is the point of interconnection on the transmission provider's transmission system where capacity and/or energy transmitted by the transmission provider will be made available to the receiving party. The POR is the point of interconnection on the transmission provider's transmission system where capacity and/or energy transmitted will be made available to the transmission provider by the delivering party.

The pair of POD and POR defines a path and the direction of flow on that path. For internal paths, this would be a specific location in the area. For an external path, this may be an area-to-area interface. Similar to the concept of POD/POR, a transfer path can also be defined as from the source to the sink.

If POD/POR (or Source/Sink) is a single unit or single injection node, the sensitivity of POR or POD is the same as the constrained shift factor, which is mentioned in Sections 3.2 and 3.3. If POD/POR (or Source/Sink) is an area, the sensitivity of POR or POD can be computed as follows.

Let PF_j be the participation factor of unit j, and the shift factor of the constraint k with respect to any unit j is S_{kj}. The area-based shift factor of the constraint k is S_{kA}, which can be computed as follows:

$$S_{kA} = \frac{\sum\limits_{j \in A}(PF_j \times S_{kj})}{\sum\limits_{j \in A} PF_j} \quad k = 1, \ldots\ldots, K_{\max}, j \in A \qquad (3.63)$$

where

S_{kA}: The area-based shift factor of constraint k
PF_j: The participation factor of unit j

Similarly, if considering the effect of the outage, the area-based shift factor of constraint k can be computed as follows.

$$S_{kA} = \frac{\sum\limits_{j \in A}(PF_j \times \text{OTDF}_{kj})}{\sum\limits_{j \in A} PF_j} \quad k = 1, \ldots\ldots, K_{\max}, j \in A \qquad (3.64)$$

If a transfer path is from area A to area B, the sensitivity of the transfer path will be computed as:

$$S_{TP}(A \to B) = S_{kA} - S_{kB} \qquad (3.65)$$

If a transfer path is from an injection node i to another injection node j, the sensitivity of the transfer path will be computed as:

$$S_{TP}(I \to J) = \text{OTDF}_{ki} - \text{OTDF}_{kj} \qquad (3.66)$$

If a transfer path is from injection node i to area A, or from area A to injection node i, the corresponding sensitivities of the transfer path will be computed as:

$$S_{TP}(I \to A) = \text{OTDF}_{ki} - S_{kA} \qquad (3.67)$$

$$S_{TP}(A \to I) = S_{kA} - \text{OTDF}_{ki} \qquad (3.68)$$

3.4 PERTURBATION METHOD FOR SENSITIVITY ANALYSIS

So far, the sensitivity analysis methods described in this chapter are based on the matrix (either B′ matrix or Jacobian matrix). The sensitivity values that are computed based on partial differential term will be stable, or will not be changed as long as the system topology is the same.

Sometimes, the perturbation method is also used in the sensitivity calculation.

3.4.1 Loss Sensitivity

The perturbation method for loss sensitivity calculation is shown as below.

(a) Perform power flow calculation, and obtain the initial system power loss P_{L0}.
(b) Simulate the calculation of the loss sensitivity with respect to generator i. Increase the power output of the generator i for ΔP_{Gi} (if computing the loss sensitivity of load k, reduce the power demand of load k for ΔP_{Dk}), and the slack unit will absorb the same amount of ΔP_{Gi}.
(c) Run power flow again, and get the new system power loss P_L.
(d) Compute the loss sensitivity as below:

For unit loss sensitivity:

$$LS_{Gi} = \frac{P_L - P_{L0}}{\Delta P_{Gi}} \quad i \in NG \tag{3.69}$$

For load loss sensitivity:

$$LS_{Dk} = \frac{P_L - P_{L0}}{\Delta P_{Dk}} \quad i \in ND \tag{3.70}$$

Where LS_{Gi}, and LS_{Dk} are the loss sensitivity values with respect to the unit i and load k, respectively.

3.4.2 Generator Shift Factor Sensitivity

The perturbation method for generator shift factor sensitivity calculation is shown below.

(a) Chose a unit i and a branch constraint j.
(b) Perform power flow calculation, and obtain the initial power flow P_{j0} for branch j.
(c) Simulate the calculation of the generator shift factor sensitivity of branch j with respect to generator i. Increase the power output of

generator i for ΔP_{Gi}, and the slack unit will absorb the same amount of ΔP_{Gi}.

(d) Run power flow again, and get the new power flow P_j for branch j.

(e) Compute the generator shift factor sensitivity as below:

$$GSF_{j,i} = \frac{P_j - P_{j0}}{\Delta P_{Gi}} \quad i \in NG \tag{3.71}$$

Where $GSF_{j,i}$ is the generator shift factor sensitivity of branch j with respect to unit i.

The calculation of the load shift factor sensitivity is similar to that of the generator shift factor sensitivity by handling the load as the negative generation.

3.4.3 Shift Factor Sensitivity for the Phase Shifter

The perturbation method for the phase shifter shift factor sensitivity calculation is shown as below.

(a) Chose a phase shifter t and a branch constraint j.

(b) Perform power flow calculation, and obtain the initial power flow P_{j0} for branch j.

(c) Simulate the calculation of the shift factor sensitivity of branch j with respect to phase shifter t. Increase the taps of the phase shifter i for ΔT_t (or angle change $\Delta\theta_t$), which can be simulated by change the suseptance of the phase shifter.

(d) Run power flow again, and get the new power flow P_j for branch j.

(e) Compute the phase shifter shift factor sensitivity as below.

$$SF_{j,t} = \frac{P_j - P_{j0}}{\Delta T_t}$$

$$\text{or} \quad SF_{j,t} = \frac{P_j - P_{j0}}{\Delta\theta_t} \tag{3.72}$$

where $SF_{j,t}$ is the shift factor sensitivity of branch j with respect to phase shifter t.

3.4.4 Line Outage Distribution Factor

The perturbation method for the line outage distribution factor calculation is shown below:

(a) Chose a branch l that will be simulated as an outage and a branch constraint j.

(b) Perform power flow calculation before branch l is open, and obtain the initial power flow P_{j0} for branch j and P_{l0} for branch l.

(c) Simulate the calculation of the line outage distribution factor (LODF). Open branch l while the unit power and load power are unchanged.

(d) Run power flow again, and get the new power flow P_j for branch j. The power flow P_l for branch l will be zero since branch l is in outage.

(e) Compute the line outage distribution factor of branch j as branch l is in outage as below:

$$\text{LODF}_{j,l} = \frac{P_j - P_{j0}}{P_{l0}} \tag{3.73}$$

where $\text{LODF}_{j,l}$ is the line outage distribution factor of branch j with respect to outage branch l.

3.4.5 Outage Transfer Distribution Factor

The perturbation method for the outage transfer distribution factor calculation is shown below.

(a) Choose a unit, a branch l that will be simulated as outage, and a branch constraint j.

(b) Perform power flow calculation before branch l is open, and obtain the initial power flow P_{j0} for branch j and P_{l0} for branch l.

(c) First of all, simulate the calculation of the generator shift factor sensitivity of branches j and l with respect to generator i. Increase the power output of generator i for ΔP_{Gi}, and the slack generator will absorb the same amount of ΔP_{Gi}.

(d) Conduct power flow calculation, and get the new power flow P_j for branch j and P_l for branch l.

(e) Compute the generator shift factor sensitivity for the branch j and l.

$$GSF_{j,i} = \frac{P_j - P_{j0}}{\Delta P_{Gi}} \quad i \in NG \tag{3.74}$$

$$GSF_{l,i} = \frac{P_l - P_{l0}}{\Delta P_{Gi}} \quad i \in NG \tag{3.75}$$

(f) Then simulate the calculation of LODF for branch j with respect to outage branch l. Open branch l while the unit power and load power are unchanged.

(g) Once again run power flow, and get the new power flow P_j' for branch j. The power flow P_l' for branch l will be zero since branch l is in outage.

(h) Compute the line outage distribution factor of branch j as branch l is in outage as below:

$$\text{LODF}_{j,l} = \frac{P_j' - P_j}{P_l} \tag{3.76}$$

Finally, the sensitivity OTDF of branch j after line l outage can be obtained as below:

$$\text{OTDF}_{j,i} = \text{GSF}_{j,i} + \text{LODF}_{j,l}\text{GSF}_{l,i} \tag{3.77}$$

where $\text{OTDF}_{j,i}$ is the sensitivity factor between line j and generator bus i when line l is opened.

It is noted that the perturbation method for sensitivity calculation is very straightforward, but there is a drawback. That is, the values of sensitivity depend highly on the solution in addition to the topology. Even if the system topology is not changed, the values of the sensitivity may be a little different for the different initial points. Thus, to obtain accurate sensitivity results, the approach based on a matrix is recommended. If the perturbation method is used, the amount of the perturbation should be small so that the solution is close to the initial operation points.

3.5   VOLTAGE SENSITIVITY ANALYSIS

Before we do voltage sensitivity analysis, we need to understand the concept and importance of voltage stability. Voltage stability is the ability of a power system to maintain adequate voltage magnitude so that when the system nominal load is increased, the actual power transferred to that load will increase. The main cause of voltage instability is the inability of the power system to meet the demand for reactive power. The voltage stability problem consists of two aspects: a large disturbance aspect and a small disturbance aspect. The former is called dynamic stability, and the latter is called static stability. The large disturbance involves short circuits and addresses postcontingency system response. The small disturbance investigates the stability of an operating point and applies a linearized model. The voltage sensitivity analysis herein is used for static voltage stability.

Static voltage instability is mainly associated with reactive power imbalance. This imbalance mainly occurs on a local network or a specified bus in a system. Therefore, the reactive power supports must be locally adequate. With static voltage stability, slowly developing changes in the power system occur that eventually lead to a shortage of reactive power and declining voltage. This phenomenon can be seen in Figure 3.2, a plot of power transferred versus voltage at the receiving end.
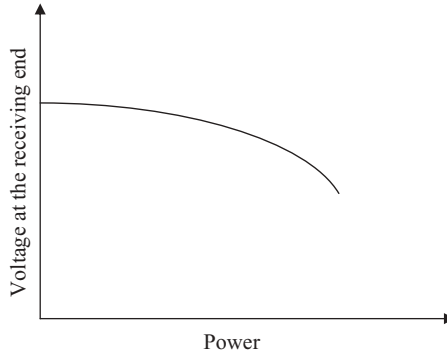
FIGURE 3.2   A plot of power versus voltage

These kinds of plots are generally called *P-V* curves or "nose" curves. As power transfer increases, the voltage at the receiving end decreases. Eventually, a critical (nose) point, the point at which the system reactive power is out of usage, is reached where any further increase in active power transfer will lead to very rapid decrease in voltage magnitude. Before reaching the critical point, a large voltage drop due to heavy reactive power losses is observed. The only way to save the system from voltage collapse is to reduce the reactive power load or add additional reactive power before reaching the point of voltage collapse.

The purpose of the voltage sensitivity analysis is to improve the voltage profile and to minimize system real power losses through the optimal reactive power controls (i.e., adding VAR supports). These goals are achieved by proper adjustments of VAR variables in power networks through seeking the weak buses in the system. Therefore, if the voltage magnitude at generator buses, VAR compensation (VAR support), and transformer tap position are chosen as the control variables, the optimal VAR control model can be represented as:

$$\min P_{\mathrm{L}}(Q_{\mathrm{s}}, V_{\mathrm{G}}, T) \tag{3.78}$$

such that

$$Q(Q_{\mathrm{s}}, V_{\mathrm{G}}, T, V_{\mathrm{D}}) = 0 \tag{3.79}$$

$$Q_{\mathrm{G\,min}} \leq Q_{\mathrm{G}}(Q_{\mathrm{s}}, V_{\mathrm{G}}, T) \leq Q_{\mathrm{G\,max}} \tag{3.80}$$

$$V_{\mathrm{D\,min}} \leq V_{\mathrm{D}}(Q_{\mathrm{s}}, V_{\mathrm{G}}, T) \leq V_{\mathrm{D\,max}} \tag{3.81}$$

$$Q_{\mathrm{s\,min}} \leq Q_{\mathrm{s}} \leq Q_{\mathrm{s\,max}} \tag{3.82}$$

$$V_{\mathrm{G\,min}} \leq V_{\mathrm{G}} \leq V_{\mathrm{G\,max}} \tag{3.83}$$

$$T_{\min} \leq T \leq T_{\max} \tag{3.84}$$

where

P_L: The system real power loss

V_G: The voltage magnitude at generator buses

Q_S: The VAR support in the system

Q_G: The VAR generation in the system

T: The tap position of the transformer

V_D: The voltage magnitude at load buses

The subscripts "min" and "max" represent the lower and upper limits of the constraint, respectively.

Two kinds of sensitivity-related factors can be computed through equations (3.78)–(3.84). Here they are called voltage benefit factors (VBF) and loss benefit factors (LBF), which are expressed as follows:

$$\text{LBF}_i = \frac{\sum_i (P_{L0} - P_L(Q_{si}))}{Q_{si}} \times 100\% \quad i \in ND \tag{3.85}$$

$$\text{VBF}_i = \frac{\sum_i (V_i(Q_{si}) - V_{i0})}{Q_{si}} \times 100\% \quad i \in ND \tag{3.86}$$

where

Q_{si}: The amount of VAR support at load bus i

LBF_i: The loss benefit factors from VAR compensation Q_{si}

VBF_i: The voltage benefit factors from VAR compensation Q_{si}

P_{L0}: The power transmission losses in the system without VAR compensation

$P_L(Q_{si})$: The power transmission losses in the system with VAR compensation Q_{si}

V_{i0}: The voltage magnitude at load bus i without VAR compensation

$V_i(Q_{si})$: The voltage magnitude at load bus i with VAR compensation Q_{si}

ND: The number of load buses

3.6   REAL-TIME APPLICATION OF THE SENSITIVITY FACTORS

In the EMS system and energy markets, the loss sensitivity factors and constraint shift factors are applied for LMP and/or alleviating overload (AOL) calculation. The above-mentioned loss sensitivities and constraint shift factors and the corresponding constraint elements (transmission lines or transformers) will be passed to the constraint logger (CLOOGER) and then passed to

the LMP calculator. The practical constraints can be divided into the following types:

(1) Automatic constraints: All branches (lines, transformers, and interfaces) violations from EMS real-time contingency analysis (RTCA) calculation

(2) Watch list constraints: The branches without violation in EMS RTCA calculation but the branch flows close to their limits

(3) Active constraints: The constraints from LMP calculator that are needed to recompute the constraint shift factors

(4) Flowgate constraints: The constraints from marketing system that are needed to compute the shift factors with respect to the flowgate constraint. The term "flowgate" refers to a single grid facility or a set of facilities.

(5) Quick selection constraints: Any branches (lines, transformers, and interfaces) that operators want to know the shift factors and monitor their branch flows

The sensitivity analysis and LMP calculation process is shown in Figure 3.3. The market will require that the LMP be determined on a periodic basis. To support this calculation, the network topology and data including loss sensitivities, network constraints, and their shift factors gathered in real time can be transferred to the LMP automatically through the SE (state estimator), RTCA, and SFT applications. If the results of the LMP calculator meet the constraints described in equations (3.3) and (3.4), the LMP calculation was successful and the LMP results may be recorded and recommended. If the LMP calculation results in any constraint violation, the violated constraint will be sent back to AOL, and the LMP recalculation will be performed until all constraints are met.

3.7   SIMULATION RESULTS

The calculation results of the several sensitivities are illustrated with the IEEE 14-bus system and AREVA T&D 60-bus system. The one-line diagram of the AREVA T&D 60-bus system is shown in Figure 3.4. The 60-bus system, which has three areas, consists of 24 generation units (15 units are available in the tests), 32 loads, 43 transmission lines, and 54 transformers.

3.7.1   Sample Computation for Loss Sensitivity Factors

The following test cases are used to analyze the loss sensitivity in this chapter.
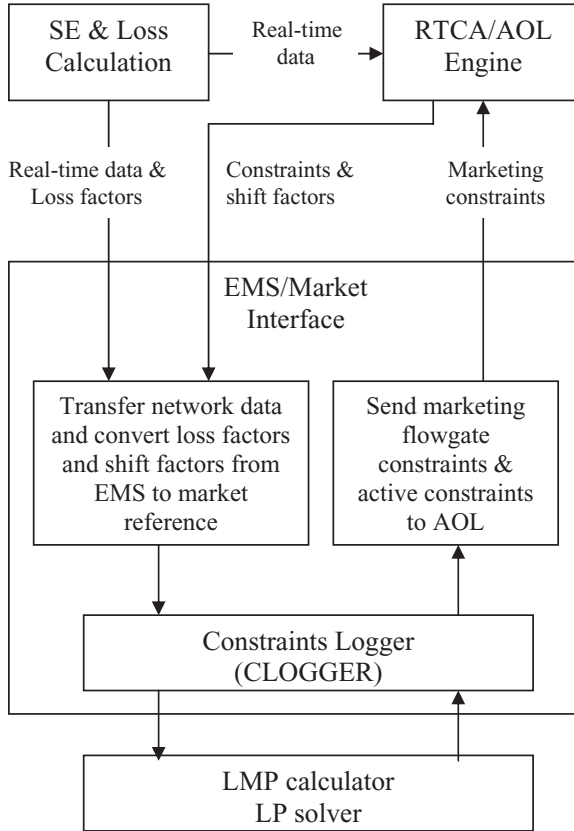
FIGURE 3.3 Application of the sensitivity factors

Case 1: Calculate loss sensitivities with the distributed generation slack and load slack, respectively. All units are AGC units (i.e., the status of unit AGC is ON).

Case 2: Calculate loss sensitivities with the distributed generation slack and load slack, respectively. All units are AGC units except the units under station DOUGLAS in Area 1.

Case 3: Calculate loss sensitivities with the distributed generation slack and load slack, respectively. All units are AGC units except the units under station HEARN in Area 1.

Case 4: Calculate loss sensitivities with the distributed generation slack and load slack, respectively. All units are AGC units except the units in Area 2.

Case 5: Calculate loss sensitivities with the distributed generation slack and load slack, respectively. All units are AGC units except the units under station HOLDEN in Area 3.
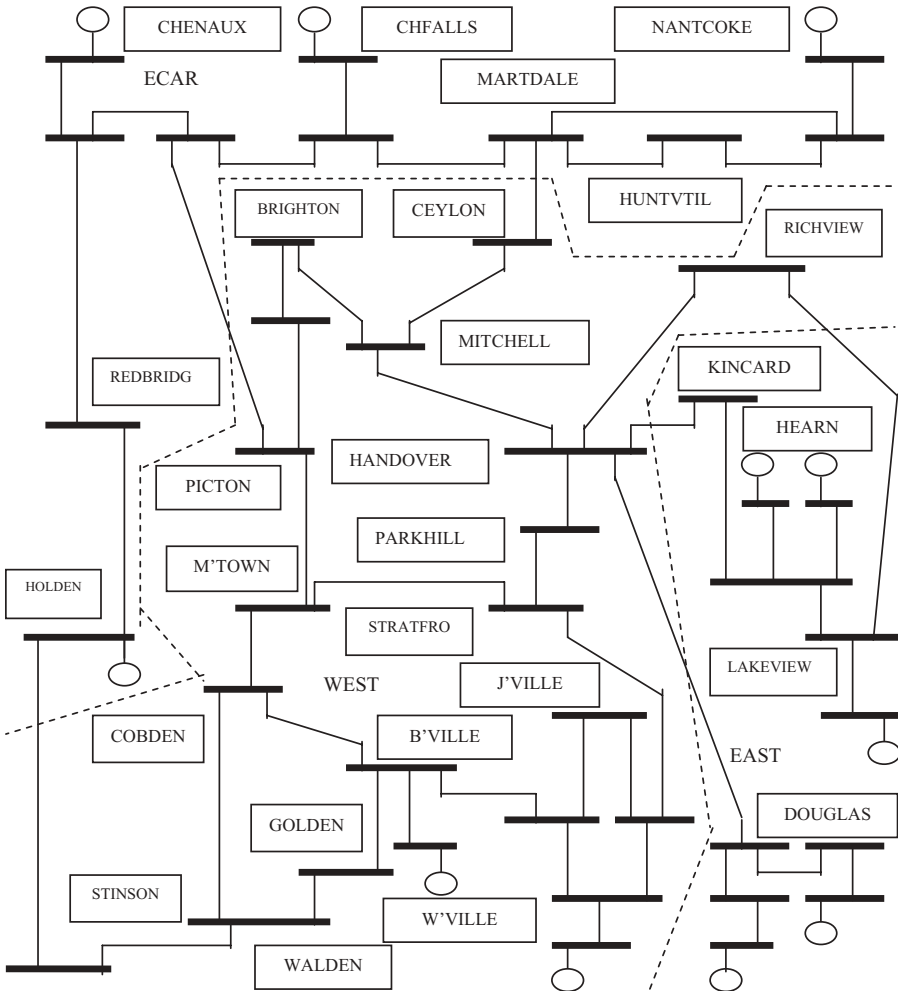
FIGURE 3.4   One-line diagram of AREVA T&D system (Area 1—EAST, Area 2—WEST, Area 3—ECAR)

Case 6: Calculate loss sensitivities for the selected single slack based on the loss factors under the distributed slack.

The simulation results are shown in Tables 3.1–3.6. All loss sensitivity factors for units and loads are computed. For the purpose of simplification, only loss sensitivities of generators are listed in Tables 3.1–3.6, in which column 1 is the name of the station and the units. Column 2 is the area number that the unit belongs to. Column 3 is the AGC status of the unit.

Tables 3.1–3.5 show the test results and comparison of loss sensitivity calculation based on the distributed generation reference and distributed load

Table 3.1   Test results and comparison of loss sensitivity calculation (Case 1: All units on AGC)

Station, Generator	Area No.	AGC Unit	Loss Sensitivity Distributed Generation Slack	Loss Sensitivity Distributed Load Slack
DOUGLAS, G2	1	YES	0.015100	0.017000
DOUGLAS, G1	1	YES	0.012100	0.014000
DOUGLAS, CT1	1	YES	0.009900	0.011800
DOUGLAS, CT2	1	YES	0.009900	0.011800
DOUGLAS, ST	1	YES	0.009700	0.011600
HEARN, G1	1	YES	−0.016500	−0.014600
HEARN, G2	1	YES	−0.016500	−0.014600
LAKEVIEW, G1	1	YES	−0.018800	−0.017000
BVILLE, 1	2	YES	−0.001000	−0.004200
WVILLE, 1	2	YES	0.000700	−0.002500
CHENAUX, 1	3	YES	−0.008900	−0.008900
CHEALLS, 1	3	YES	0.021200	0.021200
CHEALLS, 2	3	YES	0.021200	0.021200
HOLDEN, 1	3	YES	0.001000	0.001000
NANTCOKE, 1	3	YES	−0.012200	−0.012200

Table 3.2   Test results and comparison of loss sensitivity calculation (Case 2: All units on AGC except the units under station DOUGLAS in Area 1)

Station, Generator	Area No.	AGC Unit	Loss Sensitivity Distributed Generation Slack	Loss Sensitivity Distributed Lload Slack
DOUGLAS, G2	1	NO	0.032800	0.017000
DOUGLAS, G1	1	NO	0.029900	0.014000
DOUGLAS, CT1	1	NO	0.027800	0.011800
DOUGLAS, CT2	1	NO	0.027800	0.011800
DOUGLAS, ST	1	NO	0.027600	0.011600
HEARN, G1	1	YES	0.001500	−0.014600
HEARN, G2	1	YES	0.001500	−0.014600
LAKEVIEW, G1	1	YES	−0.000800	−0.017000
BVILLE, 1	2	YES	−0.001000	−0.004200
WVILLE, 1	2	YES	0.000700	−0.002500
CHENAUX, 1	3	YES	−0.008900	−0.008900
CHEALLS, 1	3	YES	0.021200	0.021200
CHEALLS, 2	3	YES	0.021200	0.021200
HOLDEN, 1	3	YES	0.001000	0.001000
NANTCOKE, 1	3	YES	−0.012200	−0.012200

Table 3.3   Test results and comparison of loss sensitivity calculation (Case 3: Only units under HEARN in Area 1 not on AGC)

Station, Generator	Area No.	AGC Unit	Loss Sensitivity Distributed Generation Slack	Loss Sensitivity Distributed Load Slack
DOUGLAS, G2	1	YES	0.012600	0.017000
DOUGLAS, G1	1	YES	0.009600	0.014000
DOUGLAS, CT1	1	YES	0.007400	0.011800
DOUGLAS, CT2	1	YES	0.007400	0.011800
DOUGLAS, ST	1	YES	0.007200	0.011600
HEARN, G1	1	NO	−0.019000	−0.014600
HEARN, G2	1	NO	−0.019000	−0.014600
LAKEVIEW, G1	1	YES	−0.021300	−0.017000
BVILLE, 1	2	YES	−0.001000	−0.004200
WVILLE, 1	2	YES	0.000700	−0.002500
CHENAUX, 1	3	YES	−0.008900	−0.008900
CHEALLS, 1	3	YES	0.021200	0.021200
CHEALLS, 2	3	YES	0.021200	0.021200
HOLDEN, 1	3	YES	0.001000	0.001000
NANTCOKE, 1	3	YES	−0.012200	−0.012200

Table 3.4   Test results and comparison of loss sensitivity calculation (Case 4: All units on AGC except the units in Area 2)

Station, Generator	Area No.	AGC Unit	Loss Sensitivity Distributed Generation Slack	Loss Sensitivity Distributed Load Slack
DOUGLAS, G2	1	YES	0.015200	0.017000
DOUGLAS, G1	1	YES	0.012200	0.014000
DOUGLAS, CT1	1	YES	0.010000	0.011800
DOUGLAS, CT2	1	YES	0.010000	0.011800
DOUGLAS, ST	1	YES	0.009900	0.011600
HEARN, G1	1	YES	−0.016700	−0.014600
HEARN, G2	1	YES	−0.016700	−0.014600
LAKEVIEW, G1	1	YES	−0.019100	−0.017000
BVILLE, 1	2	NO	−0.021000	−0.004200
WVILLE, 1	2	NO	−0.019300	−0.002500
CHENAUX, 1	3	YES	−0.008900	−0.008900
CHEALLS, 1	3	YES	0.021200	0.021200
CHEALLS, 2	3	YES	0.021200	0.021200
HOLDEN, 1	3	YES	0.001000	0.001000
NANTCOKE, 1	3	YES	−0.012200	−0.012200

Table 3.5   Test results and comparison of loss sensitivity calculation (Case 5: All units on AGC except unit 3 under station HOLDEN in Area 3)

Station, Generator	Area No.	AGC Unit	Loss Sensitivity Distributed Generation Slack	Loss Sensitivity Distributed Load Slack
DOUGLAS, G2	1	YES	0.015100	0.017000
DOUGLAS, G1	1	YES	0.012100	0.014000
DOUGLAS, CT1	1	YES	0.009900	0.011800
DOUGLAS, CT2	1	YES	0.009900	0.011800
DOUGLAS, ST	1	YES	0.009700	0.011600
HEARN, G1	1	YES	−0.016500	−0.014600
HEARN, G2	1	YES	−0.016500	−0.014600
LAKEVIEW, G1	1	YES	−0.018800	−0.017000
BVILLE, 1	2	YES	−0.001000	−0.004200
WVILLE, 1	2	YES	0.000700	−0.002500
CHENAUX, 1	3	YES	−0.008500	−0.008900
CHEALLS, 1	3	YES	0.021600	0.021200
CHEALLS, 2	3	YES	0.021600	0.021200
HOLDEN, 1	3	NO	0.001400	0.001000
NANTCOKE, 1	3	YES	−0.011800	−0.012200

reference, respectively. The loss factors computed from the distributed unit reference are listed in column 4 of Tables 3.1–3.5. The loss factors computed from the distributed load reference are listed in column 5 of Tables 3.1–3.5.

Generally, the values of loss sensitivities based on the generation reference are different from those based on the load reference, because the distribution of the units is not exactly the same as the distribution of loads in the power system. The loss factors will be close or equal if the units are close to the load locations. This can be observed from Table 3.1, where all units are on AGC status. For the 60-bus system, each load in Area 3 has at least one unit connected, so the loss factors in Area 3 are the same for both the distributed generation slack and the distributed load slack.

It is noted from Tables 3.1–3.5 that the loss sensitivity factors based on the distributed load slack are the same whether the status of the units is changed or not. But the loss factors based on the distributed generation references are changed since the AGC status of the units are different.

Generally, the change of AGC status of the units only affects the loss sensitivities in the same area that these units belong to.

It can be seen from Tables 3.2 and 3.3 that, when AGC status of the units in Area 1 changes, only the loss factors in Area 1 are affected. The loss factors in the other areas are unchanged. For Table 3.5, when AGC status of the units in Area 3 changes, only the loss factors in Area 3 are affected. The loss factors in the other areas are unchanged. But for Table 3.4, there is no

Table 3.6   Test results of loss sensitivity calculation (distributed slack vs single slack)

Station, Generator	AGC Unit	Loss Sensitivity Distributed Slack	Loss Sensitivity Single Slack, HOLDEN 1	Loss Sensitivity Single Slack, Douglas ST
DOUGLAS, G2	YES	0.017000	0.016016	0.005463
DOUGLAS, G1	YES	0.014000	0.013013	0.002428
DOUGLAS, CT1	YES	0.011800	0.010811	0.000202
DOUGLAS, CT2	YES	0.011800	0.010811	0.000202
DOUGLAS, ST	YES	0.011600	0.010611	0.000000
HEARN, G1	YES	−0.014600	−0.015616	−0.026507
HEARN, G2	YES	−0.014600	−0.015616	−0.026507
LAKEVIEW, G1	YES	−0.017000	−0.018018	−0.028936
BVILLE, 1	YES	−0.004200	−0.005205	−0.015985
WVILLE, 1	YES	−0.002500	−0.003504	−0.014265
CHENAUX, 1	YES	−0.008900	−0.009910	−0.020741
CHEALLS, 1	YES	0.021200	0.020220	0.009713
CHEALLS, 2	YES	0.021200	0.020220	0.009713
HOLDEN, 1	YES	0.001000	0.000000	−0.010724
NANTCOKE, 1	YES	−0.012200	−0.013213	−0.024079

AGC unit in Area 2; this means that there is no unit reference in Area 2. Then the AGC units in the other areas will pick up the power mismatch (i.e., Area 1 in this case). Thus the loss factors in Areas 1 and 2 are changed. The loss factors in the other areas are unchanged.

Through the above comparisons, it can be observed that the method of distributed load references for loss sensitivity calculation is superior to the method of distributed generation references in the real-time energy markets, since the AGC status of the units are changeable in the real-time system.

The results of loss sensitivity calculation for a single slack, which are computed from the proposed formula (3.24), are shown in Table 3.6. Column 3 in Table 3.6 is the set of the loss sensitivity coefficients for the distributed slack buses. Column 4 in Table 3.6 is the set of loss sensitivity factors with a single slack bus at the location of HOLDEN 1. Column 5 in Table 3.6 is the set of loss sensitivity factors with a single slack bus at the location of DOUGLAS.

It is noted that all the loss sensitivities are nonzero if the distributed slacks are selected. If the single slack is selected, the loss sensitivity of the slack equals zero.

Since the loss sensitivity values based on the distributed slacks from EMS are unchanged as long as the system topology is the same, the loss sensitivities for any market-based single slack can be easily and quickly acquired by use of the loss sensitivity formula (3.24). Therefore, a large amount of computation is avoided whenever the loss sensitivities for a market-based reference are needed in the real-time energy markets.

For example, in a practical system with 25,000 buses, the CPU time of computing loss factors is about 60 seconds with the traditional power flow calculation but less than 0.1 second if the proposed method is used. This is a huge time saving in the real-time energy markets.

To verify the correctness of the loss sensitivity equation (3.24), the loss factors are computed and compared with the traditional power flow calculation. The results and comparison are shown in Figures 3.5 and 3.6 as well as Tables 3.7 and 3.8, in which column 3 is the set of results from the power flow calculation and column 4 is the set of results from equation (3.24). Table 3.7 shows the comparison of loss factor results for single slack bus at HOLDEN-1. Table 3.8 shows the comparison of loss factor results for single slack bus at DOUGLAS-ST.
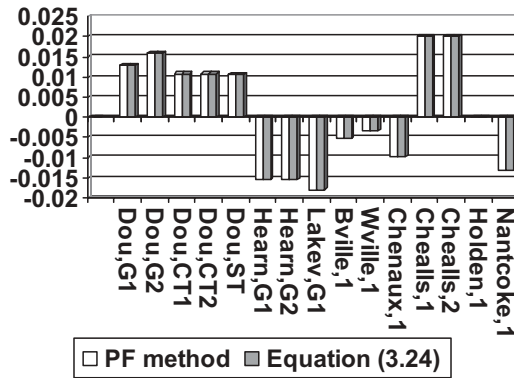
FIGURE 3.5   Comparison of loss factor results for single slack bus at HOLDEN-1
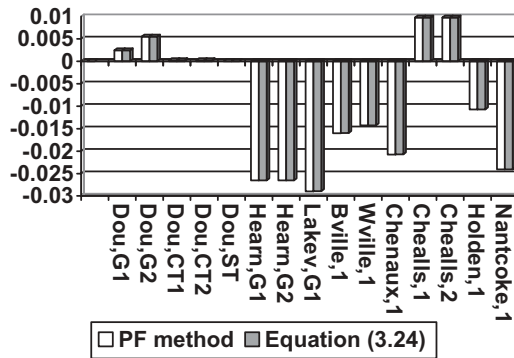
FIGURE 3.6   Comparison of loss factor results for single slack bus at DOUGLAS-ST

Table 3.7   Comparison of loss sensitivity calculation results for single slack bus at HOLDEN-1 (proposed method vs power flow method)

Station, Generator	AGC Unit	Loss Sensitivity, HOLDEN 1— PF Method	Loss Sensitivity, HOLDEN 1— Equation (3.24)	|Error %|
DOUGLAS, G2	YES	0.016029	0.016016	0.08110
DOUGLAS, G1	YES	0.013053	0.013013	0.30644
DOUGLAS, CT1	YES	0.010817	0.010811	0.05547
DOUGLAS, CT2	YES	0.010817	0.010811	0.05547
DOUGLAS, ST	YES	0.010621	0.010611	0.09415
HEARN, G1	YES	−0.015630	−0.015616	0.08957
HEARN, G2	YES	−0.015630	−0.015616	0.08957
LAKEVIEW, G1	YES	−0.018110	−0.018018	0.50801
BVILLE, 1	YES	−0.005220	−0.005205	0.23002
WVILLE, 1	YES	−0.003500	−0.003504	0.02855
CHENAUX, 1	YES	−0.009920	−0.009910	0.11088
CHEALLS, 1	YES	0.020247	0.020220	0.13335
CHEALLS, 2	YES	0.020247	0.020220	0.13335
HOLDEN, 1	YES	0.000000	0.000000	0.00000
NANTCOKE, 1	YES	−0.013240	−0.013213	0.20393

Table 3.8   Comparison of loss sensitivity calculation results for single slack bus at Douglas-ST (proposed method vs power flow method)

Station, Generator	AGC Unit	Loss Sensitivity, Douglas ST— PF Method	Loss Sensitivity, Douglas ST— Equation (3.24)	|Error %|
DOUGLAS, G2	YES	0.005467	0.005463	0.07317
DOUGLAS, G1	YES	0.002421	0.002428	0.28914
DOUGLAS, CT1	YES	0.000202	0.000202	0.14829
DOUGLAS, CT2	YES	0.000202	0.000202	0.14829
DOUGLAS, ST	YES	0.000000	0.000000	0.00000
HEARN, G1	YES	−0.026530	−0.026507	0.08669
HEARN, G2	YES	−0.026530	−0.026507	0.08669
LAKEVIEW, G1	YES	−0.028950	−0.028936	0.04836
BVILLE, 1	YES	−0.016000	−0.015985	0.09999
WVILLE, 1	YES	−0.014280	−0.014265	0.10504
CHENAUX, 1	YES	−0.020770	−0.020741	0.13962
CHEALLS, 1	YES	0.009714	0.009713	0.01029
CHEALLS, 2	YES	0.009714	0.009713	0.01029
HOLDEN, 1	YES	−0.010730	−0.010724	0.07454
NANTCOKE, 1	YES	−0.024090	−0.024079	0.02491

The difference or error of the results between the proposed method and the power flow method is obtained from the following equation:

$$|\text{Error}\%| = \left| \frac{\text{LF}_{PM}(i) - \text{LF}_{PF}(i)}{\text{LF}_{PF}(i)} \times 100\% \right| \quad i \in n \tag{3.87}$$

where

Error %: The percentage of the computation error for the proposed formula

LF_{PM}: The loss factor computed from the proposed method

LF_{PF}: The loss factor obtained with the traditional power flow calculation

It can be seen from Tables 3.7 and 3.8 that the loss sensitivity results from the two methods are very close. The maximum error is less than 0.6%.

3.7.2   Sample Computation for Constrained Shift Factors

Tables 3.9–3.12 are the results of the detected constraint and the corresponding shift factors. The results for the constraint branch T525 at Station CHENAUX are listed in Table 3.9.

In Table 3.10, column 1 is the name of the station and the units. Column 2 is the area number that the unit belongs to. Column 3 is the AGC status of the unit. Column 4 is the unit participation factors. Column 5 is the set of the shift factors of the constraint T525 with respect to the units for the EMS-based reference at station DOUGLAS.

It is noted that all the shift factors are zero for the units in Area 1 for the EMS-based reference since the reference is located in Area 1 and all units in Area 1 are close to the reference unit. If the market-based slack is selected, the shift factors for the market-based reference can be easily obtained from equations (3.57) and (3.58).

Table 3.11 shows the shift factors of the constraint T525 with respect to the units for the market-based reference at the location of HOLDEN 1 and BVILLE, respectively. The relationships of the shift factors to different references are also shown in Figure 3.7.

Table 3.12 shows the area-based shift sensitivity factors of the constraint T525, which are computed based on unit shift factors and participation factors within the area. If the unit participation factors change, the value of the area-based sensitivity will be changed.

Table 3.9   Example of the active constraint (branch T525 at station Chenaux)

Constraint Name	Rating (MVA)	Actual Flow (MVA)	Constraint Deviation	Percent of Violation
Branch T525	1171.4	1542.7	371.3	131.7

Table 3.10 Test results of shift factors for the active constraint T525 at EMS reference (station DOUGLAS)

Station, Generator	Area No.	Unit in Serve	Unit Participation Factor	Shift Factors on EMS Reference at Station DOUGLAS
DOUGLAS, G2	1	YES	1.5	0.000000
DOUGLAS, G1	1	YES	1.8	0.000000
DOUGLAS, CT1	1	YES	1.2	0.000000
DOUGLAS, CT2	1	YES	1.6	0.000000
DOUGLAS, ST	1	YES	0.9	0.000000
HEARN, G1	1	YES	0.5	0.000000
HEARN, G2	1	YES	0.8	0.000000
LAKEVIEW, G1	1	YES	1.1	0.000000
BVILLE, 1	2	YES	1.2	−0.013650
WVILLE, 1	2	YES	1.3	−0.024336
CHENAUX, 1	3	YES	1.7	0.617887
CHEALLS, 1	3	YES	0.6	0.521795
CHEALLS, 2	3	YES	1.9	0.521795
HOLDEN, 1	3	YES	2.2	0.304269
NANTCOKE, 1	3	YES	0.7	0.291815

Table 3.11 Test results of shift factors for the active constraint T525 at different market references

Station, Generator	Area No.	Unit in Serve	Shift Factors on Market Reference at Station HOLDEN	Shift Factors on Market Reference at Station BVILLE
DOUGLAS, G2	1	YES	−0.304269	0.013650
DOUGLAS, G1	1	YES	−0.304269	0.013650
DOUGLAS, CT1	1	YES	−0.304269	0.013650
DOUGLAS, CT2	1	YES	−0.304269	0.013650
DOUGLAS, ST	1	YES	−0.304269	0.013650
HEARN, G1	1	YES	−0.304269	0.013650
HEARN, G2	1	YES	−0.304269	0.013650
LAKEVIEW, G1	1	YES	−0.304269	0.013650
BVILLE, 1	2	YES	−0.317919	0.000000
WVILLE, 1	2	YES	−0.328605	0.010686
CHENAUX, 1	3	YES	0.313618	0.631537
CHEALLS, 1	3	YES	0.217526	0.535445
CHEALLS, 2	3	YES	0.217526	0.535445
HOLDEN, 1	3	YES	0.000000	0.317946
NANTCOKE, 1	3	YES	−0.012454	0.305465

Table 3.12   Test results of area-based sensitivity for the active constraint T525 at different references

Area Name	Area No.	Sensitivities on EMS Reference at Station DOUGLAS	Sensitivities on Market Reference at Station HOLDEN	Sensitivities on Market Reference at Station BVILLE
EAST	1	0.000000	−0.304269	0.013650
WEST	2	−0.019207	−0.323499	−0.005557
ECAR	3	0.454726	0.150458	0.468385
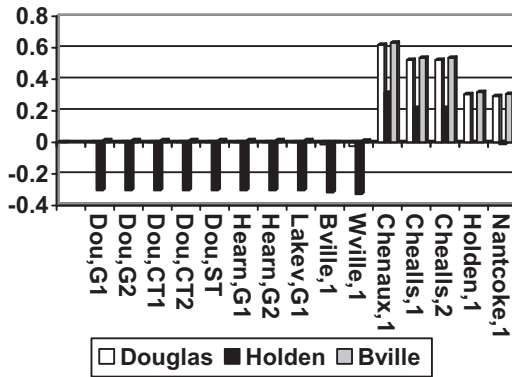
FIGURE 3.7   The shift factors with different references

Table 3.13 shows the sensitivity factors of the transfer path with respect to the constraint T525. There are four types of transfer paths:

(1) Transfer type 1—Area-Area: Both POR and POD (or SOURCE and SINK) are areas.
(2) Transfer type 2—Single point: Both POR and POD (or SOURCE and SINK) are single injection nodes.
(3) Transfer type 3—Point-Area: The POR (SOURCE) is a single injection node and POD (SINK) is an area.
(4) Transfer type 4—Area-Point: The POR (SOURCE) is an area and POD (SINK) is a single injection node.

It is noted from Table 3.13 that the sensitivity of the transfer path will be the same no matter which reference is used.

Table 3.13   Test results of sensitivity for transfer path for the active constraint T525 at different references

Transfer Path	Path Type	Sensitivities on EMS Reference at Station DOUGLAS	Sensitivities on Market Reference at Station HOLDEN	Sensitivities on Market Reference at Station BVILLE
ECAR-WEST	Area-Area	0.473933	0.473950	0.473940
WEST-EAST	Area-Area	−0.019207	−0.019230	−0.019207
ECAR-EAST	Area-Area	0.454726	0.454727	0.454735
BV1-DOUGG1	Single point	−0.013650	−0.013650	−0.013650
WV1-DOUGG1	Single point	−0.024336	−0.024336	−0.024336
CX1-DOUGG1	Single point	0.617887	0.617887	0.617887
CS1-DOUGG1	Single point	0.521795	0.521795	0.521795
CS2-DOUGG1	Single point	0.521795	0.521795	0.521795
HD1-DOUGG1	Single point	0.304269	0.304269	0.304269
NK1-DOUGG1	Single point	0.291815	0.291815	0.291815
BV1-WV1	Single point	0.010686	0.010686	0.010686
CX1-CS1	Single point	0.096092	0.096092	0.096092
HD1-NK1	Single point	0.012454	0.012454	0.012454
HD1-BV1	Single point	0.317919	0.317919	0.317919
HD1-WV1	Single point	0.328605	0.328605	0.328605
BV1-EAST	Point-Area	−0.013650	−0.013650	−0.013650
HD1-EAST	Point-Area	0.304269	0.304269	0.304269
HD1-WEST	Point-Area	0.323476	0.323476	0.323476
WV1-ECAR	Point-Area	−0.479062	−0.479062	−0.479062
EAST-WV1	Area-Point	0.024336	0.024336	0.024336
ECAR-BV1	Area-Point	0.468376	0.468376	0.468376
WEST-DOUGG1	Area-Point	−0.019207	−0.019207	−0.019207

3.7.3   Sample Computation for Voltage Sensitivity Analysis

The one line diagram of IEEE 14-bus system is shown in Figure 3.8. The corresponding parameters and data are listed in Tables 3.14 and 3.15.

Table 3.16 and Figure 3.9 show the major VAR support sites as well as the corresponding benefit factors *LBF* and *VBF* for the IEEE 14-bus system. It can be observed from Figure 3.9 that buses 9, 11, 12, and 13 have relatively big sensitivity values. The VAR supports at these locations will have bigger benefits than other locations in IEEE 14-bus system.

3.8   CONCLUSION

This chapter introduces several approaches to compute the sensitivities in the practical transmission network and energy markets. The analysis and implementation details of load sensitivity, voltage sensitivity, generator constraint
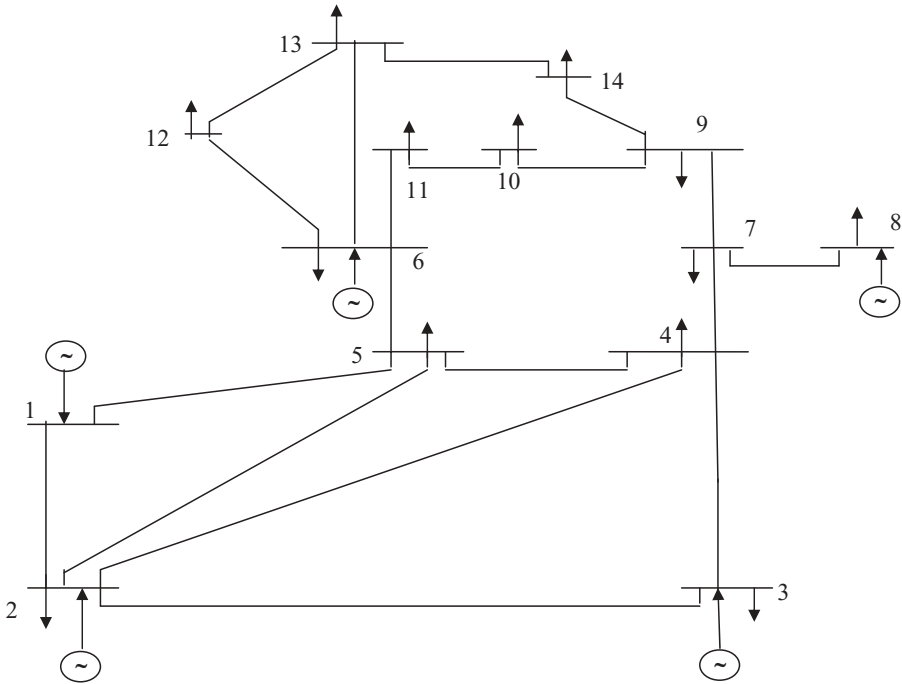
FIGURE 3.8   One-line diagram of IEEE 14-bus system
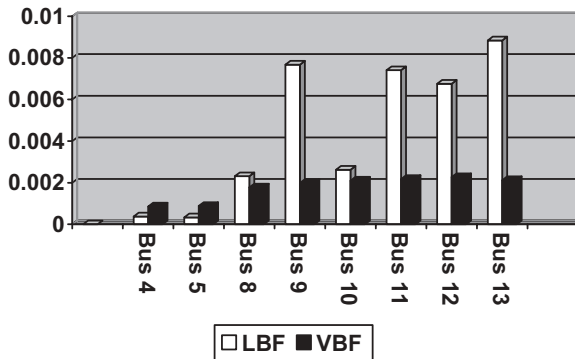
FIGURE 3.9   Voltage sensitivity analysis of 14-bus system

shift factor, and area-based constraint shift factor are presented. The chapter also comprehensively discusses how to compute the sensitivities under the different references, as well as how to convert the sensitivities based on the EMS system reference into those based on the market system reference. These sensitivity calculations can be used to determine whether the online capacity as indicated in the resource plan is located in the right place on the network

Table 3.14   IEEE 14 bus network load and generator data

Bus	MW Load	MVAr Load	Min Q_G	Max Q_G
1	0.00	0.00	0.00	10.00
2	21.70	12.70	−40.00	50.00
3	94.20	19.00	0.00	40.00
4	47.80	0.00	0.00	0.00
5	7.60	1.60	0.00	0.00
6	11.2	7.50	−6.00	24.00
7	0.00	0.00	0.00	0.00
8	0.00	0.00	−6.00	24.00
9	29.50	16.60	0.00	0.00
10	9.00	5.80	0.00	0.00
11	3.50	1.80	0.00	0.00
12	6.10	1.60	0.00	0.00
13	13.50	5.80	0.00	0.00
14	14.90	5.00	0.00	0.00

Table 3.15   IEEE 14 bus network line data

From Bus	To Bus	Resistance (p.u.)	Reactance (p.u.)	Line Charging (p.u.)
1	2	0.01938	0.05917	0.0528
1	5	0.05403	0.22304	0.0492
2	3	0.04699	0.19797	0.0438
2	4	0.05811	0.17632	0.0374
2	5	0.05695	0.17388	0.0340
3	4	0.06701	0.17103	0.0346
4	5	0.01355	0.04211	0.0128
4	7	0.00000	0.20912	0.0000
4	9	0.00000	0.55618	0.0000
5	6	0.00000	0.25202	0.0000
6	11	0.09498	0.19890	0.0000
6	12	0.12291	0.25581	0.0000
6	13	0.06615	0.13207	0.0000
7	8	0.00000	0.17615	0.0000
7	9	0.00000	0.11001	0.0000
9	10	0.03181	0.08450	0.0000
9	14	0.12711	0.27038	0.0000
10	11	0.08205	0.19207	0.0000
12	13	0.22092	0.19988	0.0000
13	14	0.17093	0.34802	0.0000

Table 3.16   Voltage sensitivity analysis results for IEEE 14-bus systems

VAR Support Site	LBF$_i$	VBF$_i$
Bus 4	0.000376	0.000855
Bus 5	0.000337	0.000884
Bus 8	0.002309	0.001775
Bus 9	0.007674	0.001989
Bus 10	0.002618	0.002097
Bus 11	0.007407	0.002175
Bus 12	0.006757	0.002268
Bus 13	0.008840	0.002122

to serve the forecasted demand. This chapter will be especially useful for power engineers since sensitivity analysis has already become daily work in the power industry. Researchers, students, and power engineers will also have the big picture on power system sensitivity analysis.

REFERENCES

[1] T.E. Dy-Liyacco, "Control Centers Are Here to Stay," *IEEE Computer Applications in Power*, Vol. 15, No. 4, pp. 18–23, 2002.

[2] N. Winser, "FERC's Standard Market Design: the ITC Perspective," 2002 IEEE PES Summer Meeting, Chicago, IL. July 22–26, 2002.

[3] A. Ott, "Experience with PJM Market Operation, System Design, and Implementation," *IEEE Trans. on Power Systems*, Vol. 18, No. 2, pp. 528–534, 2003.

[4] D. Kathan, "FERC's Standard Market Design Proposal," *2003 ACEEE/CEE National Symposium on Market Transformation*, Washington, DC, April 15, 2003.

[5] J.Z. Zhu, D. Hwang, and A. Sadjadpour, "An Approach of Generation scheduling in Energy Markets," POWERCON 2006, Chongqing, Oct. 22–28, 2006.

[6] L.K. Kirchamayer, *Economic Operation of Power Systems*, New York: John Wiley & Sons, 1958.

[7] H.W. Dommel and W.F. Tinney, "Optimal power flow solutions," *IEEE Trans. on PAS*, Vol. PAS-87, No. 10, pp. 1866–1876, 1968.

[8] M. Ilic, F.D. Galiana, and L. Fink, *Power Systems Restructuring: Engineering and Economics*. Norwell, MA: Kluwer, 1998.

[9] D. Kirschen, R. Allan, and G. Strbac, "Contributions of individual generators to loads and flows," *IEEE Trans. Power Systems*, Vol. 12, No. 1, pp. 52–60, 1997.

[10] F. Schweppe, M. Caramanis, R. Tabors, and R. Bohn, *Spot Pricing of Electricity*, Norwell, MA: Kluwer, 1988.

[11] A.J. Conejo, F.D. Galiana, and I. Kochar, "Z-Bus loss allocation," *IEEE Trans. Power Systems*, Vol. 16, No. 1, pp. 105–110, 2001.

[12] F.D. Galiana, A.J. Conjeo, and I. Korkar, "Incremental transmission loss allocation under pool dispatch," *IEEE Trans. Power Systems*, Vol. 17, No. 1, pp. 26–33, 2002.

[13] O.I. Elgerd, *Electric Energy Systems Theory: An Introduction*, New York: McGraw-Hill, 1982.

[14] J.Z. Zhu, D. Hwang, and A. Sadjadpour, "Loss Sensitivity Calculation and Analysis," *in Proc. 2003 IEEE General Meeting*, Toronto, July 13–18, 2003.

[15] J.Z. Zhu, D. Hwang, and A. Sadjadpour, "Real time loss sensitivity calculation in power systems operation," *Electric Power Systems Research*, Vol. 73, No. 1 2005, pp. 53–60.

[16] J.Z. Zhu, D. Hwang, and A. Sadjadpour, "The implementation of alleviating overload in energy markets," *IEEE/PES 2007 General Meeting*, June 24–28, 2007.

[17] J.Z. Zhu, D. Hwang, and A. Sadjadpour, "Calculation of several sensitivity in real time transmission network and energy markets," *Power-Grid Europe 2007*, Spain, June 23–26, 2007.

[18] A.J. Wood and B.F. Wollenberg, *Power Generation, Operation, and Control*, Second edition, New York, John Wiley & Sons, 1996.

[19] J.Z. Zhu and M.R. Irving, "Combined Active and Reactive Dispatch with Multiple Objectives using an Analytic Hierarchical Process," *IEE Proc. C*, Vol. 143, No. 4, pp. 344–352, 1996.

[20] J.Z. Zhu and J.A. Momoh, "Optimal VAR pricing and VAR placement using analytic hierarchy process," *Electric Power Systems Research*, Vol. 48, No. 1, pp. 11–17, 1998.

[21] M.O. Mansour and T.M. Abdel-Rahman, "Non-linear VAR Optimization Using Decomposition and Coordination," *IEEE Trans. PAS*, Vol. 103, pp. 246–255, 1984.

[22] N.H. Dandachi, M.J. Rawlins, O. Alsac, and B. Stott, "OPF for Reactive Pricing Studies on the NGC System," I*EEE Power Industry Computer Applications Conference*, PICA'95, Utah, pp. 11–17, May 1995.

[23] O. Alsac and B. Stott, "Optimal Power Flow with Steady-State Security," *IEEE Trans. PAS*, Vol. 93, pp. 745–751, 1974.

[24] J.A. Momoh and J.Z. Zhu, "Improved Interior Point Method for OPF Problems," *IEEE Trans. on Power Systems*, Vol. 14, No. 3, pp. 1114–1120, 1999.

[25] M. Begovic and A.G. Phadke, "Control of Voltage Stability using Sensitivity Analysis," *IEEE Transactions on Power Systems*, Vol. 7, Feb. 1992, pp. 114–123.

4

CLASSIC ECONOMIC DISPATCH

This chapter first introduces the input-output characteristic of a power-generating unit as well as the corresponding practical calculation method, and then presents several well-known optimization methods to solve the classic economic dispatch problem. Finally, the applications of the latest methods such as neural network and genetic algorithms to classic economic dispatch (ED) are analyzed in the chapter.

4.1 INTRODUCTION

The aim of real power economic dispatch (ED) is to make the generator's fuel consumption or the operating cost of the whole system minimal by determining the power output of each generating unit under the constraint condition of the system load demands. This is also called the classic economic dispatch, in which the line security constraints are neglected [1]. The fundamental of the economic dispatch problem is the set of input-output characteristic of a power-generating unit.

4.2 INPUT-OUTPUT CHARACTERISTIC OF GENERATOR UNITS

4.2.1 Input-Output Characteristic of Thermal Units

For thermal units, we call the input-output characteristic the generating unit fuel consumption function, or operating cost function. The unit of the

generator fuel consumption function is Btu per hour heat input to the unit (or MBtu/h). The fuel cost rate times Btu/h is the $ per hour ($/h) input to the unit for fuel. The output of the generating unit will be designed by P_G, the megawatt net power output of the unit.

In addition to the fuel consumption cost, the operating cost of a unit includes labor cost, maintenance cost, and fuel transportation cost. It is difficult to express these costs directly as a function of the output of the unit, so these costs are included as a fixed portion of the operating cost.

The thermal unit system generally consists of the boiler, the steam turbine, and the generator. The input of the boiler is fuel, and the output is the volume of steam. The relationship of the input and output can be expressed as a convex curve. The input of the turbine-generator unit is the volume of steam, and the output is the electrical power. A typical boiler-turbine-generator unit consists of a single boiler that generates steam to drive a single turbine-generator set. The input-output characteristic of the whole generating unit system can be obtained by combining directly the input-output characteristic of the boiler and the input-output characteristic of the turbine-generator unit. It is a convex curve, which is shown in Figure 4.1.

It can be observed from the input-output characteristic of the generating unit that the power output is limited by the minimal and maximal capacity of the generating unit, that is,

$$P_{G\min} \leq P_G \leq P_{G\max} \tag{4.1}$$

The minimal power output is determined by technical conditions or other factors of the boiler or turbine. Generally, the minimum load at which a unit can operate is influenced more by the steam generator and the regenerative cycle than by the turbine. The only critical parameters for the turbine are shell and rotor metal differential temperatures, exhaust hood temperature, and
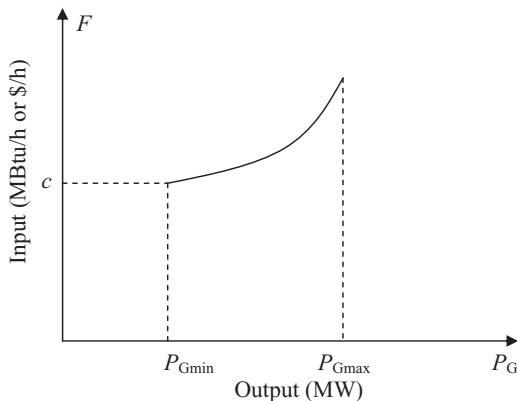
FIGURE 4.1   Input-output characteristic of the generating unit

rotor and shell expansion. Minimum load limitations of the boiler are generally caused by fuel combustion stability, and the values, which will differ with different types of boiler and fuel, are about 25–70% of design capacity. Minimum load limitations of the turbine-generator unit are caused by inherent steam generator design constraints, which are generally about 10–15%. The maximal power output of the generating unit is determined by the design capacity or rate capacity of the boiler, turbine, or generator.

Generally, the input-output characteristic of the generating unit is nonlinear. The widely used input-output characteristic of the generating unit is a quadratic function, i.e.,

$$F = aP_G^2 + bP_G + c \qquad (4.2)$$

where a, b, and c are the coefficients of the input-output characteristic. The constant c is equivalent to the fuel consumption of the generating unit operation without power output, which is shown in Figure 4.1.

4.2.2 Calculation of Input-Output Characteristic Parameters

The parameters of the input-output characteristic of the generating unit may be determined by the following approaches [2]:

(1) Based on the experiments of the generating unit efficiency
(2) Based on the historic records of the generating unit operation
(3) Based on the design data of the generating unit provided by manufacturer

In the practical power systems, we can easily obtain the fuel statistic data and power output statistic data. Through analyzing and computing a data set (F_k, P_k), we can determine the shape of the input-output characteristic and the corresponding parameters. For example, if the quadratic curve is the best match according to the statistical data, we can use the least squares method to compute the parameters. The calculation procedures are below.

Let (F_k, P_k) be obtained from the statistical data, where $k = 1, 2, \ldots n$, and the fuel curve will be a quadratic function. To determine the coefficients a, b, and c, compute the following error for each data pair (F_k, P_k):

$$\Delta F_k = \left(aP_k^2 + bP_k + c\right) - F_k \qquad (4.3)$$

According to the principle of least squares, we form the following objective function and make it minimal, i.e.,

$$J = (\Delta F_k)^2 = \sum_{k=1}^{n}\left(aP_k^2 + bP_k + c - F_k\right)^2 \qquad (4.4)$$

We will get the necessary conditions for an extreme value of the objective function when we take the first derivative of the above function J with respect to each of the independent variables a, b, and c and set the derivatives equal to zero:

$$\frac{\partial J}{\partial a} = \sum_{k=1}^{n} 2P_k^2 \left(aP_k^2 + bP_k + c - F_k \right) = 0 \tag{4.5}$$

$$\frac{\partial J}{\partial b} = \sum_{k=1}^{n} 2P_k \left(aP_k^2 + bP_k + c - F_k \right) = 0 \tag{4.6}$$

$$\frac{\partial J}{\partial c} = \sum_{k=1}^{n} 2 \left(aP_k^2 + bP_k + c - F_k \right) = 0 \tag{4.7}$$

From equations (4.5)–(4.7), we get

$$\left(\sum_{k=1}^{n} P_k^2 \right) a + \left(\sum_{k=1}^{n} P_k \right) b + nc = \sum_{k=1}^{n} F_k \tag{4.8}$$

$$\left(\sum_{k=1}^{n} P_k^3 \right) a + \left(\sum_{k=1}^{n} P_k^2 \right) b + \left(\sum_{k=1}^{n} P_k \right) c = \sum_{k=1}^{n} \left(F_k P_k \right) \tag{4.9}$$

$$\left(\sum_{k=1}^{n} P_k^4 \right) a + \left(\sum_{k=1}^{n} P_k^3 \right) b + \left(\sum_{k=1}^{n} P_k^2 \right) c = \sum_{k=1}^{n} \left(F_k P_k^2 \right) \tag{4.10}$$

Coefficients a, b, and c can be obtained by solving equations (4.8)–(4.10).

Example 4.1

We collected some statistical data for a generating unit in one power plant. The capacity limits of the generator are

$$150 \le P_G \le 200$$

Four data samples of unit fuel consumption are selected, i.e., 0.405, 0.379, 0.368, and 0.399 (Btu/MW·h), which correspond to power output of 150, 170, 185, and 200 (MW), respectively. The corresponding fuel consumptions are computed and listed in Table 4.1.

From Table 4.1, we get:

$$\sum_{k=1}^{n} P_k = 150 + 170 + 185 + 200 = 705$$

$$\sum_{k=1}^{n} P_k^2 = 150^2 + 170^2 + 185^2 + 200^2 = 1.256 \times 10^5$$

$$\sum_{k=1}^{n} P_k^3 = 150^3 + 170^3 + 185^3 + 200^3 = 2.2619 \times 10^7$$
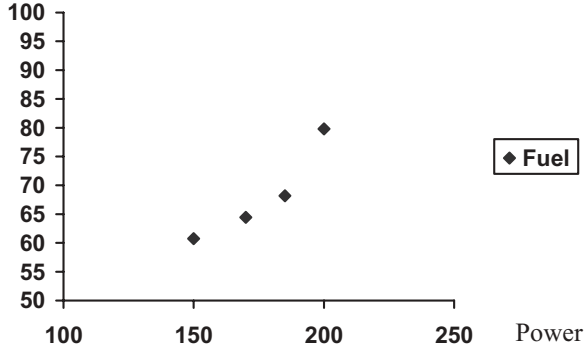
FIGURE 4.2   Four statistic data points

Table 4.1   Four data samples for a generating unit

Sample Data	K = 1	K = 2	K = 3	K = 4
Unit consume fuel (Btu/MW.h)	0.405	0.379	0.368	0.399
Power output (MW)	150.0	170.0	185.0	200.0
Consume fuel (Btu/h)	60.75	64.43	68.08	79.80

$$\sum_{k=1}^{n} P_k^4 = 150^4 + 170^4 + 185^4 + 200^4 = 4.112 \times 10^9$$

$$\sum_{k=1}^{n} F_k = 60.75 + 64.43 + 68.08 + 79.80 = 273.06$$

$$\sum_{k=1}^{n} F_k P_k = 60.75 \times 150 + 64.43 \times 170 + 68.08 \times 185 + 79.80 \times 200 = 4.86 \times 10^4$$

$$\sum_{k=1}^{n} F_k P_k^2 = 60.75 \times 150^2 + 64.43 \times 170^2 + 68.08 \times 185^2 + 79.80 \times 200^2$$
$$= 8.75 \times 10^6$$

From equations (4.8)–(4.10), we get

$$1.256 \times 10^5 a + 705b + 4c = 273.06$$

$$2.2619 \times 10^7 a + 1.26 \times 10^5 b + 705c = 4.86 \times 10^4$$

$$4.112 \times 10^9 a + 2.26 \times 10^7 b + 1.26 \times 10^5 c = 8.75 \times 10^6$$

Solving these equations, we get the coefficients of the fuel consumption function of the generating unit:

$$a = 0.0009, \quad b = 0.0457, \quad c = 31.9$$

The obtained quadratic fuel consumption function is as below:

$$F = 0.0009P_G^2 + 0.0457P_G + 31.9$$

The simulated input-output curve is shown in Figure 4.3. It is noted that the accuracy of calculation will be increased if more data samples are used.

4.2.3   Input-Output Characteristic of Hydroelectric Units

The input-output characteristic of the hydroelectric unit is similar to that of the thermal unit, but the input is different, which is expressed in terms of volume of water per unit time. The unit of water volume is m³/h. The output is the same, i.e., electric power. Figure 4.4 shows a typical input-output curve of a hydroelectric unit where the net hydraulic head is constant. This characteristic shows an almost linear curve of input water volume requirements per
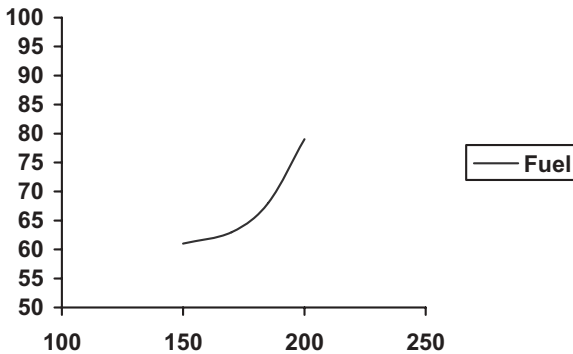
FIGURE 4.3   Simulated input-output curve
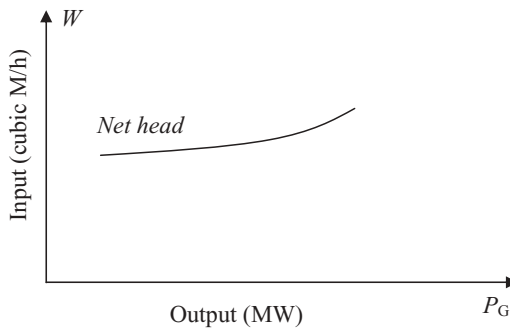
FIGURE 4.4   Hydroelectric unit input-output curve
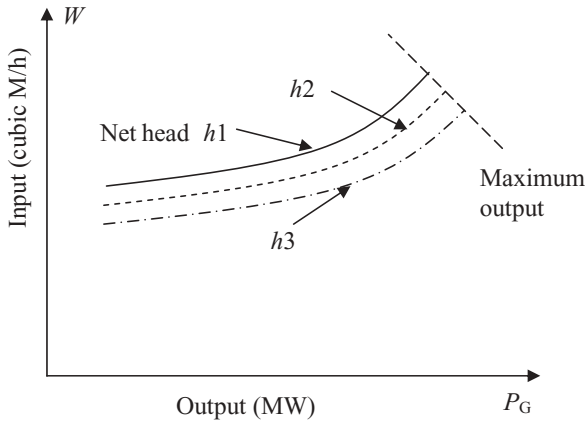
FIGURE 4.5 Hydroelectric unit input-output curve with variable water head

unit time as a function of power output as the power output increases from minimum to rated load. Above this point corresponding to the rated load, the water volume requirements increase as the efficiency of the unit falls off.

Figure 4.5 shows the input-output curve of a hydroelectric plant with variable head. This type of characteristic occurs whenever the variation in the storage pond and/or afterbay elevations is a fairly large percentage of the overall net hydraulic head.

4.3 THERMAL SYSTEM ECONOMIC DISPATCH NEGLECTING NETWORK LOSSES

4.3.1 Principle of Equal Incremental Rate

Given a system that consists of two generators connected to a single bus serving a received electrical load P_D. The input-output characteristics of two generating units are $F_1(P_{G1})$ and $F_2(P_{G2})$, respectively. The total fuel consumption of the system F is the sum of the fuel consumptions of the two generating units. Assuming there is no power output limitation for both generators, the essential constraint on the operation of this system is that the sum of the output powers must equal the load demand. The economic power dispatch problem of the system, which is to minimize F under the above-mentioned constraint, can be expressed as:

$$\min F = F_1(P_{G1}) + F_2(P_{G2}) \tag{4.11}$$

s.t.

$$P_{G1} + P_{G2} = P_D \tag{4.12}$$

According to the principle of equal incremental rate [1], the total fuel consumption F will be minimal if the incremental fuel rates of two generators are equal, that is,

$$\frac{\mathrm{d}F_1}{\mathrm{d}P_{G1}} = \frac{\mathrm{d}F_2}{\mathrm{d}P_{G2}} = \lambda \qquad (4.13)$$

where $\dfrac{\mathrm{d}F_i}{\mathrm{d}P_{Gi}}$ is the incremental fuel rate of generating unit i, which corresponds to the slope of the input-output curve of the generating unit.

If two generators operate under the different incremental fuel rate, and

$$\frac{\mathrm{d}F_1}{\mathrm{d}P_{G1}} > \frac{\mathrm{d}F_2}{\mathrm{d}P_{G2}}$$

the total output powers maintain the same. If generator 1 reduces output power ΔP, generator 2 will increase output power ΔP. Then generator 1 will reduce fuel consumption $\dfrac{\mathrm{d}F_1}{\mathrm{d}P_{G1}}\Delta P$, and generator 2 will increase fuel consumption $\dfrac{\mathrm{d}F_2}{\mathrm{d}P_{G2}}\Delta P$. The total savings of fuel consumption will be

$$\Delta F = \frac{\mathrm{d}F_1}{\mathrm{d}P_{G1}}\Delta P - \frac{\mathrm{d}F_2}{\mathrm{d}P_{G2}}\Delta P = \left(\frac{\mathrm{d}F_1}{\mathrm{d}P_{G1}} - \frac{\mathrm{d}F_2}{\mathrm{d}P_{G2}}\right)\Delta P > 0 \qquad (4.14)$$

It can be observed from equation (4.14) that ΔF will be zero when $\dfrac{\mathrm{d}F_1}{\mathrm{d}P_{G1}} = \dfrac{\mathrm{d}F_2}{\mathrm{d}P_{G2}}$, that is, the incremental fuel rates of two generators are equal.

Example 4.2

The input-output characteristics of two generating units are as follows:

$$F_1 = 0.0008P_{G1}^2 + 0.2P_{G1} + 5 \text{ Btu/h}$$
$$F_2 = 0.0005P_{G2}^2 + 0.3P_{G2} + 4 \text{ Btu/h}$$

We wish to determine the economic operation point for these two units when delivering a total of 500 MW power demand.

First of all, we can obtain the incremental fuel rate of two generating units as follows:

$$\lambda_1 = \frac{\mathrm{d}F_1}{\mathrm{d}P_{G1}} = 0.0016P_{G1} + 0.2$$

$$\lambda_2 = \frac{dF_2}{dP_{G2}} = 0.001P_{G2} + 0.3$$

According to the principle of equal incremental rate [equation (4.13)], we have

$$\lambda_1 = \lambda_2$$

That is,

$$0.0016P_{G1} + 0.2 = 0.001P_{G2} + 0.3$$

or

$$1.6P_{G1} - P_{G2} = 100$$

Given a system load of 500 MW, then

$$P_{G1} + P_{G2} = 500$$

Solving the above two equations for P_{G1}, P_{G2}, we get

$$P_{G1} = 230.77 \text{ MW}$$

$$P_{G2} = 269.23 \text{ MW}$$

Example 4.3

Suppose the input-output characteristics of two generating units are a little different from those of Example 4.2, which are as follows:

$$F_1 = 0.0008P_{G1}^2 + 0.02P_{G1} + 5 \text{ Btu/h}$$
$$F_2 = 0.0005P_{G2}^2 + 0.03P_{G2} + 4 \text{ Btu/h}$$

We still wish to determine the economic operation point for these two units when delivering a total of 500 MW power demand.

First of all, we can obtain the incremental fuel rate of two generating units as follows:

$$\lambda_1 = \frac{dF_1}{dP_{G1}} = 0.0016P_{G1} + 0.02$$

$$\lambda_2 = \frac{dF_2}{dP_{G2}} = 0.001P_{G2} + 0.03$$

According to the principle of equal incremental rate [equation (4.13)], we have

$$\lambda_1 = \lambda_2$$

that is,

$$0.0016 P_{G1} + 0.02 = 0.001 P_{G2} + 0.03$$

or

$$1.6 P_{G1} - P_{G2} = 10$$

Given a system load of 500 MW, then

$$P_{G1} + P_{G2} = 500$$

Solving the above two equations for P_{G1}, P_{G2}, we get

$$P_{G1} = 196.15 \text{ MW}$$
$$P_{G2} = 303.85 \text{ MW}$$

4.3.2 Economic Dispatch without Network Losses

4.3.2.1 Neglect the Constraints of Power Output The equal incremental principle can be used for a system with N thermal-generating units. Given that the input-output characteristics of N generating units are $F_1(P_{G1})$, $F_2(P_{G2})$, ..., $F_n(P_{Gn})$, respectively, the total system load is P_D. The problem is to minimize total fuel consumption F subject to the constraint that the sum of the power generated must equal the received load. That is,

$$\min F = F_1(P_{G1}) + F_2(P_{G2}) + \cdots + F_n(P_{Gn}) = \sum_{i=1}^{N} F_i(P_{Gi}) \tag{4.15}$$

s.t.

$$\sum_{i=1}^{N} P_{Gi} = P_D \tag{4.16}$$

This is a constrained optimization problem, and it can be solved by the Lagrange multiplier method. First of all, the Lagrange function should be formed by adding the constraint function to the objective function after the constraint function has been multiplied by an undetermined multiplier.

$$L = F + \lambda \left(P_D - \sum_{i=1}^{N} P_{Gi} \right) \tag{4.17}$$

where λ is the Lagrange multiplier.

The necessary conditions for the extreme value of the Lagrange function are to set the first derivative of the Lagrange function with respect to each of the independent variables equal to zero.

$$\frac{\partial L}{\partial P_{Gi}} = \frac{\partial F}{\partial P_{Gi}} - \lambda = 0 \quad i = 1, 2, \dots, N \tag{4.18}$$

or

$$\frac{\partial F}{\partial P_{Gi}} = \lambda \quad i = 1, 2, \dots, N \tag{4.19}$$

Since the fuel consumption function of each generating unit is only related to its own power output, equation (4.19) can be written as:

$$\frac{\mathrm{d}F_i}{\mathrm{d}P_{Gi}} = \lambda \quad i = 1, 2, \dots, N \tag{4.20}$$

or

$$\frac{\mathrm{d}F_1}{\mathrm{d}P_{G1}} = \frac{\mathrm{d}F_2}{\mathrm{d}P_{G2}} = \cdots \frac{\mathrm{d}F_N}{\mathrm{d}P_{GN}} = \lambda \tag{4.21}$$

Equation (4.20) is the principle of equal incremental rate of economic power operation for multiple generating units.

Example 4.4

Suppose the input-output characteristics of three generating units are as follows:

$$F_1 = 0.0006 P_{G1}^2 + 0.5 P_{G1} + 6 \ \text{Btu/h}$$

$$F_2 = 0.0005 P_{G2}^2 + 0.6 P_{G2} + 5 \ \text{Btu/h}$$

$$F_3 = 0.0007 P_{G3}^2 + 0.4 P_{G3} + 3 \ \text{Btu/h}$$

We wish to determine the economic operation point for these three units when delivering a total of 500 MW and 800 MW power demand, respectively.

(A) Total load $P_D = 500$ MW
The incremental fuel rates of three generating units are calculated as follows:

$$\lambda_1 = \frac{\mathrm{d}F_1}{\mathrm{d}P_{G1}} = 0.0012 P_{G1} + 0.5$$

$$\lambda_2 = \frac{\mathrm{d}F_2}{\mathrm{d}P_{G2}} = 0.001 P_{G2} + 0.6$$

$$\lambda_3 = \frac{\mathrm{d}F_3}{\mathrm{d}P_{G3}} = 0.0014 P_{G3} + 0.4$$

According to the principle of equal incremental rate, we have

$$\lambda_1 = \lambda_2 = \lambda_3$$

That is,

$$0.0012 P_{G1} + 0.5 = 0.001 P_{G2} + 0.6 = 0.0014 P_{G3} + 0.4$$

From the above equation, we get

$$1.2 P_{G1} - P_{G2} = 100$$
$$1.2 P_{G1} - 1.4 P_{G3} = -100$$

Given a system load of 500 MW, then

$$P_{G1} + P_{G2} + P_{G3} = 500$$

Solving the above three equations for P_{G1}, P_{G2}, P_{G3} we get

$$P_{G1} = 172.897 \text{ MW}$$
$$P_{G2} = 107.477 \text{ MW}$$
$$P_{G3} = 219.626 \text{ MW}$$

The corresponding system incremental fuel rate under this load level is

$$\lambda = 0.70748$$

(B) Total load $P_D = 800$ MW
Similar to (A), we get the following equations:

$$1.2 P_{G1} - P_{G2} = 100$$
$$1.2 P_{G1} - 1.4 P_{G3} = -100$$
$$P_{G1} + P_{G2} + P_{G3} = 800$$

Solving the above three equations for P_{G1}, P_{G2}, P_{G3}, we get

$$P_{G1} = 271.028 \text{ MW}$$

$$P_{G2} = 225.234 \text{ MW}$$

$$P_{G3} = 303.738 \text{ MW}$$

The corresponding system incremental fuel rate under this load level is

$$\lambda = 0.82523$$

4.3.2.2 *Consider the Constraints of Power Output*   We have discussed the equal incremental principle of economic operation. Thus we know that the necessary condition for thermal power system economic operation is that the incremental fuel rates (or incremental cost rates) of all the units are equal. However, we have not considered the two inequalities, i.e., the power output of each unit must be greater than or equal to the minimum power permitted and must also be less than or equal to the maximum power permitted on that particular unit.

Considering the inequality constraints, the problem of economic dispatch can be written as below:

$$\min F = F_1(P_{G1}) + F_2(P_{G2}) + \cdots + F_n(P_{Gn}) = \sum_{i=1}^{N} F_i(P_{Gi}) \qquad (4.22)$$

s.t.

$$\sum_{i=1}^{N} P_{Gi} = P_D \qquad (4.23)$$

$$P_{Gi\,\min} \le P_{Gi} \le P_{Gi\,\max} \qquad (4.24)$$

The equal incremental principle can be still applied to equations (4.22)–(4.24). The calculation process is as below:

(1) Neglect the inequality equation (4.24). Distribute the power among the units according to the equal incremental principle.
(2) Check the power output limits for each unit according to equation (4.24). If the power output is out of the limits, set the power output equal to the corresponding limit, that is,

$$\text{If } P_{Gk} \ge P_{Gk\,\max}, P_{Gk} = P_{Gk\,\max} \qquad (4.25)$$

$$\text{If } P_{Gk} \le P_{Gk\,\min}, P_{Gk} = P_{Gk\,\min} \qquad (4.26)$$

(3) Handle the violated unit as a negative load, i.e.,

$$P'_{Dk} = -P_{Gk} \qquad \text{for violated units } k \ (k = 1, \dots nk)$$

(4) Recompute the power balance equation as below:

$$\sum_{\substack{i=1 \\ i \notin nk}}^{N} P_{Gi} = P_D + \sum_{k=1}^{nk} P'_{Dk} \tag{4.27}$$

or

$$\sum_{\substack{i=1 \\ i \notin nk}}^{N} P_{Gi} = P_D - \sum_{k=1}^{nk} P_{Gk} \tag{4.28}$$

(5) Go back to step (1) until all inequalities of units are met.

Example 4.5

Example 4.3 is used here but considering the inequality constraints of two units, which are given as below:

$$100 \le P_{G1} \le 250 \text{ MW}$$

$$150 \le P_{G2} \le 300 \text{ MW}$$

From Example 4.3, we know the economic operation point for these two units without inequalities when delivering a total of 500 MW power demand. That is,

$$P_{G1} = 196.15 \text{ MW}$$

$$P_{G2} = 303.85 \text{ MW}$$

By checking the inequality constraints of units, we can see that the power output of unit 2 violated its upper limit. Thus we set the power output of unit 2 to its upper limit.

$$P_{G2} = 303.85 \ge 300 \, (P_{G2\max}), \ P_{G2} = 300 \text{ MW}$$

So the power dispatch becomes

$$P_{G1} = 200 \text{ MW}$$

$$P_{G2} = 300 \text{ MW}$$

Example 4.6

Example 4.4 is used here but considering the inequality constraints of three units, which are given as below.

$$100 \le P_{G1} \le 250 \text{ MW}$$

$$100 \le P_{G2} \le 250 \text{ MW}$$

$$100 \le P_{G3} \le 350 \text{ MW}$$

(A) Total load $P_D = 500\,\text{MW}$

When delivering a total of $500\,\text{MW}$ power demand, the dispatch from Example 4.4 is

$$P_{G1} = 172.897 \text{ MW}$$

$$P_{G2} = 107.477 \text{ MW}$$

$$P_{G3} = 219.626 \text{ MW}$$

By checking the inequality constraints of units, we know that all the power outputs of the units are within the limits. Thus they are the optimum results, and there is no violation of the inequality constraints.

(B) Total load $P_D = 800\,\text{MW}$

When delivering a total of $800\,\text{MW}$ power demand, the dispatch from Example 4.4 is

$$P_{G1} = 271.028 \text{ MW}$$

$$P_{G2} = 225.234 \text{ MW}$$

$$P_{G3} = 303.738 \text{ MW}$$

By checking the inequality constraints of units, we can see that the power output of unit 1 violated its upper limit. According to equation (4.25), we get

$$P_{G1} = 250 \text{ MW}$$

According to equation (4.27), we have

$$P'_{D1} = -250 \text{ MW}$$

From equation (4.28), we get the new power balance equation

$$P_{G2} + P_{G3} = 800 - 250 = 550$$

Applying the principle of equal incremental rate for units 2 and 3, we have

$$\lambda_2 = \frac{dF_2}{dP_{G2}} = 0.001 P_{G2} + 0.6$$

$$\lambda_3 = \frac{\mathrm{d}F_3}{\mathrm{d}P_{G3}} = 0.0014P_{G3} + 0.4$$

$$\lambda_2 = \lambda_3$$

that is,

$$0.001P_{G2} + 0.6 = 0.0014P_{G3} + 0.4$$

Then we can get the following two equations

$$P_{G2} - 1.4P_{G3} = -200$$
$$P_{G2} + P_{G3} = 550$$

Solving the above the equations, the power dispatch becomes

$$P_{G1} = 250.0 \text{ MW}$$
$$P_{G2} = 237.5 \text{ MW}$$
$$P_{G3} = 312.5 \text{ MW}$$

4.4 CALCULATION OF INCREMENTAL POWER LOSSES

Network losses are neglected in the previous sections on economic dispatch. It is much more difficult to solve the economic dispatch problem with network losses than the previous cases with no losses. There have been two general approaches to compute the network losses and the corresponding incremental power losses. The first is the development of a mathematical expression for the losses in the network solely as a function of the power output of each of the units. This is called the B-coefficient method. The other method is based on power flow equations. The details on how to compute incremental power losses are discussed in Chapter 3. Here, we just describe the simple B-coefficient method.

Let S_L be plural power losses of the network, and the corresponding real and reactive power losses will be P_L and Q_L. The plural power losses equal the sum of the plural power injections of nodes, which can be expressed as

$$S_L = P_L + jQ_L = \dot{V}^T \overset{*}{\dot{I}} \tag{4.29}$$

$$\dot{V} = Z\dot{I} \tag{4.30}$$

$$Z = R + jX \tag{4.31}$$

$$\dot{I} = I_P + jI_Q \tag{4.32}$$

where

    V: Node voltage
    I: Node current
    I_P: Node current component corresponding to real power
    I_Q: Node current component corresponding to reactive power
    Z: Node impedance matrix

Substituting equations (4.30)–(4.32) into equation (4.29), we get the real power losses as below:

$$P_L = I_P^T R I_P + I_Q^T R I_Q \tag{4.33}$$

The node current can also be expressed as

$$\dot{I}_i = \frac{P_i + jQ_i}{\dot{V}_i} = \frac{P_i + jQ_i}{V_i e^{-j\theta_i}} = \frac{(P_i + jQ_i)e^{j\theta_i}}{V_i} \tag{4.34}$$

Since

$$e^{j\theta_i} = \cos\theta_i + j\sin\theta_i \tag{4.35}$$

Thus

$$\dot{I}_i = \frac{(P_i + jQ_i)(\cos\theta_i + j\sin\theta_i)}{V_i} \tag{4.36}$$

From equation (4.36), we get

$$I_{Pi} = \frac{(P_i \cos\theta_i + Q_i \sin\theta_i)}{V_i} \tag{4.37}$$

$$I_{qi} = \frac{(P_i \sin\theta_i - Q_i \cos\theta_i)}{V_i} \tag{4.38}$$

Substituting equations (4.37) and (4.38) into equation (4.33), we get

$$P_L = \begin{bmatrix} P^T & Q^T \end{bmatrix} \begin{bmatrix} A & -B \\ B & A \end{bmatrix} \begin{bmatrix} P \\ Q \end{bmatrix} \tag{4.39}$$

Where the elements of A and B are

$$A_{ij} = \frac{R_{ij}\cos(\theta_i - \theta_j)}{V_i V_j} \tag{4.40}$$

$$B_{ij} = \frac{R_{ij}\sin(\theta_i - \theta_j)}{V_i V_j} \tag{4.41}$$

Suppose each node power consists of power generation and power demand. Then node power and matrices A and B can be divided into two parts, i.e.,

$$P^{\mathrm{T}} = \begin{bmatrix} P_G^{\mathrm{T}} & P_D^{\mathrm{T}} \end{bmatrix} \tag{4.42}$$

$$Q^{\mathrm{T}} = \begin{bmatrix} Q_G^{\mathrm{T}} & Q_D^{\mathrm{T}} \end{bmatrix} \tag{4.43}$$

$$A = \begin{bmatrix} A_{GG} & A_{GD} \\ A_{DG} & A_{DD} \end{bmatrix} \tag{4.44}$$

$$B = \begin{bmatrix} B_{GG} & B_{GD} \\ B_{DG} & B_{DD} \end{bmatrix} \tag{4.45}$$

Substituting equations (4.42)–(4.45) into equation (4.39), we get

$$P_{\mathrm{L}} = \begin{bmatrix} P_G^{\mathrm{T}} & Q_G^{\mathrm{T}} \end{bmatrix} \begin{bmatrix} A_{GG} & -B_{GG} \\ B_{GG} & A_{GG} \end{bmatrix} \begin{bmatrix} P_G \\ Q_G \end{bmatrix} + \begin{bmatrix} C_{GD}^{\mathrm{T}} & C_{DG}^{\mathrm{T}} \end{bmatrix} \begin{bmatrix} P_G \\ Q_G \end{bmatrix} + C \tag{4.46}$$

where

$$C = \begin{bmatrix} P_D^{\mathrm{T}} & Q_D^{\mathrm{T}} \end{bmatrix} \begin{bmatrix} A_{DD} & -B_{DD} \\ B_{DD} & A_{DD} \end{bmatrix} \begin{bmatrix} P_D \\ Q_D \end{bmatrix} \tag{4.47}$$

$$C_{GD} = 2(B_{GD}Q_D - A_{GD}P_D) \tag{4.48}$$

$$C_{DG} = 2(B_{DG}^{\mathrm{T}}P_D - A_{DG}^{\mathrm{T}}Q_D) \tag{4.49}$$

Assuming the relationship between real and reactive power output of the generator is linear, i.e.,

$$Q_{Gi} = Q_{G0i} - D_i P_{Gi} \tag{4.50}$$

equation (4.46) can be written as

$$P_{\mathrm{L}} = P_G^{\mathrm{T}} B_{\mathrm{L}} P_G + B_{\mathrm{L}0}^{\mathrm{T}} P_G + B_0 \tag{4.51}$$

where

$$B_{\mathrm{L}} = F A_{GG} F + A_{GG} + 2 F B_{GG} \tag{4.52}$$

$$B_{L0}^{T} = 2Q_{G0}^{T}(A_{GG}F + B_{GG}) + C_{DG}^{T}F + C_{GD}^{T} \qquad (4.53)$$

$$B_0 = Q_{G0}^{T}A_{GG}Q_{G0} + C_{DG}^{T}Q_{G0} + C \qquad (4.54)$$

Equation (4.51) is the B-coefficient formula of network losses. The incremental power losses can be obtained from equation (4.51):

$$\frac{\partial P_L}{\partial P_G} = 2B_L P_G + B_{L0}^{T} \qquad (4.55)$$

4.5   THERMAL SYSTEM ECONOMIC DISPATCH WITH NETWORK LOSSES

Considering the network power losses, the problem of thermal system economic dispatch can be written as below.

$$\min F = F_1(P_{G1}) + F_2(P_{G2}) + \cdots + F_n(P_{Gn}) = \sum_{i=1}^{N} F_i(P_{Gi}) \qquad (4.56)$$

s.t.

$$\sum_{i=1}^{N} P_{Gi} = P_D + P_L \qquad (4.57)$$

$$P_{Gi\min} \leq P_{Gi} \leq P_{Gi\max} \qquad (4.58)$$

The Lagrange function is written as:

$$L = F + \lambda \left(P_D + P_L - \sum_{i=1}^{N} P_{Gi} \right) \qquad (4.59)$$

The necessary conditions for the extreme value of the Lagrange function are to set the first derivative of the Lagrange function with respect to each of the independent variables equal to zero.

$$\frac{\partial L}{\partial P_{Gi}} = \frac{dF_i}{dP_{Gi}} - \lambda \left(1 - \frac{\partial P_L}{\partial P_{Gi}} \right) = 0 \quad i = 1, 2, \ldots, N \qquad (4.60)$$

or

$$\frac{dF_i}{dP_{Gi}} \times \frac{1}{\left(1 - \dfrac{\partial P_L}{\partial P_{Gi}} \right)} = \frac{dF_i}{dP_{Gi}} a_i = \lambda \quad i = 1, 2, \ldots, N \qquad (4.61)$$

where

$$a_i = \frac{1}{\left(1 - \dfrac{\partial P_L}{\partial P_{Gi}}\right)} \tag{4.62}$$

is the correction coefficient of network losses.

Considering the network losses, the equal incremental principle of classic economic dispatch can be written as

$$\frac{dF_i}{dP_{Gi}} a_i = \lambda \quad i = 1, 2, \ldots, N \tag{4.63}$$

or

$$\frac{dF_1}{dP_{G1}} a_1 = \frac{dF_2}{dP_{G2}} a_2 = \cdots \frac{dF_N}{dP_{GN}} a_N = \lambda \tag{4.64}$$

Equation (4.64) is also called the coordination equation of economic power operation.

The solution procedure of thermal system economic power dispatch is as follows.

(1) Pick a set of starting values P_{G0i} that sum to the load.
(2) Calculate the incremental fuel $\dfrac{dF_i}{dP_{Gi}}$.
(3) Calculate the incremental losses $\dfrac{\partial P_L}{\partial P_{Gi}}$ as well as the total losses.
(4) Calculate the value of λ and P_{Gi} according to the coordination equation (4.64) and the power balance equation.
(5) Compare the P_{Gi} from step (4) with the starting points P_{G0i}. If there is no significant change in any one of the values, go to step (6); otherwise go back to step 2.
(6) Done.

4.6 HYDROTHERMAL SYSTEM ECONOMIC DISPATCH

4.6.1 Neglect Network Losses

The hydrothermal system economic dispatch is usually more complex than the economic operation of an all-thermal generation system. All hydro-systems are different. The reasons for the differences are the natural differences in the watersheds, the differences in the manmade storage and release elements used to control the water flows, and the very many different types of natural and

manmade constraints imposed on the operation of hydroelectric systems. The coordination of the operation of hydroelectric plants involves the scheduling of water release. According to the scheduling period, the hydro-system operation can be divided into long-range hydro-scheduling and short-range hydro-scheduling problems.

The long-range hydro-scheduling problem involves the long-range forecasting of water availability and the scheduling of reservoir water release for an interval of time that depends on the reservoir capacities. Typical long-range scheduling goes anywhere from 1 week to 1 year or several years. For hydro schemes with a capacity of impounding water over several seasons, the long-range problem involves meteorological and statistics analysis. Here we focus on the short-range hydro-scheduling problem.

Short-range hydro-scheduling refers to time periods from 1 day to 1 week. It involves the hour-by-hour scheduling of all generations on a hydrothermal system to achieve minimum production cost (or minimum consumption fuel) for the given time period.

Let P_T, $F(P_T)$ be the power output and input-output characteristic of a thermal plant, and let P_H, $W(P_H)$ be the power output and input-output characteristic of a hydro-electric plant. The hydrothermal system economic dispatch problem can be expressed as

$$\min F_\Sigma = \int_0^T F[P_T(t)]\,dt \tag{4.65}$$

s.t.

$$P_H(t) + P_T(t) - P_D(t) = 0 \tag{4.66}$$

$$\int_0^T W[P_H(t)]\,dt - W_\Sigma = 0 \tag{4.67}$$

We divide the operation period T into s time stages

$$T = \sum_{k=1}^s \Delta t_k \tag{4.68}$$

For any time stage, suppose that the power output of the hydro plant and the thermal plant as well as load demand are constant. Then equations (4.66) and (4.67) are changed as

$$P_{Hk} + P_{Tk} - P_{Dk} = 0, \quad k = 1, 2, \ldots, s \tag{4.69}$$

$$\sum_{k=1}^s W(P_{Hk})\Delta t_k - W_\Sigma = \sum_{k=1}^s W_k \Delta t_k - W_\Sigma = 0 \tag{4.70}$$

The objective function (4.65) is also changed as

$$F_\Sigma = \sum_{k=1}^s F(P_{Tk})\Delta t_k = \sum_{k=1}^s F_k \Delta t_k \tag{4.71}$$

The Lagrange function is written as:

$$L = \sum_{k=1}^{s} F_k \Delta t_k - \sum_{k=1}^{s} \lambda_k (P_{\mathrm{H}k} + P_{\mathrm{T}k} - P_{\mathrm{D}k}) \Delta t_k + \gamma \left(\sum_{k=1}^{s} W_k \Delta t_k - W_\Sigma \right) \quad (4.72)$$

The necessary conditions for the extreme value of the Lagrange function are

$$\frac{\partial L}{\partial P_{\mathrm{H}k}} = \gamma \frac{\mathrm{d}W_k}{\mathrm{d}P_{\mathrm{H}k}} \Delta t_k - \lambda_k \Delta t_k = 0 \quad k = 1, 2, \ldots, s \qquad (4.73)$$

$$\frac{\partial L}{\partial P_{\mathrm{T}k}} = \frac{\mathrm{d}F_k}{\mathrm{d}P_{\mathrm{T}k}} \Delta t_k - \lambda_k \Delta t_k = 0 \quad k = 1, 2, \ldots, s \qquad (4.74)$$

$$\frac{\partial L}{\partial \lambda_k} = -(P_{\mathrm{H}k} + P_{\mathrm{T}k} - P_{\mathrm{D}k}) \Delta t_k = 0 \quad k = 1, 2, \ldots, s \qquad (4.75)$$

$$\frac{\partial L}{\partial \gamma} = \sum_{k=1}^{s} W_k \Delta t_k - W_\Sigma = 0 \qquad (4.76)$$

From equations (4.73) and (4.74), we get

$$\frac{\mathrm{d}F_k}{\mathrm{d}P_{\mathrm{T}k}} = \gamma \frac{\mathrm{d}W_k}{\mathrm{d}P_{\mathrm{H}k}} = \lambda_k \quad k = 1, 2, \ldots, s \qquad (4.77)$$

If the time stage is very short, equation (4.77) can be expressed as

$$\frac{\mathrm{d}F}{\mathrm{d}P_{\mathrm{T}}} = \gamma \frac{\mathrm{d}W}{\mathrm{d}P_{\mathrm{H}}} = \lambda \qquad (4.78)$$

Equation (4.78) is the equal incremental principle of hydrothermal system economic dispatch. It means that when the thermal unit increases power output ΔP, the incremental fuel consumption will be

$$\Delta F = \frac{\mathrm{d}F}{\mathrm{d}P_{\mathrm{T}}} \Delta P \qquad (4.79)$$

When the hydro unit increases power output ΔP, the incremental water consumption will be

$$\Delta W = \frac{\mathrm{d}W}{\mathrm{d}P_{\mathrm{H}}} \Delta P \qquad (4.80)$$

From equations (4.78)–(4.80), we obtain

$$\gamma = \frac{\Delta F}{\Delta W} \tag{4.81}$$

where γ is the coefficient that converts water consumption to fuel. In other words, the water consumption of a hydro unit multiplied by γ is equivalent to the fuel consumption of a thermal unit. Thus the hydro unit is equivalent to a thermal unit.

Generally, the value of γ is related to given water consumption of a hydro unit during a time period (e.g., 1 day). If the given water consumption is big, the hydro unit can produce more power output to meet the load demand. In this case, a smaller value of γ will be selected. Otherwise, a bigger value of γ will be selected. The calculation procedures of hydrothermal system economic dispatch are as below.

(1) Given a initial value $\gamma(0)$, set iteration number $k = 0$
(2) Compute power distribution for the hydrothermal system for all time stages according to equation (4.77).
(3) Check whether the total water consumption $W(k)$ equals the given water consumption, i.e.,

$$|W(k) - W_\Sigma| < \varepsilon \tag{4.82}$$

If this is met, stop calculation; otherwise, go to the next step.
(4) If $W(k) > W_\Sigma$, it means that the selected γ is too small. Make $\gamma(k + 1) > \gamma(k)$. If $W(k) < W_\Sigma$, it means that the selected γ is too big. Make $\gamma(k + 1) < \gamma(k)$. Go back to step (2).

Example 4.7

A system has one thermal plant and one hydro plant. The input-output characteristic of the thermal plant is

$$F = 0.00035 P_T^2 + 0.4 P_T + 3 \text{ Btu/h}$$

The input-output characteristic of the hydro plant is

$$W = 0.0015 P_H^2 + 0.8 P_H + 2 \text{ m}^3/\text{s}$$

The daily water consumption of the hydro plant is

$$W_\Sigma = 1.5 \times 10^7 \text{ m}^3$$

The daily load demands of the system are as shown in Figure 4.6.
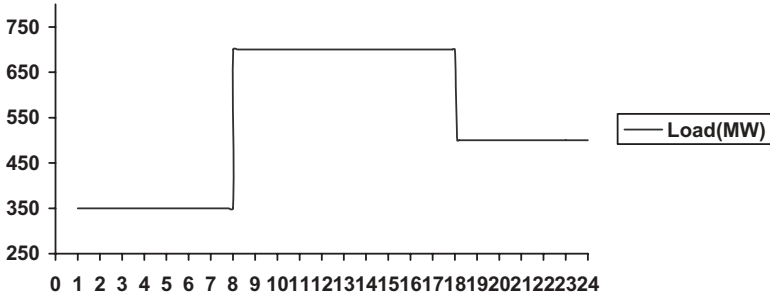
FIGURE 4.6   Daily load demands for Example 4.7

The power output limit of the thermal plant is

$$50 \le P_T \le 600 \text{ MW}$$

The power output limit of the hydro plant is

$$50 \le P_H \le 450 \text{ MW}$$

The problem is to determine the economic dispatch for this hydrothermal system.

According to the input-output characteristics of the thermal plant and the hydro plant and equation (4.78), we get the coordination equation as below:

$$0.0007 P_T + 0.4 = \gamma (0.003 P_H + 0.8)$$

From the load curve, we know that there are three time stages. The loads are the same within each time stage. Thus, for each time stage, we get the corresponding power balance equation:

$$P_{Hk} + P_{Tk} = P_{Dk} \quad k = 1, 2, 3$$

From the above two equations, we get

$$P_{Hk} = \frac{0.4 - 0.8\gamma + 0.0007 P_{Dk}}{0.003\gamma + 0.0007} \quad k = 1, 2, 3$$

$$P_{Tk} = \frac{-0.4 + 0.8\gamma + 0.003\gamma P_{Dk}}{0.003\gamma + 0.0007} \quad k = 1, 2, 3$$

Select the initial value of γ as 0.5. For the first time stage, the load level is 350 MW; we get

$$P_{H1} = \frac{0.4 - 0.8 \times 0.5 + 0.0007 \times 350}{0.003 \times 0.5 + 0.0007} = 111.36 \text{ MW}$$

$$P_{T1} = \frac{-0.4 + 0.8 \times 0.5 + 0.003 \times 0.5 \times 350}{0.003 \times 0.5 + 0.0007} = 238.64 \text{ MW}$$

For the second time stage, the load level is 700 MW; we get

$$P_{H2} = \frac{0.4 - 0.8 \times 0.5 + 0.0007 \times 700}{0.003 \times 0.5 + 0.0007} = 222.72 \text{ MW}$$

$$P_{T2} = \frac{-0.4 + 0.8 \times 0.5 + 0.003 \times 0.5 \times 700}{0.003 \times 0.5 + 0.0007} = 477.28 \text{ MW}$$

For the third time stage, the load level is 500 MW; we get

$$P_{H3} = \frac{0.4 - 0.8 \times 0.5 + 0.0007 \times 500}{0.003 \times 0.5 + 0.0007} = 159.09 \text{ MW}$$

$$P_{T3} = \frac{-0.4 + 0.8 \times 0.5 + 0.003 \times 0.5 \times 500}{0.003 \times 0.5 + 0.0007} = 340.91 \text{ MW}$$

According to the power output of the hydro plant and the input-output characteristic of the hydro plant, we can compute the daily water consumption:

$$\begin{aligned}
W_\Sigma =\ & (0.0015 \times 111.36^2 + 0.8 \times 111.36 + 2) \times 8 \times 3600 + \\
& (0.0015 \times 222.72^2 + 0.8 \times 222.72 + 2) \times 10 \times 3600 + \\
& (0.0015 \times 159.09^2 + 0.8 \times 159.09 + 2) \times 6 \times 3600 = 1.5936858 \times 10^7 \text{ m}^3
\end{aligned}$$

The water consumption is greater than the daily given amount. So increase the value of γ, say let γ = 0.52, and recompute the power output. For the first time stage, the load level is 350 MW; we get

$$P_{H1} = \frac{0.4 - 0.8 \times 0.52 + 0.0007 \times 350}{0.003 \times 0.52 + 0.0007} = 101.33 \text{ MW}$$

$$P_{T1} = \frac{-0.4 + 0.8 \times 0.52 + 0.003 \times 0.52 \times 350}{0.003 \times 0.52 + 0.0007} = 248.67 \text{ MW}$$

For the second time stage, the load level is 700 MW; we get

$$P_{H2} = \frac{0.4 - 0.8 \times 0.52 + 0.0007 \times 700}{0.003 \times 0.52 + 0.0007} = 209.73 \text{ MW}$$

Table 4.2   Iteration process of Example 4.7

Iteration	γ	P_{H1} (MW)	P_{H1} (MW)	P_{H1} (MW)	W_Σ (10^7 m^3)
1	0.5000	111.360	222.720	159.090	1.5936858
2	0.5200	101.330	209.730	147.790	1.4628090
3	0.5140	104.280	213.560	151.110	1.5009708
4	0.5145	104.207	213.463	151.031	1.5000051

$$P_{T2} = \frac{-0.4 + 0.8 \times 0.52 + 0.003 \times 0.52 \times 700}{0.003 \times 0.52 + 0.0007} = 490.27 \text{ MW}$$

For the third time stage, the load level is 500 MW; we get

$$P_{H3} = \frac{0.4 - 0.8 \times 0.52 + 0.0007 \times 500}{0.003 \times 0.52 + 0.0007} = 147.79 \text{ MW}$$

$$P_{T3} = \frac{-0.4 + 0.8 \times 0.52 + 0.003 \times 0.52 \times 500}{0.003 \times 0.52 + 0.0007} = 352.21 \text{ MW}$$

Then the daily water consumption can be computed as:

$$\begin{aligned} W_\Sigma = & \left(0.0015 \times 101.33^2 + 0.8 \times 101.33 + 2\right) \times 8 \times 3600 + \\ & \left(0.0015 \times 209.73^2 + 0.8 \times 209.73 + 2\right) \times 10 \times 3600 + \\ & \left(0.0015 \times 147.79^2 + 0.8 \times 147.79 + 2\right) \times 6 \times 3600 = 1.462809 \times 10^7 \text{ m}^3 \end{aligned}$$

The water consumption is less than the daily given amount. So reduce the value of γ and recompute the power output until the water consumption equals the daily given amount, or equation (4.82) is satisfied. The iteration process is listed in Table 4.2.

After the fourth iteration, the water consumption almost equals the daily given amount. Stop the calculation.

4.6.2   Consider Network Losses

Suppose there are m hydro plants and n thermal plants. The system load is given in the time period. The given water consumption of hydro plant j is $W_{\Sigma j}$. The hydrothermal system economic dispatch with network loss can be expressed as below:

$$\min F_\Sigma = \sum_{i=1}^{n} \int_0^T F_i[P_{Ti}(t)] \, dt \tag{4.83}$$

s.t.

$$\sum_{j=1}^{m} P_{\mathrm{H}j}(t) + \sum_{i=1}^{n} P_{\mathrm{T}i}(t) - P_{\mathrm{L}}(t) - P_{\mathrm{D}}(t) = 0 \tag{4.84}$$

$$\int_{0}^{\mathrm{T}} W_{j}[P_{\mathrm{H}j}(t)]\mathrm{d}t - W_{\Sigma j} = 0 \tag{4.85}$$

Similar to Section 4.6.1, we divide the operation period T into s time stages

$$T = \sum_{k=1}^{s} \Delta t_{k} \tag{4.86}$$

We get

$$F_{\Sigma} = \sum_{i=1}^{n} \sum_{k=1}^{s} F_{ik}(P_{\mathrm{T}ik}) \Delta t_{k} \tag{4.87}$$

$$\sum_{j=1}^{m} P_{\mathrm{H}jk} + \sum_{i=1}^{n} P_{\mathrm{T}ik} - P_{\mathrm{L}k} - P_{\mathrm{D}k} = 0 \quad k = 1, 2, \ldots, s \tag{4.88}$$

$$\sum_{k=1}^{s} W_{jk}(P_{\mathrm{H}jk}) \Delta t_{k} - W_{\Sigma j} = 0, \quad j = 1, 2, \ldots, m \tag{4.89}$$

The Lagrange function will be

$$L = \sum_{i=1}^{n} \sum_{k=1}^{s} F_{ik}(P_{\mathrm{T}ik}) \Delta t_{k} - \sum_{k=1}^{s} \lambda_{k} \left(\sum_{j=1}^{m} P_{\mathrm{H}jk} + \sum_{i=1}^{n} P_{\mathrm{T}ik} - P_{\mathrm{L}k} - P_{\mathrm{D}k} \right) \Delta t_{k} +$$
$$\sum_{j=1}^{m} \gamma_{j} \left(\sum_{k=1}^{s} W_{jk}(P_{\mathrm{H}jk}) \Delta t_{k} - W_{\Sigma j} \right) \tag{4.90}$$

The necessary conditions for the extreme value of the Lagrange function are

$$\frac{\partial L}{\partial P_{\mathrm{H}jk}} = \gamma_{j} \frac{\mathrm{d}W_{jk}}{\mathrm{d}P_{\mathrm{H}jk}} \Delta t_{k} - \lambda_{k} \left(1 - \frac{\partial P_{\mathrm{L}k}}{\partial P_{\mathrm{H}jk}} \right) \Delta t_{k} = 0 \quad j = 1, 2, \ldots, m; \quad k = 1, 2, \ldots, s \tag{4.91}$$

$$\frac{\partial L}{\partial P_{\mathrm{T}ik}} = \frac{\mathrm{d}F_{ik}}{\mathrm{d}P_{\mathrm{T}ik}} \Delta t_{k} - \lambda_{k} \left(1 - \frac{\partial P_{\mathrm{L}k}}{\partial P_{\mathrm{T}ik}} \right) \Delta t_{k} = 0 \quad i = 1, 2, \ldots, n; \quad k = 1, 2, \ldots, s \tag{4.92}$$

$$\frac{\partial L}{\partial \lambda_{k}} = -\left(\sum_{j=1}^{m} P_{\mathrm{H}jk} + \sum_{i=1}^{n} P_{\mathrm{T}ik} - P_{\mathrm{L}k} - P_{\mathrm{D}k} \right) \Delta t_{k} = 0 \quad k = 1, 2, \ldots, s \tag{4.93}$$

$$\frac{\partial L}{\partial \gamma_{j}} = \sum_{k=1}^{s} W_{jk} \Delta t_{k} - W_{j\Sigma} = 0 \quad j = 1, 2, \ldots, m \tag{4.94}$$

From equations (4.91) and (4.92), we get

$$\frac{\mathrm{d}F_{ik}}{\mathrm{d}P_{Tik}} \times \frac{1}{1 - \dfrac{\partial P_{Lk}}{\partial P_{Tik}}} = \gamma_j \frac{\mathrm{d}W_{jk}}{\mathrm{d}P_{Hjk}} \times \frac{1}{1 - \dfrac{\partial P_{Lk}}{\partial P_{Hjk}}} = \lambda_k \quad k = 1, 2, \ldots, s \qquad (4.95)$$

Equation (4.95) is true for any time stage, i.e.,

$$\frac{\mathrm{d}F_i}{\mathrm{d}P_{Ti}} \times \frac{1}{1 - \dfrac{\partial P_L}{\partial P_{Ti}}} = \gamma_j \frac{\mathrm{d}W_j}{\mathrm{d}P_{Hj}} \times \frac{1}{1 - \dfrac{\partial P_L}{\partial P_{Hj}}} = \lambda \qquad (4.96)$$

Equation (4.96) is the coordination equation of hydrothermal system economic dispatch considering network losses.

4.7   ECONOMIC DISPATCH BY GRADIENT METHOD

4.7.1   Introduction

We discussed the equal incremental principle for classical economic dispatch in the previous sections. Generally, the equal incremental principle is good only if the input-output characteristic of a generation unit is a quadratic function or the incremental input-output characteristic is a piecewise linear function [2]. But the input-output characteristic of the generating unit may be a cubic function, or more complex. For example,

$$F_{Gi} = A + BP_{Gi} + CP_{Gi}^2 + DP_{Gi}^3 + \cdots$$

Thus other methods are needed to get the optimum solution for the above function. We discuss the gradient method in this section.

4.7.2   Gradient Search in Economic Dispatch

The principle of the gradient method is that the minimum of a function, $f(x)$, can be found by a series of steps that always go to the downward direction. The gradient of the function $f(x)$ can be expressed as below:

$$\nabla f = \begin{bmatrix} \dfrac{\partial f}{\partial x_1} \\[2mm] \dfrac{\partial f}{\partial x_2} \\[1mm] \vdots \\[1mm] \dfrac{\partial f}{\partial x_n} \end{bmatrix} \qquad (4.97)$$

The gradient ∇f always points to the direction of maximum ascent. If we want to move in the direction of maximum descent, we negate the gradient. Thus the direction of steepest descent for minimizing a function can be found by use of the direction of the negative gradient. Given any starting point x^0, the new point x^1 should be obtained as below:

$$x^1 = x^0 - \varepsilon \nabla f \qquad (4.98)$$

where ε is a scale that is used to process the convergence of the gradient method.

Applying the gradient method to economic dispatch, the objective function will be

$$\min F = \sum_{i=1}^{N} f_i(P_{Gi}) \qquad (4.99)$$

The constraint is the real power balance equation, i.e.,

$$\sum_{i=1}^{N} P_{Gi} = P_D \qquad (4.100)$$

As mentioned before, to solve this classic economic dispatch problem, the Lagrange function should be constructed first, i.e.,

$$L = F + \lambda \left(P_D - \sum_{i=1}^{N} P_{Gi} \right) = \sum_{i=1}^{N} f_i(P_{Gi}) + \lambda \left(P_D - \sum_{i=1}^{N} P_{Gi} \right) \qquad (4.101)$$

The gradient of the Lagrange function is

$$\nabla L = \begin{bmatrix} \dfrac{\partial L}{\partial P_{G1}} \\[2mm] \dfrac{\partial L}{\partial P_{G2}} \\[2mm] \vdots \\[2mm] \dfrac{\partial L}{\partial P_{GN}} \\[2mm] \dfrac{\partial L}{\partial \lambda} \end{bmatrix} = \begin{bmatrix} \dfrac{df_1(P_{G1})}{dP_{G1}} - \lambda \\[2mm] \dfrac{df_2(P_{G2})}{dP_{G2}} - \lambda \\[2mm] \vdots \\[2mm] \dfrac{df_N(P_{GN})}{dP_{GN}} - \lambda \\[2mm] P_D - \sum_{i=1}^{N} P_{Gi} \end{bmatrix} \qquad (4.102)$$

To use the gradient ∇L to solve the economic dispatch problem, the starting values P_{G1}^0, P_{G2}^0, ..., P_{GN}^0, and λ^0 should be given. Then the new values will be computed by the following equation:

$$x^1 = x^0 - \varepsilon \nabla L \qquad (4.103)$$

where the vectors x^1, x^0 are

$$x^0 = \begin{bmatrix} P_{G1}^0 \\ P_{G2}^0 \\ \vdots \\ P_{GN}^0 \\ \lambda^0 \end{bmatrix} \qquad (4.104)$$

$$x^1 = \begin{bmatrix} P_{G1}^1 \\ P_{G2}^1 \\ \vdots \\ P_{GN}^1 \\ \lambda^1 \end{bmatrix} \qquad (4.105)$$

The more general expression of the gradient search is as below:

$$x^n = x^{n-1} - \varepsilon \nabla L \qquad (4.106)$$

where n is the iteration number.

The calculation steps for applying the gradient method to classic economic dispatch are summarized as below.

Step (1): Select the starting values P_{G1}^0, P_{G2}^0, ..., P_{GN}^0, where

$$P_{G1}^0 + P_{G2}^0 +, \dots, + P_{GN}^0 = P_D$$

Step (2): Compute the initial λ_i^0 for each generator.

$$\lambda_i^0 = \frac{df_i(P_{Gi})}{\partial P_{Gi}} \bigg|_{P_{Gi}^0}, \quad i = 1, \dots, N$$

Step (3): Compute the initial average incremental cost λ^0

$$\lambda^0 = \frac{1}{N} \sum_{i=1}^{N} \lambda_i^0$$

Step (4): Compute the gradient as below:

$$\nabla L^1 = \begin{bmatrix} \dfrac{df_1(P_{G1}^0)}{dP_{G1}} - \lambda^0 \\[2mm] \dfrac{df_2(P_{G2}^0)}{dP_{G2}} - \lambda^0 \\[2mm] \vdots \\[2mm] \dfrac{df_N(P_{GN}^0)}{dP_{GN}} - \lambda^0 \\[2mm] P_D - \displaystyle\sum_{i=1}^{N} P_{Gi}^0 \end{bmatrix}$$

Step (5): If $\nabla L = 0$, the solution converges. Stop the iteration. Otherwise, go to the next step.

Step (6): Select a scale ε for handling the convergence.

Step (7): Compute the new values $P_{G1}^1, P_{G2}^1, \ldots, P_{GN}^1, \lambda^1$ according to equation (4.106).

Step (8): Substitute the new values into equation (4.102) in Step 4, and recompute the gradient.

Example 4.8

For the same data as in Example 4.4, solve for the economic dispatch with a total load of 500 MW. The solution procedures are below.

Select the starting values $P_{G1}^0 = 300$, $P_{G2}^0 = 150$, $P_{GN}^0 = 250$, and

$$P_{G1}^0 + P_{G2}^0 + P_{GN}^0 = 500$$

Compute the initial λ_i^0 for each generator:

$$\lambda_1^0 = \frac{df_1(P_{G1}^0)}{dP_{G1}} = 0.0012 \times 150 + 0.5 = 0.68$$

$$\lambda_2^0 = \frac{df_2(P_{G2}^0)}{dP_{G2}} = 0.001 \times 100 + 0.6 = 0.70$$

$$\lambda_3^0 = \frac{df_3(P_{G3}^0)}{dP_{G3}} = 0.0014 \times 250 + 0.4 = 0.75$$

Compute the initial average incremental cost λ^0:

$$\lambda^0 = \frac{1}{3}\sum_{i=1}^{3}\lambda_i^0 = \frac{1}{3}(0.68 + 0.7 + 0.75) = 0.71$$

Compute the gradient as below:

$$\nabla L^1 = \begin{bmatrix} 0.68 - 0.71 \\ 0.70 - 0.71 \\ 0.75 - 0.71 \\ 500 - (150 + 100 + 250) \end{bmatrix} = \begin{bmatrix} -0.03 \\ -0.01 \\ 0.04 \\ 0.00 \end{bmatrix}$$

Select a scale $\varepsilon = 300$ for handling the convergence, and compute the new values $P_{G1}^1, P_{G2}^1, \ldots, P_{GN}^1, \lambda^1$ according to equation (4.106).

$$\begin{bmatrix} P_{G1}^1 \\ P_{G2}^1 \\ P_{G3}^1 \\ \lambda^1 \end{bmatrix} = \begin{bmatrix} 150 \\ 100 \\ 250 \\ 0.71 \end{bmatrix} - 300 \begin{bmatrix} -0.03 \\ -0.01 \\ 0.04 \\ 0.0 \end{bmatrix} = \begin{bmatrix} 159 \\ 103 \\ 238 \\ 0.71 \end{bmatrix}$$

Then compute the new gradient as below:

$$\nabla L^2 = \begin{bmatrix} (0.0012 \times 159 + 0.5) - 0.71 \\ (0.0010 \times 103 + 0.6) - 0.71 \\ (0.0014 \times 238 + 0.4) - 0.71 \\ 500 - (159 + 103 + 238) \end{bmatrix} = \begin{bmatrix} -0.0192 \\ -0.0070 \\ 0.0232 \\ 0.00 \end{bmatrix}$$

$$\begin{bmatrix} P_{G1}^2 \\ P_{G2}^2 \\ P_{G3}^2 \\ \lambda^2 \end{bmatrix} = \begin{bmatrix} 159 \\ 103 \\ 238 \\ 0.71 \end{bmatrix} - 300 \begin{bmatrix} -0.0192 \\ -0.0070 \\ 0.0232 \\ 0.0 \end{bmatrix} = \begin{bmatrix} 164.76 \\ 105.10 \\ 231.04 \\ 0.71 \end{bmatrix}$$

Once again compute the new gradient.

$$\nabla L^3 = \begin{bmatrix} (0.0012 \times 164.76 + 0.5) - 0.71 \\ (0.0010 \times 105.10 + 0.6) - 0.71 \\ (0.0014 \times 231.04 + 0.4) - 0.71 \\ 500 - (164.76 + 105.1 + 231.04) \end{bmatrix} = \begin{bmatrix} -0.0123 \\ -0.0049 \\ 0.01346 \\ -0.900 \end{bmatrix}$$

The gradient $\nabla L^3 \neq 0$, so compute new solution.

$$\begin{bmatrix} P_{G1}^3 \\ P_{G2}^3 \\ P_{G3}^3 \\ \lambda^3 \end{bmatrix} = \begin{bmatrix} 164.76 \\ 105.10 \\ 231.04 \\ 0.71 \end{bmatrix} - 300 \begin{bmatrix} -0.0123 \\ -0.0049 \\ 0.01346 \\ -0.900 \end{bmatrix} = \begin{bmatrix} 168.45 \\ 107.80 \\ 227.00 \\ 270.71 \end{bmatrix}$$

The iterations have led to no solution since the element λ in the gradient had huge jump and cannot be converged. To solve this problem, we present three methods as below.

4.7.2.1   Gradient Method 1   In the calculation of the gradient, the element λ will be removed from the gradient, that is,

$$
\nabla L = \begin{bmatrix} \dfrac{\partial L}{\partial P_{G1}} \\[1.2em] \dfrac{\partial L}{\partial P_{G2}} \\[1em] \vdots \\[1em] \dfrac{\partial L}{\partial P_{GN}} \end{bmatrix} = \begin{bmatrix} \dfrac{\mathrm{d}f_1(P_{G1})}{\mathrm{d}P_{G1}} - \lambda \\[1.2em] \dfrac{\mathrm{d}f_2(P_{G2})}{\mathrm{d}P_{G2}} - \lambda \\[1em] \vdots \\[1em] \dfrac{\mathrm{d}f_N(P_{GN})}{\mathrm{d}P_{GN}} - \lambda \end{bmatrix}
\tag{4.107}
$$

We always set the value of λ equal to the average of the incremental cost of the generators at the iterated generation values, that is,

$$
\lambda^k = \frac{1}{N} \sum_{i=1}^{N} \left[\frac{\mathrm{d}f_i(P_{Gi}^k)}{\mathrm{d}P_{Gi}} \right]
\tag{4.108}
$$

Example 4.9

Reworking example 4.8 using gradient method 1, the results are shown in Table 4.3.

This solution is much more stable and is converging to the optimum solution. However, gradient method 1 cannot guarantee that the total outputs of the generators meet the total load demand.

4.7.2.2   Gradient Method 2   This method is modified from method 1, but we need to check the power balance equation each time when we finish the iteration of gradient calculation. The method is as follows.

Table 4.3   Gradient method 1 results ($\varepsilon = 300$)

Iteration	P_{G1}	P_{G2}	P_{G3}	λ
0	150	100	250	0.71
1	159	103	238	0.709
2	164.46	104.8	230.74	0.708396
3	169.7388	105.5388	226.348	0.7086
4	171.21	106.4688	223.888	0.7085
5	172.11	107.0688	222.418	0.7083
6	172.65	107.4288	221.518	0.7082

If $\sum_{i=1}^{N}(P_{Gi}^{k}) > P_D$, select the unit with the maximal incremental generation cost to pick up the power difference:

$$P_{GS}^{k}{}'\Big|_{\lambda_{max}} = P_{GS}^{k} - \left(\sum_{i=1}^{N}(P_{Gi}^{k}) - P_D\right) \qquad (4.109)$$

If $\sum_{i=1}^{N}(P_{Gi}^{k}) < P_D$, select the unit with the minimal incremental generation cost to pick up the power difference:

$$P_{GS}^{k}{}'\Big|_{\lambda_{max}} = P_{GS}^{k} + \left(P_D - \sum_{i=1}^{N}(P_{Gi}^{k})\right) \qquad (4.110)$$

Then recompute the average incremental generation cost, and conduct a new iteration.

Example 4.10

Reworking Example 4.9 using gradient method 2, the results are shown in Table 4.4.

This solution is much more stable and is converging to the optimum solution. Obviously, gradient method 2 can guarantee that the total outputs of generators meet the total load.

4.7.2.3 Gradient Method 3   This method is similar to method 2 but with some simplification. One fixed unit is selected as the slack machine. For example, selecting the last unit as the slack generator, we get

$$P_{GN} = P_D - \sum_{i=1}^{N-1}(P_{Gi}) \qquad (4.111)$$

Table 4.4   Gradient method 2 results ($\varepsilon = 300$)

Iteration	P_{G1}	P_{G2}	P_{G3}	P_{total}	λ
0	150	100	250	500	0.71
1	159	103	238	500	0.709
2	164.46	104.8	230.74	500	0.708396
3	169.7388	105.5388	224.7224*	500	0.70793
4	171.0108*	106.2678	222.7214	500	0.7078

*The corresponding unit is selected to balance the total generations and total load.

The objective function becomes

$$F = f_1(P_{G1}) + f_2(P_{G2}) +, \ldots, f_N(P_{GN})$$

$$= f_1(P_{G1}) + f_2(P_{G2}) +, \ldots, f_N\left(P_D - \sum_{i=1}^{N-1}(P_{Gi})\right) \qquad (4.112)$$

The gradient will become

$$\nabla F = \begin{bmatrix} \dfrac{dF}{dP_{G1}} \\ \dfrac{dF}{dP_{G2}} \\ \vdots \\ \dfrac{dF}{dP_{G(N-1)}} \end{bmatrix} = \begin{bmatrix} \dfrac{df_1(P_{G1})}{dP_{G1}} - \dfrac{df_N(P_{GN})}{dP_{GN}} \\ \dfrac{df_2(P_{G2})}{dP_{G2}} - \dfrac{df_N(P_{GN})}{dP_{GN}} \\ \vdots \\ \dfrac{df_{(N-1)}(P_{G(N-1)})}{dP_{G(N-1)}} - \dfrac{df_N(P_{GN})}{dP_{GN}} \end{bmatrix} \qquad (4.113)$$

The gradient iteration will be the same as before:

$$x^n = x^{n-1} - \varepsilon \nabla F \qquad (4.114)$$

and

$$x = \begin{bmatrix} P_{G1} \\ P_{G2} \\ \vdots \\ P_{G(N-1)} \end{bmatrix} \qquad (4.115)$$

Example 4.11

Reworking Example 4.8 using gradient method 3, the results are shown in Table 4.5.

This solution is also stable and is converging to the optimum solution, which is similar to method 2. Obviously, gradient method 3 can also guarantee that the total outputs of generators meet the total load.

Table 4.5   Gradient method 5 results ($\varepsilon = 300$)

Iteration	P_{G1}	P_{G2}	P_{G3}	P_{total}
0	150	100	250	500
1	171	115	214	500
2	169.32	110.38	220.3	500
3	170.8908	109.792	219.3172	500
4	171.4728	108.937	219.59	500

4.8   CLASSIC ECONOMIC DISPATCH BY GENETIC ALGORITHM

4.8.1   Introduction

Another type of method that is used to solve the classic economic dispatch problem is Genetic Algorithm (GA) [3–5]. The theoretical foundation for GA was first described by Holland and was extended by Goldberg. GA provides a solution to a problem by working with a population of individuals each representing a possible solution. Each possible solution is termed a "chromosome." New points of the search space are generated through GA operations, known as reproduction, crossover, and mutation. These operations consistently produce fitter offspring through successive generations, which rapidly lead the search toward global optima. The features of GA are different from other search techniques in the following aspects:

(1) The algorithm is a multipath that searches many peaks in parallel, hence reducing the possibility of local minimum trapping.
(2) GA works with a bit string encoding instead of the real parameters. The coding of parameter will help the genetic operator to evolve the current state into the next state with minimum computations.
(3) GA evaluates the fitness of each string to guide its search instead of the optimization function. The genetic algorithm only needs to evaluate objective function (fitness) to guide its search. There is no requirement for the operation of derivatives.
(4) GA explores the search space where the probability of finding improved performance is high.

The main operators of GA used are:

- **Crossover operator** is applied with a certain probability. The parent generations are combined (exchange bits) to form two new generations that inherit solution characteristics from both parents. Crossover, although being the primary search operator, cannot produce information that does not already exist within the population.
- **Mutation operator** is also applied with a small probability. Randomly chosen bits of the offspring genotype flip from 0 to 1 and vice versa to give characteristics that do not exist in the parent population. Generally, mutation is considered as a secondary but not useless operator that gives a nonzero probability to every solution to be considered and evaluated.
- **Elitism** is implemented so that the best solution of every generation is copied to the next so that the possibility of its destruction through a genetic operator is eliminated.
- **Fitness scaling** is referred to a nonlinear transformation of genotype fitness in order to emphasize small differences between near-optimal qualities in a converged population.

The GA-type algorithms are actually unconstrained optimization; all information must be expressed in a fitness function. As mentioned at the beginning of this chapter, the classic economic dispatch problem neglects the network losses and network constraints. Thus the fitness function for classic ED can be easily formed.

4.8.2 GA-Based ED Solution

According to Section 4.3, the classic economic dispatch problem can be stated as below:

$$\min F = \sum_{i=1}^{N} F_i(P_{Gi}) \tag{4.116}$$

s.t.

$$\sum_{i=1}^{N} P_{Gi} = P_D \tag{4.117}$$

In the application of GA to economic dispatch, the outputs of the $N - 1$ "free generators" can be chosen arbitrarily within limits while the output of the "reference generator" (or slack bus generator) is constrained by the power balance. It is assumed that the Nth generator is the reference generator. GAs do not work on the real generator outputs themselves, but on bit string encoding of them. The output of the free generators is encoded in string, for example, an 8-bit string (an unsigned 8-bit integer) that gives a resolution of 2^8 discrete power values in the range (P_{Gmin}, P_{Gmax}). These $(N-1)$ strings are concatenated to form a consolidated solution bit string of $8*(N-1)$ bits called the genotype. A population of m genotypes must be initially generated at random. Each genotype is decoded to a power output vector. The output of the reference unit is

$$P_{GN} = P_D - \sum_{i=1}^{N-1} P_{Gi} \tag{4.118}$$

Adding penalty factors h_1, h_2 to the violation of power output of the slack bus unit, we can combine equations (4.117) and (4.118) as below:

$$F_A = \sum_{i=1}^{N} F_i(P_{Gi}) + h_1(P_{GN} - P_{GN\max})^2 + h_2(P_{GN\min} - P_{GN})^2 \tag{4.119}$$

where $P_{GN\min}$, $P_{GN\max}$ are the lower and upper limits of the power output of the slack bus unit, respectively. The value of the penalty factors should be large so that there is no violation for unit output at the final solution.

Since GA is designed for the solution of maximization problems, the GA fitness function is defined as the inverse of equation (4.119).

$$F_{\text{fitness}} = \frac{1}{F_A} \tag{4.120a}$$

In the economic dispatch problem, the problem variables correspond to the power generations of the units. Each string represents a possible solution and is made of substrings, each corresponding to a generating unit. The length of each substring is decided based on the maximum/minimum limits on the power generation of the corresponding unit and the solution accuracy desired. The string length, which depends on the length of each substring, is chosen based on a trade-off between solution accuracy and solution time. Longer strings may provide better accuracy but result in more solution time. Thus the step size of the unit can be computed as follows:

$$\varepsilon_i = \frac{P_{Gi\max} - P_{Gi\min}}{2^n - 1} \tag{4.120b}$$

where n is the length of the substring in binary codes corresponding to a unit.

For example, there are six units in a system, and the sixth unit is selected as the slack bus unit. The power output limits of the five free units are.

$$20 \le P_{G1} \le 100 \, (\text{MW})$$

$$10 \le P_{G2} \le 100 \, (\text{MW})$$

$$50 \le P_{G3} \le 200 \, (\text{MW})$$

$$20 \le P_{G4} \le 120 \, (\text{MW})$$

$$50 \le P_{G5} \le 250 \, (\text{MW})$$

If the length of the substring in binary codes is selected as 4, the step size of each unit will be

$$\varepsilon_1 = \frac{P_{G1\max} - P_{G1\min}}{2^4 - 1} = \frac{100 - 20}{15} = 5.33 \, \text{MW}$$

$$\varepsilon_2 = \frac{P_{G2\max} - P_{G2\min}}{2^4 - 1} = \frac{100 - 10}{15} = 6.00 \, \text{MW}$$

$$\varepsilon_3 = \frac{P_{G3\max} - P_{G3\min}}{2^4 - 1} = \frac{200 - 50}{15} = 10.00 \, \text{MW}$$

$$\varepsilon_4 = \frac{P_{G4\max} - P_{G4\min}}{2^4 - 1} = \frac{120 - 20}{15} = 6.67 \, \text{MW}$$

$$\varepsilon_5 = \frac{P_{G5\max} - P_{G5\min}}{2^4 - 1} = \frac{250 - 50}{15} = 13.33 \, \text{MW}$$

If the length of the substring in binary codes is selected as 5, the step size of each unit will be

$$\varepsilon_1 = \frac{P_{G1max} - P_{G1min}}{2^5 - 1} = \frac{100 - 20}{31} = 2.58 \text{ MW}$$

$$\varepsilon_2 = \frac{P_{G2max} - P_{G2min}}{2^5 - 1} = \frac{100 - 10}{31} = 2.90 \text{ MW}$$

$$\varepsilon_3 = \frac{P_{G3max} - P_{G3min}}{2^5 - 1} = \frac{200 - 50}{31} = 4.84 \text{ MW}$$

$$\varepsilon_4 = \frac{P_{G4max} - P_{G4min}}{2^5 - 1} = \frac{120 - 20}{31} = 3.23 \text{ MW}$$

$$\varepsilon_5 = \frac{P_{G5max} - P_{G5min}}{2^5 - 1} = \frac{250 - 50}{31} = 6.45 \text{ MW}$$

It can be observed that the long string has a smaller step size, which verifies that the length of the substring in binary codes has an effect on the solution accuracy and solution speed.

In standard GAs, all the strings in the population are reformed during a generation. Parents are crossed on the basis of their performance in comparison to the average fitness of the population, and mutation is allowed to occur on the offspring. The selective pressure is provided by the fitness measure; the differential need not be great to achieve good results. Both selective pressure and initial population sizes may be tuned to match the problem space. The type of crossover and rate of mutation need to be selected based on the problem type. For a large-scale power system, there are many generators. If the standard GA is used to economic dispatch, it appears to increase performance. Little improvement on GA operator is needed; that is, we do not replace the entire population with each generation. Instead, it probabilistically chooses two parents to reform into two offspring. Recombination and mutation occur, and then one of the offspring is discarded randomly. The remaining offspring is placed in the population according to its fitness in relation to the rest of the strings. The lowest-valued string is discarded. This keeps high-valued strings within the population, directly accumulating high-performance hyperplanes. It also bases the reproductive opportunity on rank within the population, not on a string's fitness value in comparison with the average of the population, reducing the impact of selective pressure fluctuation. It also reduces the importance of choosing a proper evaluation function for fitness in that the difference in the fitness function between two adjacent strings is irrelevant.

To use GA programming to solve classic economic dispatch, the following parameters are needed for data input.

· Number of chromosomes (that comprise a generation)
· Bit resolution per generator

- Number of cross-points
- Number of generations
- Initial crossover probability (%)
- Initial mutation probability (%)
- Minimal power output of each unit
- Maximal power output of each unit
- Status of the unit
- Coefficient of unit cost function
- Total load demand

Example 4.12

For example 4.6, using genetic algorithm to distribute the 500-MW load to three units. The GA parameters are selected as follows

- Number of chromosomes = 100
- Bit resolution per generator = 8
- Number of cross-points = 2
- Number of generations = 9000
- Initial crossover probability = 92%
- Initial mutation probability = 0.1%

The total load is 500 MW; the output results are as below:

$$P_{G1} = 172.897 \text{ MW}$$

$$P_{G2} = 107.477 \text{ MW}$$

$$P_{G3} = 219.626 \text{ MW}$$

4.9 CLASSIC ECONOMIC DISPATCH BY HOPFIELD NEURAL NETWORK

Since Hopfield introduced the neural network in the early 1980s [6], the Hopfield neural networks (HNNs) have been used in many different applications. This section presents the application of HNN to the classic economic dispatch problem [7–10].

4.9.1 Hopfield Neural Network Model

Let u_i be the ith input of the neuron and V_i its output. Suppose there are N neurons that are connected together; the nonlinear differential equations of HNN are described as below:

$$\begin{cases} C_i \dfrac{du_i}{dt} = \sum_{j=1}^{N} T_{ij} V_j + \dfrac{u_i}{R_i} + I_i \\ V_i = g(u_i) \quad i = 1, 2, \dots, N \end{cases} \tag{4.121}$$

where

$$\frac{1}{R_i} = \theta_i + \sum_{j=1}^{N} T_{ij} \tag{4.122}$$

$$V_i = g(u_i)$$

are the nonlinear characteristic of the neuron.

For a very high gain parameter λ of the neuron, the output equation can be defined as

$$V_i = g(\lambda u_i) = g\left(\frac{u_i}{u_0}\right) = \frac{1}{1 + \exp\left(-\dfrac{u_i + \theta_i}{u_0}\right)} \tag{4.123}$$

where θ_i is threshold bias.

The energy function of the system (4.121) is defined as

$$E = -\frac{1}{2} \sum_{i=1}^{N} \sum_{j=1}^{N} T_{ij} V_i V_j - \sum_{i=1}^{N} V_i I_i + \sum_{i=1}^{N} \frac{1}{R_i} \int_{0}^{V_i} g^{-1}(V) \, dV \tag{4.124}$$

From equation (4.124), we get

$$\frac{dE}{dt} = \sum_{i} \frac{\partial E}{\partial V_i} \frac{dV_i}{dt} \tag{4.125}$$

where

$$\begin{aligned} \frac{\partial E}{\partial V_i} &= -\frac{1}{2} \sum_{j} T_{ij} V_j - \frac{1}{2} \sum_{j} T_{ji} V_j + \frac{u_i}{R_i} - I_i \\ &= -\frac{1}{2} \sum_{j} (T_{ji} - T_{ij}) V_j - \left(\sum_{j} T_{ij} V_j - \frac{u_i}{R_i} + I_i \right) \\ &= -\frac{1}{2} \sum_{j} (T_{ji} - T_{ij}) V_j - C_i \frac{du_i}{dt} \\ &= -\frac{1}{2} \sum_{j} (T_{ji} - T_{ij}) V_j - C_i \left[g^{-1}(V_i) \right]' \frac{dV_i}{dt} \end{aligned} \tag{4.126}$$

Substituting equation (4.126) into equation (4.125), we get

$$\frac{\mathrm{d}E}{\mathrm{d}t} = -\frac{1}{2}\sum_j (T_{ji} - T_{ij})V_j \frac{\mathrm{d}V_i}{\mathrm{d}t} - C_i[g^{-1}(V_i)]'\left(\frac{\mathrm{d}V_i}{\mathrm{d}t}\right)^2 \qquad (4.127)$$

Since the weight parameter matrix T in equation (4.121) is symmetric, we have

$$T_{ji} = T_{ij} \qquad (4.128)$$

Substituting equation (4.128) into equation (4.127), we get

$$\frac{\mathrm{d}E}{\mathrm{d}t} = -C_i[g^{-1}(V_i)]'\left(\frac{\mathrm{d}V_i}{\mathrm{d}t}\right)^2 \qquad (4.129)$$

Since g^{-1} is a monotone increasing function, and $C_i > 0$, thus

$$\frac{\mathrm{d}E}{\mathrm{d}t} = -C_i[g^{-1}(V_i)]'\left(\frac{\mathrm{d}V_i}{\mathrm{d}t}\right)^2 \leq 0 \qquad (4.130)$$

This shows that the time evolution of the system is a motion in state space that seeks out minima in E and comes to a stop at such points.

4.9.2   Mapping of Economic Dispatch to HNN

As discussed above, the classic economic dispatch problem without line security can be written as:

$$\min F = F_1(P_{G1}) + F_2(P_{G2}) + \cdots + F_n(P_{Gn}) = \sum_{i=1}^N F_i(P_{Gi}) \qquad (4.131)$$

s.t.

$$\sum_{i=1}^N P_{Gi} = P_D + P_L \qquad (4.132)$$

$$P_{Gi\,min} \leq P_{Gi} \leq P_{Gi\,max} \qquad (4.133)$$

assuming that the generator cost function is a quadratic function, that is,

$$F_i(P_{Gi}) = a_i P_{Gi}^2 + b_i P_{Gi} + c_i \qquad (4.134)$$

and the network loss can be represented by the B-coefficient

$$P_L = \sum_{i=1}^N \sum_{j=1}^N P_{Gi} B_{ij} P_{Gj} \qquad (4.135)$$

To apply HNN to solve the above classic economic dispatch problem, the following energy function is defined by augmenting the objective function (4.131) with the constraint (4.132):

$$E = \frac{1}{2} A \left(P_D + P_L - \sum_i P_{Gi} \right)^2 + \frac{1}{2} B \sum_i (a_i P_{Gi}^2 + b_i P_{Gi} + c_i) \qquad (4.136)$$

By comparing equation (4.136) with equation (4.124), whose threshold is assumed to be zero, the weight parameters and external input of neuron I in the network [7] are given by

$$T_{ii} = -A - Bc_i \qquad (4.137)$$

$$T_{ij} = -A \qquad (4.138)$$

$$I_i = A(P_D + P_L) - \frac{Bb_i}{2} \qquad (4.139)$$

where the diagonal weights are nonzero.

The sigmoid function (4.123) can be modified to meet the power limit constraint as follows [7]:

$$V_i(k+1) = (P_{i\max} - P_{i\min}) \frac{1}{1 + \exp\left(-\dfrac{u_i(k) + \theta_i}{u_0}\right)} + P_{i\min} \qquad (4.140)$$

To speed up convergence of the ED problem solved by HNN, two adjustment methods can be used [9].

4.9.2.1 Slope Adjustment Method

Since energy is to be minimized and its convergence depends on the gain parameter u_0, the gradient descent method can be applied to adjust the gain parameters.

$$u_0(k+1) = u_0(k) - \eta_s \frac{\partial E}{\partial u_0} \qquad (4.141)$$

where η_s is a learning rate.

From equations (4.136) and (4.140), the gradient of energy with respect to the gain parameter can be computed as

$$\frac{\partial E}{\partial u_0} = \sum_i \frac{\partial E}{\partial P_i} \frac{\partial P_i}{\partial u_0} \qquad (4.142)$$

The update rule of equation (4.141) needs a suitable choice of the learning rate η_s. For a small value of η_s, convergence is guaranteed but the speed is too

slow. On the other hand, if the learning rate is too big, the algorithm becomes unstable. The suggested learning rate will be

$$0 < \eta_s < \frac{2}{g_{s,max}^2} \tag{4.143}$$

where

$$g_{s,max} = \max \|g_s(k)\|$$
$$g_s(k) = \frac{\partial E(k)}{\partial u_0} \tag{4.144}$$

Moreover, the optimal convergence is corresponding to

$$\eta_s^* = \frac{1}{g_{s,max}^2} \tag{4.145}$$

4.9.2.2   *Bias Adjustment Method*   There is a limitation in the slope adjust-ment method, in which the slopes are small near the saturation region of the sigmoid function. If every input can use the same maximum possible slope, convergence will be much faster. This can be achieved by changing the bias to shift the input near the center of the sigmoid function, that is,

$$\theta_i(k+1) = \theta_i(k) - \eta_b \frac{\partial E}{\partial \theta_i} \tag{4.146}$$

where η_b is a learning rate.

The bias can be applied to every neuron as in equation (4.123). Thus, from equations (4.136) and (4.140), the derivate of energy with respect to a bias can be computed as

$$\frac{\partial E}{\partial \theta_i} = \frac{\partial E}{\partial P_i} \frac{\partial P_i}{\partial \theta_i} \tag{4.147}$$

The suggested learning rate will be

$$0 < \eta_b < -\frac{2}{g_b(k)} \tag{4.148}$$

where

$$g_b(k) = \sum_i \sum_j T_{ij} \frac{\partial V_i}{\partial \theta} \frac{\partial V_j}{\partial \theta} \tag{4.149}$$

Moreover, the optimal convergence is corresponding to

$$\eta_b = -\frac{1}{g_b(k)} \tag{4.150}$$

4.9.3 Simulation Results

The test example and results of applying HNN to ED are taken from reference [9]. The system data are shown in Table 4.6. Each generator has three types of fuels. There are four values of load demand, that is, 2400, 2500, 2600, and 2700 MW.

Table 4.6 Cost coefficients for piecewise quadratic cost function

Unit	Min	Generation P1 F1	P2 F2	Max F3	F	c	b	a
1	100	196	250	250	1	.2697e2	−.3975e0	.2176e-2
		1	2	2	2	.2113e2	−.3059e0	.1861e-2
					2	.2113e2	−.3059e0	.1861e-2
2	50	114	157	230	1	.1184e3	−.1269e1	.4194e-2
		2	3	1	2	.1865e1	−.3988e-1	.1138e-2
					3	.1365e2	−.1980e-1	.1620e-2
3	200	332	388	500	1	.3979e2	−.3116e0	.1457e-2
		1	2	3	2	−.5914e2	.4864e0	.1176e-4
					3	−.2876e1	.3389e-1	.8035e-3
4	99	138	200	265	1	.1983e1	−.3114e-1	.1049e-2
		1	2	3	2	.5285e2	−.6348e0	.2758e-2
					3	.2668e3	−.2338e1	.5935e-2
5	190	338	407	490	1	.1392e2	−.8733e-1	.1066e-2
		1	2	3	2	.9976e2	−.5206e0	.1597e-2
					3	.5399e2	.4462e0	.1498e-3
6	85	138	200	265	1	.5285e2	−.6348e0	.2758e-2
		2	1	3	2	.1983e1	−.3114e-1	.1049e-2
					3	.2668e3	−.2338e1	.5935e-2
7	200	331	391	500	1	.1893e2	−.1325e0	.1107e-2
		1	2	3	2	.4377e2	−.2267e0	.1165e-2
					3	−.4335e2	.3559e0	.2454e-3
8	99	138	200	265	1	.1983e1	−.3114e-1	.1049e-2
		1	2	3	2	.5285e2	−.6348e0	.2758e-2
					3	.2668e3	−.2338e1	.5935e-2
9	130	213	370	440	1	.8853e2	−.5675e0	.1554e-2
		3	1	2	2	.1530e2	−.4514e-1	.7033e-2
					3	.1423e2	−.1817e-1	.6121e-3
10	200	362	407	490	1	.1397e2	−.9938e-1	.1102e-2
		1	3	2	2	−.6113e2	.5084e0	.4164e-4
					3	.4671e2	−.2024e0	.1137e-2

Table 4.7   Results for slope adjustment method with fixed learning rate, 1.0 (A) and adaptive learning rate (B)

Unit	2400 MW A	2400 MW B	2500 MW A	2500 MW B	2600 MW A	2600 MW B	2700 MW A	2700 MW B
1	196.8	189.9	205.6	205.1	215.7	214.5	223.2	224.6
2	202.7	202.9	206.7	206.5	211.1	211.4	216.1	215.7
3	251.2	252.1	265.3	266.4	278.9	278.8	292.5	291.9
4	232.5	232.9	236.0	235.8	239.2	239.3	242.6	242.6
5	240.4	241.7	257.9	256.8	276.1	276.1	294.1	293.6
6	232.5	232.9	236.0	235.9	239.2	239.1	242.4	242.5
7	252.5	253.4	269.5	269.3	286.0	286.7	303.5	303.0
8	232.5	232.9	236.0	235.8	239.2	239.3	242.7	242.6
9	320.2	321.0	331.8	334.0	343.4	343.6	355.8	355.7
10	238.9	240.4	255.5	254.4	271.2	271.2	287.3	287.8
Total P	2400.0	2400.0	2500.0	2500.0	2600.0	2600.0	2700.0	2700.0
Cost	481.83	481.71	526.23	526.23	574.36	574.37	626.27	626.24
Iters	99,992	84,791	80,156	86,081	72,993	79,495	99,948	99,811
u_0	95.0	110.0	120.0	100.0	130.0	120.0	160.0	120.0
n	1.5	1.0E-04	1.0	1.0E-04	1.0	1.0E-04	1.0	1.0E-04

The ED results based on the slope adjustment method are shown in Table 4.7. Compared with the conventional Hopfield network, the number of iterations is reduced to about one-half, and oscillation is drastically reduced from about 40,000 to less than 100 iterations. In addition, the degree of freedom of the system increases from 1, which is u_0, to 2. It can be observed that the final results of the adaptive learning rate are close to those of the fixed learning rate.

The ED results based on the bias adjustment method are shown in Table 4.8, which are similar to those based on the slope adjustment method. For the adaptive learning rate, the number of iterations is reduced and the final results of the adaptive learning rate are better than those of the fixed learning rate.

APPENDIX: OPTIMIZATION METHODS USED IN ECONOMIC OPERATION

Here we introduce several methods [10–17] that are used for economic power operation of power systems.

Although a wide spectrum of methods exists for optimization, methods can be broadly categorized in terms of the derivative information that is, or is not, used. Search methods that use only function evaluations are most suitable for problems that are very nonlinear or have a number of discontinuities. Gradient

Table 4.8   Results for the bias adjustment method with fixed learning rate, 1.0 (A) and adaptive learning rate (B)

Unit	2400 MW A	2400 MW B	2500 MW A	2500 MW B	2600 MW A	2600 MW B	2700 MW A	2700 MW B
1	197.6	189.4	208.3	206.7	212.4	217.9	221.4	228.8
2	201.6	201.8	206.2	205.8	209.6	210.5	213.8	214.1
3	252.3	253.5	265.2	265.6	280.0	278.8	293.3	292.0
4	232.7	232.9	235.9	235.8	238.8	239.0	242.1	242.2
5	239.9	242.1	257.1	258.2	277.9	275.8	295.4	293.6
6	232.7	232.9	235.9	235.8	238.6	239.0	242.0	242.1
7	251.5	253.8	268.3	269.4	288.1	285.5	305.3	302.6
8	232.7	232.9	235.8	235.8	238.8	239.0	242.1	242.1
9	318.8	319.3	330.9	330.1	341.9	342.1	345.2	352.3
10	240.3	241.6	256.4	256.9	274.0	272.3	290.4	290.1
Total P	2400.0	2400.0	2500.0	2500.0	2600.0	2600.0	2700.0	2700.0
Cost	481.83	481.72	526.24	526.23	574.43	574.37	626.32	626.27
Iters	99,960	99,904	99,987	88,776	99,981	99,337	99,972	73,250
u_0	100.0	100.0	100.0	100.0	100.0	100.0	100.0	100.0
theta	0.0	50.0	0.0	50.0	0.0	50.0	0.0	100.0
n	1.0	1.0	1.0	5.0	1.0	5.0	1.0	5.0

methods are generally more efficient when the function to be minimized is continuous in its first derivative. Higher-order methods, such as Newton's method, are only really suitable when the second-order information is readily and easily calculated, because calculation of second-order information, using numerical differentiation, is computationally expensive.

Gradient Method

Gradient methods use information about the slope of the function to dictate a direction of search where the minimum is thought to lie. The simplest of these is the method of steepest descent in which a search is performed in a direction.

$$S^k = -\nabla f(x^k) \tag{4A.1}$$

where $\nabla f(x^k)$ is the gradient of the objective function.
   The optimum search step can be computed as follows:

$$\varepsilon^{*k} = \frac{[\nabla f(x^k)]^T \nabla f(x^k)}{[\nabla f(x^k)]^T H(x^k) \nabla f(x^k)} \tag{4A.2}$$

where $H(x^k)$ is the Hessian matrix of the objective function.

The gradient method based on equation (4A.2) is also called the optimum gradient method. However, this method is very inefficient when the function to be minimized has long, narrow valleys.

Line Search

Line search is a search method that is used as part of a larger optimization algorithm. At each step of the main algorithm, the line search method searches along the line containing the current point, x^k, parallel to the **search direction**, which is a vector determined by the main algorithm. That is, the iteration form of the method can be expressed as:

$$x^{k+1} = x^k + \varepsilon d^k \tag{4A.3}$$

where x^k denotes the current iterate, d^k is the search direction, and ε is a scalar step length parameter.

The line search method attempts to decrease the objective function along the line $x^k + \varepsilon d^k$ by repeatedly minimizing polynomial interpolation models of the objective function. The line search procedure has two main steps:

The **bracketing** phase determines the range of points on the line $x^{k+1} = x^k + \varepsilon d^k$ to be searched. The **bracket** corresponds to an interval specifying the range of values of ε.

The **sectioning** step divides the bracket into subintervals, on which the minimum of the objective function is approximated by polynomial interpolation.

The resulting step length ε satisfies the Wolfe conditions:

$$f\left(x^k + \varepsilon d^k\right) \le f\left(x^k\right) + \alpha_1 \varepsilon \left(\nabla f^k\right)^T d^k \tag{4A.4}$$

$$\nabla f\left(x^k + \varepsilon d^k\right)^T d_k \ge \alpha_2 \varepsilon \left(\nabla f^k\right)^T d^k \tag{4A.5}$$

where α_1 and α_2 are constants with $0 < \alpha_1 < \alpha_2 < 1$.

The first condition (4A.4) requires that ε sufficiently decreases the objective function. The second condition (4A.5) ensures that the step length is not too small. Points that satisfy both conditions (4A.4) and (4A.5) are called **acceptable points**.

Newton–Raphson Optimization

The **Newton-Raphson optimization** is also called the Newton method or the Hessian matrix method.

The objective function can be approximately expressed by use of the second-order Taylor series expansion at the point x^k, that is,

$$f(x) \approx f\left(x^k\right) + \left[\nabla f\left(x^k\right)\right]^T \Delta x + \frac{1}{2} \Delta x^T H\left(x^k\right) \Delta x \tag{4A.6}$$

The necessary condition that a quadratic function achieves the minimum value is that its gradient equals zero.

$$\nabla f(x) = \nabla f(x^k) + H(x^k)\Delta x = 0 \tag{4A.7}$$

Thus the general iteration expression is as below:

$$x^{k+1} = x^k - [H(x^k)]^{-1}\nabla f(x^k) \tag{4A.8}$$

It is noted that the Hessian matrix $H(x)$ will be constant if the original non-linear objective function is a quadratic function. In this case, the minimum value of the function will be obtained through one iteration only. Otherwise, the Hessian matrix $H(x)$ will not be constant, and multiple iterations are needed to obtain the minimum of the function. The formula of the search direction is

$$S^k = -[H(x^k)]^{-1}\nabla f(x^k) \tag{4A.9}$$

The advantage of the Hessian matrix method is fast convergence. The disadvantage is that it needs to compute the inverse of the Hessian matrix, which leads to an expensive memory and calculation burden.

Trust-Region Optimization

The convergence of the Newton optimization method can be made more robust by using **trust regions** (TR) [11]. TR-based methods generate steps based on a quadratic model of the objective function. A region around the current solution is defined, within which the model is supposed to be an adequate representation of the objective function. Then a step is selected to minimize this approximate model in the trust region. Both the direction and the length of the step are chosen simultaneously. If a step is not acceptable, the size of the region is reduced and a new solution is found. In general, the step direction changes whenever the size of the trust region is altered [11].

Since the trust-region method uses the gradient $g(x^k)$ and the Hessian matrix $H(x^k)$, it requires that the objective function $f(x)$ have continuous first- and second-order derivatives inside the feasible region. The general trust-region problem is expressed as

$$\min f = g^T(x^k)\Delta x + \frac{1}{2}\Delta x^T H(x^k)\Delta x \tag{4A.10}$$

s.t.

$$\|\Delta x\| \le \delta \tag{4A.11}$$

where δ is the trust region radius.

The general idea of the trust region is to solve the subproblem represented by equations (4A.10) and (4A.11) to obtain a point y^k. Then the value of the true objective function is calculated at y^k and compared to the value predicted by the quadratic model, to verify whether the point located in the trust region represents effective progress toward the optimal solution. For this purpose, the size of the trust region is critical to the effectiveness of each step.

In practice, the size of the region is determined according to the evolution of the iterative process. If the model is sufficiently accurate, the size of the trust region is steadily increased to allow bigger steps. Otherwise, the quadratic model is inadequate, so that the size of the trust region must be reduced. To establish an algorithm to control the trust region radius, define the **reduction ratio** evaluated at the kth iteration

$$\rho^k = \frac{J(x^k) - J(x^{k+1})}{Q(x^k) - Q(x^{k+1})} \tag{4A.12}$$

where $J(x^k)$ and $Q(x^k)$ are the values of the summation of the weighted squared residuals for the actual objective function and the corresponding approximated quadratic model, respectively, evaluated at the kth iteration.

Newton-Raphson Optimization with Line Search

This technique uses the gradient $g(x^k)$ and the Hessian matrix $H(x^k)$ and thus requires that the objective function have continuous first- and second-order derivatives inside the feasible region. If second-order derivatives are computed efficiently and precisely, the method may perform well for medium-sized to large problems, and it does not need many function, gradient, and Hessian calls.

This algorithm uses a pure Newton step when the Hessian is positive definite and when the Newton step reduces the value of the objective function successfully. Otherwise, a combination of ridging and line search is done to compute successful steps. If the Hessian is not positive definite, a multiple of the identity matrix is added to the Hessian matrix to make it positive definite. In each iteration, a line search is done along the search direction to find an approximate optimum of the objective function. The default line-search method uses quadratic interpolation and cubic extrapolation.

Quasi-Newton Optimization

The (dual) quasi-Newton method uses the gradient $g(x^k)$ and does not need to compute second-order derivatives since they are approximated. It works well for medium to moderately large optimization problems where the objective function and the gradient are much faster to compute than the Hessian.

The method builds up curvature information at each iteration to formulate a quadratic model problem of the form

$$\min f(x) = b + c^T x + \frac{1}{2} x^T H x \tag{4A.13}$$

where the Hessian matrix, H, is a positive definite symmetric matrix, c is a constant vector, and b is a constant. The optimal solution for this problem occurs when the partial derivatives of x go to zero, i.e.,

$$\nabla f(x^*) = H x^* + c = 0 \tag{4A.14}$$

The optimal solution point, x^*, can be written as

$$x^* = -H^{-1} c \tag{4A.15}$$

Newton-type methods (as opposed to quasi-Newton methods) calculate H directly and proceed in a direction of descent to locate the minimum after a number of iterations. Calculating H numerically involves a large amount of computation. Quasi-Newton methods avoid this by using the observed behavior of $f(x)$ and $\nabla f(x)$ to build up curvature information to make an approximation to H with an appropriate updating technique.

A large number of Hessian updating methods have been developed. However, the formula of Broyden, Fletcher, Goldfarb, and Shanno (BFGS) is thought to be the most effective for use in a general purpose method [12–17].

The formula given by BFGS is

$$H^{k+1} = H^k + \frac{q^k (q^k)^T}{(q^k)^T S^k} - \frac{(H^k)^T (S^k)^T S^k H^k}{(S^k)^T H^k S^k} \tag{4A.16}$$

where

$$S^k = x^{k+1} - x^k \tag{4A.17}$$

$$q^k = \nabla f(x^{k+1}) - \nabla(x^k) \tag{4A.18}$$

As a starting point, H^0 can be set to any symmetric positive definite matrix, for example, the identity matrix I. To avoid the inversion of the Hessian H, we can derive an updating method that avoids the direct inversion of H by using a formula that makes an approximation of the inverse Hessian H^{-1} at each update. A well-known procedure is the DFP formula of Davidon, Fletcher, and Powell. This uses the same formula as the BFGS method (4A.16) except that q^k is substituted for S^k.

The gradient information is either supplied through analytically calculated gradients or derived by partial derivatives using a numerical differentiation method via finite differences. This involves perturbing each of the design variables, x, in turn and calculating the rate of change in the objective function.

At each major iteration, k, a line search is performed in the direction

$$d = -\left(H^k\right)^{-1}\nabla f\left(x^k\right) \tag{4A.19}$$

Double Dogleg Optimization

The double dogleg optimization method combines the ideas of quasi-Newton and trust region methods. The double dogleg algorithm computes in each iteration the step S^k as the linear combination of the steepest descent or ascent search direction S_1^k and a quasi-Newton search direction S_2^k,

$$S^k = \alpha_1 S_1^k + \alpha_2 S_2^k \tag{4A.20}$$

The step is requested to remain within a prespecified trust region radius. The double dogleg optimization technique works well for medium to moderately large optimization problems where the objective function and the gradient are much faster to compute than the Hessian.

Conjugate Gradient Optimization

Second-order derivatives are not used by conjugate gradient optimization. As we discussed above the method of steepest descent (or gradient method) converges slowly. The method of conjugate gradients is an attempt to mend this problem. "Conjugacy" means that two unequal vectors, S_i and S_j, are orthogonal with respect to any symmetric positive definite matrix, for example, Q, i.e.,

$$S_i^T Q S_j = 0 \tag{4A.21}$$

This can be looked upon as a generalization of orthogonality, for which Q is the unity matrix. The idea is to let each search direction S_i be dependent on all the other directions searched to locate the minimum of $f(x)$ through equation (4A.21). A set of such search directions is referred to as a Q-orthogonal, or conjugate, set, and it will take a positive definite n-dimensional quadratic function to its minimum point in, at most, n exact linear searches. This method is often referred to as **conjugate directions**, and a short description follows.

The conjugate gradients method is a special case of the method of conjugate directions in which the conjugate set is generated by the gradient vectors. This seems to be a sensible choice since the gradient vectors have proved their applicability in the steepest descent method, and they are orthogonal to the previous search direction.

Subsequently, the mutually conjugate directions are chosen so that

$$S^{k+1} = -\nabla f\left(x^{k+1}\right) + \beta^k S^k \tag{4A.22}$$

where the coefficient β^k is given by, for example, the so called Fletcher–Reeves formula:

$$\beta^k = \frac{\left[\nabla f\left(x^{k+1}\right)\right]^T \nabla f\left(x^{k+1}\right)}{\left[\nabla f\left(x^k\right)\right]^T \nabla f\left(x^k\right)} \tag{4A.23}$$

The optimum search step can be computed as follows.

$$\varepsilon^{*k} = -\frac{\left[\nabla f\left(x^k\right)\right]^T S^k}{\left(S^k\right)^T H\left(x^k\right) S^k} \tag{4A.24}$$

During n successive iterations, uninterrupted by restarts or changes in the working set, the conjugate gradient algorithm computes a cycle of n conjugate search directions. In each iteration, a line search is done along the search direction to find an approximate optimum of the objective function. The default line-search method uses quadratic interpolation and cubic extrapolation to obtain a step size ε satisfying the Goldstein conditions. One of the Goldstein conditions can be violated if the feasible region defines an upper limit for the step size.

Lagrange Multipliers Method

Suppose there are M constraints to be met; then the optimization problem can be written as below:

$$\min f\left(x_i\right), \quad i = 1, 2, \ldots, N \tag{4A.25}$$

s.t.

$$h_1\left(x_i\right) = 0, \quad i = 1, 2, \ldots, N \tag{4A.26}$$

$$h_2\left(x_i\right) = 0, \quad i = 1, 2, \ldots, N \tag{4A.27}$$

$$\ldots \ldots$$

$$h_M\left(x_i\right) = 0, \quad i = 1, 2, \ldots, N \tag{4A.28}$$

The optimum point would posses the property that the gradient of $f(x)$ and the gradient of h_1, h_2, and h_M are linear dependent, i.e.,

$$\nabla f + \lambda_1 \nabla h_1 + \lambda_2 \nabla h_2, \ldots, + \lambda_M \nabla h_M = 0 \tag{4A.29}$$

The scaling variable λ is called a Lagrange multiplier.

In addition, we can write the Lagrange equation according to equations (4A.25)–(4A.28).

$$L(x_i, \lambda_M) = f(x_i) + \lambda_1 h_1(x_i) + \lambda_2 h_2(x_i), \dots, + \lambda_M h_M(x_i) \quad i = 1, 2, \dots, N \tag{4A.30}$$

To meet the conditions stated in equation (4A.29), we simply require that the partial derivate of the Lagrange function with respect to each of the unknown variables, $x_1, x_2, \dots, x_N$ *and* $\lambda_1, \lambda_2, \dots, \lambda_M$, be equal to zero. That is,

$$\frac{\partial L}{\partial x_1} = 0$$

$$\frac{\partial L}{\partial x_2} = 0$$

$$\vdots$$

$$\frac{\partial L}{\partial x_N} = 0$$

$$\frac{\partial L}{\partial \lambda_1} = 0 \tag{4A.31}$$

$$\frac{\partial L}{\partial \lambda_2} = 0$$

$$\vdots$$

$$\frac{\partial L}{\partial \lambda_M} = 0$$

Kuhn–Tucker Conditions

If inequality constraints are involved in the optimization problem, the optimum is reached if the Kuhn–Tucker conditions are met, which can be stated as below:

$$\min f(x_i), \quad i = 1, 2, \dots, N \tag{4A.32}$$

s.t.

$$h_j(x_i) = 0, \quad j = 1, 2, \dots, M_h \tag{4A.33}$$

$$g_j(x_i) \le 0, \quad j = 1, 2, \dots, M_g \tag{4A.34}$$

The Lagrange function can be formed based on equations (4A.32)–(4A.34).

$$L(x, \lambda, \mu) = f(x) + \sum_{j=1}^{M_h} \lambda_j h_j(x) + \sum_{j=1}^{M_g} \mu_j g_j(x) \tag{4A.35}$$

The Kuhn–Tucker conditions for the optimum for the points x^*, λ^*, μ^* are

1. $\dfrac{\partial L}{\partial x_i}(x^*, \lambda^*, \mu^*) = 0, \quad \mathrm{i} = 1, 2, \ldots, N$

2. $h_j(x^*) = 0, \quad j = 1, 2, \ldots, M_h$

3. $g_j(x^*) \leq 0, \quad j = 1, 2, \ldots, M_g$

4. $\mu_j^* g_j(x^*) = 0, \quad \mu_j^* \geq 0, \quad j = 1, 2, \ldots, M_g$

The first condition is the set of partial derivatives of the Lagrange function that must equal zero at the optimum. The second and third expressions are a restatement of the constraint conditions on the problem. The fourth is the complementary slackness condition. Since the product $\mu_j^* g_j(x^*)$ equals zero, μ_j^* equals to zero, $g_j(x^*)$ equals to zero, or both equal to zero. If μ_j^* equals to zero, $g_j(x^*)$ is free to be nonbinding; if μ_j^* is positive, $g_j(x^*)$ must be zero. Thus we can know whether the inequality constraint is binding or not by looking at the value of μ_j^*.

REFERENCES

[1] L.K. Kirchamayer, *Economic Operation of Power Systems*, New York: Wiley, 1958.

[2] J.Z. Zhu, "Power System Optimal Operation," Tutorial of Chongqing University, 1990.

[3] J. Nanda, R.B. Narayanan, "Application of genetic algorithm to economic load dispatch with Line-flow constraints," *Electrical Power and Energy Systems*, Vol. 24, 2002, pp. 723–729.

[4] D.C. Walters, G.B. Sheble, "Genetic algorithm solution of economic dispatch with valve point loading," *IEEE Trans on Power System* Vol. 8, No. 3, 1993.

[5] G.B. Sheble, K. Brittig, "Refined genetic algorithm-economic dispatch example," *IEEE Trans on Power System*, Vol. 10, No. 1, 1995.

[6] J.I. Hopfield, "Neural Networks and Physical Systems with Emergent Collective Computational Abilities," *Proceedings of National Academy of Science, USA*, Vol. 79, 1982, pp. 2554–2558.

[7] J.H. Park, Y.S. Kim, I.K. Eom, and K.Y. Lee, "Economic load dispatch for piecewise quadratic cost function using Hopfield neural networks," *IEEE Trans on Power System*, Vol. 8, No. 3, 1993, pp. 1030–1038.

[8] T.D. King, M.E. El-Hawary, and F. El-Hawary, "Optimal environmental dispatching of electric power system via an improved Hopfield neural network model," *IEEE Trans on Power System*, Vol. 10, No. 3, 1995, pp. 1559–1565.

[9] K.Y. Lee, A.S. Yome, and J.H. Park, "Adaptive neural networks for economic load dispatch," *IEEE Trans on Power System*, Vol. 13, No. 2, 1998, pp. 519–526.

[10] K.P. Wong and C.C. Fung, "Simulated-annealing-based economic dispatch algorithm," *IEE Proc. Part C*, Vol. 140, No. 6, 1993, pp. 509–515.

[11] J. Nocedal and S.J. Wright, *Numerical Optimization*. Springer, 1999.

[12] R. Fletcher, *Practical Methods of Optimization*, John Wiley and Sons, 1987.

[13] C.G. Broyden, "The Convergence of a Class of Double-rank Minimization Algorithms," *J. Inst. Maths. Applics.*, Vol. 6, pp. 76–90, 1970.

[14] R. Fletcher, "A New Approach to Variable Metric Algorithms," *Computer Journal*, Vol. 13, pp. 317–322, 1970.

[15] D. Goldfarb, "A Family of Variable Metric Updates Derived by Variational Means," *Mathematics of Computing*, Vol. 24, pp. 23–26, 1970.

[16] D.F. Shanno, "Conditioning of Quasi-Newton Methods for Function Minimization," *Mathematics of Computing*, Vol. 24, pp. 647–656, 1970.

[17] R. Fletcher and M.J.D. Powell, "A Rapidly Convergent Descent Method for Minimization," *Computer Journal*, Vol. 6, pp. 163–168, 1963.

[18] J.H. Holland, *Adaptation in Nature and Artificial Systems*, The University of Michigan Press, 1975.

[19] D.E. Goldberg, *Genetic Algorithms in Search, Optimization and Machine Learning*, Addision-Wesley, Reading, 1989.

5

SECURITY-CONSTRAINED ECONOMIC DISPATCH

The security-constrained economic dispatch (SCED) is one of the simplified optimal power flow (OPF) problems. It is widely used in power industry. This chapter first introduces several major approaches to solve the SCED problem such as linear programming, network flow programming, and quadratic programming. Then, nonlinear convex network flow programming and the genetic algorithm are added to attack the security-constrained economic dispatch problem. The implementation details of these methods and a great number of numerical examples are provided in this chapter.

5.1 INTRODUCTION

Chapter 4 analyzes the model and algorithm of the classic economic dispatch, where the network security constraints are neglected. In practical power systems, it is very important to solve the economic dispatch with network security constraints. Mathematical optimization methods such as linear programming, quadratic programming, and network flow programming as well as genetic algorithms are applied to solve this problem [1–19].

5.2 LINEAR PROGRAMMING METHOD

5.2.1 Mathematical Model of Economic Dispatch with Security

The mathematical model of real power economic dispatch with security constraints can be written as follows (model M-1):

$$\text{Min } F = \sum_{i \in NG} f_i(P_{Gi}) \tag{5.1}$$

Such that

$$\text{s.t.} \quad \sum_{i \in NG} P_{Gi} = \sum_{k \in ND} P_{Dk} + P_L \tag{5.2}$$

$$|P_{ij}| \le P_{ij\max} \quad ij \in NT \tag{5.3}$$

$$P_{Gi\min} \le P_{Gi} \le P_{Gi\max} \quad i \in NG \tag{5.4}$$

Where

P_D: The real power load
P_{ij}: The power flow of transmission line ij
$P_{ij\max}$: The power limits of transmission line ij
P_{Gi}: The real power output at generator bus i
$P_{Gi\min}$: The minimal real power output at generator i
$P_{Gi\max}$: The maximal real power output at generator i
P_L: The network losses
f_i: The cost function of the generator i
NT: The number of transmission lines
NG: The number of generators

Since the input-output characteristic of generator units and system power losses are nonlinear functions, the real power economic dispatch model is a nonlinear model. To use a linear programming method to solve security constrained economic dispatch, it needs to linearize the objective function and constraints in the model.

5.2.2   Linearization of ED Model

5.2.2.1   Linearization of Objective Function   Let the initial operation point of generator i be P_{Gi}^0. The nonlinear objective function can be expressed by use of Taylor series expansion, and only the first two terms are considered, that is,

$$f_i(P_{Gi}) \approx f_i\left(P_{Gi}^0\right) + \left.\frac{\mathrm{d}f_i(P_{Gi})}{\mathrm{d}P_{Gi}}\right|_{P_{Gi}^0} \Delta P_{Gi} = b\Delta P_{Gi} + c$$
$$\text{or} \tag{5.5}$$
$$f_i(\Delta P_{Gi}) = b\Delta P_{Gi}$$

where

$$b = \frac{\mathrm{d}f_i(P_{Gi})}{\mathrm{d}P_{Gi}}\bigg|_{P_{Gi}^0} \tag{5.6}$$

$$c = f_i(P_{Gi}^0) \tag{5.7}$$

are constant and

$$\Delta P_{Gi} = P_{Gi} - P_{Gi}^0 \tag{5.8}$$

5.2.2.2 *Linearization of Power Balance Equation* Since loads are constant for the given time, we can get the following expression through linearizing the real power balance equation:

$$\sum_{i \in NG} \left(1 - \frac{\partial P_L}{\partial P_{Gi}}\right)\bigg|_{P_{Gi}^0} \Delta P_{Gi} = 0 \tag{5.9}$$

5.2.2.3 *Linearization of Branch Flow Constraints* The real power flow equation of a branch can be written as follows:

$$P_{ij} = V_i^2 g_{ij} - V_i V_j (g_{ij} \cos\theta_{ij} + b_{ij} \sin\theta_{ij}) \tag{5.10}$$

where

P_{ij}: The sending end real power on transmission branch ij

V_i: The node voltage magnitude of node i

θ_{ij}: The difference of node voltage angles between the sending end and receiving end of the line ij

b_{ij}: The susceptance of transmission branch ij

g_{ij}: The conductance of transmission branch ij

Through linearizing equation (5.10), we get the incremental branch power expression as below:

$$\Delta P_{ij} = -V_i^0 V_j^0 (-g_{ij} \sin\theta_{ij}^0 \Delta\theta_{ij} + b_{ij} \cos\theta_{ij}^0 \Delta\theta_{ij}) \tag{5.11}$$

In a high-voltage power network, the value of θ_{ij} is very small, and the following approximate equations are easily obtained:

$$\sin\theta_{ij} \cong 0 \tag{5.12}$$

$$\cos\theta_{ij} \cong 1 \tag{5.13}$$

In addition, assume that the magnitudes of all bus voltages are the same and equal to 1.0 p.u. Furthermore, suppose the reactance of the branch is

much bigger than the resistance of the branch, so that we can neglect the resistance of the branch. Thus,

$$g_{ij} = \frac{R_{ij}}{R_{ij}^2 + X_{ij}^2} \approx 0 \tag{5.14}$$

$$b_{ij} = -\frac{X_{ij}}{R_{ij}^2 + X_{ij}^2} \approx -\frac{X_{ij}}{X_{ij}^2} \approx -\frac{1}{X_{ij}} \tag{5.15}$$

Substituting equations (5.12)–(5.15) into equation (5.11), we get

$$\Delta P_{ij} = -b_{ij}\Delta\theta_{ij} = -b_{ij}\left(\Delta\theta_i - \Delta\theta_j\right) = \frac{\Delta\theta_i - \Delta\theta_j}{X_{ij}} \tag{5.16}$$

The above equation can also be written in matrix form, i.e.,

$$\Delta P_b = B'\Delta\theta \tag{5.17}$$

Where the elements of the susceptance matrix B′ are

$$B'_{ij} = b_{ij} = -\frac{1}{X_{ij}} \tag{5.18}$$

$$B'_{ii} = -\sum_{\substack{j=1 \\ j\neq i}}^{n} b_{ij} \tag{5.19}$$

From chapter 1, the bus power injection equation can be written as

$$P_{Gi} - P_{Di} = V_i \sum_{j=1}^{n} V_j \left(g_{ij}\cos\theta_{ij} + b_{ij}\sin\theta_{ij}\right) \tag{5.20}$$

Since the load demand is constant, the linearization expression of the equation (5.20) can be written as below:

$$\Delta P_{Gi} = V_i^0 \sum_{j=1}^{n} V_j^0 \left(-g_{ij}\sin\theta_{ij}^0 \Delta\theta_{ij} + b_{ij}\cos\theta_{ij}^0 \Delta\theta_{ij}\right)$$

$$= V_i^0 \sum_{j=1}^{n} V_j^0 \left(-g_{ij}\sin\theta_{ij}^0 + b_{ij}\cos\theta_{ij}^0\right)\Delta\theta_{ij} \tag{5.21}$$

The above equation can also be written in the following matrix form

$$\Delta P_G = H\Delta\theta \tag{5.22}$$

Equation (5.22) stands for the relationship between the incremental generator output power (except for the generator that is taken as slack unit) and the incremental bus voltage angle. Matrix H can also be simplified by using equations (5.12)–(5.15).

According to equations (5.17) and (5.22), we can get the direct linear relationship between the incremental branch power flow and incremental generator output power, i.e.,

$$\Delta P_b = B'\Delta\theta = B'H^{-1}\Delta P_G = D\Delta P_G \tag{5.23}$$

where

$$D = B'H^{-1} \tag{5.24}$$

is also called as the linear sensitivity of the branch power flow with respect to the generator power output.

Thus the linear expression of the branch power flow constraints can be written as

$$|D\Delta P_G| \le \Delta P_{b\max} \tag{5.25}$$

The element of the matrix $\Delta P_{b\max}$ is the incremental power flow limit $\Delta P_{ij\max}$ of the branch ij, i.e.,

$$\Delta P_{ij\max} = P_{ij\max} - P_{ij}^0 \tag{5.26}$$

If the branch outage is considered in the real power economic dispatch, the outage transfer distribution factors (OTDF) in Chapter 3 will be used. So the sensitivity factor OTDF between branch ij and generator bus i when line l is opened is written as

$$\text{OTDF}_{ij,i} = \frac{\Delta P_{ij}}{\Delta P_{Gi}} = (S_{ij,i} + \text{LODF}_{ij,i}S_{l,i}) \tag{5.27}$$

In this case, the branch power flow can be written as

$$\Delta P_{ij} = (S_{ij,i} + \text{LODF}_{ij,i}S_{l,i})\Delta P_{Gi} \tag{5.28}$$

The matrix form of the above equation is

$$\Delta P_b = D'\Delta P_G \tag{5.29}$$

The corresponding branch power flow constraints are written as

$$|D'\Delta P_G| \le \Delta P'_{b\max} \tag{5.30}$$

Comparing with D, $\Delta P_{b\max}$ in equation (5.25), D', $\Delta P'_{b\max}$ in equation (5.30) consider the effect of the branch outage. In this case, we call the real power economic dispatch the $N-1$ security economic dispatch.

5.2.2.4 *Generator Output Power Constraint*   The incremental form of the generator output power constraint is

$$P_{G i\min} - P_{Gi}^0 \le \Delta P_{Gi} \le P_{G i\max} - P_{Gi}^0 \quad i \in NG \tag{5.31}$$

5.2.3 Linear Programming Model

The linearized economic dispatch model can be written as the standard linear programming form:

$$\min Z = c_1 x_1 + c_2 x_2 + \cdots + c_N x_N$$

s.t.

$$a_{11} x_1 + a_{12} x_2 + \cdots + a_{1N} x_N \ge b_1$$
$$a_{21} x_1 + a_{22} x_2 + \cdots + a_{2N} x_N \ge b_2$$
$$\vdots$$
$$a_{N1} x_1 + a_{N2} x_2 + \cdots + a_{NN} x_N \ge b_N$$
$$x_{i\min} \le x_i \le x_{i\max}$$

The basic algorithm of LP can be found in the Appendix in Chapter 9.

5.2.4 Implementation

5.2.4.1 *Solution Steps of ED by LP*   The above-mentioned method for solving economic dispatch by LP uses an iterative technique to obtain the optimal solution, so it is also called a successive linear programming (SLP) method. The solution procedures of SLP for economic dispatch are summarized below:

Step 1. Select the set of initial control variables.

Step 2. Solve the power flow problem to obtain a feasible solution that satisfies the power balance equality constraint.

Step 3. Linearize the objective function and inequality constraints around the power flow solution and formulate the LP problem.

Step 4. Solve the LP problem and obtain optimal incremental control variables ΔP_{Gi}.

Step 5. Update the control variables: $P_{Gi}^{(k+1)} = P_{Gi}^{(k)} + \Delta P_{Gi}$.

Step 6. Obtain the power flow solution with updated control variables.

Step 7. Check the convergence. If ΔP_{Gi} in step 4 are below the user-defined tolerance, the solution converges. Otherwise, go to step 3.

5.2.4.2 *Test Results*
The linear programming-based economic dispatch method is tested on IEEE 5-bus and 30-bus systems. The network topologies of the IEEE test systems are shown in Figure 5.1. The corresponding system data and parameters are listed in Tables 5.1–5.3. The data and parameters of the 30-bus system are listed in Tables 5.4–5.6.

The calculation results of economic dispatch with *N* security for the IEEE 5-bus system are shown in Table 5.7. The calculation results of economic dispatch with *N* security for the IEEE 30-bus system are shown in Table 5.8, and *N* − 1 security economic dispatch results are listed in Table 5.9.

Table 5.1   Generator data of 5-bus system

Generators	#1	#2
P_{Gimax}(p.u.)	1.00	1.00
P_{Gimin}(p.u.)	0.20	0.20
Q_{Gimax}(p.u.)	0.80	0.80
Q_{Gimin}(p.u.)	−0.20	−0.20
Quadratic cost function		
a_i	50.00	50.00
b_i	351.00	389.00
c_i	44.40	40.60

Table 5.2   Load data of 5-bus system

Load Bus	#3	#4	#5
MW load P_D(p.u.)	0.60	0.40	0.60
MVAR load Q_D(p.u.)	0.30	0.10	0.20

Table 5.3   Line data of 5-bus system

Line No.	From-To Bus	Resistance	Reactance	Line Charge
1	1–3	0.10	0.40	0.00
2	4–1	0.15	0.60	0.00
3	5–1	0.05	0.20	0.00
4	3–2	0.05	0.20	0.00
5	2–5	0.05	0.20	0.00
6	3–4	0.10	0.40	0.00
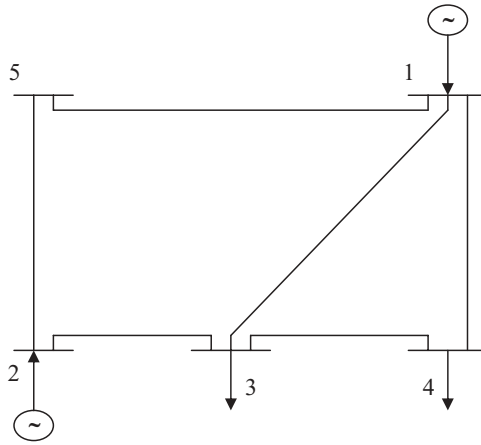
(a) IEEE 5-bus system
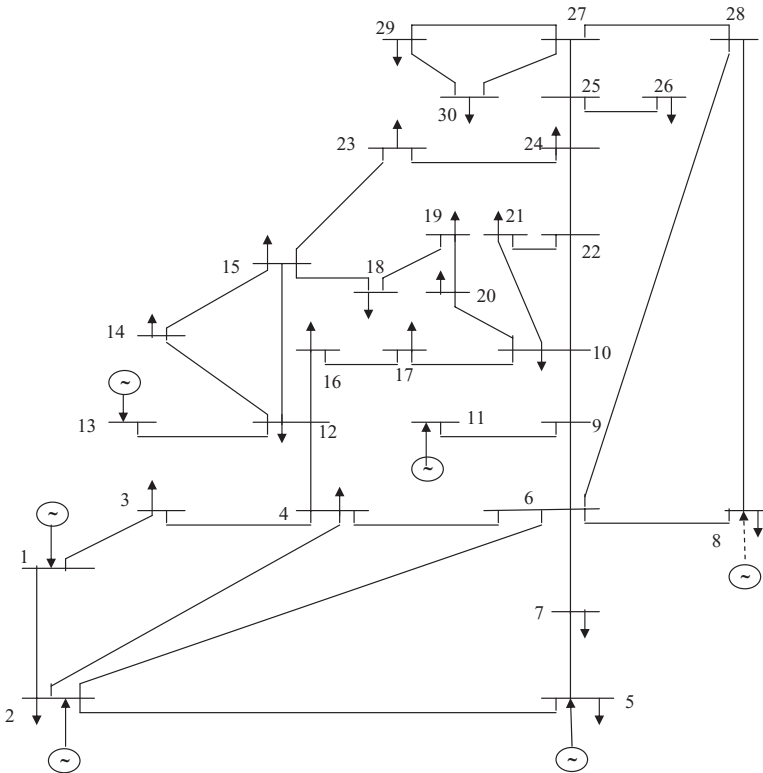
(b) One-line diagram of IEEE 30-bus system

FIGURE 5.1   IEEE test systems

Table 5.4   Generator data of 30-bus system

Generators	#1	#2	#5	#8	#11	#13
P_{Gimax}(p.u.)	2.00	0.80	0.50	0.35	0.30	0.40
P_{Gimin}(p.u.)	0.50	0.20	0.15	0.10	0.10	0.12
Q_{Gimax}(p.u.)	2.50	1.00	0.80	0.60	0.50	0.60
Q_{Gimin}(p.u.)	−0.20	−0.20	−0.15	−0.15	−0.10	−0.15
Quadratic cost function						
a_i	0.00375	0.0175	0.0625	0.0083	0.0250	0.0250
b_i	2.00000	1.7500	1.0000	3.2500	3.0000	3.0000
c_i	0.00000	0.0000	0.0000	0.0000	0.0000	0.0000

Table 5.5   Load data of 30-bus system

Bus No.	P_D(p.u.)	Q_D(p.u.)	Bus No.	P_D(p.u.)	Q_D(p.u.)
1	0.000	0.000	16	0.035	0.016
2	0.217	0.127	17	0.090	0.058
3	0.024	0.012	18	0.032	0.009
4	0.076	0.016	19	0.095	0.034
5	0.942	0.190	20	0.022	0.007
6	0.000	0.000	21	0.175	0.112
7	0.228	0.109	22	0.000	0.000
8	0.300	0.300	23	0.032	0.016
9	0.000	0.000	24	0.087	0.067
10	0.058	0.020	25	0.000	0.000
11	0.000	0.000	26	0.035	0.023
12	0.112	0.075	27	0.000	0.000
13	0.000	0.000	28	0.000	0.000
14	0.062	0.016	29	0.024	0.009
15	0.082	0.025	30	0.106	0.019

5.2.5   Piecewise Linear Approach

Assuming that the objective function is a quadratic characteristic, the objective function can also be linearized by a piecewise linear approach.

If the objective function is divided into N linear segments, the real power variable of each generator will also be divided into N variables. Figure 5.2 is an objective function with three linear segments. The corresponding slopes are b_1, b_2, and b_3, respectively.

From Figure 5.2, the generator power output variables for each segment can be presented as below:

$$P_{Gimin} \leq P_{Gi1} \leq P_{G1max} \tag{5.32}$$

$$P_{G1min} \leq P_{Gi2} \leq P_{G2max} \tag{5.33}$$

$$P_{G2min} \leq P_{Gi3} \leq P_{Gimax} \tag{5.34}$$

Table 5.6   Line data of 30-bus system

Line No.	From-To Bus	Resistance (p.u.)	Reactance (p.u.)	Line Limit (p.u.)
1	1–2	0.0192	0.0575	1.30
2	1–3	0.0452	0.1852	1.30
3	2–4	0.0570	0.1737	0.65
4	3–4	0.0132	0.0379	1.30
5	2–5	0.0472	0.1983	1.30
6	2–6	0.0581	0.1763	0.65
7	4–6	0.0119	0.0414	0.90
8	5–7	0.0460	0.1160	0.70
9	6–7	0.0267	0.0820	1.30
10	6–8	0.0120	0.0420	0.32
11	6–9	0.0000	0.2080	0.65
12	6–10	0.0000	0.5560	0.32
13	9–10	0.0000	0.2080	0.65
14	9–11	0.0000	0.1100	0.65
15	4–12	0.0000	0.2560	0.65
16	12–13	0.0000	0.1400	0.65
17	12–14	0.1231	0.2559	0.32
18	12–15	0.0662	0.1304	0.32
19	12–16	0.0945	0.1987	0.32
20	14–15	0.2210	0.1997	0.16
21	16–17	0.0824	0.1932	0.16
22	15–18	0.1070	0.2185	0.16
23	18–19	0.0639	0.1292	0.16
24	19–20	0.0340	0.0680	0.32
25	10–20	0.0936	0.2090	0.32
26	10–17	0.0324	0.0845	0.32
27	10–21	0.0348	0.0749	0.32
28	10–22	0.0727	0.1499	0.32
29	21–22	0.0116	0.0236	0.32
30	15–23	0.1000	0.2020	0.16
31	22–24	0.1150	0.1790	0.16
32	23–24	0.1320	0.2700	0.16
33	24–25	0.1885	0.3292	0.16
34	25–26	0.2544	0.3800	0.16
35	25–27	0.1093	0.2087	0.16
36	28–27	0.0000	0.3960	0.65
37	27–29	0.2198	0.4153	0.16
38	27–30	0.3202	0.6027	0.16
39	29–30	0.2399	0.4533	0.16
40	8–28	0.0636	0.2000	0.32
41	6–28	0.0169	0.0599	0.32
42	10–10	0.0000	−5.2600	
43	24–24	0.0000	−25.0000	

Table 5.7 Economic dispatch results for 5-bus system

Method	LP	P_{imin}	P_{imax}
P_{G1}(p.u.)	0.97864	0.2	1.0
P_{G2}(p.u.)	0.66622	0.2	1.0
Total Cost ($/hr)	757.74	/	/
Total loss (p.u.)	0.04490	/	/

Table 5.8 *N* security economic dispatch results by LP for IEEE 30-bus system

Generation No.	Economic Dispatch	P_{Gimin}	P_{Gimax}
P_{G1}	1.7626	0.50	2.00
P_{G2}	0.4884	0.20	0.80
P_{G5}	0.2151	0.15	0.50
P_{G8}	0.2215	0.10	0.35
P_{G11}	0.1214	0.10	0.30
P_{G13}	0.1200	0.12	0.40
Total generation	2.9290	/	/
Total real power losses	0.0948	/	/
Total generation cost ($)	802.4000	/	/

Table 5.9 *N* – 1 security economic dispatch results by LP for IEEE 30-bus system

Generator No.	Economic Dispatch	P_{Gimin}	P_{Gimax}
P_{G1}(p.u.)	1.38540	0.50	2.00
P_{G2}(p.u.)	0.57560	0.20	0.80
P_{G5}(p.u.)	0.24560	0.15	0.50
P_{G8}(p.u.)	0.35000	0.10	0.35
P_{G11}(p.u.)	0.17930	0.10	0.30
P_{G13}(p.u.)	0.16910	0.12	0.40
Total generation(p.u.)	2.90500	/	/
Total Cost ($/hr)	813.74	/	/
Total loss (p.u.)	0.0711	/	/
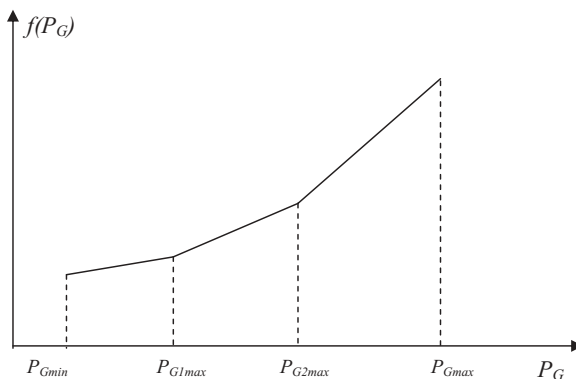
FIGURE 5.2 Piecewise linear objective function

If $P_{Gi\min}$ is selected as the initial generator output power, the incremental generator power outputs for each segment can be expressed as

$$\Delta P_{Gi1} = P_{Gi1} - P_{Gi\min} \tag{5.35}$$

$$\Delta P_{Gi2} = P_{Gi2} - P_{Gi1\min} \tag{5.36}$$

$$\Delta P_{Gi3} = P_{Gi3} - P_{Gi2\min} \tag{5.37}$$

Thus the constraint equations (5.32)–(5.34) become

$$0 \le \Delta P_{Gi1} \le P_{Gi1\max} - P_{Gi\min} \tag{5.38}$$

$$0 \le \Delta P_{Gi2} \le P_{Gi2\max} - P_{Gi1\max} \tag{5.39}$$

$$0 \le \Delta P_{Gi3} \le P_{Gi\max} - P_{Gi2\max} \tag{5.40}$$

The piecewise linear objective function becomes

$$F = \sum_{i=1}^{NG} f_i(P_{Gi}) = \sum_{k=1}^{3} \sum_{i=1}^{NG} b_k \Delta P_{Gik} \tag{5.41}$$

Replacing the incremental generator power output ΔP_{Gi} in constraints (5.9) and (5.30) in Section 5.2.2 by $\sum_{k=1}^{3} \Delta P_{Gik}$, we can also obtain the linear programming model for the economic dispatch problem.

5.3   QUADRATIC PROGRAMMING METHOD

A quadratic programming (QP) model contains a quadratic objective function and linear constraints. As mentioned above in this chapter, the economic dispatch problem is a nonlinear mathematical model. We discuss the successive linear programming method for solving the economic dispatch problem in Section 5.2. The successive linear programming method can also be used in the quadratic programming model of economic dispatch.

5.3.1   QP Model of Economic Dispatch

Let the initial operation point of generator i be P_{Gi}^0. The nonlinear objective function can be expressed by use of Taylor series expansion, and only the first three terms are considered, that is,

$$f_i(P_{Gi}) \approx f_i(P_{Gi}^0) + \frac{\mathrm{d}f_i(P_{Gi})}{\mathrm{d}P_{Gi}}\bigg|_{P_{Gi}^0} \Delta P_{Gi} + \frac{1}{2}\frac{\mathrm{d}f_i^2(P_{Gi})}{\mathrm{d}P_{Gi}^2}\bigg|_{P_{Gi}^0} \Delta P_{Gi}^2$$

$$= a\Delta P_{Gi}^2 + b\Delta P_{Gi} + c \tag{5.42}$$

or

$$f_i(\Delta P_{Gi}) = a\Delta P_{Gi}^2 + b\Delta P_{Gi} \tag{5.43}$$

where

$$a = \frac{1}{2}\frac{\mathrm{d}f_i'(P_{Gi})}{\mathrm{d}P_{Gi}}\bigg|_{P_{Gi}^0} \tag{5.44}$$

$$b = f_i'(P_{Gi}) = \frac{\mathrm{d}f_i(P_{Gi})}{\mathrm{d}P_{Gi}}\bigg|_{P_{Gi}^0} \tag{5.45}$$

$$c = f_i(P_{Gi}^0) \tag{5.46}$$

are constant and

$$\Delta P_{Gi} = P_{Gi} - P_{Gi}^0 \tag{5.47}$$

Linearizing the constraints using the same approach used in Section 5.2, the quadratic programming model of real power economic dispatch can be written as below.

$$\min f_i(\Delta P_{Gi}) = \sum_{i=1}^{N}\left(a\Delta P_{Gi}^2 + b\Delta P_{Gi}\right) \tag{5.48}$$

s.t.

$$\sum_{i \in NG}\left(1 - \frac{\partial P_L}{\partial P_{Gi}}\right)\bigg|_{P_{Gi}^0} \Delta P_{Gi} = 0 \tag{5.49}$$

$$P_{Gi\min} - P_{Gi}^0 \leq \Delta P_{Gi} \leq P_{Gi\max} - P_{Gi}^0 \quad i \in NG \tag{5.50}$$

$$|D'\Delta P_G| \leq \Delta P_{b\max}' \tag{5.51}$$

5.3.2 QP Algorithm

The economic dispatch model in equations (5.48)–(5.51) can be written as the standard quadratic programming model.

$$\min f(X) = \mathbf{C}X + X^{\mathrm{T}}\mathbf{Q}X \tag{5.52}$$

s.t.

$$\mathbf{A}X \le \mathbf{B} \tag{5.53}$$

$$X \ge 0 \tag{5.54}$$

where $\mathbf{C}$ is an n-dimensional row vector describing the coefficients of the linear terms in the objective function, and $\mathbf{Q}$ is an $(n \times n)$ symmetric matrix describing the coefficients of the quadratic terms.

As in linear programming, the decision variables are denoted by the n-dimensional column vector $\mathbf{X}$, and the constraints are defined by an $(m \times n)$ $\mathbf{A}$ matrix and an m-dimensional column vector $\mathbf{B}$ of right-hand-side coefficients. For the real power economic dispatch problem, we know that a feasible solution exists and that the constraint region is bounded.

When the objective function $f(\mathbf{X})$ is strictly convex for all feasible points, the problem has a unique local minimum, which is also the global minimum. A sufficient condition to guarantee strict convexity is for $\mathbf{Q}$ to be positive definite. This is generally true for most of economic dispatch problems.

Equation (5.53) can be expressed as

$$g(X) = (\mathbf{A}X - \mathbf{B}) \le 0 \tag{5.55}$$

Form the Lagrange function for equations (5.52) and (5.55), i.e.,

$$L(X, \mu) = \mathbf{C}X + X^{\mathrm{T}}\mathbf{Q}X + \mu g(X) \tag{5.56}$$

where μ is an m-dimensional row vector.

According to the optimization theory, the Kuhn–Tucker (KT) conditions for a local minimum are given as follows:

$$\begin{cases} \dfrac{\partial L}{\partial X_j} \ge 0, j = 1, \dots, n \\[2mm] \mathbf{C} + 2X^{\mathrm{T}}\mathbf{Q} + \mu\mathbf{A} \ge 0 \end{cases} \tag{5.57}$$

$$\begin{cases} \dfrac{\partial L}{\partial \mu_i} \le 0, i = 1, \dots, m \\[2mm] \mathbf{A}X - \mathbf{B} \le 0 \end{cases} \tag{5.58}$$

$$\begin{cases} X_j \dfrac{\partial L}{\partial X_j} = 0, j = 1, \dots, n \\[2mm] X^{\mathrm{T}}(\mathbf{C}^{\mathrm{T}} + 2\mathbf{Q}X + \mathbf{A}^{\mathrm{T}}\mu) = 0 \end{cases} \tag{5.59}$$

$$\begin{cases} \mu_i g_i(X) = 0, i = 1, \dots, m \\[2mm] \mu(\mathbf{A}X - \mathbf{B}) = 0 \end{cases} \tag{5.60}$$

$$\begin{cases} X \geq 0 \\ \mu \geq 0 \end{cases} \qquad (5.61)$$

If we introduce nonnegative surplus variables **y** to the inequalities in equation (5.57) and nonnegative slack variables **v** to the inequalities in equation (5.58), we get the following equivalent form.

$$\mathbf{C}^{\mathrm{T}} + 2\mathbf{Q}X + \mathbf{A}^{\mathrm{T}}\mu^{\mathrm{T}} - y = 0 \qquad (5.62)$$

$$\mathbf{A}X - \mathbf{B} + v = 0 \qquad (5.63)$$

Then, the KT conditions can be written as below:

$$2\mathbf{Q}X + \mathbf{A}^{\mathrm{T}}\mu^{\mathrm{T}} - y = -\mathbf{C}^{\mathrm{T}} \qquad (5.64)$$

$$\mathbf{A}X + v = \mathbf{B} \qquad (5.65)$$

$$X \geq 0, \mu \geq 0, y \geq 0, v \geq 0 \qquad (5.66)$$

$$y^{\mathrm{T}}X = 0, \mu v = 0 \qquad (5.67)$$

The first two expressions are linear equalities, the third restricts all the variables to be nonnegative, and the fourth is the complementary slackness condition.

Obviously, the KT conditions in equations (5.64)–(5.67) have a linear form with the variables X, μ, y, and v. An approach similar to the modified simplex can be used to solve equations (5.64)–(5.67). The procedures of the algorithm are as below:

(1) Let the structural constraints be equations (5.64) and (5.65) defined by the KT conditions.
(2) If any of the right-hand-side values are negative, multiply the corresponding equation by –1.
(3) Add an artificial variable to each equation.
(4) Let the objective function be the sum of the artificial variables.
(5) Put the resultant problem into simplex form.

The goal is to find the solution to the linear programming problem that minimizes the sum of the artificial variables with the additional requirement that the complementary slackness conditions be satisfied at each iteration. If the sum is zero, the solution will satisfy equations (5.64)–(5.67). To accommodate equation (5.67), the rule for selecting the entering variable must be modified with the following relationships:

$$X_j \text{ and } y_j \text{ are complementary for } j = 1, \ldots, n$$

$$\mu_i \text{ and } v_i \text{ are complementary for } i = 1, \ldots, m$$

The entering variable will be that whose reduced cost is most negative provided that its complementary variable is not in the basis or would leave the basis on the same iteration. At the conclusion of the algorithm, the vector **x** defines the optimal solution and the vector μ defines the optimal dual variables.

This approach has been shown to work well when the objective function is positive definite, and requires computational effort comparable to a linear programming problem with $m + n$ constraints, where m is the number of constraints and n is the number of variables in the QP. Fortunately, the objective function in economic power dispatch is positive definite. Thus this approach is very good for solving the QP model of economic dispatch.

5.3.3 Implementation

The first example is to solve the following QP problem using the mentioned algorithm in Section 5.3.2.

$$\min f(x) = x_1^2 + 4x_2^2 - 8x_1 - 16x_2$$

subject to

$$x_1 + x_2 \leq 5$$

$$x_1 \leq 3$$

$$x_1 \geq 0, \quad x_2 \geq 0$$

Solution: Convert the problem into the following quadratic programming model:

$$\min f(X) = \mathbf{C}X + X^{\mathrm{T}}\mathbf{Q}X$$

s.t.

$$\mathbf{A}X \leq \mathbf{B}$$

$$X \geq 0$$

where

$$\mathbf{C}^{\mathrm{T}} = \begin{bmatrix} -8 \\ -16 \end{bmatrix}$$

$$\mathbf{Q} = \begin{bmatrix} 1 & 0 \\ 0 & 4 \end{bmatrix}$$

$$\mathbf{A} = \begin{bmatrix} 1 & 1 \\ 1 & 0 \end{bmatrix}$$

$$\mathbf{B} = \begin{bmatrix} 5 \\ 3 \end{bmatrix}$$

$$\mathbf{X} = \begin{bmatrix} x_1 \\ x_2 \end{bmatrix}$$

As can be seen, the **Q** matrix is positive definite so the KT conditions are necessary and sufficient for a global optimum.

Let

$$y = \begin{bmatrix} y_1 \\ y_2 \end{bmatrix}$$

$$v = \begin{bmatrix} v_1 \\ v_2 \end{bmatrix}$$

$$\mu = \begin{bmatrix} \mu_1 \\ \mu_2 \end{bmatrix}$$

According to equations (5.64) and (5.65), we get

$$2x_1 + \mu_1 + \mu_2 - y_1 = 8$$
$$8x_2 + \mu_1 - y_2 = 16$$
$$x_1 + x_2 + v_1 = 5$$
$$x_1 + v_2 = 3$$

To create the appropriate linear programming problem, we add artificial variables to each constraint and minimize their sum.

$$\min Z = w_1 + w_2 + w_3 + w_4$$

s.t.

$$2x_1 + \mu_1 + \mu_2 - y_1 + w_1 = 8$$
$$8x_2 + \mu_1 - y_2 + w_2 = 16$$
$$x_1 + x_2 + v_1 + w_3 = 5$$
$$x_1 + v_2 + w_4 = 3$$
$$x_1 \geq 0, x_2 \geq 0, y_1 \geq 0, y_2 \geq 0, v_1 \geq 0, v_2 \geq 0, \mu_1 \geq 0, \mu_2 \geq 0,$$

Applying the presented algorithm to this example, the optimal solution to the original problem is $(x_1^*, x_2^*) = (3, 2)$. Table 5.10 shows the iterations of the solution.

The second example is to apply the presented QP algorithm to solve the real power economic dispatch problem. The testing system is the IEEE 30-bus system, the data of which are given in Section 5.2. The following testing cases are conducted.

Case 1: IEEE 30-bus system with the original data
Case 2: IEEE 30-bus system with the original data, but the limit of line 1 is reduced to 1.0 p.u.

The security economic dispatch results for two cases are shown in Table 5.11. The results of case 1 are also compared with those obtained by using linear programming, which are shown in Table 5.12. It can be observed that the ED results obtained by QP are a little better than those obtained by LP.

Table 5.10   Iterations for QP example

Iterations	Basic Variables	Solution	Objective Values	Entering Variable	Leaving Variable
1	(w_1, w_2, w_3, w_4)	(8,16,5,3)	32	x_2	w_2
2	(w_1, x_2, w_3, w_4)	(8,2,3,3)	14	x_1	w_3
3	(w_1, x_2, x_1, w_4)	(2,2,3,0)	2	μ_1	w_4
4	(w_1, x_2, x_3, μ_1)	(2,2,3,0)	2	μ_1	w_1
5	(μ_1, x_2, x_3, μ_1)	(2,2,3,0)	0	/	/

Table 5.11   Economic dispatch results by QP for IEEE 30-bus system

Generation No.	Case 1	Case 2
P_{G1}	1.7586	1.5174
P_{G2}	0.4883	0.5670
P_{G5}	0.2151	0.2326
P_{G8}	0.2233	0.3045
P_{G11}	0.1231	0.1517
P_{G13}	0.1200	0.1400
Total generation	2.9285	2.9132
Total real power losses	0.0945	0.0792
Total generation cost ($)	802.3900	807.2400

Table 5.12   ED results and comparison between QP and LP for IEEE 30-bus system

Generation No.	QP Method	LP Method
P_{G1}	1.7586	1.7626
P_{G2}	0.4883	0.4884
P_{G5}	0.2151	0.2151
P_{G8}	0.2233	0.2215
P_{G11}	0.1231	0.1214
P_{G13}	0.1200	0.1200
Total generation	2.9285	2.9290
Total real power losses	0.0945	0.0948
Total generation cost ($)	802.3900	802.4000

5.4   NETWORK FLOW PROGRAMMING METHOD

5.4.1   Introduction

Network flow programming (NFP) is a specialized linear programming. It is characterized by simple manipulation and rapid convergence. NFP models of N security economic dispatch have been proposed in recent years.

This section first presents a network flow model and uses the out-of-kilter algorithm (OKA) for solving the online economic power dispatch with N and $N-1$ security. A fast $N-1$ security analysis method solved by OKA is applied to seek out all the overconstrained cases for all possible single line outages, and then an "N − 1 constrained zone" is formed that is coordinated with the network flow model. Based on the normal operating state a corrective incremental network flow model for economic dispatch is established for the over-constrained cases. Consequently, the calculation burden is reduced significantly and the shortcoming of the NFP, imprecision, is mitigated to some extent.

5.4.2   Out-of-Kilter Algorithm

5.4.2.1   OKA Model   According to graph theory, a network with n nodes and m arcs (branches) can be shown as in Figure 5.3(a). The corresponding minimum cost flow problem can be expressed as follows:

$$\min C = \sum_{ij} C_{ij} f_{ij} \quad ij \in m \tag{5.68}$$

such that

$$\sum_{j \in n} (f_{ij} - f_{ji}) = r_i \quad i \in n \tag{5.69}$$

$$L_{ij} \le f_{ij} \le U_{ij} \quad ij \in m \tag{5.70}$$
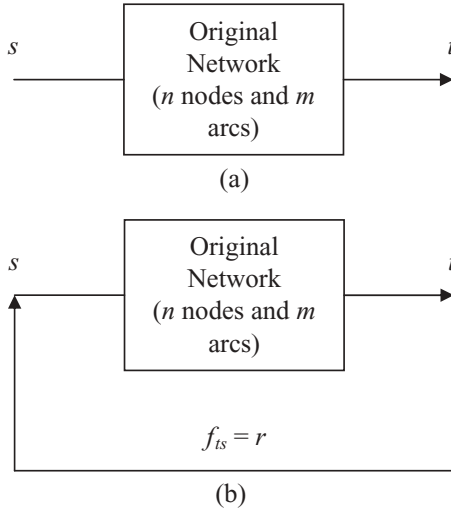
FIGURE 5.3   OKA network model with one source s and one sink t

where

C_{ij}: The arc cost per unit flow
f_{ij}: The flow on arc ij in the network
L_{ij}: The lower bound of the flow on arc ij in the network
U_{ij}: The upper bound of flow on arc ij in the network
n: The total number of the nodes in the network
m: The total number of the arcs in the network

According to the "out-of-kilter" algorithm (OKA) of network flow pro-gramming, we can transform the original network into an OKA network by introducing a "return arc" from sink node t to source node s, while the internal flows remain unchanged. The return arc flow f_{ts} equals the original network flow r. The OKA network model is shown in Figure 5.3(b).

Similarly, if the original network has multiple sources and multiple sinks, which is shown in Figure 5.4(a), the corresponding OKA model can be formed as shown in Figure 5.4(b), where each source corresponds to a source arc con-necting to a total source node s and each sink forms a sink arc connecting to the total sink node t.

The corresponding mathematical model for OKA is given below:

$$\min C = \sum_{ij} C_{ij} f_{ij} \quad ij \in (m + ss + tt + 1) \tag{5.71}$$

such that
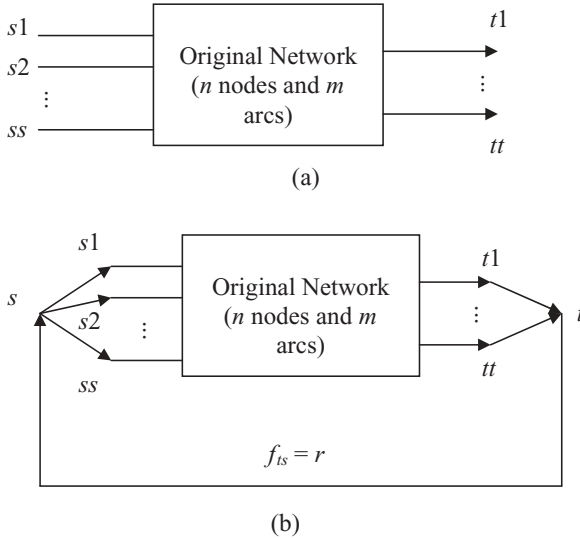
FIGURE 5.4   OKA network model with multiple sources *ss* and multiple sinks *tt*

$$\sum_{j\in n}(f_{ij} - f_{ji}) = 0 \quad i \in n \tag{5.72}$$

$$L_{ij} \leq f_{ij} \leq U_{ij} \quad ij \in (m + ss + tt + 1) \tag{5.73}$$

where *m* is the total number of arcs other than the return arc.

5.4.2.2 Complementary Slackness Conditions for Optimality of OKA

The model consisting of equations (5.71)–(5.73) is a specialized linear pro-gramming model. According to the dual theory, the corresponding primary problem and dual problem can be expressed as below:

Primary Problem

$$\max F' = -\sum_{ij} C_{ij} f_{ij} \tag{5.74}$$

such that

$$\sum_{j\in n}(f_{ij} - f_{ji}) = 0 \tag{5.75}$$

$$L_{ij} \leq f_{ij} \leq U_{ij} \quad i \in n, j \in n, ij \in (m + ss + tt + 1) \tag{5.76}$$

Dual Problem

$$\min G = \sum_{ij} U_{ij}\alpha_{ij} - \sum_{ij} L_{ij}\beta_{ij} \tag{5.77}$$

such that

$$C_{ij} + \pi_i - \pi_j + \alpha_{ij} - \beta_{ij} \geq 0 \tag{5.78}$$

$$\alpha_{ij} \geq 0, \quad \beta_{ij} \geq 0 \quad i \in n, \, j \in n, \, ij \in (m + ss + tt + 1) \tag{5.79}$$

where π is the dual variable of the variable f of the primary problem; α and β correspond to the dual variables of the upper and lower limits of the primary problem.

When all the variables f, π, α, and β meet the requirements of the constraints, there exists the following relationship between the objective functions of primary and dual problems:

$$
\begin{aligned}
G - F' &= \sum_{ij} U_{ij}\alpha_{ij} - \sum_{ij} L_{ij}\beta_{ij} + \sum_{ij} C_{ij}f_{ij} \\
&= 0 \cdot (\pi_s - \pi_t) + \sum_{ij} U_{ij}\alpha_{ij} - \sum_{ij} L_{ij}\beta_{ij} + \sum_{ij} C_{ij}f_{ij} \\
&= \sum_{j}\sum_{i} \pi_i(f_{ij} - f_{ji}) + \sum_{ij} U_{ij}\alpha_{ij} - \sum_{ij} L_{ij}\beta_{ij} + \sum_{ij} C_{ij}f_{ij} \\
&= \sum_{ij} [\pi_i - \pi_j + \alpha_{ij} - \beta_{ij} + C_{ij}]f_{ij} + \sum_{ij} (U_{ij} - f_{ij})\alpha_{ij} + \sum_{ij} (f_{ij} - L_{ij})\beta_{ij} \geq 0
\end{aligned}
\tag{5.80}
$$

It will be true that $G - F' = 0$ if the solution is optimal. Thus from equation (5.80) we get

$$(U_{ij} - f_{ij})\alpha_{ij} = 0 \tag{5.81}$$

$$(f_{ij} - L_{ij})\beta_{ij} = 0 \tag{5.82}$$

$$(C_{ij} + \pi_i - \pi_j + \alpha_{ij} - \beta_{ij})f_{ij} = 0 \tag{5.83}$$

That is,

$$(\overline{C_{ij}} + \alpha_{ij} - \beta_{ij})f_{ij} = 0 \tag{5.84}$$

From equations (5.81)–(5.84), we get:

Case 1: $\overline{C_{ij}} > 0$
If $\beta_{ij} = \overline{C_{ij}} + \alpha_{ij}, f_{ij} \neq 0$
Furthermore, if $\alpha_{ij} \geq 0, \beta_{ij} \neq 0$, then from equation (5.82) we can get

$$f_{ij} = L_{ij}$$

Case 2: $\overline{C_{ij}} < 0$
If $\beta_{ij} = \overline{C_{ij}} + \alpha_{ij}$, then $f_{ij} \neq 0$, and $\alpha_{ij} > \beta_{ij}$

Furthermore, if $\beta_{ij} \geq 0$, $\alpha_{ij} \neq 0$, then from equation (5.81) we can get

$$f_{ij} = U_{ij}$$

Case 3: $\overline{C}_{ij} = 0$

From (5.84), we get $(\alpha_{ij} - \beta_{ij})f_{ij} = 0$, which can be analyzed as follows:

(3a) If $f_{ij} = 0$, then $(\alpha_{ij} - \beta_{ij}) \neq 0$

When $\alpha_{ij} > \beta_{ij}$, then $\alpha_{ij} > 0$, in this way, we get the following expression from equation (5.81):

$$f_{ij} = U_{ij} \neq 0$$

When $\beta_{ij} > \alpha_{ij}$, then $\beta_{ij} > 0$, in this way, we get the following expression from equation (5.82):

$$f_{ij} = L_{ij} \neq 0$$

Both situations are conflicted with the assumption $f_{ij} = 0$. So we can be sure $f_{ij} \neq 0$ for this case.

(3b) Assuming $\alpha_{ij} = 0$, then $\beta_{ij} f_{ij} = 0$

Since $f_{ij} \neq 0$ from (3a), we have $\beta_{ij} = 0$

Therefore, from equation (5.81) we get

$$f_{ij} \leq U_{ij}$$

From equation (5.82) we get

$$f_{ij} \geq L_{ij}$$

that is, if $\overline{C}_{ij} = 0$, then $L_{ij} \leq f_{ij} \leq U_{ij}$

According to the three cases described above, the complementary slackness conditions for optimality of OKA are summarized as follows:

$$f_{ij} = L_{ij} \quad \text{for} \quad \overline{C}_{ij} > 0 \tag{5.85}$$

$$L_{ij} \leq f_{ij} \leq U_{ij} \quad \text{for} \quad \overline{C}_{ij} = 0 \tag{5.86}$$

$$f_{ij} = U_{ij} \quad \text{for} \quad \overline{C}_{ij} < 0 \tag{5.87}$$

where the relative cost is

$$\overline{C}_{ij} = C_{ij} + \pi_i - \pi_j \tag{5.88}$$

According to equations (5.85)–(5.87) and labeling technique, the arcs have nine kinds of states, which are shown in Table 5.13.

Table 5.13   States of OKA arcs

Symbol	$\overline{C}_{ij}$	f_{ij}	State of Arcs
I_1	$\overline{C}_{ij} > 0$	$f_{ij} = L_{ij}$	In-kilter
I_2	$\overline{C}_{ij} = 0$	$L_{ij} < f_{ij} < U_{ij}$	In-kilter
		$f_{ij} = U_{ij}, f_{ij} = L_{ij}$	In-kilter
I_3	$\overline{C}_{ij} < 0$	$f_{ij} = U_{ij}$	In-kilter
II_1	$\overline{C}_{ij} > 0$	$f_{ij} < L_{ij}$	Out-of-kilter
II_2	$\overline{C}_{ij} = 0$	$f_{ij} < L_{ij}$	Out-of-kilter
II_3	$\overline{C}_{ij} < 0$	$f_{ij} < U_{ij}$	Out-of-kilter
III_1	$\overline{C}_{ij} > 0$	$f_{ij} > L_{ij}$	Out-of-kilter
III_2	$\overline{C}_{ij} = 0$	$f_{ij} > U_{ij}$	Out-of-kilter
III_3	$\overline{C}_{ij} < 0$	$f_{ij} > U_{ij}$	Out-of-kilter

The complementary slackness conditions for optimality of OKA shown in equations (5.85)–(5.87) correspond to the three "in-kilter" states of the arcs. In addition, there are six "out-of-kilter" states that do not satisfy conditions (5.85)–(5.87). If all the arcs are in kilter, then the optimal solution is obtained. Otherwise, we must vary the relevant arc flows or node potentials (parameter π) by the labeling technique so that the out-of-kilter states of the arcs come into kilter.

The states of arcs and labeling rules can be explained with Figure 5.5.

In Figure 5.5, if the arc is in the in-kilter state, the point $(f_{ij}, \overline{C}_{ij})$ will be located on one of three dark lines I_1, I_2, and I_3, where the dark line I_1 corresponds to the lower bound L_{ij} of flow f_{ij}; the dark line I_3 corresponds to the upper bound U_{ij} of flow f_{ij}; and the dark line I_2 corresponds to the flow f_{ij} that is within $L_{ij} < f_{ij} < U_{ij}$.

If the flow of the arc is violated at the upper or lower limits, the point $(f_{ij}, \overline{C}_{ij})$ will be located out of three dark lines, which correspond to six "out-of-kilter" states in Figure 5.5. In these situations, the value of flow of the arc will be either less than its lower limit or higher than its upper limit, that is, $f_{ij} > U_{ij}$ or $f_{ij} < L_{ij}$.

5.4.2.3   Labeling Rules and Algorithm of OKA   According to labeling technique, the labeling rules of OKA for the forward arc and backward arc under nine OKA states in Table 5.13 are listed in Table 5.14, where symbol "↑" stands for increase, "↓" stands for reduce, "→" stands for change, and "f_k" indicates that the flow is outside of the feasible region.
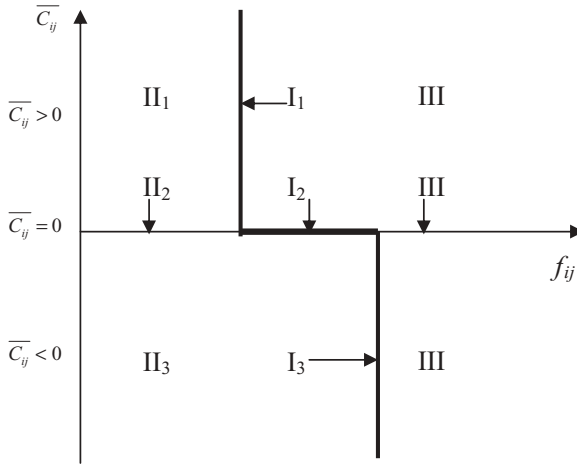
FIGURE 5.5 States of OKA arcs

Table 5.14 Labeling rules of OKA algorithm

Symbol	f_{ij}	Forward Arc f^+ Labeling? Why?	Backward arc f^- Labeling? Why?
I_1	$f_{ij} = L_{ij}$	No, $f^+ \uparrow \to f_k^+$	No, $f^- \downarrow \to f_k^-$
I_2	$L_{ij} < f_{ij} < U_{ij}$	Yes, $f^+ \uparrow \to U$	Yes, $f^- \downarrow \to L$
	$f_{ij} = U_{ij}\, f_{ij} = L_{ij}$	No, $f^+ \uparrow \to f_k^+$	No, $f^- \downarrow \to f_k^-$
I_3	$f_{ij} = U_{ij}$	No, $f^+ \uparrow \to f_k^+$	No, $f^- \downarrow \to f_k^-$
II_1	$f_{ij} < L_{ij}$	Yes, $f^+ \uparrow \to U$	No, $f^- \downarrow \to f_k^-$
II_2	$f_{ij} < L_{ij}$	Yes, $f^+ \uparrow \to U$	No, $f^- \downarrow \to f_k^-$
II_3	$f_{ij} < U_{ij}$	Yes, $f^+ \uparrow \to U$	No, $f^- \downarrow \to f_k^-$
III_1	$f_{ij} > L_{ij}$	No, $f^+ \uparrow \to f_k^+$	Yes, $f^- \downarrow \to L$
III_2	$f_{ij} > U_{ij}$	No, $f^+ \uparrow \to f_k^+$	Yes, $f^- \downarrow \to L$
III_3	$f_{ij} > U_{ij}$	No, $f^+ \uparrow \to f_k^+$	Yes, $f^- \downarrow \to U$

According to the labeling rules mentioned above, the out-of-kilter algorithm is implemented as follows.

5.4.2.3.1 With incremental flow Loop When there exists an incremental flow loop, correct the values of flow for all arcs in the loop. The process is as below:

(1) For forward arcs
    (a) If $\overline{C_{ij}} \geq 0, f_{ij} < L_{ij}$, the node j is able to be labeled. The incremental flow to the node j will be computed as

$$q_j = \min[q_i, L_{ij} - f_{ij}] \tag{5.89}$$

(b) If $\overline{C_{ij}} \leq 0$, $f_{ij} < U_{ij}$, the node j is able to be labeled. The incremental flow to the node j will be computed as

$$q_j = \min[q_i, U_{ij} - f_{ij}] \tag{5.90}$$

(2) For backward arcs

(a) If $\overline{C_{ji}} \geq 0$, $f_{ji} > L_{ji}$, the node j is able to be labeled. The incremental flow to the node j will be computed as

$$q_j = \min[q_i, f_{ji} - L_{ji}] \tag{5.91}$$

(b) If $\overline{C_{ji}} \leq 0$, $f_{ji} > U_{ji}$, the node j is able to be labeled. The incremental flow to the node j will be computed as

$$q_j = \min[q_i, f_{ji} - U_{ji}] \tag{5.92}$$

5.4.2.3.2 Without Incremental Flow Loop When there does not exist an incremental flow loop, correct the values of the relative cost $\overline{C_{ij}}$, or $\overline{C_{ji}}$ by increasing the cost of the vertex π. This is because the change of $\overline{C_{ij}}$, or $\overline{C_{ji}}$ causes the change of the path of minimum cost flow. Consequently, a new incremental flow loop will be produced. The process of computing the incremental vertex cost is as below.

Let B and $\overline{B}$ stand for the set of the labeled vertexes and unlabeled vertexes, respectively. Obviously, the super source $s \in B$, and super sink $t \in \overline{B}$. In addition, define two sets of arcs A_1 and A_2:

$$A_1 = \{ij, i \in B, j \in \overline{B}, \overline{C_{ij}} > 0, f_{ij} \leq U_{ij}\} \tag{5.93}$$
$$A_2 = \{ji, i \in B, j \in \overline{B}, \overline{C_{ji}} < 0, f_{ji} \geq L_{ij}\} \tag{5.94}$$

The incremental vertex cost is determined as below

$$\delta = \min\{\delta_1, \quad \delta_2\} \tag{5.95}$$

where

$$\delta_1 = \min\{|\overline{C_{ij}}|\} > 0 \tag{5.96}$$
$$\delta_2 = \min\{|\overline{C_{ji}}|\} > 0 \tag{5.97}$$

If A_1 is an empty set, make $\delta_1 = \infty$; If A_2 is an empty set, make $\delta_2 = \infty$. When $\delta = \infty$, it means there is no feasible flow, which is no solution for the given NFP problem. When $\delta < \infty$, update the vertex costs for all unlabeled vertexes, that is,

$$\delta' = \pi_j + \delta \quad j \in \bar{B} \tag{5.98}$$

In this way, the out-of-kilter arc will be changed into an in-kilter arc. When all arcs are in in-kilter states, the optimum solution is obtained.

The procedures of the OKA algorithm are as follows:

Step 1. Set the initial values of the arc flows. The initial flows are requested to satisfy constraint (5.72) only, but not necessarily constraint (5.73).

Step 2. Check the state of the arcs. If all arcs are in kilter, then the optimal solution has been found. Terminate the iteration. Otherwise, go to step 3.

Step 3. Revise the state of the arcs. Arbitrarily choose an arc from the set of arcs, which is out of kilter, to be revised. Using the labeling technique, when a flow-augmenting loop exists, vary the values of flow f_{ij} for all arcs in this loop. If no flow-augmenting loop is found, adjust the values of π at unlabeled nodes, and hence change the relative cost $\overline{C}_{ij}$, or $\overline{C}_{ji}$. This may need some cross-iterations between flow and the relative cost so that the out-of-kilter arc can be become an in-kilter arc. Once the arc state has been revised, go back to step 2.

It should be noted that the revision process converges after a finite number of iterations.

In comparison with the general algorithm of the minimum cost flow, the main features of the OKA are:

(1) The nonzero lower bound of flow may be allowable.
(2) The initial flow does not have to be feasible or zero flow.
(3) Nonnegative constraints, $f_{ij} \geq 0$, are released.
(4) It is easy to imitate a change in network topology by changing the specified bound values of the flows as the branch outage occurs.

5.4.3 *N* Security Economic Dispatch Model

In the normal operating case, the NFP model of real power economic dispatch with N security can be written as follows:

$$\min F^0 = \sum_{i \in NG} (a_i P_{Gi}^{0\,2} + b_i P_{Gi}^0 + c_i) + h \sum_{j \in NT} R_j P_{Tj}^{0\,2} \tag{5.99}$$

such that

$$\sum_{i(\omega)} P_{Gi}^0 + \sum_{j(\omega)} P_{Tj}^0 + \sum_{k(\omega)} \hat{P}_{Dk}^0 = 0 \quad \omega \in n \tag{5.100}$$

$$\underline{P_{Gi}} \leq P_{Gi}^0 \leq \overline{P_{Gi}} \tag{5.101}$$

$$P_{\mathrm{T}j} \leq P_{\mathrm{T}j}^0 \leq \overline{P_{\mathrm{T}j}} \quad i \in NG, j \in NT, k \in ND \tag{5.102}$$

where

   a_i, b_i, and c_i: The cost coefficients of the ith generator.

   $P_{\mathrm{G}i}^0$: The real power flow of generation arc i in the normal operating case

   $P_{\mathrm{T}i}^0$: The real power flow of transmission arc j in the normal operating case

   $P_{\mathrm{D}k}^0$: The real power flow of load arc k in the normal operating case

   NG: The total number of generation arcs

   NT: The total number of transmission arcs

   ND: The total number of load arcs

   N: The total number of nodes

   R_j: The resistance of transmission arc (line) j

   $\underline{P}$: The lower bound of the real power flow through the arc

   $\overline{P}$: The upper bound of the real power flow through the arc

The positive direction of flow is specified as the flow enters into the node and the negative as it leaves the node. The symbol $i(w)$ means that arc i is adjacent to node w; so do $j(w)$ and $k(w)$.

The following points should be noted.

(1) The second term of the objective,

$$h \sum_{j \in NT} R_j P_{\mathrm{T}j}^{0\,2} \tag{5.103}$$

is the penalty on transmission losses with the system marginal cost h (in \$ per MWh). The total transmission loss is represented approximately, but validly, as the sum of the products of the line resistance and the square of the transmitted power on the line. This is obtained from the following real power loss expression of the transmission line:

$$P_{\mathrm{L}j} = \frac{P_{\mathrm{T}j}^2 + Q_{\mathrm{T}j}^2}{V_{\mathrm{T}j}^2} \times R_j \tag{5.104}$$

under the assumptions of 1.0 p.u. flat voltage across the line and local supply of the reactive power.

(2) The power loss of an individual line is assumed to be distributed equally to its ends. Thus the real load $P_{\mathrm{D}k}^0$ in equation (5.100) would involve half the transmission losses on all the lines connected to node k, which are estimated preliminarily from the power flow calculation of the normal operation and kept constant, or modified if necessary, that is,

$$\hat{P}_{Dk}^0 = P_{Dk}^0 + \frac{1}{2}\sum_{j \to k} R_j P_{Tj}^{0\,2} \tag{5.105}$$

Another half of the loss of the line that is not related to load will be added on the flow of the return arc of the OKA network model.

(3) The transmitted real power acts as the independent variable, and the line security constraints are introduced into the model straight away. The secure line limit is based on its SIL and its length, and not on the thermal limit.

(4) The topology of the power system is preserved since the penalty factors are not calculated in the usual sense. Therefore, the model can be solved easily by NFP as well as the OKA.

Although this model is different from the traditional economic dispatch model, it is verified that they are equivalent [4, 10].

The objective function of economic power dispatch in equation (5.99) is a quadratic function. It can be linearized by use of the average cost. From the previous section, we know that the OKA network model of economic power dispatch consists of three types of arcs. These are the generation arc, the transmission arc and the load arc. Obviously, each generation arc corresponds to a generator, each transmission arc corresponds to a line or transformer, and each load arc corresponds to a real power demand. In addition, there is a return arc. The total arcs in a power network will be $m + 1$, where $m = NG + NT + ND$.

Comparing the economic dispatch model shown in equations (5.99)–(5.102) with the OKA model shown in equations (5.71)–(5.73), the average cost and flow limits of each type of arc are

(a) The generation arc:

$$\overline{C_{ij}} = a_i P_{Gi} + b_i \tag{5.106}$$

$$L_{ij} = \underline{P_{Gi}} \tag{5.107}$$

$$U_{ij} = \overline{P_{Gi}} \tag{5.108}$$

(b) The transmission arc:

$$\overline{C_{ij}} = h R_j P_{Tj} \tag{5.109}$$

$$L_{ij} = \underline{P_{Tj}} \tag{5.110}$$

$$U_{ij} = \overline{P_{Tj}} \tag{5.111}$$

(c) The load arc:

$$\overline{C_{ij}} = 0 \tag{5.112}$$

$$L_{ij} = \hat{P}_{Dk}^0 \tag{5.113}$$

$$U_{ij} = \hat{P}_{Dk}^0 \tag{5.114}$$

(d) The return arc:

$$\overline{C_{ij}} = 0 \tag{5.115}$$

$$L_{ij} = \sum_{k \in ND} \hat{P}_{Dk}^0 + \frac{1}{2} \sum_{j \in NT} R_j P_{Tj}^{0\,2} \tag{5.116}$$

$$U_{ij} = \sum_{k \in ND} \hat{P}_{Dk}^0 + \frac{1}{2} \sum_{j \in NT} R_j P_{Tj}^{0\,2} \tag{5.117}$$

If the network loss is neglected in the economic dispatch OKA model, the cost of transmission arc will be zero; load $\hat{P}_{Dk}$ will be replaced by P_{Dk}. Meanwhile, the part of power loss in the return arc will be zero, too.

It is noted that the flow P_{ts} on the return arc contains the total loads and network losses, i.e.,

$$P_{ts} = \sum_{k \in ND} \hat{P}_{Dk}^0 + \frac{1}{2} \sum_{j \in NT} R_j P_{Tj}^{0\,2} \tag{5.118}$$

Substituting equation (5.105) into equation (5.118), we get

$$
\begin{aligned}
P_{ts} &= \sum_{k \in ND} \left(P_{Dk}^0 + \frac{1}{2} \sum_{j \to k} R_j P_{Tj}^{0\,2} \right) + \frac{1}{2} \sum_{j \in NT} R_j P_{Tj}^{0\,2} \\
&= \sum_{k \in ND} \left(P_{Dk}^0 \right) + \frac{1}{2} \sum_{j \in NT} R_j P_{Tj}^{0\,2} + \frac{1}{2} \sum_{j \in NT} R_j P_{Tj}^{0\,2} \\
&= \sum_{k \in ND} \left(P_{Dk}^0 \right) + \sum_{j \in NT} R_j P_{Tj}^{0\,2} \\
&= P_D + P_L
\end{aligned}
\tag{5.119}
$$

Obviously, the KCL law at the super source node that connects to the return arc will be

$$\sum_{i=1}^{NG} P_{Gi} = P_D + P_L \tag{5.120}$$

This is exactly the real power balance equation in the traditional real power economic dispatch model. Thus it is very easy to compute network losses in the economic dispatch OKA model, which becomes to adjust the flow in the flow-augmenting loop that contains the return arc.

5.4.4   Calculation of *N* – 1 Security Constraints

In the theoretical sense, the total number of $N-1$ security constraints is very large and equals $n(n-1)$ for the system with n transmission and transformer branches. In the practical sense, power transmission systems are usually designed well within the capacity of the system load and generation. Only a small proportion of lines may be overloaded, even if a single branch outage occurs. Therefore, it is neither necessary nor reasonable to incorporate all the $N-1$ security constraints into the calculation model directly. To detect all the possible overconstrained cases, which must be considered, a fast contingency analysis for a single line outage must be performed [20, 21].

Based on the normal generation schedule obtained from model M-1, the NFP model M-2 of $N-1$ security analysis is presented as

$$\min F_l = \sum_{j \in NT} R_j P_{\mathrm{T}j}^{\;2}(l) \tag{5.121}$$

such that

$$\sum_{i(\omega)} P_{\mathrm{G}i}^{0} + \sum_{j(\omega)} P_{\mathrm{T}j}(l) + \sum_{k(\omega)} P_{\mathrm{D}k}^{0} = 0 \quad \omega \in n \tag{5.122}$$

$$|P_{\mathrm{T}j}(l)| \le \gamma \overline{P_{\mathrm{T}j}} \quad l \in NL \tag{5.123}$$

$$P_{\mathrm{T}l} = 0 \tag{5.124}$$

where

$P_{\mathrm{T}j}(l)$: The real power transmitted in line j while line l is in outage

NL: The set of the outage lines

γ: A constant greater than unity (say $1 < \gamma < 1.3$)

The differences between models M-1 and M-2 are the following:

(1) The generation production costs in the objective equation (5.99) and the inequality constraint equation (5.100) vanish, since all the generations and loads remain unchanged.
(2) Only the transmitted real power $P_{\mathrm{T}j}(l)$ acts as a variable to adjust the power flows. The inequality constraint equation (5.123) has replaced equation (5.102). The constant γ is introduced to find the overloaded line when line l appears as an outage.

Once the overconstrained cases have been detected, the maximum value of the violation in line j can be determined by the following equations:

$$\Delta \overline{P_{\mathrm{T}j}} = \max_{l \in NL} \left\{ P_{\mathrm{T}j}(l) - \overline{P_{\mathrm{T}j}} \right\} \quad j \in NT1 \tag{5.125}$$

$$\Delta \underline{P_{Tj}} = \min_{l \in NL} \left\{ P_{Tj}(l) - \underline{P_{Tj}} \right\} \quad j \in NT2 \tag{5.126}$$

where $NT1$ and $NT2$ represent the number of lines that violate their upper and lower bounds, respectively, as line l appears as an outage.

5.4.5 $N - 1$ Security Economic Dispatch

There is no guarantee that the economic schedules with N security in normal operation will not violate the line limits if a single contingency occurs (or multiple contingencies occur). If such a situation does arise, it is necessary to reallocate the generations so that the line constraints are satisfied. An efficient approach to incorporating $N - 1$ security constraints as a part of economic dispatch is therefore desirable. Based on the normal case with consideration of N security and the fast contingency analysis, the network flow model M-3 of $N - 1$ security economic power dispatch is presented as follows:

$$\min \Delta F = \sum_{i \in NG} \left(\left. \frac{\partial f_i}{\partial P_{Gi}} \right|_{P_{Gi}^0} \Delta P_{Gi} \right) + h \sum_{j \in NT} \left(\left. \frac{\partial P_{Lj}}{\partial P_{Tj}} \right|_{P_{Tj}^0} \Delta P_{Tj} \right) \tag{5.127}$$

such that

$$\sum_{i(\omega)} \Delta P_{Gi} + \sum_{j(\omega)} \Delta P_{Tj} = 0 \quad \omega \in (NG + NT) \tag{5.128}$$

$$\underline{P_{Gi}} - P_{Gi}^0 \le \Delta P_{Gi} \le \overline{P_{Gi}} - P_{Gi}^0 \quad i \in NG \tag{5.129}$$

$$|\Delta P_{Gi}| \le \Delta \overline{P_{Grci}} \quad i \in NG \tag{5.130}$$

$$\Delta P_{Tj} = -\Delta \overline{P_{Tj}} \quad j \in NT1 \tag{5.131}$$

$$\Delta P_{Tj} = -\Delta \underline{P_{Tj}} \quad j \in NT2 \tag{5.132}$$

$$\underline{P_{Tj}} - P_{Tj}^0 \le \Delta P_{Tj} \le \overline{P_{Tj}} - P_{Tj}^0 \quad j \in (NT - NT1 - NT2) \tag{5.133}$$

where ΔP_{Gi} and ΔP_{Tj} are the incremental generations and transmissions, respectively. The incremental generation and transmission costs are

$$\left. \frac{\partial f_i}{\partial P_{Gi}} \right|_{P_{Gi}^0} = 2a_i P_{Gi}^0 + b_i \tag{5.134}$$

$$\left. \frac{\partial P_{Lj}}{\partial P_{Tj}} \right|_{P_{Tj}^0} = 2R_j P_{Tj}^0 \tag{5.135}$$

ΔF is the objective that is the total incremental product cost.

Obviously, M-3 is an incremental optimization model. The following issues should be noted.

(1) The objective equation (5.127) and the equality constraint equation (5.128) are obtained under the assumption that the loads are held constant, that is, $\Delta P_{Dk} = 0$. Exceptionally, if there is no feasible solution for problem M-3 in the preventive control, some loads would be curtailed partially or completely, so that the problem becomes solvable. In this case, the incremental loads may act as the variable introduced into M-3 without the cost. The contents of load shedding can be found in Chapter 11.

(2) To realize the transition from the N to the $N-1$ security schedule successfully, the limits of the real power generation regulations (regulating speeds), ΔP_{Grci} must be considered. These are determined from the product of the relevant regulating speed and the regulating time specified. Thus the regulating value of the generation is restricted by the two inequality equations (5.129) and (5.130), which can be combined into one expression:

$$\max\left\{-\Delta\overline{P_{Grci}}, \underline{P_{Gi}} - P_{Gi}^0\right\} \le \Delta P_{Gi} \le \min\left\{\Delta\overline{P_{Grci}}, \overline{P_{Gi}} - P_{Gi}^0\right\} \quad i \in NG \quad (5.136)$$

(3) If any critical single line outage occurs, then the line security zone will be contracted to some extent. Equations (5.131)–(5.133) reflect the changing number of line security constraints. Recalling equations (5.125) and (5.126), an "$N-1$ constrained zone," which is in fact formed by the intersection of the secure zones for all single contingencies, can be determined from these equations. This means that an $N-1$ security problem with the same number of constraints as in the N security problem can be introduced into the network flow model.

Substituting equations (5.125), (5.126), and (5.134)–(5.136) into model M-3, the incremental network flow model of economic dispatch with $N-1$ security, model M-4, becomes

$$\min \Delta F = \sum_{i \in NG} \left(2a_i P_{Gi}^0 + b_i\right)\Delta P_{Gi} + h\sum_{j \in NT}\left(2R_j P_{Tj}^0\right)\Delta P_{Tj} \quad (5.137)$$

such that

$$\sum_{i(\omega)}\Delta P_{Gi} + \sum_{j(\omega)}\Delta P_{Tj} = 0 \quad \omega \in (NG + NT) \quad (5.138)$$

$$\max\left\{-\Delta\overline{P_{Grci}}, \underline{P_{Gi}} - P_{Gi}^0\right\} \le \Delta P_{Gi} \le \min\left\{\Delta\overline{P_{Grci}}, \overline{P_{Gi}} - P_{Gi}^0\right\} \quad i \in NG \quad (5.139)$$

$$\Delta\overline{P_{Tj}} = -\max_{l \in NL}\left\{P_{Tj}(l) - \overline{P_{Tj}}\right\} \quad j \in NT1 \quad (5.140)$$

$$\Delta\underline{P_{Tj}} = -\min_{l \in NL}\left\{P_{Tj}(l) - \underline{P_{Tj}}\right\} \quad j \in NT2 \quad (5.141)$$

$$\underline{P_{Tj}} - P_{Tj}^0 \le \Delta P_{Tj} \le \overline{P_{Tj}} - P_{Tj}^0 \quad j \in (NT - NT1 - NT2) \quad (5.142)$$

The linear model M-4 corresponds to the OKA model and it can be solved easily by the out-of-kilter algorithm.

It is noted that model M-4 can provide the bigeneration schedule, that is, the normal generation schedule from model M-1 is used in the normal operation state, while the postfault generation schedule from model M-4 is only used in the postcontingency case. Furthermore, it can also be used as a single generation schedule, which is applied both in the normal case and in post-contingency, that is, the unique generation schedule not only guarantees secure operation in the normal case but it also avoids the occurrence of an overload in a possible single contingency. This scheme is easy to implement because no rescheduling is needed. However, because all the $N-1$ line security constraints have to be satisfied, the constraint region is very narrow, and hence the operating cost increases.

5.4.6   Implementation

5.4.6.1   *Major Procedures of the OKA*   The essence of the OKA is to revise the out-of-kilter states of arcs to in-kilter states according to complementary slackness conditions for optimality equations (5.85)–(5.87). It should be noted that the correction process converges after a finite number of iterations. A numerical example, which is taken from reference [2] to illustrate the solution procedures, is given below.

The problem is to solve a secure economic dispatch of a simple power system shown in Figure 5.6. There are two generators (PG_1 and PG_2) and three transmission lines to supply a load P_D. The system parameters are as follows.

$$F_1(P_{G1}) = C_1 P_{G1} = 2P_{G1}$$

$$F_2(P_{G2}) = C_2 P_{G2} = 5P_{G2}$$

$$0 \le P_{Gi} \le 2$$

$$0 \le P_{G2} \le 2$$
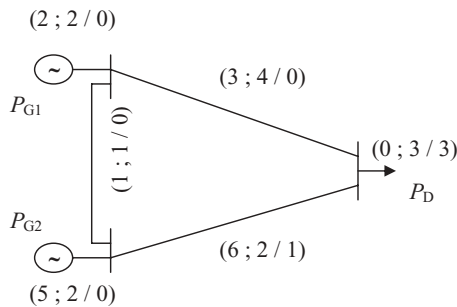
FIGURE 5.6   A simple power system (C_{ij}; U_{ij}/L_{ij})

$$P_D = 3$$

$$0 \le P_{l1} \le 1$$

$$0 \le P_{l2} \le 4$$

$$1 \le P_{l1} \le 2$$

where, $l1$ is the line between the two generators PG_1 and PG_2; $l2$ is the line from the generator PG_1 to load P_D; and $l3$ is the line from the generator PG_2 to the load P_D.

For simplification, the network loss is neglected. Then the economic dispatch model for this example can be written as follows:

$$\min F = 2P_{G1} + 5P_{G2}$$

s.t.

$$P_{G1} + P_{G2} = 3$$

$$0 \le P_{Gi} \le 2$$

$$0 \le P_{G2} \le 2$$

$$0 \le P_{l1} \le 1$$

$$0 \le P_{l2} \le 4$$

$$1 \le P_{l1} \le 2$$

This economic dispatch problem can be expressed as the OKA network flow model as mentioned above.

The corresponding network flow model for the OKA is depicted in Figure 5.7. The solution process of the OKA is demonstrated below:

(1) Assign the initial values: $f_{13} = f_{32} = f_{24} = f_{41} = 2$, $f_{12} = f_{34} = 0$, and $\pi_1 = \pi_2 = \pi_3 = \pi_4 = 0$. These values and the relevant parameters are given in Figure 5.8(a). Then calculate the relative cost $\overline{C_{ij}}$.
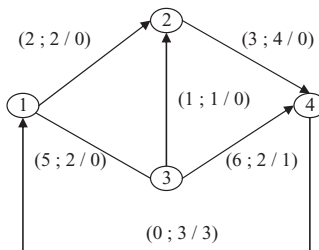
FIGURE 5.7 Network flow model for the OKA corresponding to Figure 5.6
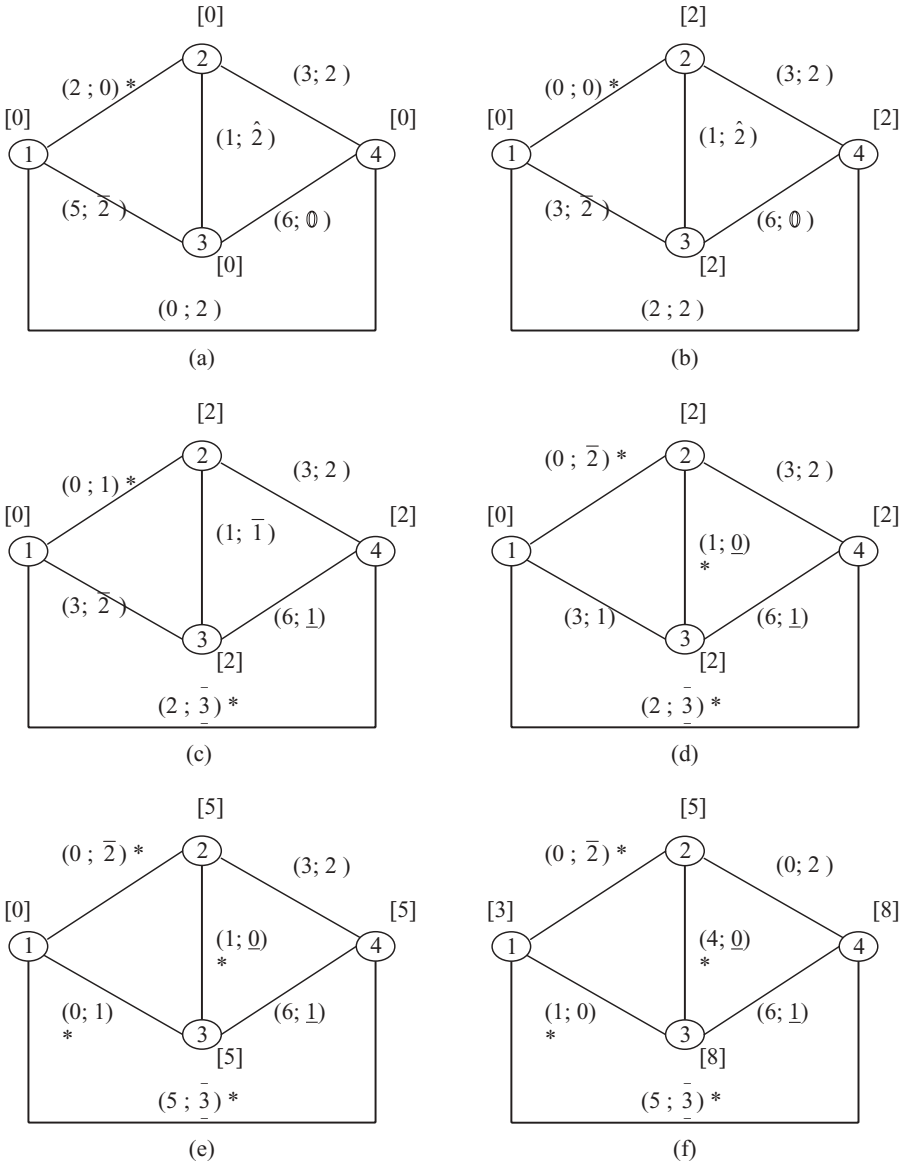
FIGURE 5.8 The solution process of the OKA

(2) Check the state of the arcs. From Figure 5.8(a) we know that all the arcs are out of kilter except arc 1-2 marked with a star.

(3) Choose an out-of-kilter arc, say arc 4-1. By the labeling technique, no flow-augmenting loop exists, since only node 1 can be labeled, but

nodes 2-4 cannot. Then change the value of π at nodes 2-4 as shown in Figure 5.8(b). In this case, arc 4-1 is still out of kilter, but all the nodes can be labeled. Then, a flow-augmenting loop 1-2-3-4-1 is found and the augmenting value is equal to unity. After the flows in this loop are adjusted, the result is shown in Figure 5.8(c). Now, arc 4-1 comes into kilter, and so does arc 3-4 at the same time.

(4) Again check the state of the arcs. We can observe that arcs 1-3, 3-2, and 2-4 are out of kilter.

(5) Choose arc 1-3 to be revised. The flow-augmenting loop 1-2-3-1 is obtained since nodes 1, 2, and 3 can be labeled. Then modify the relevant flows; the results are given in Figure 5.8(d). In this case, arc 1-3 is still out of kilter and the nodes cannot be labeled, except node 1. Through changing the values of π and $\overline{C_{ij}}$, arc 1-3 comes into kilter, as shown in Figure 5.8(e).

(6) Check the state of the arcs once more. Only arc 2-4 is in the out-of-kilter state.

(7) Revise the state of arc 2-4. No flow-augmenting loop exists since only node 2 can be labeled. After the values of π and $\overline{C_{ij}}$ at nodes 1, 3, and 4 have been changed, arc 2-4 comes into kilter, as shown in Figure 5.8(f).

(8) By checking the state of the arcs, we see that all the arcs are in kilter and all conditions for optimality have been satisfied. This shows that the optimal (minimum cost) power flow of the system is obtained. Stop the iteration.

The optimal results are:

(1) The relevant cost:

$$\overline{C_{12}} = 0, \overline{C_{13}} = 0, \overline{C_{23}} = 4, \overline{C_{24}} = 0, \overline{C_{34}} = 6, \overline{C_{41}} = 5$$

(2) The vertex cost:

$$\pi_1 = 3, \pi_2 = 5, \pi_3 = 8, \pi_4 = 8,$$

(3) Flow on the arcs:

$$f_{12} = 2, f_{13} = 1, f_{23} = 0, f_{24} = 2, f_{34} = 1, f_{41} = 3$$

5.4.6.2 *Numerical Example of Economic Dispatch with* N *Security* The proposed model and algorithm are also tested on IEEE 5-bus and 30-bus systems. Table 5.15 is the economic dispatch results of the 5-bus system obtained by OKA algorithm, where the total generation costs are 757.50 \$/hr,

Table 5.15   Economic dispatch by OKA (5-bus system)

Generators or Lines	Real Power (p.u.)	Lower Limit (p.u.)	Upper Limit (p.u.)
P_{G1}	0.9270	0.3000	1.2000
P_{G2}	0.7160	0.3000	1.2000
P_{13}	0.2160	0.0000	1.0000
P_{41}	−0.4110	0.0000	0.5000
P_{51}	−0.3000	0.0000	0.3000
P_{32}	−0.4000	0.0000	0.4000
P_{25}	0.3160	0.0000	1.0000
P_{34}	0.0000	0.0000	0.5000

Table 5.16   Economic dispatch by OKA (30-bus system)

Case	Case 1	Case 2	Case 3	Case 4
P_{G1}(p.u.)	1.7588	1.75000	1.34665	1.69665
P_{G2}(p.u.)	0.4881	0.26236	0.64571	0.33295
P_{G5}(p.u.)	0.2151	0.15000	0.15000	0.15000
P_{G8}(p.u.)	0.2236	0.31270	0.31270	0.31270
P_{G11}(p.u.)	0.1230	0.30000	0.30000	0.30000
P_{G13}(p.u.)	0.12000	0.12000	0.12000	0.12000
Total cost ($/hr)	802.51	813.75	814.24	809.68
Total loss (p.u.)	0.0950	0.0782	0.0793	0.0783

and the total system losses are 0.043 p.u. The results are almost the same as those obtained by linear programming.

The following simulation cases are conducted for 30-bus system.

Case 1: The original data including the power limit of the line.

Case 2: The original data, but the power limit of the lines 2 and 6 are reduced to 0.45 and 0.35 p.u., respectively.

Case 3: The original data, but the power limit of the line 1 is reduced to 0.65 p.u.

Case 4: The original data, but the power limit of the line 1 is reduced to 1.00 p.u.

The corresponding economic dispatch results are shown in Table 5.16.

To analyze the impact of the weighting h to the calculation result, the data of case 3 are used and the different values of h are selected. The results are listed in Table 5.17, which shows that the optimal results are reached when the weighting h equals to 20–25.

Table 5.17 Economic dispatch with different *h* by OKA (30-bus system)

h	>1600	200–1600	29–200	20–25
P_{G1}(p.u.)	0.56236	0.84236	1.34665	1.34665
P_{G2}(p.u.)	0.80000	0.80000	0.29571	0.64571
P_{G5}(p.u.)	0.50000	0.50000	0.15000	0.15000
P_{G8}(p.u.)	0.31270	0.31270	0.31270	0.31270
P_{G11}(p.u.)	0.30000	0.30000	0.30000	0.30000
P_{G13}(p.u.)	0.40000	0.12000	0.12000	0.12000
Total cost ($/hr)	964.86	915.21	872.52	814.24
Total loss (p.u.)	0.0594	0.0620	0.0691	0.0793
Iteration No.	1	1	2	3

Table 5.18 *N* – 1 security analysis and calculation results (IEEE 30-bus system)

Outage Line Number	Overloaded Lines Caused by Outage
1	L_1(1.75662), L_4(1.73162), L_7(−1.08480)
2	L_1(1.75662), L_{10}(0.56510), L_{12}(−0.39087)
4	L_1(1.73162), L_{10}(0.56510), L_{12}(0.39087)
5	L_1(1.73162), L_6(1.30000), L_8(−0.72573), L_{10}(0.56508)

Table 5.19 Results and comparison of economic dispatch with *N* – 1 security (IEEE 30-bus system)

Generator No.	OKA	LP
P_{G1}(p.u.)	1.40625	1.38540
P_{G2}(p.u.)	0.60638	0.57560
P_{G5}(p.u.)	0.25513	0.24560
P_{G8}(p.u.)	0.30771	0.35000
P_{G11}(p.u.)	0.17340	0.17930
P_{G13}(p.u.)	0.16154	0.16910
Total generation(p.u.)	2.91041	2.90500
Total cost ($/hr)	813.44	813.74
Total loss (p.u.)	0.07641	0.0711

5.4.6.3 Numerical Example of Economic Dispatch with* N – 1 *Security The same data of the IEEE 30-bus system are used to compute the economic dispatch with *N* − 1 security. The results are listed in Tables 5.18 and 5.19.

From Table 5.18, through the *N* − 1 security analysis and calculation, the *N* − 1 security cannot be satisfied as four single line outages (line number 1, 2, 4 and 5) appear. Thus, these violated constraints need to be introduced in the *N* − 1 security economic dispatch model to readjust the generators output until no any violation appears. The final results are shown in Table 5.19.

Through comparing with the conventional linear programming method that is used to solve economic dispatch, the OKA network flow programming can achieve almost the same results as LP, although sometimes the precision of OKA may be a littler lower than that of the LP method, which can be neglected from the view of the engineering.

It should be noted that the amount of calculation of the $N - 1$ security economic dispatch is greatly reduced with the presented method because of the use of the "$N - 1$ constrained zone", which is formed by the fast $N - 1$ security analysis.

5.5   NONLINEAR CONVEX NETWORK FLOW PROGRAMMING METHOD

5.5.1   Introduction

This section presents a new nonlinear convex network flow programming (NLCNFP) model of EDC, which is solved by a combination approach of quadratic programming (QP) and network flow programming (NFP). First of all, a new NLCNFP model of economic power dispatch with security is deduced, based on the load flow equations. Then, a new incremental NLCNFP model of secure and economic dispatch can be set up. The new EDC model can be transformed into a QP model, in which the search direction in the space of the flow variables is found. The concept of a maximum basis in the network flow graph is introduced, allowing the constrained QP model to be changed into an unconstrained QP model that is then solved with the reduced gradient method.

5.5.2   NLCNFP Model of EDC

5.5.2.1   *Mathematical Model*   It is well known that the active power flow equations of a transmission line can be written as follows:

$$P_{ij} = V_i^2 g_{ij} - V_i V_j g_{ij} \cos\theta_{ij} - V_i V_j b_{ij} \sin\theta_{ij} \tag{5.143}$$

$$P_{ji} = V_j^2 g_{ij} + V_i V_j \left(-g_{ij} \cos\theta_{ij} + b_{ij} \sin\theta_{ij}\right) \tag{5.144}$$

where

P_{ij}: The sending end active power on transmission line ij

P_{ji}: The receiving end active power on transmission line ij

V_i: The node voltage magnitude of node i

θ_{ij}: The difference of node voltage angles between the sending end and receiving end of line ij

b_{ij}: The susceptance of transmission line ij

g_{ij}: The conductance of transmission line ij

In a high-voltage power network, the value of θ_{ij} is very small, and the following approximate equations are easily obtained

$$V \cong 1.0 \text{ p.u.} \tag{5.145}$$

$$\sin\theta_{ij} \cong \theta_{ij} \tag{5.146}$$

$$\cos\theta_{ij} \cong 1 - \theta_{ij}^2/2 \tag{5.147}$$

Substituting equations (5.145)–(5.147) into equations (5.143) and (5.144), the active power load flow equations of a line can be simplified and deduced as follows:

$$P_{ij} = P_{ijC} + \frac{1}{2}\left(-\frac{P_{ijC}}{b_{ij}}\right)^2 g_{ij} \tag{5.148}$$

$$P_{ji} = P_{ijC} + \frac{1}{2}\left(-\frac{P_{ijC}}{b_{ij}}\right)^2 g_{ij} \tag{5.149}$$

where

$$P_{ijC} = -b_{ij}\theta_{ij} \tag{5.150}$$

is called an equivalent power flow on transmission line ij.

The active power loss on transmission line ij can be obtained according to equations (5.148) and (5.149), i.e.,

$$\begin{aligned} P_{Lij} = P_{ij} + P_{ji} &= \left(-\frac{P_{ijC}}{b_{ij}}\right)^2 g_{ij} \\ &= P_{ijC}^2 \frac{(R_{ij}^2 + X_{ij}^2)}{X_{ij}^2} R_{ij} \end{aligned} \tag{5.151}$$

where

R_{ij}: The resistance of transmission line ij
X_{ij}: The reactance of transmission line ij

Let

$$Z_{ijC} = \frac{(R_{ij}^2 + X_{ij}^2)}{X_{ij}^2} R_{ij} \tag{5.152}$$

The active power loss on the transmission line ij can be expressed as follows:

$$P_{Lij} = P_{ijC}^2 Z_{ijC} \tag{5.153}$$

The traditional NFP model for economic dispatch problem can be written as follows, i.e., model M-5,

$$\min F = \sum_{i \in NG} \left(a_i P_{Gi}^2 + b_i P_{Gi} + c_i \right) + h \sum_{ij \in NT} P_{Lij} \tag{5.154}$$

such that

$$P_{Gi} = P_{Di} + \sum_{j \to i} P_{ij} \tag{5.155}$$

$$P_{Gim} \leq P_{Gi} \leq P_{GiM} \quad i \in NG \tag{5.156}$$

$$-P_{ijM} \leq P_{ij} \leq P_{ijM} \quad j \in NT \tag{5.157}$$

where

P_{Gi}: The active power of generator i

P_{Di}: The active power demand at load bus i

P_{ij}: The flow in the line connected to node i; would have a negative value for a line in which the flow is toward node i

a_i, b_i, c_i: The cost coefficients of the ith generator

NG: The number of generators in the power network

NT: The number of transmission lines in the power network

P_{ijM}: The active power flow constraint on transmission line ij

P_{Lij}: The active power loss on transmission line ij

h: The weighting coefficient of the transmission losses

$j \to i$ represents node j connected to node i through transmission line ij.

Subscripts m and M represent the lower and upper bounds of the constraint.

The second term of the objective function (equation 5.154) is a penalty on transmission losses based on the system marginal cost h (in \$ per MWh). Equation (5.157) is the line security constraint. Equation (5.156) defines the generator power upper and lower limits. Equation (5.155) is Kirchhoff's first law (i.e., node current law, KCL).

Substituting equation (5.151) or (5.153) into equation (5.154), and substituting equation (5.148) into equation (5.155), the new NLCNFP model M-6 can be written as follows:

$$\min F = \sum_{i \in NG} \left(a_i P_{Gi}^2 + b_i P_{Gi} + c_i \right) + h \sum_{ij \in NT} P_{ijC}^2 Z_{ijC} \tag{5.158}$$

such that

$$P_{Gi} = P_{Di} + \sum_{j \to i} \left[P_{ijC} + \frac{P_{ijC}^2}{2b_{ij}^2} g_{ij} \right] \tag{5.159}$$

$$P_{Gim} \le P_{Gi} \le P_{GiM} \quad i \in NG \tag{5.156}$$

$$-P_{ijCM} \le P_{ijC} \le P_{ijCM} \quad j \in NT \tag{5.160}$$

where Z_{ijC} is called an equivalent impedance of transmission line ij, as shown in equation (5.152).

Obviously, equation (5.159) is equivalent to the general system active balance equation in the traditional EDC model, i.e.,

$$\sum_{i \in NG} P_{Gi} = \sum_{k \in ND} P_{Dk} + P_L \tag{5.161}$$

where

ND: The number of load nodes

P_L: The total system active power losses, which is obtained through the computation of equation (5.162), rather than usual power flow calculations

$$P_L = \sum_{ij \in NT} P_{Lij} = \sum_{ij \in NT} P_{ijC}^2 Z_{ijC} \tag{5.162}$$

The limit value of the equivalent line power flow P_{ijCM} in equation (5.160) can be obtained from equation (5.148), i.e.,

$$P_{ijM} = P_{ijCM} + \frac{1}{2} \left(-\frac{P_{ijCM}}{b_{ij}} \right)^2 g_{ij} \tag{5.163}$$

According to equation (5.163), we can get the positive limit value of the equivalent line power flow P_{ijCM} (the negative root of P_{ijCM} is neglected), i.e.,

$$P_{ijCM} = \frac{\left[\sqrt{1 + (2g_{ij} P_{ijM} / b_{ij}^2)} - 1 \right]}{g_{ij}} \tag{5.164}$$

5.5.2.2 *Consideration of KVL* It is well known that Kirchhoff's second law (i.e., loop voltage law, KVL) has not been considered in the study of secure economic power dispatch using general NFP. This is why there always exists some modeling error when secure economic power dispatch is solved with traditional linear NFP. KVL is considered in this section.

The voltage drop on transmission line ij can be approximately expressed as

$$V_{ij} = P_{ijC} Z_{ijC} \tag{5.165}$$

In this way, the voltage equation of the lth loop can be obtained, i.e.,

$$\sum_{ij} (P_{ijC} Z_{ijC}) \mu_{ij,l} = 0 \quad l = 1, 2, \ldots, NM \tag{5.166}$$

where NM is the number of loops in the network and $\mu_{ij,l}$ is the element in the related loop matrix, which takes the value 0 or 1.

Introducing the KVL equation into model M-6, we get the following model M-7, in which the augmented objective function is obtained from KVL equation (5.166) and objective function (5.158) in model M-6.

$$\min F_{\mathrm{L}} = \sum_{i \in NG} (a_i P_{Gi}^2 + b_i P_{Gi} + c_i)$$
$$+ h \sum_{ij \in NT} P_{ijC}^2 Z_{ijC} - \lambda_l \sum_{ij} (P_{ijC} Z_{ijC}) \mu_{ij,l} \quad l = 1, 2, \ldots, NM \tag{5.167}$$

subject to constraints in equations (5.156), (5.159), (5.160) where λ_l is the Lagrange multiplier, which can be obtained through minimizing equation (5.167) with respect to variable P_{ijC}, i.e.,

$$2h P_{ijC} Z_{ijC} - \lambda_l \sum_{ij} Z_{ijC} \mu_{ij,l} = 0 \quad l = 1, 2, \ldots, NM \tag{5.168}$$

$$\lambda_l = 2h P_{ijC} \bigg/ \sum_{ij} \mu_{ij,l} \quad l = 1, 2, \ldots, NM \tag{5.169}$$

By solving optimization NLCNFP model M-7, the generator power output P_{Gi} and the equivalent line power flow P_{ijC} can be obtained. Therefore, the line power P_{ij}, angle θ_{ij}, which is the difference of node voltage angles between the sending end and the receiving end of the line, and system active power losses P_{L} can be computed from equations (5.148), (5.150) and (5.162), respectively, rather than from the usual power flow calculations.

Similarly, the method of handling $N - 1$ security constraints in Section 5.4 is adopted here. Thus the incremental NLCNFP model of economic dispatch with $N - 1$ security, model M-8, becomes

$$\min \Delta F = \sum_{i \in NG} (2a_i P_{Gi}^0 + b_i) \Delta P_{Gi} + h \sum_{ij \in NT} (2 Z_{ijC} P_{ijC}^0) \Delta P_{ijC} + \lambda_l \sum_{ij} Z_{ijC} \mu_{ij,l} \tag{5.170}$$

such that

$$\Delta P_{Gi} = \sum_{j \to i} \left(1 + \frac{P_{ijC}}{b_{ij}^2} g_{ij} \right) \Delta P_{ijC} \tag{5.171}$$

$$\max \{ -\Delta P_{\mathrm{GRC}iM}, P_{Gim} - P_{Gi}^0 \} \le \Delta P_{Gi} \le \min \{ \Delta P_{\mathrm{GRC}iM}, P_{GiM} - P_{Gi}^0 \}, \quad i \in NG \tag{5.172}$$

$$\Delta P_{ijC} = -\max_{l \in NL} \{ P_{ijC}(l) - P_{ijCM} \} \quad j \in NT1 \tag{5.173}$$

$$\Delta P_{ijC} = -\min_{l \in NL}\{P_{ijC}(l) + P_{ijCM}\} \quad j \in NT2 \tag{5.174}$$

$$-P_{ijCM} - P_{ijC}^0 \leq \Delta P_{ijC} \leq P_{ijCM} - P_{ijC}^0 \quad j \in (NT - NT1 - NT2) \tag{5.175}$$

It is noted that the $N-1$ security region may be very narrow since all constraints that are produced by all kinds of single outages are introduced in the $N-1$ security economic dispatch. In other words, the feasible range of the generator's power output becomes very small. Consequently, $N-1$ security is met, but the system economy may not be satisfied. Thus the idea of multigeneration plans is used. The method is to solve the economic dispatch model by considering one single outage only each time. This means that each effective single outage corresponds to one generation plan. Generally, there are not too many effective single outages in a system. Therefore, it will not have many generation plans. The incremental NLCNFP model of multigeneration plans can be written as below:

$$\min \Delta F = \sum_{i \in NG}(2a_i P_{Gi}^0 + b_i)\Delta P_{Gi}(l) + h\sum_{ij \in NT}(2Z_{ijC}P_{ijC}^0)\Delta P_{ijC}(l) + \lambda_l \sum_{ij}Z_{ijC}\mu_{ij,l} \tag{5.176}$$

such that

$$\Delta P_{Gi}(l) = \sum_{j \to i}\left(1 + \frac{P_{ijC}^0}{b_{ij}^2}g_{ij}\right)\Delta P_{ijC}(l) \tag{5.177}$$

$$\max\{-\Delta P_{GRCiM}, P_{Gim} - P_{Gi}^0\} \leq \Delta P_{Gi}(l) \leq \min\{\Delta P_{GRCiM}, P_{GiM} - P_{Gi}^0\}, \quad i \in NG \tag{5.178}$$

$$\Delta P_{ijC}(l) = -(P_{ijC}(l) - P_{ijCM}) \quad j \in NT1, l \in NL \tag{5.179}$$

$$\Delta P_{ijC}(l) = -(P_{ijC}(l) + P_{ijCM}) \quad j \in NT2, l \in NL \tag{5.180}$$

$$-P_{ijCM} - P_{ijC}^0 \leq \Delta P_{ijC} \leq P_{ijCM} - P_{ijC}^0 \quad j \in (NT - NT1 - NT2) \tag{5.181}$$

5.5.3 Solution Method

Because of the special form of model M-7 or M-8, we introduce the following algorithm for solving it.

Model M-7 or M-8 is easily changed into a standard model of nonlinear convex network flow programming, i.e., model M-9,

$$\min C = \sum_{ij}c(f_{ij}) \tag{5.182}$$

such that

$$\sum_{j \in n}(f_{ij} - f_{ji}) = r_i \quad i \in n \tag{5.183}$$

$$L_{ij} \leq f_{ij} \leq U_{ij} \quad ij \in m \tag{5.184}$$

Equation (5.183) can be written as

$$Af = r \tag{5.185}$$

where A is a matrix with $n \times (n + m)$, in which every column corresponds to an arc in the network and every row corresponds to a node in the network.

Matrix A can be divided into a basic submatrix and a nonbasic submatrix, which is similar to the convex simplex method, i.e.,

$$A = [B, S, N] \tag{5.186}$$

where the columns of B form a basis; both S and N correspond to the nonbasic arcs. S corresponds to the nonbasic arcs in which the flows are within the corresponding constraints. N corresponds to the nonbasic arcs in which the flows reach the corresponding bounds.

A similar division can be made for the other variables. i.e.,

$$f = [f_B, f_S, f_N] \tag{5.187}$$

$$g(f) = [g_B, g_S, g_N] \tag{5.188}$$

$$G(f) = \text{diag}[G_B, G_S, G_N] \tag{5.189}$$

$$D = [D_B, D_S, D_N] \tag{5.190}$$

where

$g(f)$: The first-order gradient of the objective function
$G(f)$: The Hessian matrix of the objective function
D: The search direction in the space of the flow variables

To solve model M-9, Newton's method can first be used to calculate the search direction in the space of the flow variables. The idea behind Newton's method is that the function being minimized is approximated locally by a quadratic function, and this approximate function is minimized exactly.

Suppose that f is a feasible solution and the search step along the search direction in the space of flow variables $\beta = 1$. Then the new feasible solution can be obtained.

$$f' = f + D \tag{5.191}$$

Substituting equation (5.191) into the equations in model M-9, the nonlinear convex network flow programming model M-9 can be changed into the

following quadratic programming model M-10, in which the search direction in the space of the flow variables is to be solved:

$$\min C(D) = \frac{1}{2} D^{\mathrm{T}} G(f) D + g(f)^{\mathrm{T}} D \qquad (5.192)$$

such that

$$AD = 0 \qquad (5.193)$$

$$D_{ij} \geq 0, \quad \text{when } f_{ij} = L_{ij} \qquad (5.194)$$

$$D_{ij} \leq 0, \quad \text{when } f_{ij} = U_{ij} \qquad (5.195)$$

Model M-10 is a special quadratic programming model that has the form of network flow programming. To enhance the calculation speed, we present a new approach, in place of the general quadratic programming algorithm, to solve the model M-10. The main calculation steps are described below.

5.5.3.1   *Temporarily Neglect Equations (5.194) and (5.195)*   This means that $L_{ij} < f_{ij} < U_{ij}$ in this case. Thus $D_N = 0$ according to the definition of the corresponding nonbasic arc.

From equation (5.193), we know that

$$AD = [B, S, N] \begin{bmatrix} D_B \\ D_S \\ 0 \end{bmatrix} = 0 \qquad (5.196)$$

From equation (5.196), we can obtain

$$D_B = -B^{-1} S D_S \qquad (5.197)$$

$$D = \begin{bmatrix} -B^{-1}S \\ I \\ 0 \end{bmatrix} D_S = Z D_S \qquad (5.198)$$

Substituting equation (5.198) into equation (5.192), we get

$$\min C(D) = \frac{1}{2}(Z D_S)^{\mathrm{T}} G(f)(Z D_S) + g(f)^{\mathrm{T}}(Z D_S) \qquad (5.199)$$

Through minimizing equation (5.199) to variable D_S, the model M-10 can be changed into an unconstrained problem, the optimization solution of which can be solved from the following equations:

$$D_N = 0 \tag{5.200}$$

$$BD_B = -SD_B \tag{5.201}$$

$$(Z^\mathrm{T}GZ)D_S = -Z^\mathrm{T}g \tag{5.202}$$

5.5.3.2 Introduction of Equations (5.194) and (5.195) According to equations (5.200)–(5.202), D_S can be solved from equation (5.202), and then D_B can be solved from equation (5.201). If D_B violates the constraint equations (5.194) and (5.195), a new basis must be sought to calculate the new search direction in the space of flow variables. This step will not be terminated until D_B satisfies constraint equations (5.194) and (5.195).

5.5.3.3 Introduction of Maximum Basis in Network Obviously, the general repeated calculation of D_B and D_S, which is similar to that of pivoting in linear programming, is not only time-consuming but also does not improve the value of the objective function. To speed up the calculation, we adopt a new method to form a basis in advance so that D_B and D_S can satisfy the constraints (5.194) and (5.195). Therefore, the maximum basis in the network, which consists of as many free basic arcs as possible, is introduced in this chapter.

The maximum basis in a network can be obtained by solving the following model M-11:

$$\max_B \sum_{ij} d_{ij} A_{ij} \tag{5.203}$$

where

$$d_{ij} = \begin{cases} 1, & \text{when arc } ij \text{ is a free one, i.e., the flow in arc } ij \text{ is within its bounds} \\ 0, & \text{when arc } ij \text{ is not a free one, i.e., the flow in arc } ij \text{ reaches its} \\ & \text{bounds} \end{cases}$$

$$A_{ij} = \begin{cases} 1, & \text{when arc } ij \text{ is in the basis } B \\ 0, & \text{when arc } ij \text{ is not in basis } B \end{cases}$$

Suppose that basis B is the maximum basis from equation (5.203), only the flows on the free arcs in basis B need to be adjusted in order to satisfy equation (5.203), if the flow on a free nonbasic arc needs to be adjusted [22].

The introduction of the maximum base indicates the adjusting direction of flow, i.e., the change of flow is carried out according to the maximum basis. Through selecting the maximum basis, equations (5.194) and (5.195) in model M-10 can always be satisfied in the calculation of the search direction in the space of the flow variables. Therefore, the quadratic programming model M-10 is equivalent to unconstrained problem equations (5.200)–(5.202). To enhance the calculation speed further, equations (5.200)–(5.202) can be solved by the reduced gradient method.

5.5.3.4 *Reduced Gradient Algorithm with Weight Factor* Equations (5.200)–(5.202) can be written in compact format as below:

$$(Z^{T}GZ)D = -Z^{T}g \tag{5.204}$$

If we use a unit matrix to replace the Hessian matrix $(Z^{T}GZ)$, we get

$$V = -Z^{T}g \tag{5.205}$$

$$D = ZV \tag{5.206}$$

where

V: The negative reduced gradient
D: The direction of the reduced gradient

The main advantages of the reduced gradient method are: (1) the calculation is simple and (2) the required storage space is relatively small. The disadvantage is that it is an approximation. Thus the reduced gradient algorithm has a linear convergence speed.

To improve the convergence speed of the reduced gradient method, select a positive matrix that is not a unit matrix but can be easily inversed and use it to replace the Hessian matrix $(Z^{T}GZ)$. In this way, we get a new reduced gradient with weight, that is,

$$MV = -Z^{T}g \tag{5.207}$$

where

M: the weight of the reduced gradient.

Select the initial value of Z as

$$Z = \begin{bmatrix} -B^{-1}S \\ I \\ 0 \end{bmatrix} \tag{5.208}$$

Substituting equation (5.208) into equation (5.207), we get

$$MV = -Z^{T}g = -\left[-S^{T}\left(B^{T}\right)^{-1}, I, 0\right]\begin{bmatrix} g_{B} \\ g_{S} \\ g_{N} \end{bmatrix} = S^{T}\left(B^{T}\right)^{-1}g_{B} - g_{S} \tag{5.209}$$

According to equations (5.182) and (5.185), the following Lagrange function can be obtained:

$$L = C(f) - \lambda(Af - r) \tag{5.210}$$

where

λ: The Lagrange multiplier

According to the condition of optimization, we have

$$\frac{\partial L}{\partial f} = 0 \tag{5.211}$$

$$\frac{\partial C(f)}{\partial f} - A^{\mathrm{T}}\lambda = 0 \tag{5.212}$$

That is,

$$g(f) = A^{\mathrm{T}}\lambda \tag{5.213}$$

Expanding the above equation, we get

$$\begin{bmatrix} B^{\mathrm{T}}\lambda \\ S^{\mathrm{T}}\lambda \\ N^{\mathrm{T}}\lambda \end{bmatrix} = \begin{bmatrix} g_B \\ g_S \\ g_N \end{bmatrix} \tag{5.214}$$

$$B^{\mathrm{T}}\lambda = g_B \tag{5.215}$$

Substituting equation (5.215) into equation (5.209), we get

$$MV = S^{\mathrm{T}}(B^{\mathrm{T}})^{-1} B^{\mathrm{T}}\lambda - g_S = S^{\mathrm{T}}\lambda - g_S \tag{5.216}$$

In summary, the calculation steps of nonlinear convex network flow programming model, which is solved by reduced gradient algorithm with weight, are as follows:

(1) Compute λ from equation (5.215).
(2) Compute V from equation (5.216).
(3) Compute D_S from the following expression:

$$D_S = \begin{cases} 0, & \text{when } (f_S)_{ij} = L_{ij}, \text{and } V_{ij} < 0. \\ 0, & \text{when } (f_S)_{ij} = U_{ij}, \text{and } V_{ij} > 0. \\ V_{ij}, & \text{otherwise} \end{cases} \tag{5.217}$$

(4) Compute D_B from equation (5.201).

(5) Compute the new value of flow $f' = f + D_B$

In the practical calculation, several parameters related to the algorithm must be addressed.

(1) The convergence criteria

The convergence criteria are given as below:

$$\max\left|(S^{\mathrm{T}}\lambda - g_S)_j\right| \leq \sigma \tag{5.218}$$

where σ is determined according to the required calculation precision.

(2) The selection of weighting matrix M

We can select the diagonal matrix of the Hessian matrix $Z^{\mathrm{T}}GZ$ as the weighting matrix M, i.e.,

$$M = \mathrm{diag}(Z^{\mathrm{T}}GZ) \tag{5.219}$$

(3) The selection of the search step

We assumed that the search step along the search direction in the space of flow variables $\beta = 1$. To speed up the convergence, we can use the following approach to compute the optimum search step along the search direction in the space of flow variables. First of all, compute the initial step as below:

$$\beta^0 = -\frac{g^{\mathrm{T}}D}{D^{\mathrm{T}}GD} \tag{5.220}$$

Then compute the optimum step according to the following equation:

$$\frac{g(f + \beta * D)^{\mathrm{T}}D}{\left|g(f)^{\mathrm{T}}D\right|} \leq \omega, \quad 0 < \omega < 1 \tag{5.221}$$

Meanwhile, the $\beta*$ must meet the following equation:

$$C(f + \beta * D) - C(f) \leq \eta, \quad 0 < \eta < 1 \tag{5.222}$$

If the above equation is not satisfied, use half of $\beta*$ to recompute the flow until the equation is met.

5.5.4   Implementation

For examining the NLCNFP model and algorithm, the numerical simulations have been carried out on IEEE 5-bus and 30-bus systems. The results and comparison of secure EDC are listed on Tables 5.20–5.22. To further raise the precision of EDC and check the operation states of the system, the fast

Table 5.20   Economic dispatch results comparison (5-bus system)

Method	OKA	NLCNFP
P_{G1}(p.u.)	0.92700	0.97800
P_{G2}(p.u.)	0.71600	0.66670
Total cost ($/hr)	757.500	757.673
Total loss (p.u.)	0.04300	0.04470

Table 5.21   ED results and comparison between NLCNFP and OKA for IEEE 30-bus system

Scenario	Scenario 1	Scenario 1	Scenario 2	Scenario 2
Method	NLCNFP	OKA	NLCNFP	OKA
P_{G1}(p.u.)	1.7595	1.7588	1.5018	1.69665
P_{G2}(p.u.)	0.4884	0.4881	0.5645	0.33295
P_{G5}(p.u.)	0.2152	0.2151	0.2321	0.15000
P_{G8}(p.u.)	0.2229	0.2236	0.3207	0.31270
P_{G11}(p.u.)	0.1227	0.1230	0.1518	0.30000
P_{G13}(p.u.)	0.1200	0.12000	0.1413	0.12000
Total generation	2.9286	2.9290	2.9121	2.9151
Total real power losses	0.0946	0.0950	0.0781	0.0783
Total generation cost ($)	802.3986	802.51	807.80	809.68

Table 5.22   ED results and comparison among NLCNFP, QP, and LP for IEEE 30-bus system

Generation No.	NLCNFP Method	QP Method	LP Method
P_{G1}	1.7595	1.7586	1.7626
P_{G2}	0.4884	0.4883	0.4884
P_{G5}	0.2152	0.2151	0.2151
P_{G8}	0.2229	0.2233	0.2215
P_{G11}	0.1227	0.1231	0.1214
P_{G13}	0.1200	0.1200	0.1200
Total generation	2.9286	2.9285	2.9290
Total real power losses	0.0946	0.0945	0.0948
Total generation cost ($)	802.3986	802.3900	802.4000

decoupled power flow is also used in the calculation, but only in the first and final stages.

Table 5.20 shows the economic dispatch results of the 5-bus system with use of nonlinear convex network flow programming. The ED results with use of out-of-kilter algorithm are also listed in Table 5.20 (column 3).

The simulation results of the 30-bus system by NLCNFP are also compared with those obtained by OKA in Section 5.4. The following two cases are used to do comparison.

Scenario 1: The original data
Scenario 2: The original data, but the power limit value of the line 1 is reduced to 1.00 p.u.

The corresponding calculation results and comparison based on two different network flow techniques (NLCNFP and OKA) for these two scenarios are listed in Table 5.21. Obviously, the ED solved by NLCNFP has higher precision than the ED solved by OKA.

Table 5.22 lists the ED results comparison among the NLCNFP method and the conventional linear programming and quadratic programming methods. The agreement between the conventional ED method through power flow calculations and the NLCNFP method can be observed.

According the $N - 1$ security analysis in Section 5.4, there are four single outages that cause the line violation for the 30-bus system. They are outage lines 1, 2, 4, and 5. Applying the idea of multigeneration plans to the 30-bus system, there will be five generation plans: one for the normal operation state and four for the effective single outages, respectively. The detailed results of the multigeneration plans are shown in Table 5.23.

Table 5.23 Multigeneration plans for IEEE 30-bus system

Generation No.	Normal State	Line 1 Outage	Line 2 Outage	Line 4 Outage	Line 5 Outage
P_{G1}	1.7595	1.42884	1.40919	1.41584	1.57840
P_{G2}	0.4884	0.55222	0.57188	0.56521	0.38880
P_{G5}	0.2152	0.24135	0.24135	0.24135	0.25512
P_{G8}	0.2229	0.35000	0.35000	0.35000	0.35000
P_{G11}	0.1227	0.17340	0.17340	0.17340	0.17340
P_{G13}	0.1200	0.16154	0.16154	0.16154	0.16154
Total generation	2.9286	2.90735	2.90736	2.90734	2.90726
Total real power losses	0.0946	0.07335	0.07336	0.07334	0.07326
Total generation cost ($)	802.3986	811.36192	812.64862	812.18859	808.30441
N security	Satisfied	/	/	/	/
$N - 1$ security	Not satisfied when one of lines #1,2,3,5 is in outage	Satisfied	Satisfied	Satisfied	Satisfied

5.6 TWO-STAGE ECONOMIC DISPATCH APPROACH

5.6.1 Introduction

This section presents a two-stage economic dispatch approach according to the practical operation situation of power systems. The first stage involves the classic economic power dispatch without consideration of network loss. The initial generation plans of the generator units are determined according to the rank of fuel consumption characteristic of the units or the principle of equal incremental rate. The second stage involves economic dispatch with consideration of system power loss and network security constraints. Three objectives can be used for the second stage. They are (1) minimize the fuel consumption, (2) minimize system loss, and (3) minimize the movement of generator output from the initial generation plans.

5.6.2 Economic Power Dispatch—Stage One

The equal incremental principle, which is introduced in Chapter 4, can be used for the first stage of economic power dispatch. Given that the input-output characteristic of NG generating units are $F_1(P_{G1})$, $F_2(P_{G2})$, ..., $F_n(P_{Gn})$, respectively, the total system load is P_D. The problem is to minimize the total fuel consumption of generators F subject to the constraint that the sum of the power generated must equal the received load. That is,

$$\min F = F_1(P_{G1}) + F_2(P_{G2}) + \cdots + F_n(P_{Gn}) = \sum_{i=1}^{NG} F_i(P_{Gi}) \qquad (5.223)$$

s.t.

$$\sum_{i=1}^{NG} P_{Gi} = P_D \qquad (5.224)$$

This is a constrained optimization problem, and it can be solved by the Lagrange multiplier method. According to Chapter 4, the principle of equal incremental rate of economic power operation for multiple generating units can be obtained as

$$\frac{dF_i}{dP_{Gi}} = \lambda \quad i = 1, 2, \ldots, N \qquad (5.225)$$

or

$$\frac{dF_1}{dP_{G1}} = \frac{dF_2}{dP_{G2}} = \cdots \frac{dF_N}{dP_{GN}} = \lambda \qquad (5.226)$$

The economic operation points P_{Gi}^0 of the first stage can be obtained from the above equations (5.225) or (5.226).

5.6.3 Economic Power Dispatch—Stage Two

The second stage of the economic power dispatch includes loss correction and network security constraints. On one hand, the system loss minimization or the fuel consumption minimization can be selected as objective function. On the other hand, the operators expect optimal dispatch points close to the economic operation points P_{Gi}^0 obtained from the first stage. Thus the following three objectives may be adopted in the second stage of economic dispatch.

(1) Minimize the fuel consumption

$$\min F_1 = \sum_{i=1}^{NG} F_i(P_{Gi}) \tag{5.227}$$

(2) Minimize the system loss

$$\min F_2 = P_L \tag{5.228}$$

(3) Minimize the adjustment of generator output

$$\min F_3 = \sum_{i=1}^{NG} \left(P_{Gi} - P_{Gi}^0\right)^2 \tag{5.229}$$

The constraints include real power balance, generator power output limits, and branch power flow constraints, that is,

$$\sum_{i \in NG} P_{Gi} = \sum_{k \in ND} P_{Dk} + P_L \tag{5.230}$$

$$P_{Gi\min} \leq P_{Gi} \leq P_{Gi\max} \quad i \in NG \tag{5.231}$$

$$|P_{ij}| \leq P_{ij\max} \quad ij \in NT \tag{5.232}$$

where

P_D: The real power load.
P_{ij}: The power flow of transmission line ij
$P_{ij\,\max}$: The power limits of transmission line ij
P_{Gi}: The real power output at generator bus i
$P_{Gi\,\min}$: The minimal real power output at generator i
$P_{Gi\,\max}$: The maximal real power output at generator i

P_L: The network losses

F_i: The fuel consumption function of the generator unit i

NT: The number of transmission lines

NG: The number of generators

It is noted that the two-stage approach for economic dispatch can be used for dynamic economic dispatch or daily dispatch in the practical operation of the power systems. To actualize the transition from the time point t to $t + 1$ schedule successfully, the real power generation regulations constraint, $\Delta P_{GRCimax}$, must be considered, i.e.,

$$\left|P_{Gi} - P_{Gi}^0\right| \le \Delta P_{GRCimax} \quad i \in NG \tag{5.233}$$

or

$$-\Delta P_{GRCimax} + P_{Gi}^0 \le P_{Gi} \le \Delta P_{GRCimax} + P_{Gi}^0 \quad i \in NG \tag{5.234}$$

Thus the regulating value of the generation is restricted by the two inequality equations (5.231) and (5.234), which can be combined into one expression:

$$\max\left\{-\Delta P_{GRCimax} + P_{Gi}^0, P_{Gimin}\right\} \le P_{Gi} \le \min\left\{\Delta P_{GRCimax} + P_{Gi}, P_{Gimax}\right\} \quad i \in NG \tag{5.235}$$

The economic dispatch model for the second stage can be written as

$$\min F = h_1 F_1 + h_2 F_2 + h_3 F_3 \tag{5.236}$$

s.t.

$$\sum_{i \in NG} P_{Gi} = \sum_{k \in ND} P_{Dk} + P_L \tag{5.237}$$

$$\max\left\{-\Delta P_{GRCimax} + P_{Gi}^0, P_{Gimin}\right\} \le P_{Gi} \le \min\left\{\Delta P_{GRCimax} + P_{Gi}, P_{Gimax}\right\} \quad i \in NG \tag{5.238}$$

$$\left|P_{ij}\right| \le P_{ijmax} \quad ij \in NT \tag{5.239}$$

where

$$h_1 + h_2 + h_3 = 1 \tag{5.240}$$

h_1: The weighting factor of the fuel consumption objective function

h_2: The weighting factor of the loss minimization objective function

h_3: The weighting factor of the generator output adjustment objective function

The weighting factors can be determined according to the practical situation of the specific system. For example, if the network loss is the only concern in a system, we can select $h_2 = 1$, and $h_1 = h_3 = 0$. If the network loss is not a concern, and the economy is primary in a system, we can select $h_1 = 1$, and $h_2 = h_3 = 0$.

The economic dispatch model for the second stage can be solved by any algorithm mentioned in previous sections.

5.6.4   Evaluation of System Total Fuel Consumption

In practical system operation, the system total fuel consumption is mainly concerned. Generally, the system total fuel consumption includes two parts:

(1) The total fuel consumption of the generators
(2) The equivalent fuel consumption of the system power losses

Generally, the system total fuel consumption before optimization is taken as a reference point. It is expected that the system total fuel consumption obtained after stage two is less than that in the reference point.

For the reference point, the initial system power losses P_L^0 are obtained from a power flow solution. In addition, since the line constraints are not considered before optimization, there may be a branch flow violation. Thus the penalty term for the power violation should be introduced in the calculation of the system total fuel consumption in the reference point. The system total power violation can be computed as below:

$$\Delta P_{\text{Viol}} = \sum_{ij=1}^{Nl} \left(P_{ij}^0 - P_{ij\,\text{max}} \right) \tag{5.241}$$

where Nl is the set of violated branches.

The equivalent fuel consumption for the power violation is computed as

$$F_{\text{viol}} = \gamma_2 \Delta P_{\text{Viol}} \tag{5.242}$$

Obviously, equivalent fuel consumption for the power violation F_{viol} will be zero if there is no branch violation (i.e., Nl is empty set).

Thus the system total fuel consumption before optimization will be

$$F_T^1 = \sum_{i=1}^{NG} F_i \left(P_{Gi}^0 \right) + \gamma_1 P_L^0 + \gamma_2 \Delta P_{\text{Viol}} \tag{5.243}$$

After stage two, the system power losses P_L and the economic operation points are computed by solving model equations (5.236)–(5.239) and power flow. That is,

$$F_T^2 = \sum_{i=1}^{NG} F_i(P_{Gi}) + \gamma_1 P_L \tag{5.244}$$

where

γ_1, γ_2: The coefficient's of converting the system power loss and branch power violation to the fuel consumption, respectively.

The requirement of the two-stage economic dispatch will be

$$F_T^2 \leq F_T^1 \tag{5.245}$$

where

F_T^1: The initial system total fuel consumption
F_T^2: The final system total fuel consumption

Example 5.1

The test example is the IEEE 30-bus system with some data change. The modified 30 bus system consists of 5 generation units, 21 loads, 41 transmission lines and transformers.

The fuel consumption functions of the generators are quadratic curves and are shown in Table 5.24. The two-stage economic dispatch results are shown in Tables 5.25 and 5.26.

Table 5.24   The fuel consumption function of generators for IEEE 30-bus system

Gen. No.	a	b	c
1	0.00984	0.33500	0.00000
2	0.00834	0.22500	0.00000
5	0.00850	0.18500	0.00000
11	0.00884	0.13500	0.00000
13	0.00834	0.22500	0.00000

where: $F_1 = a_i P_{Gi}^2 + b_i P_{Gi} + c_i$

Table 5.25   The results of generation scheduling for IEEE 30-bus system

Gen. No.	Initial Point	Stage Two for ED
1	54.645	51.305
2	59.480	60.330
5	60.570	61.440
11	57.370	58.190
13	59.480	60.190

Table 5.26   The results of system fuel consumption for IEEE 30-bus system

Stage	Initial Point	Stage Two for ED
Total system loss (MW)	4.120	4.030
Total system fuel consumption	216.686	215.906

Table 5.25 shows the generation plans for the two stages, respectively. Tables 5.26 shows system total losses and fuel consumption for the two stages, respectively.

It can be observed from Table 5.26 that the system losses and fuel consumption of the second stage are lower than those before optimization, where loss is about 2.18% reduction, and total system fuel consumption is about 0.36% reduction.

5.7   SECURITY-CONSTRAINED ED BY GENETIC ALGORITHMS

Genetic algorithms (GAs) are adaptive search techniques that derive their models from the genetic processes of biological organisms based on evolution theory. In Chapter 4, GAs are applied to solve the classic economic dispatch problem, where the network losses and security constraints are neglected.

Considering the network losses P_L, and selecting unit N as the slack bus unit, then the real power balance equation can be written as

$$P_{GN} = P_D + P_L - \sum_{i=1}^{N-1} P_{Gi} \tag{5.246}$$

The network security constraints can be written as

$$|P_{ij}| \leq P_{ij\max} \quad ij = 1, 2, \ldots, NL \tag{5.247}$$

Adding penalty factors h_1, h_2 to the violation of power output of the slack bus unit and h_3 to the violation of line power, we get the augmented cost

$$F_A = \sum_{i=1}^{N} F_i(P_{Gi}) + h_1(P_{GN} - P_{GN\max})^2 + h_2(P_{GN\min} - P_{GN})^2 + h_3 \sum_{ij=1}^{NL} (|P_{ij}| - P_{ij\max})^2 \tag{5.248}$$

GA is designed for the solution of maximization problem, so the fitness function for solving security economic dispatch problem is defined as the inverse of equation (5.248):

$$F_{\text{fitness}} = \frac{1}{F_A} \tag{5.249}$$

The GA operations are stated in Chapter 4. The calculation steps for solving GA-based ED with line flow constraints are as follows.

(1) Select the parameters related to GA such as population size, number of generations, substring length, and number of trials.

(2) Generate initially random coded strings as population members in the first generation.

(3) Decode the population to get power generations of the units in the strings.

(4) Perform power flow analysis considering the unit generations in step (3), so that GA is able to evaluate system transmission loss, slack bus generation, line flows, and hence any violation for the slack bus generation and violation for the line flow limits.

(5) Check whether the number of trials reaches the maximal.

   If the number of trials reaches the maximal, and there is no any generator power violation or line flow violation, stop and output the results.

   If the number of trials reaches the maximal, but there exists a generator power violation or line flow violation, this means that the given trial number is too small. Increase the trial numbers and recompute.

   If the number of trials does not reach the maximal, go to the next step.

(6) Evaluate the fitness of population members (i.e., strings).

(7) Execute selection of strings based on reproduction considering the roulette wheel procedure with embedded elitism followed by crossover with embedded mutation to create the new population for the next generation. Go to step (2).

Example 5.2

The method of GAs for solving security economic dispatch problem is tested on the IEEE 30-bus system. The test case is normal operation state only. The parameters related to GAs are selected as below:

- Number of chromosomes = 100
- Bit resolution per generator = 8
- Number of cross-points = 2
- Number of generations = 18,000
- Initial crossover probability = 92%
- Initial mutation probability = 0.1%

The total load is 283.4 MW; the output results are listed in Table 5.27. The GA-based ED results are also compared with those obtained by traditional optimization method (quadratic programming and linear programming). The same results are obtained.

Table 5.27 ED results by genetic algorithm and comparison for IEEE 30-bus system

Generation No.	GA Method	QP Method	LP Method
P_{G1}	1.7612	1.7586	1.7626
P_{G2}	0.4884	0.4883	0.4884
P_{G5}	0.2152	0.2151	0.2151
P_{G8}	0.2223	0.2233	0.2215
P_{G11}	0.1221	0.1231	0.1214
P_{G13}	0.1200	0.1200	0.1200
Total generation	2.9292	2.9285	2.9290
Total real power losses	0.0952	0.0945	0.0948
Total generation cost ($)	802.4634	802.3900	802.4000

APPENDIX: NETWORK FLOW PROGRAMMING

Network flow programming (NFP) is a special form of linear programming (LP). The algorithms for LP including the simplex method can also be used for NFP problem. However, since the specialization of NFP, especially when NFP is applied to the economic dispatch problem of a power system, some simplified algorithms are more efficient to solve NFP problem. Here we only introduce several most important applications of network flow problems that are used in power system optimal operation [22–27].

The Transportation Problem

The transportation problem is to find the amounts of goods to ship from the supply site to the demand site to minimize the total transportation cost. As we describe in Section 5.4, in the economic dispatch of a power system, the supply sites correspond to the generator sources, the demand sites correspond to load demands, and the transportation paths correspond to transmission lines.

In the transportation problem, the supply node is called the source and the demand node is called the sink. The mathematical representation of the transportation problem is as below:

$$\min C = \sum_{i=1}^{S} \sum_{j=1}^{D} c_{ij} x_{ij} \qquad (5A.1)$$

such that

$$\sum_{j \in D} x_{ij} \leq s_i \quad i \in S \qquad (5A.2)$$

$$\sum_{i \in S} x_{ij} \geq r_j \quad j \in D \qquad (5A.3)$$

$$x_{ij} \geq 0 \quad i \in S, j \in D \qquad (5A.4)$$

where

c_{ij}: The cost of supply from source i to sink j

x_{ij}: The supply from source i to sink j. It must be nonnegative.

s_i The supply from the source

r_j The supply received at the sink

S The total number of source nodes in the network

D The total number of sink nodes in the network

Obviously, the transportation problem is not feasible unless supply is at least as great as demand

$$\sum_{i \in S} s_i \geq \sum_{j \in D} r_j \qquad (5A.5)$$

If this inequality is satisfied, then the transportation problem is feasible. This is generally true for the economic dispatch problem of power systems, in which the total generations equal the total load demands plus the system power loss.

For simplification of the transportation problem it can be assumed that the total demand is equal to the total supply, that is,

$$\sum_{i \in S} s_i = \sum_{j \in D} r_j \qquad (5A.6)$$

Under this assumption, the inequalities in constraints (5A.2) and (5A.3) must be satisfied with equalities, that is,

$$\sum_{j \in D} x_{ij} = s_i \quad i \in S \qquad (5A.7)$$

$$\sum_{i \in S} x_{ij} = r_j \quad j \in D \qquad (5A.8)$$

This corresponds to the economic dispatch problem neglecting network loss. We also can use this assumption even for economic dispatch with transmission loss as we analyze in Section 5.4.

This problem can, of course, be solved by the simplex method described in the Appendix of Chapter 9. However, the simplex tableau for this problem involves an IJ by I + J constraint matrix. Instead, we use a more efficient algorithm to solve it. The algorithm consists of four steps.

(1) Form a transportation array or table as in Table A1.
(2) Find a basic feasible shipping schedule, x_{ij}.
    (2a) Choose any available square from the table, say (i_0, j_0), specify $x_{i_0 j_0}$ as large as possible subject to the constraints, and circle this variable.

Table A1   **Transportation array**

	D_1		D_2			D_D		
P_1	c_{11}	x_{11}	c_{12}	x_{12}	$\cdots$	c_{1D}	x_{1D}	s_1
P_2	c_{21}	x_{21}	c_{22}	x_{22}	$\cdots$	c_{2D}	x_{2D}	s_2
	$\vdots$		$\vdots$			$\vdots$		
P_S	c_{S1}	x_{S1}	c_{S2}	x_{S2}	$\cdots$	c_{SD}	x_{SD}	s_S
	r_1		r_2			r_D		

(2b) Delete from consideration whichever row or column has its constraint satisfied, but not both. If there is a choice, do not delete a row (column) if it is the last row (resp. column) undeleted.

(2c) Repeat steps (2a) and (2b) until the last available square is filled with a circled variable, and then delete from consideration both row and column.

(3) Test for optimality.

Given a feasible shipping schedule x_{ij}, we can use the equilibrium theorem to check for optimality. This entails finding feasible u_i and v_j that satisfy the equilibrium conditions

$$v_j - u_i = c_{ij}, \quad \text{for } x_{ij} > 0 \tag{5A.9}$$

where u_i and v_j are nonnegative dual variables of the primal problem and satisfy the following constraint:

$$v_j - u_i < c_{ij}, \quad \text{for all } i \text{ and } j \tag{5A.10}$$

Then, the method for checking the optimality is as below:

(3a) Set one of the u_i and v_j, and use equation (A9) for squares containing circled variables to find all the u_i and v_j.

(3b) Check feasibility, $v_j - u_i \leq c_{ij}$, for the remaining squares. If feasible, the solution is optimal for the problem and its dual problem.

(4) If the test fails, find an improved basic feasible shipping schedule, and repeat step (3).

(4a) Choose any square (i, j) with $v_j - u_i > c_{ij}$, set $x_{ij} = \theta$, but keep the constraints satisfied by subtracting and adding θ to appropriate circled variables.

(4b) Choose θ to be the minimum of the variables in the squares in which θ is subtracted.

(4c) Determine the new variable and remove from the circled variables one of the variables from which θ was subtracted that is now zero.

Example A1

There is a simplified power system that consists of three generators ($G_1 = 6$ p.u., $G_2 = 7$ p.u., and $G_3 = 9$ p.u.) and four load demands ($D_1 = 3$ p.u., $D_2 = 9$ p.u., $D_3 = 4$ p.u., $D_4 = 6$ p.u.). Each generator connects to all loads, respectively. Assume network loss is neglected. To compute the minimal transmission cost flow P_{ij} for this network:

1. We can form the transportation table in Table A2, where the number in the table is the transmission cost for transfer the power from the generator to load.
2. Find an initial power flow P_{ij}.

Choose any square, say the upper left corner, (1, 1), and make P_{11} as large as possible subject to the constraints. In this case, P_{11} is chosen equal to 3 (we delete the unit for simplification). It means that supply load D_1 receives its demands from PG_1. Thus, $P_{21} = P_{31} = 0$.

We choose another square, say (1, 2), and make P_{12} as large as possible subject to the constraints. Then $P_{12} = 3$, since there are only three units left at PG_1. Hence, $P_{13} = P_{14} = 0$. Next, choose square (2, 2), say, and put $P_{22} = 6$, so that load D_2 receives all of its demands, 3 units from PG_1 and 6 units from PG_2. Hence, $P_{32} = 0$. One continues in this way until all the variables P_{ij} are determined. The results are shown in Table A3.

It is noted that this method of finding an initial feasible solution is simple but may not be efficient. Here we introduce another approach that is called the least cost method.

Table A2   Transportation array for Example A1

	D_1	D_2	D_3	D_4	
PG_1	4	10	12	3	6
PG_2	8	5	6	4	7
PG_3	1	3	4	7	9
	3	9	4	6	

Table A3   Feasible flow for Example A1

	D_1	D_2	D_3	D_4	
PG_1	4 (3)	10 (3)	12	3	6
PG_2	8	5 (6)	6 (1)	4	7
PG_3	1	3	4 (3)	7 (6)	9
	3	9	4	6	

Table A4   Feasible flow using least cost rule for Example A1

	D_1	D_2	D_3	D_4	
PG_1	4	10	12	3 (6)	6
PG_2	8	5 (3)	6 (4)	4 (0)	7
PG_3	1 (3)	3 (6)	4	7	9
	3	9	4	6	

We choose a different order for selecting the squares in the example above. We try to find a good initial solution by choosing the squares with the smallest transmission costs first.

It can be observed from Table A3 that the smallest transmission cost is in the lower left square, which is $c_{31} = 1$. Thus it will be most economical to supply power from generator 3 to load 1. Since the maximal load is 3 for D_1, the maximal power flow $P_{31} = 3$ is determined and D_1 is satisfied, which can be deleted for the other computation. Of the remaining squares, 3 is the lowest transmission cost (there are two). We might choose the upper right corner next. Thus $P_{14} = 6$ is determined, and we may delete either PG_1 or D_4, but not both, according to rule (2b). Say we delete PG_1. Next $P_{32} = 6$ is determined and PG_3 is deleted. Of the generators, only PG_2 remains, so we can determine $P_{22} = 3$, $P_{23} = 4$ and $P_{24} = 0$. The results are shown in Table A4.

3. Check optimality of the results

We check the feasible power flow in Table A4 for optimality. First solve for u_i and v_j. We put $u_2 = 0$ because that allows us to solve quickly for $v_2 = 5$, $v_3 = 6$, and $v_4 = 4$. [Generally, it is a good idea to start with a $u_i = 0$ (or $v_j = 0$) for which there are many determined variables in the corresponding

Table A5 Optimality check for Example A1

	3	5	6	4	
1	4	8	12	3 6	6
0	8	5 3	6 4	4 0	7
2	1 3	3 6	4	7	9
	3	9	4	6	

row (column).] Knowing $v_4 = 4$ allows us to solve for $u_1 = 1$. Knowing $v_2 = 5$ allows us to solve for $u_3 = 2$, which allows us to solve for $v_1 = 3$. We write the v_j variables across the top of the array and u_i along the left, as shown in Table A5.

Then, check the feasibility of the remaining six squares. The upper left square satisfies the constraint $v_j - u_i \le c_{ij}$, since $3 - 1 = 2 \le 4$. Similarly, all the squares may be seen to satisfy the constraints, and hence the above gives the solution to both primal and dual problems. The optimal shipping schedule is as noted, and the value is

$\Sigma\Sigma c_{ij}x_{ij} = 3 \cdot 1 + 6 \cdot 3 + 3 \cdot 5 + 4 \cdot 6 + 0 \cdot 4 + 6 \cdot 3 = 78$.

We can check whether the solution is optimal by computing $\Sigma v_j r_j - \Sigma u_i s_i$, which is the objective function of the dual problem. According to Corollary 2 of the duality theorem described in Appendix A, we have

$$\sum\sum c_{ij}x_{ij} = \sum v_j r_j - \sum u_i s_i \tag{5A.11}$$

If both primal and dual problems have the optimal solution.

$$\sum v_j r_j - \sum u_i s_i = 78$$

Thus the above solution is optimal.

Example A2

Example A2 is computed as for example A1 with the transmission cost shown in Table A6.

According to the least cost rule, we get the feasible flow table in Table A7.

According to the equilibrium condition, we can compute u_i and v_j. The corresponding results are shown in Table A8.

Through checking the optimality in Table A8, we find that the block $(2, 1)$ in Table A8 cannot satisfy the constraint $v_j - u_i \le c_{ij}$, since

Table A6   Transportation array for Example A2

	D_1	D_2	D_3	D_4	
PG_1	4	8	13	3	6
PG_2	2	5	6	5	7
PG_3	1	3	4	15	9
	3	9	4	6	

Table A7   Least cost flow for Example A2

	D_1	D_2	D_3	D_4	
PG_1	4	8	13	3 6	6
PG_2	2	5 3	6 4	5	7
PG_3	1 3	3 6	4	15	9
	3	9	4	6	

Table A8   Optimality check for Example A2

	3	5	6	5	
2	4	8	13	3 6	6
0	2	5 3	6 4	5	7
2	1 3	3 6	4	15	9
	3	9	4	6	

$v_1 - u_2 = 3 - 0 = 3 \geq c_{12} = 2$. Thus the solution in Table A8 is not optimal. We need to find an improved basic feasible shipping schedule and recheck the optimality.

Choose any square (i, j) with $v_j - u_i > c_{ij}$, set $x_{ij} = \theta$, but keep the constraints satisfied by subtracting and adding θ to appropriate selected variables. We would like to add θ to block $(2, 1)$. This requires subtracting θ from squares $(3, 1)$ and $(2, 2)$ and adding θ to square $(3, 2)$, which are shown in Table A9.

Table A9 Optimality check for Example A2

	3	5	6	5	
2	4	8	13	3	
				6	6
0	2 +θ	5 −θ 3	6 4	5	7
2	1 −θ 3	3 +θ 6	4	15	9
	3	9	4	6	

Table A10 Optimality check for Example A2

	2	5	6	5	
2	4	8	13	3	
				6	6
0	2 3	5 0	6 4	5	7
2	1 0	3 9	4	15	9
	3	9	4	6	

We choose θ to be the minimum of the x_{ij} in the squares in which we are subtracting θ. In the example, θ = 3. Determine the new variable and remove from the selected variables one of the variables from which θ was subtracted that is now zero. Thus we get Table A10. We can check whether all the constraints are met, and the optimal solution is 75.

Dijkstra Label Setting Algorithm

Dijkstra's algorithm is a widely used label method for solving network flow problems such as the shortest-path problem. The data structures that are carried from one iteration to the next are a set F of *finished* nodes and two arrays indexed by the nodes of the graph. The first array, $v_j, j \in N$, is just the array of labels. The second array, $h_i, i \in N$, indicates the next node to visit from node i in a shortest path. As the algorithm proceeds, the set F contains those nodes for which the shortest path has already been found. This set starts out empty. Each iteration of the algorithm adds one node to it. This is why the algorithm is called a label-setting algorithm, since each iteration sets one label to its optimal value. For finished nodes, the labels are fixed at their optimal values. For each unfinished node, the label has a temporary value, which represents the length of the shortest path from that node to the root, subject to the condition that all intermediate nodes on the path must be fin-

ished nodes. At those nodes for which no such path exists, the temporary label is set to infinity (or, in practice, a large positive number).

The algorithm is initialized by setting all the labels to infinity except for the root node (or source node), whose label is set to 0. Also, the set of finished nodes is initialized to the empty set. Then, as long as there remain unfinished nodes, the algorithm selects an unfinished node j having the smallest temporary label, adds it to the set of finished nodes, and then updates each unfinished "upstream" neighbor i by setting its label to $c_{ij} + v_j$ if this value is smaller than the current value v_i. For each neighbor i whose label gets changed, h_i is set to j.

REFERENCES

[1] O. Alsac and B. Stott, "Optimal load flow with steady-state security," *IEEE Trans., PAS*, 1974, pp. 745–751.

[2] J.Z. Zhu and G.Y. Xu, "A new economic power dispatch method with security," *Electric Power Systems Research*, 1992, Vol. 25, pp. 9–15.

[3] J.Z. Zhu, "Power System Optimal Operation," Tutorial of Chongqing University, 1990.

[4] M.R. Irving and M.J.H. "Sterling, Economic dispatch of Active power with constraint relaxation," *IEE Proceedings*. C, 1983, Vol. 130, pp. 172–177.

[5] T.H. Lee, D.H. Thorne, and E.F. Hill, "A transportation method for economic dispatching—Application and comparison," *IEEE Trans., PAS*, 1980, Vol. 99, pp. 2372–2385.

[6] E. Hobson, D.L. Fletcher, and W.O. Stadlin, "Network flow linear programming techniques and their application to fuel scheduling and contingency analysis," *IEEE Trans., PAS*, 1984, Vol. 103, pp. 1684–1691.

[7] A.J. Elacqua and S.L. Corey, "Security constrained dispatch at the New York power pool," *IEEE Trans., PAS*, 1982, Vol. 101, pp. 2876–2884.

[8] J.A. Momoh, G.F. Brown, and R. Adapa, "Evaluation of interior point methods and their application to power system economic dispatch," Proceedings of the 1993 North American Power Symposium, October 11–12, 1993.

[9] J.Z. Zhu and M.R. Irving, "Combined active and reactive dispatch with multiple objectives using an analytic hierarchical process," *IEE Proceedings* C, 1996, Vol. 143, No. 4, pp. 344–352.

[10] J.Z. Zhu and G.Y. Xu, "Application of out-of-kilter algorithm in network programming technology to real power economic dispatch," *Journal of Chongqing University*, Vol. 11, No. 2, 1988.

[11] J.Z. Zhu and G.Y. Xu, "The convex network flow programming model and algorithm of real power economic dispatch with security," *Control & Decision*, Vol. 6, No. 1, 1991, pp. 48–52.

[12] J.Z. Zhu and C.S. Chang, "A new model and algorithm of secure and economic automatic generation control," *Electric Power Systems Research*, 1998, Vol. 45, No. 2, pp. 119–127.

[13] J.Z. Zhu, *Application of Network Flow Techniques to Power Systems*, WA: Tianya Press, Technology, Dec. 2005.

[14] J.Z. Zhu, M.R. Irving, and G.Y. Xu, "A new approach to secure economic power dispatch," *International Journal of Electric Power & Energy System*, 1998, Vol. 20, No. 8, pp. 533–538.

[15] J.Z. Zhu and G.Y. Xu, "Network flow model of multi-generation plan for on-line economic dispatch with security," *Modeling, Simulation & Control*, A, Vol. 32, No. 1, 1991, pp. 49–55.

[16] J.Z. Zhu and G.Y. Xu, "Secure economic power reschedule of power systems," *Modeling, Measurement & Control*, D, Vol. 10, No. 2, 1994, pp. 59–64.

[17] J. Nanda and R.B. Narayanan, "Application of genetic algorithm to economic load dispatch with Line flow constraints," *Electrical Power and Energy Systems*, Vol. 24, 2002, pp. 723–729.

[18] T.D. King, M.E. El-Hawary, and F. El-Hawary, "Optimal environmental dispatching of electric power system via an improved Hopfield neural network model," *IEEE Trans on Power System*, Vol. 10, No. 3, 1995, pp. 1559–1565.

[19] K.P. Wong and C.C. Fung, "Simulated-annealing-based economic dispatch algorithm," *IEE Proc.* Part C, Vol. 140, No. 6, 1993, pp. 509–515.

[20] J.Z. Zhu and G.Y. Xu, "Approach to automatic contingency selection by reactive type performance index," *IEE Proceedings* C, 1991, Vol. 138, pp. 65–68.

[21] J.Z. Zhu and G.Y. Xu, "A unified model and automatic contingency selection algorithm for the P and Q sub-problems," *Electric Power Systems Research*, 1995, Vol. 32, pp. 101–105.

[22] D.K. Smith, *Network optimization practice*, Ellis Horwood, Chichester, UK, 1982.

[23] G. B. Dantzig, *Linear Programming and Extensions*, Princeton University Press, 1963.

[24] D.G. Luenberger, *Introduction to linear and nonlinear programming*, Addison-Wesley Publishing Company, Inc. USA, 1973.

[25] G. Hadley, *Linear programming*, Addison—Wesley, Reading, MA, 1962.

[26] J.K. Strayer, *Linear Programming and Applications*, Springer-Verlag, 1989.

[27] M. Bazaraa, J. Jarvis, and H. Sherali, *Linear Programming and Network Flows*, 2 edn, Wiley, New York, 1977.

6

MULTIAREA SYSTEM ECONOMIC DISPATCH

This chapter focuses on the operation of the multiarea system. In addition to the introduction of the wheeling model, multiarea wheeling, the total transfer capability computation in multiareas, this chapter introduces the multiarea economic dispatch algorithms based on nonlinear convex network flow programming, as well as the nonlinear optimization neural network approach.

6.1 INTRODUCTION

Many countries have more than one major generation-transmission utility with local distribution utilities. Because of the recent deregulation of power industry, the industry structure is important in discussing the interchange of power and energy since the purchase and sale of power and energy is a commercial business in which the parties to any transaction expect to enhance their own economic positions under nonemergency situations. The multiarea system economic dispatch or interconnected systems economic dispatch is for this purpose.

At present, many approaches have been considered for multiarea economic dispatch (MAED) [1–5], which is an extension of economic dispatch. All kinds of optimization algorithms and heuristic approaches have been used in economic dispatch [6–18], which we also describe in Chapter 5.

6.2   ECONOMY OF MULTIAREA INTERCONNECTION

Electric power systems are interconnected or multiple areas are intercon-
nected to one big system because the interconnected system is more reliable.
Here we use the term multiarea system to stand for the interconnected system.
In a multiarea system, generations and loads are coordinated with each other
through the tie-lines among the areas. A load change in any one of the areas
is taken care of by all generators in all areas. Similarly, if a generator is lost
in one control area, governing action from generators in all connected areas
will increase generation outputs to make up the mismatch. Another advantage
of a multiarea system is that it may be operated at less cost than if left as sepa-
rate parts. As we describe in Chapter 4, it will improve the operating econom-
ics if two generators that have different incremental costs are operating
together. This concept is also suited for the interconnected multiarea system
since the generator cost functions are different for different areas.

For example, the companies that are members of the broker system send
hourly buy-and-sell offers for energy to the broker, who matches them accord-
ing to certain market rules. Hourly, each member transmits an incremental
cost and the number of MWh it is willing to sell or its decremental cost and
the number of MWh it will buy. The broker sets up the transactions by match-
ing the lowest-cost seller with the highest-cost purchaser, proceeding in this
manner until all offers are processed. A common arrangement set up by the
broker for the buyers and sellers is to compensate the seller for the incremen-
tal generation costs and split the savings of the buyer equally with the seller.
The pricing formula for this arrangement is similar to the operation of two
generators with different incremental cost rates in a system. But we handle
the two generators like two utilities with one selling and the other buying.
Then, the transaction's cost rate is computed as below [19]:

$$\lambda_c = \lambda_s + \frac{1}{2}(\lambda_b - \lambda_s)$$

$$= \frac{1}{2}(\lambda_b + \lambda_s) \tag{6.1}$$

where

λ_s: Incremental cost of the selling utility ($/MWh)
λ_b: Decremental cost of the buying utility ($/MWh)
λ_c: Cost rate of the transaction ($/MWh)

Example 6.1

There are four utilities, with two selling and two buying. The related data
are listed in Tables 6.1 and 6.2. The maximum pool savings possible is
computed as below:

Table 6.1   Data of utilities A and B

Utilities Selling Energy	Incremental Cost ($/MWh)	MWh for Sale	Seller's Total Increase in Cost ($)
A	20	120	2400
B	28	80	2240

Table 6.2   Data of utilities C and D

Utilities Buying Energy	Decremental Cost ($/MWh)	MWh for Purchase	Buyer's Total Decrease in Cost ($)
C	32	60	1920
D	46	140	6440

Net pool savings = (1920 + 6440) − (2440 + 2240) = 3720 ($)
   The broker sets up transactions as shown below:

1. Transaction: A sells 120 MWh to D
   Transaction saving $\Delta F_{A-D} = 120 \times (46 - 20) = 3120$ ($)
2. Transaction: B sells 20 MWh to D
   Transaction saving $\Delta F_{B-D} = 20 \times (46 - 28) = 360$ ($)
3. Transaction: B sells 60 MWh to C
   Transaction saving $\Delta F_{B-C} = 60 \times (32 - 28) = 240$ ($)

The total transaction savings are

$$\Delta F_T = 60 \times (32 - 28) = 3120 + 360 + 240 = 3720 \ (\$)$$

Then the rate and payment of each transaction are computed as follows:

1. Transaction: A sells 120 MWh to D
   Rate $\lambda_{A-D} = (46 + 20)/2 = 33$ ($/MWh)
   Payment: $F_{A-D} = 33 \times 120 = 3960$ ($)
2. Transaction: B sells 20 MWh to D
   Rate $\lambda_{A-D} = (46 + 28)/2 = 37$ ($/MWh)
   Payment: $F_{A-D} = 37 \times 20 = 740$ ($)
3. Transaction: B sells 60 MWh to C
   Rate $\lambda_{A-D} = (32 + 28)/2 = 30$ ($/MWh)
   Payment: $F_{A-D} = 30 \times 60 = 1800$ ($)

This means that utility A receives payment of $3960 from utility D, and utility B receives payment of $2540 from C and D. The each participant obtains benefit.

$$\Delta F_A = 3960 - 2400 = 1560 \ (\$)$$

$$\Delta F_B = 2540 - 2240 = 300 \ (\$)$$

$$\Delta F_C = 1920 - 1800 = 120 \ (\$)$$

$$\Delta F_D = 6440 - 3960 - 740 = 1740 \ (\$)$$

Obviously, $\Delta F_A + \Delta F_B + \Delta F_C + \Delta F_D = \Delta F_T$.

Therefore, there exist transactions among areas if the areas belong to different companies. One area may have a surplus of power and energy and may wish to sell it to other areas with different companies on a long-term firm supply basis. If excess this agreed amount, it will be on a "when and if available" basis with a different price. Meanwhile, some area may wish to buy energy from the other areas in the connected system. It is possible that the interconnected system will have interchange power being bought and sold simultaneously within several areas. Thus the price for the interchange must be set while taking account of the other transactions. For example, if one area were to sell interchange power to two different areas in sequence, it would probably quote a higher price for the second sale since the first sale would have raised its incremental cost. On the other hand, if the selling utility was a member of a power pool, the sale price might be set by the power and energy pricing portions of the pool agreement to be at a level such that the seller receives the cost of the generation for the sale plus one-half the total savings of all the purchasers. In this case, it is assumed that a pool control center exists and the sale price would be computed by this center and would differ from the prices under multiple interchange contracts. In the United States, the independent system operator (ISO) plays this kind of role.

The power pool or ISO is administered from a central location that has responsibility for setting up interchange between members, as well as other administrative tasks. The pool members relinquish certain responsibilities to the pool operating office in return for greater economy in operation. The agreement that the pool members sign is usually very complex. The complexity arises because the members of the pool are attempting to gain greater benefits from the pool operation and to allocate these benefits equitably among the members. In addition to maximizing the economic benefits of interchange between the members, the pool helps member companies by coordinating unit commitment and maintenance scheduling, providing a centralized assessment of system security and reliability, as well as marketing rules, and so on. The increased reliability provided by the pool allows the members to draw energy from the pool transmission network during emergencies as well as covering each others' reserves when generating units are down for maintenance or in outage.

The agreements among the pool members are very important for the operation of a pool system. Obviously, the agreements will become more

complicated if the members try to push for maximum economic operation. Nevertheless, the savings obtainable are quite significant and have led many interconnected utility systems (i.e., multiarea systems) throughout the world to form centrally dispatched power pools when feasible. At present, there are several organizations similar to the power pool in the United States. These are MISO, ISONE, CAISO, PJM, NYISO, ERCOT, SPP, Entergy, etc. These ISOs have SCADA and EMS systems, as well as a market system. They use real-time data telemetered to central computers that calculate the best economic dispatch for the whole organization (within footprint) and provide signals to the member companies.

Example 6.2

For example 6.1, assume that four utilities were scheduled to transact energy by a central dispatching scheme and 12% of the gross system savings was to be set aside to compensate those systems that provided transmission facilities to the pool. The maximum pool savings possible is computed as below.

The net pool savings without transmission compensation is 3720 ($). Thus the transmission compensation $F_{Tcomp} = 3720 \times 12\% = 446.4$ ($)

The weighted average incremental cost for selling can be computed as below:

$$\bar{\lambda}_s = \frac{\sum\limits_{i=1}^{NS} \lambda_{si} P_{si}}{\sum\limits_{i=1}^{NS} P_{si}} \tag{6.2}$$

where

$\bar{\lambda}_s$: The weighted average incremental cost for selling utilities ($/MWh)
λ_{si}: The incremental cost for selling utility i ($)
P_{si}: The selling power for selling utility i (MWh)
NS: The number of selling utilities

The weighted average decremental cost for buying can be computed as below:

$$\bar{\lambda}_b = \frac{\sum\limits_{j=1}^{NB} \lambda_{bj} P_{bj}}{\sum\limits_{j=1}^{NB} P_{bj}} \tag{6.3}$$

where

$\overline{\lambda}_b$: The weighted average incremental cost for buying utilities ($/MWh)
λ_{bj}: The decremental cost for buying utility j ($)
P_{bj}: The selling power for buying utility j (MWh)
NB: The number of buying utilities

For this example, the seller's weighted average incremental cost is

$$\overline{\lambda}_s = \frac{20 \times 120 + 28 \times 80}{120 + 80} = 23.2 \text{ ($/MWh)}$$

The buyer's weighted average decremental cost is

$$\overline{\lambda}_b = \frac{32 \times 60 + 46 \times 140}{60 + 140} = 41.8 \text{ ($/MWh)}$$

Considering the transmission compensation, the transaction savings for seller and buyer can be computed as below:

$$\Delta F_{si} = (1 - \eta\%) \frac{\overline{\lambda}_b - \lambda_{si}}{2} P_{si} \tag{6.4}$$

$$\Delta F_{bi} = (1 - \eta\%) \frac{\lambda_{bi} - \overline{\lambda}_s}{2} P_{bi} \tag{6.5}$$

where

$\eta\%$: The transmission compensation rate

For utility A that sells 120 MWh to the pool, the transaction savings are

$$\Delta F_{sA} = (1 - 12\%) \frac{41.8 - 20}{2} \times 120 = 1151.04 \text{ ($)}$$

For utility B that sells 80 MWh to the pool, the transaction savings are

$$\Delta F_{sB} = (1 - 12\%) \frac{41.8 - 28}{2} \times 80 = 485.76 \text{ ($)}$$

For utility C that buys 60 MWh from the pool, the transaction savings are

$$\Delta F_{bC} = (1 - 12\%) \frac{32 - 23.2}{2} \times 60 = 232.32 \text{ ($)}$$

For utility D that buys 140 MWh from pool, the transaction savings are

$$\Delta F_{bD} = (1 - 12\%)\frac{46 - 23.2}{2} \times 140 = 1404.48 \ (\$)$$

The total savings are

$$\Delta F_T = \Delta F_{sA} + \Delta F_{sB} + \Delta F_{bC} + \Delta F_{bD}$$
$$= 1151.04 + 485.76 + 232.32 + 1404.48 = 3273.6$$

The practical costs in the transactions for this hour are:

For A, it sells 120 MWh and obtains

$$F_A = 120 \times 23.2 + 1151.04 = 3935.04 \ (\$)$$

For B, it sells 80 MWh and obtains

$$F_B = 80 \times 23.2 + 485.76 = 2341.76 \ (\$)$$

For C, it buys 60 MWh with payment

$$F_C = 60 \times 41.8 - 232.32 = 2275.68 \ (\$)$$

For D, it buys 140 MWh with payment

$$F_D = 140 \times 41.8 - 1404.48 = 4447.52 \ (\$)$$

The total payments for this transaction are $F_C + F_D = 2275.68 + 4447.52 = 6723.2$.

The total costs that sellers obtained are $F_A + F_B = 3935.04 + 2341.76 = 6276.8$

The difference between the total payments and the costs that sellers obtained is 446.4, which equals the transmission charge or compensation.

6.3   WHEELING

6.3.1   Concept of Wheeling

Wheeling is the heart of the operational and economic issues of an open access transmission. Let us use the following example to explain what "wheeling" is. Assume utility A (e.g., in area A) needs to sell 200 MW to another utility B (e.g., in area B) through its own transmission (line 1) shown in Figure 6.1(a). For simplification of explanation, the network power loss is
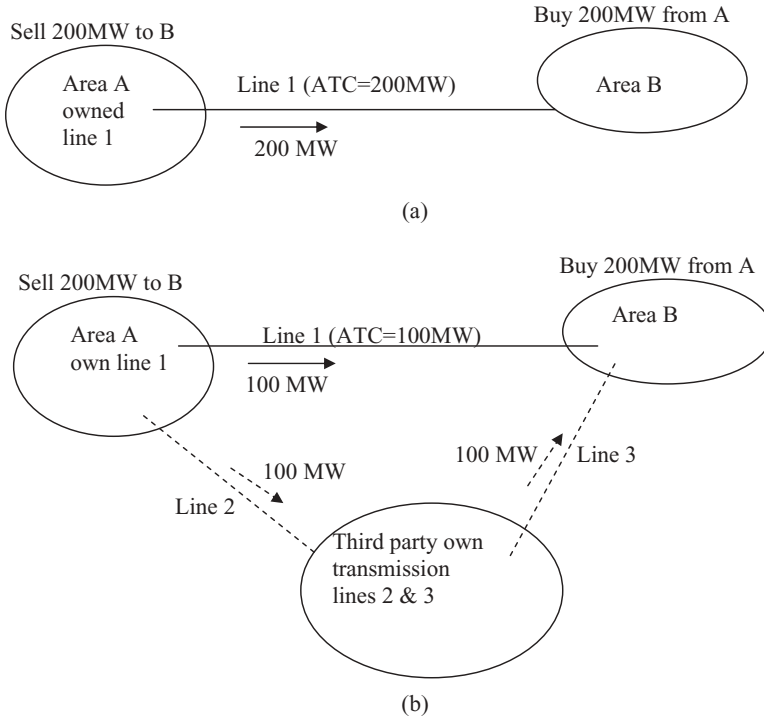
FIGURE 6.1   Explanation of wheeling

neglected. If the available transfer capacity (ATC) of line 1 is greater than 200 MW, the transaction is simple and there is no "wheeling." But if the ATC of line 1 is only 100 MW and the same amount of transaction is required, utility A cannot complete the transaction through its own transmission lines. Utility A has to "borrow" the path from the third party that owns transmission lines 2 and 3, which connect to utilities A and B (unless utility A constructs a new transmission line, which is an expensive investment). Thus the transaction between utilities A and B is completed through the third party, which is shown in Figure 6.1(b). This case involves "wheeling." The corresponding cost or pricing for this transaction is more complicated than that for the case shown in Figure 6.1(a).

Thus we can simply say that "wheeling" is the use of some party's (or parties') transmission system for the benefit of other parties. Each wheeling utility is termed a wheel. Wheeling occurs on the interconnected areas or systems that contain more than two utilities (or parties) whenever a transaction takes place. When the contracted energy flow enters and leaves the wheeling utility, the flows throughout the wheeling utility's network will change. The transmission losses incurred in the wheeling utility will change. Wheeling rates are the prices it charges for use of its network, which determine the

payments by the buyers or sellers, or both, to the wheeling utility to compensate it for the generation and network costs incurred.

There are four major types of wheeling depending on the relationships between the wheeling utility and the buyer-seller parties [20].

- *Utility to utility:* This is usually a case of area-to-area wheeling.
- *Utility to private user or requirements customer:* The former is usually a case of area-to-bus wheeling, while the latter is usually a case of area-to-area wheeling, unless the requirements customer is small enough to be fed only at one bus, and thus it becomes area-to-bus wheeling.
- *Private generator to utility:* Bus-to-area wheeling.
- *Private generator to private generator:* Bus-to-bus wheeling.

Wheeling power may either increase or decrease transmission losses depending on whether the power wheeled flows in the same direction as, or counter to, the native load on the wheeler's lines. Wheeling power on a heavily loaded line causes more energy loss.

The cost of wheeling is a current high-priority problem throughout the power industry for utilities, independent power producers, as well as regulators. The following factors have led to the importance of the cost of the wheeling problem in the United States:

(1) Enormous growth in transmission facilities at 230 KV and above since 1960s
(2) Cost differentials for electric energy between different but interconnected electric utilities
(3) High cost of new plant construction versus long-term, off-system capacity purchase
(4) Dramatic growth in nonutility generation (NUG) capacity, which includes independent power producers (IPP) and cogenerators, due to the passage: of the Public Utility Regulatory Act in 1978 and the subsequent introduction of competitive bidding for generation capacity and energy.

Wheeling is necessary and important for any NUG, unless the customer of a NUG is the utility itself to which it is directly connected.

It is noted that not all of the transaction flows over the direct interconnections between the two systems. The other systems are all wheeling some amount of the transaction. These are called "parallel path or loop flows" in the United States, where various arrangements have been worked out between the utilities in different regions to facilitate interutility transactions that involve wheeling. These past agreements would generally ignore flows over parallel paths where the two systems were contiguous and owned sufficient transmission capacity to permit the transfer [19]. In this case, wheeling was not

taking place, by mutual agreement. The extension of this agreement to non-contiguous utilities led to the artifice known as the "contract path." To make arrangements for wheeling, the two utilities would rent the capability needed to any path that would interconnect these two utilities.

6.3.2 Cost Models of Wheeling

We considered energy transaction prices based on the split-savings concept earlier in this book. Both the sellers and wheeling systems would want to recover their cost and would wish to receive a profit by splitting the savings of the purchaser. The transmission services may be offered on the basis of a "cost plus" price. Other pricing schemes have been used. Most are based upon simplified models that allow such fictions as the "contract path." Some are based on an attempt to mimic a power flow, in that they would base prices on incremental power flows determined in some cases by using DC power flow models. The very simplest rate is a charge per MWh transferred and ignores any path considerations. More complex schemes are based on the marginal cost of transmission that is based on the use of bus incremental costs [19]. The numerical evaluation of bus incremental costs is straightforward for a system in economic dispatch. In that case, the bus penalty factor times the incremental cost of power at the bus is equal to the system λ, except for the generator buses that are at upper or lower limits. This concept is not only for the generator buses, but also for the load buses, even any bus that does not have any generator or load connected to it. In the practical marketing system, this kind of bus or node is called the pricing bus or pricing node. It is noted that this method is only good for a small increment of power at a bus, rather than a large increment. If the increment of power is large, the optimal power dispatch must be recalculated and the cost is not equal to the incremental cost. We treat this case in next sections as well as Chapter 8 on optimal power flow.

In this section, several cost models of wheeling are discussed.

6.3.2.1 Short-Run Marginal Cost Model   The short-run marginal costs (SRMC) of wheeling are the costs of the last MWh of energy wheeled, which can be computed from the difference in the marginal costs of electricity at the entry and exit buses, that is, the difference in the spot prices of these buses.

Figure 6.2 gives a wheeling example with system A selling ΔP_W MW to system C and system B wheeling that amount. As we mentioned above, if the operators were to purchase the block of wheeled power at bus i at the incremental cost, and sell it to system C at the incremental cost of power at bus j, the wheeling costs, using marginal cost pricing and related computations can be obtained as below [21]:

$$\lambda_W = \frac{\partial F_i}{\partial P_{Gi}} - \frac{\partial F_j}{\partial P_{Gj}} \tag{6.6}$$
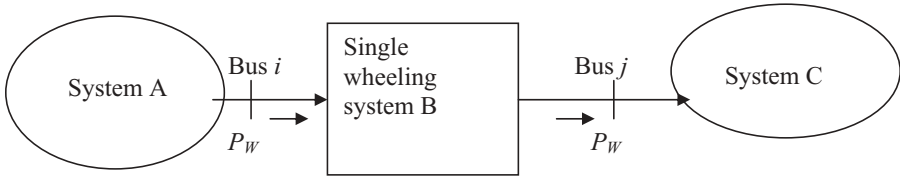
FIGURE 6.2   Wheeling example

where

λ_W: Short-run marginal costs of wheeling

Equation (6.6) is simply the equation of the spot prices. The total wheeling costs with wheeling power ΔP_W MW will be

$$\Delta F_W = \lambda_W \Delta P_W = \left[\frac{\partial F_i}{\partial P_{Gi}} - \frac{\partial F_j}{\partial P_{Gj}} \right] \Delta P_W \tag{6.7}$$

6.3.2.2   Embedded Cost Model   The embedded cost of wheeling methods, used throughout the utility industry, allocates the embedded capital costs and the average annual operation (not production) maintenance costs of existing facilities to a particular wheel; these facilities include transmission, subtransmission, and substation facilities. Happ has given a detailed treatment of all the methods as well as their algorithms. There are four types of embedded methods [22, 23]:

(1) Rolled-in-embedded method
     This method assumes that the entire transmission system is used in wheeling, regardless of the actual transmission facilities that carry the wheel. The cost of wheeling as determined by this method is independent of the distance of the wheel, which is the reason that the method is also known as the postage stamp method. The embedded capital costs correspondingly reflect the entire transmission system.
(2) Contract path method
     This method is based upon the assumption that the wheel is confined to flow along a specified electrically continuous path through the wheeling company's transmission system. Changes in flows in facilities that are not along the identified path are ignored. Thus this method is limited to those facilities that lie along assumed path.
(3) Boundary flow method
     This method incorporates changes in MW boundary flows of the wheeling company due to a wheel, either on a line basis or on a net interchange basis, into the cost of wheeling. Two power flows, executed

successively for every year with and without each wheel, yield the changes in either individual boundary line or net interchange MW flows. The load level represented in the power flows can be at peak load or any other appropriate load.

(4) Line-by-line method

This method considers changes in MW flows due to the wheel in all transmission lines of the wheeling company and the line lengths in miles. Two power flows executed with and without the wheel yield the changes in MW flows in all transmission lines.

There are two limitations common to all four embedded cost methods:

(1) The methods consider only the costs of existing transmission facilities.

(2) The methods do not consider changes in production costs as a result of required changes in dispatch and or unit commitment due to the presence of the wheel.

Other cost factors may exist that contribute to the cost of wheeling. In particular, the available transfer capacity of the transmission network is not considered, for example, the economic purchases or sales of power, which have to be curtailed to accommodate the wheel because of transmission limits.

6.3.2.3 Long-Run Incremental Cost Model
Long-run incremental transmission costs for wheeling account for:

(1) The investment costs for reinforcement to accommodate the wheel, or credit for delaying or avoiding reinforcements, and

(2) The charge in operating costs and incremental operation and maintenance costs incurred because of the wheel.

There are currently two models for the LRIC methodologies: standard long-run incremental cost (SLRIC) methodology and long-run fully incremental cost (LRFIC) methodology.

The standard long-run incremental cost method uses traditional system planning approaches to determine reinforcements that are required, and corresponding investment schedules with and without each wheel, throughout the study period. If more than one wheel is present in the study period, the cost of each reinforcement and the change in operating costs have to be accurately allocated to each wheel.

The long-run fully incremental cost method does not allow excess transmission capacity to be used by a wheel but forces a reinforcement along the path of the wheel to accommodate it; if more than one wheel is present in the study period, a reinforcement is required for each separate wheel [23].
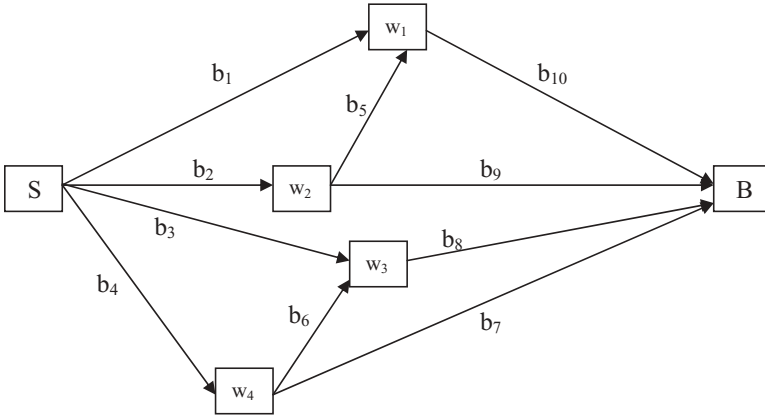
FIGURE 6.3   Multiarea wheeling topology

6.4   MULTIAREA WHEELING

Multiarea wheeling is a real-world practical concern, because wheeling from a seller to a buyer involves power flow through several intermediate networks. How much power should be wheeled through each path, what wheeling should be applied to each such transaction, and how can these decisions be made optimal?

Consider an interconnected system with multiple intermediate wheeling utilities and multiple seller-buyer couples. An OKA network flow model, which is described in Chapter 5, can be used to represent this energy transaction system [24], where one seller can be treated as one source and one buyer can be treated as a sink. OKA is able to introduce a super source (seller) and a super sink (buyer) and make multiple seller-buyer pairs become one simple seller-buyer pair.

Figure 6.3 is a simple system with four intermediate wheeling utilities W_1, W_2, W_3, and W_4 and one buyer and seller pair (S-B). There are 10 interutility wheeling paths, given by the directed path b_1 through b_{10}.

Suppose that the energy to be transported through each path is arbitrarily set; then the computation of wheeling rates for each path can be obtained from the solution of an economic dispatch problem using OKA network flow programming [24]. To decide the optimal power flow on each path, the power flows can be set as variables and the wheeling rates can be used to improve the initial set values. The total operating costs must be minimized considering the topological structure of multiwheeling areas and the feasible region of wheeling power flow. The topological relation can be reflected in the following matrix equation:

$$\begin{bmatrix} 1 & 1 & 1 & 1 & 0 & 0 & 0 & 0 & 0 & 0 \\ 1 & 0 & 0 & 0 & 1 & 0 & 0 & 0 & 0 & -1 \\ 0 & 1 & 0 & 0 & -1 & 0 & 0 & 0 & -1 & 0 \\ 0 & 0 & 1 & 0 & 0 & 1 & 0 & -1 & 0 & 0 \\ 0 & 0 & 0 & 1 & 0 & -1 & -1 & 0 & 0 & 0 \\ 0 & 0 & 0 & 0 & 0 & 0 & 1 & 1 & 1 & 1 \end{bmatrix} \begin{bmatrix} b_1 \\ b_2 \\ b_3 \\ b_4 \\ b_5 \\ b_6 \\ b_7 \\ b_8 \\ b_9 \\ b_{10} \end{bmatrix} = \begin{bmatrix} 1 \\ 0 \\ 0 \\ 0 \\ 0 \\ 1 \end{bmatrix}$$

The assumptions made for the relation are [25]:

(1) Power inflow is given a positive sign and power outflow is given a negative sign and
(2) We are only concerned with the sale of unit power from S to B.

Each row-column multiplication represents one power balance equation for a particular utility (there are a total of 6 utilities in this example).

6.5 MAED SOLVED BY NONLINEAR CONVEX NETWORK FLOW PROGRAMMING

6.5.1 Introduction

This section proposes a new nonlinear convex network flow programming (NLCNFP) to solve the problem of security-constrained interconnected MAED. The proposed MAED model considers tie-line security and transfer constraints in each area. In addition, a simple analysis of buying and selling contract in a MAED is also made. The NLCNFP model of security-constrained MAED is set up and solved by using a combined method of quadratic programming (QP) and network flow programming (NFP). For examining the proposed approach, a network model of four interconnected areas is constructed. Computation results are given below in the chapter.

6.5.2 NLCNFP Model of MAED

The aim of MAED is to minimize the total production cost of supplying loads to all areas within security constraints. Initially, a basic formulation M-1 is formulated

$$\text{Min}F = \sum_{k=1}^{n} \sum_{i=1}^{NG(k)} f_{ik}(P_{Gik}) + h\sum_{k=1}^{n} \sum_{ij \in NT} P_{Lijk} \tag{6.8}$$

such that

$$\sum_{k=1}^{n} \sum_{i=1}^{NG(k)} P_{Gik} - \sum_{k=1}^{n} \sum_{i=1}^{ND(k)} P_{Dik} - P_{L} = 0 \tag{6.9}$$

$$P_{Gik\,\text{min}} \leq P_{Gik} \leq P_{Gik\,\text{max}} \tag{6.10}$$

$$|\Delta P_{Gik}| \leq \Delta P_{GikGRC} \quad k = 1, \ldots, n; i = 1, \ldots, NG(k) \tag{6.11}$$

$$|P_{ijk}| \leq P_{ijk\,\text{max}} \quad k = 1, \ldots, n; j = 1, \ldots, NL(k) \tag{6.12}$$

$$|P_{T}| \leq P_{T\,\text{max}} \quad T = 1, \ldots, NT \tag{6.13}$$

where

f_{ik}: The generation cost function of the ith generator in area k

P_{Gik}: The active power output of the ith generator in area k

P_{Dik}: The active load at node i in area k

P_{ijk}: The active power on branch j in area k

P_{T}: The active power on the tie-line

P_{L}: The active power loss of the system

P_{Lijk}: The active power loss of branch j in area k

ΔP_{GikGRC}: The limit of the generation rate constraint (GRC)

NT: The number of tie-lines

n: The number of areas

$NG(k)$: The number of generators in area k

$ND(k)$: The number of loads in area k

$NL(k)$: The number of transmission lines in area k

Subscripts "min" and "max" stand for the lower and upper bounds of a constraint.

According to Chapter 5, we have the following approximate equations:

$$V \cong 1.0 \text{ p.u.} \tag{6.14}$$

$$\sin \theta_{ij} \cong \theta_{ij} \tag{6.15}$$

$$\cos \theta_{ij} \cong 1 - \theta_{ij}^2 / 2 \tag{6.16}$$

Then, the active power loss on branch ij can be expressed as follows.

$$P_{Lijk} = P_{ijk}^2 Z_{ijk} \tag{6.17a}$$

where

$$Z_{ijk} = \frac{\left(R_{ijk}^2 + X_{ijk}^2\right)}{X_{ijk}^2} R_{ijk} \tag{6.18a}$$

$$P_{ijk} = -b_{ijk}\theta_{ijk} \tag{6.19a}$$

R_{ij}: The resistance of branch j in area k

X_{ij}: The reactance of branch j in area k

θ_{ijk}: The difference of node voltage angles between the sending end and receiving end of branch j in area k

b_{ijk}: The susceptance of branch j in area k

The active power loss on tie-line T can also be expressed as follows.

$$P_{LT} = P_T^2 Z_T \tag{6.17b}$$

where

$$Z_T = \frac{\left(R_T^2 + X_T^2\right)}{X_T^2} R_T \tag{6.18b}$$

$$P_T = -b_T\theta_T \tag{6.19b}$$

R_T: The resistance of tie-line branch T

X_T: The reactance of tie-line branch T

θ_T: The difference of node voltage angles between the sending end and receiving end of tie-line branch T

b_T: The susceptance of tie-line branch T

Thus the total system power loss can be written as below:

$$
\begin{aligned}
P_L &= \sum_{k=1}^{n} \sum_{ij=1}^{Nl(k)} P_{Lijk} + \sum_{T=1}^{NT} P_{LT} \\
&= \sum_{k=1}^{n} \sum_{ij=1}^{Nl(k)} P_{ijk}^2 Z_{ijk} + \sum_{T=1}^{NT} P_T^2 Z_T
\end{aligned} \tag{6.20}
$$

Similar to Chapter 5, we can get the power flow limit for each branch in area k, as well as each tie-line.

$$P_{ijk\,\max} = \frac{\left[\sqrt{1+(2g_{ijk}P_{ijk}/b_{ijk}^2)}-1\right]}{g_{ijk}} \tag{6.21}$$

$$P_{T\,\max} = \frac{\left[\sqrt{1+(2g_T P_T/b_T^2)}-1\right]}{g_T} \tag{6.22}$$

where g_{ij} and g_T are the conductance of branch j in area k and the tie-line, respectively.

If the KVL law is considered in the NFP model of MAED, the voltage equation of the lth loop can be written as.

$$\sum_{ij}(P_{ijk}Z_{ijk})\mu_{ij,l}=0 \quad l=1,2,\ldots,NM \tag{6.23}$$

where

NM: The number of loops in the network

$\mu_{ij,l}$: The element in the related loop matrix, which takes the value 0 or 1.

Furthermore, assume that the input-output characteristics of the generators in all areas are quadratic functions.

$$f_{ik}(P_{Gik}) = a_{ik}P_{Gik}^2 + b_{ik}P_{Gik} + c_{ik} \tag{6.24}$$

Therefore, we can obtain the following nonlinear convex network flow programming model for the MAED problem (M-2).

$$\mathrm{Min}F = \sum_{k=1}^{n}\sum_{i=1}^{NG(k)}\left(a_{ik}P_{Gik}^2+b_{ik}P_{Gik}+c_{ik}\right)+h\sum_{k=1}^{n}\sum_{ij}P_{ijk}^2 Z_{ijk}-\lambda_l\sum_{ij}(P_{ijk}Z_{ijk})\mu_{ij,l} \tag{6.25}$$

$$\sum_{k=1}^{n}\sum_{i=1}^{NG(k)}P_{Gik}-\sum_{k=1}^{n}\sum_{i=1}^{ND(k)}P_{Dik}-\left(\sum_{k=1}^{n}\sum_{ij=1}^{NI(k)}P_{ijk}^2 Z_{ijk}+\sum_{T=1}^{NT}P_T^2 Z_T\right)=0 \tag{6.26}$$

$$P_{Gik\,\min}\le P_{Gik}\le P_{Gik\,\max} \tag{6.27}$$

$$|\Delta P_{Gik}|\le \Delta P_{GikGRC} \quad k=1,\cdots,n; i=1,\ldots,NG(k) \tag{6.28}$$

$$|P_{ijk}|\le \frac{\left[\sqrt{1+(2g_{ijk}P_{ijk}/b_{ijk}^2)}-1\right]}{g_{ijk}} \quad k=1,\ldots,n; j=1,\ldots,NL(k) \tag{6.29}$$

$$|P_T|\le \frac{\left[\sqrt{1+(2g_T P_T/b_T^2)}-1\right]}{g_T} \quad T=1,\ldots,NT \tag{6.30}$$

In the MAED model, equation (6.26) defines the total power balance of multiarea systems. Equation (6.29) is the line security constraint in area k.

Equation (6.30) is the tie line capacity constraint. Equation (6.27) defines the generator power upper and lower limits. Equation (6.28) is the generation rate constraint and can be written as

$$P_{Gik}^0 - \Delta P_{GikGRC} \leq P_{Gik} \leq P_{Gik}^0 + \Delta P_{GikGRC} \tag{6.31}$$

where P_{Gik}^0 is the initial power of the ith generator in area k.

Thus the generation is regulated between two inequality equations (6.27) and (6.31), which can be combined into one expression:

$$\max\left\{P_{Gik}^0 - \Delta P_{GikGRC}, P_{Gik\,\min}\right\} \leq P_{Gik} \leq \min\left\{P_{Gik}^0 + \Delta P_{GikGRC}, P_{Gik\,\max}\right\} \tag{6.32}$$

There can be contracts of buying and selling among areas. Suppose area A sells electricity to area B, and P_{ABsell} represents the amount of power sold or P_{BAbuy} represents the amount of power purchased. The following constraints are introduced into the MAED model:

$$\sum_T P_{TAB} = +P_{ABsell} \tag{6.33}$$

$$\sum_T P_{TBA} = -P_{BAbuy} \tag{6.34}$$

or

$$(1-\eta)\% P_{ABsell} \leq \sum_T P_{TAB} \leq (1+\eta)\% P_{ABsell} \tag{6.35}$$

$$(1-\eta)\% P_{BAbuy} \leq \left|\sum_T P_{TBA}\right| \leq (1+\eta)\% P_{BAbuy} \tag{6.36}$$

where

> P_{TAB}: The tie-line transfer between areas A and B. Power transfer from the area is considered to be positive if it is an export.
> P_{ABsell}: The amount of power sold from area A to area B
> P_{BAbuy}: The amount of power purchased
> η: The trading error that is permitted in interconnected power system operation

In this way, MAED model M-2 can be written into the following model M-3 that contains the contract constraints of buying and selling electricity among areas.

$$\text{Min}F = \sum_{k=1}^{n}\sum_{i=1}^{NG(k)}\left(a_{ik}P_{Gik}^2 + b_{ik}P_{Gik} + c_{ik}\right) + h\sum_{k=1}^{n}\sum_{ij}P_{ijk}^2 Z_{ijk} - \lambda_l\sum_{ij}\left(P_{ijk}Z_{ijk}\right)\mu_{ij,l}$$

$$+ \beta\left(\sum_T P_{TAB} - P_{ABsell}\right)^2 + \gamma\left(\left|\sum_T P_{TBA}\right| - P_{BAbuy}\right)^2 \tag{6.37}$$

Subject to

$$\sum_{k=1}^{n}\sum_{i=1}^{NG(k)}P_{Gik} - \sum_{k=1}^{n}\sum_{i=1}^{ND(k)}P_{Dik} - \left(\sum_{k=1}^{n}\sum_{ij=1}^{Nl(k)}P_{ijk}^2 Z_{ijk} + \sum_{T=1}^{NT}P_T^2 Z_T\right) = 0 \tag{6.26}$$

$$\max\left\{P_{Gik}^0 - \Delta P_{GikGRC}, P_{Gik\,min}\right\} \le P_{Gik} \le \min\left\{P_{Gik}^0 + \Delta P_{GikGRC}, P_{Gik\,max}\right\} \tag{6.32}$$
$$k = 1, \ldots, n; i = 1, \ldots, NG(k)$$

$$|P_{ijk}| \le \frac{\left[\sqrt{1+(2g_{ijk}P_{ijk}/b_{ijk}^2)}-1\right]}{g_{ijk}} \quad k = 1, \ldots, n; j = 1, \ldots, NL(k) \tag{6.29}$$

$$|P_T| \le \frac{\left[\sqrt{1+(2g_T P_T/b_T^2)}-1\right]}{g_T} \quad T = 1, \ldots, NT \tag{6.30}$$

$$(1-\eta)\% P_{ABsell} \le \sum_T P_{TAB} \le (1+\eta)\% P_{ABsell} \tag{6.35}$$

$$(1-\eta)\% P_{BAbuy} \le \left|\sum_T P_{TBA}\right| \le (1+\eta)\% P_{BAbuy} \tag{6.36}$$

where β and γ are the penalty factors, which are large positive constants.

6.5.3 Solution Method

MAED model M-3 is easily changed into a standard model of nonlinear convex network flow programming, i.e., model M-4

$$\min C = \sum_{ij} c(f_{ij}) \tag{6.38}$$

such that

$$\sum_{j\in n}(f_{ij} - f_{ji}) = r_i \quad i \in n \tag{6.39}$$

$$L_{ij} \le f_{ij} \le U_{ij} \quad ij \in m \tag{6.40}$$

where

f_{ij}: The flow on arc ij in the network

L_{ij}: The lower bound of the flow on arc ij in the network

U_{ij}: The upper bound of flow on arc ij in the network

n: The total number of nodes in the network

m: The total number of arcs in the network

According to Chapter 5 (Section 5.5), the nonlinear convex network flow programming model M-4 can be changed into the following quadratic programming model M-5, in which the search direction in the space of the flow variables is to be solved:

$$\min C(D) = \frac{1}{2} D^{\mathrm{T}} G(f) D + g(f)^{\mathrm{T}} D \tag{6.41}$$

such that

$$AD = 0 \tag{6.42}$$

$$D_{ij} \geq 0, \quad \text{when} \quad f_{ij} = L_{ij} \tag{6.43}$$

$$D_{ij} \leq 0, \quad \text{when} \quad f_{ij} = U_{ij} \tag{6.44}$$

Model M-5 is a special quadratic programming model, which has the form of network flow. To enhance the calculation speed, we present a new approach, in place of the general quadratic programming algorithm, to solve model M-5. The details of the calculation steps are described in Chapter 5.

6.5.4 Test Results

For examining the proposed approach, a network of four interconnected areas is constructed as shown in Figure 6.4. Area A1 is an IEEE 30-bus system. It has 6 generators, 21 loads, and 41 transformation branches, in which 1, 2, 5, 8, 11, and 13 are generators. The generator data of IEEE 30-bus system are
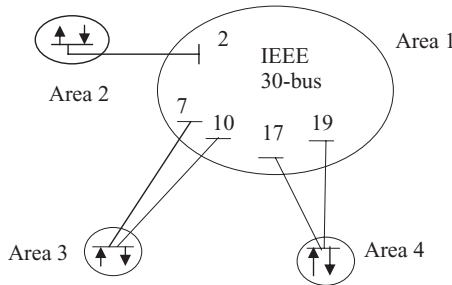
FIGURE 6.4   The network model of four interconnected power systems

Table 6.3   Data of generator nodes for IEEE 30-bus system (p.u.)

Node	a_i	b_i	c_i	P_{Gimin}	P_{Gimax}	ΔP_{GiGRC}
1	37.5	200	0.0	0.50	2.00	0.35
2	175	175	0.0	0.20	0.80	0.25
5	625	100	0.0	0.15	0.50	0.15
8	83.4	325	0.0	0.10	0.35	0.15
11	250	300	0.0	0.10	0.30	0.15
13	250	300	0.0	0.12	0.40	0.15

Note: The generation cost function is: $f_i = a_i P_{Gi}^2 + b_i P_{Gi} + c_i$.

listed in Table 6.3. The network parameters, including network constraints of the 30-bus system, are shown in Chapter 5. Parameters of areas A2, A3, A4 and tie lines are given as follows.

Fuel cost function and power upper and lower limits are:

$$F_{A2} = 80P_{A2}^2 + 175P_{A2} \quad 0.2 \le P_{A2} \le 1.0$$

$$F_{A3} = 90P_{A3}^2 + 150P_{A3} \quad 0.2 \le P_{A3} \le 1.0$$

$$F_{A4} = 600P_{A4}^2 + 300P_{A4} \quad 0.2 \le P_{A2} \le 1.0$$

Loads of areas A2, A3, and A4 are $P_{DA2} + jQ_{DA2} = 0.44 + j0.21$; $P_{DA3} + jQ_{DA3} = 0.312 + j0.14$; and $P_{DA4} + jQ_{DA4} = 0.396 + j0.18$, respectively. Parameters and capacity constraints of the tie line are:

$$R_{A2\text{-}20} = 0.0340; X_{A2\text{-}20} = 0.0680; P_{A2\text{-}20Tmax} = 0.7$$

$$R_{A3\text{-}17} = 0.0192; X_{A3\text{-}17} = 0.0575; P_{A3\text{-}17max} = 0.7$$

$$R_{A3\text{-}19} = 0.0192; X_{A3\text{-}19} = 0.0575; P_{A3\text{-}19Tmax} = 0.7$$

$$R_{A4\text{-}10} = 0.0267; X_{A4\text{-}10} = 0.8200; P_{A4\text{-}10Tmax} = 0.6$$

$$R_{A4\text{-}7} = 0.0267; X_{A4\text{-}7} = 0.8200; P_{A4\text{-}7Tmax} = 0.6$$

The following test cases for MAED are performed in the study, in which the symbol "+" represents the selling contract and "−" represents the purchase contract.

Case 1: Neglecting the buying and selling contract among areas

Case 2: Considering the buying and selling contract among areas

$$P_{A3\text{-}A1sell} = +0.5; P_{A4\text{-}A1buy} = -0.0$$

Case 3: Considering the buying and selling among areas

$$P_{A3\text{-}A1sell} = +0.55; P_{A4\text{-}A1buy} = -0.10$$

Table 6.4   Test results of security-constrained MAED for four interconnected systems (NLCNFP method)

Test Cases	Case 1 (p.u)	Case 2 (p.u.)	Case 3 (p.u.)
Area A1			
P_{G1}	1.1523	1.0718	1.1146
P_{G2}	0.3569	0.3471	0.3539
P_{G5}	0.1792	0.1839	0.1833
P_{G8}	0.1053	0.1163	0.1124
P_{G11}	0.1248	0.1358	0.1319
P_{G13}	0.1253	0.1363	0.1324
Area A2			
P_{GA2}	0.8832	0.8504	0.8684
Area A3			
P_{GA3}	0.9297	0.8120	0.8620
Area A4			
P_{GA4}	0.2053	0.3965	0.2964
Total Gen.	4.06176	4.04987	4.05534
Power losses	0.07975	0.06787	0.07333
Total gen. cost ($)	1041.987	1109.621	1068.4117
Tie-line power P_{A2-20}	0.4432	0.4104	0.4284
P_{A3-17}	0.4988	0.4086	0.4487
P_{A3-19}	0.1189	0.0914	0.1013
P_{A4-7}	0.1364	0.2088	0.1684
P_{A4-10}	−0.3272	−0.2083	−0.2680
Line security	Satisfied	Satisfied	Satisfied

To evaluate the calculation accuracy, the following performance index (PI) on trading error is proposed, i.e.,

$$PI_{EAB}\% = \frac{|P_{TAB} - P_{ABsell}|}{P_{ABsell}} \times \% \qquad (6.45)$$

or

$$PI_{EAB}\% = \frac{|P_{TAB} - P_{ABbuy}|}{P_{ABbuy}} \times \% \qquad (6.46)$$

The calculation results of the security-constrained MAED for the above three test cases are listed in Table 6.4. From Table 6.4 we can get:

Case 2:

$$P_{TA3-A1} = P_{A3-17} + P_{A3-19} = 0.4086 + 0.0914 = 0.5$$

$$PI_{EA3-A1}\% = 0.0$$

$$P_{TA4-A1} = P_{A4-7} + P_{A4-10} = 0.2088 - 0.2083 = 0.0005$$

$$PI_{EA4-A1}\% = 0.05\%$$

Case 3:

$$P_{\text{TA3-A1}} = P_{\text{A3-17}} + P_{\text{A3-19}} = 0.4487 + 0.1013 = 0.55$$

$$PI_{\text{EA3-A1}}\% = 0.0$$

$$P_{\text{TA4-A1}} = P_{\text{A4-7}} + P_{\text{A4-10}} = 0.1684 - 0.2680 = -0.0996$$

$$PI_{\text{EA4-A1}}\% = 0.04\%$$

The maximum trading error is only 0.05%. Therefore, the proposed MAED approach not only satisfies all security constraints, but also has high accuracy.

6.6 NONLINEAR OPTIMIZATION NEURAL NETWORK APPROACH

6.6.1 Introduction

This section presents a new nonlinear optimization neural network approach to solve the problem of security-constrained interconnected multiarea economic dispatch (MAED). The optimization neural network (ONN) can be used to solve mathematical programming problems. It has attracted much attention in recent years. In 1986, Tank and Hopfield first proposed an optimization neural network—TH model, which was used to solve linear programming problems. ONN is totally different from traditional optimization methods. It changes the solution of an optimization problem into an equilibrium point (or equilibrium state) of a nonlinear dynamic system, and changes optimal criteria into energy functions for dynamic system. Because of its parallel computational structure and the evolution of dynamics, the ONN approach is superior to traditional optimization methods.

6.6.2 The Problem of MAED

According to the previous section, a basic formulation of MAED is formulated as

$$\text{Min}F = \sum_{k=1}^{n} \sum_{i=1}^{NG(k)} f_{ik}(P_{Gik}) \tag{6.47}$$

such that

$$\sum_{k=1}^{n} \sum_{i=1}^{NG(k)} P_{Gik} - \sum_{k=1}^{n} \sum_{i=1}^{ND(k)} P_{Dik} - P_{L} = 0 \tag{6.48}$$

$$P_{Gik\,\text{min}} \leq P_{Gik} \leq P_{Gik\,\text{max}} \tag{6.49}$$

$$|\Delta P_{Gik}| \leq \Delta P_{GikGRC} \quad k = 1, \dots, n; i = 1, \dots, NG(k) \tag{6.50}$$

$$|P_{ijk}| \leq P_{ijk\,\max} \quad k = 1, \ldots, n; ij = 1, \ldots, NL(k) \tag{6.51}$$

$$|P_T| \leq P_{T\,\max} \quad T = 1, \ldots, NT \tag{6.52}$$

The generation is regulated between two inequality equations (6.49) and (6.50), which can be combined into one expression:

$$\max\{P_{Gik}^0 - \Delta P_{GikGRC}, P_{Gik\,\min}\} \leq P_{Gik} \leq \min\{P_{Gik}^0 + \Delta P_{GikGRC}, P_{Gik\,\max}\} \tag{6.53}$$

There can be contracts of buying and selling among areas. Suppose area A sells electricity to area B, and P_{ABsell} represents the amount of power sold or P_{BAbuy} represents the amount of power purchased. The following constraints are introduced into the MAED model, which are the same as in Section 6.5.

$$\sum_T P_{TAB} = +P_{ABsell} \tag{6.54}$$

$$\sum_T P_{TBA} = -P_{BAbuy} \tag{6.55}$$

or

$$(1 - \eta)\% P_{ABsell} \leq \sum_T P_{TAB} \leq (1 + \eta)\% P_{ABsell} \tag{6.56}$$

$$(1 - \eta)\% P_{BAbuy} \leq \left| \sum_T P_{TBA} \right| \leq (1 + \eta)\% P_{BAbuy} \tag{6.57}$$

The above MAED model can be written into the following model M-6, which contains the contract constraints of buying and selling electricity among areas.

$$\text{Min} F = \sum_{k=1}^{n} \sum_{i=1}^{NG(k)} f_{ik}(P_{Gik}) + \beta \left(\sum_T P_{TAB} - P_{ABsell} \right)^2 + \gamma \left(\left| \sum_T P_{TBA} \right| - P_{BAbuy} \right)^2 \tag{6.58}$$

such that

$$\sum_{k=1}^{n} \sum_{i=1}^{NG(k)} P_{Gik} - \sum_{k=1}^{n} \sum_{i=1}^{ND(k)} P_{Dik} - P_L = 0 \tag{6.59}$$

$$\max\{P_{Gik}^0 - \Delta P_{GikGRC}, P_{Gik\,\min}\} \leq P_{Gik} \leq \min\{P_{Gik}^0 + \Delta P_{GikGRC}, P_{Gik\,\max}\} \tag{6.60}$$
$$k = 1, \ldots, n; i = 1, \ldots, NG(k)$$

$$|P_{bjk}| \leq P_{bjk\,\max} \quad k = 1, \ldots, n; j = 1, \ldots, NL(k) \tag{6.61}$$

$$|P_T| \leq P_{T\max} \quad T = 1, \ldots, NT \tag{6.62}$$

$$(1-\eta)\%P_{\text{ABsell}} \leq \sum_T P_{\text{TAB}} \leq (1+\eta)\%P_{\text{ABsell}} \tag{6.63}$$

$$(1-\eta)\%P_{\text{BAbuy}} \leq \left|\sum_T P_{\text{TBA}}\right| \leq (1+\eta)\%P_{\text{BAbuy}} \tag{6.64}$$

where β and γ are the penalty factors.

It is noted that there are some differences between the above MAED model M-6 and the model M-3 described in Section 6.5, where some approximations are applied in order to use the nonlinear convex network flow programming algorithm.

6.6.3   Nonlinear Optimization Neural Network Algorithm

6.6.3.1   Nonlinear Optimization Neural Network Model of MAED   The above MAED model M-6 can be solved by a new approach of the nonlinear optimization neural network. The neural network approach is a penalty minimizing neural network approach with weights based on optimization theory and the neural optimization method. It can be used to solve the nonlinear problem with equality and inequality constraints.

The MAED model M-6 can be rewritten into a general form of constrained optimization, i.e., model M-7:

$$\min f(x) \tag{6.65}$$

such that

$$h_j(x) = 0 \quad j = 1, \ldots, m \tag{6.66}$$

$$g_i(x) \geq 0 \quad i = 1, \ldots, k \tag{6.67}$$

To change the inequality constraints of equation (6.67) into equality constraints, new variables $y_1, \ldots, y_m$ (i.e., relaxation variables) are introduced into equation (6.67). In this way, model M-7 can be written as model M-8, i.e.,

$$\min f(x) \tag{6.65}$$

such that

$$h_j(x) = 0 \quad j = 1, \ldots, m \tag{6.66}$$

$$g_i(x) - y_i^2 = 0 \quad i = 1, \ldots, k \tag{6.68}$$

The optimization neural network is applied to the solution of M-8. The approach is totally different from traditional optimization methods. It changes the solution of optimization problems into an equilibrium point of nonlinear dynamic system, and changes optimal criteria into energy functions for dynamic system. Therefore, the energy function of NNLONN must be formed at the beginning.

According to optimization theory as described in Reference [26], we can construct the following energy function of neural network for model M-8:

$$E(x, y, \lambda, \mu, S) = f(x) - \mu^{T} h(x) - \lambda^{T} [g(x) - y^2] + (S/2) \|h(x)\|^2$$
$$+ (S/2) \|g(x) - y^2\|^2 \tag{6.69}$$

where λ and μ are Lagrange multipliers.

It is possible to construct a different energy function from the above, e.g., in an energy function as used in reference [27]. It is noted that a different energy function will produce a different neural network and distinct characteristics. There are two advantages for the proposed NNLONN approach. One is that the first three terms in the energy function of equation (6.69) are just an expanded Langrage functions as in conventional nonlinear programming. Methods to guarantee optimal solution of such functions are well understood. Another advantage is due to the quadratic penalties, which are formulated to become part of the energy function (6.69) and equality constraints (6.66)–(6.68). These penalties behave very effectively against any violation of constraint.

Dynamic equations of the neural network can be obtained according to equation (6.69).

$$dx/dt = -\left\{ \nabla_x f(x) + (Sh(x) - \mu)^{T} \nabla_x h(x) + [S(g(x) - y^2) - \lambda]^{T} \nabla_x (g(x) - y^2) \right\} \tag{6.70}$$

$$dy/dt = -\left\{ \nabla_y f(x) + (Sh(x) - \mu)^{T} \nabla_y h(x) + [S(g(x) - y^2) - \lambda]^{T} \nabla_y (g(x) - y^2) \right\} \tag{6.71}$$

$$\partial\mu/\partial t = Sh(x) \tag{6.72}$$

$$\partial\lambda/\partial t = S(g(x) - y^2) \tag{6.73}$$

From equation (6.69) we know that the variables x and y are separable. So we can get

$$\min_{x,y} E(x, y, \lambda, \mu, S) = \min_x \min_y E(x, y, \lambda, \mu, S)$$
$$= \min_x E(x, y^*(x, \lambda, \mu, S), \lambda, \mu, S) \tag{6.74}$$

where, $y^*(x, \lambda, \mu, S)$ satisfies the following equation:

$$\min_{y} E(x, y, \lambda, \mu, S) = E(x, y^*(x, \lambda, \mu, S), \lambda, \mu, S) \qquad (6.75)$$

To obtain $y^*(x, \lambda, \mu, S)$, we set $dE/dy = 0$. Then, from equation (6.69) we get

$$2y^{\mathrm{T}}[\lambda + Sy^2 - Sg(x)] = 0 \qquad (6.76)$$

Obviously, from equation (6.76) we know if $\lambda - Sg(x) \geq 0$, then $y = 0$; if $\lambda - Sg(x) < 0$, then $y = 0$, or $y^2 = (Sg(x) - \lambda)/S$, i.e.,

$$y^2 = \begin{cases} 0, & \text{if} \quad \lambda - Sg(x) \geq 0 \\ [Sg(x) - \lambda]/S, & \text{if} \quad \lambda - Sg(x) < 0 \end{cases} \qquad (6.77)$$

or

$$y^2 - g(x) = \begin{cases} -g(x), & \text{if} \quad -g(x) \geq -\lambda/S \\ -\lambda/S, & \text{if} \quad -g(x) < -\lambda/S \end{cases} \qquad (6.78)$$

From equation (6.78), we can get the following expressions:

$$y^2 - g(x) = \max(-g(x), -\lambda/S) \qquad (6.79)$$
$$y^2 - g(x) = -\min(g(x), \lambda/S) \qquad (6.80)$$
$$g(x) - y^2 = \min(g(x), \lambda/S) \qquad (6.81)$$

Substituting equation (6.79) into equation (6.69), we get

$$
\begin{aligned}
E(x, \lambda, \mu, S) &= f(x) - \mu^{\mathrm{T}} h(x) + (S/2)\|h(x)\|^2 - \lambda^{\mathrm{T}}[-\max(-g(x), -\lambda/S)] \\
&\quad + (S/2)\|\max(-g(x), -\lambda/S)\|^2 \\
&= f(x) - \mu^{\mathrm{T}} h(x) + (S/2)\|h(x)\|^2 - (1/2S)[2\lambda^{\mathrm{T}} \max(-Sg(x), -\lambda)] \\
&\quad + (1/2S)\|\max(-Sg(x), -\lambda)\|^2 \\
&= f(x) - \mu^{\mathrm{T}} h(x) + (S/2)\|h(x)\|^2 + (1/2S)\{-\|\lambda\|^2 + \|\lambda\|^2 \\
&\quad + 2\lambda^{\mathrm{T}} \max[-Sg(x), -\lambda] + \|\max[-Sg(x), -\lambda]\|^2\} \\
&= f(x) - \mu^{\mathrm{T}} h(x) + (S/2)\|h(x)\|^2 \\
&\quad + (1/2S)\{\|\lambda + \max[-Sg(x), -\lambda]\|^2 - \|\lambda\|^2\} \\
&= f(x) - \mu^{\mathrm{T}} h(x) + (S/2)\|h(x)\|^2 \\
&\quad + (1/2S)\{\|\max[0, \lambda - Sg(x)]\|^2 - \|\lambda\|^2\}
\end{aligned} \qquad (6.82)
$$

Substituting equation (6.79) into equation (6.80), we get

$$
\begin{aligned}
\mathrm{d}x/\mathrm{d}t &= -\left\{\nabla_x f(x) + [Sh(x) - \mu]^{\mathrm{T}} \nabla_x h(x) + [S(-\max(-g(x), -\lambda/S) - \lambda]^{\mathrm{T}} \nabla_x g(x)\right\} \\
&= -\left\{\nabla_x f(x) + [Sh(x) - \mu]^{\mathrm{T}} \nabla_x h(x) + [-\max(-Sg(x), -\lambda) - \lambda]^{\mathrm{T}} \nabla_x g(x)\right\} \\
&= -\left\{\nabla_x f(x) + [Sh(x) - \mu]^{\mathrm{T}} \nabla_x h(x) - [\max(-g(x), -\lambda) + \lambda]^{\mathrm{T}} \nabla_x g(x)\right\} \\
&= -\left\{\nabla_x f(x) + [Sh(x) - \mu]^{\mathrm{T}} \nabla_x h(x) - \max[0, \lambda - Sg(x)]^{\mathrm{T}} \nabla_x g(x)\right\} \quad (6.83)
\end{aligned}
$$

Substituting equation (6.81) into equation (6.73), we get

$$
\mathrm{d}\lambda/\mathrm{d}t = S \cdot \min(g(x), \lambda/S) = \min[Sg(x), \lambda] \quad (6.84)
$$

According to equations (6.82), (6.83), (6.72), and (6.84), we have deduced a new nonlinear optimization neural network model M-9, which can be used to solve the optimization problem with equality and inequality constraints. The NLONN model M-9 can be written as

$$
\begin{aligned}
E(x, \lambda, \mu, S) &= f(x) - \mu^{\mathrm{T}} h(x) + (S/2)\|h(x)\|^2 \\
&\quad + (1/2S)\left\{\|\max[0, \lambda - Sg(x)]\|^2 - \|\lambda\|^2\right\} \quad (6.85)
\end{aligned}
$$

$$
\mathrm{d}x/\mathrm{d}t = -\left\{\nabla_x f(x) + [Sh(x) - \mu]^{\mathrm{T}} \nabla_x h(x) - \nabla_x g(x)\max[0, \lambda - Sg(x)]^{\mathrm{T}}\right\} \quad (6.86)
$$

$$
\mathrm{d}\mu/\mathrm{d}t = Sh(x) \quad (6.87)
$$

$$
\mathrm{d}\lambda/\mathrm{d}t = \min[Sg(x), \lambda] \quad (6.88)
$$

The Appendix to this chapter shows that the energy function equation (6.85) in NNLONN model M-9 is a Lyapunov function, and the equilibrium point of the neural network corresponds to the optimal solution of the constrained optimization problem M-7.

6.6.3.2 *Numerical Simulation of NLONN Network*   The first-order Euler method can be used in the numerical analysis of the NLONN network, i.e.,

$$
\mathrm{d}Z/\mathrm{d}t = [Z(t + \Delta t) - Z(t)]/\Delta t \quad (6.89)
$$

$$
Z(t + \Delta t) = Z(t) + (\mathrm{d}Z/\mathrm{d}t)\Delta t \quad (6.90)
$$

So dynamic equations (6.86)–(6.88) of the NLONN network can be made equivalent to the following equations:

$$
\begin{aligned}
x(t + \Delta t) &= x(t) - \Delta t\left\{\nabla_x f(x(t)) + [Sh(x(t)) - \mu]^{\mathrm{T}} \nabla_x h(x(t)) \right. \\
&\quad \left. - \nabla_x g(x(t))\max[0, \lambda - Sg(x(t))]^{T}\right\} \quad (6.91)
\end{aligned}
$$

$$\mu(t+\Delta t)=\mu(t)+\Delta t Sh(x(t)) \tag{6.92}$$

$$\lambda(t+\Delta t)=\lambda(t)+\Delta t \min[Sg(x(t)),\lambda(t)] \tag{6.93}$$

The calculation steps of the NLONN method are given below.

Step 1: Select a set of initial values $x(0)$ and parameters $\lambda(0)$, $\mu(0)$, as well as a set of positive ordinal numbers $\{S(k)\}\cdot S(k+1)=\rho S(k)$.

Step 2: Calculate gradients.

$$\begin{aligned}
\Phi(x)&=\nabla_x E[x(k),\lambda(k),\mu(k),S(k)]\\
&=\nabla_x f(x(k))+[S(k)h(x(k))-\mu(k)]^T\nabla_x h(x(k))]\\
&\quad-\max[0,\lambda(k)-S(k)g(x(k))]^T\nabla_x g(x(k))
\end{aligned} \tag{6.94}$$

Step 3: Compute new state

$$x(k+1)=x(k)-\Delta t\phi_x(k) \tag{6.95}$$

Step 4: Perform multiplier iteration

$$\mu(k+1)=\mu(k)+\Delta t S(k)h(x(k+1)) \tag{6.96}$$

$$\lambda(k+1)=\lambda(k)+\Delta t \min[S(k)g(x(k+1)),\lambda(k)] \tag{6.97}$$

$$S(k+1)=\rho S(k) \tag{6.98}$$

Step 5: Perform convergence check, using criteria

$$\|x(k+1)-x(k)\|\leq\varepsilon_1 \tag{6.99}$$

$$\|\mu(k+1)-\mu(k)\|\leq\varepsilon_2 \tag{6.100}$$

$$\|\lambda(k+1)-\lambda(k)\|\leq\varepsilon_3 \tag{6.101}$$

Stop if equations (6.99)–(6.101) are satisfied. Otherwise, let $k=k+1$, go back to step 2.

6.6.4 Test Results

For examining the presented approach, a network of three interconnected areas is constructed as shown in Figure 6.5. Area A1 is an IEEE 30-bus system. The generator and load data of the IEEE 30-bus system are listed in Tables 6.5 and 6.6. The other data and parameters of the IEEE 30-bus system are listed in Chapter 5. Parameters of areas A2, A3, and tie-lines are given as follows.
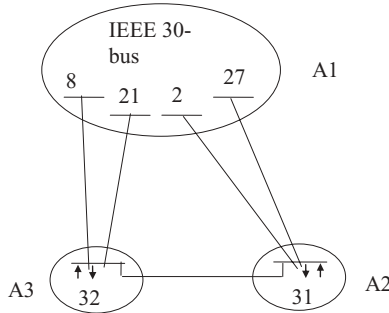
FIGURE 6.5 The network model of three interconnected power systems

Table 6.5 Data of generator nodes for IEEE 30-bus system (p.u.)

Node	a_i	b_i	c_i	P_{Gimin}	P_{Gimax}	ΔP_{GiGRC}
1	37.5	200	0.0	0.50	2.00	0.50
2	175	175	0.0	0.20	0.80	0.30
5	625	100	0.0	0.15	0.50	0.25
8	83.4	325	0.0	0.10	0.35	0.25
11	250	300	0.0	0.10	0.30	0.15
13	250	300	0.0	0.12	0.40	0.15

Note: The generation cost function is: $f_i = a_i P_{Gi}^2 + b_i P_{Gi} + c_i$.

Table 6.6 Data of load nodes for IEEE 30-bus system (p.u.)

Node No.	Real Power	Reactive Power	Node No.	Real Power	Reactive Power
1	0.000	0.000	16	0.035	0.018
2	0.217	0.127	17	0.090	0.058
3	0.024	0.012	18	0.032	0.009
4	0.076	0.016	19	0.095	0.034
5	0.942	0.190	20	0.022	0.007
6	0.000	0.000	21	0.175	0.112
7	0.228	0.109	22	0.000	0.000
8	0.300	0.300	23	0.032	0.016
9	0.000	0.000	24	0.087	0.067
10	0.058	0.020	25	0.000	0.000
11	0.000	0.000	26	0.035	0.023
12	0.112	0.075	27	0.000	0.000
13	0.000	0.000	28	0.000	0.000
14	0.062	0.016	29	0.024	0.009
15	0.082	0.025	30	0.106	0.019

Fuel cost function and power upper and lower limits are:

$$F_{31} = 650P_{31}^2 + 325P_{31} \quad 0.1 \le P_{31} \le 0.9$$
$$F_{32} = 30P_{32}^2 + 100P_{32} \quad 0.1 \le P_{32} \le 0.9$$

Loads of areas A2 and A3 are $P_{DA2} + jQ_{DA2} = 0.5 + j0.26$ and $P_{DA3} + jQ_{DA3} = 0.4 + j0.21$, respectively. Parameters and capacity constraints of the tie line are:

$$R_{2\text{-}31} = 0.0192; X_{2\text{-}31} = 0.0575; P_{2\text{-}31\text{Tmax}} = 0.6$$
$$R_{8\text{-}32} = 0.0192; X_{8\text{-}32} = 0.0575; P_{8\text{-}32\text{Tmax}} = 0.5$$
$$R_{31\text{-}27} = 0.057; X_{31\text{-}27} = 0.1737; P_{31\text{-}27\text{Tmax}} = 0.6$$
$$R_{32\text{-}21} = 0.057; X_{32\text{-}21} = 0.1737; P_{32\text{-}21\text{Tmax}} = 0.5$$
$$R_{31\text{-}32} = 0.0192; X_{31\text{-}32} = 0.0575; P_{31\text{-}32\text{Tmax}} = 0.5$$

The following test cases of security-constrained MAED are performed in the study.

Case 1: Neglecting the buying and selling among areas
Case 2: Considering the buying and selling among areas. $P_{A3-A1sell} = 0.4$; $P_{A1-A2sell} = 0.3$; $P_{A3-A2sell} = 0.0$.
Case 3: Considering the buying and selling among areas. $P_{A3-A1sell} = 0.32$; $P_{A1-A2sell} = 0.32$; $P_{A3-A2sell} = 0.0$.

To evaluate the calculation precision, the performance index (PI) on trading error is used, i.e.,

$$PI_{EAB}\% = \frac{|P_{TAB} - P_{ABsell}|}{P_{ABsell}} \times \% \tag{6.102}$$

The calculation results of the security-constrained MAED for the above three test cases are listed in Table 6.7. From Table 6.7 we get:

Case 2:

$$P_{TA3\text{-}A1} = P_{32\text{-}8} + P_{32\text{-}21} = 0.172 + 0.228 = 0.4$$
$$PI_{EA3\text{-}A1}\% = 0$$
$$P_{TA1\text{-}A2} = P_{2\text{-}31} + P_{27\text{-}31} = 0.4584 - 0.1585 = 0.2999$$
$$PI_{EA1\text{-}A2}\% = 0.0333\%$$
$$P_{TA3\text{-}A2} = P_{32\text{-}31} = 0.0$$
$$PI_{EA3\text{-}A2}\% = 0$$

Table 6.7   Test results of security-constrained MAED for three interconnected systems (NLONN method)

Test Cases	Case 1 (p.u.)	Case 2 (p.u.)	Case 3 (p.u.)
Area A1			
P_{G1}	1.5971	1.6588	1.5951
P_{G2}	0.4377	0.4636	0.4304
P_{G5}	0.2096	0.2122	0.2133
P_{G8}	0.2903	0.2252	0.3324
P_{G11}	0.1459	0.1322	0.1748
P_{G13}	0.1366	0.1287	0.1699
Area A2			
P_{G31}	0.1000	0.2001	0.1801
Area A3			
P_{G32}	0.9000	0.8000	0.7200
Total Gen.	3.81722	3.82081	3.81602
Power losses	0.08322	0.08681	0.08202
Total gen. cost ($)	923.0356	957.5161	974.6212
Tie-line power			
P_{32-8}	0.1827	0.1720	0.1123
P_{32-21}	0.2364	0.2280	0.2077
P_{2-31}	0.4687	0.4584	0.4624
P_{27-31}	−0.1422	−0.1585	−0.1425
P_{32-31}	0.0808	0.0000	0.0000
Line security	Satisfied	Satisfied	Satisfied

Case 3:

$$P_{TA3\text{-}A1} = P_{32\text{-}8} + P_{32\text{-}21} = 0.1123 + 0.2077 = 0.32$$

$$PI_{EA3\text{-}A1}\% = 0$$

$$P_{TA1\text{-}A2} = P_{2\text{-}31} + P_{27\text{-}31} = 0.4624 - 0.1425 = 0.3199$$

$$PI_{EA1\text{-}A2}\% = 0.03125\%$$

$$P_{TA3\text{-}A2} = P_{32\text{-}31} = 0.0$$

$$PI_{EA3\text{-}A2}\% = 0$$

The maximum trading error is only 0.0333%. Therefore, the proposed MAED approach not only satisfies all security constraints but also has high precision.

6.7   TOTAL TRANSFER CAPABILITY COMPUTATION IN MULTIAREAS

As we analyzed in previous sections that the transfer capability limits affect the wheeling. It is useful to compute the total transfer capability (TTC) of the multiareas.

6.7.1   Continuation Power Flow Method

The general method to compute the TTC is the continuation power flow (CPF) or repeated power flow (RPF) method [28–31]. It is sometimes called the perturbation method.

The net active and reactive power injections at the sink and source buses are functions of λ.

$$P_i = P_{i0} + \lambda L_{Pi} \tag{6.103}$$

$$Q_i = Q_{i0} + \lambda L_{Qi} \tag{6.104}$$

where

λ: The parameter controlling the amount of injection
P_{i0}: The base case real power injections at the bus
Q_{i0}: The base case reactive power injections at the bus
L_{Pi}: The real power load participation factors
L_{Qi}: The reactive power load participation factors

The traditional power flow equations augmented by an extra equation for λ are expressed as

$$f(\theta, V, \lambda) = 0 \tag{6.105}$$

where

V: The vector of bus voltage magnitudes
θ: The vector of bus voltage angles

Once a base case (for $\lambda = 0$) solution is found, the next solution can be predicted by taking an appropriately sized step in a direction tangent to the solution path. The tangent vector is obtained as below:

$$d[f(\theta, V, \lambda)] = f_\theta d\theta + f_V dV + f_\lambda d\lambda \tag{6.106}$$

Since equation (6.106) is rank deficient, an arbitrary value such as 1 can be assigned as one of the elements of the tangent vector $t = [d\theta, dV, d\lambda]^T = \pm 1$, i.e., $t_k = \pm 1$. Thus

$$\begin{bmatrix} f_\theta & f_V & f_\lambda \\ & e_k & \end{bmatrix}[t] = \begin{bmatrix} 0 \\ \pm 1 \end{bmatrix} \tag{6.107}$$

Where e_k is a row vector with all elements zero, except for the kth entry, which is equal to 1.

The new solution after perturbation will then be computed as

$$\begin{bmatrix} \theta^* \\ V^* \\ \lambda^* \end{bmatrix} = \begin{bmatrix} \theta \\ V \\ \lambda \end{bmatrix} + \varepsilon \begin{bmatrix} d\theta \\ dV \\ d\lambda \end{bmatrix} \tag{6.108}$$

Where ε is a scalar used to adjust the step size.

The new solution obtained in equation (6.108) may violate the limits. Thus it is necessary to correct the continuation parameter. The corrector is a slightly modified Newton power flow algorithm in which the Jacobian matrix is augmented by an equation to account for the continuation parameter.

Let $x = [\theta, V, \lambda]^T$, $x_k = \eta$, then the new set of equations will take the form

$$\begin{bmatrix} f(x) \\ e_k - \eta \end{bmatrix} = [0] \tag{6.109}$$

Therefore, for a specific source/sink transfer case, the steps for computing the TTC are summarized as below [28]:

(1) Input power system data.
(2) Select the contingency from the contingency list.
(3) Initialize:
    (a) Run power flows to ensure that the initial point does not violate any limits.
    (b) Set the tolerance for the change of transfer power.
(4) Prediction step size of CPF:
    (a) Calculate the tangent vector $t = [d\theta, dV, d\lambda]^T$
    (b) Choose the scalar ε to design the prediction step size.
    (c) Make a step of increase of the transfer power to predict the next solution using equation (6.108).
(5) Correct step size of CPF with generator Q limits. Solve equation (6.109).
(6) Check for limit violations: Check the solution of step (5) for violations of operational or physical limits—line flow limit, voltage magnitude limit, and voltage stability limit. If there are violations, reduce the transfer power increment by $\varepsilon = 0.5\varepsilon$; then go back to step (5) until the change of the transfer power is smaller than the tolerance. The maximum transfer power for the selected contingency is reached. Otherwise, go to prediction step (4).
(7) Check whether all contingencies are processed. If they are, compare the maximum transfer powers for all the contingencies and choose the

smallest one as the TTC for this specific source/sink transfer case and terminate the procedure. Otherwise, go to step (2).

6.7.2 Multiarea TTC Computation

In a multiarea system, it is assumed that each area operates autonomously by its own independent operator. Each area carries out its own CPF calculation and maintains its own detailed system model. Furthermore, each area uses network equivalents to represent the buses in other areas, except for the boundary. One of the equivalent methods is the REI equivalent. The basic idea of the REI equivalent is to aggregate the injections of a group of buses into a single bus. The aggregated injection is distributed to these buses via a radial network called the REI network. After the aggregation, all buses with zero injections are eliminated, yielding the equivalent [32, 33]. For example, all PV and PQ buses except for the seller and buyer buses of outer external area are grouped into two different REI equivalent networks, which are assigned the corresponding bus types (PQ or PV) accordingly [28]. In this way, systemwide TTC can be computed without exchanging information with each other. However, the admittances of the REI network are functions of the operating point for which the equivalent is constructed. Doing so will also introduce errors in the multiarea TTC result. In light of this, the equivalent must be properly updated during the TTC computation.

In the case of the multiarea CPF implementation, each area carries out its own CPF, and the continuation parameter for each area may be different at each step. Therefore, a strategy for choosing and updating the continuation parameter that ensures synchronized CPF calculation in different areas is introduced.

Another issue related to updating the equivalents is the generator Q limits. As the power transfer increases at a chosen PQ bus, generator buses will continue to hit their Q limits in succession. As each limit is reached, the generated reactive power will be held at the Q limit, bus type will be switched to PQ, and the bus voltage will become an unknown increasing the dimension of the Jacobian by one. While updating the equivalents, these generator buses that are now of type PQ are grouped with other PQ buses in each area. This will continue until other limits are reached.

A self-adaptive step size control is implemented for the sink area. λ is chosen as the continuation parameter when starting from the base case. Then the continuation parameter is chosen from the voltage increment vector $[dV]^T$. A constant voltage magnitude decrease is used to predict the next solution. Usually, the scalar ε in equation (6.118) is set as 0.02 [28]. Therefore, a constant decrease in voltage magnitude will result in a large increase in load at the beginning and a small increase in load as the nose point is approached.

After each correction step, the load change at the sink area will be broadcast to all other areas. The continuation parameter continues to be λ in all

other areas, and the scalar ε is set as the load change of the sink area at each step. Hence, different areas will have the same load increase at each discrete step of CPF calculation.

If contingencies are considered in the calculation of multiareas TTC, contingencies associated with the tie lines must be comonitored by all areas. However, contingencies caused by topology changes within individual areas do not have to be modeled directly by others. Instead, when a contingency occurs within one area, only the network model of this area will be changed. As a result, the tie-line power flows and buyer bus voltages calculated from different areas will have very large mismatches during the synchronized computation. After updating the equivalents for the area experiencing the contingency, the updated equivalent buses will reflect the effects of the contingency. This way, other areas can account for the effects of the contingency indirectly.

APPENDIX: COMPARISON OF TWO OPTIMIZATION NEURAL NETWORK MODELS

Reference [27] also presented an optimization neural network model, which can be written as M-10.

$$L(S, x) = f(x) + \lambda^{\mathrm{T}} g(x) + \mu^{\mathrm{T}} h(x) (S/2) \left(\|g^+(x)\|^2 + \|h(x)\|^2 \right) \tag{6A.1}$$

$$\mathrm{d}x/\mathrm{d}t = -\nabla f(x) - \nabla h(x)[Sh(x) + \mu] - \nabla g(x)^{\mathrm{T}} (Sg^+(x) + \lambda) \tag{6A.2}$$

$$\mathrm{d}\mu/\mathrm{d}t = \varepsilon (Sh(x)) \tag{6A.3}$$

$$\mathrm{d}\lambda/\mathrm{d}t = \varepsilon \left(Sg^+(x) \right) \tag{6A.4}$$

where ε is a very small positive number and

$$g^+(x) = \max[0, g(x)] \tag{6A.5}$$

It is noted that the proposed NLONN model M-9 is different from the traditional optimization neural network model M-10. This can be seen by analyzing the stability and optimization of two neural networks.

For Proposed Neural Network M-9

The derivative of energy function in M-9 to time t can be obtained from the following calculation:

$$\frac{\mathrm{d}E}{\mathrm{d}t} = \frac{\partial E}{\partial x}\frac{\mathrm{d}x}{\mathrm{d}t} + \frac{\partial E}{\partial \mu}\frac{\mathrm{d}\mu}{\mathrm{d}t} + \frac{\partial E}{\partial \lambda}\frac{\partial \lambda}{\partial t}$$

$$= -\left\|\frac{\mathrm{d}x}{\mathrm{d}t}\right\|^2 - S\|h(x)\|^2 + \frac{1}{S}\{\max[0, \lambda - Sg(x)] - \lambda\}^{\mathrm{T}} \min[Sg(x), \lambda)$$

$$= -\left\|\frac{\mathrm{d}x}{\mathrm{d}t}\right\|^2 - S\|h(x)\|^2 + \frac{1}{S}\{\max[-\lambda, Sg(x)]\}^{\mathrm{T}}[-\max(-Sg(x), -\lambda)]$$

$$= -\left\|\frac{\mathrm{d}x}{\mathrm{d}t}\right\|^2 - S\|h(x)\|^2 - \frac{1}{S}\|\max[-Sg(x), -\lambda]\|^2 \qquad (6A.6)$$

Obviously, from equation (6A.6) we can know that $\mathrm{d}E/\mathrm{d}t \leq 0$. When and only when

$$h(x) = 0; \quad \max[-\lambda, -Sg(x)] = 0; \quad \mathrm{d}x/\mathrm{d}t = 0 \qquad (6A.7)$$

then

$$\mathrm{d}E/\mathrm{d}t = 0 \qquad (6A.8)$$

The meaning of $\max[-\lambda, -Sg(x)] = 0$ is that

$$Sg(x) \geq 0 \quad \text{when} \quad \lambda = 0 \qquad (6A.9)$$

$$\lambda \geq 0 \quad \text{when} \quad Sg(x) = 0 \qquad (6A.10)$$

Equations (6A.9) and (6A.10) are just the Kuhn–Tucker conditions in optimization theory. Thus $\max[-\lambda, -Sg(x)] = 0$ is tenable.

Certainly, any feasible solutions including the optimal solution satisfy the equation $h(x) = 0$. So from equation (6.96) of M-9 we get the following expression:

$$\mathrm{d}x/\mathrm{d}t = -\{\nabla_x f(x) - \mu\nabla_x h(x) - \max[0, \lambda - Sg(x)]\nabla_x g(x)\} \qquad (6A.11)$$

According to equations (6A.9) and (6A.10), we get

$$\max[0, \lambda - Sg(x)]\nabla_x g(x) = \lambda\nabla_x g(x) \qquad (6A.12)$$

According to equations (6A.11) and (6A.12), we get

$$\mathrm{d}x/\mathrm{d}t = -\{\nabla_x f(x) - \mu\nabla_x h(x) - \lambda\nabla_x g(x)\} \qquad (6A.13)$$

If $\mathrm{d}x/\mathrm{d}t = 0$, when and only when

$$\nabla_x f(x) - \mu\nabla_x h(x) - \lambda\nabla_x g(x) = 0 \qquad (6A.14)$$

Equation (6A.14) is just the optimality conditions of optimization problem M-7. So this condition is tenable. It means that $dx/dt = 0$ is also tenable. Now we have demonstrated that all conditions in equation (6A.7) are satisfied. Therefore, equation (6A.8) is also satisfied. This has proved that the energy function of the proposed NLONN neural network is a Lyapunov function. The corresponding neural network is certainly stable and the equilibrium point of neural network corresponds to the optimal solution of the constrained optimization problem M-7.

For Neural Network M-10 in Reference [27]

According to equations (6A.1)–(6A.5), the derivative of energy function in M-10 to time t can be obtained from the following calculation:

$$\frac{dL}{dt} = \frac{\partial L}{\partial x}\frac{dx}{dt} + \frac{\partial L}{\partial \mu}\frac{d\mu}{dt} + \frac{\partial L}{\partial \lambda}\frac{\partial \lambda}{\partial t}$$

$$= -\left\|\frac{dx}{dt}\right\|^2 + \varepsilon \cdot S \cdot \|h(x)\|^2 + \varepsilon \cdot S \cdot g^T(x) \cdot g^+(x) \qquad (6A.15)$$

Since ε is a very small positive number, and $g^+(x) = \max[0, g(x)]$, the last two terms in the right side of equation (6A.15) are not negative. This means that $dL/dt \leq 0$ is untenable all along. Therefore, there exists a stability problem in the neural network M-10.

REFERENCES

[1] J.Z. Zhu, "Multi-area power systems economic dispatch using a nonlinear optimization neural network approach," *Electric Power Components and Systems*, Vol. 31, 2002, pp. 553–563.

[2] J.Z. Zhu and J.A. Momoh, "Multi-area power systems economic dispatch using nonlinear convex network flow programming," *Electric Power Systems Research*, Vol. 59, No. 1, 2001, pp. 13–20.

[3] C.S. Chang, A.C. Liew, J.X. Xu, X.W. Wang, and B. Fan, "Dynamic security constrained multiobjective generation dispatch of longitudinally interconnected power systems using bicriterion global optimization," IEEE/PES Summer Meeting, 1995, SM 578-5.

[4] D. Streiffert, "Multi-area economic dispatch with tie line constraints," IEEE/PES Winter Meeting, 1995, WM 179-2.

[5] C. Wang and S.M. Shahidehpour, "Power generation scheduling for multi-area hydro-thermal systems with tie line constraints, cascaded reservoirs and uncertain data," *IEEE Trans., PAS*, Vol. 08, No. 3, 1993, pp. 1333–1340.

[6] O. Alsac and B. Stott, "Optimal power flow with steady-state security," *IEEE Trans., PAS*, Vol. 93, 1974, pp. 745–751.

[7] J.Z. Zhu and M.R. Irving, "Combined active and reactive dispatch with multiple objectives using an analytic hierarchical process," *IEE Proc. C*, Vol. 143, No. 4, 1996, pp. 344–352.

[8] H.W. Dommel and W.F. Tinney, "Optimal power flow solutions," *IEEE Trans., PAS*, Vol. 87, No. 10, 1968, pp. 1866–1876.

[9] D.I. Sun, B. Ashley, A. Hughes, and W.F. Tinney, "Optimal power flow by Newton approach," *IEEE Trans., PAS*, Vol. 103, No. 10, pp. 2864–2880.

[10] M.R. Irving and M.J.H. Sterling, "Economic dispatch of active power with constraint relaxation," *IEE Proc. C*, Vol. 130, No. 4, 1983.

[11] M.R. Irving and M.J.H. Sterling, "Efficient Newton-Raphson algorithm for load flow calculation in transmission and distribution networks," *IEE Proc. C*, Vol. 134, 1987.

[12] J.Z. Zhu and G.Y. Xu, "A new real power economic dispatch method with security," *Electric Power Systems Research*, Vol. 25, No. 1, 1992, pp. 9–15.

[13] D.C. Walters and Z.C. Sheble, "Genetic algorithm solution of economic dispatch with valve point loading," *IEEE Trans., on Power Systems*, Vol. 8, No. 3, 1993.

[14] M. Salami and G. Cain, "Multiple genetic algorithm processor for the economic power dispatch problem," Procs. of Intern. Conf. on Genetic Algorithm in Engineering Systems, UK, Sep., 1995, pp. 188–193.

[15] T.D. King, M.E. El-Hawary, and F. El-Hawary, "Optimal environmental dispatching of electric power system via an improved Hopfield neural network model," *IEEE Trans on Power System*, Vol. 10, No. 3, 1995, pp. 1559–1565.

[16] K.P. Wong and C.C. Fung, "Simulated-annealing-based economic dispatch algorithm," *IEE Proc. Part C*, Vol. 140, No. 6, 1993, pp. 509–515.

[17] T.H. Lee, D.H. Thorne, and E.F. Hill, "A transportation method for economic dispatching—Application and comparison," *IEEE Trans., PAS*, 1980, Vol. 99, pp. 2372–2385.

[18] E. Hobson, D.L. Fletcher, and W.O. Stadlin, "Network flow linear programming techniques and their application to fuel scheduling and contingency analysis," *IEEE Trans., PAS*, 1984, Vol. 103, pp. 1684–1691.

[19] A.J. Wood and B.F. Wollenberg, *Power Generation, Operation, and Control*, Second edition, New York: John Wiley & Sons, 1996.

[20] K.L. Lo and S.P. Zhu, "A Theory for Pricing Wheeled Power," *Electric Power Systems Research*, 1994, Vol. 28.

[21] M.C. Caramanis, R.E. Bohn, and F.C. Schweppe, "The Costs of Wheeling and Optimal Wheeling Rates," *IEEE Transactions on Power Systems*, Vol. PWRS, No. 1, 1986.

[22] H.H. Happ, "Cost of Wheeling Methodology," *IEEE Transactions on Power Systems*, Vol. 9, No. 1, February 1994.

[23] Purdue ECE Technical Reports, "Real Time Pricing of Electric Power," 1995, http://docs.lib.purdue.edu/ecetr/120.

[24] J.Z. Zhu and C.S. Chang, "Energy transaction scheduling with network constraints and transmission losses", Proc. of Intern. Conf. On Advances in Power System Control, Operation & Management, APSCOM-97, Nov. 11–14, 1997, Hong Kong.

[25] Y.Z. Li and A.K. David, "Optimal Multi-Area Wheeling," *IEEE Transactions on Power Systems*, Vol. 9, No. 1, February 1994.

[26] M.S. Bazaraa, H.D. Aherali, and C.M. Shetty, *Nonlinear Programming: Theory and Algorithms*, John Wiley & Sons, New York, 1993.

[27] C.Y. Maa and M.A. Shanblatt, "A Two-phase Optimization Neural Network," *IEEE Trans. On Neural Network*, Vol. 3, No. 6, 1992.

[28] L. Min and A. Abur, "Total Transfer Capability Computation for Multi-Area Power Systems," *IEEE Transactions on Power Systems*, Vol. 21, No. 3, 2006, pp. 1141–1147.

[29] V. Ajjarapu and C. Christy, "The continuation power flow: A tool for steady state voltage stability analysis," *IEEE Trans. Power Syst*, Vol. 7, No. 1, pp. 416–423, Feb. 1992.

[30] C.A. Canizares and F.L. Alvarado, "Point of collapse and continuation methods for large ACDC systems," *IEEE Trans. Power Syst*, Vol. 8, No.1, pp. 1–8, Feb. 1993.

[31] H.D. Chiang, A.J. Flueck, K.S. Shah, and N. Balu, "CPFLOW: A practical tool for tracing power system steady-state stationary behavior due to load and generation variations," *IEEE Trans. Power Syst*, Vol. 10, No. 2, pp. 623–634, May 1995.

[32] P. Dimo, *Nodal Analysis of Power System*. Turnbridge Wells, Kent, U.K.: Abacus Press, 1975.

[33] W.F. Tinney and W.L. Powell, "The REI Approach to Power Network Equivalents," Transl.: 1977 PICA Conf. Toronto, ON, Canada, May 1977, pp. 312–320.

7

UNIT COMMITMENT

This chapter first introduces several major techniques for solving the unit commitment problem such as the priority method, dynamic programming, and the Lagrange relaxation method. Several new algorithms are then added to attack the unit commitment problems. These are the evolutionary programming-based Tabu search method, particle swarm optimization, and the analytic hierarchy process. A great deal of numerical examples and analysis are provided in the chapter.

7.1 INTRODUCTION

Since generators cannot instantly turn on and produce power, unit commitment (UC) must be planned in advance so that enough generation is always available to handle system demand with an adequate reserve margin in the event that generators or transmission lines go out or load demand increases. Unit commitment handles the unit generation schedule in a power system for minimizing operating cost and satisfying prevailing constraints such as load demand and system reserve requirements over a set of time periods [1–20]. The classic UC problem is aimed at determining the start-up and shutdown schedules of thermal units to meet forecasted demand over certain time periods (24 h to 1 week) and belongs to a class of combinatorial optimization problems. The methods that have been studied so far fall into roughly three categories: heuristic search, mathematical programming, and hybrid methods. Optimization techniques such as the priority list, augmented Lagrangian

relaxation, dynamic programming, and the branch–and–bound algorithm have been used to solve the classic UC problem. Genetic algorithms (GA), simulated annealing (SA), analytic hierarchy process (AHP), and particle swarm optimization (PSO) have also been used for UC problem since the beginning of the last decade.

7.2 PRIORITY METHOD

The classic UC problem is to minimize total operational cost and is subject to minimum up- and downtime constraints, crew constraints, unit capability limits, generation constraints, and reserve constraints. Thus the objective function of UC consists of the generation cost function and start-up cost function of the generators. The former is described in Chapter 4. The latter involves the cost of the energy that brings the unit online.

There are two types of startup cost model: one is bringing the unit online from a cold start and the other is bringing it from bank status, in which the unit is turned off but still close to operating temperature. The start-up cost model when cooling can be expressed in the exponential function below:

$$F_{Sc}(t) = \left(1 - e^{-t/\alpha}\right) \times F + C_f \tag{7.1}$$

where

F_{Sc}: The cold start cost for the cooling model
C_f: The fixed cost of generator operation including crew expense, maintenance expense
F: The fuel cost
t: Time that the unit was cooled
α: Thermal time constant for the unit

The start-up cost model when banking can be expressed as a linear function as below:

$$F_{Sb}(t) = F_0 \times t + C_f \tag{7.2}$$

where

F_{Sb}: The start-up cost for banking model
F_0: The cost of maintaining unit at operating temperature

The simplest unit commitment solution is to list all combinations of units on and off, as well as the corresponding total cost to create a rank list, and then make the decision according to the rank table. This method is called the

priority list. The rank is based on the minimum average production cost of the unit. The average production cost of the unit is defined as

$$\mu = \frac{F(P_G)}{P_G} \tag{7.3}$$

where

μ: The average production cost of the unit

$F(P_G)$: The generation cost function of the unit

P_G: The generator real power output

From Chapter 4, the incremental rate of the unit is defined as

$$\lambda = \frac{\mathrm{d}F(P_G)}{\mathrm{d}P_G} \tag{7.4}$$

When the average production cost of the unit equals the incremental rate of the unit, the corresponding average production cost is called the minimum average production cost, μ_{min}. Generally, the power output is close to rated power when the unit is at the minimum average production cost.

Example 7.1

There are five generator units, and the minimum average production costs μ_{min} are computed as shown in Table 7.1.

The priority order for these units based on the minimum average production cost is shown in Table 7.2.

The steps of the priority list method are summarized as below:

Step (1): Compute the minimum average production cost of all units, and order the units from the smallest value of μ_{min}. Form the priority list.

Step (2): If the load is increasing during that hour, determine how many units can be started up according to the minimum downtime of the unit.

Table 7.1   The minimum average production cost

Unit	Minimum Average Production Cost μ_{min}	Min MW	Max MW
G1	10.56	100	400
G2	9.76	120	500
G3	11.95	100	300
G4	8.90	50	600
G5	12.32	150	250

Table 7.2   The priority order for 5 units

Priority Order	Unit	μ_{min}	Min MW	Max MW
1	G4	8.90	50	600
2	G2	9.76	120	500
3	G1	10.56	100	400
4	G3	11.95	100	300
5	G5	12.32	150	250

Then select the top units for turning on from the priority list according to the amount of load increasing.

Step (3): If the load is dropping during that hour, determine how many units can be stopped according to the minimum up time of the unit. Then select the last units for stopping from the priority list according to the amount of load dropping.

Step (4): Repeat the process for the next hour.

There are other priority list methods such as ranking units based on the full-load average production cost of each unit [21] as well as based on the incremental cost rate of each unit [22].

7.3   DYNAMIC PROGRAMMING METHOD

Suppose a system has n units. If the enumeration approach is used, there would be $2^n - 1$ combinations. The dynamic programming (DP) method consists in implicitly enumerating feasible schedule alternatives and comparing them in terms of operating costs. Thus DP has many advantages over the enumeration method, such as reduction in the dimensionality of the problem.

There are two DP algorithms. They are forward dynamic programming and backward dynamic programming. The forward approach, which runs forward in time from the initial hour to the final hour, is often adopted in the unit commitment. The advantages of the forward approach are:

- Generally, the initial state and conditions are known.
- The start-up cost of a unit is a function of the time. Thus the forward approach is more suitable since the previous history of the unit can be computed at each stage.

The recursive algorithm is used to compute the minimum cost in hour t with feasible state I, that is

$$F_{tc}(t, I) = \min_{\{L\}}[F(t, I) + S_c(t-1, L \Rightarrow t, I) + F_{tc}(t-1, I)] \tag{7.5}$$

where

$F_{tc}(t, I)$: The total cost from initial state to hour t state I
$S_c(t - 1, L \Rightarrow t, I)$: The transition cost from state $(t - 1, L)$ to state (t, I)
$\{L\}$: The set of feasible states at hour $t - 1$
$F(t, I)$: The production cost for state (t, I)

The following constraints should be satisfied for the UC problem solved by dynamic program:

$$\sum_{i=1}^{n} P_{Gi}^t = P_D^t \tag{7.6}$$

$$x_i^t P_{Gimin}^t \leq P_{Gi}^t \leq x_i^t P_{Gimax}^t \tag{7.7}$$

where

P_D^t: The system load at hour t
P_{Gimin}^t: The lower limit of the unit power output
P_{Gimax}^t: The upper limit of the unit power output
x_i^t: The 0–1 variable

As we mentioned before, there are $2^n - 1$ combinations or states for n units. The computation amount is large. We can combine the DP algorithm and priority list method to discard some infeasible states as well as high-cost states. In addition, we add the unit minimum uptime and minimum downtime constraints, which can also reduce the states. For example, before we perform unit commitment using the forward DP algorithm, we first order the units according to the priority list and the unit minimum up-/downtime. The first part of the units order is the must-up units, the last part is the must-down units, and middle part is the unit ranking based on the minimum average production cost of the rest of units. In this way, the computation amount of DP will be reduced.

Example 7.2

We use priority list and dynamic programming to solve the unit commitment for a simple four-unit system [21]. The data of the units and the load pattern are listed in Tables 7.3 and 7.4, respectively.

In Table 7.3, the symbol "–" in the initial state means the unit is offline. For example, "8" means the unit has been online for 8 hours, and "–6" means the unit has been offline for 6 hours.

The total combinations of four units are $2^n - 1 = 2^4 - 1 = 15$. If we order the unit combinations or states by the maximum net capacity of each combination, we get Table 7.5.

Table 7.3   The data of units

Unit	Max (MW)	Min (MW)	Cost ($/h)	Ave. Cost	Start-up Cost	Initial State	Min Up Times (h)	Min Down Times (h)
1	80	25	213.00	23.54	350	−5	4	2
2	250	60	585.62	20.34	400	8	5	3
3	300	75	684.74	19.74	1100	8	5	4
4	60	20	252.00	28.00	0	−6	1	1

Table 7.4   The load pattern

Hour	Load (MW)
1	450
2	530
3	600
4	540
5	400
6	280
7	290
8	500

Table 7.5   The ordering of the unit combinations

State	Unit Combination	Max Net Capacity (MW)
15	1 1 1 1	690
14	1 1 1 0	630
13	0 1 1 1	610
12	0 1 1 0	550
11	1 0 1 1	440
10	1 1 0 1	390
9	1 0 1 0	380
8	0 0 1 1	360
7	1 1 0 0	330
6	0 1 0 1	310
5	0 0 1 0	300
4	0 1 0 0	250
3	1 0 0 1	140
2	1 0 0 0	80
1	0 0 0 1	60
0	0 0 0 0	0
(Unit)	1 2 3 4	

Table 7.6   UC results by priority list

Hour	Load (MW)	Units On-Line	Generation Cost
1	450	Units 3, and 2	9208
2	530	Units 3, and 2	10648.36
3	600	Units 3, 2 and 1	12265.36
4	540	Units 3, and 2	10828.36
5	400	Units 3, and 2	8308.36
6	280	Unit 3	5573.54
7	290	Unit 3	5748.14
8	500	Units 3, and 2	10108.36

In the combinations of Table 7.5, "1" means committed (unit operating), and "0" means uncommitted (unit shut down). For example, "0001" for state 1 means unit 4 is committed, and units 1, 2, 3 are uncommitted; "1001" for state 3 means units 1 and 4 are committed and units 2 and 3 are uncommitted.

Case 1: Neglecting the constraints of unit minimum up/down time. Solve UC problem using the priority list order.

In case 1, units are committed in order until the load is satisfied. The total cost for the interval is the sum of the eight dispatch costs plus the transitional costs for starting any units. It can be known from the average production cost in Table 7.3 that the priority order for the four units is unit 3, unit 2, unit 1, unit 4. All possible commitments start from state 12 since the load at first hour is 450 MW, and maximum net capacity from state 1 to state 11 is only 440 MW. In addition, state 13 is discarded since it does not satisfy the order of the priority list. The UC results for the priority ordered method are listed in Table 7.6.

Case 2: Neglecting the constraints of unit minimum up/down time. Solve UC problem using dynamic programming.

In case 2, first select the feasible states, using the priority list order. For first 4 hours, the feasible states have only 12, 14, and 15 in Table 7.5. For last 4 hours, the feasible states have 5, 12, 14, and 15. Thus the total feasible states are {5, 12, 14, 15}, and the initial state is 12. According to the recursive algorithm of the dynamic programming, we can compute the minimum total cost.

$$F_{tc}(t, I) = \min_{\{L\}}[F(t, I) + S_c(t-1, L \Rightarrow t, I) + F_{tc}(t-1, I)]$$

For $t = 1$: $\{L\} = \{12\}$, and $\{I\} = \{12, 14, 15\}$

$$F_{tc}(1, 12) = F(1, 12) + S_c(0, 12 \Rightarrow 1, 12) + F_{tc}(1, 12)$$
$$= F(1, 12) + S_c(0, 12 \Rightarrow 1, 12) + 0 = 9208 + 0 = 9208$$

$$F_{tc}(1, 14) = F(1, 14) + S_c(0, 14 \Rightarrow 1, 14) + F_{tc}(1, 14) = 9493 + 350 = 9843$$

$$F_{tc}(1, 15) = F(1, 15) + S_c(0, 15 \Rightarrow 1, 15) + F_{tc}(1, 15) = 9861 + 350 = 10211$$

$$\text{For } t = 2: \{L\} = \{12, 14\}, \text{ and } \{I\} = \{12, 14, 15\}$$

$$F_{tc}(2, 15) = \min_{\{12, 14\}} [F(2, 15) + S_c(1, L \Rightarrow 2, 15) + F_{tc}(1, L)]$$

$$= 11301 + \min \left[\begin{array}{c} (350 + 9208) \\ (0 + 9843) \end{array} \right] = 20859$$

And so on.

The UC results are the same as those in case 1.

7.4 LAGRANGE RELAXATION METHOD

Since the enumeration approach is involved in unit commitment solved by dynamic programming, the computation burden is huge for large power systems with many generators. The priority list is very simple, and has a fast calculation speed, but it may discard the optimum scheme. The Lagrange relaxation method can overcome the above-mentioned disadvantages.

The mathematical problem of the unit commitment can be expressed as below.

1. Objective function

$$\min \sum_{t=1}^{T} \sum_{i=1}^{n} [F_i(P_{Gi}^t) x_i^t + F_{si}(t) x_i^t] = F(P_{Gi}^t, x_i^t) \tag{7.8}$$

2. Constraints
   1) Load balance equation

$$\sum_{i=1}^{n} P_{Gi}^t x_i^t = P_D^t, \quad t = 1, 2, \ldots, T \tag{7.9}$$

   2) Generator power output limits

$$x_i^t P_{Gi\min}^t \leq P_{Gi}^t \leq x_i^t P_{Gi\max}^t, \quad t = 1, 2, \ldots, T \tag{7.10}$$

   3) Power reserve constraint

$$\sum_{i=1}^{n} P_{Gi\max} x_i^t \geq P_D^t + P_R^t, \quad t = 1, 2, \ldots, T \tag{7.11}$$

4) Minimum up-/downtime

$$\left(U_{t-1,i}^{\mathrm{up}} - T_i^{\mathrm{up}}\right)\left(x_i^{t-1} - x_i^t\right) \geq 0, \quad t = 1, 2, \ldots, T, i = 1, 2, \ldots, n \tag{7.12}$$

$$\left(U_{t-1,i}^{\mathrm{down}} - T_i^{\mathrm{down}}\right)\left(x_i^t - x_i^{t-1}\right) \geq 0, \quad t = 1, 2, \ldots, T, i = 1, 2, \ldots, n \tag{7.13}$$

where

$F_{\mathrm{S}i}$: Start-up cost of unit i at time period t

P_{R}^t: Power reserve at time period t

T_i^{up}: Minimum uptime for unit i in hours

T_i^{down}: Minimum downtime for unit i in hours

$U_{t-1,i}^{\mathrm{up}}$: Number of consecutive uptime periods until time period t, measured in hours

$U_{t-1,i}^{\mathrm{down}}$: Number of consecutive downtime periods until time period t, measured in hours

The UCP has two kinds of constraints: separable and coupling constraints. Separable constraints such as capacity and minimum up- and downtime constraints are related to one single unit. On the other hand, coupling constraints involve all units. A change in one unit affects the other units. The power balance and power reserve constraints are examples of coupling constraints. The LR framework relaxes the coupling constraints and incorporates them into the objective function by a dual optimization procedure. Thus the objective function can be separated into independent functions for each unit, subject to unit capacity and minimum up and down time constraints. The resulting Lagrange function of the UCP is as follows:

$$L(P, x, \lambda, \beta) = F\left(P_{\mathrm{G}i}^t, x_i^t\right) + \sum_{t=1}^{T} \lambda_t \left(P_{\mathrm{D}}^t - \sum_{i=1}^{n} P_{\mathrm{G}i}^t x_i^t\right) + \sum_{t=1}^{T} \beta_t \left(P_{\mathrm{D}}^t + P_{\mathrm{R}}^t - \sum_{i=1}^{n} P_{\mathrm{G}i\max} x_i^t\right)$$
$$\tag{7.14}$$

The unit commitment problem becomes the minimization of the Lagrange function (7.14), subject to constraints (7.10), (7.12), and (7.13). For the sake of simplicity, we have used the symbol P, without the subscripts $\mathrm{G}i$ and t, to denote any appropriate vector of elements $P_{\mathrm{G}i}^t$. The symbols x, λ, and β are handled the same way. The LR approach requires minimizing the Lagrange function given as:

$$q(\lambda, \beta) = \min_{P, x} L(P, x, \lambda, \beta) \tag{7.15}$$

Since $q(\lambda, \beta)$ provides a lower bound for the objective function of the original problem, the LR method requires us to maximize the objective function over the Lagrange multipliers:

$$q*(\lambda, \beta) = \max_{\lambda, \beta} q(\lambda, \beta) \qquad (7.16)$$

After eliminating constant terms such as $\lambda_t P_D^t$ and $\beta_t(P_D^t + P_R^t)$ in equation (7.14), equation (7.15) can be written as

$$q(\lambda, \beta) = \min_{P, x} \sum_{i=1}^{n} \sum_{t=1}^{T} \left\{ [F_i(P_{Gi}^t) + F_{Si}(t)] x_i^t - \lambda_t P_{Gi}^t x_i^t - \beta_t P_{Gi\max}^t x_i^t \right\} \qquad (7.17)$$

subject to

$$x_i^t P_{Gi\min}^t \leq P_{Gi}^t \leq x_i^t P_{Gi\max}^t, \quad t = 1, 2, \ldots, T$$

$$\left(U_{t-1,i}^{\mathrm{up}} - T_i^{\mathrm{up}}\right)\left(x_i^{t-1} - x_i^t\right) \geq 0, \quad t = 1, 2, \ldots, T, i = 1, 2, \ldots, n$$

$$\left(U_{t-1,i}^{\mathrm{down}} - T_i^{\mathrm{down}}\right)\left(x_i^t - x_i^{t-1}\right) \geq 0, \quad t = 1, 2, \ldots, T, i = 1, 2, \ldots, n$$

There are two basic steps for the Lagrange procedure to solve the UC problem. They are:

(1) Initializing the Lagrange multipliers with values that try to make $q(\lambda, \beta)$ larger.
(2) Assuming the values of the Lagrange multipliers in step (1) are fixed and the Lagrange function (L) is minimized by adjusting P_{Gi}^t and x_i^t.

This minimization is done separately for each unit, and different techniques such as LP and dynamic programming can be used. The solutions for the N independent subproblems are used in the master problem to find a new set of Lagrange multipliers. This involves dual optimization. As we know for dual optimization, the function to be optimized is convex and the variables are continuous, then the maximization of the dual function gives the identical result as minimizing the primal function. However, for unit commitment problem, there are 0–1 integer variables that indicate the status of the units, which are not continuous, or nonconvex. Thus the dual theory is not exactly satisfied in UC problem. The application of the dual optimization method to the UC problem has been given the name "Lagrange relaxation." There exists a gap between the results of the maximization of the dual function and minimizing the primal function. The aim of the Lagrange relaxation method is to reduce the duality gap by iterations. If a criterion is prespecified, this iterative procedure continues until a duality gap criterion is met. The duality gap is also used as a measure of convergence. If the relative duality gap between the primal and the dual solutions is less than a specific tolerance, it is considered that the optimum has been reached. The procedure then ends with finding a feasible UC schedule.

Actually, the multipliers can be updated by using a subgradient method with a scaling factor and tuning constants, which are determined heuristically. This method is as follows:

A vector g is called a subgradient of $L(\cdot)$ at λ^* if

$$L(\lambda) \le L(\lambda^*) + (\lambda - \lambda^*)^{\mathrm{T}} g \tag{7.18}$$

If the subgradient is unique at a point λ, then it is the gradient at that point. The set of all subgradients at λ is called the subdifferential, $\partial L(\lambda)$, and is a closed convex set. A necessary and sufficient condition for optimality in subgradient optimization is $0 \in \partial L(\lambda)$. The value of λ can be adjusted by the subgradient optimization algorithm as below:

$$\lambda_t^{k+1} = \lambda_t^k + \alpha g^k \tag{7.19}$$

where g^k is any subgradient of $L(\cdot)$ at λ_t^k. The step size, α, must be chosen carefully to achieve good performance by the algorithm. Here g^k is calculated as follows:

$$g^k = \frac{\partial L(\lambda_t^k)}{\partial L\lambda_t^k} = P_D^t - \sum_{i=1}^{n} x_i^k P_{Gi}^t \tag{7.20}$$

Example 7.3

The data for the three-unit, four-hour unit commitment problem are as below, which is solved with Lagrange relaxation technique [21].

1. Units data

$$F_1(P_{G1}) = 0.002 P_{G1}^2 + 10 P_{G1} + 500$$

$$F_2(P_{G2}) = 0.0025 P_{G2}^2 + 8 P_{G2} + 300$$

$$F_3(P_{G3}) = 0.005 P_{G1}^2 + 6 P_{G1} + 100$$

$$100 \le P_{G1} \le 600$$

$$100 \le P_{G2} \le 400$$

$$50 \le P_{G3} \le 200$$

2. Hourly load data shown in Table 7.7

For simplification, there are no startup costs, no minimum up- or downtime constraints. The results of several iterations are shown in Tables 7.8–7.13, starting from an initial condition where all λ^t values are set to zero. An economic dispatch is performed for each hour, provided there is

Table 7.7 Hourly load data

Hour (t)	Load P_D^t (MW)
1	170
2	520
3	1100
4	330

Table 7.8 Iteration 1

Hour	λ	u_1	u_2	u_3	P_{G1}	P_{G2}	P_{G3}	ΔP	P_{G1}^{ed}	P_{G2}^{ed}	P_{G3}^{ed}
1	0	0	0	0	0	0	0	170	0	0	0
2	0	0	0	0	0	0	0	520	0	0	0
3	0	0	0	0	0	0	0	1100	0	0	0
4	0	0	0	0	0	0	0	330	0	0	0

Where $\Delta P = P_D^t - \sum_{i=1}^{n} P_{Gi}^t x_i^t$.

Table 7.9 Iteration 2

Hour	λ	u_1	u_2	u_3	P_{G1}	P_{G2}	P_{G3}	ΔP	P_{G1}^{ed}	P_{G2}^{ed}	P_{G3}^{ed}
1	1.7	0	0	0	0	0	0	170	0	0	0
2	5.2	0	0	0	0	0	0	520	0	0	0
3	11.0	0	1	1	0	400	200	500	0	0	0
4	3.3	0	0	0	0	0	0	330	0	0	0

Table 7.10 Iteration 3

Hour	λ	u_1	u_2	u_3	P_{G1}	P_{G2}	P_{G3}	ΔP	P_{G1}^{ed}	P_{G2}^{ed}	P_{G3}^{ed}
1	3.4	0	0	0	0	0	0	170	0	0	0
2	10.4	0	1	1	0	400	200	−80	0	320	200
3	16.0	1	1	1	600	400	200	−100	500	400	200
4	6.6	0	0	0	0	0	0	330	0	0	0

Table 7.11 Iteration 4

Hour	λ	u_1	u_2	u_3	P_{G1}	P_{G2}	P_{G3}	ΔP	P_{G1}^{ed}	P_{G2}^{ed}	P_{G3}^{ed}
1	5.1	0	0	0	0	0	0	170	0	0	0
2	10.24	0	1	1	0	400	200	−80	0	320	200
3	15.8	1	1	1	600	400	200	−100	500	400	200
4	9.9	0	1	1	0	380	200	−250	0	130	200

Table 7.12   Iteration 5

Hour	λ	u_1	u_2	u_3	P_{G1}	P_{G2}	P_{G3}	ΔP	P_{G1}^{ed}	P_{G2}^{ed}	P_{G3}^{ed}
1	6.8	0	0	0	0	0	0	170	0	0	0
2	10.08	0	1	1	0	400	200	−80	0	320	200
3	15.6	1	1	1	600	400	200	−100	500	400	200
4	9.4	0	0	1	0	0	200	130	0	0	200

Table 7.13   Iteration 6

Hour	λ	u_1	u_2	u_3	P_{G1}	P_{G2}	P_{G3}	ΔP	P_{G1}^{ed}	P_{G2}^{ed}	P_{G3}^{ed}
1	8.5	0	0	1	0	0	200	−30	0	0	170
2	9.92	0	1	1	0	384	200	−64	0	320	200
3	15.4	1	1	1	600	400	200	−100	500	400	200
4	10.7	0	1	1	0	400	200	−270	0	130	200

sufficient generation committed that hour. The primal value J^* represents the total generation cost summed over all hours as calculated by economic dispatch. $q(\lambda)$ stands for the dual value. The duality gap will be $J^* - q^*$, or the relative duality gap will be $\dfrac{J^* - q^*}{q^*}$.

For iteration 1, $q(\lambda) = 0, j^* = 40,000$, and $\dfrac{J^* - q^*}{q^*} =$ undefined. In the next iteration, the λ^t values have been increased as 1.7, 5.2, 11.0, and 3.3. The results as well as the relative duality gap for the several iterations are shown below.

For iteration 2, $q(\lambda) = 14,982, j^* = 40,000$, and $\dfrac{J^* - q^*}{q^*} = 1.67$.

For iteration 3, $q(\lambda) = 18,344, j^* = 36,024$, and $\dfrac{J^* - q^*}{q^*} = 0.965$.

For iteration 4, $q(\lambda) = 19,214, j^* = 28,906$, and $\dfrac{J^* - q^*}{q^*} = 0.502$.

For iteration 5, $q(\lambda) = 19,532, j^* = 36,024$, and $\dfrac{J^* - q^*}{q^*} = 0.844$.

For iteration 6, $q(\lambda) = 19,442, j^* = 20,170$, and $\dfrac{J^* - q^*}{q^*} = 0.037$.

After 10 iterations, $q(\lambda) = 19,485, j^* = 20,017$, and $\dfrac{J^* - q^*}{q^*} = 0.027$. The relative duality gap is still not zero. The solution will not converge to a final value. Therefore, a tolerance ε for the relative duality gap should be

introduced if the Lagrange relaxation algorithm is used. It means that when $\dfrac{J^* - q^*}{q^*} \leq \varepsilon$ the Lagrange relaxation algorithm will be stopped.

7.5   EVOLUTIONARY PROGRAMMING-BASED TABU SEARCH METHOD

7.5.1   Introduction

Tabu search (TS) is a powerful optimization procedure that has been successfully applied to a number of combinatorial optimization problems. It has the ability to avoid entrapment in local minima. The TS method uses a flexible memory system (in contrast to "memory-less" systems such as simulated annealing and genetic algorithm and rigid memory systems such as in branch-and-bound). Specific attention is given to the short-term memory component of TS, which has provided solutions superior to the best obtained with other methods for a variety of problems.

Research endeavors, therefore, have been focused on efficient, near-optimal UC algorithms, which can be applied to large-scale power systems and have reasonable storage and computation time requirements. The major limitations of the numerical techniques are the problem dimensions, the large computational time, and the complexity in programming.

The LR approach introduced in the previous section to solve the short-term UC problems was found to provide a faster solution but will fail to obtain solution feasibility and solution quality problems and becomes complex if the number of the units increases.

Evolutionary programming (EP) is capable of determining a global or near-global solution. It is based on the basic genetic operation of human chromosomes. It operates with the stochastic mechanics, which combine offspring creation based on the performance of current trial solutions and competition and selection based on the successive generations, from a considerably robust scheme for large-scale real-valued combinational optimization. This section will introduce the EP-based TS method to solve the unit commitment problem.

7.5.2   Tabu Search Method

The same mathematical model of a UC problem in Section 7.4 is adopted.

The UC problem is a combinatorial problem with integer variables and continuous variables. It can be decomposed into two subproblems, a combinatorial problem in integer variables and a nonlinear optimization problem in output power variables. The Tabu Search (TS) method is used to solve the combinatorial optimization, and the nonlinear optimization is solved via a quadratic programming [14]. The steps of the TS are as follows.

Step (1): Assume that the fuel costs are fixed for each hour and all of the generators share the loads equally.

Step (2): By optimum allocation, find the initial feasible solution on unit status.

Step (3): Demand is taken as the control parameter.

Step (4): Generate the trial solution.

Step (5): Calculate the total operating cost as the summation of running cost and startup–shutdown cost.

Step (6): Tabulate the fuel cost for each unit for every hour.

About the trial solution, the neighbors should be randomly generated. Because of the constraints in the UCP, this is not a simple matter. The most difficult constraints to satisfy are the minimum up-/downtimes. The TS algorithm requires a starting feasible schedule that satisfies all of the system and units constraints. This schedule is randomly generated.

Once a trial solution is obtained, the corresponding total operating cost is determined. Since the production cost is a quadratic function, a quadratic programming method can be used to solve the subproblem. The startup cost is then calculated for the given schedule. The calculation is stopped if the following conditions are satisfied:

- The load balance constraints are satisfied.
- The spinning reserve constraints are satisfied.

The Tabu list (TL) is controlled by the trial solutions in the order in which they are made. Each time a new element is added to the "bottom" of a list, the oldest element on the list is dropped from the "top." Empirically, TL sizes, which provide good results, often grow with the size of the problem, and stronger restrictions are generally coupled with smaller sizes [14]. The best sizes of TL lie in an intermediate range between these extremes. In some applications, a simple choice of TL size in a range centered on seven seems to be quite effective.

Another important criterion of TS arises when the move under consideration has been found to be tabu. Associated with each entry in the TL there is a certain value for the evaluation function called the "aspiration level." Normally, the aspiration level criteria are designed to override tabu status if a move is "good enough" [14].

7.5.3 Evolutionary Programming

Evolutionary programming (EP) is a mutation-based evolutionary algorithm applied to discrete search spaces. Real-parameter EP is similar in principle to evolution strategy (ES), in which normally distributed mutations are performed in both algorithms. Both algorithms encode mutation strength (or

variance of the normal distribution) for each decision variable, and a self-adapting rule is used to update the mutation strengths. For the case of evolutionary strategies, Fogel remarks that "evolution can be categorized by several levels of hierarchy: the gene, the chromosome, the individual, the species, and the ecosystem" [24–26]. Thus, while genetic algorithms stress models of genetic operators, ES emphasizes mutational transformation that maintains behavioral linkage between each parent and its offspring at the level of the individual.

The general EP algorithm is shown below [15, 24–26].

(1) The initial population is determined by setting

$$s_i = S_i \sim U(a_k, b_k)^k, \quad i = 1, \dots, m \tag{7.21}$$

where

S_i: A random vector
s_i: The outcome of the random vector
$U(a_k, b_k)^k$: A uniform distribution ranging over $[a_k, b_k]$ in each of k dimensions
m: The number of parents

(2) Each s_i is assigned a fitness score

$$\varphi(s_i) = G(F(s_i), v_i), \quad i = 1, \dots, m \tag{7.22}$$

where F maps $s_i \rightarrow R$ and denotes the true fitness of s_i. v_i represents random alteration in the instantiation of s_i. $G(F(s_i), v_i)$ describes the fitness score to be assigned. In general, the functions F and G can be as complex as required. For example, F may be a function not only of a particular s_i but also of other members of the population, conditioned on a particular.

(3) Each s_i is altered and assigned to s_{i+m} such that

$$s_{i+m} = s_{i,j} + N(0, \beta_j \varphi(s_i) + z_j), \quad j = 1, \dots, k \tag{7.23}$$

where $N(0, \beta_j \varphi(s_i) + z_j)$ represents a Gaussian random variable. β_j is a constant of proportionality of scale $\varphi(s_i)$, and z_j represents an offset to guarantee a minimum amount of variance.

(4) Each s_{i+m} is assigned a fitness score

$$\varphi(s_{i+m}) = G(F(s_{i+m}), v_{i+m}), \quad i = 1, \dots, m \tag{7.24}$$

(5) For each s_i, $i = 1, \dots, 2m$, a value a value w_i is assigned according to

$$w_i = \sum_{t=1}^{c} w_t^* \tag{7.25}$$

$$w_t^* = \begin{cases} 1, & \text{if } \varphi(s_t^*) \le \varphi(s_i) \\ 0, & \text{otherwise} \end{cases} \tag{7.26}$$

where c is the number of competitions.

(6) The solutions $s_i, i = 1, \dots , 2m$ are ranked in descending order of their corresponding value w_i. The first m solutions are transcribed along with their corresponding values $\varphi(s_i)$ to be the basis of the next generation.

(7) The process proceeds to step (3) unless the available execution time is exhausted or an acceptable solution has been discovered.

Applying the above mentioned evolutionary programming to unit commitment problem, the calculation steps are shown below.

(1) Initialize the parent vector $p = [p_1, p_2, \dots , p_n], i = 1, 2, \dots , N_p$ such that each element in the vector is determined by $p_j \sim \text{random}(p_{j\min}, p_{j\max}), j = 1, 2, \dots , N$ with one generator as dependent generator.

(2) Calculate the overall objective function of the UC problem, using the trail vector p_i, and find the minimum of the objective function F_{Ti}.

(3) Create the offspring trail solution p_i' as follows.
(a) Compute the standard deviation

$$\sigma_j = \beta \left(\frac{F_{Tij}}{\min(F_{Ti})} \right) (P_{j\max} - P_{j\min}) \tag{7.27}$$

(b) Add a Gaussian random variable $N(0, \sigma_j^2)$ to all of the state variables of p_i, to get p_i'.

(4) Select the first N_p individuals from the total $2N_p$ individuals of both p_i and p_i' through evaluating each trail vector by $W_{pi} = \text{sum}(W_x)$, where $x = 1, 2, \dots , N_p, i = 1, 2, \dots , 2N_p$ such that

$$W_x = \begin{cases} 1, & \text{if } \dfrac{F_{Tij}}{F_{Tij} + F_{Tir}} < \text{random}(0, 1) \\ 0, & \text{otherwise} \end{cases} \tag{7.28}$$

(5) Sort the W_{pi} in descending order, and the first N_p individuals will survive and be transcribed along with their elements to form the basis of the next generation.

(6) Back to step 2 until a maximum number of generations N_m is reached.

7.5.4   EP-Based TS for Unit Commitment

In the TS technique for solving the UC problem, the initial operating schedule status in terms of maximum real power generation of each unit is given as input. As we know that TS is used to improve any given status by avoiding entrapment in local minima, the offspring obtained from the EP algorithm is given as input to TS, and the refined status is obtained. Considering the features of EP and TS algorithms, the EP-based TS method is used for solving unit commitment problem.

(1) Get the demand for 24 hours and number of iterations to be carried out.
(2) Generate a population of parents (N) by adjusting the existing solution to the given demand to the form of state variables.
(3) Unit downtime makes a random recommitment.
(4) Check for constraint in the new schedule by TS. If the constraints are not met, then repair the schedule. A repair mechanism to restore the feasibility of the constraints is applied and described as follows:
   - Pick at random one of the OFF units at one of the violated hours.
   - Apply the rules in Section 7.5.2 to switch the selected unit from OFF to ON, keeping the feasibility of the downtime constraints.
   - Check for the reserve constraints at this hour. Otherwise, repeat the process at the same hour for another unit.
(5) Solve the master problem of UC and calculate total production cost for each parent.
(6) Add the Gaussian random variable to each state variable and, hence, create an offspring. This will further undergo some repair operations. After these, the new schedules are checked in order to verify that all constraints are met.
(7) Improve the status of the evolved offspring, and verify the constraints by TS.
(8) Formulate the rank for the entire population.
(9) Select the best N number of population for next iteration.
(10) Has the iteration count been reached? If yes, go to step 11; otherwise, go to step (2).
(11) Select the best population (s) by evolutionary strategy.
(12) Print the optimum schedule.

7.6   PARTICLE SWARM OPTIMIZATION FOR UNIT COMMITMENT

7.6.1   Algorithm

Particle swarm optimization (PSO) was introduced by Kennedy and Eberhart in 1995 [23] as an alternative to GAs. The PSO technique has turned out to

be a competitor in the field of numerical optimization ever since. Similar to GA, a PSO consists of a population refining its knowledge of the given search space. PSO is inspired by particles moving around in the search space. The individuals in a PSO thus have their own positions and velocities. These individuals are denoted as particles. Traditionally, PSO has no crossover between individuals and has no mutation, and particles are never substituted by other individuals during the run. Instead, the PSO refines its search by attracting the particles to positions with good solutions. Each particle remembers its own best position found so far in the exploration. This position is called the personal best and is denoted by P_{bi}^{t} in equation (7.29). Additionally, among these P_{bi}^{t}, there is only one particle that has the best fitness, called the global best, which is denoted by P_{gbi}^{t} in equation (7.29). The velocity and position update equations of PSO are given by

$$V_i^t = wV_i^{t-1} + C_1 \times r_1 \times \left(P_{bi}^{t-1} - X_i^{t-1}\right) + C_2 \times r_2 \times \left(P_{gbi}^{t-1} - X_i^{t-1}\right) \tag{7.29}$$

$$X_i^t = X_i^{t-1} + V_i^t \quad i = 1, \dots, N_D \tag{7.30}$$

where

w: The inertia weight

C_1, C_2: The acceleration coefficients

N_D: The dimension of the optimization problem (number of decision variables)

r_1, r_2: Two separately generated uniformly distributed random numbers between 0 and 1

X: The position of the particle

V_i: The velocity of the ith dimension

PSO has the following key features compared with the conventional optimization algorithms.

- It only requires a fitness function to measure the "quality" of a solution instead of complex mathematical operations like gradient, Hessian, or matrix inversion. This reduces the computational complexity and relieves some of the restrictions that are usually imposed on the objective function like differentiability, continuity, or convexity.
- It is less sensitive to a good initial solution since it is a population-based method.
- It can be easily incorporated with other optimization tools to form hybrid ones.
- It has the ability to escape local minima since it follows probabilistic transition rules.

More interesting PSO advantages can be emphasized when compared to other members of evolutionary algorithms like the following.

- It can be easily programmed and modified with basic mathematical and logic operations.
- It is inexpensive in terms of computation time and memory.
- It requires less parameter tuning.
- It works with direct real-valued numbers, which eliminates the need to do binary conversion of a classical canonical genetic algorithm.

The simplest version of PSO lets every individual move from a given point to a new point that is a weighted combination of the individual's best position ever found and of the individual's best position, P_{bi}^t. The choice of the PSO algorithm's parameters (such as the inertia weight) seems to be of utmost importance for the speed and efficiency of the algorithm.

If economic power dispatch (EPD) is also considered in the unit commitment, a hybrid PSO (HPSO) can be used [20]. The blending real-valued PSO (solving EPD) with binary-valued PSO (solving UC) are operated independently and simultaneously. The binary PSO (BPSO) is made possible with a simple modification to the particle swarm algorithm. This BPSO solves binary problems similar to the traditional method. In binary particle swarm X_i and P_{bi}^t can take on values of 0 or 1 only. The velocity V_i will determine a probability threshold. If V_i is higher, the individual is more likely to choose 1, and lower values favor the 0 choice. Such a threshold needs to stay in the range $[0.0, 1.0]$. One straightforward function for accomplishing this is common in neural networks. The function is called the sigmoid function and is defined as follows:

$$s(V_i) = \frac{1}{1 + \exp(-V_i)} \tag{7.31}$$

The function squashes its input into the requisite range and has properties that make it agreeable for use as a probability threshold. A random number (drawn from a uniform distribution between 0.0 and 1.0) is then generated, whereby X_i is set to 1 if the random number is less than the value from the sigmoid function, that is,

$$X_i = \begin{cases} 1, & \text{if } r < s(V_i) \\ 0, & \text{otherwise} \end{cases} \tag{7.32}$$

In the UC problem, X_i represents the on or off state of generator i. To ensure that there is always some chance of a bit flipping (on and off of generators), a V_{max} constant the start of a trial to limit the range of V_i. A large V_{max} results in a low frequency of changing state of generator, whereas a small value increases the frequency of on/off of a generator.

7.6.2 Implementation

The mathematical model of the UC problem, which is described in Section 7.4, can be expressed as the general form:

$$\min f(x) \tag{7.33}$$

such that

$$h_j(x) = 0 \quad j = 1, \ldots, m \tag{7.34}$$

$$g_i(x) \geq 0 \quad i = 1, \ldots, k \tag{7.35}$$

To handle the infeasible solutions, the cost function is used to evaluate a feasible solution, that is,

$$\Phi_f(x) = f(x) \tag{7.36}$$

The constraint violation measure $\Phi_u(x)$ for the $r + m$ constraints are usually defined as

$$\Phi_u(x) = \sum_{i=1}^{r} g_i^+(x) + \sum_{j=1}^{m} |h_j^+(x)| \tag{7.37}$$

or

$$\Phi_u(x) = \frac{1}{2} \left[\sum_{i=1}^{r} (g_i^+(x))^2 + \sum_{j=1}^{m} (h_j^+(x))^2 \right] \tag{7.38}$$

where

$g_i^+(x)$: The magnitude of the violation of the ith inequality constraint
$h_j^+(x)$: The magnitude of the violation of the jth equality constraint
r: The number of inequality constraints
m: The number of equality constraints

Then the total evaluation of an individual x, which can be interpreted as the error (for a minimization problem) of an individual x, is obtained as

$$\Phi(x) = \Phi_f(x) + \gamma \Phi_u(x) \tag{7.39}$$

where γ is a penalty parameter of a positive (or negative) constant for the minimization (or maximization) problem, respectively. By associating a penalty with all constraint violations, a constrained problem is transformed into an unconstrained problem such that we can deal with candidates that

violate the constraints to generate potential solutions without considering the constraints.

According to equation (7.39), we formulate the objective of the UC problem as a combination of total production cost as the main objective with power balance and spinning reserve as inequality constraints; then we get

$$\Phi(x) = F\left(P_{Gi}^t, x_i^t\right) + \frac{\gamma}{2}\sum_{t=1}^{T}\left[C_1\left(P_D^t - \sum_{i=1}^{n}P_{Gi}^t x_i^t\right)^2 + C_2\left(P_D^t + P_R^t - \sum_{i=1}^{n}P_{Gimax}^t x_i^t\right)^2\right]$$

(7.40)

The penalty factor γ is computed at the kth generation defined by

$$\gamma = \gamma_0 + \log(k+1)$$

(7.41)

The choice of γ determines the accuracy and speed of convergence. From the experiment, a greater value of γ increases its speed and convergence rate. For this reason, a value of 100 for γ_0 is selected. The pressure on the infeasible solution can be increased with the number of generations, as discussed in the Kuhn–Tucker optimality theorem, and the penalty function theorem provides guidelines to choose the penalty term. In equation (7.40), C_1 is set to 1 if a violation to constraint (7.9) occurs and $C_1 = 0$ whenever equation (7.9) is not violated. Similarly, C_2 is also set to 1 whenever a violation of equation (7.11) is detected, and it remains 0 otherwise.

Substituting equation (7.8) into equation (7.40), we get

$$\Phi(x) = \sum_{t=1}^{T}\sum_{i=1}^{n}\left[F_i(P_{Gi}^t)x_i^t + F_{si}(t)x_i^t\right]$$
$$+ \frac{\gamma}{2}\sum_{t=1}^{T}\left[C_1\left(P_D^t - \sum_{i=1}^{n}P_{Gi}^t x_i^t\right)^2 + C_2\left(P_D^t + P_R^t - \sum_{i=1}^{n}P_{Gimax}^t x_i^t\right)^2\right]$$
$$= \sum_{t=1}^{T}\left\{\sum_{i=1}^{n}[F_i(P_{Gi}^t) + F_{si}(t)]x_i^t + \frac{\gamma}{2}\left[C_1\left(P_D^t - \sum_{i=1}^{n}P_{Gi}^t x_i^t\right)^2\right.\right.$$
$$\left.\left. + C_2\left(P_D^t + P_R^t - \sum_{i=1}^{n}P_{Gimax}^t x_i^t\right)^2\right]\right\}$$

(7.42)

Equation (7.42) is the fitness function for evaluating every particle in the population of PSO for time period T. The initial values of power are generated randomly within the power limits of a generator. As particles explore the searching space, starting from initial values, which are generated randomly within the power limit as shown in equation (7.10), they do encounter cases whereby the power generated exceeds the boundary (minimum or maximum capacity) and therefore violate the constraint in equation (7.10). To avoid the boundary violation, we reinitialize the value whenever it is greater than the

maximum capacity or smaller than the minimum capacity of a generator. Again, the reinitialization is done within the power limits of a generator.

The minimum-up and minimum-down time can be easily handled. As the solution is based upon the best particle (P_{gbi}^t) in the history of the entire population, constraints are taken care of by forcing the binary value in P_{gbi}^t to change its state whenever either the minimum up or the minimum down constraint is violated. However, this may change the current fitness, which is evaluated with equation (7.42). It implies that the current P_{gbi}^t might no longer be the best among all the other particles. To avoid this situation, the P_{gbi}^t will be revaluated with the same equation. Ramping can be incorporated by adding the ramping cost into the total production cost in equation (7.8).

7.7   ANALYTIC HIERARCHY PROCESS

The classical UC problem is aimed at determining the startup and shutdown schedules of thermal units to meet forecasted demand over certain time periods (24 h to 1 week) and belongs to a class of combinatorial optimization problems. The previous sections introduced several methods.

Although these techniques are effective for the problem posed, they do not handle network constraints and bidding issues. This section addresses future UC requirements in a deregulated environment where network constraints, reliability, value of generation, and variational changes in demands and other costs may be factors.

The classical UC Lagrange method cannot solve this problem because of combinatorial explosion. Accordingly, as an initial approach to solve this complex problem, we attempt to find a method for solving UC considering network limitation and generation bids as a daily operational planning problem. This approach supports the decision making effectively of ranking units in terms of their values by using the analytic hierarchy process (AHP) and the analytic network process (ANP) techniques. The scheduled generation over time is studied as input into the optimal power flow (OPF) problem for optimal dispatch within the network and generation constraint. The OPF problem is deeply discussed in Chapter 8.

7.7.1   Explanation of Proposed Scheme

The basic concept of proposed optimal generation scheduling is as follows.

First, it is assumed that the ranking of generating units, and their priority as well as demand, is known. As a result, the preferred generators for competitive scheduling and pricing will be known. Therefore, the number of generators whose fuel consumption constraints must be considered can be reduced considerably. This reduces the difficulties of unit commitment and optimal power flow. The proposed scheme addresses adequate ranking and prioritizing of units before optimizing the pricing of generation units to meet

a given demand. By incorporating the interaction of factors such as load demand, generating cost curve, bid/sale price, unit up/down cost, and the relative importance of different generation units, the scheme can be implemented to address the technical and nontechnical constraints in the unit commitment problem. This information is easily augmented with the optimization scheme for effective optimal decisions. The scheme consists of the three following stages:

(1) Ranking of units in terms of their values by AHP/ANP
(2) Checking the constraints by rule–based method
(3) Solving optimization problem by interior point optimal power flow

Next, for all generators committed, the network availability for transfer power, the constraints on startup and shutdown, and generated output and reserve are determined for daily operational planning. In the daily UC calculation, a Lagrange method is used without network constraints. Since the majority of connected generators include network constraints, and other equipment limitation to ensure feasibility, an OPF technique based on the modified quadratic interior point (MQIP) method [27] is adopted for solving the resulting optimal generation scheduling problem. This gives the proposed scheme a significant advantage over classical heuristic or Lagrange methods. Further work to evaluate this technique is ongoing for multiutility areas where reliability and stability constraints on the networks are requirements.

According to the above discussion, the scheme for optimal generation scheduling can be represented as in Figure 7.1.
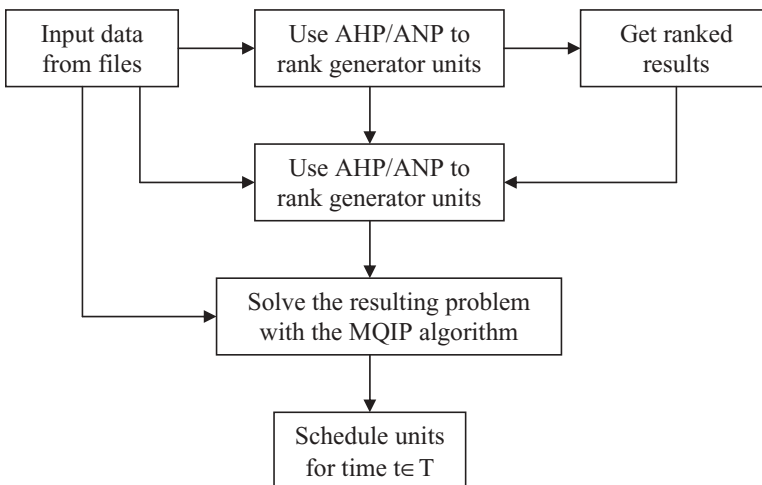
FIGURE 7.1 Scheme for optimal generation scheduling

7.7.2 Formulation of Optimal Generation Scheduling

7.7.2.1 Objective Functions   In general, in UC problems, the objective function to be minimized is the sum of the operation and startup costs. First, the fuel cost of the generation is a function of its output P_i.

For simplicity, we assume that the generation production cost is a quadratic function. Thus the total generation cost can be expressed as

$$F_g(P_{gi}(t)) = \sum_{i=1}^{NG} \left(a_i P_{gi}(t)^2 + b_i P_{gi}(t) + c_i \right) \qquad (7.43)$$

where $P_{gi}(t)$ is the real power output of the ith generator in period t.

$P_{gi}(t)$ is assumed to be within the maintenance schedule, i.e., considered to be at an acceptable efficiency to meet the prescribed load. It should be noted that machines being committed are not operating at 100% efficiency because of imperfect operating conditions and aging.

The startup cost, on the other hand, increases with shutdown time of generator. We assume that the boiler and turbine cool down after shutdown and the cost of preheating increases with shutdown time and is embedded in $F_{Si}(t)$ (startup cost of generator i at time t).

Therefore, if the number of generators is NG and the duration of the period under consideration is T, the objective function is

$$\min F = \sum_{i=1}^{NG} \sum_{t=1}^{T} \left[\left(a_i P_{gi}(t)^2 + b_i P_{gi}(t) + c_i \right) + F_{Si}(t) \right] x_i(t) \qquad (7.44)$$

7.7.2.2 Constraints   The constraints can be classified as coupling constraints and local constraints. The coupling constraints are related to all generators (in service) under consideration, regardless of age or efficiency, and the following are considered.

7.7.2.2.1 Demand-Supply Balance Constraint   The sum of the generator outputs must be equal to the demand $P_D(t)$

$$\sum_{i=1}^{NG} (x_i(t) P_{gi}(t)) = P_D(t) \qquad (7.45)$$

Again, $x_i(t)$ is a 0–1 variable expressing the state, i.e., (0: shutdown, 1: startup) of the ith generator in period t.

7.7.2.2.2 Reserve Power Constraint   To deal with unpredictable disturbances (interruption of generation and transmission lines or unexpected increase in demand), the output of generators in operation must increase, and

hence the instantaneous reserve power shown in the equation below must be required

$$\sum_{i=1}^{NG}(X_{si}(t)\,r_{si}(t)) \geq R_S(t) \tag{7.46}$$

where $r_{si}(t)$ is the contribution of unit i to spinning reserve at hour t, and $R_s(t)$ is the operational reserve requirement at period t.

7.7.2.2.3 *Generator Output Constraint*   When the generator is in the midst of startup, its output must be between the upper limit P_{gimax} and the lower limit P_{gimin}.

$$x_i(t)\,P_{gi\min} \leq P_{gi}(t) \leq x_i(t)\,P_{gi\max} \tag{7.47}$$

For unit ramp rate conditions

$$P_{gi}(t) - P_{gi}(t-1) \leq UP_{gi}; \quad \text{for unit ramp up of unit } i \tag{7.48}$$

$$P_{gi}(t-1) - P_{gi}(t) \leq DR_{gi}; \quad \text{for unit ramp down of unit } i \tag{7.49}$$

For each selected generator for bid.
    The constraint on bid price for unit i at period t is

$$B_{gi}(t) > BP_{gi\min}(t); \quad i \in NG \tag{7.50}$$

where $B_{gi}(t)$ is the bid price of unit i at time t.

7.7.2.3 *Network Limitation*   To account for network limitation during UC dispatch, the network and operation constraints are specified as additional constraints below.
    Power Flow Equation:
    The power flow equations at bus i with losses are given as

$$P_{gi}(t) - P_{di}(t) = F_{pi}(V, \theta, t) \tag{7.51}$$

$$Q_{gi}(t) - Q_{di}(t) = F_{qi}(V, \theta, t) \tag{7.52}$$

where

$$F_{pi}(t) = V_i(t)\sum_{j=1}^{NG}(V_j(t)\,Y_{ij}\cos(\theta_i - \theta_j - \delta_{ij})) \tag{7.53}$$

$$F_{qi}(t) = V_i(t)\sum_{j=1}^{NG}(V_j(t)\,Y_{ij}\sin(\theta_i - \theta_j - \delta_{ij})) \tag{7.54}$$

The transformer taps in the circuit within limits to minimum loss or voltage deviation

$$T_{i\min} \leq T_i(t) \leq T_{i\max} \tag{7.55}$$

where

$T_{i\min}$: The minimum tap ratio of the transformer
$T_{i\max}$: The maximum tap ratio of the transformer

The minimum operation time and minimum shutdown due to fatigue limit of the generator are

$$t_{\mathrm{upmin}} \leq t_i \leq t_{\mathrm{upmax}} \tag{7.56}$$

$$t_{\mathrm{downmin}} \leq t_i \leq t_{\mathrm{downmax}} \tag{7.57}$$

The limits on line flow are defined as

$$\frac{V_i^2 + V_j^2 - 2V_i V_j \cos(\theta_i - \theta_j)}{Z_L^2} \leq I_{L\max}^2 \tag{7.58}$$

where

Z_L: The impedance of the transmission line
$I_{L\max}$: The maximum current limit of the transmission line

Also, each generator is also required to maintain one of the following generator limits for reactive power constraints:

$$x_i(t) Q_{gi\min} \leq Q_{gi}(t) \leq x_i(t) Q_{gi\max} \tag{7.59}$$

$$V_{gi\min}(t) \leq V_{gi}(t) \leq P_{gi\max}(t) \tag{7.60}$$

and for load buses, we have the following constraint:

$$V_{di\min}(t) \leq V_{di}(t) \leq P_{di\max}(t) \tag{7.61}$$

The problem posed can be solved by many optimization methods such as Lagrange relaxation methods, heuristic rules, and optimal power flow with decomposition techniques. The Lagrange method utilizes the following primal problem:
Given

$$\mathrm{Min}\, F\left(x_i(t),\, P_{gi}(t),\, F_{si}(t)\right) \tag{7.62}$$

s.t.

1) local coupling constraints (7.45) to (7.49);
2) power flow constraints (7.51) and (7.54), given as
   $g_i(x_i(t), P_{gi}(t)) \leq 0, i = 1; \ldots ; NG.$

The function F expresses the sum of fuel consumption and startup cost. Using the Lagrange multiplier, we determine λ and μ, which are introduced in the Lagrange function as follows:

$$L[x_i(t), P_{gi}(t), \lambda(t), \mu(t)] = F[x_i(t), P_{gi}(t), F_{Si}(t)] - \lambda(t) \sum_{i=1}^{NG} (x_i(t) P_{gi}(t) - P_D(t))$$

$$+ \mu(t) \sum_{i=1}^{NG} (x_i(t) P_{gi\max}(t) - R_s(t)) \tag{7.63}$$

This is usually converted to a dual problem where

$$\max\{\min L[x_i(t), P_{gi}(t), \lambda(t), \mu(t)]\} \tag{7.64}$$

s.t.

$$g_i(x_i(t), P_{gi}(t)) \leq 0 \tag{7.65}$$

To include the network constraints and bidding of generators, a new UC–based OPF/AHP is proposed [7]. Namely, we solve for the UC problem over time, using OPF to account for the network voltage, transformer, and flow constraints. Application of the MQIP optimization method solves for the optimal operating point at each time period. The second phase of the algorithm uses AHP/ANP to determine the value and merit of each generation bid to be submitted for commitment.

7.7.3   Application of AHP to Unit Commitment

7.7.3.1   AHP Algorithm   The AHP is a decision-making approach [28–30]. It presents the alternatives and criteria, evaluates trade-off, and performs a synthesis to arrive at a final decision. AHP is especially appropriate for cases that involve both qualitative and quantitative analysis. The ANP is the extension of AHP. It makes decisions when alternatives depend on criteria with multiple interactions.

The steps of the AHP algorithm may be written as follows:

Step 1: Set up a hierarchy model.
Step 2: Form a judgment matrix.

The value of elements in the judgment matrix reflects the user's knowledge about the relative importance between every pair of factors.

Step 3: Calculate the maximal eigenvalue and the corresponding eigenvector of the judgment matrix.

Step 4: Hierarchy ranking and consistency check of results.

We can perform the hierarchy ranking according to the value of elements in the eigenvector, which represents the relative importance of the corresponding factor. The consistency index of a hierarchy ranking CI is defined as

$$CI = \frac{\lambda_{\max} - n}{n - 1} \tag{7.66}$$

where $\lambda_{\max}$ is the maximal eigenvalue of the judgment matrix and n is the dimension of the judgment matrix.

The stochastic consistency ratio is defined as:

$$CR = \frac{CI}{RI} \tag{7.67}$$

where RI is a set of given average stochastic consistency indices and CR is the stochastic consistency ratio.

For matrices with 1–9 dimension, respectively, the values of RI will be as below.

n:	1	2	3	4	5	6	7	8	9
RI	0.00	0.00	0.58	0.90	1.12	1.24	1.32	1.41	1.45

It is obvious that a matrix with 1 or 2 dimension is not necessary to check the stochastic consistency ratio. Generally, the judgment matrix is satisfied if the stochastic consistency ratio CR < 0.10.

It is possible to precisely calculate the eigenvalue and the corresponding eigenvector of a matrix, but this would be time-consuming. Moreover, it is not necessary to precisely compute the eigenvalue and the corresponding eigenvector of the judgment matrix. The reason is that the judgment matrix, which is formed by the subjective judgment of the user, itself has some range of error. Therefore, the following two approximate approaches are adopted to compute the maximal eigenvalue and the corresponding eigenvector.

(A) Root Method

(1) Multiply all elements of each row in the judgment matrix

$$M_i = \Pi_i X_{ij}, \quad i = 1, \ldots, n; \quad j = 1, \ldots, n \tag{7.68}$$

where

n: The dimension of the judgment matrix A

X_{ij}: An element in the judgment matrix A

(2) Calculate the nth root of M_i

$$W_i^* = \sqrt[n]{M_i}, \quad i = 1, \ldots, n \tag{7.69}$$

We can obtain the vector

$$W^* = [W_1^*, W_2^*, \ldots, W_n^*]^T \tag{7.70}$$

(3) Normalize the vector W^*

$$W_i = \frac{W_i^*}{\sum\limits_{j=1}^{n} W_j^*} \quad i = 1, \ldots, n \tag{7.71}$$

In this way, we obtain the eigenvector of the judgment matrix A, that is,

$$W = [W_1, W_2, \ldots, W_n]^T \tag{7.72}$$

(4) Calculate the maximal eigenvalue $\lambda_{\max}$ of the judgment matrix

$$\lambda_{\max} = \sum\limits_{i=1}^{n} \frac{(AW)_j}{nW_i} \quad j = 1, \ldots, n \tag{7.73}$$

Where $(AW)_i$ represents the ith element in vector AW.

Example 7.4

Compute the maximal eigenvalue $\lambda_{\max}$ and the corresponding eigenvector for the following judgment matrix.

$$A = \begin{bmatrix} 1 & 1/5 & 1/3 \\ 5 & 1 & 3 \\ 3 & 1/3 & 1 \end{bmatrix}$$

The calculation steps of root method are as follows.

(1) Multiply all elements of each row in the judgment matrix

$$M_1 = 1 \times \frac{1}{5} \times \frac{1}{3} = \frac{1}{15} = 0.067$$

$$M_2 = 5 \times 1 \times 3 = 15$$

$$M_3 = 3 \times \frac{1}{3} \times 1 = 1$$

(2) Calculate the nth root of M_i

$$W_1^* = \sqrt[3]{M_1} = \sqrt[3]{0.067} = 0.405$$

$$W_2^* = \sqrt[3]{M_2} = \sqrt[3]{15} = 2.466$$

$$W_3^* = \sqrt[3]{M_3} = \sqrt[3]{1} = 1$$

We can obtain the vector

$$W^* = [W_1^*, W_2^*, W_3^*]^{\mathrm{T}} = [0.405, 2.466, 1]^{\mathrm{T}}$$

(3) Normalize the vector W^*

$$\sum_{j=1}^{3} W_j^* = 0.405 + 2.466 + 1 = 3.871$$

$$W_1 = \frac{W_1^*}{\sum_{j=1}^{3} W_j^*} = \frac{0.405}{3.871} = 0.105$$

$$W_2 = \frac{W_2^*}{\sum_{j=1}^{3} W_j^*} = \frac{2.466}{3.871} = 0.637$$

$$W_3 = \frac{W_3^*}{\sum_{j=1}^{3} W_j^*} = \frac{1}{3.871} = 0.258$$

The eigenvector of the judgment matrix A is obtained, that is,

$$W = [W_1, W_2, W_3]^{\mathrm{T}} = [0.105, 0.637, 0.258]^{\mathrm{T}}$$

(4) Calculate the maximal eigenvalue $\lambda_{\max}$ of the judgment matrix

$$AW = \begin{bmatrix} 1 & 1/5 & 1/3 \\ 5 & 1 & 3 \\ 3 & 1/3 & 1 \end{bmatrix} \begin{bmatrix} 0.105 \\ 0.637 \\ 0.258 \end{bmatrix}$$

$$AW_1 = 1 \times 0.105 + \frac{1}{5} \times 0.637 + \frac{1}{3} \times 0.258 = 0.318$$

$$AW_2 = 5 \times 0.105 + 1 \times 0.637 + 3 \times 0.258 = 1.936$$

$$AW_3 = 3 \times 0.105 + \frac{1}{3} \times 0.637 + 1 \times 0.258 = 0.785$$

$$\lambda_{\max} = \sum_{i=1}^{n} \frac{(AW)_j}{nW_i} = \frac{(AW)_1}{3W_1} + \frac{(AW)_2}{3W_2} + \frac{(AW)_3}{3W_3}$$

$$= \frac{0.318}{3 \times 0.105} + \frac{1.936}{3 \times 0.637} + \frac{0.785}{3 \times 0.258} = 3.037$$

(B) Sum Method

(1) Normalize every column in the judgment matrix

$$X_{ij}^* = \frac{X_{ij}}{\sum\limits_{k=1}^{n} X_{kj}} \quad i, j = 1, \dots, n \tag{7.74}$$

Now the judgment matrix A is changed into a new matrix A^*, in which each column has been normalized.

(2) Add the all elements of each row in matrix A^*

$$W_i^* = \sum_{j=1}^{n} X_{ij}, \quad i = 1, \dots, n \tag{7.75}$$

(3) Normalizing the vector W^*, we have

$$W_i = \frac{W_i^*}{\sum\limits_{j=1}^{n} W_j^*} \quad i = 1, \dots, n \tag{7.76}$$

Hence, we obtain the eigenvector of the judgment matrix A,

$$W = [W_1, W_2, \dots, W_n]^T \tag{7.77}$$

(4) Calculate the maximal eigenvalue $\lambda_{\max}$ of the judgment matrix

$$\lambda_{\max} = \sum_{i=1}^{n} \frac{(AW)_j}{nW_i} \quad j = 1, \ldots, n \tag{7.78}$$

Where $(AW)_i$ represents the i-th element in vector AW.

Example 7.5

The judgment matrix A is the same as in Example 7.4. Compute the maximal eigenvalue $\lambda_{\max}$ and the corresponding eigenvector with the sum method. The calculation steps are as follows.

(1) Normalize every column in the judgment matrix.

$$\sum_{k=1}^{3} X_{k1} = 1 + 5 + 3 = 9$$

$$X_{11}^{*} = \frac{X_{11}}{\sum\limits_{k=1}^{3} X_{k1}} = \frac{1}{9} = 0.111$$

$$X_{21}^{*} = \frac{X_{21}}{\sum\limits_{k=1}^{3} X_{k1}} = \frac{5}{9} = 0.556$$

$$X_{31}^{*} = \frac{X_{31}}{\sum\limits_{k=1}^{3} X_{k1}} = \frac{3}{9} = 0.333$$

$$\sum_{k=1}^{3} X_{k2} = \frac{1}{5} + 1 + \frac{1}{3} = 1.533$$

$$X_{12}^{*} = \frac{X_{12}}{\sum\limits_{k=1}^{3} X_{k2}} = \frac{0.2}{1.533} = 0.130$$

$$X_{22}^{*} = \frac{X_{22}}{\sum\limits_{k=1}^{3} X_{k2}} = \frac{0.2}{1.533} = 0.652$$

$$X_{32}^{*} = \frac{X_{32}}{\sum\limits_{k=1}^{3} X_{k2}} = \frac{0.333}{1.533} = 0.217$$

$$\sum_{k=1}^{3} X_{k3} = \frac{1}{3} + 3 + 1 = 4.333$$

$$X_{13}^{*} = \frac{X_{13}}{\sum\limits_{k=1}^{3} X_{k3}} = \frac{0.333}{4.333} = 0.077$$

$$X_{23}^{*} = \frac{X_{23}}{\sum\limits_{k=1}^{3} X_{k3}} = \frac{3}{4.333} = 0.692$$

$$X_{33}^{*} = \frac{X_{33}}{\sum\limits_{k=1}^{3} X_{k3}} = \frac{1}{4.333} = 0.231$$

Now the judgment matrix A is changed into a new matrix A^{*}, in which each column has been normalized.

$$A^{*} = \begin{bmatrix} 0.111 & 0.130 & 0.077 \\ 0.556 & 0.652 & 0.692 \\ 0.333 & 0.217 & 0.231 \end{bmatrix}$$

(2) Add the all elements of each row in matrix A^{*}

$$W_{1}^{*} = \sum_{j=1}^{3} X_{1j}^{*} = 0.111 + 0.130 + 0.077 = 0.317$$

$$W_{2}^{*} = \sum_{j=1}^{3} X_{2j}^{*} = 0.556 + 0.652 + 0.692 = 1.900$$

$$W_{3}^{*} = \sum_{j=1}^{3} X_{3j}^{*} = 0.333 + 0.217 + 0.231 = 0.781$$

(3) Normalizing the vector W^{*}, we have

$$\sum_{j=1}^{3} W_{j}^{*} = 0.317 + 1.900 + 0.781 = 2.998$$

$$W_{1} = \frac{W_{1}^{*}}{\sum\limits_{j=1}^{3} W_{j}^{*}} = \frac{0.317}{2.998} = 0.106$$

$$W_2 = \frac{W_2^*}{\sum\limits_{j=1}^{3} W_j^*} = \frac{1.900}{2.998} = 0.634$$

$$W_3 = \frac{W_3^*}{\sum\limits_{j=1}^{3} W_j^*} = \frac{0.781}{2.998} = 0.261$$

The eigenvector of the judgment matrix A is obtained as below:

$$W = [W_1, W_2, W_3]^{\mathrm{T}} = [0.106, 0.634, 0.261]^{\mathrm{T}}$$

(4) Calculate the maximal eigenvalue $\lambda_{\max}$ of the judgment matrix

$$AW = \begin{bmatrix} 1 & 1/5 & 1/3 \\ 5 & 1 & 3 \\ 3 & 1/3 & 1 \end{bmatrix} \begin{bmatrix} 0.106 \\ 0.634 \\ 0.261 \end{bmatrix}$$

$$AW_1 = 1 \times 0.106 + \frac{1}{5} \times 0.634 + \frac{1}{3} \times 0.261 = 0.320$$

$$AW_2 = 5 \times 0.106 + 1 \times 0.634 + 3 \times 0.261 = 1.941$$

$$AW_3 = 3 \times 0.106 + \frac{1}{3} \times 0.634 + 1 \times 0.261 = 0.785$$

$$\lambda_{\max} = \sum_{i=1}^{n} \frac{(AW)_j}{nW_i} = \frac{(AW)_1}{3W_1} + \frac{(AW)_2}{3W_2} + \frac{(AW)_3}{3W_3}$$

$$= \frac{0.320}{3 \times 0.106} + \frac{1.941}{3 \times 0.634} + \frac{0.785}{3 \times 0.261} = 3.036$$

It is noted from examples 7.4 and 7.5 that the root method and the sum method can achieve similar results.

7.7.3.2 AHP-Based Unit Commitment   According to the theory of AHP/ANP, the following AHP/ANP model in Figure 7.2 is devised to handle ranking of the generator units.

The hierarchical network model of units ranking consists of three sections:

(1) The unified ranking of units
(2) The ranking criteria or performance indices, in which the PI_C reflects the relative importance of units
(3) The generating units $G_1, \dots, G_m$
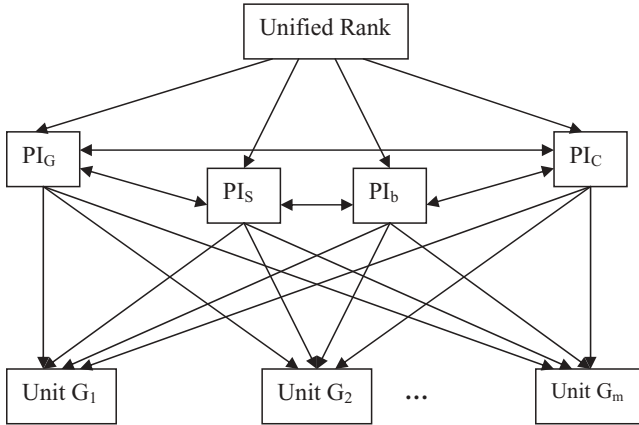
FIGURE 7.2   Hierarchical network model of units rank

The performance indices PI_G, PI_S, and PI_b are defined as

$$PI_G = \frac{1}{F_{gi}(P_{gi}(t))} \tag{7.79}$$

$$PI_S = \frac{1}{F_{Si}(t)} \tag{7.80}$$

$$PI_b = \frac{1}{BP_{gi}(t)} \tag{7.81}$$

The four ranking criteria PI_G, PI_S, PI_b, and PI_C are interacted. The basic principle of AHP/ANP is to calculate the eigenvector of the alternatives for each criterion. For qualitative factors such as the relative importance of units and criteria, the corresponding eigenvectors can be obtained by computing the judgment matrix. The judgment matrix can be formed based on some scaling method such as the 9-scaling method. For two performance indices A and B, their relationship can be expressed as follows if the 9-scaling method is used.

If both performance indices A and B are equally important, then the scaling factor will be "1."

If performance index A is slightly more important compared with performance index A B, then the scaling factor of A to B will be "3."

If performance index A is more important than performance index B, then the scaling factor of A to B will be "5."

If performance index A is far more important than performance index B, then the scaling factor of A to B will be "7."

If performance index A is extremely important compared with performance index B, then the scaling factor of A to B will be "9."

Table 7.14   Judgment matrix *A–PI*

A	PI_G	PI_S	PI_b	PI_C
PI_G	1	3	1	3
PI_S	1/3	1	1/2	1/2
PI_b	1	1/2	1	2
PI_C	1/3	2	1/2	1

Naturally, "2," "4," "6," "8" are the median of both neighboring judgments, respectively.

With the above 9-scaling, the judgment matrix for representing the relative importance of four criteria is given as Table 7.14.

The ranking results of units for each time stage will be obtained from AHP/ANP calculation. The list of unit ranking shows the priority of units to be committed at each time stage. However, it has not considered the constraints such as system real power balance and system spinning reserve requirement. This chapter adopts the rule-based method to solve this problem.

AHP/ANP is used to decide total ranking of all units for each time stage, and rule-based system decides the commitment state of units according to the system power balance and system spinning reserve requirement. So the final unit commitment results are obtained through the communication between AHP/ANP ranking and rule–based constraints checking.

As mentioned above, the priority ranking of all units for each time stage can be obtained by AHP/ANP. This priority rank considers the nontechnical constraints and nonquantitative factors, but it does not involve the constraints of power balance and reserve requirements in the unit commitment. Therefore, the rule-based method is used to coordinate this problem. The implementation steps of the rule-based unit commitment are as follows.

Step 1: Select the number 1 unit from the priority rank of units at hour t.

Step 2: Check the constraints of the ramp up/down of the unit.

If the constraints are satisfied, go to step 4.

Step 3: If the constraints of the ramp up/down of the unit are not satisfied, discard this unit at hour t. Select the next unit from the priority rank of units, and go to step 2.

Step 4: Check the power balance. If system power can be balanced, go to step 5. Otherwise, add one more unit according to the priority of units, and go to step 2.

Step 5: Check the spinning reserve at hour t. If the system has enough spinning reserve, go to the next step. Otherwise, add one more unit according to the priority rank of units, and go to step 2.

Step 6: Stop. All units that were not selected as well as those that have been discarded in the selection will not be committed at hour t. The other units will be committed at hour t.

7.7.3.2 Mathematical Demonstration of AHP   It is noted that the AHP method relies highly on the judgment matrix, which is formed according to the experiences of the users using the some scaling method. It is possible that consistency is not obtained. The higher the order of the judgment matrix, the more serious this problem becomes. In this case, a series of problems must be answered, as follows:

(A) Does there exist a single maximal eigenvalue of the judgment?
(B) Are all the components of the eigenvector of the judgment matrix corresponding to the maximal eigenvalue positive?
(C) Is it necessary to check the consistency of the judgment matrix?

7.7.3.2.1 Maximal Eigenvalue and Corresponding Eigenvector of Judgment Matrix   To answer these questions, let us calculate the maximal eigenvalue and corresponding eigenvector of the judgment matrix.

Generally, the judgment matrix A has the following characteristics:

$$a_{ij} > 0$$

$$a_{ji} = \frac{1}{a_{ij}}, \quad i \neq j \tag{7.82}$$

$$a_{ii} = 1 \quad i, j = 1, 2, \dots, n$$

where

a_{ij}: The element of the judgment matrix A
n: The dimension of the judgment matrix

Obviously, judgment matrix A is positive. Naturally, it is also a nonnegative and irreducible matrix [31, 32].

According to Reference [33], we can prove that the judgment matrix is primitive [31]. Therefore, judgment matrix A has a largest positive eigenvalue $\lambda_{\max}$, which is unique, and the eigenvector W of matrix A corresponding to the maximal eigenvalue $\lambda_{\max}$ has positive components and is essentially unique by the theorem of Perron–Frobenius and the properties of the judgment matrix [31].

7.7.3.2.2 Consistency of Judgment Matrix   We first give the definition of the consistency matrix.

Definition: We say matrix $A = [a_{ij}]$ is consistent if there exist $a_{ij} = \dfrac{a_{ik}}{a_{jk}}$, for all i, j and k.

If a positive matrix A is consistent, it has the following properties:

(a) $a_{ij} = \dfrac{1}{a_{ji}}$ (7.83)

$a_{ii} = 1 \quad i, j = 1, 2, \ldots, n$

(b) The transposition of A is also consistent.

(c) Each row in A can be obtained by multiplying any row by a positive number.

(d) The maximal eigenvalue of A is $\lambda_{\max}$ = n. The other eigenvalues of A are all zero.

(e) If the eigenvector of A corresponding to the largest eigenvalue $\lambda_{\max}$ is $X = [X_1, X_2, \ldots X_n]^T$,

$$a_{ij} = \frac{X_i}{X_j}; \quad i, j = 1, 2, \ldots, n \qquad (7.84)$$

Now, we discuss the case that the elements of the positive consistent matrix are perturbed but still satisfy property (a). Obviously, the judgment matrix, which we presented in this section, is such a case.

Suppose the eigenvector of the judgment matrix A corresponding to the maximal eigenvalue $\lambda_{\max}$ is $W = [W_1, W_2, \ldots, W_n]^T$. Let

$$a_{ij} = \left(\frac{W_i}{W_j}\right) \times \varepsilon_{ij}; \quad i, j = 1, 2, \ldots, n \qquad (7.85)$$

where

$$\begin{aligned} \varepsilon_{ii} &= 1, \\ \varepsilon_{ij} &= \frac{1}{\varepsilon_{ji}} \end{aligned} \qquad (7.86)$$

When $\varepsilon_{ij} = 1$ for all i and j, equation (7.85) is converted into equation (7.84). In this case, the judgment matrix is consistent. When $\varepsilon_{ij} \neq 1$ ($i \neq j, i, j = 1, 2, \ldots, n$), judgment matrix A is regarded as a perturbed matrix based on the consistency.

According to property (d) of the consistent positive matrix and n eigenvalues of the judgment matrix, λ_1 ($=\lambda_{\max}$), $\lambda_2, \ldots, \lambda_n$, we can obtain

$$\sum_i \lambda_i = n, \quad i = 1, 2, \ldots, n \qquad (7.87)$$

We define the following equation as a matrix, which reflects that the judgment matrix deviates from the consistent matrix:

$$\mu = -\left(\frac{1}{n-1}\right)\sum_i \lambda_i, \quad i = 1, 2, \ldots, n \qquad (7.88)$$

From equation (7.87), we get

$$\mu = \frac{\lambda_{\max} - n}{n - 1} \tag{7.89}$$

In fact, we can obtain the following theorem.

Theorem 1: If the positive eigenvector of the judgment matrix A corresponding to the largest eigenvalue $W = [W_1, W_2, \ldots, W_n]^T$, $a_{ij} = \left(\dfrac{W_i}{W_j}\right) \times \varepsilon_{ij}$, $\varepsilon_{ij} > 0$, we have

$$\mu = -1 + \left(\frac{1}{n(n-1)}\right) \sum_{1 \le i \le j \le n} \left[\varepsilon_{ij} + \frac{1}{\varepsilon_{ij}}\right] \tag{7.90}$$

Proof: According to Perron–Frobenius' theorem, we obtain

$$\lambda_{\max} = \sum_j a_{ij}\left(\frac{W_j}{W_i}\right), \quad i, j = 1, 2, \ldots, n \tag{7.91}$$

$$\lambda_{\max} - 1 = \sum_{j \ne i} a_{ij}\left(\frac{W_j}{W_i}\right), \quad i, j = 1, 2, \ldots, n \tag{7.92}$$

then

$$n\lambda_{\max} - n = \sum_{1 \le i \le j \le n} \left[a_{ij}\left(\frac{W_j}{W_i}\right) + a_{ji}\left(\frac{W_i}{W_j}\right)\right] \tag{7.93}$$

Consequently, we get

$$\mu = \frac{\lambda_{\max} - n}{n - 1} = -1 + \frac{1}{n(n-1)} \sum_{1 \le i \le j \le n} \left[a_{ij}\left(\frac{W_j}{W_i}\right) + a_{ji}\left(\frac{W_i}{W_j}\right)\right] \tag{7.94}$$

Substitute $a_{ij} = \left(\dfrac{W_i}{W_j}\right) \times \varepsilon_{ij}$ into equation (7.94), completing the proof of *Theorem 1*.

We know from *Theorem 1* that the smallest extremum of μ is zero under the condition of $\varepsilon_{ij} = 1$ for all i and j.

Theorem 2: Let $\lambda_{\max}$ be the maximal eigenvalue of the judgment matrix A. Then

$$\lambda_{\max} \ge n \tag{7.95}$$

Let

$$\varepsilon_{ij} = 1 + \delta_{ij}$$
$$\delta_{ij} > -1 \tag{7.96}$$

Then

$$a_{ij} = \frac{W_j}{W_i} + \left(\frac{W_i}{W_j}\right)\delta_{ij} \tag{7.97}$$

Thus δ_{ij} can be regarded as the relative change of the consistency matrix disturbed.

From equation (7.94), we have

$$\mu = \left(\frac{1}{n(n-1)}\right)\sum_{1 \le i \le j \le n}\left[\frac{\delta_{ij}^2}{1+\delta_{ij}}\right] \tag{7.98}$$

According to equations (7.89) and (7.98), we can obtain *Theorem 2*.

When $\delta = \max_{ij}\delta_{ij}$,

$$\lambda_{\max} - n < \frac{1}{n}\sum_{1 \le i \le j \le n}\delta_{ij}^2 \le \frac{(n-1)\delta^2}{2} \tag{7.99}$$

From equations (7.95) and (7.99), we have

$$n \le \lambda_{\max} \le n + \frac{(n-1)\delta^2}{2} \tag{7.100}$$

Therefore, in order to make the judgment matrix nearly consistent, we always hope that μ is near to zero, or $\lambda_{\max}$ is near n. Generally, the smaller δ_{ij} is, the nearer $\lambda_{\max}$ is to n. This is why we check the consistency of the judgment matrix when we apply the analytic hierarchy process to power system problems.

Example 7.6

The proposed approach is examined with the IEEE 39-bus test system, which is taken from Reference [7]. The test system has 10 generators, i.e., G30, G31, G32, G33, G34, G35, G36, G37, G38, and G39. The daily load demands are given in Table 7.15. The generating unit data are given in Table 7.16. Table 7.17 shows the bid price of generation power over a set of time periods.

The calculation results of unit commitment are listed in Tables 7.18 and 7.19. Table 7.18 is the unit commitment schedule obtained from AHP/ANP

Table 7.15   Daily load demands in MW

Hour	P_D	R_S	Hour	P_D	R_S	Hour	P_D	R_S
1	4878	244	9	6341	317	17	6524	326
2	5061	253	10	6585	329	18	6585	329
3	5183	259	11	6707	335	19	6402	320
4	5486	274	12	6768	338	20	6219	311
5	5610	281	13	6707	335	21	5792	290
6	5792	290	14	6646	332	22	5486	274
7	5853	293	15	6585	329	23	5183	259
8	6079	503	16	6463	323	24	4939	247

Table 7.16   Generating unit data

Unit No.	a_i	b_i	c_i	P_{imax}	P_{imin}	$F_{Si}(t)$
30	0.834	2.50	0.00	500.0	0.00	800
31	0.650	0.00	0.00	999.0	0.00	900
32	0.834	0.00	0.00	700.0	0.00	850
33	0.824	0.00	0.00	700.0	0.00	850
34	0.814	0.00	0.00	700.0	0.00	850
35	0.804	0.00	0.00	700.0	0.00	850
36	0.830	0.00	0.00	700.0	0.00	850
37	0.800	0.00	0.00	700.0	0.00	850
38	0.650	0.00	0.00	900.0	0.00	870
39	0.600	0.00	0.00	1200.0	0.00	920

Table 7.17   Bid price of generation power over a set of time periods in dollars per MW per hour

Unit	0–3	4–6	7–9	10–12	13–15	16–18	19–21	22–24
30	40	42	38	45	42	36	38	44
31	26	29	32	28	26	30	32	28
32	30	32	33	30	34	36	33	36
33	32	34	32	36	34	32	36	38
34	42	38	37	34	36	38	40	45
35	31	33	35	32	34	36	35	37
36	29	31	34	37	35	39	41	43
37	35	37	39	35	37	40	37	39
38	33	35	37	39	41	37	42	45
39	24	26	28	28	30	32	30	28

and the rule–based method. It has not considered the voltage security and transmission security constraints. The corresponding power flow solution also violates voltage limits and transmission security limits.

From Table 7.18, we find that power flows at hours 1, 2, 4, 5, 8, 22, and 24 are infeasible. Table 7.19 is the final unit commitment schedule with OPF corrections. It satisfies the voltage security and transmission security

Table 7.18   Unit commitment without transmission security and voltage constraints

Unit No.	Hour (0–24)
30	0 0 0 0 0 0 0 0 0 0 0 0 0 0 0 0 0 0 0 0 0 0 0 0
31	1 1 1 1 1 1 1 1 1 1 1 1 1 1 1 1 1 1 1 1 1 1 1 1
32	0 0 1 1 1 1 1 1 1 1 1 1 1 1 1 1 1 1 1 1 1 1 1 1
33	1 1 1 1 1 1 1 1 1 1 1 1 1 1 1 1 1 1 1 1 1 1 1 1
34	0 0 0 0 0 0 0 1 1 1 1 1 1 1 1 1 1 1 1 1 1 0 0 0
35	1 1 1 1 1 1 1 1 1 1 1 1 1 1 1 1 1 1 1 1 1 1 1 1
36	1 1 1 1 1 1 1 1 1 1 1 1 1 1 1 1 1 1 1 0 0 0 0 0
37	0 0 0 0 0 0 1 0 1 1 1 1 1 1 1 1 1 1 1 1 1 1 1 0
38	1 1 1 1 1 1 1 1 1 1 1 1 1 1 1 1 1 1 1 1 1 1 1 1
39	1 1 1 1 1 1 1 1 1 1 1 1 1 1 1 1 1 1 1 1 1 1 1 1

Table 7.19   Unit commitment with transmission security and voltage constraints

Unit No.	Hour (0–24)
30	0 0 0 0 0 0 0 0 0 0 0 0 0 0 0 0 0 0 0 0 0 0 0 0
31	1 1 1 1 1 1 1 1 1 1 1 1 1 1 1 1 1 1 1 1 1 1 1 1
32	1 1 1 1 1 1 1 1 1 1 1 1 1 1 1 1 1 1 1 1 1 1 1 1
33	1 1 1 1 1 1 1 1 1 1 1 1 1 1 1 1 1 1 1 1 1 1 1 1
34	0 0 0 0 0 0 0 1 1 1 1 1 1 1 1 1 1 1 1 1 1 0 0 0
35	1 1 1 1 1 1 1 1 1 1 1 1 1 1 1 1 1 1 1 1 1 1 1 1
36	1 1 1 1 1 1 1 1 1 1 1 1 1 1 1 1 1 1 0 0 1 0 0
37	0 0 0 0 1 1 1 0 1 1 1 1 1 1 1 1 1 1 1 1 1 1 1 1
38	1 1 1 1 1 1 1 1 1 1 1 1 1 1 1 1 1 1 1 1 1 1 1 1
39	1 1 1 1 1 1 1 1 1 1 1 1 1 1 1 1 1 1 1 1 1 1 1 1

constraints. The total generation cost for unit commitment schedule in Table 7.19 is $11, 391.00. If the commitment states of units are taken as the input of OPF, the total optimal generation cost will be reduced to $11 159.60.

REFERENCES

[1] A.I. Cohen and M. Yoshimura, "A branch and bound algorithm for unit commitment," *IEEE Trans. Power Syst.*, vol. PAS–101, pp. 444–451, 1982.

[2] A.I. Cohen and S.H. Wan, "A method for solving the fuel constrained unit commitment," *IEEE Trans. Power Syst.*, vol. 1, pp. 608–614, Feb. 1987.

[3] W.L. Snyder, H.D. Powell, and C. Rayburn, "Dynamic programming approach to unit commitment," *IEEE Trans. Power Syst.*, vol. PWRS-2, pp. 339–350, May 1987.

[4] S. Vemuri and L. Lemonidis, "Fuel constrained unit commitment," *IEEE Trans. Power Syst.*, vol. 7, pp. 410–415, Feb. 1992.

[5] S. Ruzic and N. Rajakovic, "A new approach for solving extended unit commitment problem," *IEEE Trans. Power Syst.*, vol. 6, pp. 269–277, Feb. 1991.

[6] E.H. Allen and M.D. Ilic, "Stochastic unit commitment in a deregulated utility industry," in *Proc. 29th North Amer. Power Symp.,* Laramie, Wyoming, Oct. 1997, pp. 105–112.

[7] J.A. Momoh and J.Z. Zhu, "Optimal generation scheduling based on AHP/ANP," *IEEE Trans. on Systems, Man, and Cybernetics—Part B:*, vol. 33, No.3, June 2003.

[8] G.S. Lauer, D.P. Bertsekas, N.R. Sandell, Jr., and T.A. Posbergh, "Solution of large-scale optimal unit commitment problems," *IEEE Trans. Automat. Contr.*, vol. AC-28, pp. 1–11, 1982.

[9] A. Merlin and P. Sandrin, "A new method for commitment at electricité de France," *IEEE Trans. Power Syst.*, vol. PAS-102, pp. 1218–1255, May 1983.

[10] Z. Ouyang and S.M. Shahiderpour, "Short term unit commitment expert system," *Int. J. Elect. Power Syst. Res.*, vol. 20, pp. 1–13, 1990.

[11] C.C. Su and Y.Y. Hsu, "Fuzzy dynamic programming: an application to unit commitment," *IEEE Trans. Power Syst.*, vol. 6, pp. 1231–1237, Aug. 1991.

[12] H. Sasaki, M. Watanabe, J. Kubokawa, and N. Yorino, "A solution method of unit commitment by artificial neural networks," *IEEE Trans. Power Syst.*, vol. 7, pp. 974–981, Aug. 1992.

[13] N.P. Padhy, "Unit commitment using hybrid models: a comparative study for dynamic programming, expert systems, fuzzy system and genetic algorithms," *Int. J. Elect. Power Energy Syst.*, vol. 23, no. 1, pp.827–836, 2000.

[14] A.H. Mantawy, Y.L. Youssef, L. Abdel-Magid, and S.Z. Shokri, Z. Selim, "A unit commitment by Tabu search," *Proc. Inst. Elect. Eng. Gen. Transm. Dist.*, vol. 145, no. 1, pp. 56–64, 1998.

[15] K.A. Juste, H. Kita, E. Tanaka, and J. Hasegawa, "An evolutionary programming solution to the unit commitment problem," *IEEE Trans. Power Syst.*, vol. 14, pp. 1452–1459, Nov. 1999.

[16] H.T. Yang, P.C. Yang, and C.L. Huang, "Evolutionary programming based economic dispatch for units with nonsmooth fuel cost functions," *IEEE Trans. Power Syst.*, vol. 11, pp. 112–117, Feb. 1996.

[17] A.H. Mantawy, Y.L. Abdel-Magid, and S.Z. Selim, "Integrating genetic algorithm, Tabu search and simulated annealing for the unit commitment problem," *IEEE Trans. Power Syst.*, vol. 14, pp. 829–836, Aug. 1999.

[18] C.C.A. Rajan and M.R. Mohan, "An evolutionary programming-based tabu search method for solving the unit commitment problem," *IEEE Trans. Power Syst.*, vol. 19, No. 1, pp. 577–585, 2004.

[19] H.H. Balci and J.F. Valenzuela, "Scheduling electric power generators using particle swarm optimization combined with the lagrangian relaxation method," *Int. J. Appl. Math. Comput. Sci.*, Vol. 14, No. 3, 2004.

[20] T.O. Ting, M.V.C. Rao, and C.K. Loo, "A novel approach for unit commitment problem via an effective hybrid particle swarm optimization," *IEEE Trans. Power Syst.*, vol. 21, No. 1, pp. 411–418, 2006.

[21] A.J. Wood and B. Wollenberg, *Power Generation Operation and Control*, 2nd ed. New York: John Wiley & Sons, 1996.

[22] W.Y. Li, *Power Systems Security Economic Operation*, Chongqing University Press, 1989.

[23] J. Kennedy and R. Eberhart, Particle swarm optimization. Presented at Proc. IEEE Int. Conf. Neural Networks. [Online]. Available: http://www.engr.iupui.edu/~shi/Conference/psopap4.html.

[24] D.B. Fogel, *Evolutionary Computation, Toward a New Philosophy of Machine Intelligence*. Piscataway, NJ: IEEE Press, 1995.

[25] T. Back, *Evolutionary Algorithms in Theory and Practice*. New York: Oxford Univ. Press, 1996.

[26] L.J. Fogel, A.J. Owens, and M.J. Walsh, *Artificial Intelligence Through Simulated Evolution*. New York: John Wiley & Sons, 1996.

[27] J.A. Momoh and J.Z. Zhu, "Improved interior point method for OPF problems", *IEEE Trans Power Syst*, Vol. 14, No. 3, Aug. 1999, pp. 1114–1120.

[28] J.Z. Zhu and M.R. Irving, "Combined active and reactive dispatch with multiple objectives using an analytic hierarchical process", *IEE Proceedings-C*, Vol. 143, No. 4, 1996, pp. 344–352.

[29] J.Z. Zhu and J.A. Momoh, "Optimal VAr pricing and VAr placement using analytic hierarchy process," *Elec. Power Syst. Res.*, vol. 48, pp. 11–17, Dec. 1998.

[30] T.L. Satty, *The Analytic Hierarchy Process*. McGraw Hill, Inc, 1980.

[31] J.Z. Zhu and M.R. Irving, "The development of Combined active and reactive dispatch, Part I: Mathematical model and algorithm," Research Report, Brunel Institute of Power Systems, Brunel University, March, 1995.

[32] W. Ledermann, *Handbook of Applicable Mathematics, Vol. I: Algebra*, Wiley-Interscience, 1980.

[33] H.S. Wilf, *Mathematics for the Physical Sciences*, Wiley, 1962.

8

OPTIMAL POWER FLOW

This chapter selects several classic optimal power flow algorithms and gives the implementation details. These algorithms include traditional methods such as Newton method, gradient method, linear programming as well as latest methods such as modified interior point method, analytic hierarchy process, and particle swarm optimization method.

8.1 INTRODUCTION

The optimal power flow (OPF) was first introduced by Carpentier in 1962 [1]. The goal of OPF is to find the optimal settings of a given power system network that optimize the system objective functions such as total generation cost, system loss, bus voltage deviation, emission of generating units, number of control actions, and load shedding while satisfying its power flow equations, system security, and equipment operating limits. Different control variables, some of which are generators' real power outputs and voltages, transformer tap changing settings, phase shifters, switched capacitors, and reactors, are manipulated to achieve an optimal network setting based on the problem formulation.

According to the selected objective functions, and constraints, there are different mathematical formulations for the OPF problem. They can be broadly classified as follows [1–65]:

(1) Linear problem in which objectives and constraints are given in linear forms with continuous control variables

(2) Nonlinear problem where either objectives or constraints or both combined are nonlinear with continuous control variables

(3) Mixed-integer linear problems when control variables are both discrete and continuous

Various techniques were developed to solve the OPF problem. The algorithms may be classified into three groups: (1) conventional optimization methods, (2) intelligence search methods, and (3) nonquantity approach to address uncertainties in objectives and constraints.

8.2   NEWTON METHOD

8.2.1   Neglect Line Security Constraints

If the line security constraints are neglected, the optimal power flow problem with real and reactive power variables can be represented as below:

$$\min F = \sum_{i=1}^{NG} f_i(P_{Gi}) \tag{8.1}$$

such that

$$P_i(V, \theta) = P_{Gi} - P_{Di} \tag{8.2}$$

$$Q_i(V, \theta) = Q_{Gi} - Q_{Di} \tag{8.3}$$

$$P_{Gi\min} \le P_{Gi}(V, \theta) \le P_{Gi\max} \tag{8.4}$$

$$Q_{Gi\min} \le Q_{Gi}(V, \theta) \le Q_{Gi\max} \tag{8.5}$$

$$V_{i\min} \le V_i \le V_{i\max} \tag{8.6}$$

where

P_{Gi}: The real power output of the generator connecting to bus i

Q_{Gi}: The reactive power output of the generator connecting to bus i

P_{Di}: The real power load connecting to bus i

Q_{Di}: The reactive power load connecting to bus i

P_i: The real power injection at bus i

Q_i: The reactive power injection at bus i

V_i: The voltage magnitude at bus i

f_i: The generator fuel cost function

The subscripts "min" and "max" in the equations represent the lower and upper limits of the constraint, respectively.

Equations (8.2) and (8.3) are power flow equations, and can be written as follows:

$$P_i(V, \theta) = V_i \sum_{j=1}^{N} V_j (G_{ij} \cos\theta_{ij} + B_{ij} \sin\theta_{ij}) \tag{8.7}$$

$$Q_i(V, \theta) = V_i \sum_{j=1}^{N} V_j (G_{ij} \sin\theta_{ij} - B_{ij} \cos\theta_{ij}) \tag{8.8}$$

Substituting equations (8.7) and (8.8) into equations (8.2)–(8.6), we get

$$\text{Min } F(V, \theta) \tag{8.9}$$

s.t.

$$W_{Pi} = V_i \sum_{j=1}^{N} V_j (G_{ij} \cos\theta_{ij} + B_{ij} \sin\theta_{ij}) - P_{Gi} + P_{Di} = 0 \tag{8.10}$$

$$W_{Qi} = V_i \sum_{j=1}^{N} V_j (G_{ij} \sin\theta_{ij} - B_{ij} \cos\theta_{ij}) - Q_{Gi} + Q_{Di} = 0 \tag{8.11}$$

$$W_{PMi} = V_i \sum_{j=1}^{N} V_j (G_{ij} \cos\theta_{ij} + B_{ij} \sin\theta_{ij}) - P_{Gi\max} \leq 0 \tag{8.12}$$

$$W_{PNi} = V_i \sum_{j=1}^{N} V_j (G_{ij} \cos\theta_{ij} + B_{ij} \sin\theta_{ij}) - P_{Gi\min} \geq 0 \tag{8.13}$$

$$W_{QMi} = V_i \sum_{j=1}^{N} V_j (G_{ij} \sin\theta_{ij} - B_{ij} \cos\theta_{ij}) - Q_{Gi\max} \leq 0 \tag{8.14}$$

$$W_{QNi} = V_i \sum_{j=1}^{N} V_j (G_{ij} \sin\theta_{ij} - B_{ij} \cos\theta_{ij}) - Q_{Gi\min} \geq 0 \tag{8.15}$$

$$W_{VMi} = V_i - V_{i\max} \leq 0 \tag{8.16}$$

$$W_{VNi} = V_i - V_{i\min} \geq 0 \tag{8.17}$$

We construct the new augmented objective function by introducing constraints (8.10)–(8.17) into the original objective function (8.9) with penalty factors.

$$L(X) = F(X) + \sum_{i=1}^{N} r_{Pi} W_{Pi}^2(X) + \sum_{i=1}^{N} r_{Qi} W_{Qi}^2(X) + \sum_{i=1}^{N} r_{Vi} W_{Vi}^2(X) \tag{8.18}$$

where

X: The vector that consists of V and θ

W_{Pi}: Includes all constraints related to real power variables such as equations (8.10), (8.12), and (8.13)

W_{Qi}: Includes all constraints related to reactive power variables such as equations (8.11), (8.14), and (8.15)

W_{Vi}: Includes all constraints related to voltage variables such as equations (8.16) and (8.17)

r_{Pi}: The penalty factor for violated constraints related to real power variable. If there is no constraint violation, $r_{Pi} = 0$.

r_{Qi}: The penalty factor for violated constraints related to reactive power variable. If there is no constraint violation, $r_{Qi} = 0$.

r_{Vi}: The penalty factor for violated constraints related to voltage variable. If there is no constraint violation, $r_{Vi} = 0$.

N: The total number of buses

In this way, the OPF problem represented in equations (8.1)–(8.6) becomes an unconstrained optimization problem (8.18). It is noted that only violated constraints are introduced in equation (8.18) since the penalty factor will be zero if the constraint is not violated. The unconstrained optimization problem can be solved by the Newton method or the Hessian matrix method (see Appendix in Chapter 4).

8.2.1.1 Calculation of Hessian Matrix and Gradient

From equation (8.18) as well as equations (8.10)–(8.17), we can get the gradient and Hessian matrix of the augmented objective function as below:

Gradient:

$$\frac{\partial L}{\partial V_j} = \frac{\partial F}{\partial V_j} + 2\left[\sum_{i=1}^{N} r_{Pi} W_{Pi} \frac{\partial P_i}{\partial V_j} + \sum_{i=1}^{N} r_{Qi} W_{Qi} \frac{\partial Q_i}{\partial V_j} + r_{Vj} W_{Vj}\right] \qquad (8.19)$$

$$\frac{\partial L}{\partial \theta_j} = \frac{\partial F}{\partial \theta_j} + 2\left[\sum_{i=1}^{N} r_{Pi} W_{Pi} \frac{\partial P_i}{\partial \theta_j} + \sum_{i=1}^{N} r_{Qi} W_{Qi} \frac{\partial Q_i}{\partial \theta_j}\right] \qquad (8.20)$$

Hessian Matrix:

$$\frac{\partial^2 L}{\partial V_i^2} = \frac{\partial^2 F}{\partial V_i^2} + 2\sum_{i=1}^{N} r_{Pi}\left[W_{Pi} \frac{\partial^2 P_i}{\partial V_i^2} + \left(\frac{\partial P_i}{\partial V_j}\right)^2\right] + 2\sum_{i=1}^{N} r_{Qi}\left[W_{Qi} \frac{\partial^2 Q_i}{\partial V_i^2} + \left(\frac{\partial Q_i}{\partial V_j}\right)^2\right] + 2r_{Vj}$$

$$(8.21)$$

$$\frac{\partial^2 L}{\partial V_j \partial V_k} = \frac{\partial^2 F}{\partial V_j \partial V_k} + 2\sum_{i=1}^{N} r_{Pi}\left[W_{Pi} \frac{\partial^2 P_i}{\partial V_j \partial V_k} + \frac{\partial P_i}{\partial V_j} \frac{\partial P_i}{\partial V_k}\right]$$

$$+ 2\sum_{i=1}^{N} r_{Qi}\left[W_{Qi} \frac{\partial^2 Q_i}{\partial V_j \partial V_k} + \frac{\partial Q_i}{\partial V_j} \frac{\partial Q_i}{\partial V_k}\right] \quad j \neq k \qquad (8.22)$$

$$\frac{\partial^2 L}{\partial V_j \partial \theta_k} = \frac{\partial^2 F}{\partial V_j \partial \theta_k} + 2\sum_{i=1}^{N} r_{Pi} \left[W_{Pi} \frac{\partial^2 P_i}{\partial V_j \partial \theta_k} + \frac{\partial P_i}{\partial V_j} \frac{\partial P_i}{\partial \theta_k} \right]$$

$$+ 2\sum_{i=1}^{N} r_{Qi} \left[W_{Qi} \frac{\partial^2 Q_i}{\partial V_j \partial \theta_k} + \frac{\partial Q_i}{\partial V_j} \frac{\partial Q_i}{\partial \theta_k} \right] \quad j \neq k \tag{8.23}$$

$$\frac{\partial^2 L}{\partial V_j \partial \theta_j} = \frac{\partial^2 F}{\partial V_j \partial \theta_j} + 2\sum_{i=1}^{N} r_{Pi} \left[W_{Pi} \frac{\partial^2 P_i}{\partial V_j \partial \theta_j} + \frac{\partial P_i}{\partial V_j} \frac{\partial P_i}{\partial \theta_j} \right]$$

$$+ 2\sum_{i=1}^{N} r_{Qi} \left[W_{Qi} \frac{\partial^2 Q_i}{\partial V_j \partial \theta_j} + \frac{\partial Q_i}{\partial V_j} \frac{\partial Q_i}{\partial \theta_j} \right] \tag{8.24}$$

$$\frac{\partial^2 L}{\partial \theta_i^2} = \frac{\partial^2 F}{\partial \theta_i^2} + 2\sum_{i=1}^{N} r_{Pi} \left[W_{Pi} \frac{\partial^2 P_i}{\partial \theta_i^2} + \left(\frac{\partial P_i}{\partial \theta_i}\right)^2 \right] + 2\sum_{i=1}^{N} r_{Qi} \left[W_{Qi} \frac{\partial^2 Q_i}{\partial \theta_i^2} + \left(\frac{\partial Q_i}{\partial \theta_i}\right)^2 \right] \tag{8.25}$$

$$\frac{\partial^2 L}{\partial \theta_j \partial \theta_k} = \frac{\partial^2 F}{\partial \theta_j \partial \theta_k} + 2\sum_{i=1}^{N} r_{Pi} \left[W_{Pi} \frac{\partial^2 P_i}{\partial \theta_j \partial \theta_k} + \frac{\partial P_i}{\partial \theta_j} \frac{\partial P_i}{\partial \theta_k} \right]$$

$$+ 2\sum_{i=1}^{N} r_{Qi} \left[W_{Qi} \frac{\partial^2 Q_i}{\partial \theta_j \partial \theta_k} + \frac{\partial Q_i}{\partial \theta_j} \frac{\partial Q_i}{\partial \theta_k} \right] \tag{8.26}$$

where the derivatives of the bus power injection with respect to variables V and θ can be obtained from the power flow equations, that is,

$$V_j \frac{\partial P_i}{\partial V_j} = \begin{cases} V_i V_j \left(G_{ij} \cos \theta_{ij} + B_{ij} \sin \theta_{ij} \right) & i \neq j \\ V_i^2 G_{ii} + P_i & i = j \end{cases} \tag{8.27}$$

$$\frac{\partial P_i}{\partial \theta_j} = \begin{cases} V_i V_j \left(G_{ij} \sin \theta_{ij} - B_{ij} \cos \theta_{ij} \right) & i \neq j \\ -V_i^2 B_{ii} - Q_i & i = j \end{cases} \tag{8.28}$$

$$V_j \frac{\partial Q_i}{\partial V_j} = \begin{cases} V_i V_j \left(G_{ij} \sin \theta_{ij} - B_{ij} \cos \theta_{ij} \right) & i \neq j \\ -V_i^2 B_{ii} - Q_i & i = j \end{cases} \tag{8.29}$$

$$\frac{\partial Q_i}{\partial \theta_j} = \begin{cases} -V_i V_j \left(G_{ij} \cos \theta_{ij} + B_{ij} \sin \theta_{ij} \right) & i \neq j \\ -V_i^2 G_{ii} + P_i & i = j \end{cases} \tag{8.30}$$

$$\frac{\partial^2 P_i}{\partial V_i^2} = \begin{cases} 0 & i \neq j \\ 2 G_{ii} & i = j \end{cases} \tag{8.31}$$

$$\frac{\partial^2 P_i}{\partial V_j \partial V_k}_{j \neq k} = \begin{cases} 0 & i \neq j, i \neq k \\ G_{ij} \cos \theta_{ij} + B_{ij} \sin \theta_{ij} & i = k \\ G_{ik} \cos \theta_{ik} + B_{ik} \sin \theta_{ik} & i = j \end{cases} \tag{8.32}$$

$$V_j \frac{\partial^2 P_i}{\partial V_j \partial \theta_j} = \begin{cases} V_i V_j \left(G_{ij} \sin \theta_{ij} - B_{ij} \cos \theta_{ij} \right) & i \neq j \\ -V_i^2 B_{ii} - Q_i & i = j \end{cases} \tag{8.33}$$

$$\frac{\partial^2 P_i}{\partial V_j \partial \theta_k}_{j \neq k} = \begin{cases} 0 & i \neq j, i \neq k \\ V_i(-G_{ij} \sin \theta_{ij} + B_{ij} \cos \theta_{ij}) & i = k \\ V_k(G_{ik} \sin \theta_{ik} - B_{ik} \cos \theta_{ik}) & i = j \end{cases} \tag{8.34}$$

$$\frac{\partial^2 P_i}{\partial \theta_i^2} = \begin{cases} V_i V_j(-G_{ij} \cos \theta_{ij} - B_{ij} \sin \theta_{ij}) & i \neq j \\ V_i^2 G_{ii} - P_i & i = j \end{cases} \tag{8.35}$$

$$\frac{\partial^2 P_i}{\partial \theta_j \partial \theta_k}_{j \neq k} = \begin{cases} 0 & i \neq j, i \neq k \\ V_i V_j(G_{ij} \cos \theta_{ij} + B_{ij} \sin \theta_{ij}) & i = k \\ V_i V_k(G_{ik} \cos \theta_{ik} + B_{ik} \sin \theta_{ik}) & i = j \end{cases} \tag{8.36}$$

$$\frac{\partial^2 Q_i}{\partial V_i^2} = \begin{cases} 0 & i \neq j \\ -2B_{ii} & i = j \end{cases} \tag{8.37}$$

$$\frac{\partial^2 Q_i}{\partial V_j \partial V_k}_{j \neq k} = \begin{cases} 0 & i \neq j, i \neq k \\ G_{ij} \sin \theta_{ij} - B_{ij} \cos \theta_{ij} & i = k \\ G_{ik} \sin \theta_{ik} - B_{ik} \cos \theta_{ik} & i = j \end{cases} \tag{8.38}$$

$$V_j \frac{\partial^2 Q_i}{\partial V_j \partial \theta_j} = \begin{cases} V_i V_j(-G_{ij} \cos \theta_{ij} - B_{ij} \sin \theta_{ij}) & i \neq j \\ -V_i^2 G_{ii} + P_i & i = j \end{cases} \tag{8.39}$$

$$\frac{\partial^2 Q_i}{\partial V_j \partial \theta_k}_{j \neq k} = \begin{cases} 0 & i \neq j, i \neq k \\ V_i(G_{ij} \cos \theta_{ij} + B_{ij} \sin \theta_{ij}) & i = k \\ -V_k(G_{ik} \cos \theta_{ik} + B_{ik} \sin \theta_{ik}) & i = j \end{cases} \tag{8.40}$$

$$\frac{\partial^2 Q_i}{\partial \theta_i^2} = \begin{cases} -V_i V_j(G_{ij} \sin \theta_{ij} - B_{ij} \cos \theta_{ij}) & i \neq j \\ -V_i^2 B_{ii} - Q_i & i = j \end{cases} \tag{8.41}$$

$$\frac{\partial^2 Q_i}{\partial \theta_j \partial \theta_k}_{j \neq k} = \begin{cases} 0 & i \neq j, i \neq k \\ V_i V_j(G_{ij} \sin \theta_{ij} - B_{ij} \cos \theta_{ij}) & i = k \\ V_i V_k(G_{ik} \sin \theta_{ik} - B_{ik} \cos \theta_{ik}) & i = j \end{cases} \tag{8.42}$$

8.2.1.2 *Computation of Search Direction*   The formula of the search direction of the Newton method or the Hessian matrix method is

$$S^k = -[H(X^k)]^{-1} g(X^k) \tag{8.43}$$

where

  g: The gradient of the augmented function
  H: The Hessian matrix of the augmented function
  S: The search direction

The advantage of the Hessian matrix method is fast convergence. The disadvantage is that it requires computation of the inverse of the Hessian matrix, which leads to an expensive memory and calculation burden. Thus we rewrite equation (8.43) as below.

$$H(X^k)S^k = -g(X^k) \tag{8.44}$$

For a given gradient and Hessian matrix of the objective function at the X^k, the search direction S^k can be obtained by solving equation (8.44) with the Gauss elimination method. Since the Hessian matrix of the augmented function is a sparse matrix in the OPF problem, the sparsity programming technique can be used.

The iteration calculation based on the search direction is as follows:

$$X^{k+1} = X^k + \beta^k S^k \tag{8.45}$$

where β is a scalar step length.

The iteration calculation will be stopped if the following convergence condition is satisfied:

$$\|X^{k+1} - X^k\| \le \varepsilon_1 \tag{8.46}$$

or

$$\frac{|L(X^{k+1}) - L(X^k)|}{|L(X^k)|} \le \varepsilon_2 \tag{8.47}$$

where ε_1, ε_2 are the permitted tolerances.

8.2.1.3 *Steps of the Newton method*   The calculation steps of the Newton method are summarized as below.

(1) Given the initial values for the penalty factors
(2) Given the permitted calculation tolerances
(3) Solve the initial power flow to get the values of the state variables X^0, and set the iteration number $k = 0$.
(4) Compute the augmented objective function $L(X^k)$ and its gradient g^k and Hessian matrix H^k.
(5) Compute the search direction S^k according to equation (8.43).
(6) Compute the step length β, using quadratic interpolation.
(7) Compute the new state variable X^{k+1} according to equation (8.45).
(8) Compute the augmented objective function $L(X^{k+1})$ and its gradient g^{k+1} and Hessian matrix H^{k+1}, and check the convergence conditions. If

either equation (8.46) or (8.47) is met, go to next step. Otherwise, set $k = k + 1$, go back to step (5).

(9) Check whether all constraints are met. If yes, stop the calculation. Otherwise, double the penalty factor for the violated constraint, and reset $k = 0$. Go back to step (4).

8.2.2 Consider Line Security Constraints

The line power constraints can be expressed as

$$P_{l\min} \le P_l \le P_{l\max} \tag{8.48}$$

Where P_l is the power flow at the line l from bus j to bus k.

Similarly, the above constraint can be written as

$$W_{\text{PM}l} = P_l - P_{l\max} \le 0 \tag{8.49}$$

$$W_{\text{PN}l} = P_l - P_{l\min} \ge 0 \tag{8.50}$$

We use W_{Pl} to express the above line power constraints and introduce it into the augmented objective function (8.18). The new objective function will be

$$L^*(X) = L(X) + \sum_{l=1}^{Nl} r_{Pl} W_{Pl}^2(X) \tag{8.51}$$

where

r_{Pl}: The penalty factor for violated line security constraints. If there is no line power flow constraint violation, $r_{Pl} = 0$.

Nl: The total number of lines

Since the augmented objective function includes a new penalty term on line power flow violation, the gradient and Hessian matrix equations (8.19)–(8.26) will be updated to add the corresponding term, that is,

$$\frac{\partial L^*}{\partial V_j} = \frac{\partial L}{\partial V_j} + 2\sum_{l=1}^{Nl} r_{Pl} W_{Pl} \frac{\partial P_l}{\partial V_j} \tag{8.52}$$

$$\frac{\partial L^*}{\partial \theta_j} = \frac{\partial L}{\partial \theta_j} + 2\sum_{l=1}^{Nl} r_{Pl} W_{Pl} \frac{\partial P_l}{\partial \theta_j} \tag{8.53}$$

$$\frac{\partial^2 L^*}{\partial V_i^2} = \frac{\partial^2 L}{\partial V_i^2} + 2\sum_{l=1}^{Nl} r_{Pl} \left[W_{Pl} \frac{\partial^2 P_l}{\partial V_i^2} + \left(\frac{\partial P_l}{\partial V_j} \right)^2 \right] \tag{8.54}$$

$$\frac{\partial^2 L^*}{\partial V_j \partial V_k} = \frac{\partial^2 L}{\partial V_j \partial V_k} + 2\sum_{l=1}^{Nl} r_{Pl} \left[W_{Pl} \frac{\partial^2 P_l}{\partial V_j \partial V_k} + \frac{\partial P_l}{\partial V_j} \frac{\partial P_l}{\partial V_k} \right] \quad j \neq k \qquad (8.55)$$

$$\frac{\partial^2 L^*}{\partial V_j \partial \theta_k} = \frac{\partial^2 L}{\partial V_j \partial \theta_k} + 2\sum_{l=1}^{Nl} r_{Pl} \left[W_{Pl} \frac{\partial^2 P_l}{\partial V_j \partial \theta_k} + \frac{\partial P_l}{\partial V_j} \frac{\partial P_l}{\partial \theta_k} \right] \quad j \neq k \qquad (8.56)$$

$$\frac{\partial^2 L^*}{\partial V_j \partial \theta_j} = \frac{\partial^2 L}{\partial V_j \partial \theta_j} + 2\sum_{l=1}^{Nl} r_{Pl} \left[W_{Pl} \frac{\partial^2 P_l}{\partial V_j \partial \theta_j} + \frac{\partial P_l}{\partial V_j} \frac{\partial P_l}{\partial \theta_j} \right] \qquad (8.57)$$

$$\frac{\partial^2 L^*}{\partial \theta_i^2} = \frac{\partial^2 L}{\partial \theta_i^2} + 2\sum_{l=1}^{Nl} r_{Pl} \left[W_{Pl} \frac{\partial^2 P_l}{\partial \theta_i^2} + \left(\frac{\partial P_l}{\partial \theta_i} \right)^2 \right] \qquad (8.58)$$

$$\frac{\partial^2 L^*}{\partial \theta_j \partial \theta_k} = \frac{\partial^2 L}{\partial \theta_j \partial \theta_k} + 2\sum_{l=1}^{Nl} r_{Pl} \left[W_{Pl} \frac{\partial^2 P_l}{\partial \theta_j \partial \theta_k} + \frac{\partial P_l}{\partial \theta_j} \frac{\partial P_l}{\partial \theta_k} \right] \quad j \neq k \qquad (8.59)$$

Letting the branch admittance of line l be $g_{jk} + jb_{jk}$, and neglecting the line charging, the line power flow can be expressed as

$$P_l = P_{jk} = V_j^2 g_{jk} - V_j V_k \left(g_{jk} \cos\theta_{jk} + b_{jk} \sin\theta_{jk} \right) \qquad (8.60)$$

The derivatives of the line power with respect to variables V and θ in equations (8.52)–(8.59) can be obtained from equation (8.60).

$$\frac{\partial P_l}{\partial V_j} = g_{jk}(2V_j - V_k \cos\theta_{jk}) - b_{jk}V_k \sin\theta_{jk} \qquad (8.61)$$

$$\frac{\partial P_l}{\partial V_k} = -g_{jk}V_j \cos\theta_{jk} - b_{jk}V_j \sin\theta_{jk} \qquad (8.62)$$

$$\frac{\partial P_l}{\partial \theta_j} = g_{jk}V_jV_k \sin\theta_{jk} - b_{jk}V_jV_k \cos\theta_{jk} \qquad (8.63)$$

$$\frac{\partial P_l}{\partial \theta_k} = -g_{jk}V_jV_k \sin\theta_{jk} + b_{jk}V_jV_k \cos\theta_{jk} \qquad (8.64)$$

$$\frac{\partial^2 P_l}{\partial V_j^2} = 2g_{jk} \qquad (8.65)$$

$$\frac{\partial^2 P_l}{\partial V_k^2} = 0 \qquad (8.66)$$

$$\frac{\partial^2 P_l}{\partial V_j \partial V_k} = -g_{jk} \cos\theta_{jk} - b_{jk} \sin\theta_{jk} \qquad (8.67)$$

$$\frac{\partial^2 P_l}{\partial V_j \partial \theta_j} = g_{jk}V_k \sin\theta_{jk} - b_{jk}V_k \cos\theta_{jk} \qquad (8.68)$$

$$\frac{\partial^2 P_l}{\partial V_k \partial \theta_j} = g_{jk} V_j \sin\theta_{jk} - b_{jk} V_j \cos\theta_{jk} \tag{8.69}$$

$$\frac{\partial^2 P_l}{\partial V_j \partial \theta_k} = -g_{jk} V_k \sin\theta_{jk} - b_{jk} V_k \cos\theta_{jk} \tag{8.70}$$

$$\frac{\partial^2 P_l}{\partial V_k \partial \theta_k} = -g_{jk} V_j \sin\theta_{jk} + b_{jk} V_j \cos\theta_{jk} \tag{8.71}$$

$$\frac{\partial^2 P_l}{\partial \theta_j^2} = \frac{\partial^2 P_l}{\partial \theta_k^2} = g_{jk} V_j V_k \cos\theta_{jk} + b_{jk} V_j V_k \sin\theta_{jk} \tag{8.72}$$

$$\frac{\partial^2 P_l}{\partial \theta_j \partial \theta_k} = -g_{jk} V_j V_k \cos\theta_{jk} - b_{jk} V_j V_k \sin\theta_{jk} \tag{8.73}$$

The same calculation steps given in the previous section can be used when line power flow constraints are considered.

Example 8.1

The test example is a 5-bus system, which is taken from reference [17]. The data of generators are shown in Table 8.1. The generator fuel cost is a quadratic function, that is, $f_i = a_i P_{Gi}^2 + b_i P_{Gi} + c_i$. The other data and parameters are shown in Figure 8.1, where the p.u. is used. Table 8.2 shows the initial power flow results with the initial system cost of 4518.04. The OPF results solved by the Newton method are shown in Table 8.3. The system minimum cost is 4236.5.

Table 8.1 Data of generators for 5-bus system

Unit No.	c_i	b_i	a_i	P_{Gimin}	P_{Gimax}	Q_{Gimax}	Q_{Gimax}
1	44.4	351	50	2.0	3.5	1.5	2.5
2	40.0	389	50	4.0	5.5	1.0	2.0

Table 8.2 Initial power flow results for 5-bus system

Bus No.	P_i	Q_i	V_i	θ_i
1	2.5794	2.2993	1.05	0
2	5.0	1.8130	1.05	21.84
3	−1.6	−0.8	0.8621	−4.38
4	−2.0	−1.0	1.0779	17.85
5	−3.7	−1.3	1.0364	−4.28
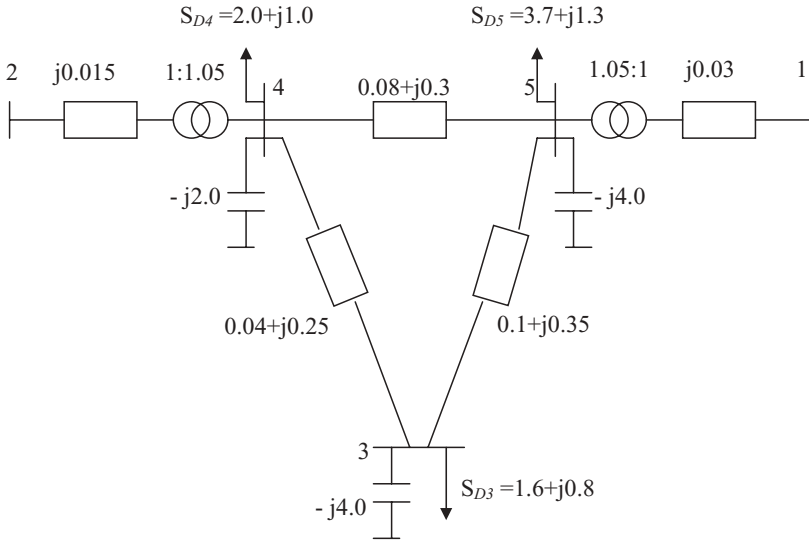
FIGURE 8.1   A 5-bus system

Table 8.3   OPF results by Newton method for 5-bus system

Bus No.	P_i	Q_i	V_i	θ_i	$V_{i\max}$	$V_{i\min}$
1	3.4351	2.0707	1.0999	0	1.1	0.9
2	3.9997	1.2000	1.0634	8.67	1.1	0.9
3	−1.6	−0.8	0.9324	−10.96	1.1	0.9
4	−2.0	−1.0	1.1003	5.59	1.1	0.9
5	−3.7	−1.3	1.1000	−5.13	1.1	0.9

8.3   GRADIENT METHOD

8.3.1   OPF Problem without Inequality Constraints

The optimal power flow problem without inequality constraints can be represented as below:

$$\min F = \sum_{i=1}^{NG} f_i(P_{Gi})$$

such that

$$P_i(V, \theta) = P_{Gi} - P_{Di}$$
$$Q_i(V, \theta) = Q_{Gi} - Q_{Di}$$

Before we solve the above OPF problem, we first define the state variables X as

$$X = \begin{bmatrix} \left. \begin{matrix} \theta \\ V \end{matrix} \right\} & \text{on each } PQ \text{ bus} \\ \theta & \text{on each } PV \text{ bus} \end{bmatrix} \tag{8.74}$$

And all specified variables Y as

$$Y = \begin{bmatrix} \left. \begin{matrix} \theta_{\text{ref}} \\ V_{\text{ref}} \end{matrix} \right\} & \text{on reference bus} \\ \left. \begin{matrix} P_{\text{D}} \\ Q_{\text{D}} \end{matrix} \right\} & \text{on each } PQ \text{ bus} \\ \left. \begin{matrix} P_{\text{G}} \\ V_{\text{G}} \end{matrix} \right\} & \text{on each } PV \text{ bus} \end{bmatrix} \tag{8.75}$$

For the parameters in the Y vector, some are adjustable, such as generator power output and generator bus voltage, and some are fixed, such as P and Q at each load bus. Thus vector Y can be partitioned into a vector U of control parameters and a vector W of fixed parameters,

$$Y = \begin{bmatrix} U \\ W \end{bmatrix} \tag{8.76}$$

Then power flow equations can be expressed as

$$g(X,Y) = \begin{bmatrix} \left. \begin{matrix} P_i(V,\theta) - (P_{\text{G}i} - P_{\text{D}i}) \\ Q_i(V,\theta) - (Q_{\text{G}i} - Q_{\text{D}i}) \end{matrix} \right\} & \text{on each bus} \\ P_k(V,\theta) - (P_{\text{G}k} - P_{\text{D}k}) & \begin{matrix} \text{on each } PV \text{ bus } k, \text{ not} \\ \text{including the reference bus} \end{matrix} \end{bmatrix} \tag{8.77}$$

Thus the OPF problem without inequality constraints can be expressed as

$$\text{Min } f(X,U) \tag{8.78}$$

s.t.

$$g(X,U,W) = 0 \tag{8.79}$$

The unconstrained Lagrange function for the OPF problem is obtained.

$$L(X,U,W) = f(X,U) + \lambda^{\text{T}} g(X,U,W) \tag{8.80}$$

or

$$L(X, U, W) = \sum_{\substack{i=1 \\ i \neq ref}}^{NG} f_i(P_{Gi}) + f_{ref}[P_{ref}(V, \theta)]$$

$$+ [\lambda_1, \lambda_1, \ldots, \lambda_m] \begin{bmatrix} P_i(V, \theta) - P_{inet} \\ Q_i(V, \theta) - Q_{inet} \\ P_k(V, \theta) - P_{knet} \\ \vdots \end{bmatrix} \qquad (8.81)$$

where

$$P_{inet} = P_{Gi} - P_{Di}$$
$$Q_{inet} = Q_{Gi} - Q_{Di}$$

The number of Lagrange multipliers is m since there are m power flow equations. According to the necessary conditions for a minimum, we get

$$\nabla L_X = \frac{\partial L}{\partial X} = \frac{\partial f}{\partial X} + \left[\frac{\partial g}{\partial X}\right]^T \lambda = 0 \qquad (8.82)$$

$$\nabla L_U = \frac{\partial L}{\partial U} = \frac{\partial f}{\partial U} + \left[\frac{\partial g}{\partial U}\right]^T \lambda = 0 \qquad (8.83)$$

$$\nabla L_\lambda = \frac{\partial L}{\partial \lambda} = g(X, U, W) = 0 \qquad (8.84)$$

Since the objective function itself is not a function of the state variable except for the reference bus, the derivatives of the objective function with respect to the state variables become

$$\frac{\partial f}{\partial X} = \begin{bmatrix} \dfrac{\partial f_{ref}(P_{ref})}{\partial P_{ref}} \dfrac{\partial P_{ref}}{\partial \theta_1} \\ \dfrac{\partial f_{ref}(P_{ref})}{\partial P_{ref}} \dfrac{\partial P_{ref}}{\partial V_1} \\ \vdots \end{bmatrix} \qquad (8.85)$$

The $\dfrac{\partial g}{\partial X}$ in equation (8.82) is the Jacobian matrix for the Newton power flow, which was discussed in Chapter 2. That is,

$$\frac{\partial g}{\partial X} = \begin{bmatrix} \dfrac{\partial P_1}{\partial \theta_1} & \dfrac{\partial P_1}{\partial V_1} & \dfrac{\partial P_1}{\partial \theta_2} & \dfrac{\partial P_1}{\partial V_2} & \cdots \\[2mm] \dfrac{\partial Q_1}{\partial \theta_1} & \dfrac{\partial Q_1}{\partial V_1} & \dfrac{\partial Q_1}{\partial \theta_2} & \dfrac{\partial Q_1}{\partial V_2} & \cdots \\[2mm] \dfrac{\partial P_2}{\partial \theta_1} & \dfrac{\partial P_2}{\partial V_1} & \cdots & \cdots & \cdots \\[2mm] \dfrac{\partial Q_2}{\partial \theta_1} & \dfrac{\partial Q_2}{\partial V_1} & \cdots & \cdots & \cdots \\[2mm] \vdots & \vdots & \vdots & \vdots & \vdots \end{bmatrix} \tag{8.86}$$

Equation (8.83) is the gradient of the Lagrange function with respect to the control variables, in which the vector $\dfrac{\partial f}{\partial U}$ is a vector of derivatives of the objective function with respect to the control variables.

$$\frac{\partial f}{\partial U} = \begin{bmatrix} \dfrac{\partial f_1(P_1)}{\partial P_1} \\[2mm] \dfrac{\partial f_2(P_2)}{\partial P_2} \\[2mm] \vdots \end{bmatrix} \tag{8.87}$$

The other term in equation (8.83), $\dfrac{\partial g}{\partial U}$, consists of a matrix of all zeros with some -1 terms on the diagonals, which correspond to equations in $g(X, U, W)$ where a control variables is present.

The solution steps of the gradient method of OPF are as follows [2, 13].

(1) Given a set of fixed parameters W, assume a starting set of control variables U.
(2) Solve a power flow. This makes sure that equation (8.84) is satisfied.
(3) Solve equation (8.82) for λ:

$$\lambda = -\left[\left(\frac{\partial g}{\partial X} \right)^T \right]^{-1} \frac{\partial f}{\partial X} \tag{8.88}$$

(4) Substitute λ into equation (8.83), and compute the gradient of the Lagrange function with respect to the control variables.

$$\nabla L_U = \frac{\partial f}{\partial U} + \left[\frac{\partial g}{\partial U} \right]^T \lambda = \frac{\partial f}{\partial U} + \left[\frac{\partial g}{\partial U} \right]^T \left\{ -\left[\left(\frac{\partial g}{\partial X} \right)^T \right]^{-1} \frac{\partial f}{\partial X} \right\}$$

$$= \frac{\partial f}{\partial U} - \left[\frac{\partial g}{\partial U} \right]^T \left[\left(\frac{\partial g}{\partial X} \right)^T \right]^{-1} \frac{\partial f}{\partial X} \tag{8.89}$$

The gradient will give the direction of maximum increase in the cost function as a function of the adjustments in each of the control variables. Since the objective is minimization of cost function, it needs to move in the negative direction of the gradient.

(5) If $|\nabla L_U|$ is sufficiently small, the minimum has been reached. Otherwise, go to next step.

(6) Find a new set of control parameters from

$$U^{k+1} = U^k + \Delta U = U^k - \beta|\nabla L_U|$$

where β is the step length. Go back to step 2 with new values of control variables.

8.3.2 Consider Inequality Constraints

8.3.2.1 Inequality Constraints on Control Parameters
The inequality constraints on control parameters such as generator bus voltage limits can be expressed as follows.

$$U_{\min} \leq U \leq U_{\max} \tag{8.90}$$

These constraints can be easily handled during the calculation of the new control parameters in equation (8.89). If the control variable i exceeds one of its limit, it will be set to the corresponding limit, that is,

$$U_i^{k+1} = \begin{cases} U_{i\max}, & \text{if } U_i^k + \Delta U_i > U_{i\max} \\ U_{i\min}, & \text{if } U_i^k + \Delta U_i < U_{i\max} \\ U_i^k + \Delta U_i, & \text{otherwise} \end{cases} \tag{8.91}$$

At the minimum the components $\dfrac{\partial f}{\partial U}$ of ∇L_U will be

$$\begin{aligned} \frac{\partial f}{\partial U_i} &= 0, \quad \text{if } U_{i\min} < U_i > U_{i\max} \\ \frac{\partial f}{\partial U_i} &\leq 0, \quad \text{if } U_i = U_{i\max} \\ \frac{\partial f}{\partial U_i} &\geq 0, \quad \text{if } U_i = U_{i\min} \end{aligned} \tag{8.92}$$

The Kuhn–Tucker theorem proves that the conditions of equation (8.92) are necessary for a minimum, provided the functions involved are convex.

8.3.2.2   *Functional Inequality Constraints*   The upper and lower limits on the state variables such as bus voltages on PQ buses can also be functional inequality constraints, which can be expressed as

$$h(X,U) \leq 0 \tag{8.93}$$

Compared with the inequality constraints on control variables, the functional inequality constraints are difficult to handle; the method can become very time consuming or practically impossible at some situations. Basically, a new direction, different from the negative gradient, must be found when confronting a functional inequality constraint. The method often used is the penalty method, in which the objective function is augmented by penalties for functional constraint violations. This forces the solution back sufficiently close to the constraint. The reasons that the penalty method is selected are as below.

(1) Generally, the functional constraints are seldom rigid limits in the strict mathematical sense but are, rather, soft limits. For example, $V \leq 1.0$ on a PQ bus means V should not exceed 1.0 by too much, and $V = 1.01$ may still be permissible. The penalty method produces just such soft limits.

(2) The penalty method adds very little to the algorithm, as it simply amounts to adding terms to $\dfrac{\partial f}{\partial X}$, and also to $\dfrac{\partial f}{\partial U}$ if the functional constraint is also a function of U.

(3) It produces feasible power flow solutions, with the penalties signaling the trouble spots, where poorly chosen rigid limits would exclude solutions.

Example 8.2

The test example is a 5-bus system, which was shown in Figure 8.1 in Example 8.1. The data and parameters of the system are the same as Example 8.1. The OPF results solved by the gradient method are shown in Table 8.4. The system minimum cost is 4235.7

Table 8.4   OPF results by gradient method for 5-bus system

Bus No.	P_i	Q_i	V_i	θ_i	$V_{i\max}$	$V_{i\min}$
1	3.4351	2.0359	1.0938	0	1.1	0.9
2	3.9987	1.2487	1.0650	8.53	1.1	0.9
3	−1.6	−0.8	0.9300	−11.10	1.1	0.9
4	−2.0	−1.0	1.1014	5.45	1.1	0.9
5	−3.7	−1.3	1.0944	−5.18	1.1	0.9

8.4 LINEAR PROGRAMMING OPF

The early LP-based OPF method was limited to network constrained economic power dispatch, which we introduced in Chapter 5. The earliest versions used the fixed constraint approximations, based on the purely DC power flow. Later on, incremental formulations were introduced, whereby constraint linearization is iterated with AC power flow, to model and enforce the constraints exactly [18]. The advantages of the LP based OPF are:

(1) Reliability of the optimization
(2) Ability to recognize problem infeasibility quickly, so that appropriate strategies can be put into effect
(3) The range of operating limits can be easily accommodated and handled, including contingency constraints
(4) Convergence to engineering accuracy is rapid, and also accepted when the changes in the controls have become very small.

The large-scale application of LP-based methods has traditionally been limited to network constrained real and reactive dispatch calculations whose objectives are separable, comprising the sum of convex cost curves. The accuracy of calculation may be lost if the oversimplified approximation is adopted in LP-based OPF. The piecewise linear segmentation of the generator fuel cost curve should be good for avoiding this problem. The piecewise approach can fit an arbitrary curve convexly to any desired accuracy with a sufficient number of segments. Originally, a separable LP variable had to be used for each segment, with the resulting large problems with multisegments cost curve modeling were prohibitively time and storage consuming. The difficulty was alleviated considerably by a separable programming procedure that uses a single variable per cost curve, regardless of the number of the segments. However, the number of segments still affects the solution speed and precision. If the segment sizes are large, the following issues may be appeared.

(1) Even a very small change in an OPF problem can cause some optimized controls to jump to adjacent segment breakpoints.
(2) Discrete jumps between segment breakpoints occasionally produce solution oscillations when iterating with AC power flow.

The technique of successive segment refinement can be used to overcome the above problems. The idea is that the nonlinear cost curves are approximated with relatively large segments at the beginning. Then, at each subsequent iteration, each cost curve is modeled with a smaller segment size, until the final degree of refinement has been reached.

For LP-based OPF, in addition to the linearization of the objective function, the constraints also need to be linearized. Generally, the linearized

power flow equations are used in LP-based OPF either based on a linear sensitivity matrix or the fast decoupled power flow model. The latter can be written as

$$[B']\Delta\theta = \Delta P \tag{8.94}$$

$$[B'']\Delta V = \Delta Q \tag{8.95}$$

These provide accurate enforcement of the network constraints in the real or reactive subproblems through the iterative process. The real power subproblem in OPF based on equation (8.94) is restricted to the "real power" constraints that are strong functions of angle "θ," and the reactive power subproblem in OPF based on equation (8.95) is restricted to the "reactive power" constraints that are strong functions of the magnitude of voltage "V." Tests on a large power system have demonstrated that successive constrained P and Q subproblems for OPF are effective in achieving practical overall optimization. If only a real power subproblem is considered in OPF, it becomes the security-constrained economic power dispatch, which was introduced in Chapter 5.

For inequality constraints in LP-based OPF, the sensitivity approach is used to express each selected constraint in terms of the control variables. Let U, X, and P be the control, state variables, and bus power injections, respectively. Y is the constraint whose sensitivities are to be computed. The incremental relationships between these variables are:

$$\Delta Y = C\Delta X + D\Delta U \tag{8.96}$$

$$\Delta P = [B]\Delta U \tag{8.97}$$

$$\Delta X = [A]^{-1}\Delta P \tag{8.98}$$

From the above equations, we get the following sensitivity vector:

$$\frac{\Delta Y}{\Delta U} = C[A]^{-1}[B]\Delta U + D \tag{8.99}$$

The row vectors C and D are usually extremely sparse, and are specific to the particular constraint Y. The power flow Jacobian matrix $[A]$ and matrix $[B]$ are constant throughout the OPF iteration. The main work in calculating the sensitivity vector from equation (8.99) is the repeat solution $C[A]^{-1}$ using fast-forward substitution.

After the above handlings on OPF objective function and constraints, the linear OPF model can be constructed and, consequently, solved by linear programming algorithm.

8.5   MODIFIED INTERIOR POINT OPF

8.5.1   Introduction

Optimal power flow (OPF) calculations determine optimal control variables and system quantities for efficient power system planning and operation. OPF has now become a useful tool in power system operation as well as in planning. Over the years, different objective functions have emerged, and the constraints and size of systems to be solved have increased. An efficient OPF tool is required to solve both the operations problem and the planning problem. The operational OPF problem, considering a time duration from one-half hour to a day, consists of many objective functions such as economic dispatch and loss minimization. For VAR planning, the time duration can be up to 5 years. VAR planning can also consider the operational cost of losses, thus forming a hybrid planning/operation problem.

An OPF package must handle large, interconnected power systems. In some instances, the area to be optimized needs to be identified and the type of optimization needs to be established before optimization. Generally the available OPF packages do not determine the type of problem, recommend the type of objective, or identify the area to be optimized. Also, in most OPF packages, the model is predetermined and cannot be modified by the user without access to the source code [27]. An OPF package that allows the user to pick certain constraints from a specified list is useful for adapting the package to the user's needs.

To implement the above requirements, a more versatile OPF package is necessary. Obviously, the conventional OPF algorithms are limited and too slow for this purpose. The increasing burden being imposed on the optimization is handled by rapidly advancing computer technology as well as through the development of more efficient algorithms exploiting the sparse nature of the power system structure. The interior point (IP) method is one of the most efficient algorithms, as evidenced by the list of references [27–45]. The IP method classification is a relatively new optimization approach that was applied to solve power system optimization problems in the late 1980s and early 1990s. This method is essentially a linear programming method, and, as expected, linear programming problems dominate the IP classification. When compared with other well-known linear programming techniques, IP methods maintain their accuracy while achieving great advantages in speed of convergence of as much as 12:l in some cases. However, the IP methods, in general, suffer from bad initial, termination, and optimality criteria and, in most cases, are unable to solve nonlinear and quadratic objective functions. The extended quadratic interior point (EQIP) method described here can handle quadratic objective functions subject to linear and nonlinear constraints.

The optimization technique used in this section is an improved quadratic interior point (IQIP) method. The IQIP method features a general starting point (rather than a good point as in the former EQIP as well as general IP

methods) and is even faster than the EQIP optimization scheme. Consequently, the OPF approach described in this section offers great improvements in speed, accuracy, and convergence in solving multiobjective and multi-constraint optimization problems. It is also capable of solving the global optimization of an interconnected system and a partitioned system for local optimization. The scheduled generation, transformer taps, bus voltages, and reactors are used to achieve a feasible and optimized power flow solution.

8.5.2 OPF Formulation

8.5.2.1 *Objective Functions* Three objective functions are considered. They are fuel cost minimization, VAR planning, and loss minimization.

(1) Fuel cost minimization

$$\text{Min } F_g = \sum_{i=1}^{NG} \left(a_i P_{gi}^2 + b_i P_{gi} + c_i \right) \tag{8.100}$$

(2) VAR planning

$$\text{Min } F_q = \sum_{i=1}^{Nc} S_{ci} \left(q_{ci}^{\text{tot}} - q_{ci}^{\text{exist}} \right) - \sum_{i=1}^{Nr} S_{ri} \left(q_{ri}^{\text{tot}} - q_{ri}^{\text{exist}} \right) + S_\omega P_L \tag{8.101}$$

(3) Loss minimization

$$\min P_L = F\left(P_{\text{gslack}} \right) \tag{8.102}$$

where

P_{gi}: The real power generation at generator i

P_L: The system real power loss

P_{gslack}: The real power of slack generator

S_c: The cost of unit capacitive VAR

S_r: The cost of unit inductive VAR

q_c: The capacitive VAR support

q_r: The inductive VAR support

l: The contingency case, $l = 0$, means the intact case or base case

S_w: The coupling coefficient between the VAR and loss portions in the VAR planning objective function

8.5.2.2 *Constraints* The linear and nonlinear constraints that include voltage, flows, real generation, reactive sources and transformer taps are considered as follows:

$$P_{gi,l}^{\min} \le P_{gi,l} \le P_{gi,l}^{\max}, \quad i \in NG \tag{8.103}$$

$$\sum_{i=1}^{NG} P_{gi} = \sum_{k=1}^{ND} P_{dk} + P_L \tag{8.104}$$

$$P_{gi} - P_{di} - F_i(V, \theta, T) = 0$$
$$i = 1, 2, \ldots, N_{\text{bus}}, i \ne Slack \tag{8.105}$$

$$Q_{gi} - Q_{di} - G_i(V, \theta, T) = 0$$
$$i = 1, 2, \ldots, N_{\text{bus}}, i \ne \text{Slack} \tag{8.106}$$

$$\frac{V_i^2 + V_j^2 - 2V_iV_j \cos(\theta_i - \theta_j)}{Z_L(l)^2} - I_{L\max}^2(l) \le 0 \quad l = 0, 1, 2, \ldots, Nl \tag{8.107}$$

$$Q_{gi\min} \le Q_{gi} \le Q_{gi\max}, \quad i \in NG \tag{8.108}$$

$$0 \le q_{ci}^{\text{exist}} \le q_{ci\max}^{\text{exist}}, \quad i \in \text{VAR sites} \tag{8.109}$$

$$0 \le q_{ri}^{\text{exist}} \le q_{ri\max}^{\text{exist}}, \quad i \in \text{VAR sites} \tag{8.110}$$

$$q_{ci}^{\text{tot}} - q_{ci}^{\text{exist}} \ge 0, \quad i \in \text{VAR sites} \tag{8.111}$$

$$q_{ri}^{\text{tot}} - q_{ri}^{\text{exist}} \ge 0, \quad i \in \text{VAR sites} \tag{8.112}$$

$$V_{gi\min} \le V_{gi} \le V_{gi\max}, \quad i \in NG \tag{8.113}$$

$$V_{di\min} \le V_{di} \le V_{di\max}, \quad i \in ND \tag{8.114}$$

$$T_{i\min} \le T_i \le T_{i\max}, \quad i \in NT \tag{8.115}$$

$$P_{\text{slack}} = F_{\text{slack}}(V, \theta, T) \tag{8.116}$$

where

P_{dk}: The real power load at load bus k

Q_{di}: The reactive power load at load bus i

V_{gi}: The voltage magnitude at generator bus i

V_{di}: The voltage magnitude at load bus i

Q_{gi}: The VAR generation of generator i

Z_L: The impedance of transmission line L

$I_{L\max}$: The maximal current limit through transmission line L

T: The transformer tap position

θ: The bus voltage angle

P_L: The system real power loss

NG: The set of generation buses

NT: The set of transformer branches

ND: The set of load buses

N_{bus}: The set of total network buses

ϕ_i: The angle of phase shifter transformer i

$NM\phi$: The adjustment numbers of the phase shifter

Nl: The set of the outage line ($l = 0$ means no line outage)

The subscripts "min" and "max" stand for the lower and upper bounds of a constraint, respectively.

We can pick certain constraints from equations (8.103)–(8.116) according to the particular needs of the practical system. Generally, the constraints in equations (8.103)–(8.108) and (8.113)–(8.115) are considered for economic dispatch. The constraints in equations (8.104)–(8.116) are considered for VAR planning. For loss minimization, the constraints in equations (8. 104)–(8.108) and (8.113)–(8.116) are considered.

8.5.3 IP OPF Algorithms

8.5.3.1 General Interior Point Algorithm The OPF problem can be expressed as general form as below:

$$\text{Min } f(x) \tag{8.117}$$

s.t.

$$d(x) \geq 0 \tag{8.118}$$

$$x \geq 0$$

There are several primal–dual interior point (IP) methods. Here we introduce the logarithmic barrier function-based IP method. For the above problem, the logarithmic barrier function is given by

$$b(x, \mu) = f(x, \mu) - \mu \sum_{j=1}^{m} \ln d_j(x) - \mu \sum_{i=1}^{n} \ln x_i \tag{8.119}$$

where

μ: A positive parameter

m: The number of constraints

n: The number of variables

The barrier gradient and Hessian are

$$\nabla b(x, \mu) = g - \mu B^T D^{-1} I - \left(\mu X^{-1} I \right) \tag{8.120}$$

$$\nabla^2 b(x, \mu) = \nabla^2 f - \sum_{j=1}^{m} \frac{\mu}{d_j} \nabla^2 d_j + \mu B^T D^{-2} B + \mu X^{-2} \tag{8.121}$$

where

> *I:* A column vector of ones
> *D:* Diagonal matrix diag$\{d(x)\}$
> *X:* Diagonal matrix diag$\{x\}$

The solution to the above problem can be obtained via a sequence of solutions to the unconstrained subproblem.

$$\text{Minimize } b(x, \mu) \tag{8.122}$$

According to KT conditions, we have

$$\nabla b(x, \mu) = 0 \tag{8.123}$$

$$\nabla^2 b(x, \mu) = 0 \quad \text{is positive definite} \tag{8.124}$$

$$\lim_{\mu \to 0} (x_\mu) = x^*$$

$$\lim_{\mu \to 0} \frac{\mu}{x_{j\mu}} = s_j^* \tag{8.125}$$

$$\lim_{\mu \to 0} \frac{\mu}{d_j(x_\mu)} = z_j^*$$

where s_j^* and z_j^* are the Lagrange multipliers. The points (x_μ) define a barrier trajectory, or a local central path for equation (8.125). If we introduce the slack variable

$$v_\mu = d(x_\mu), \quad v_\mu \geq 0 \tag{8.126}$$

and define

$$z_\mu = \mu D(x_\mu)^{-1} I, \quad z_\mu \geq 0 \tag{8.127}$$

$$s_\mu = \mu X_\mu^{-1} I, \quad s_\mu \geq 0 \tag{8.128}$$

then the central path is equivalent to

$$g_\mu - B_\mu^{\mathrm{T}} z_\mu - s_\mu = 0 \tag{8.129}$$

$$d_\mu - v_\mu = 0 \tag{8.130}$$

$$\nabla^2 f_\mu - \sum_{j=1}^{m} z_{j\mu} \nabla^2 d_{j\mu} + B_\mu^{\mathrm{T}} V_\mu^{-1} Z_\mu B_\mu + X_\mu^{-1} S_\mu = 0 \tag{8.131}$$

$$V_\mu z_\mu = \mu I, \quad v_\mu, z_\mu \geq 0 \tag{8.132}$$

$$X_\mu s_\mu = \mu I, \quad x_\mu, s_\mu \geq 0 \tag{8.133}$$

The above nonlinear equations can be expressed as below, which hold at $(x_\mu, v_\mu, z_\mu, s_\mu)$:

$$\begin{bmatrix} -g + B^{\mathrm{T}} z - s \\ d - v \\ V z - \mu I \\ S x - \mu I \end{bmatrix} = 0 \tag{8.134}$$

Applying Newton's method to the above, we obtain

$$\begin{bmatrix} -W & B^{\mathrm{T}} \\ B & 0 \end{bmatrix}\begin{bmatrix} \Delta x \\ \Delta z \end{bmatrix} + \begin{bmatrix} \Delta s \\ -\Delta v \end{bmatrix} = \begin{bmatrix} g - B^{\mathrm{T}} z - s \\ v - d \end{bmatrix} \tag{8.135}$$

and

$$V \Delta z + Z \Delta v = \mu I - Zv \tag{8.136}$$

$$S \Delta x + X \Delta s = \mu I - Xs \tag{8.137}$$

The solution of the above linear systems can be obtained as follows.

First, compute Δs and Δv.

$$\Delta v = -v - Z^{-1} V \Delta z + \mu Z^{-1} I \tag{8.138}$$

$$\Delta s = -s - X^{-1} S \Delta x + \mu X^{-1} I \tag{8.139}$$

Then substitute the above two equations into equation (8.135) to get the augmented system

$$\begin{bmatrix} -D_x & B^{\mathrm{T}} \\ B & Z^{-1} V \end{bmatrix}\begin{bmatrix} \Delta x \\ \Delta z \end{bmatrix} = \begin{bmatrix} g - B^{\mathrm{T}} z - \mu X^{-1} I \\ \mu Z^{-1} I - d \end{bmatrix} \tag{8.140}$$

where

$$D_x = W + X^{-1} S \tag{8.141}$$

Solving the above equation, we get Δz as below:

$$\Delta z = -V^{-1} Z B \Delta x + V^{-1}(\mu I - Zd) \tag{8.142}$$

The solution Δx can be obtained by solving the following normal system:

$$-K\Delta x = h \tag{8.143}$$

where

$$K = D_x + B^T V^{-1} Z B \tag{8.144}$$

$$h = g - B^T z + B^T V^{-1}(Zd - \mu I) - \mu X^{-1} I \tag{8.145}$$

8.5.3.1.1 Calculation of the Step Length   It should be noted that if started far from a solution (or start point is not good), the primal–dual IP methods may fail to converge to a solution [31–39]. For this reason, primal–dual methods usually use a merit function in order to induce convergence. There are, however, problems associated with the merit function, particularly with the choice of the penalty parameter [66]. The filter technique [42] may be used to handle convergence issue.

There are two competing aims in the primal–dual solution of equation (8.117). The first aim is to minimize the objective, and the second is the satisfaction of the constraints. These two conflicting aims can be written as

$$\text{Min } f(x) \tag{8.146}$$

s.t.

$$\text{Min } \delta = (d - v)^2 \tag{8.147}$$

A merit function usually combines equations (8.146) and (8.147) into a single objective. Instead, we see equations (8.146) and (8.147) as two separate objectives, similar to multiobjective optimization. However, the situation here is different since it is essential to find a point where $d = v$ if possible. In this sense, the second objective has priority. Nevertheless, we will make use of the principle of domination from multiobjective programming in order to introduce the concept of the filter.

Definition 1 [66]: A pair (f^k, δ^k) is said to dominate another pair (f^j, δ^j) if and only if $f^k \leq f^j$ and $\delta^k \leq \delta^j$.

In the context of the primal–dual method, this implies that the kth iterate is at least as good as the jth iterate with respect to equations (8.146) and (8.147). Next, we define the filter which will be used in the line search to accept or reject a step.

Definition 2 [66]: A filter is a list of pairs (f^j, δ^j) such that no pair dominates any other. A point (f^k, δ^k) is said to be accepted for inclusion in the filter if it is not dominated by any point in the filter.

The filter therefore accepts any point that either improves optimality or infeasibility.

In most primal–dual methods, the separate step lengths are used for the primal and dual variables [67]. A standard ratio test is used to ensure that nonnegative variables remain nonnegative

$$\alpha_P = \min\{\alpha_x, \alpha_v\} \tag{8.148}$$

$$\alpha_D = \min\{\alpha_z, \alpha_s\} \tag{8.149}$$

where

$$\alpha_j = \min\left\{1, 0.9995 \times \min\left\{\frac{\omega_j}{-\Delta\omega_j}, \text{ if } \Delta\omega_j < 0\right\}\right\} \tag{8.150}$$

$$\omega = x, v, z, s$$

The step lengths in the above are successively halved until the following iteration becomes acceptable to the filter:

$$x' = x + \alpha_P \Delta x \tag{8.151}$$

$$v' = v + \alpha_P \Delta v \tag{8.152}$$

$$z' = z + \alpha_D \Delta z \tag{8.153}$$

$$s' = s + \alpha_D \Delta s \tag{8.154}$$

8.5.3.1.2 Selection of the Barrier Parameter Another important issue in the primal–dual method is the choice of the barrier parameter. Many methods are based on approximate complementarity where the centering parameter is fixed a priori [68]. Mehrotra [69] suggested a scheme for linear programming in which the barrier parameter is estimated dynamically during the iteration. The heuristic originally proposed in may be used. First, the Newton equations system is solved with the barrier μ set to zero. The direction obtained in this case (Δx^α, Δv^α, Δz^α, Δs^α) is called the **affine-scaling direction**. The barrier parameter is estimated dynamically from the estimated reduction in the complementarity gap along the affine-scaling direction

$$\mu = \left(\frac{g^\alpha}{z^T v + s^T x}\right)^2 \left(\frac{z^T v + s^T x}{m + n}\right) \tag{8.155}$$

where

$$g^\alpha = \left(z + \alpha_D^\alpha \Delta z^\alpha\right)^T \left(v + \alpha_P^\alpha \Delta v^\alpha\right) + \left(s + \alpha_D^\alpha \Delta s^\alpha\right)^T \left(x + \alpha_P^\alpha \Delta x^\alpha\right) \tag{8.156}$$

The step lengths in the affine-scaling direction are obtained by using equations (8.155) and (8.156). To avoid numerical instability, the above equation

is used to compute μ when the absolute complementarity gap $z^Tv + s^Tx \geq 1$. But if $z^Tv + s^Tx \leq 1$, we use following equation to compute μ, that is,

$$\mu = \left(\frac{1}{m+n}\right)^2 \left(\frac{z^Tv + s^Tx}{m+n}\right) \tag{8.157}$$

8.5.3.2 *The Improved Quadratic Interior Point Method*   The OPF model discussed in this section is a nonlinear mathematical programming problem. It can be reduced by an elimination procedure. The reduction of the OPF model is based on the linearized load flow around base load flow solution for small perturbation. The reduced OPF model can be expressed as

$$\min F = \frac{1}{2}X^TQX + G^TX + C \tag{8.158}$$

such that

$$AX = B \tag{8.159}$$

$$X \geq 0$$

Equation (8.158) is a scalar objective function, which corresponds to the objective functions of OPF. Equation (8.159) corresponds to constraints (8.103)–(8.116) with linearization handling. X in (8.158) and (8.159) is a vector of controllable variables, which is defined as $X = [V_g^T, T^T, P_g^T]^T$ in economic dispatch, or $X = [V_g^T, T^T, q_c^T, q_r^T, P_L^T]^T$ in VAR planning, or $X = [V_g^T, T^T, P_L^T]^T$ in loss minimization.

The model (8.158)–(8.159) has a quadratic objective function subject to the linear constraints that satisfy the basic requirements of quadratic interior point (QIP) scheme. The barrier-like IP methods discussed in the previous section and the enhanced projection method used in quadratic interior point have the enough speed and accuracy to solve optimal power flow problems such as economic dispatch, loss minimization, and VAR optimization. However, the effectiveness of these IP methods depends on a good starting point [27]. The improved quadratic interior point (IQIP) is presented in this section. It features the general starting point (rather than a good point) and faster convergence. The calculation steps of IQIP are as follows.

S1   Given a starting point X_1,

S2 $X_1 := AX_1$

S3 $\Delta := B - AX_1$

S4 $\Delta\text{max} := \max|\Delta i|$

S5   if $\Delta\text{max} < \varepsilon_0$, go to S10. Otherwise, go to next step.

S6 $U := \left\lfloor A_1 \left(A_1 A_1^{\mathrm{T}} \right)^{-1} \right\rfloor \Delta$

S7 $R := \min\{Ui\}$

S8   if $R + 1 \geq 0$, $X_1 := X_1 \times (1 + U)$, go to S3. Otherwise, go to next step.

S9 $QB := -1/R$, $X_1 := X_1 * (1 + QB * U)$, go to S3.

S10 $D_k := \mathrm{diag}[x_1, x_2, \ldots, x_n]$

S11 $B_k := A D_k$

S12 $dp^k := \left\lfloor B_k^{\mathrm{T}} \left(B_k B_k^{\mathrm{T}} \right)^{-1} B_k - 1 \right\rfloor D_k \left[Q X^k + G \right]$

S13 $\beta_1 := -\dfrac{1}{\gamma}$, $\gamma < 0$; $\beta_1 := 10^6$, $\gamma > 0$ where $\gamma = \min\left[dp_j^k \right]$

S14

     $\beta_2 := \dfrac{\left(dp^k \right)^{\mathrm{T}} \left(dp^k \right)}{W}$ if $W > 0$; $\beta_2 := 10^6$ if $W \leq 0$ where $W = \left(D_k dp^k \right)^T Q \left(D_k dp^k \right)$

S15 $X^{k+1} := X^k + \alpha(\beta D_k dp^k)$, where $\beta = \min[\beta_1, \beta_2]$; $\alpha(<0)$ is a variable step.
Set $k := k + 1$, and go to S11. End when $dp^k < m$, where k is the iteration counter.

The partitioning scheme and optimization modules are adopted here. The partitioning scheme provides the objective function and the optimizable area. The optimization module selects the default constraints for the selected objective unless otherwise specified. The user can add or remove constraints from the default constraint set equations (8.103)–(8.116). The optimization is carried out with the improved quadratic interior point (IQIP) method described above. The nonlinear constraints are handled via successive linearization in conjunction with an area power flow.

IQIP handles the initial value of the state variables before the optimization so that it can solve the bad initial conditions encountered in other interior point methods. Consequently, IQIP has a faster convergence speed than other IP methods. IQIP achieves an optimum in the linearized space while the power flow adjusts for the approximation caused by the linearization. The check of the power flow mismatch should be performed in the optimization area first. In this way, the optimization calculation accuracy will be increased. This ensures local optimization with all violations removed. Then the check of the power flow mismatch will be performed in the whole system including the external areas, which adjusts the changes in the boundary injections caused by the local optimization. The overall scheme ensures a local optimum, with no violation in the optimized area, while satisfying a global power flow. The local optimum will be the global optimum if there is only one area in the system.

If the region formed by the constraints is very narrow, the solution may be declared infeasible. Three options are available for infeasibility handling. They are:

(1) The bounds option, which allows the program to widen the bounds on violating soft constraints. The new limits or a percent increase/decrease from the current limits can be prespecified by the user for all objective functions.

(2) VAR option I, which allows the program to add new VAR sites at buses with big contributions to improving system performance (only for VAR optimization).

(3) VAR option II, which allows the program to add new VAR sites at buses with severe voltage violations (only for VAR optimization).

For economic dispatch or loss minimization, if infeasibility is detected the bounds option is selected. The bounds on violating constraints are widened accordingly. For VAR optimization, or planning, if infeasibility is detected VAR option I is first selected, and the new VAR sites are added at buses with big contributions to improve system performance such as reducing system loss or voltage violations. If further infeasibilities occur, VAR option II is selected, and other new VAR sites are added at buses with severe voltage violations.

8.5.3.3 Simulation Calculations The simulation examples are taken from reference [27]. The two interior point-based OPF methods are tested on IEEE 14-bus systems and modified IEEE 30-bus systems. One is the extended quadratic interior point (EQIP); another is improved quadratic interior point (IQIP). For comparison, the solution method of MINOS is also used to solve the OPF problem with the same data and same conditions. MINOS is a Fortran-based optimization package developed by Stanford University, which is designed to solve large-scale optimization problems. The solution method in the MINOS program is a reduced gradient algorithm or a projected augmented Lagrange algorithm.

The data and parameters of the 14-bus system are shown in Chapter 3. The optimization data used for simulating the IEEE 14-bus system using the three objective functions are given in Tables 8.5–8.7.

Table 8.5 represents the generator data used for the IEEE 14-bus system. Tables 8.6 and 8.7 represent the capacitor and inductor VAR allocation data of the IEEE 14-bus system, respectively.

In the following calculations, optimization iteration will be stopped when the difference of objective value ΔF is less than $\varepsilon (\varepsilon = 10^{-6})$.

Table 8.5   Generator data for 14-bus system (p.u.)

Unit No.	a	b	c	$P_{gi\min}$	$P_{gi\max}$
1	0.0784	0.1350	0.0000	0.0000	3.0000
2	0.0834	0.2250	0.0000	0.0000	1.3000
6	0.0875	0.1850	0.0000	0.2000	2.0000

Table 8.6   Capacitive VAR data for 14-bus system (p.u.)

VAR Site Bus	Fixed Unit Cost	Variable Unit Cost	Max. Capacitive VAR	Max. Inductive VAR
5	2.3500	0.1500	0.8000	0.0000
9	3.4500	0.2000	0.8000	0.0000
13	3.4500	0.2000	0.8000	0.0000

Table 8.7   Inductive VAR data for 14-bus system (p.u.)

VAR Site Bus	Fixed Unit Cost	Variable Unit Cost	Max. Capacitive VAR	Max. Inductive VAR
5	6.0000	0.2500	0.4000	0.0000
9	6.0000	0.2500	0.4000	0.0000
13	6.0000	0.2500	0.4000	0.0000

Table 8.8   Three test cases for OPF objective 1

Initial Value	Case 1	Case 2	Case 3
PG1	0.0000	0.0000	0.0000
PG2	0.4000	0.3500	0.0000
PG6	0.7000	0.7000	0.7000
VG1	1.0500	1.0500	1.0500
VG2	1.0450	1.0450	1.0450
VG6	1.0500	1.0500	1.0500

8.5.3.3.1   Sample set of Results with IQIP/EQIP/MINOS Options (minimization of the total generation cost as objective function)   Three test cases are given here for the 14-bus system for OPF with minimization of generation cost as objective function (i.e., objective 1 in OPF model, Section 8.5.2). The initial values of real power for the three cases are different as shown in Table 8.8. The comparisons of results for three test cases using IQIP/EQIP/MINOS methods are listed in Tables 8.9–8.11.

It can be observed from Tables 8.9–8.11 that the MINOS method cannot converge for these test cases, while the other two methods evaluated the optimization solutions. The improved IQIP method has high accuracy, fewer iteration numbers, and fast calculation speed compared with OPF based on the EQIP method. The maximum speed ratio between IQIP and EQIP can reach 1:8 (see Table 8.9 and Table 8.10). If the initial starting point is good (as in case 3), the OPF based on the EQIP method has a fast convergence speed but the convergence speed is still slower than that of IQIP based OPF. Meanwhile, for the same iteration number, the objective value obtained by IQIP is less than that by EQIP. Therefore, the improved IQIP method is

Table 8.9   Optimization results and comparison for case 1 (p.u.)

Control Option	IQIP	EQIP	MINOS
PG1	1.53414	2.18319	/
PG2	0.93357	0.34326	/
PG6	0.38141	0.35392	/
VG1	1.05000	1.05000	/
VG2	1.04997	1.04683	/
VG6	1.05000	1.05000	/
T4-7	0.98454	0.97513	/
T4-9	1.01278	0.98307	/
T5-6	0.98454	0.94992	/
Total PG	2.84912	2.88037	/
Power loss	0.10912	0.14037	/
Total PG cost	0.7578562	0.8272073	/
Objective value	0.7578562	0.8272073	/
PF mismatch	0.1402E-6	0.4370E-4	/
Iteration no.	12	26	/
CPU time (s)	30.0	252.9	No convergence

Table 8.10   Optimization results and comparison for case 2 (p.u.)

Control Option	IQIP	EQIP	MINOS
PG1	1.65313	2.21476	/
PG2	0.84114	0.31538	/
PG6	0.35920	0.35192	/
VG1	1.05000	1.05000	/
VG2	1.04997	1.04588	/
VG6	1.04996	1.05000	/
T4-7	0.98208	0.97525	/
T4-9	1.01269	0.98293	/
T5-6	0.98853	0.94962	/
Total PG	2.85347	2.88206	/
Power loss	0.11347	0.14206	/
Total PG cost	0.7632329	0.8340057	/
Objective value	0.7632329	0.8340057	/
PF mismatch	0.1866E-4	0.4357E-4	/
Iteration no.	12	26	/
CPU time (s)	30.2	253.8	No convergence

superior to the EQIP method. It features a general starting point and fast convergence.

Since the MINOS program cannot converge under specific operating conditions and constraints, the other test case, the 30-bus system, is used to further demonstrate the effectiveness of the IQIP method. The data and parameters of the 30-bus system are taken from reference [3]. The optimization results and comparison for IQIP/EQIP/MINOS methods are listed in Table 8.12. It

Table 8.11   Optimization results and comparison for case 3 (p.u.)

Control Option	IQIP	EQIP	MINOS
PG1	1.55607	1.58973	/
PG2	0.93372	0.88235	/
PG6	0.36034	0.37895	/
VG1	1.05000	1.05000	/
VG2	1.04993	1.05000	/
VG6	1.04956	1.04987	/
T4-7	1.00047	0.99398	/
T4-9	1.00715	1.01298	/
T5-6	0.99392	0.97887	/
Total PG	2.85319	2.85100	/
Power loss	0.11319	0.11100	/
Total PG cost	0.7609503	0.7583547	/
Objective value	0.7609503	0.7583547	/
PF mismatch	0.9630E-6	0.1622E-4	/
Iteration no.	3	11	/
CPU time (s)	21.3	35.9	No convergence

Table 8.12   Optimization results and comparison for IEEE 30-bus system (p.u.)

Control Option	IQIP	EQIP	MINOS
PG1	0.73357	0.73921	0.75985
PG2	0.59838	0.59999	0.38772
PG5	0.61117	0.61412	0.66590
PG11	0.58787	0.57562	0.60000
PG13	0.34092	0.34321	0.40355
VG1	1.05000	1.05000	1.05000
VG2	1.04999	1.05000	1.03984
VG5	1.04998	1.05000	1.01709
VG11	1.04867	1.04915	1.05000
VG13	1.05000	1.05000	1.05000
T6-9	1.05160	1.08149	1.05461
T6-10	1.07615	1.01465	0.92151
T4-12	1.06768	1.09528	1.03377
T28-27	0.97443	0.94345	0.97217
Total PG	2.87190	2.87215	2.87120
Power loss	0.03790	0.03815	0.03720
Total PG cost	0.6575824	0.6581953	0.6572583
Objective value	0.6575824	0.6581953	0.6572583
PF mismatch	0.9447E-6	0.3988E-4	0.5734E-7
Iteration no.	7	12	9
CPU time (s)	147.0	267.4	567.9

can be observed that the proposed IQIP method has the fastest convergence speed, followed by the EQIP method. The MINOS method has the slowest convergence speed.

8.5.3.3.2 Sample Set of Results with IQIP/EQIP/MINOS Options (VAR optimal placement as objective function)   The test case given here is for the 14-bus system for OPF with VAR optimal placement as objective function (i.e., objective 2 in OPF model, Section 8.5.2). The initial voltages on load buses are shown in Table 8.13. The optimization results and comparisons for the IQIP/EQIP/MINOS methods are listed in Table 8.14.

Table 8.13   Initial voltages on load bus for 14-bus system (p.u.)

Bus No.	Initial V	V_{min}	V_{max}
3	0.94410	0.95000	1.05000
5	0.99220	0.95000	1.05000
7	0.94250	0.95000	1.05000
8	0.93270	0.95000	1.05000
9	0.93330	0.95000	1.05000
10	0.93910	0.95000	1.05000
13	0.98720	0.95000	1.05000
14	0.93530	0.95000	1.05000

Table 8.14   Optimization results and comparison for objective 2 (p.u.)

Control Option	IQIP	EQIP	MINOS
VG1	1.05000	1.05000	1.05000
VG2	1.05000	1.05000	1.04248
VG6	1.05000	1.05000	1.04430
T4-7	0.97001	0.97000	0.97000
T4-9	0.96001	0.96001	0.96000
T5-6	1.03000	1.03000	0.93000
VD3	0.98340	0.98340	0.97610
VD5	1.02600	1.02600	1.02030
VD7	1.00200	1.00200	0.99530
VD8	0.99270	0.99280	0.98600
VD9	0.98970	0.98970	0.98300
VD10	0.99130	0.99130	0.98470
VD13	1.02180	1.02180	1.01580
VD14	0.98320	0.98320	0.97670
Power loss	0.110866	0.110868	0.110459
Objective value	0.110866	0.110868	0.110459
PF mismatch	0.1596E-6	0.4634E-8	0.4225E-6
Iteration no.	4	4	8
CPU time (s)	115.9	150.4	184.4

Table 8.15   Optimization results and comparison for loss minimization (p.u.)

Control Option	IQIP	EQIP	MINOS
VG1	1.05000	1.05000	1.05000
VG2	1.05000	1.05000	1.02837
VG6	1.05000	1.05000	1.03330
T4-7	0.97001	0.97001	0.97000
T4-9	0.96001	0.96001	0.96000
T5-6	1.03000	1.02999	1.03000
VD5	1.02600	1.02600	1.00930
VD9	0.98970	0.98970	0.97040
VD13	1.02180	1.02180	1.00430
Initial loss	0.1164598	0.1164598	0.1164598
Final loss	0.1108663	0.1108664	0.1118670
Objective value	0.1108663	0.1108664	0.1118670
PF mismatch	0.4132E-6	0.4634E-8	0.4339E-6
Iteration no.	3	3	8
CPU time (s)	22.2	27.0	70.7

It is observed from Table 8.14 that IQIP and EQIP have almost the same optimization results, which are better than those obtained from the MINOS method. The comparison of the results shows that three methods alleviate the voltage violations satisfactorily. The convergence speed of the IQIP method ranks first, followed by the EQIP method. The MINOS method ranks last.

8.5.3.3.3   Sample Set of Results with IQIP/EQIP/MINOS Options (loss minimization as objective function)   The test case given here is for the 14-bus system for OPF with loss minimization as objective function (i.e., objective 3 in OPF model, Section 8.5.2). The optimization results and comparison for loss minimization with IQIP/EQIP/MINOS methods are listed in Table 8.15.

From Table 8.15, IQIP and EQIP have almost the same optimization results for loss minimization objective. In view of loss reduction, load voltage modification, and convergence speed, both IQIP and EQIP methods appear superior to the MINOS method. Similarly, the IQIP method has the fastest convergence speed for loss minimization.

8.6   OPF WITH PHASE SHIFTER

The problem of power system security has obtained much attention in the deregulated power industry. To meet the load demand in a power system and satisfy the stability and reliability criteria, either the existing transmission lines must be utilized more efficiently or new line(s) should be added to the system. The latter is often impractical. The reason is that building a new power transmission line is in many countries a very time-consuming process and some-
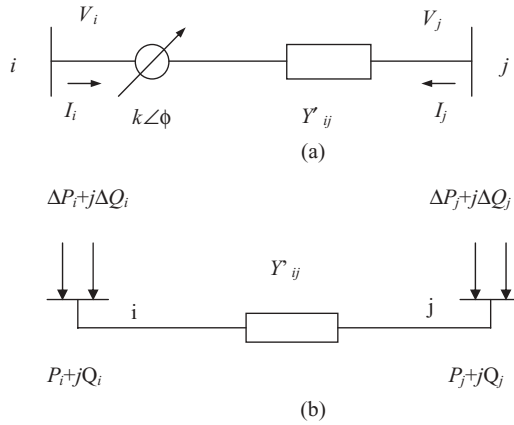
FIGURE 8.2 Phase shifter model

times an impossible task, because of environmental problems. Therefore, the first alternative provides an economically and technically attractive solution to power system security problem by use of some efficient controls, such as controllable series capacitors, phase shifters, and load shedding, etc. This chapter introduces power system security enhancement through optimal power flow with phase shifter. The objective functions of OPF include minimum line overloads and minimum adjustment of numbers of phase shifters. It is noted that general OPF calculations are hourly based and the control variables of OPF are continuous. However, the calculations of phase shifter are daily based. The control variables associated with the phase shifter transformers are discrete. To solve this problem, a rule-based OPF with a phase shifter scheme can be adopted for practical system operation [25].

8.6.1 Phase Shifter Model

A phase shifter model can be represented by an equivalent circuit, which is shown in Figure 8.2(a). It consists of an admittance in series with an ideal transformer having a complex turns ratio $k \angle \phi$.

The mathematical model of the phase shifter can be derived from Figure 8.2(a), i.e.,

$$\begin{bmatrix} \tilde{I}_i \\ \tilde{I}_j \end{bmatrix} = \begin{bmatrix} Y'_{ij} + Y_i & -Y'_{ij} \\ -Y'_{ij} & Y'_{ij} + Y_j \end{bmatrix} \begin{bmatrix} \tilde{V}_i \\ \tilde{V}_j \end{bmatrix} \tag{8.160}$$

where

$$Y_i = Y'_{ij} \left[\frac{1}{k^2} - 1 + \left(1 - \frac{1}{K \angle (-\phi)} \right) \frac{V_j}{V_i} \right] \tag{8.161}$$

$$Y_j = Y'_{ij}\left[\left(1 - \frac{1}{k\angle\phi}\right)\frac{V_i}{V_j}\right] \tag{8.162}$$

It can be known from equation (8.160) that the mathematical model of the phase shifter makes the Y bus unsymmetrical. To make the Y bus symmetrical, the phase shifter can be simulated by installing the additional injections at the buses. The additional injections can be simplified as follows.

$$\Delta P_i = |V_i||V_j|B'_{ij}\cos(\theta_i - \theta_j)\sin\phi_{ij}$$
$$\Delta P_j = -|V_i||V_j|B'_{ij}\cos(\theta_i - \theta_j)\sin\phi_{ij}$$
$$\Delta Q_i = |V_i||V_j|B'_{ij}\sin(\theta_i - \theta_j)\sin\phi_{ij}$$
$$\Delta Q_j = |V_i||V_j|B'_{ij}\sin(\theta_i - \theta_j)\sin\phi_{ij}$$

where

I_i, P_i: Current and real power flow at bus i

I_j, P_j: Current and real power flow at bus j

Q_i: Reactive power at bus i

Q_j: Reactive power at bus j

$V_i \angle \theta_i$: Complex voltage at bus i

$V_j \angle \theta_j$: Complex voltage at bus j

$k \angle \phi$: Complex turn ratio of the phase shifter

$Y'_{ij} = G'_{ij} + jB'_{ij}$: Series admittance of line ij

Therefore, the phase shifter model can be simulated by increasing the injections at the terminal buses as shown in Figure 8.2(b).

8.6.2   Rule-Based OPF with Phase Shifter Scheme

8.6.2.1   OPF Formulation with Phase Shifter

8.6.2.1.1 Objective Functions   Because of the installation of the phase shifter, the system will have lots of benefits such as overload release, system loss reduction, generation cost reduction, and generation adjustment reduction. All these benefits may be selected as objective functions for OPF with phase shifter. However, the primary purpose of installing the phase shifter is to remove the line overload. Thus the minimal line overload is selected as the primary objective function. In addition, since the adjustment numbers of the phase shifter are limited in the practical system, the minimal adjustment number of phase shifters is also selected as the objective function. Two objective functions are given as follows.

(1) Minimal line overloads

$$\text{Min } F_\text{O} = \sum_{ij=1}^{NB} \left(P_{ij}(t) - P_{ij\text{max}} \right)^2 \tag{8.163}$$

where

F_o: The overload objective function
$P_{ij}(t)$: The overload flow on transmission line ij at time stage t
$P_{ij\text{max}}$: The transmission limit of line ij
NB: The set of overload lines

(2) Minimal adjustment number of phase shifters

$$\text{Min } F_\phi = \sum_{i=1}^{NS} W_i \phi_i \tag{8.164}$$

where

F_ϕ: The phase shifter adjustment objective function
ϕ_i: The angle of phase shifter transformer
W_i: The priority coefficient of phase shifter transformers
NS: The set of phase shifter transformers
NG: The set of generators

8.6.2.1.2 Constraints   In addition to the general linear/nonlinear constraints, the constraints relating to phase shifter variables such as phase shifter angle and maximal adjustment numbers should be included in the OPF formulation with phase shifter. The candidate constraints are as follows:

Constraint 1: Real power flow equation
Constraint 2: Reactive power flow equation
Constraint 3: Upper and lower limits of real power output of the generators
Constraint 4: Upper and lower limits of reactive power output of the generators
Constraint 5: Upper and lower limits of node voltages
Constraint 6: Available transfer capacity of the transmission lines
Constraint 7: Upper and lower limits of transformer taps
Constraint 8: Upper and lower limits of phase shifter taps
Constraint 9: Maximal adjustment times of phase shifters per day

It is noted that constraints 8 and 9 are the phase shifter constraints that were used in the rule-based search technique, and the limits of all control and state variables are determined for the specific system under study.

The above-mentioned OPF model with phase shifter is a nonlinear mathematical programming problem. It can be reduced by an elimination procedure and solved by improved quadratic interior point method, which was introduced in the previous section.

8.6.2.2   Rule-Based Scheme   To determine the best location for installing the phase shifter, sensitivity analysis is adopted. The formulation of sensitivity analysis of objective function with respect to phase shifter variable can be expressed as follows:

$$S_{F-\phi} = \frac{\partial F_o}{\partial \phi_i} = \frac{F_o(0) - F_o(\phi_i)}{|\Delta\phi_i|} \tag{8.165}$$

where

$F_o(0)$: The total line overload before phase shifter i is installed

$F_o(\phi_i)$: The total line overload after phase shifter i is installed

In equation (8.165), the value of sensitivity $S_{F-\phi}$ will be greater than zero if a power violation is reduced by the use of a phase shifter, i.e., $F_o((\phi_i) < F_o(0)$. Obviously, if phase shifter i is not helpful in alleviating line overload $F_o(\phi_i) \geq F_o(0)$. In this case, we define the value of the sensitivity $S_{F-\phi} = 0$.

In the rule-based system, the following rules are defined.

Rule 1: If the system operates in the normal state without load change, then none of the existing phase shifters will change tap.

Rule 2: If the system load increases, or the system operates in contingency state, then judge:
If no line overload appeared, then none of the existing phase shifters will change tap.
If line overload occurred in system, then go to rule 3 to adjust the tap of some phase shifters.

Rule 3: If the phase shifter leads to maximal overload reduce at time stage t, then this phase shifter will be recommended at this time.

Rule 4: If phase shifters i and j lead to same overload reduce at time stage t, then check the other benefits:
If phase shifter i makes less generation cost benefit than phase shifter j, then phase shifter j will be recommended at this time.
If phase shifter i makes less system loss benefit than phase shifter j, then phase shifter j will be recommended at this time.

Rule 5: Phase shifter I is recommended and the line overloads are still exist, then the next priority phase shifter in the rank will be joined to remove the violations until there is no more available phase shifter.

Rule 6: If OPF suggests a solution, and RBS confirms that phase shifter constraints are met, then the problem at this time stage is solved.

Rule 7: If RBS checks OPF solution and OPF solution violates phase shifter constraints, then freeze the corresponding tap of phase shifter.

Rule 8: If RBS checks state of phase shifters and phase shifter k has a frozen tap, then phase shifter k will be out of service in the subsequent time stages.

A phase shifter tap will be frozen when the tap number of the phase shifter at the time reaches its maximum. The IQIP algorithm then uses that which was fixed or scheduled by the rule-based engine. The solution steps of the integrated algorithm for OPF with phase shifter are as follows.

Step 1: Assume several contingencies.

Step 2: OPF calculation without phase shifter for each given contingency from time stage t ($t = 1$, first time stage).

Step 3: Judge whether OPF is solvable. If the answer is "Yes," there is no need to use phase shifter. If "No," go to step 4.

Step 4: Contingency analysis through power flow calculation. Check the overload state of lines.

Step 5: Conduct sensitivity analysis for obtaining a list of phase shifter ranking according to the amount of releasing the line overload for each phase shifter. Then decide the corresponding weighting factor.

Step 6: OPF calculation with the available phase shifter.

Step 7: Use the rule-based method to check the operation limitation of the phase shifter. Calculate the operation times, $NM\phi_i = NM\phi_i + 1$, if phase shifter i is operated in this time stage.

Step 8: If $NM\alpha_i(t) = NM\phi_{i\max}$, freeze the corresponding taps of the phase shifter. That is, this phase shifter will be out of service in subsequent times.

Step 9: Check time stages. If $t = t_{\max}$ (e.g., 24 h), stop. Otherwise, $t = t + 1$, go to step 2.

Finally, in the search technique, the phase shifters are adjusted sequentially and their direction of adjustments is governed by the impact on the primary objective function of minimal line overload. The engineering rules are such that the least number of phase shifters are adjusted at a time, provided that they have the greatest impact in reducing the line flow overloads. The phase shifter constraints, which are handled by the rule-based search technique, are adjusted to produce discrete settings and in turn pass on to the IQIP module of the algorithm.

Example 8.3

The integrated scheme of OPF with phase shifter is tested on the IEEE 30-bus system. The data and parameters of the 30-bus system are the same

as in the previous section, and the limits of the installed phase shifters were taken as $\pm 10^0$ [25].

The total system load of the IEEE 30-bus system is 283.4 MW. The corresponding load scaling factor (LSF) is 1.0. The daily load demands of the IEEE 30-bus system are shown in Table 8.16. To determine the degree of line violations at the line L_{i-j}, the following performance index is defined [25]:

$$PI_{ij} = \frac{P_{ij} - P_{ij\,max}}{P_{ij\,max}}, \quad ij \in NOL \tag{8.166}$$

where

> PI_{ij}: The performance index of line overloads
> P_{ij}: The overload flow on transmission line
> NOL: The set of overloaded lines

Through power flow analysis for each time stage, line overloads only appeared at hours 8, 15, 16, 17, 18, and 19, which are peak load periods. The violation amounts of line flow for each time stage are summarized in Table 8.17.

The line overloads will become more serious if system contingency scenarios are considered. Therefore, OPF with phase shifter adjustment should be employed for enhancing power system security.

For the purpose of simulation, the following line contingency scenarios are given, that is, L_{12-14}, L_{10-21}, L_{22-25}, L_{24-27}, and L_{29-30}.

Table 8.18 is the summary of contingency analysis, and the total power violations for all time stages are shown. It can be observed from Table 8.18 that the line L_{10-21} outage is the most serious contingency case, where the total line violation is 107.26 MW.

Table 8.19 gives the details of contingency calculation under the peak load (at hour 18). The calculation results show that although the contingency ranks

Table 8.16   Daily load curve for IEEE 30-bus system

Time (hour)	Load (LSF)	Time Stage	Load (LSF)	Time Stage	Load (LSF)
1	0.90	9	1.30	17	1.50
2	0.96	10	1.15	18	1.55
3	1.00	11	1.10	19	1.40
4	1.05	12	1.05	20	1.20
5	1.10	13	1.16	21	1.12
6	1.15	14	1.30	22	1.03
7	1.30	15	1.40	23	0.96
8	1.40	16	1.45	24	0.90

Table 8.17 Total power flow violation without contingency

Time (hour)	Overload (MW)	Time (hour)	Overload (MW)	Time (hour)	Overload (MW)
1–7	0.00	15	5.12	18	13.08
8	5.12	16	6.78	19	5.12
9–14	0.00	17	9.62	20–24	0.00

Table 8.18 Summary of contingency analysis

Outage line	L_{12-14}	L_{10-21}	L_{22-25}	L_{24-27}	L_{29-30}
Overloaded lines	L_{1-2} L_{6-8} L_{9-10} L_{9-11}	L_{1-2} L_{6-8} L_{9-11} L_{10-20}	L_{1-2} L_{6-8} L_{9-11} L_{10-20}	L_{1-2} L_{6-8} L_{9-10} L_{9-11} L_{10-21}	L_{1-2} L_{6-8} L_{9-10} L_{9-11} L_{27-30}
Overloaded time stage	T8, T15–T19	T7–9, T14–T20	T8, T15–T19	T8, T15–T19	T8, T15–T19
Total line MW violation	50.68	102.76	52.73	57.18	50.53

Table 8.19 Contingency analysis results at peak load time stage 18

Outage Line	Overload Line (MW)	Line Flow Limit (MW)	Overload Index (PI)	Power Violation	Contingency Ranking
L_{12-14}	L_{1-2}	130	0.144	33.63	4
	L_{6-8}	55	0.167		
	L_{9-10}	65	0.042		
	L_{9-11}	65	0.046		
L_{10-21}	L_{1-2}	130	0.144	43.38	1
	L_{6-8}	55	0.176		
	L_{9-11}	65	0.034		
	L_{10-20}	32	0.390		
L_{22-25}	L_{1-2}	130	0.144	31.665	5
	L_{6-8}	55	0.187		
	L_{9-11}	65	0.021		
	L_{10-20}	16	0.096		
L_{24-27}	L_{1-2}	130	0.139	38.53	2
	L_{6-8}	55	0.135		
	L_{9-10}	65	0.045		
	L_{9-11}	65	0.063		
	L_{10-21}	32	0.188		
L_{29-30}	L_{1-2}	130	0.144	33.86	3
	L_{6-8}	55	0.167		
	L_{9-10}	65	0.037		
	L_{9-11}	65	0.027		
	L_{27-30}	19	0.108		

Table 8.20   Ranking of phase shifter locations based on sensitivity analysis (LSF = 1.55, outage line L_{10-21})

Phase Shifter Location (L_{ij})	Phase Shifter Angle (deg.)	Over-Loaded Lines (L_{ij})	Line Flow Limit (MW)	Performance Indices (PI_{ij})	Sensitivity Values S_{ij} (MW/deg.)	Phase Shifter Ranking (Rk_{ij})
L_{1-3}	+5	L_{6-8}	55	0.172	1.87	7
		L_{9-11}	65	0.026		
		L_{10-22}	32	0.382		
L_{6-8}	+1	L_{1-2}	130	0.145	2.30	5
		L_{9-11}	65	0.033		
		L_{10-22}	32	0.383		
L_{15-18}	−3	L_{6-8}	55	0.147	4.45	3
		L_{9-11}	65	0.007		
		L_{10-22}	32	0.257		
L_{2-4}	+1	L_{1-2}	130	0.125	1.99	6
		L_{6-8}	55	0.178		
		L_{9-11}	65	0.039		
		L_{10-22}	32	0.393		
L_{10-22}	+1	L_{6-8}	55	0.160	15.5	1
		L_{9-11}	65	0.009		
		L_{10-20}	16	0.055		
		L_{10-21}	32	0.094		
L_{2-6}	+3	L_{6-8}	55	0.169	3.15	4
		L_{9-11}	65	0.019		
		L_{10-22}	32	0.383		
L_{24-25}	+3	L_{9-11}	65	0.003	7.87	2
		L_{24-27}	32	0.040		

for different time stages are not totally the same, the selected worst contingency case is the same, i.e., the line L_{10-21} outage. The worst scenario for this example is that the line L_{10-21} outage happens under the peak load (at hour 18).

To determine the priority of phase shifters, the sensitivity analysis of phase shifters is conducted under the peak load and the worst contingency case. Simulation results show that system security will be greatly enhanced if the phase shifter is installed at locations L_{1-3}, L_{2-4}, L_{2-6}, L_{6-8}, L_{10-22}, L_{15-18}, L_{24-25}, respectively.

For the specified worst contingency, it can be seen from Table 8.20 that the best three locations for installing phase shifter are L_{10-22}, L_{15-18}, L_{24-25}.

Table 8.21 lists the results of phase shifter adjustments during the operation period (24h) based on optimal power flow. Simulation results show that all the line overloads are removed because of the use of the phase shifters.

Table 8.21 Results of phase shifter adjustments

Time (hour)	Phase Shifter Site (located at line L_{ij})	Phase shifter angle (degree)	Overload (MW)
1–6	None	/	/
7	L_{10-22}	+1	0.00
8	L_{10-22}	+1	0.00
9	L_{10-22}	+1	0.00
10–13	None	/	/
14	L_{10-22}	+1	0.00
15	L_{10-22}	+1	0.00
16	L_{10-22}	+1	0.00
17	L_{24-25}	+1	0.00
18	L_{10-22}	+1	0.00
	L_{24-25}	+1	0.00
	L_{15-18}	−2	0.00
19	L_{10-22}	+1	0.00
20	L_{10-22}	+1	0.00
21–24	None	None	/

8.7 MULTIPLE-OBJECTIVES OPF

The optimal power flow problem may have all kinds of objectives, which create the complication in the implementation since these objectives do not have a consistent goal to produce the optimum solution. This section introduces the OPF problem that is a fully coupled active and reactive dispatch or a combined active and reactive dispatch (CARD). The purpose of this OPF is to achieve the overall objective of minimum generation cost and to improve the distribution of reactive power and voltage, subject to constraints that ensure system security. Security is defined as the maintenance of individual circuit flows, generator real and reactive power output, and system voltages within limits under normal system conditions and contingency cases. Five different objective functions are considered [11]. They are minimization of generator fuel cost, maximization of reactive power reserve margins, voltage maximization, avoidance of voltage collapse, and improvement in the ability of the system to maintain a higher system load level. The analytic hierarchical process (AHP) is sued to handle these objectives during the implementation of combined active and reactive dispatch (CARD).

8.7.1 Formulation of Combined Active and Reactive Dispatch

8.7.1.1 Objective Functions Five objective functions that are used in combined active and reactive dispatch (CARD) are as follows [11, 12].

8.7.1.1.1 Minimization of Generator Fuel Costs   Generally, the generator fuel cost can be expressed as a quadratic function:

$$F_1 = \sum_{j \in NSTEP} \sum_{i \in NG} \left(a_i P_{ij}^2 + b_i P_{ij} + c_i \right) \tau_j \tag{8.167}$$

where

NG: The number of generators
NSTEP: The number of time steps
τ_j: The approximate integration coefficients

Linearizing equation (8.167), we get

$$\Delta F_1 = \sum_{j \in NSTEP} \sum_{i \in NG} \left(2a_i P_{ij} + b_i \right) \Delta P_{ij} \tau_j \tag{8.168}$$

If the generator fuel costs are modeled by linear functions relating monetary units to energy supplied, the following expression can be used:

$$\Delta F_1 = \sum_{j \in NSTEP} \sum_{i \in NG} \left(c_i \Delta P_{ij} \right) \tau_j \tag{8.169}$$

where

$$
\begin{aligned}
\tau_1 &= 0.5 T_1 \\
\tau_2 &= 0.5 (T_1 + T_2) \\
&\dots \\
\tau_{NSTEP} &= 0.5 T_{\text{NSTEP}}, \text{ and} \\
T_j &= \text{duration of time stage } j
\end{aligned}
$$

The time factors τ_j correspond to the integration of the fuel costs over the operation period by means of the trapezoidal rule.

8.7.1.1.2 Maximization of Reactive Power Reserve Margins   This objective aims to maximize the reactive power reserve margins and seeks to distribute the reserve among the generators and SVCs in proportion to ratings. It can be expressed as

$$F_2 = \sum_{j \in NSTEP} \sum_{i \in NG} \left(\frac{Q_{ij}^2}{Q_{i\max}} \right) \tag{8.170}$$

Linearizing the above equation, we get

$$\Delta F_2 = 2 \sum_{j \in NSTEP} \sum_{i \in NG} \left(\frac{Q_{ij}^0 \Delta Q_{ij}}{Q_{i\max}} \right) \tag{8.171}$$

8.7.1.1.3 Maximization of Load Voltage This objective aims to optimize the voltage profile by maximizing the sum of the load voltage.

$$\Delta F_3 = \sum_{j \in NSTEP} \sum_{i \in ND} \Delta V_{ij} \tag{8.172}$$

where ND is the number of loads.

8.7.1.1.4 Avoidance of Voltage Collapse This objective aims to optimize the voltage profile by maximizing the voltage collapse proximity indicator for the whole system. It can be expressed as

$$\Delta F_4 = \sum_{j \in NSTEP} \sum_{k \in NCTG} \Delta \lambda_{kj} \tag{8.173}$$

where λ_{kj} is a scalar (to be maximized) less than any bus voltage collapse proximity indicator at time stage j, contingency k ($k = 0$, refer to base case).

8.7.1.1.5 Ability to Maintain Higher System Load Level This objective aims to allow the generators to respond efficiently to system load changes by optimizing the ability of the system to maintain a higher system load level, while constraining generators within their reactive limits. It can be expressed as.

$$\Delta F_5 = \sum_{j \in NSTEP} \sum_{k \in NCTG} \Delta \alpha_{kj} \tag{8.174}$$

where α_{kj} is a system load increment (to be maximized) at time stage j, contingency k.

The objective function of CARD can be written as

$$\Delta F = w_1 \Delta F_1 + w_2 \Delta F_2 + w_3 \Delta F_3 + w_4 \Delta F_4 + w_5 \Delta F_5 \tag{8.175}$$

where w_i is the weighting coefficient of the ith objective function. The calculation of w_i is discussed later.

8.7.1.2 Constraints At each time step, the following constraints are taken into account:

(a) Active Power Constraints

- The active power balance equation
- The generator active power upper and lower limits
- The generator active power reserve upper and lower limits group import and export constraints
- The active power-reserve relationship constraints

- The system active power reserve constraint
- The line active power flow upper and lower limits.

(b) Reactive Power Constraints

- The reactive power balance equation
- The generator reactive power upper and lower limits network voltage limits
- The transformer tap changer ranges
- Q- V characteristics of SVCs
- The additional constraints aimed at avoiding voltage collapse
- The additional constraints aimed at improving the ability of the system to maintain higher system load.

(c) Constraints That Are a Combined Function of Active and Reactive Power

- The generator capability chart limits (other than simple MW or MVAr limits)
- The branch current flow limits, modeled at midpoint of the branch.
- The additional constraints aimed at improving the ability of the system to maintain higher system load taking into account generator capability chart limits.

Some of the constraints are straightforward constraints (constraints regarding system variables) and others are functional constraints that are stated as follows.

8.7.1.2.1 Group Limits Station limits and approximate network security limits may be expressed by a number of group import and export constraints:

$$\left(\sum_i P_{ij}\right) - P_{Djlocal} \leq P_{exp} \tag{8.176}$$

$$\left(\sum_i P_{ij}\right) - P_{Djlocal} \geq P_{imp} \tag{8.177}$$

Write the above equations in incremental form, that is,

$$\sum_i \Delta P_{ij} \leq P_{exp} - \sum_i P_{ij0} + P_{Djlocal} \tag{8.178}$$

$$\sum_i \Delta P_{ij} \geq P_{imp} - \sum_i P_{ij0} + P_{Djlocal} \tag{8.179}$$

where $P_{Djlocal}$ is the local load demand within the group at time stage j.

8.7.1.2.2 Spinning Reserve Constraints The reserve available from a generator may be modeled as a trapezoidal function of generation [11, 12]. The allocation of the corresponding independent variable ΔR_{ij} is then subject to

$$R_{i\min} - R_{ij0} \leq \Delta R_{ij} \leq R_{i\max} - R_{ij0} \tag{8.180}$$

$$\Delta R_{ij} + \Delta P_{ij} \leq P_{i\max} - P_{ij0} - R_{ij0} \tag{8.181}$$

$$\sum_{\text{gen}} \Delta R_{ij} \geq S_{\text{total}} - \sum_{\text{gen}} R_{ij0} \tag{8.182}$$

8.7.1.2.3 Operating Chart Limits for Generators The ability of generators to absorb reactive power is generally limited by the machine minimum excitation limit. A further limit is determined so as to provide an adequate margin of safety for the machine thermal limit. A simplified generator capability chart can be defined in which the leading and lagging limits of machine reactive output are expressed as a function of the real power output. Using a trapezoidal approximation, this can be represented as:

$$P_{ij} + \left(\frac{\beta_{i1}}{\alpha_{i1}}\right)Q_{ij} - \beta_{i1} \leq 0 \tag{8.183}$$

$$P_{ij} + \left(\frac{\beta_{i2}}{\alpha_{i2}}\right)Q_{ij} - \beta_{i2} \leq 0 \tag{8.184}$$

Linearizing the above equations around the current operating point, we obtain

$$\Delta P_{ij} + \left(\frac{\beta_{i1}}{\alpha_{i1}}\right)\Delta Q_{ij} + P_{ij0} + \left(\frac{\beta_{i1}}{\alpha_{i1}}\right)Q_{ij0} - \beta_{i1} \leq 0 \tag{8.185a}$$

$$\Delta P_{ij} + \left(\frac{\beta_{i2}}{\alpha_{i2}}\right)\Delta Q_{ij} + P_{ij0} + \left(\frac{\beta_{i2}}{\alpha_{i2}}\right)Q_{ij0} - \beta_{i2} \leq 0 \tag{8.185b}$$

where α_{i1}, α_{i2} are the intersections with the Q-axis, and β_{i1}, β_{i2} are the intersection with the P-axis.

8.7.1.2.4 Maintaining Higher System Load Constraints Every generator i should contribute its share of reactive power output to meet a prospective increase in system demand in such a way that the generator output does not exceed its reactive limits

$$Q_{ij} + \left(\frac{\delta Q_{ij}}{\delta \alpha_j}\right)\alpha_j \leq Q_{ij\max} \tag{8.186}$$

When considering generators with active power control, the operating chart limits for the generators are taken into account.

Linearizing equation (8.186) around the current operating point, we obtain

$$\Delta Q_{ij} + \left(\frac{\delta Q_{ij}}{\delta \alpha_j}\right) \Delta \alpha_j \leq Q_{ij\,max} - Q_{ij0} - \left(\frac{\delta Q_{ij}}{\delta \alpha_j}\right) \alpha_{j0} \tag{8.187}$$

where $\dfrac{\delta Q_{ij}}{\delta \alpha_j}$ represents the change in the reactive power output of generator i as a fraction of the change in load demand at time stage j evaluated with a load flow algorithm. α_j represents the increase in system demand.

8.7.1.2.5 Avoidance of Voltage Collapse Constraints

For a network with n buses, Thevenin's equivalent impedance looking into the port between bus i and ground is $Z_{ii} \angle \theta_i$, which equals the ith diagonal element of $[Z] = [Y]^{-1}$. Therefore, for permissible power transfer to the load at bus i we must have $Z_i/Z_{ii} > 1$, where $Z_i \angle \gamma_i$ is the impedance for load $i (Z_i = V_i^2 \cos\gamma_i / P_i)$.

The idea is to constrain the voltage collapse proximity indicators at the load nodes in order to maintain an acceptable system voltage profile. This has been done by finding a parameter greater than 1, at each time interval, such that the voltage collapse proximity indicators at the load nodes specified by the user are greater than this parameter. These parameters λ_j form part of the objective function. The corresponding constraints can be written as:

$$Z_i / Z_{ii} \geq \lambda^2 \tag{8.188}$$

$$V_i \geq \lambda \sqrt{Z_{ii} P_i / \cos\gamma_i} \tag{8.189}$$

Linearizing equation (8.189) around the current operating point, we obtain

$$\Delta V_{ij} - \Delta\lambda_j \sqrt{Z_{ii} P_i / \cos\gamma_i} \geq -V_{ij0} + \Delta\lambda_{j0}\sqrt{Z_{ii} P_i / \cos\gamma_i} \tag{8.190}$$

8.7.1.2.6 Static VAR Compensators

SVCs are high-speed variable reactive power sources and sinks connected to the system. Their electrical characteristic is such that MVAR output (or absorption) is related to voltage in a linear manner; normally for a small change in voltage the compensator will go from zero to full output. This is known as the slope. Thus the constraint of SVCs can be modeled as:

$$V_{ij\,min} \leq V_{ij} - a_i Q_{ij} \leq V_{ij\,max} \tag{8.191}$$

$$Q_{ij\,min} \leq Q_{ij} \leq Q_{ij\,max} \tag{8.192}$$

The linearized incremental model is

$$V_{ij\min} - V_{ij0} + a_i Q_{ij0} \leq \Delta V_{ij} - a_i \Delta Q_{ij} \leq V_{ij\max} - V_{ij0} + a_i Q_{ij0} \qquad (8.193)$$

where a_i is the slope.

8.7.1.2.7 Dynamic Constraints In the dynamic dispatch case additional generation rate limit constraints can be considered:

$$-P_{\mathrm{rd}i} T_j \leq P_{ij} - P_{i(j-1)} \leq P_{\mathrm{ru}i} T_j \qquad (8.194)$$

The linearized incremental form of the above equation is

$$-P_{\mathrm{rd}i} T_j \leq P_{ij0} + \Delta P_{ij} - P_{i(j-1)0} + \Delta P_{i(j-1)} \leq P_{\mathrm{ru}i} T_j \qquad (8.195)$$

where $P_{\mathrm{rd}i}$, $P_{\mathrm{ru}i}$ are the vector limits for decreasing and increasing output, respectively, and T_j is the length of the time step.

For every contingency at every time step, the constraints regarding the slack bus will be included in addition to the constraints for the normal case.

8.7.2 Solution Algorithm

8.7.2.1 AHP Model of CARD Obviously, the mathematical model of combined active and reactive dispatch mentioned in Section 8.7.1 is a linear model based on multiobjective functions. It is not appropriate to use an equal weighting coefficient for the various kinds of objectives in (8.175) because the importance of these objectives is different in a practical power system. Therefore, the weighting coefficients of the various objective functions in the CARD model must be determined before CARD can be executed. However, it is very difficult to decide precisely the weighting coefficient of each objective in the CARD model unless only one or two objectives are considered. There are two reasons for this. One is that the objectives are interrelated and interact with each other. The other is that the relative importance of these objectives is not the same, not only for different power systems but also within the same power system in different circumstances. An analytic hierarchical process was recommended to solve this challenging problem [11].

The principle and method of the analytic hierarchy process (AHP) are introduced in Chapter 7. AHP transforms the complex problem into rank calculation within the hierarchy structure. In the ranking computation, the ranking in each hierarchy can also be converted into the judgment and comparison of a series of pairs of factors. The judgment matrix can be formed according to the quantified judgment of pairs of factors by some ratio scale method. Consequently, the value of the weighting coefficients of all factors can be obtained through calculating the maximal eigenvalue and the corresponding eigenvector of the judgment matrix. The judgment matrix A of the CARD hierarchy model can be written as follows:

$$
A = \begin{bmatrix}
1 & \dfrac{W_1}{W_2} & \dfrac{W_1}{W_3} & \dfrac{W_1}{W_4} & \dfrac{W_1}{W_5} \\[2mm]
\dfrac{W_2}{W_1} & 1 & \dfrac{W_2}{W_3} & \dfrac{W_2}{W_4} & \dfrac{W_2}{W_5} \\[2mm]
\dfrac{W_3}{W_1} & \dfrac{W_3}{W_2} & 1 & \dfrac{W_3}{W_4} & \dfrac{W_3}{W_5} \\[2mm]
\dfrac{W_4}{W_1} & \dfrac{W_4}{W_2} & \dfrac{W_4}{W_3} & 1 & \dfrac{W_4}{W_5} \\[2mm]
\dfrac{W_5}{W_1} & \dfrac{W_5}{W_2} & \dfrac{W_5}{W_3} & \dfrac{W_5}{W_4} & 1
\end{bmatrix}
\tag{8.196}
$$

where W_i is the weighting coefficient of the ith subobjective in the hierarchy model of CARD.

The AHP algorithm and the selection of the judgment matrix can be found in Chapter 7.

8.7.2.2 Solution Algorithm The solution algorithm adopted for the AHP-based combined active and reactive dispatch may be described as follows:

(a) Either perform a merit order dispatch or use an existing active power generation pattern provided by the user to satisfy active power demand. The same active generation pattern applies for contingency cases.

(b) Perform a Newton–Raphson power flow for normal and defined contingency cases at every time step. If power flow analysis only is requested, then stop; otherwise proceed to step (c).

(c) For every contingency case, at every time step, include a new set of variables and constraints relating that case to the variables and constraints of the intact case.

(d) Set up a hierarchy model for CARD.

(e) Form a judgment matrix according to the experiences and needs of the user.

(f) Perform the AHP calculation to obtain the optimum weighting coefficients of the various objective functions.

(g) Linearize the objective function and constraints around the operating point.

(h) Execute the LP algorithm (sparse dual revised simplex method with relaxation) to obtain the optimum state of the linearized system.

(i) Apply constraint limit squeezing automatically, or as necessary depending on the option to be selected.

(j) Iterate between LP and power flow until the system converges.

The AHP-based CARD algorithm is designed to satisfy the following convergence criteria simultaneously:

- The consistency of the weighting coefficients is satisfactory.
- No violation of constraint limit occurs.
- Changes in control variables over two consecutive iterations are within specified tolerances.
- Changes in objective function value over two consecutive iterations are within specified tolerance.

8.8 PARTICLE SWARM OPTIMIZATION FOR OPF

As we discussed above, various traditional optimization techniques were developed to solve the OPF problem. Some of these techniques have excellent convergence characteristics, and some are widely used in the industry. It is noted that each technique may be tailored to suit a specific OPF optimization problem based on the mathematical nature of the objectives and/or constraints. In addition, some of these techniques might converge to local solutions instead of global ones if the initial guess happens to be in the neighborhood of a local solution. This occurs as a result of using Kuhn–Tucker conditions as termination criteria to detect stationary points. This practice is commonly used in most commercial nonlinear optimization programs [70].

In recent years, a new optimization method, particle swarm optimization (PSO), has been applied to solve the OPF problem [59–64]. This section introduces several major PSO methods that are used in OPF.

8.8.1 Mathematical Model

Generally, the following OPF model is used in various particle swarm optimization approaches. The objective function may be one of the following

(1) Fuel cost minimization

$$\text{Min } F_g = \sum_{i=1}^{NG} \left(a_i P_{gi}^2 + b_i P_{gi} + c_i \right) \tag{8.197}$$

(2) Fuel emission minimization

$$\text{Min } E_g = \sum_{i=1}^{NG} \left(a_i P_{gi}^2 + \beta_i P_{gi} + \gamma_i \right) \tag{8.198}$$

(3) Loss minimization

$$\text{Min } P_L = \sum_{i=1}^{NL} P_l \tag{8.199}$$

(4) Voltage deviation minimization at load buses

$$\text{Min } VD = \sum_{i=1}^{ND} \left(V_i - V_i^{\text{sp}}\right)^2 \qquad (8.200)$$

where

V_i^{sp}: The pre-specified reference value at load bus i
P_{gi}: The real power generation at generator i
P_L: System real power loss
P_l: Real power loss on line l
P_{gslack}: The real power of slack generator
a_i, b_i, c_i: The coefficients of generator fuel cost
α_i, β_i, γ_i: The coefficients of generator emission function
VD: The total voltage deviation at load buses
NG: The number of generating units
ND: The number of load buses
NL: The number of lines

The constraints are as follows.

$$P_{gi} - P_{di} - f_{Pi}(V, \theta, T) = 0 \qquad (8.201)$$

$$Q_{gi} - Q_{di} - f_{Qi}(V, \theta, T) = 0 \qquad (8.202)$$

$$P_{gi\min} \le P_{gi} \le P_{gi\max}, \quad i \in NG \qquad (8.203)$$

$$Q_{gi\min} \le Q_{gi} \le Q_{gi\max}, \quad i \in NG \qquad (8.204)$$

$$Q_{ci\min} \le Q_{ci} \le Q_{ci\max}, \quad i \in NC \qquad (8.205)$$

$$V_{gi\min} \le V_{gi} \le V_{gi\max}, \quad i \in NG \qquad (8.206)$$

$$V_{di\min} \le V_{di} \le V_{di\max}, \quad i \in ND \qquad (8.207)$$

$$T_{i\min} \le T_i \le T_{i\max}, \quad i \in NT \qquad (8.208)$$

$$S_{Lj} \le S_{Lj\max}, \quad j \in NL \qquad (8.209)$$

where

S_{Lj}: The transmission line loadings
$S_{lj\max}$: The limit of transmission line loadings
Q_{di}: Switchable VAR compensations at bus i
NC: The number of switchable VAR sources
V_{gi}: The voltage magnitude at generator bus i

The subscripts "min" and "max" stand for the lower and upper bounds of a constraint, respectively.

Several PSO methods can be used to solve the above-mentioned OPF problem, which are introduced in the next section.

8.8.2 PSO Methods

The PSO has been used to solve the unit commitment, which is introduced in Chapter 7. Here, we focus on applying PSO methods to solve OPF problem [59, 71–75].

8.8.2.1 *Conventional Particle Swarm Optimization*   In PSO algorithms, each particle moves with an adaptable velocity within the regions of decision space and retains a memory of the best position it ever encountered. The best position ever attained by each particle of the swarm is communicated to all other particles. The conventional PSO assumes an n-dimensional search space $S \subset R^n$, where n is the number of decision variables in the optimization problem, and a swarm consisting of N particles.

In PSO, a number of particles form a swarm that evolves or flies throughout the problem hyperspace to search for optimal or near-optimal solution. The coordinates of each particle represent a possible solution with two vectors associated with it, the position X and velocity V vectors. During their search, particles interact with each others in a certain way to optimize their search experience. There are different variants of the particle swarm paradigms, but the most general one is the P_{gb} model, where the whole population is considered as a single neighborhood throughout the optimization process. In each iteration, the particle with the best solution shares its position coordinates (P_{gb}) information with the rest of the swarm.

Thus the variables are defined as follows.

The position of the ith particle at time t is an n-dimensional vector denoted by

$$X_i(t) = (x_{i,1}, x_{i,2}, \ldots, x_{i,n}) \in S \tag{8.210}$$

The velocity of this particle at time t is also an n-dimensional vector denoted by

$$V_i(t) = (v_{i,1}, v_{i,2}, \ldots, v_{i,n}) \in S \tag{8.211}$$

The best previous position of the ith particle at time t is a point in S, which is denoted by

$$P_i = (p_{i,1}, p_{i,2}, \ldots, p_{i,n}) \in S \tag{8.212}$$

The global best position ever attained among all particles is a point in S, which is denoted by

$$P_{gb} = (p_{gb,1}, p_{gb,2}, \ldots, p_{gb,n}) \in S \tag{8.213}$$

Then, each particle updates its coordinates based on its own best search experience (P_i) and P_{gb} according to the following velocity and position update equations:

$$V_i^{t+1} = wV_i^t + C_1 \times r_1 \times (P_i - X_i^t) + C_2 \times r_2 \times (P_{gb} - X_i^t) \tag{8.214}$$

$$X_i^{t+1} = X_i^t + V_i^{t+1} \tag{8.215}$$

where

> w: Inertia weight
>
> C_1, C_2: Acceleration coefficients
>
> r_1, r_2: Two separately generated uniformly distributed random numbers in the range [0,1] added in the model to introduce stochastic nature.

The inertia weighting factor for the velocity of particle is defined by the inertial weight approach

$$w^t = w_{max} - \frac{w_{max} - w_{min}}{t_{max}} \times t \tag{8.216}$$

where t_{max} is the maximum number of iterations and t is the current number of iterations. w_{max} and w_{min} are the upper and lower limits of the inertia weighting factor, respectively.

Moreover, in order to guarantee the convergence of the PSO algorithm, the constriction factor k is defined as.

$$k = \frac{2}{\left|2 - \varphi - \sqrt{\varphi^2 - 4\varphi}\right|} \tag{8.217}$$

where $\varphi = C_1 + C_2$, $\varphi \geq 4$.

In this constriction factor approach (CFA), the basic system equations of the PSO, (8.214) and (8.215), can be considered as difference equations. Therefore, the system dynamics, namely, the search procedure, can be analyzed by the eigenvalue analysis and can be controlled so that the system behavior has the following features.

(1) The system converges.
(2) The system can search different regions efficiently.

In the CFA, the φ must be greater than 4.0 to guarantee stability. However, as φ increases, the factor k decreases and diversification is reduced, yielding

slower response. Therefore, we choose 4.1 as the smallest φ that guarantees stability but yields the fastest response. It has been observed that $4.1 \leq \varphi \leq 4.2$ leads to good solutions [59].

8.8.2.2 Passive Congregation-Based PSO

According to the local-neighborhood variant of the PSO algorithm (L-PSO) [75], each particle moves toward its best previous position and toward the best particle in its restricted neighborhood. As the local-neighborhood leader of a particle, its nearest particle (in terms of distance in the decision space) with the better evaluation is considered. Since the constriction factor approach generates higher-quality solutions in the basic PSO, some enhancements are presented. Specifically, Parrish and Hammer [76] have proposed mathematical models to show how these forces organize the swarms. These can be classified in two categories: the **aggregation** and the **congregation** forces.

Aggregation refers to the swarming of particles by nonsocial, external physical forces. There are two types of aggregation: passive aggregation and active aggregation. Passive aggregation is a swarming by physical forces, as the water currents in the open sea group the plankton [76].

Congregation, on the other hand, is a swarming by social forces, which is the source of attraction of a particle to others and is classified in two types: social and passive. Social congregation usually happens when the swarm's fidelity is high, such as genetic relation. Social congregation necessitates active information transfer, e.g., ants that have high genetic relation use antennal contacts to transfer information about location of resources.

According to references [59, 75, 76], passive congregation is an attraction of a particle to other swarm members, where there is no display of social behavior since particles need to monitor both environment and their immediate surroundings such as the position and the speed of neighbors. Such information transfer can be employed in the passive congregation. A hybrid L-PSO with passive congregation operator (PAC) is called LPAC PSO [59]. Moreover, the global variant-based passive congregation PSO (GPAC) can also be enhanced with the constriction factor approach.

The swarms of the enhanced GPAC and LPAC are manipulated by the following velocity update:

$$V_i^{t+1} = k\left[w^t V_i^t + C_1 \times r_1 \times (P_i - X_i^t) + C_2 \times r_2 \times (P_k - X_i^t) + C_3 \times r_3 \times (P_r - X_i^t)\right]$$

$$i = 1, 2, \ldots, N \tag{8.218}$$

where

C_1, C_2, C_3: The cognitive, social, and passive congregation parameters, respectively

P_i: The best previous position of the ith particle;

P_k: Either the global best position ever attained among all particles in the case of enhanced GPAC or the local best position of particle i, namely, the position of its nearest particle k with better evaluation in the case of LPAC

P_i: The position of passive congregator (position of a randomly chosen particle r)

The positions are updated with the same equation (8.215). The positions of the ith particle in the n-dimensional decision space are limited by the minimum and maximum positions expressed by vectors

$$X_{i\min} \le X_i \le X_{i\max} \tag{8.219}$$

The velocities of the ith particle in the n-dimensional decision space are limited by

$$V_{i\max} \le V_i \le V_{i\max} \tag{8.220}$$

where the maximum velocity in the mth dimension of the search space is computed as

$$V_{i\max}^m = \frac{s_{i\max}^m - s_{i\min}^m}{Nr}, \quad m = 1, 2, \dots, n \tag{8.221}$$

where $s_{i\max}^m$, *and* $s_{i\min}^m$ are the limits in the m-dimension of the search space. The maximum velocities are constricted in small intervals in the search space for better balance between exploration and exploitation. Nr is a chosen number of search intervals for the particles. It is an important parameter in the enhanced GPAC and LPAC PSO algorithms. A small Nr facilitates global exploration (searching new areas), while a large Nr tends to facilitate local exploration. A suitable value for the Nr usually provides balance between global and local exploration abilities and consequently results in a reduction of the number of iterations required to locate the optimum solution. The basic steps of the enhanced GPAC and LPAC are listed below [59].

Step (1) Generate a swarm of N particles with uniform probability distribution, initial positions $X_i(0)$, and velocities $V_i(0)$, ($i = 1,2, \dots, N$), and initialize the random parameters. Evaluate each particle i, using objective function f (e.g., to be minimized).

Step (2) For each particle i, calculate the distance d_{ij} between its position and the position of all other particles:

$$d_{ij} = \|X_i - X_j\|(i = 1, 2, \dots, N, i \ne j)$$

where X_i and X_j are the position vectors of particle i and particle j, respectively.

Step (3) For each particle i, determine the nearest particle, particle k, with better evaluation than its own, i.e., $d_{ik} = \min_j (d_{ij})$, $f_k \leq f_i$ and set it as the leader of particle i.

In the case of enhanced GPAC, particle k is considered the global best.

Step (4) For each particle i, randomly select a particle r and set it as the passive congregator of particle i.

Step (5) Update the velocities and positions of particles, using (8.218) and (8.215), respectively.

Step (6) Check whether the limits of positions in equation (8.219) and velocities in equations (8.220) and (8.221) are enforced. If the limits are violated, then they are replaced by the respective limits.

Step (7) Evaluate each particle, using the objective function f. The objective function f is calculated by running a power flow. In the case where for a particle no power flow solution exists, an error is returned and the particle retains its previous achievement.

Step (8) If the stopping criteria are not satisfied, go to Step (2).

The enhanced GPAC and LPAC PSO algorithms will be terminated if one of the following criteria is satisfied: (1) no improvement of the global best in the last 30 generations is observed, or (2) the maximum number of allowed iterations is achieved.

Finally, we can indicate that the last term of equation (8.218), added in the conventional PSO velocity update equation (8.214), displays the information transferred via passive congregation of particle i with a randomly selected particle r. This passive congregation operator can be regarded as a stochastic variable that introduces perturbations to the search process. For each particle i, the perturbation is proportional to the distance between itself and a randomly selected particle r rather than an external random number, namely, the turbulence factor introduced in reference [77]. The constriction factor approach helps the convergence of algorithm more than the turbulence factor because (1) in the early stages of the process, where distance between particles is large, the turbulence factor should be large, avoiding premature convergence; and (2) in the last stages of process, as the distance between particles becomes smaller, the turbulence factor should be smaller, too, enabling the swarm to converge in the global optimum [77] Therefore, LPAC is more capable of probing the decision space, avoiding suboptimums and improving information propagation in the swarm, than other conventional PSO algorithms.

8.8.2.3 *Coordinated Aggregation-Based PSO*   The coordinated aggregation is a completely new operator introduced in the swarm, where each particle moves considering only the positions of particles with better achievements than its own, with the exception of the best particle, which moves randomly. The coordinated aggregation can be considered as a type of

active aggregation where particles are attracted only by places with the most food.

Let $X_i(t)$ and $X_j(t)$ be the positions of particle i and particle j at iterative cycle t, respectively. The differences between the position of particles i and the position of particle j, $X_i(t) - X_j(t)$, are defined as **coordinators** of particle i velocity. The ratios of differences between the achievement of particle i, $A(X_i)$ and the better achievements by particles j, $A(X_j)$ to the sum of all these differences are called achievement's weighting factors ω_{ij}^t

$$\omega_{ij} = \frac{A(X_j) - A(X_i)}{\sum_l A(X_l) - A(X_i)}, \quad j, l \in \Omega_i \tag{8.222}$$

where Ω_i represents the set of particles j with better achievement than particle i.

The velocity of particle i is adapted by means of coordinators multiplied by weighting factors.

The steps of the coordinated aggregation–based PSO (CAPSO) algorithm are listed below [59].

Step (1) **Initialization**: Generate N particles. For each particle i, choose initial position $X_i(0)$ randomly. Calculate its initial achievement $A(X_i(0))$, using the objective function f and find the maximum $A_g(0) = \max_i A(X_i(0))$, called the global best achievement. Then, particles update their positions in accordance with the following steps.

Step (2) **Swarm's manipulation**: The particles, except the best of them, regulate their velocities in accordance with the equation

$$V_i^{t+1} = w^t V_i^t + \sum_j r_j \omega_{ij}^t (X_j^t - X_i^t) \quad j \in \Omega_i, i = 1, 2, \dots, N \tag{8.223}$$

where ω_{ij}^t are achievement's weighting factors and the inertia weighting factor w^t is defined by equation (8.216). The role of the inertia weighting factor is considered critical for the CAPSO convergence behavior. It is employed to control the influence of the previous history of the velocities on the current one. Accordingly, the inertia weighting function regulates the trade-off between the global and local exploration abilities of the swarms.

Step (3) **Best particle's manipulation (craziness)**: The best particle in the swarm updates its velocity with a **random coordinator** calculated between its position and the position of a randomly chosen particle in the swarm. The manipulation of the best particle seems like the crazy agents or the turbulence factor introduced in reference [77] and helps the swarm escape from the local minima.

Step (4) Check whether the limits of velocities in equations (8.220) and (8.221) are enforced. If the limits are violated, then they are replaced by the respective limits.

Step (5) **Position update**: The positions of particles are updated with equation (8.215). Check whether the limits of positions in equation (8.219) are enforced.

Step (6) **Evaluation**: Calculate the achievement $A(X_i(t))$ of each particle i, using the objective function f. The achievement is calculated by running a power flow. In the case where for a particle no power flow solution exists, an error is returned and the particle retains its previous achievement.

Step (7) If the stopping criteria are not satisfied, go to Step 2. The CAPSO algorithm will be terminated if no more improvement of the global best achievement in the last 30 generations is observed or the maximum number of allowed iterations is achieved.

Step (8) **Global optimal solution**: Choose the optimal solution as the global best achievement.

8.8.3 OPF Considering Valve Loading Effects

Generally, the generator fuel cost function in the OPF model ignores the valve point loading that introduces rippling effects to the actual input–output curve. The overall fuel cost function for a number of thermal generating units is modeled by a quadratic function, which is shown in equation (8.197). The valve effects can be expressed as a sine function [49] and added into equation (8.197), that is,

$$\text{Min} F_g = \sum_{i=1}^{NG} \left[a_i P_{gi}^2 + b_i P_{gi} + c_i + \left| e_i \sin \left(f_i \left(P_{gi\min} - P_{gi} \right) \right) \right| \right] \tag{8.224}$$

This more accurate modeling adds more challenges to most derivative-based optimization algorithms in finding the global solution since the objective is no longer convex or differentiable everywhere.

A hybrid PSO (HPSO) approach can be used to solve this problem [64]. This approach combines PSO technique with a Newton–Raphson-based power flow program in which the former technique is used as a global optimizer to find the best combinations of the mixed-type control variables while the latter serves as a minimizer to reduce the nonlinear power flow equation mismatch. The Newton–Raphson method used in this implementation is the one with the full Jacobian evaluated and updated at each iteration. The HPSO utilizes a population of particles or possible solutions to explore the feasible solution hyperspace in its search for an optimal solution. Each particle's position is used as a feasible initial guess for the power flow subroutine. This mechanism of multiple initial solutions can provide a better probability of detecting an optimal solution to the power flow equations that would globally minimize a given objective function. The importance of such hybridization is

signified by realizing the fact that in a transmission system the solution to the power flow equation is not unique, i.e., multiple solutions within the stability margins may exist and only one can globally optimize a certain objective.

The same OPF constraints in equations (8.201)–(8.209) are used here. Within the context of PSO applications to the OPF, inequality constraints that represent the permissible operating range of each optimization variable are typically handled in the following two ways [59–64]:

(1) Set to limit approach (SLA): If any optimization variable exceeds its upper or lower bound, the value of the variable is set to the violated limit. This resembles the idea found in operating all generating units at equal incremental principle to reach economic dispatch, which is described in Chapter 4. It is important to note that PSO has some randomness in the update equation that might cause several variables to exceed their limits during the optimization process. Thus this approach may fix multiple optimization variables to their operating limits for which global solution may not be reached. Also, this approach fails to utilize the memory element that each particle has once it exceeds its boundaries.

(2) Penalty factor: The other approach is to use penalty factors to incorporate the inequality constraints with the objective, which we used in Section 8.2. The main problem with this approach is introducing new parameters that need to be properly selected in order to reach acceptable PSO performance. Values of the penalty factors are problem dependent; thus this approach requires proper adjustments of the penalty factors in addition to tuning the PSO parameters.

Another approach is combining these two methods to handle the inequality constraints [64]. This combines the ideas of preserving feasible solution and infeasible solution rejection methods to retain only feasible solutions throughout the optimization process without the need to introduce penalty factors in the objective function. In most of the evolutionary computation optimization methods that employ the infeasible solution rejection method to handle constraints, any solution candidate among the population is randomly reinitialized once it crosses the boundaries of the feasible region. The majority of methods do not have memory elements associated with each candidate in the population. However, in the case of HPSO, each particle has a memory element (P_i) that recalls the best visited location through its own flying experience to search for the optimal solution and may use this information once it violates the problem boundaries. Thus this hybridization makes use of the memory element that each particle has to maintain its feasibility status. This restoration operation keeps the infeasible particle *alive* as a possible candidate that could locate the optimal solution instead of a complete rejection that eliminates its potential in the swarm.

For the control variables in equations (8.201)–(8.209), there are two types: continuous and discrete. The continuous variables are initialized with uni-

formly distributed pseudorandom numbers that take the range of these variables, e.g.,

$$P_{gi} = \text{random}[P_{gi\,min}, P_{gi\,max}], \text{ and } V_i = \text{random}[V_{i\,min}, V_{i\,max}]$$

However, in the case of the discrete variables, an additional operator was needed to account for the distinct nature of these variables. A rounding operator was included to ensure that each discrete variable is rounded to its nearest decimal integer value that represents the physical operating constraint of a given variable. Each transformer tap setting was rounded to its nearest decimal integer value of 0.01 by utilizing the rounding operator as: round (random $[T_{i\,min}, T_{i\,max}], 0.01$). The same principle applies to the discrete reactive injection due capacitor banks with the difference being the step size, i.e., round (random $[Q_{ci\,min}, Q_{ci\,max}], 1$). This ensures that the fitness of each solution is measured only when all elements of the solution vector are properly represented to reflect the real-world nature of each variable. Since the particle update equation has some uniformly distributed random operators built into it and because of the addition of two different types of vectors, the rounding operator is called again after each update to act only on the discrete variables as: round (T_i, 0.01) and round (Q_{ci}, 1). Once the rounding process is over, all solution elements go through a feasibility check. This simple rounding method guarantees that power flow calculations and fitness measurements are obtained only when all problem variables are properly addressed and their nature types are accounted for.

Example 8.4

The example is extracted from reference [64]. The test system is a IEEE 30-bus system with modified unit data and bus data, which are shown in Tables 8.22 and 8.23. The line data are the same as Table 5.6 in Chapter 5. There are two capacitor banks installed at buses 5 and 24 with ratings of 19 and 4 MVAR, respectively. A series of experiments were conducted to properly tune the HPSO parameters to suit the targeted OPF problem. The most noticeable observation from this groundwork is that the optimal settings for C_1 and C_2 are found to be 1.0. These values are relatively small since most of the values reported in the previously related work are in the range of 1.4–2 [59–63]. The best settings for number of particles and particle's maximum velocity (V_{max}) are 20 and 0.1, respectively. The inertia weight is kept fixed throughout the simulation process between the upper and lower bounds of 0.9 and 0.4, respectively.

The following three cases are conducted.

Case 1: Considering only the continuous control variables. The objective is to minimize the generator fuel costs, which are the quadratic fuel cost functions. The OPF results solved by HPSO are listed in Table 8.24. For comparison, the OPF results solved by sequential quadratic programming (SQP) are also listed in Table 8.24. Comparison of the results shows that

Table 8.22   Data of the generator for IEEE 30-bus system

Unit	1	2	3	4	5	6
Bus no.	1	2	22	27	23	13
A	0.02	0.0175	0.0625	0.00834	0.025	0.025
B	2	1.75	1	3.25	3	3
C	0	0	0	0	0	0
E	300	200	150	100	200	200
F	0.2	0.22	0.42	0.3	0.35	0.35
P_{min}(MW)	0	0	0	0	0	0
P_{max}(MW)	80	80	50	55	30	40
Q_{min}(Mvar)	−20	−20	−15	−15	−10	−15
Q_{max}(Mvar)	150	60	62.5	48.7	40	44.7

Table 8.23   Bus data for IEEE 30-bus system (p.u.)

Bus No.	P_D	Q_D	V_{min}	V_{max}	Bus No.	P_D	Q_D	V_{min}	V_{max}
1	0.000	0.000	0.95	1.1	16	0.035	0.016	0.90	1.05
2	0.217	0.127	0.95	1.1	17	0.090	0.058	0.90	1.05
3	0.024	0.012	0.90	1.05	18	0.032	0.009	0.90	1.05
4	0.076	0.016	0.90	1.05	19	0.095	0.034	0.90	1.05
5	0.942	0.190	0.90	1.05	20	0.022	0.007	0.90	1.05
6	0.000	0.000	0.90	1.05	21	0.175	0.112	0.90	1.05
7	0.228	0.109	0.90	1.05	22	0.000	0.000	0.95	1.1
8	0.300	0.300	0.90	1.05	23	0.032	0.016	0.95	1.1
9	0.000	0.000	0.90	1.05	24	0.087	0.067	0.90	1.05
10	0.058	0.020	0.90	1.05	25	0.000	0.000	0.90	1.05
11	0.000	0.000	0.90	1.05	26	0.035	0.023	0.90	1.05
12	0.112	0.075	0.90	1.05	27	0.000	0.000	0.95	1.1
13	0.000	0.000	0.95	1.1	28	0.000	0.000	0.90	1.05
14	0.062	0.016	0.90	1.05	29	0.024	0.009	0.90	1.05
15	0.082	0.025	0.90	1.05	30	0.106	0.019	0.90	1.05

HPSO achieves a better solution when only continuous optimization variables are used.

Case 2: Considering both the continuous and discrete control variables. The test system is modified by introducing four tap-changing transformers between buses 6–9, 6–10, 4–12, and 27–28. The operating range of all transformers is set between 0.9 and 1.05, with a discrete step size of 0.01. The capacitor banks at buses 5 and 24 are also considered as new discrete control variables with a range of 0–40 MVAR and a step size of 1. With this modification, the problem now has both continuous and discrete control variables that can be troublesome to most conventional optimization methods. The results are shown in the last column in Table 8.24.

Case 3: Considering the valve loading effects. The fuel cost function is augmented with an additional sine term as in equation (8.224). HPSO is applied to solve this kind of optimization problem. Table 8.25 lists the

Table 8.24   OPF results of IEEE 30-bus system for cases 1 and 2

Case	Case 1	Case 1	Case 2
Method	SQP	PSO	PSO
P_{g1}	41.51	43.611	42.180
P_{g2}	55.4	58.060	57.013
P_{g13}	16.2	17.555	17.305
P_{g22}	22.74	22.998	22.025
P_{g23}	16.27	17.056	17.872
P_{g27}	39.91	32.567	35.060
V_{g1}	0.982	1.000	1.000
V_{g2}	0.979	1.000	0.999
V_{g13}	1.064	1.059	1.061
V_{g22}	1.016	1.012	1.071
V_{g23}	1.026	1.021	1.076
V_{g27}	1.069	1.037	1.10
Q_{c5}	/	/	4.000
Q_{c24}	/	/	8.000
T_{6-9}	/	/	0.900
T_{6-10}	/	/	0.950
T_{4-12}	/	/	0.930
T_{27-28}	/	/	0.950
Total cost ($/hr)	576.892	575.411	574.143
Total losses (MW)	2.860	2.647	2.255

Table 8.25   OPF results of IEEE 30-bus system for case 3

Swarm's Size	20	30	100
Method	PSO	PSO	PSO
P_{g1}	47.068	47.059	47.126
P_{g2}	42.911	42.359	71.366
P_{g13}	8.790	35.902	8.972
P_{g22}	44.728	37.359	37.391
P_{g23}	8.983	8.826	8.993
P_{g27}	42.044	20.959	20.777
V_{g1}	1.000	1.000	1.000
V_{g2}	1.099	1.009	1.097
V_{g13}	1.091	1.017	1.037
V_{g22}	1.087	1.082	0.982
V_{g23}	1.048	1.057	1.048
V_{g27}	1.029	1.080	1.088
Q_{c5}	33.000	16.000	29.000
Q_{c24}	35.000	15.000	12.000
T_{6-9}	1.040	1.010	1.020
T_{6-10}	1.010	1.000	0.950
T_{4-12}	1.040	0.990	1.020
T_{27-28}	0.990	1.030	1.040
Total cost ($/hr)	658.416	645.333	615.250

results obtained with different swarm sizes. Increasing the swarm's size improved the HPSO performance in achieving better results at the expense of computational time.

REFERENCES

[1] J. Carpentier, "Contribution e létude do Dispatching Economique," *Bull. Soc. Franc. Elect.*, pp. 431–447, 1962.

[2] H.W. Dommel and W.F. Tinney, "Optimal power flow solutions", *IEEE Trans. Power Syst.*, Vol. 87, NO. 10, 1968, pp. 1866–1876.

[3] O. Alsac and B. Stott, "Optimal power flow with steady-state security", *IEEE Trans. Power Syst.*, Vol. 93, 1974, pp. 745–75.

[4] D.I. Sun, B. Ashley, A. Hughes, and W.F. Tinney, "Optimal power flow by Newton approach", *IEEE Trans. Power Syst.*, Vol. 103, 1984, pp. 2864–2880.

[5] M.R. Irving and M.J.H. Sterling, "Economic dispatch of active power with constraint relaxation", *IEE Proceedings, Part C*, Vol. 130, No. 4, 1983.

[6] L.G. Dias and M.E. El-Hawary, "Security-constrained OPF: Influence of fixed tap transformer fed loads," *IEEE Trans. Power Syst.*, vol. 6, no. 4, pp. 1366–1372, Nov. 1991.

[7] J.Z. Zhu and G.Y. Xu, "Network flow model of multi-generation plan for on-line economic dispatch with security," *Modeling, Simulation & Control, A*, Vol. 32, No. 1, 1991, pp. 49–55.

[8] J.Z. Zhu and G.Y. Xu, "Comprehensive investigation of real power economic dispatch with N and N-1 security," Proc. of 1991 Intern. Conf. on Power Systems Technology, Beijing, 1991.

[9] J.Z. Zhu and G.Y. Xu, "A new real power economic dispatch method with security", *Electric Power Systems Research*, Vol. 25, No. 1, 1992, pp. 9–15.

[10] A.D. Papalexopoulos, C.F. Imparato, and F.F. Wu, "Large Scale Optimal Power Flow: Effects of Initialization Decoupling and Discretization," *IEEE Trans. Power Syst.*, Vol. 4, 1989, pp. 748–759.

[11] J.Z. Zhu and M.R. Irving, "Combined active and reactive dispatch with multiple objectives using an analytic hierarchical process", *IEE Proceedings, Part C*, Vol. 143, NO. 4, 1996, pp. 344–352.

[12] A.M. Chebbo and M.R. Irving, "Combined active and reactive dispatch, Part I: problem formulation and solution", *IEE Proceedings, Part C*, Vol. 142, NO. 4, 1995, pp. 393–400.

[13] A.J. Wood and B. Wollenberg, *Power Generation Operation and Control*, 2nd ed. New York: Wiley, 1996.

[14] J.Z. Zhu and C.S. Chang, "Security-constrained multiarea economic load dispatch using nonlinear optimization neural network approach", 1997 Intern. Conf. on Intelligent System Applications to Power Systems, Seoul Korea, July, 1997.

[15] T.H. Lee, D.H. Thorne, and E.F. Hill, "A transportation method for economic dispatching – Application and comparison", *IEEE Trans. Power Syst.*, 1980, Vol. 99, pp. 2372–2385.

[16] E. Hobson, D.L. Fletcher, and W.O. Stadlin, "Network flow linear programming techniques and their application to fuel scheduling and contingency analysis", *IEEE Trans. Power Syst.*, 1984, Vol. 103, pp. 1684–1691.

[17] W.Y. Li, *Secure Economic Operation of Power Systems*, Chongqing University Press, 1989.

[18] O. Alsac, J. Bright, M. Prais, and B. Stott, "Further Developments in LP-Based Optimal Power Flow," *IEEE Trans. Power Syst.*, Vol. 5, 1990, pp. 697–711.

[19] Y.L. Chen and C.C. Liu, "Optimal Multi-Objective VAR Planning using an Interactive Satisfying Method" IEEE PES, 1994 Summer Meeting, July, 1994, pp. 24–28.

[20] K. Mamandur and R. Chenoweth, "Optimal Control of Reactive Power Flow for Improvements in Voltage Profiles and for Real Power Loss Minimization," *IEEE Trans. Power Syst.*, Vol. 100, 1981, pp. 3185–3194.

[21] M.O. Mansour and T.M. Abdel-Rahman, "Non-linear VAR Optimization Using Decomposition and Coordination," *IEEE Trans. Power Syst.*, Vol. 103, 1984, pp. 246–255.

[22] E. Acha, H.A. Perez, and C.R. Esquivel, "Advanced transformer control modeling in an optimal power flow using Newton's method," *IEEE Trans. Power Syst.*, Vol. 15, No. 1, 2000, pp. 290–298.

[23] J.Z. Zhu and M.R. Irving, "A new approach to secure economic power dispatch," *International Journal of Electric Power & Energy System*, 1998, Vol. 20, No. 8, pp. 533–538.

[24] J.Z. Zhu and J.A. Momoh, "Multi-area power systems economic dispatch using nonlinear convex network flow programming," *Electric Power Systems Research*, Vol. 59, No. 1, 2001, pp. 13–20.

[25] J.A. Momoh, J.Z. Zhu, G.D. Boswell, and S. Hoffman, "Power system security enhancement by OPF with phase shifter," *IEEE Trans. Power Syst.*, Vol. 16, No. 2, May. 2001, pp. 287–293.

[26] J.A. Momoh, J.Z. Zhu, and J.L. Dolce, "Optimal allocation with network limitation for autonomous space power system," *AIAA Journal – Journal of Propulsion and Power*, Vol. 16, No. 6, Nov.–Dec., 2000, pp. 1112–1117.

[27] J.A. Momoh and J.Z. Zhu, "Improved interior point method for OPF problems", *IEEE Trans. Power Syst.*, Vol. 14, No. 3, Aug. 1999, pp. 1114–1120.

[28] J.A. Momoh, R. Adapa, and M.E. El-Hawary, "A review of selected optimal power flow literature to 1993—I: Nonlinear and quadratic programming approaches," *IEEE Trans. Power Syst.*, vol. 14, no. 1, pp. 96–104, Feb. 1999.

[29] J.A. Momoh, M.E. El-Hawary, and R. Adapa, "A review of selected optimal power flow literature to 1993—II: Newton, linear programming and interior point methods," *IEEE Trans. Power Syst.*, vol. 14, no. 1, pp. 105–111, Feb. 1999.

[30] K.A. Clements, P.W. Davis, and K.D. Frey, "An Interior Point Algorithm for Weighted Least Absolute value Power System State Estimation", IEEE PES Winter Meeting, 1991.

[31] K. Ponnambalam, V.H. Quintana, and A. Vannelli, "A Fast Algorithm for Power System Optimization Problems Using an Interior Point Method", IEEE PES Winter Meeting, 1991.

[32] L.S. Vargas, V.H. Quintana, and A. Vannelli, "A Tutorial Description of an Interior Point Method and its Application to Security-Constrained Economic Dispatch", IEEWPES 1992 Summer Meeting.

[33] J.A. Momoh, S.X. Guo, C.E. Ogbuobiri, and R. Adapa, "The Quadratic Interior Point Method for Solving Power System Optimization Problems", *IEEE Trans. on Power Syst.*, Vol. 9, 1994.

[34] N.C. Lu and M.R. Unum, "Network Constrained Security Control using an Interior Point Algorithm", *IEEE Trans. Power Syst.*, Vol. 8, 1993.

[35] S. Granville, "Optimal reactive dispatch through interior-point methods," *IEEE Trans. Power Syst.*, vol. 9, pp. 136–146, Feb. 1994.

[36] J.A. Momoh, G.F. Brown, and R.A. Adapa, "Evaluation of Interior Point Methods and Their Application to Power Systems Economic Dispatch," Proceedings of North American Power Symposium, Washington, D.C., Oct. 1993, pp. 116–123.

[37] H. Wei, H. Sasaki, and R. Yokoyama, "An application of interior point quadratic programming algorithm to power system optimization problems", *IEEE Trans. Power Syst.*, Vol. 11, 1996, pp. 260–266.

[38] S. Granville, J.C.O. Mello, and A.C.G. Melo, "Application of interior point methods to power flow un-solvability", *IEEE Trans. Power Syst.*, Vol. 11, 1996, pp. 1096–1103.

[39] Y.C. Wu, A.S. Debs, and R.E. Marsten, "A direct nonlinear predictor-corrector primal–dual interior point algorithm for optimal power flows," *IEEE Trans. Power Syst.*, vol. 9, pp. 876–883, May 1994.

[40] G.L. Torres and V.H. Quintana, "An interior-point method for nonlinear optimal power flow using voltage rectangular coordinates," *IEEE Trans. Power Syst.*, vol. 13, pp. 1211–1218, Nov. 1998.

[41] E.D. Castronuovo, J.M. Campagnolo, and R. Salgado, "Optimal power flow solutions via interior point method with high-performance computation techniques," in Proc. 13th PSCC in Trondheim, June 28–July 2, 1999, pp. 1207–1213.

[42] R.A. Jabr, A.H. Coonick, and B.J. Cory, "A prime-dual interior point method for optimal power flow dispatching," *IEEE Trans. Power Syst.*, vol. 17, no. 3, pp. 654–662, 2002.

[43] K. Xie, Y.H. Song, J. Stonham, E. Yu, and G. Liu, "Decomposition model and interior point methods for optimal spot pricing of electricity in deregulation environments," *IEEE Trans. Power Syst.*, vol. 15, no. 1, pp. 39–50, Feb. 2000.

[44] J.Z. Zhu, W. Yan, C.S. Chang, and G.Y. Xu, "Reactive power optimization using an analytic hierarchical process and a nonlinear optimization neural network approach," *IEE Proceedings: Generation, Transmission and Distribution*. Vol. 145 No. 1, 1998 pp. 89–96.

[45] J.Z. Zhu and J.A. Momoh, "Optimal VAR pricing and VAR placement using analytic hierarchy process," *Electric Power Systems Research*, 1998, Vol. 48, No. 1, pp. 11–17.

[46] J.Z. Zhu and X.F. Xiong, "Optimal Reactive Power Control using Modified Interior Point Method", *Electric Power Systems Research*, Volume 66, 2003, Pages 187–192.

[47] J.Z. Zhu, "Multi-area power systems economic dispatch using a nonlinear optimization neural network approach," *Electric Power Components and Systems*, Vol. 31, 2002, pp. 553–563.

[48] T. Kulworawanichpong and S. Sujitjorn, "Optimal power ?ow using tabu search," *IEEE Power Eng. Rev.*, vol. 22, no. 6, pp. 37–55, Jun. 2002.

[49] D.C. Walters and G.B. Sheble, "Genetic algorithm solution of economic dispatch with valve point loading," *IEEE Trans. Power Syst.*, vol. 8, no. 3, pp. 1325–1332, Aug. 1993.

[50] K.P. Wong, A. Li, and T.M.Y. Law, "Advanced constrained genetic algorithm load flow method," *IEE Proc. C*, Vol. 146, No. 6, 1999, pp. 609–618.

[51] K.H. Abdul-Rahman and S.M. Shahidehpour, "Application of fuzzy sets to optimal reactive power planning with security constraints," *IEEE Trans. Power Syst.*, vol. 9, no. 2, pp. 589–597, May 1994.

[52] L.L. Lai and J.T. Ma, "Application of evolutionary programming to reactive power planning-comparison with nonlinear programming approach," *IEEE Trans. Power Syst.*, vol. 12, no. 1, pp. 198–206, Feb. 1997.

[53] W.S. Jwo, C.W. Liu, C.C. Liu, and Y.T. Hsiao, "Hybrid expert system and simulated annealing approach to optimal reactive power planning," *IEE Proc. Generation, Transmission and Distribution*, vol. 142, no. 4, pp. 381–385, Jul. 1995.

[54] W.J. Zhang, F.X. Li, and L.M. Tolbert, "Review of reactive power planning: objectives, constraints, and algorithms," *IEEE Trans. Power Syst.*, vol. 22, no. 4, 2007, pp. 2177–2186.

[55] R. Yokoyama, S.H. Bae, T. Morita, and H. Sasaki, "Multiobjective optimal generation dispatch based on probability security criteria," *IEEE Trans. Power Syst.*, vol. 3, no. 1, pp. 317–324, Feb. 1988.

[56] W.-M. Lin, F.-S. Cheng, and M.-T. Tsay, "An improved Tabu search for economic dispatch with multiple minima," *IEEE Trans. Power Syst.*, vol. 17, pp. 108–112, Feb. 2002.

[57] N. Deeb, "Simulated annealing in power systems," in Proc. IEEE Int. Conf. Man and Cybernetics, Oct. 1992, vol. 2, pp. 1086–1089.

[58] A.J. Korsak, "On the question of uniqueness of stable load-flow solutions," *IEEE Trans. Power App. Syst.*, vol. PAS-91, no. 3, pp. 1093–1100, May 1972.

[59] J.G. Vlachogiannis and K.Y. Lee, "A comparative study on particle swarm optimization for optimal steady-state performance of power systems," *IEEE Trans. Power Syst.*, vol. 21, no. 4, pp. 1718–1728, Nov. 2006.

[60] J.B. Park, K.S. Lee, J.R. Shin, and K.Y. Lee, "A particle swarm optimization for economic dispatch with nonsmooth cost functions," *IEEE Trans. Power Syst.*, vol. 20, no. 1, pp. 34–42, Feb. 2005.

[61] Z.L. Gaing, "Constrained optimal power flow by mixed-integer particle swarm optimization," in Proc. IEEE Power Eng. Soc. General Meeting, San Francisco, CA, 2005, pp. 243–250.

[62] B. Zhao, C.X. Guo, and Y.J. Cao, "Improved particle swarm optimization algorithm for OPF problems," in Proc. IEEE/PES Power Systems Conf. Exposition, New York, 2004, pp. 233–238.

[63] M.A. Abido, "Optimal power flow using particle swarm optimization," *Int. J. Elect. Power Energy Syst.*, vol. 24, no. 7, pp. 563–571, 2002.

[64] M.R. AlRashidi and M.E. El-Hawary, "Hybrid particle swarm optimization approach for solving the discrete OPF problem considering the valve loading effects," *IEEE Trans. Power Syst.*, vol. 22, no. 4, 2007, pp. 2030–2038.

[65] S.K.M. Kodsi and C.A. Cañizares, "Application of a stability-constrained optimal power flow to tuning of oscillation controls in competitive electricity markets," *IEEE Trans. Power Syst.*, vol. 22, no. 4, 2007, pp. 1944–1954.

[66] R. Fletcher and S. Leyffer, "Nonlinear programming without a penalty function," Univ. of Dundee, Dundee, U.K., Numeric. Anal. Rep. NA/171, Sept. 22, 1997.

[67] S.J. Wright, *Primal Dual Interior Point Methods*. Philadelphia, PA: SIAM, 1997.

[68] D.M. Gay, M.L. Overton, and M.H. Wright, "A primal–dual interior method for non-convex nonlinear programming," Computing Sciences Research Center, Bell Laboratories, Murray Hill, NJ, Tech. Rep. 97–4-08, July 1997.

[69] S. Mehrotra, "On the implementation of a primal–dual interior point method," *SIAM J. Optim.*, vol. 2, pp. 575–601, 1992.

[70] M. Avriel and B. Golany, *Mathematical Programming for Industrial Engineers*. New York: Marcel Dekker, 1996.

[71] R. Eberhart and J. Kennedy, "A new optimizer using particle swarm theory," in Proc. 6th Int. Symp. Micro Machine and Human Science, Nagoya, Japan, 1995, pp. 39–43.

[72] J. Kennedy and R. Eberhart, "Particle swarm optimization," in Proc. IEEE Int. Conf. Neural Networks, Perth, Australia, 1995, vol. 4, pp. 1942–1948.

[73] X. Hu, Y. Shi, and R. Eberhart, "Recent advances in particle swarm," in Proc. Congr. Evolutionary Computation, Portland, OR, 2004, vol. 1, pp. 90–97.

[74] R.C. Eberhart and Y. Shi, "Guest editorial special issue on particle swarm optimization," *IEEE Trans. Evol. Comput.*, vol. 8, no. 3, pp. 201–203, Mar. 2004.

[75] J. Kennedy and R.C. Eberhart, *Swarm Intelligence*. San Francisco, CA: Morgan Kaufmann, 2001.

[76] J.K. Parrish and W.M. Hammer, *Animal Groups in Three Dimensions*. Cambridge, U.K.: Cambridge Univ. Press, 1997.

[77] S. He, Q.H. Wu, J.Y. Wen, J.R. Saunders, and P.C. Patton, "A particle swarm optimizer with passive congregation," *Biosystems*, vol. 78, pp. 135–147, 2004.

9

STEADY-STATE SECURITY REGIONS

Steady state security region analysis is important in power system operation. This chapter presents the concept and definition of the security region and introduces several major methods used in steady-state security region analysis: the security corridor, the traditional expansion method, the enhanced expansion method, linear programming, and the fuzzy set theory.

9.1 INTRODUCTION

In the steady state, a power system is designed by the so-called power flow equations or the steady-state network relationships. Given a set of power injections (generators, loads), the power flow equations may be solved to obtain the operation point (voltages, angles). Therefore, a lot of power flow calculations are needed in the traditional steady-state security analysis, and the corresponding amount of computations is very huge. A method of steady-state security analysis, "steady-state security regions," has caused more attention over the last decades [1–14]. The main idea of security regions is to obtain a set of security injections explicitly so that for security assessment one need only check whether a given injection vector lies within the security region. By doing so, the solution of power flow equations can be avoided.

The approach for steady-state security regions of power systems was first proposed by Hnyilicza et al. in 1975 [1]. Fischl et al. developed methods to identify steady-state security regions [2, 3]. The idea of steady-state security

regions was expanded by Banakar and Galiana, who suggest a method to construct the so-called "security corridors" for security assessment [5]. The previous security region, which was formed by using the active constraints, was implicit and was difficult to use in power system security analysis and security operation. Wu and Kumagai deduced a hyperbox to approximately express the steady-state security regions, so that the disadvantage of the former methods for security regions could be overcome [6]. However, such steady-state security regions were very conservative. To avoid being conservative, Liu proposed an expanding method to obtain the hyperbox, which tended to achieve maximal security regions [7]. The expanding speed, however, was very slow because of the adoption of fixed expanding steps. Moreover, the fuzzy branch power constraints and $N-1$ security constraints have not been considered in these investigations of steady-state security regions.

Zhu proposed a new expanding method of the steady-state security regions of power system based on the fast decoupled load flow model [8, 9]. For the first time, the fuzzy branch power constraints and the $N-1$ security constraints are introduced into the study of the steady-state security regions [10–12]. Recently, Zhu also applied the optimization method to compute the steady-state security regions [13, 14].

9.2 SECURITY CORRIDORS

9.2.1 Concept of Security Corridor [4, 5]

In terms of x, the rectangular coordinate components of the complex bus voltages, the load flow equations can be expressed by

$$z = [L(x)]x \tag{9.1}$$

where $L(x)$ is a real matrix equal to half the Jacobian of the load flow equations and z is the vector of specified nodal injections. Without loss of generality, one can assume that there is no mixed (hybrid) bus in the system, which implies that

$$z = \begin{bmatrix} u \\ -d \end{bmatrix} \tag{9.2}$$

where u is the vector of control variables (voltage levels at the generation buses and real power generations at the PV buses) and d is the demand vector (real and reactive loads at PQ buses).

In terms of x, a load flow-dependent variable can be expressed in the general form

$$y = x^{\mathrm{T}}[Y]x \tag{9.3}$$

where Y represents the functional dependence of y on the network parameters, which is the sparse, constant, symmetric matrix. In the conventional load flow formulation, the line power flows, reactive power generations, the square of voltage levels at the load buses, and the real power injection at the slack bus are among the dependent variables.

Considering the network constraints, equation (9.3) will be restricted as below:

$$y_{j\min} \leq y_j \leq y_{j\max}, \quad j = 1, \ldots, N_{dp} \tag{9.4}$$

where $y_{j\min}$, $y_{j\max}$ are the lower and upper bounds of the constraint, respectively. N_{dp} is the total number of such dependent variables in the system.

Since each point in the x-space can be mapped into the z-space through equation (9.1), one can define the set of all injections, z, that satisfy a specific operating constraint. For instance, the set z^j defined by

$$z^j = \{z | z = [L(x)]x; x \in x^j\} \tag{9.5}$$

represents the map of the following set

$$x^j = \{x | y_{j\min} \leq x^T[y_j]x \leq y_{j\max}\} \tag{9.6}$$

This is into the z-space. Let S_z be the set of the collection of all the injections satisfying the various operating constraints on the intact system. It can be defined as below:

$$S_z = H_z \cap \left(\bigcap_{j=1}^{2N_{dp}} z^j \right) \tag{9.7}$$

The hyperbox H is defined by the known limitations on the control variables and conservative bounds on the load variables, namely,

$$H_z = \{z | z_{\min} \leq z \leq z_{\max}\} \tag{9.8}$$

If we select an expansion point, the constraints (9.4) can be explicitly expressed through a Taylor series expansion of y.

A more demanding security set is the invulnerability set. This set contains all the injection vectors that do not violate any of the system's operating limits, while it is intact or subjected to a list of probable outages.

Since the variations of the loads, $d(t)$, can be predicted with a bus-load forecast, and a control vector, $u(t)$, can be computed that satisfies the security requirements, a predicted trajectory of the injection vector, $z(t)$, can be established. Therefore, one can introduce the concept of a security corridor. Such a corridor can be thought of as a "tube of varying width" in z-space surrounding
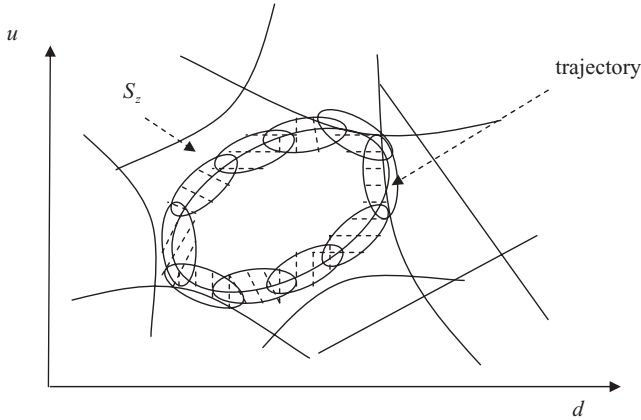
FIGURE 9.1 A pictorial representation of a nominal daily trajectory and its associated security corridor (shaded) inside the security set

the predicted trajectory and lying entirely within the security region, S_z. The security corridor, E_S^c, has two important properties:

(1) It is characterized by a very small number of inequalities compared to S_z.

(2) Since the security corridor, E_S^c, is a subset of S_z with some "width" in al1 directions, the actual trajectory can deviate from the predicted one while still remaining inside E_S^c and hence in S_z.

The security corridor then permits the monitoring of security by the very simple task of verifying that the actual injection vector, z, belongs to E_S^c. If z is inside the corridor, then it becomes unnecessary to test all other security inequalities or to run repeated load flows. In the infrequent cases when the actual trajectory deviates beyond the limits of the corridor, a conventional security analysis based on load flow computations would have to be carried out. The advantage gained is that most of the time quite wide excursions in the trajectory are needed to go outside the security corridor. The typical periodic and stochastic load behavior will normally not violate the security corridor limits. Finally, the security corridor greatly facilitates the computation, as well as verification, of the effectiveness of control actions such as emergency or preventive rescheduling.

The corridor can be characterized via a small number of overlapping ellipsoids whose centers lie on the predicted trajectory [5]. A pictorial illustration of such an arrangement is given in Figure 9.1.

Since the ellipsoids are expressible by simple, explicit functions and they can be oriented to lie along the trajectory, they seem to be the logical choice for this purpose. The N ellipsoids forming the corridor are defined by

$$E^i = \left\{ z \,\middle|\, (z - z_i)^{\mathrm{T}}[A_i](z - z_i) \le c_i \right\} \quad i = 1, \dots, N \tag{9.9}$$

where A is a constant, symmetric, positive definite matrix representing the orientation of E^i. The vector z_i represents the center of E^i, while the constant c_i controls its size. The union of the ellipsoids denoted by E^c forms the corridor, i.e,

$$E^c = \bigcup_{i=1}^{N} E^i \tag{9.10}$$

The secure part of E^c is then referred to as the "security corridor," and is defined by

$$E_s^c = S_z \cap E^c = \bigcup_{i=1}^{N} E_s^i \tag{9.11}$$

where E_s^i is the secure part of E^i.

9.2.2   Construction of Security Corridor [5]

It can be known from equations (9.9) and (9.10) that the key to constructing a security corridor is to select z_i and A. To have the predicted trajectory surrounded by the corridor, the center of the ellipsoids z_i, $i = I, \dots, N$, must be on the trajectory. These points should be selected inside S_z so that E is not empty.

The number of ellipsoids, N, needed to cover a trajectory is small when the ellipsoids are oriented properly along the trajectory. Let the unit tangent to the trajectory at z_i be represented by a_i. The ellipsoid E^i is laid along the trajectory by making sure that its major axis lies along a_i. This can be accomplished by defining A_i as below:

$$[A_i] = \lambda_{i\max}[I] - (\lambda_{i\max} - \lambda_{i\min})[a_i a_i^{\mathrm{T}}], \quad \lambda_{i\max} > \lambda_{i\min} > 0 \tag{9.12}$$

One can easily show that the eigenvalues of A_i are all $\lambda_{i\max}$ except one, which is $\lambda_{i\min}$, and that the engenvector corresponding to $\lambda_{i\min}$ is a_i. In addition, the storage requirements of A_i are very low; its inverse can be analytically obtained as follows:

$$[A_i]^{-1} = \frac{[I] + \left(\dfrac{\lambda_{i\max}}{\lambda_{i\min}} - 1 \right)[a_i a_i^{\mathrm{T}}]}{\lambda_{i\max}} \tag{9.13}$$

According to the expression of the security corridor in equation (9.11) and the expression of the security sets in equation (9.7), we get

$$E_s^i = S_z \cap E^i = H_z \cap \left(\bigcap_{j=1}^{2N_{dp}} z^j \right) \cap E^i \tag{9.14}$$

or

$$E_s^i = H_z \cap \left\{ \bigcap_{j=1}^{2N_{dp}} z^j \cap E^i \right\} \tag{9.15}$$

For a relatively small E^i, (i.e., small c_i) the majority of the sets z^i contain the entire set E^i. For such sets one can write

$$z^j \supset E^i \Rightarrow z^j \cap E^i = E^i \tag{9.16}$$

Those few that intersect E^i must be identified and characterized explicitly. This can be accomplished by solving the following optimization problem:

$$\min c_{ij} = (z - z_i)^T [A_i](z - z_i), z \in \text{Ext}(z^j) \quad \text{for } j = 1, \dots, 2 N_{dp} \tag{9.17}$$

Since $z_i \in S_z$, the intersection $z_i \cap E^i$ is always nonempty. In terms of x, the above problem can be written as

$$\min c_{ij} = \{[L(x)]x - z_i\}^T [A_i]\{[L(x)]x - z_i\} \tag{9.18}$$

s.t.

$$y_{j\min} \le x^T [y_j] x \le y_{j\max} \tag{9.19}$$

To simplify the above optimization problem, z^i can be approximated as below:

$$\hat{z}^j = \{z | D_j^T(x_j) z \le y_{j\lim it}\} \tag{9.20}$$

The solution to equation (9.17) with $z \in \text{Ext}(\hat{z}^j)$ is simply

$$\hat{c}_{ij}^* = [y_{j\lim it} - D_j^T(x_j) z_i]^2 / \delta_{ij} \tag{9.21}$$

where x_i is the load flow solution to z_i and

$$\delta_{ij} = D_j^T(x_i)[A_i]^{-1} D_j(x_i) \tag{9.22}$$

Thus the corresponding approximated security corridor E_s^i is expressed explicitly as follows:

$$\hat{E}_s^i = H_z \cap E^j \cap \{z | D_j^T(x_i) z \le y_{j\lim it}, \forall j \in I^i\} \tag{9.23}$$

where I^i is an integer set and its elements are defined as below:

$$j \in I^i \quad \text{if } \hat{c}^*_{ij} < c_i$$

It is noted that this approximation requires that the solution point is relatively close to z_i.

A relatively simple but sufficiently indicative measure of the size of E^i is $\Delta P_{d\max}\%$, the maximum percent change that the total real demand, P_d, can have inside E^i with respect to P_{di}, the total demand at z_i. To compute this quantity, we need to solve the following problem:

$$\text{Max} P_d = -\alpha^T z \tag{9.24}$$

s.t.

$$(z - z_i)^T [A_i](z - z_i) = c_i \tag{9.25}$$

The entries of the vector α are either zero or 1, with ones appearing at locations that correspond to real power demands z.

In summary, the steps of constructing a security corridor are as follows.

(1) Choose z_i from the trajectory and run a load flow to make sure that $z_i \in S_z$.
(2) Compute a_i and define the matrix A_i.
(3) Compute values of $\hat{c}^*_{ij}, j = 1, 2, \ldots, N_{dp}$ using equation (9.21), and tabulate them in ascending order.
(4) Decide on $N_{i\max}$, the maximum number of elements that I^i can have.
(5) Assign to c_i the first $N_{i\max} + 1$ values of $\hat{c}^*_{ij}$ in the list, one at a time. For each value, compute and tabulate $\Delta P_{d\max}\%$, as well as the times when the trajectory enters and leaves the resulting E^i.
(6) Compare the results to establish what value of c_i chosen from those examined could offer a reasonable $\Delta P_{d\max}\%$ and sufficient overlapping with E^{i-1} while the number of elements in I^i is small ($\leq N_{i\max}$). If such a c_i cannot be found, then either change the eigenvalues of A_i or choose z_i closer to z_{i-1} and repeat the relevant steps.

Note that in the last step it is assumed that the value of c_{i-1} is already fixed, and the time when the trajectory enters and leaves E^{i-1} as well as its associated $\Delta P_{d\max}\%$ are known. Sufficient overlapping is achieved between E^i and E^{i-1} when a significant portion (normally 25%) of the time spent by the trajectory inside E^{i-1} is also part of the time that it spends inside E^i. Since the trajectory is usually available in a piecewise linear form, the computation of the trajectory's "arrival" and "departure" times for a given ellipsoid is quite simple to calculate.

The number of elements in I^i is limited here by N_{imax}, mainly because of the nonsparsity of the vectors $D_j(x_i)$, $j \in I^i$ $f:..$; $(\sim i)$, $i = 1, ..., N$, which have to be computed and stored. The vectors $D_j(x_i)$ can be obtained by performing one constant Jacobian Newton power flow iteration. That is,

$$[L(x_0)]^T D_j(x_0) = [Y_j] x_0 \tag{9.26}$$

9.3   TRADITIONAL EXPANSION METHOD

9.3.1   Power Flow Model

Given a power system, suppose the total number of branches is m; the total number of buses is n. Bus n is the slack bus, buses 1 to n_d are load buses and buses $n_d + 1$ to $n - 1$ are PV buses (the number of PV buses is NG). According to fast decoupled power flow, the active power flow equations can be written as follows:

$$[P] = [B'][\theta] \tag{9.27}$$

$$[\theta_L] = [A]^T[\theta] \tag{9.28}$$

where P is the vector of active power injections, θ is the vector of node voltage angle, θ_L is the vector of node voltage angle differences across lines, and A is the relation matrix between nodes and branches.

From equations (9.27) and (9.28) we can obtain

$$[\theta_L] = [A]^T[B']^{-1}[P] \tag{9.29}$$

where

$$B'_{ij} = -1/X_{ij} \tag{9.30}$$

$$B'_{ii} = \sum_{\substack{j=1 \\ j \neq i}}^{n} \left(\frac{1}{X_{ij}} \right) \tag{9.31}$$

X_{ij} and B_{ij} are the reactance and susceptance of branch ij, respectively.

If we use reactive injection current to replace the reactive injection power, the reactive power flow equations can be written as follows:

$$[I] = [B''][V] \tag{9.32}$$

$$[V] = [B'']^{-1}[I] \tag{9.33}$$

where

$$I_i \approx \frac{Q_i}{V_i} \tag{9.34}$$

$$B''_{ij} = -\frac{X_{ij}}{R_{ij}^2 + X_{ij}^2} \tag{9.35}$$

$$B''_{ii} = \sum_{\substack{j=1 \\ j \neq i}}^{n} (-B_{ij}) \tag{9.36}$$

9.3.2 Security Constraints

The following security constraints will be considered in the study of steady-state security regions:

(1) Generator power output constraints

$$P_{Gi\min} \leq P_{Gi} \leq P_{Gi\max} \tag{9.37}$$

$$\frac{Q_{Gi\min}}{V_i} \leq I_{Gi} \leq \frac{Q_{Gi\max}}{V_i} \tag{9.38}$$

For the slack bus unit, the power output constraints are

$$P_{Gn\min} \leq -\sum_{i=1}^{n-1} P_i \leq P_{Gn\max} \tag{9.39}$$

$$\frac{Q_{Gn\min}}{V_n} \leq -\sum_{i=1}^{n-1} I_i \leq \frac{Q_{Gn\max}}{V_n} \tag{9.40}$$

where subscripts "*min*" and "*max*" represent the lower and upper bounds of the constraints, respectively. nth bus is the slack bus.

(2) Branch power flow constraints

$$-\theta_{ij\max} \leq \theta_{ij} \leq \theta_{ij\max} \tag{9.41}$$

In the normal operation status of power systems, the branch reactive power constraints can be neglected.

9.3.3 Definition of Steady-State Security Regions

The aim of steady-state security analysis is to analyze and check whether all elements in the system would operate within constraints as defined by a given set of input data and information. Therefore, the steady-state security regions can be represented by a set of power injections, which satisfy the power flow equations and security constraints.

$$R_P = \{P / \exists \theta \in R, \text{and } (f_P(\theta) = P) \in R\} \tag{9.42}$$

$$R_Q = \{I / \exists V \in R, \text{and } (f_Q(V) = I) \in R\} \tag{9.43}$$

where R_P and R_Q are the active and reactive power steady-state security regions, R is the set of security constraints, and f is the set of load flows.

One hand, the calculation methods of active and reactive power steady-state security regions are the same. On the other hand, the active power security is relatively more important since the reactive power problem is generally a local issue. Thus we focus on active security regions in this chapter.

Practically, it is desired to obtain each security region to cover as many operating points as possible. Hence, the idea of maximal security region was proposed. $\Omega_P^* \in R_P$ is said to be a maximal security region if there exists no hyperbox Ω_P in R_P, such that Ω_P strictly contains Ω_P^*, i.e., $\Omega_P^* \not\subset \Omega_P$. In other words, a hyperbox Ω_P^* is maximal if it is impossible to extend it in any dimension with R_P.

9.3.4 Illustration of Calculation of Steady-State Security Region

Generally, the expanding method is used to compute the maximal security region. The idea is to select the initial operation point first, and then expand the initial point by adding the fixed step until we reach any limit of constraints.

For example, there is a simple system with two generators. The feasible region is shown in Figure 9.2. The steady-state security region obtained by the expanding method is shown in Figure 9.3.
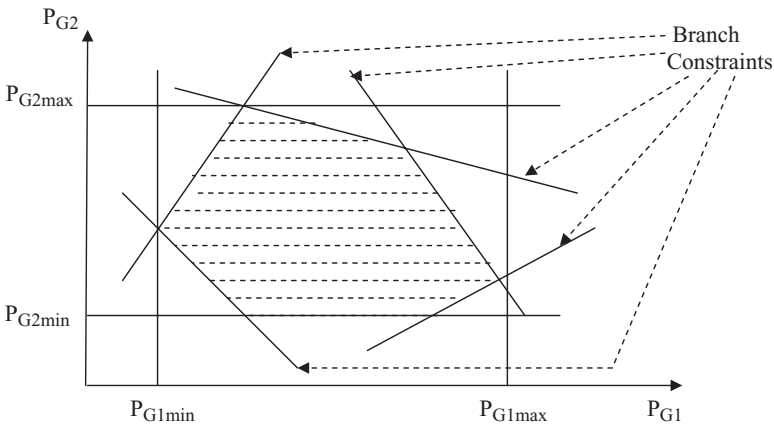

FIGURE 9.2 Feasible region of illustrating system
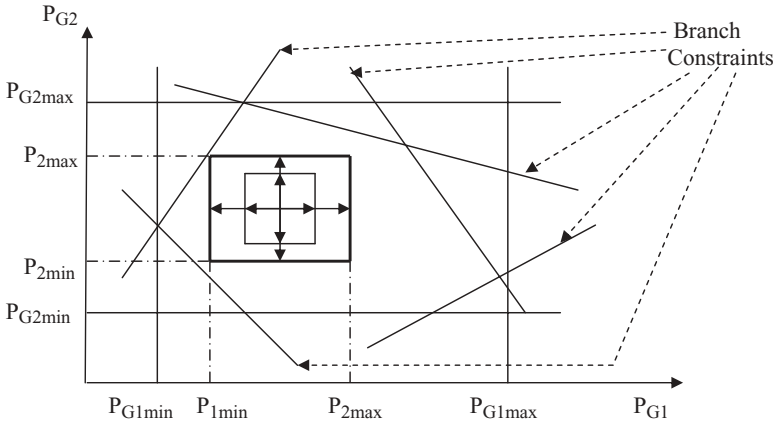
FIGURE 9.3 Security region obtained by the expanding method

Table 9.1   Security region results for IEEE 6-Bus System (p.u.)

Regions	P_{G4}	P_{G5}	P_{G6}
P_{imax}	3.7500	2.6490	2.5510
P_{imin}	2.4490	1.4000	0.0000

Table 9.2   Security region results for IEEE 30-Bus System (p.u.)

Regions	P_{G2}	P_{G5}	P_{G8}	P_{G11}	P_{G13}
P_{imax}	0.7120	0.4020	0.3500	0.3000	0.4000
P_{imin}	0.4280	0.1500	0.1480	0.1000	0.1770

9.3.5   Numerical Examples

The expanding method for computing power steady-state security region is further illustrated by IEEE 6-bus and 30-bus systems. The parameters of systems are taken from references [6, 8, 11]. The obtained security regions for two systems are shown in Tables 9.1 and 9.2, respectively.

9.4   ENHANCED EXPANSION METHOD

9.4.1   Introduction

Since computing speed is very slow in the previous expanding methods, a new expanding method is presented in this section. In this expanding method,

security constraints are divided into two groups and the expanding calculations are first carried out in the first group of constraints with small constraint margins. In addition, the failure probability of branch temporary overload and the capability of tapping the potentialities for branch power capacity are considered based on fuzzy sets. Furthermore, an idea of the "$N-1$ constraint zone" is also adopted to calculate all $N-1$ security constraints so as to reduce the computation burden.

9.4.2 Extended Steady-State Security Region

9.4.2.1 Security Constraints The same power flow model as in Section 9.3 is used here. The following security constraints will be taken in the study of steady-state security regions:

(1) Generator active power output constraints

$$P_{Gi\min} \leq P_{Gi} \leq P_{Gi\max} \qquad (9.44)$$

$$P_{Gn\min} \leq -\sum_{i=1}^{n-1} P_i \leq P_{Gn\max} \qquad (9.45)$$

(2) Fuzzy branch load flow constraints

$$-\theta_{ij\max} \leq \theta_{ij} \leq \theta_{ij\max} \qquad (9.46)$$

or

$$-P_{ij\max}/b_{ij} \leq \theta_{ij} \leq P_{ij\max}/b_{ij} \qquad (9.47)$$

When the limits of branch power flow are not determined beforehand, equations (9.46) and (9.47) cannot be directly adopted. During the stage of planning and system design, values of branch power flow limits are given to allow for some margin of security and reliability. In fact, it is possible to tap extra potentialities of branch power flow capacity in some cases, so as to allow some margins to be expanded. However, overtapping of potentialities for branch power flow capacity will lead to some problems such as high power losses and unreliability. Hence, it is conceptually sound to replace equation (9.46) or (9.47) by fuzzy constraints. By changing each bilateral inequality constraint into two single inequality constraints, the branch active power constraints can be expressed as follows:

$$\mu_{\theta_{ij}}(\theta ij) = \begin{cases} 1, & \text{if } \theta_{ij} \leq \theta_{ij\max} \\ L(\theta_{ij\max}, \theta'_{ij\max}; \theta_{ij}), & \text{if } \theta_{ij\max} \leq \theta_{ij} \leq \theta'_{ij\max} \\ 0, & \text{if } \theta_{ij} \geq \theta'_{ij\max} \end{cases} \qquad (9.48)$$
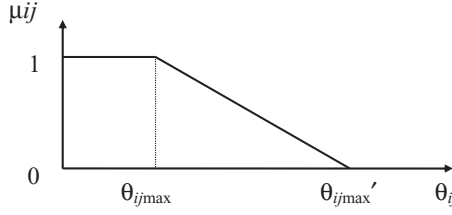
FIGURE 9.4 Fuzzy branch power flow constraint

where L is a droop function in which θ_{ijM}, θ'_{ijM} are its parameters and $L = 1$ when $\theta_{ij} = \theta_{ijM}$; $L = 0$ when $\theta_{ij} = \theta'_{ijM}$. The fuzzy branch power constraint is as shown in Figure 9.4, in which θ'_{ijM} represents the tapping limit of potentialities for the branch power capacity.

Substituting equation (9.29) into equations (9.46) and (9.47), and similarly changing each bilateral inequality constraint into two single inequality constraints, the fuzzy branch active power constraints can be expressed as follows:

$$[A_1][P] \leq [\theta] \tag{9.49}$$

where

$$[A_1] = [A]^{\mathrm{T}}[B']^{-1} \tag{9.50}$$

Dividing the matrix A_1 into the generator node submatrix and the load node submatrix, i.e., A_G and A_d, equation (9.49) can be written as follows.

$$[A_G][P_G] \leq [\theta_G] \tag{9.51}$$

where

$$[\theta_G] = [\theta] - [A_d][P_d] \tag{9.52}$$

According to Figure 9.4, equation (9.52) can be implemented with fuzzy operation under the λ-cut of fuzzy set (see below).

9.4.2.2 Definition of Steady-State Security Regions As defined in Section 9.3, the active power steady-state security regions can be represented by a set of active power injections, which satisfy the load flow equations and security constraints.

$$R_P = \{P/\exists \theta \in R, \text{ and } (f_P(\theta) = P) \in R\} \tag{9.53}$$

where R includes the set of fuzzy security constraints.

In addition, from the economic point of view, the operating regions expressed in terms of power injections may still be conservative. This is because load variations are allowed in constructing the regions, which can be known from the definition of power injection $P_i = P_{Gi} - P_{Di}$. The bigger the range of the load positive variations (i.e., increase), the smaller the obtained region is (i.e., more conservative). If the load demands are fixed at, say, the base values, a security region in terms of the generators, which is equivalent to the region of power injections under the load determination, can be considered.

9.4.3   Steady-State Security Regions with *N* – 1 Security

$N - 1$ security means that the line flows will not exceed the settings of protective devices for the intact lines when any branch has an outage. Many works have been done pertaining to $N - 1$ security in the study of power system economic dispatch [15–19], but less in the study of steady-state security regions.

The $N - 1$ steady-state security region is defined as a set of node power injections that satisfies not only the load flow equations and N security constraints, but also $N - 1$ security constraints.

$$R_{PN} = \{P/\exists\theta \in R_N, \text{ and } (f_P(\theta) = P) \in R_N\} \qquad (9.54)$$

where R_{PN} is the active power steady-state security regions with $N - 1$ security. R_N is the set of N and $N - 1$ security constraints.

Obviously, the crux of the $N - 1$ steady-state security regions is to perform the $N - 1$ security analysis (i.e., the calculation of $N - 1$ security constraints). The "$N - 1$ constrained zone," which is discussed in Chapter 5, will be coordinated with the steady-state security regions.

9.4.4   Consideration of Failure Probability of Branch Temporary Overload

In Section 9.4.2, we discussed the problem of tapping the potentialities of branch power flow capacity. In fact, it corresponds to the problem of whether the branch may temporarily overload in a practical power system under some case. Therefore, the value of θ'_{ijM}, which is the limit of the capability of tapping the potentialities for branch power capacity, will be determined according to the particular case of a practical power system.

Suppose the average overloading time of a branch is AOT. The average overloading ratio of the branch can be written as follows:

$$\eta_{ij} = \frac{1}{(\text{AOT})_{ij}} \quad ij \in NL \qquad (9.55)$$

It is assumed that the failure probability of branch temporary overloading is Poisson distributed. It can be expressed as
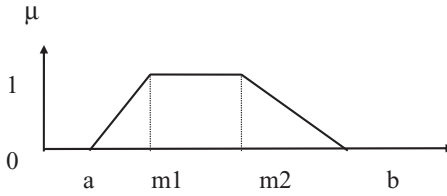
FIGURE 9.5   Trapezoidal fuzzy number

$$p_{ij} = 1 - e^{-\eta_{ij}T} \tag{9.56}$$

where p_{ij} is the failure probability of branch ij overload; T is system operation time.

Obviously, the average overloading time AOT of the branch is random and uncertain. It is dealt with a fuzzy number in this case. If AOT is a trapezoidal fuzzy number, as shown in Figure 9.5, the fuzzy number η_{ij} from equation (9.55) is also trapezoidal. Moreover, the fuzzy failure probability of branch temporary overload p_{ij} computed from equation (9.56) is also dealt with a trapezoidal fuzzy number.

The all-branches failure probability $p_{ij}(ij = 1, 2, \ldots\ldots NL)$ under any λ-cut of fuzzy set μ can be obtained from the equation (9.56). A ranking list, which reflects the relative capability of tapping potentialities for different branches, is acquired according to the value of p_{ij}. So the limit of the capability of tapping the potentialities for branch power capacity θ'_{ijM} can be determined easily according to the ranking list.

To acquire the higher security and reliability when fuzzy steady-state security regions are used in the practical operation of power systems, the branches with big failure probability will not be allowed to be temporarily overloaded. This it means that the branch power capacity of these branches cannot be changed, i.e., $\theta'_{ijM} = \theta_{ijM}$ in this case. Therefore, we give a performance index *PI*. If the failure probability of branch overload under the λ-cut of fuzzy set μ is bigger than *PI*, i.e.,

$$\mu_{pij} > PI \tag{9.57}$$

then the corresponding branches will not be allowed to be temporarily overloaded.

9.4.5   Implementation

In the enhanced expanding method, security constraints are divided into two groups and the expanding calculations are first carried out in the first group of constraints with small constraint margins. If the maximal region has not obtained after the calculation is finished in the first group, the expanding

computation will be continued in the second group until the security regions cannot be further expanded.

9.4.5.1 Method of Step-Size Calculation

Assuming that there are m inequalities in equation (9.47), in which the ith inequality constraint (under λ-cut of fuzzy set) is as follows:

$$\sum_j a_{Gij} P_{Gi} < \mu_{\theta ij}(\theta_{ij}) \quad i = 1, \dots, NG \tag{9.58}$$

Suppose Ω is a hyperbox, in which the generator power outputs are control variables. If not all summits of Ω have reached the boundary of R, Ω can still be expanded by solving the following m equations.

$$\sum_i a_{Gij} P_{Gi}^* = \mu_{\theta ij}(\theta_{ij}) \quad j = 1, \dots, m \tag{9.59}$$

where,

$$P_{Gi}^* = \begin{cases} P_{i\max} + \varepsilon, & \text{if } a_{Gij} > 0 \\ P_{i\min} - \varepsilon, & \text{if } a_{Gij} < 0 \\ 0, & \text{if } a_{Gij} = 0 \end{cases} \tag{9.60}$$

P_{Gi}^* and ε can be obtained from equation (9.60). Let $\varepsilon_{\min} = \min\{\varepsilon_j, j = 1, 2, \dots, m\}$, which is taken as the calculation step; the new expanding security region can be obtained as follows:

$$\Omega = \{P_G / P_{i\min}^* \leq P_{Gi} \leq P_{i\max}^*\} \quad i = 1, 2, \dots NG \tag{9.61}$$

$$P_{i\min}^* = P_{i\min} - \varepsilon_{\min} \tag{9.62}$$

$$P_{i\max}^* = P_{i\max} + \varepsilon_{\min} \tag{9.63}$$

9.4.5.2 Steps of New Expanding Method

The calculation steps of the new expanding method are given as follows [8].

Step (1): Select the generators operating point P_{Gi}^0 as the initial expanding point. Then the initial security regions can be expressed as

$$\Omega^0 = \{P_G | P_{i\min}^0 \leq P_{Gi} \leq P_{i\max}^0, i = 1, \dots, NG\} \tag{9.64}$$

$$P_{i\min}^0 = P_{i\max}^0 = P_{Gi}^0 \tag{9.65}$$

Let iteration number $K = 0$, and mark the variables (or indices) $V_i^M = V_i^m = 1$, $i = 1, \dots, NG$.

Step (2): obtain $\varepsilon_j(j = 1, \ldots, m)$ according to the method of step calculation (section 9.4.5.1). Then $\varepsilon_{\min}$ can be found. A threshold value is defined as follows:

$$\varepsilon_h = \frac{\varepsilon_{\min}}{\beta} \tag{9.66}$$

where β is a constant.

Then the m constraints will be divided into two groups based on the threshold value ε_h. Suppose that the number of constraints with $\varepsilon \le \varepsilon_h$ is m_1, which is called group one, and the number of constraints with $\varepsilon > \varepsilon_h$ is m_2, which is called group two.

Step (3): Calculate $\varepsilon_{\min}$ in m_1 constraints as Section 9.4.5.1. i.e.,

$$P_{Gi}^* = \begin{cases} P_{i\max} + \varepsilon, & \text{if } a_{Gij} > 0, \text{ and } V_i^M \neq 0 \\ P_{i\max} & \text{if } a_{Gij} > 0, \text{ and } V_i^M = 0 \\ P_{i\min} - \varepsilon, & \text{if } a_{Gij} < 0, \text{ and } V_i^m \neq 0 \\ P_{i\min}, & \text{if } a_{Gij} < 0, \text{ and } V_i^m = 0 \\ 0, & \text{if } a_{Gij} = 0 \end{cases} \tag{9.67}$$

then $\varepsilon_{\min} = \min\{\varepsilon_j\}$ $(j = 1, 2, \ldots, m_1)$,

Step (4). Let $K = k$; then the security regions can be obtained, i.e.,

$$\Omega^k = \{P_G | P_{i\min}^k \le P_{Gi} \le P_{i\max}^k, i = 1, \ldots, NG\} \tag{9.68}$$

$$P_{i\max}^k = P_{i\max}^{k-1} + \varepsilon_{\min} V_i^M \tag{9.69}$$

$$P_{i\min}^k = P_{i\min}^{k-1} - \varepsilon_{\min} V_i^m \tag{9.70}$$

Step (5): Find the inequality constraint with $\varepsilon_j = \varepsilon_{\min}$ and let the corresponding $V_i^M = V_i^m = 0$.

Step (6): Stop if $V_i^M = V_i^m = 0$ for all $i = 1, 2, \ldots, NG$. Otherwise, let $k = k + 1$, go back to step 3.

Step (7): If $k = m_1$ but some V_i^M and V_i^m are still not zero, steps 3–6 will be repeated in the second group of constraints, i.e., m_2 until $V_i^M = V_i^m = 0$ for all $i = 1, \ldots, NG$.

In this way, the maximal security regions are obtained as follows:

$$\Omega = \{P_G | P_{i\min} \le P_{Gi} \le P_{i\text{Max}}, i = 1, \ldots, NG\} \tag{9.71}$$

9.4.6 Test Results and Analysis

The enhanced steady-state security region technique including the model and its algorithm are tested with the IEEE 6-bus and 30-bus systems. Suppose the

system operation time is 150 hours. The performance index of branch failure probability PI is 0.085.

To enhance the calculation speed, the following two measures are adopted in the new expanding method. The first is the adoption of the calculation step (not fixed step), and the second is that the constraints are divided into two groups based on the threshold value shown in equation (9.54). Obviously, the value of β will produce some effects to expanding speed. We found from a great deal of numerical examples and calculations that satisfactory results can be obtained when β is selected as a gold separation constant, i.e., $\beta = 0.618$.

The IEEE 6-bus system contains 8 branches. The average overloading time (ACTs) of the branches are assumed as in Table 9.3. The failure probability of branch temporary overloading for the IEEE 6-bus system can be computed and shown in Table 9.4. It can be known from Table 9.4 that the values of failure probability for all branches are less than PI. It means that the power capacity for all branches in the IEEE 6-bus system can be tapped the potentialities. The fuzzy line power capacities are given as $P_{ij\max} = 1.0, 3.0, 3.0, 1.6, 1.6, 0.95, 3.0, 0.25$, respectively; and $P'_{ij\max} = 1.08$, respectively.

Table 9.3   Average overloading time for IEEE 6-bus system

Branch No.	AOT (h)			
	a	m_1	m_2	b
1	1834	1868	1898	1922
2	1888	1922	1959	2027
3	1845	1882	1907	1949
4	2081	2127	2150	2190
5	1992	2048	2081	2123
6	2108	2152	2196	2240
7	1888	1922	1959	2027
8	1854	1896	1919	1961

Table 9.4   Branch failure probability for IEEE 6-bus system

Branch No.	p_{ij}			
	a	m_1	m_2	b
1	0.075	0.076	0.077	0.079
2	0.071	0.074	0.075	0.076
3	0.074	0.076	0.077	0.078
4	0.066	0.067	0.067	0.070
5	0.068	0.070	0.070	0.072
6	0.065	0.066	0.067	0.069
7	0.071	0.074	0.075	0.076
8	0.074	0.075	0.076	0.078

The IEEE 30-bus system contains 41 branches. The corresponding average overloading time (AOTs) of the branches are assumed as in Table 9.5. The failure probability of branch temporary overloading for the IEEE 30-bus system can be computed and shown in Table 9.6.

It can be observed from Table 9.6 that the values of failure probability for branches 1, 2, 4, and 5 are bigger than *PI*. This means that the power capacity for these branches cannot be tapped the potentialities. The fuzzy line power capacities of the 30-bus test system are listed in Table 9.7.

The calculating results are shown in Tables 9.8–9.13. Tables 9.8 and 9.11 provide the calculation results of security regions for the IEEE 6-bus and 30-bus systems when the λ-cuts of fuzzy branch power capacity set $\mu(\theta ij)$ equal 0.0, 0.5, 0.6, and 1, respectively.

It can be found from Tables 9.8 and 9.11 that the bigger the value of λ-cut of fuzzy set $\mu(\theta ij)$, the higher will be the system reliability requirements and

Table 9.5   Average overloading time for IEEE 30-bus system

Branch No.	AOT (h)			
	a	m_1	m_2	b
1	1600	1640	1685	1725
2	1622	1655	1690	1750
3	1992	2048	2081	2123
4	1606	1640	1685	1725
5	1655	1690	1730	1780
6	1888	1922	1959	2027
7	1725	1750	1790	1834
8	2300	2365	2410	2470
9	1750	1800	1855	1888
Others	2300	2365	2410	2470

Table 9.6   Branch failure probability for IEEE 30-bus system

Branch No.	p_{ij}			
	a	m_1	m_2	b
1	0.0833	0.0852	0.0874	0.0895
2	0.0821	0.0849	0.0866	0.0883
3	0.0680	0.0700	0.0700	0.0720
4	0.0833	0.0852	0.0874	0.0892
5	0.0808	0.0831	0.0849	0.0866
6	0.0710	0.0740	0.0750	0.0760
7	0.0790	0.0804	0.0821	0.0833
8	0.0589	0.0603	0.0615	0.0631
9	0.0760	0.0777	0.0800	0.0821
Others	0.0589	0.0603	0.0615	0.0631

Table 9.7 Fuzzy line power capacities for IEEE 30-bus system

Branch No.	$P_{ij\max}$ (p.u.)	$P'_{ij\max}$ (p.u.)
1	1.30	1.30
2	1.30	1.30
3	0.65	0.80
4	1.30	1.30
5	1.30	1.30
6	0.60	0.80
7	0.90	1.20
8	0.70	1.00
9	1.30	1.50
Others #A	0.65	0.80
Others #B	0.32	0.50
Others #C	0.16	0.25

#A—the power capacities of these lines are 0.65.
#B—the power capacities of these lines are 0.32.
#C—the power capacities of these lines are 0.16.

Table 9.8 Results for security regions on IEEE 6-bus system (p.u.)

λ-Cut	Regions	PG4	PG5	PG6
1	$P_{i\max}$	3.9760	2.4240	3.8990
	$P_{i\min}$	2.0250	0.4740	0.0000
0.6	$P_{i\max}$	3.9755	2.4245	4.5480
	$P_{i\min}$	1.7010	0.1500	0.0000
0.5	$P_{i\max}$	3.9755	2.4245	4.7100
	$P_{i\min}$	1.6200	0.0693	0.0000
0	$P_{i\max}$	3.9755	2.4245	5.1849
	$P_{i\min}$	1.2151	0.000	0.0000

Table 9.9 Comparison of security region results for IEEE 6-bus system (p.u.)

Method	Regions	PG4	PG5	PG6
Method 1	$P_{i\max}$	3.9760	2.4240	3.8990
	$P_{i\min}$	2.0250	0.4740	0.0000
Method 2	$P_{i\max}$	3.7500	2.6490	2.5510
	$P_{i\min}$	2.4490	1.4000	0.0000

Method 1: enhanced expanding method.
Method 2: traditional expanding method.

Table 9.10   Results for $N-1$ security regions on IEEE 6-bus system

Gen. Node	Base Value P^0	Security $P_{i\min}$	Regions $P_{i\max}$
PG4	2.514	2.378	3.301
PG5	1.523	1.369	1.654
PG6	2.363	1.400	2.645

Table 9.11   Results for security regions on IEEE 30-bus system (p.u.)

λ-Cut		1	0.6	0.5	0.0
P_{G2}	$P_{i\max}$	0.7350	0.7550	0.7600	0.7710
	$P_{i\min}$	0.3712	0.3700	0.3656	0.3513
P_{G5}	$P_{i\max}$	0.4622	0.4733	0.4744	0.4895
	$P_{i\min}$	0.1500	0.1500	0.1500	0.1500
P_{G8}	$P_{i\max}$	0.3500	0.3500	0.3500	0.3500
	$P_{i\min}$	0.1110	0.1080	0.1000	0.1000
P_{G11}	$P_{i\max}$	0.3000	0.3000	0.3000	0.3000
	$P_{i\min}$	0.1000	0.1000	0.1000	0.1000
P_{G13}	$P_{i\max}$	0.4000	0.4000	0.4000	0.4000
	$P_{i\min}$	0.1200	0.1200	0.1200	0.1200

Table 9.12   Comparison of security region results for IEEE 30-bus system (p.u.)

Method	Method 1		Method 2	
Regions	$P_{\max}$	$P_{\min}$	$P_{\max}$	$P_{\min}$
P_{G2}	0.7350	0.3712	0.7120	0.4280
P_{G5}	0.4622	0.1500	0.4020	0.1500
P_{G8}	0.3500	0.1110	0.3500	0.1480
P_{G11}	0.3000	0.1000	0.3000	0.1000
P_{G13}	0.4000	0.1200	0.4000	0.1770

Method 1: enhanced expanding method.
Method 2: traditional expanding method.

Table 9.13   Results for $N-1$ security regions on IEEE 30-bus system (p.u.)

Gen. Node	Base Value P_{Gi}^0	Lower Bound of Regions $P_{i\min}$	Upper Bound of Regions $P_{i\max}$
P_{G2}	0.566	0.2000	0.7350
P_{G5}	0.293	0.1500	0.3500
P_{G8}	0.306	0.1000	0.3500
P_{G11}	0.154	0.1540	0.1600
P_{G13}	0.295	0.2950	0.3000

the smaller will be the acquired security regions. On the contrary, the smaller the value of λ-cut of fuzzy set μ(θ*ij*), the lower will be the system reliability requirements and the larger will be the acquired security regions. Therefore, it is very convenient to select the corresponding security regions to judge whether the power system operation is secure according to the given reliability requirements.

Tables 9.9 and 9.12 are the comparisons of results for the IEEE 6-bus and 30-bus systems with previous work. It can be observed from Tables 9.9 and 9.12 that steady-state security regions without the fuzzy line power flow capacity constraints (i.e., the value of λ-cut of fuzzy set μ(θ*ij*) = 1) computed by enhanced method are bigger than those computed by the general expanding method. Therefore, power security regions in this section are relatively less conservative than those of the previous work.

Tables 9.10 and 9.13 provide the calculation results of $N-1$ security regions for the IEEE 6-bus and 30-bus systems when the λ-cut of fuzzy branch power capacity set μ(θ*ij*) equals 1. It can be observed that the $N-1$ security regions for both 6-bus and 30-bus systems are far smaller than N security regions. Especially for the IEEE 30-bus system, the range of expanding for generators 11 and 13 is almost zero in the calculation of $N-1$ security regions. The reason is that the feasible region became narrow because of the introduction of $N-1$ security constraints.

The results show that it is very important to calculate security regions with fuzzy line power flow constraints. It can provide more information for real-time security analysis and security operation in power system compared with the previous methods. This is because different reliability requirements correspond to different security regions with fuzzy constraint, while only one reliability requirement corresponds to one security region in the previous method. Because of the adoption of the new expanding method, the computing time is also shorter than that of the traditional expansion method.

9.5 FUZZY SET AND LINEAR PROGRAMMING

9.5.1 Introduction

This section presents a new approach to constructing the steady-state security regions of power systems, i.e., the maximal security regions are directly computed with optimization method [13, 14]. First of all, the security regions model is converted into a linear programming (LP) optimization model, in which the upper and lower limits of each component forming hyperbox are taken as unknown variables, and the objective is to maximize the sum of generator' power adjustment ranges. The fuzzy branch power constraints and the $N-1$ security constraints are also introduced into the optimization model of the steady-state security regions. The IEEE 6-bus and 30-bus systems are used as test examples.

9.5.2 Steady-State Security Regions Solved by LP

9.5.2.1 Objective Function In the practical operation of power systems, it is desired to obtain each security region to cover as many points of operation as possible. This means that it is desired to make the volume of the hyperbox as big as possible. However, it will be very complicated if the volume of the hyperbox is directly taken as an objective function. In fact, there exists some approximately corresponding relation between the size of the hyperbox's volume and the sum of all sides of the hyperbox. Especially for the practical operation of power systems, operators are mainly concerned about the secure and adjustable range of generator power output, rather than the size of Ω_P's volume. Therefore, in the optimization model for Ω_P, we do not directly select the volume of Ω_P as an objective function. The objective for optimization calculation Ω_P is to maximize the sum of generators' power adjustment ranges, i.e.,

$$\text{Max} Z = \sum_{i=\text{nd}+1}^{n-1} W_i \big(P_{Gi}^M - P_{Gi}^m \big) \tag{9.72}$$

where W_i is the weighting coefficient of the ith generator.

$\big(P_{Gi}^M - P_{Gi}^m \big)$ is the secure and adjustable range of the ith generator power output. It is also the length of the ith side of hyperbox. Obviously, it must satisfy the rated adjustable range of the ith generator power output $(P_{Gi\max} - P_{Gi\min})$, i.e.,

$$\big(P_{Gi}^M - P_{Gi}^m \big) \le (P_{Gi\max} - P_{Gi\min}) \tag{9.73}$$

9.5.2.2 Security Constraints In the optimization calculation of hyperbox Ω_P, the unknown variables are upper and lower limits of each component in hyperbox Ω_P. This is different from the ordinary expanding method. Therefore, the constraints for constructing Ω_P must be changed in the optimization method.

(1) Generation constraints
   According to the definition of security regions, we get

$$P_{Gi} \ge P_{Gi}^m \ge P_{Gi\min} \quad i = n_d + 1, \ldots\ldots, n - 1 \tag{9.74}$$

$$P_{Gi} \le P_{Gi}^M \le P_{Gi\max} \quad i = n_d + 1, \ldots\ldots, n - 1 \tag{9.75}$$

where buses $1 \sim n_d$ are PQ buses, buses $n_d + 1 \sim n - 1$ are PV buses, and the nth bus is the slack bus.
   For the slack generator, we have the following equations:

$$\sum_{i=1}^{nd} P_i - \sum_{i=nd+1}^{n-1} P_{Gi}^{M} = P_{Gnm} \tag{9.76}$$

$$\sum_{i=1}^{nd} P_i - \sum_{i=nd+1}^{n-1} P_{Gi}^{m} = P_{GnM} \tag{9.77}$$

where P_{Gnm} and P_{GnM} are the lower and upper limits of the slack generator, respectively.

(2) Branch constraints

According to equation (9.39), the security constraints of branch ij can be written as

$$\theta_{ij\,\min} \leq \sum_{k=nd+1}^{n-1} (A_{ik} - A_{jk})P_{Gk} \leq \theta_{ij\,\max} \tag{9.78}$$

For equation (9.78), the power injection of the kth generator P_{Gk} can be replaced by P_{Gk}^{m} and P_{Gk}^{M} under the following conditions:

$$P_{Gk} = \begin{cases} P_{Gk}^{m}, & \text{when} \quad A_{ik} - A_{jk} \geq 0 \\ P_{Gk}^{M}, & \text{when} \quad A_{ik} - A_{jk} \leq 0 \end{cases} \tag{9.79}$$

In this way, the unknown variables in security constraints are all changed into P_{Gk}^{m} and P_{Gk}^{M} ($k = n_{d}+1, \ldots\ldots, n-1$).

9.5.2.3 Linear Programming Model and Implementation

9.5.2.3.1 LP Model for Computing Ω_P According to equations (9.72)–(9.79), the optimization model for computing Ω_P is set up, i.e., model M-1,

$$\text{Max}Z = \sum_{k=nd+1}^{n-1} W_k(P_{Gk}^{M} - P_{Gk}^{m}) \tag{9.80}$$

subject to constraints in equations (9.73)–(9.79)

Obviously, M-1 is a linear programming model. It can be expressed by the standard form of linear programming, i.e., model M-2

$$\text{Max}Z = CX \tag{9.81}$$

such that

$$AX \leq B \tag{9.82}$$

$$X \geq 0 \tag{9.83}$$

Model M-2 can be solved by simplex method. The details of the LP algorithm are shown in the Appendix to this chapter.

9.5.2.3.2 Calculation of Security Regions Wthout Basic Operation Point
The steady-state security regions can be obtained directly through solving model M-1 without a basic operation point. With this method, it is very convenient to judge whether there a security region exists under the given operation state. Meanwhile, it is easy to find the "security center point" of power system operation when security region Ω_P is obtained. Therefore, this method can provide useful information for system operation.

9.5.2.3.3 Calculation of Security Regions Considering Basic Operation Point
As described in the previous paragraph, the biggest hyperbox Ω_P can be acquired when the basic operation point has not been considered in the calculation of security regions. However, in some cases, it is possible that the obtained hyperbox Ω_P has not covered the basic operation point. Thus this Ω_P is not practical. For this reason, we introduce the following constraints into model M-1, i.e.,

$$[P_G^M] \geq [P_{G0}] \tag{9.84}$$

$$[P_G^m] \leq [P_{G0}] \tag{9.85}$$

where $[P_{G0}]$ is the basic operation point.

Then we can obtain optimization model M-3, which considers the basic operation point $[P_{G0}]$, i.e.,

$$\text{Max} Z = \sum_{k=\text{nd}+1}^{n-1} W_k (P_{Gk}^M - P_{Gk}^m) \tag{9.86}$$

sbject to constraints in equations (9.73)–(9.79), (9.84), and (9.85)

In this way, the hyperbox Ω_P obtained from model M-3 certainly covers $[P_{G0}]$. If there a solution does not exist in M-3, then we can judge that the given operation point $[P_{G0}]$ is not secure.

It is noted that the optimal solution of LP is certainly located at the summit on the feasible region. So, at some cases, it is possible that $[P_{G0}]$ will be located at some boundary of the hyperbox Ω_P, although Ω_P contains the $[P_{G0}]$. This means that the security adjustable amount of the generator at some direction in Ω_P is zero in this situation. In other cases, although $[P_{G0}]$ is in Ω_P and is also not at the boundary of Ω_P, it is possible that the security adjustable amount of the generator at some direction in Ω_P is very small. Under the above-mentioned cases, it is very difficult to judge whether the operation point is still secure when some perturbation occurs in the power system operation. For this reason, we adopt the following constraints to remedy this disadvantage.

$$[P_G^M] \ge [P_{G0}] + [\Delta P_{G0}] \tag{9.87}$$

$$[P_G^m] \le [P_{G0}] + [\Delta P_{G0}] \tag{9.88}$$

where $[\Delta P_{G0}]$ is the vector of generation power deviation from basic operation point $[P_{G0}]$. This is an estimate value and can be determined according to the requirements of system operation and experiences of operators.

Introducing constraints (9.87) and (9.88) into M-1, the new optimization model M-4 for computing Ω_P can be expressed as follows.

$$\text{Max} Z = \sum_{k=n_d+1}^{n-1} W_k \left(P_{Gk}^M - P_{Gk}^m \right) \tag{9.89}$$

such that

$$\left(P_{Gi}^M - P_{Gi}^m \right) \le \left(P_{Gi\max} - P_{Gi\min} \right) \tag{9.90}$$

$$P_{Gi} \ge P_{Gi}^m \ge P_{G\min} \quad i = n_d + 1, \ldots\ldots, n-1 \tag{9.91}$$

$$P_{Gi} \le P_{Gi}^M \le P_{Gi\max} \quad i = n_d + 1, \ldots\ldots, n-1 \tag{9.92}$$

$$\left(\sum_{i=1}^{n_d} P_i - \sum_{i=n_d+1}^{n-1} P_{Gi}^M \right) = P_{Gnm} \tag{9.93}$$

$$\left(\sum_{i=1}^{n_d} P_i - \sum_{i=n_d+1}^{n-1} P_{Gi}^m \right) = P_{GnM} \tag{9.94}$$

$$\theta_{ij\min} \le \sum_{k=n_d+1}^{n-1} \left(A_{ik} - A_{jk} \right) P_{Gk} \le \theta_{ij\max} \tag{9.95}$$

$$P_{Gk} = \begin{cases} P_{Gk}^m, & \text{when} \quad A_{ik} - A_{jk} \ge 0 \\ P_{Gk}^M, & \text{when} \quad A_{ik} - A_{jk} \le 0 \end{cases} \tag{9.96}$$

$$[P_G^M] \ge [P_{G0}] + [\Delta P_{G0}] \tag{9.97}$$

$$[P_G^m] \le [P_{G0}] + [\Delta P_{G0}] \tag{9.98}$$

The above model is a linear model, which can be solved by a linear programming algorithm.

9.5.3 Numerical Examples

9.5.3.1 *Comparison of LP and Expanding Method for Ω_P* The calculation of the maximal security region, hyperbox Ω_P, by the optimization method is examined with the IEEE 6-bus and 30-bus systems.

To assess or compare the size of Ω_P for different means, the following performance index is introduced:

$$PI = \frac{\sum\limits_{i=n_d+1}^{n-1} \left(P_{Gi}^{M} - P_{Gi}^{m} \right)}{\sum\limits_{i=n_d+1}^{n-1} \left(P_{Gi\max} - P_{Gi\min} \right)} \qquad (9.99)$$

or

$$PI_i = \frac{P_{Gi}^{M} - P_{Gi}^{m}}{P_{Gi\max} - P_{Gi\min}} \quad i = n_d + 1, \ldots, n-1 \qquad (9.100)$$

The calculation results for a steady-state security region are given in Tables 9.14 and 9.15, where the optimization approach for constructing the maximal security region is identified as method 1 and the expanding method is identified as method 2. Table 9.14 represents the results for security regions on the IEEE 6-bus system. Table 9.15 represents the results for security regions on the IEEE 30-bus system. For comparison, we also use the traditional expanding method to calculate the maximal security region for the IEEE 30-bus

Table 9.14   Comparison of security region results for IEEE 6-bus system

Methods	Security Regions	Generator PG4	Generator PG5	Total PI%
Method 1	P_{Gi}^{M}	4.200	2.200	71%
	P_{Gi}^{m}	0.184	1.378	
	$PI_i\%$	96%	31%	
Method 2	P_{Gi}^{M}	3.750	2.649	37%
	P_{Gi}^{m}	2.449	1.400	
	$PI_i\%$	31%	47%	

Method 1: optimization method.
Method 2: the expanding method.

Table 9.15   Comparison of security region results for IEEE 30-bus system

Methods	Security Regions	Gen. PG2	Gen. PG5	Gen. PG8	Gen. PG11	Gen. PG13	Total PI%
Method 1	P_{Gi}^{M}	0.800	0.500	0.350	0.300	0.384	85%
	P_{Gi}^{m}	0.439	0.150	0.100	0.100	0.120	
	$PI_i\%$	80%	100%	100%	100%	94%	
Method 2	P_{Gi}^{M}	0.712	0.402	0.350	0.300	0.400	70%
	P_{Gi}^{m}	0.428	0.150	0.148	0.100	0.177	
	$PI_i\%$	47%	72%	81%	100%	80%	

Method 1 is optimization method.
Method 2 is the expanding method.

system under the same system parameters and conditions. The results are listed in Table 9.15.

From Tables 9.14 and 9.15, we know that the security region Ω_P obtained by the optimization method in this section is far bigger than that obtained by the traditional expanding method described in Section 9.3. Therefore, the conservation of the maximal security regions computed based on the optimization approach is relatively small. The computation time needed in this approach is also very short (only 1.1 second for IEEE 6-bus system, and 4.37 seconds for IEEE 30-bus system).

The calculation results and comparison show that the linear programming method is superior to the expanding method for computing security regions.

9.5.3.2 Applying LP for Ω_P Considering Fuzzy Constraints

The optimization computation of steady-state security region with fuzzy constraints is examined with the IEEE 6-bus system. The parameters of systems including the fuzzy branch power capacities, the branch average contingency time (ACTs), probability of branch temporary overload are the same as those in Section 9.3. Suppose the system operation time is 150 hours. The performance index of branch failure probability *PI* is 0.085.

Table 9.16 provides the calculation results of security regions for the IEEE 6-bus system when the λ-cut of fuzzy branch power capacity set $\mu(\theta ij)$ equals 0.0, 0.5, 0.6, and 1, respectively.

It can be observed from Table 9.16 that the bigger the value of the λ-cut of fuzzy set $\mu(\theta ij)$, the higher will be the system reliability requirements and the smaller will be the acquired security regions. On the contrary, the smaller the value of the λ-cut of fuzzy set $\mu(\theta ij)$, the lower will be the system reliability requirements and the larger will be the acquired security regions. Therefore, it is very convenient to select the corresponding security regions to judge whether the power system operation is secure according to the given reliability requirements.

Calculation of security regions with fuzzy line power flow constraints can provide more information for real-time security analysis and security

Table 9.16 Results for security regions on IEEE 6-bus system (p.u.)

λ-Cut	Regions	PG4	PG5	PG6
1	P_{Gi}^M	4.2000	2.2240	3.8990
	P_{Gi}^m	0.1840	1.3700	0.0000
0.6	P_{Gi}^M	4.0050	2.2245	4.5480
	P_{Gi}^m	0.1701	1.1500	0.0000
0.5	P_{Gi}^M	4.0050	2.2245	4.7100
	P_{Gi}^m	0.1620	1.0693	0.0000
0	P_{Gi}^M	3.9755	2.4245	5.1849
	P_{Gi}^m	0.1215	1.000	0.0000

operation in power system compared with existing methods. Because of the adoption of the optimization method, the computing time of security regions is also shorter than that of the expanding methods.

APPENDIX: LINEAR PROGRAMMING

Linear programming (LP) is widely used in power systems problem. Hence, we briefly describe the basic algorithm of LP [22–28].

Standard Form of LP

Not all linear programming problems are so easily solved. There may be many variables and many constraints. Some variables may be constrained to be non-negative and others unconstrained. Some of the main constraints may be equalities and others inequalities. However, two classes of problems, called here the standard maximum problem and the standard minimum problem, play a special role. In these problems, all variables are constrained to be non-negative, and all main constraints are inequalities.

Given an m-vector, $b = (b_1, \ldots, b_m)^T$, an n-vector, $c = (c_1, \ldots, c_n)^T$, and an $m \times n$ matrix,

$$A = \begin{pmatrix} a_{11} & a_{12} & \ldots & a_{1n} \\ a_{21} & a_{22} & \ldots & a_{2n} \\ \vdots & \vdots & \ddots & \vdots \\ a_{m1} & a_{m1} & \ldots & a_{mn} \end{pmatrix}$$

The standard maximum problem of the linear programming can be formulated as follows:

$$\text{maximize} \quad c_1 x_1 + c_2 x_2 + \cdots + c_n x_n$$

$$\text{subject to} \quad a_{11} x_1 + a_{12} x_2 + \cdots + a_{1n} x_n \leq b_1$$

$$a_{21} x_1 + a_{22} x_2 + \cdots + a_{2n} x_n \leq b_2$$

$$\cdots$$

$$a_{m1} x_1 + a_{m2} x_2 + \cdots + a_{mn} x_n \leq b_m$$

$$x_1, x_2, \ldots x_n \geq 0$$

or

$$\text{Max} \quad c^T x$$

$$\text{s.t.} \quad Ax \leq b$$

$$x \geq 0$$

We shall always use m to denote the number of constraints and n to denote the number of decision variables.

The standard minimum problem of the linear programming can be formulated as follows:

$$\text{minimize} \quad y_1 b_1 + y_2 b_2 + \cdots + y_m b_m$$

$$\text{subject to} \quad y_1 a_{11} + y_2 a_{12} + \cdots + y_m a_{m1} \geq c_1$$

$$y_1 a_{12} + y_2 a_{22} + \cdots + y_m a_{m2} \geq c_2$$

$$\cdots$$

$$y_1 a_{1n} + y_2 a_{2n} + \cdots + y_m a_{mn} \geq c_n$$

$$y_1, y_2, \ldots y_m \geq 0$$

or

$$\text{Min} \quad y^{\mathrm{T}} b$$

$$\text{s.t.} \quad y^{\mathrm{T}} A \geq c$$

$$y \geq 0$$

The following terminologies are used in LP:

- The function to be maximized or minimized is called the objective function.
- A vector, x for the standard maximum problem or y for the standard minimum problem, is said to be feasible if it satisfies the corresponding constraints.
- The set of feasible vectors is called the constraint set.
- A linear programming problem is said to be feasible if the constraint set is not empty; otherwise it is said to be infeasible.
- A feasible maximum (resp. minimum) problem is said to be unbounded if the objective function can assume arbitrarily large positive (resp. negative) values at feasible vectors; otherwise, it is said to be bounded. Thus there are three possibilities for a linear programming problem. It may be bounded feasible, it may be unbounded feasible, and it may be infeasible.
- The value of a bounded feasible maximum (resp, minimum) problem is the maximum (resp. minimum) value of the objective function as the variables range over the constraint set.
- A feasible vector at which the objective function achieves the value is called optimal.

Example A1

The following linear programming problem:

$$\text{maximize} \quad 7x_1 + 5x_2$$
$$\text{subject to} \quad x_1 + x_2 \le 1$$
$$-3x_1 - 3x_2 \le -15$$
$$x_1, x_2 \ge 0$$

Indeed, the second constraint implies that $x_1 + x_2 \ge 5.0$, which contradicts the first constraint. If a problem has no feasible solution, then the problem itself is called **infeasible**.

At the other extreme from infeasible problems, one finds unbounded problems. A problem is **unbounded** if it has feasible solutions with arbitrarily large objective values. For example, consider

$$\text{maximize} \quad 3x_1 - 4x_2$$
$$\text{subject to} \quad -2x_1 + 3x_2 \le -1$$
$$-x_1 - 2x_2 \le -5$$
$$x_1, x_2 \ge 0$$

Here, we could set x_2 to zero and let x_1 be arbitrarily large. As long as x_1 is greater than 5 the solution will be feasible, and as it gets larger the objective function does, too. Hence, the problem is unbounded. In addition to finding optimal solutions to linear programming problems, we shall also be interested in detecting when a problem is infeasible or unbounded.

A linear programming problem was defined as maximizing or minimizing a linear function subject to linear constraints. All such problems can be converted into the form of a standard maximum problem by the following techniques.

A minimum problem can be changed to a maximum problem by multiplying the objective function by –1. Similarly, constraints of the form $\sum_{j=1}^{n} a_{ij} x_j \ge b_i$ can be changed into the form $\sum_{j=1}^{n} (-a_{ij}) x_j \le -b_i$. Two other problems arise.

(1) Some constraints may be equalities. An equality constraint $\sum_{j=1}^{n} a_{ij} x_j = b_i$ may be removed by solving this constraint for some x_j for which $a_{ij} \ne 0$ and substituting this solution into the other constraints and into the objective function wherever x_j appears. This removes one constraint and one variable from the problem.

(2) Some variables may not be restricted to be nonnegative. An unrestricted variable, x_j, may be replaced by the difference of two non-negative variables, $x_j = u_j - v_j$, where $u_j \geq 0$ and $v_j \geq 0$. This adds one variable and two nonnegativity constraints to the problem.

Any theory derived for problems in standard form is therefore applicable to general problems. However, from a computational point of view, the enlargement of the number of variables and constraints in (2) is undesirable and, as will be seen later, can be avoided.

Duality

For every linear program there is a dual linear program with which it is intimately connected. We first state this duality for the standard programs.

Definition: The dual of the standard maximum problem

$$\text{maximize } c^T x \tag{9A.1}$$

$$\text{subject to the constraints } Ax \geq b$$

$$\text{and} \quad x \geq 0$$

is defined to be the standard minimum problem

$$\text{minimize } y^T b \tag{9A.2}$$

$$\text{subject to the constraints } y^T A \leq c^T$$

$$\text{and} \quad y \geq 0$$

Example A2

Find x_1 and x_2 to maximize $2x_1 + x_2$ subject to the constraints $x_1 \geq 0$, $x_2 \geq 0$, and

$$3x_1 + 2x_2 \leq 9$$

$$4x_1 + 3x_2 \leq 18$$

$$-x_1 + x_2 \leq 2$$

The dual of this standard maximum problem is therefore the standard minimum problem: Find y_1, y_2, and y_3 to minimize $9y_1 + 18y_2 + 2y_3$ subject to the constraints $y_1 \geq 0$, $y_2 \geq 0$, $y_3 \geq 0$, and

$$3y_1 + 4y_2 - y_3 \geq 2$$

$$2y_1 + 3y_2 + y_3 \geq 1$$

If the standard minimum problem (A2) is transformed into a standard maximum problem (by multiplying $A, b,$ and c by -1), its dual by the definition above is a standard minimum problem that, when transformed to a standard maximum problem (again by changing the signs of all coefficients) becomes exactly (A1). Therefore, the dual of the standard minimum problem (A2) is the standard maximum problem (A1). The problems (A1) and (A2) are said to be duals.

The general standard maximum problem and the dual standard minimum problem may be simultaneously exhibited in the display:

	x_1	x_2	$\cdots$	x_n	
y_1	a_{11}	a_{12}	$\ldots$	a_{1n}	$\leq b_1$
y_2	a_{21}	a_{22}	$\ldots$	a_{2n}	$\leq b_2$
$\vdots$	$\vdots$	$\vdots$	$\ddots$	$\vdots$	$\vdots$
y_m	a_{m1}	a_{m2}	$\ldots$	a_{mn}	$\leq b_m$
	$\geq c_1$	$\geq c_2$	$\cdots$	$\geq c_n$	

(9A.3)

The relation between a standard problem and its dual is seen in the following theorem and its corollaries.

Theorem 1: If x is feasible for the standard maximum problem (9A.1) and if y is feasible for its dual (A2), then

$$c^{\mathrm{T}}x \leq y^{\mathrm{T}}b \tag{9A.4}$$

Proof:

$$c^{\mathrm{T}}x = y^{\mathrm{T}}Ax \leq y^{\mathrm{T}}b$$

The first inequality follows from $x \geq 0$ and $c^{\mathrm{T}} \leq y^{\mathrm{T}}A$. The second inequality follows from $y \geq 0$ and $Ax \leq b$.

Corollary 1: If a standard problem and its dual are both feasible, then both are bounded feasible.

Proof: If y is feasible for the minimum problem, then (9A.4) shows that $y^{\mathrm{T}}b$ is an upper bound for the values of $c^{\mathrm{T}}x$ for x feasible for the maximum problem, and similarly for the converse.

Corollary 2: If there exists feasible x^* and y^* for a standard maximum problem (9A.1) and its dual (9A.2) such that $c^{\mathrm{T}}x^* = y^{*\mathrm{T}}b$, then both are optimal for their respective problems.

Proof: If x is any feasible vector for (9A.1), then $c^{\mathrm{T}}x \le y^{*\mathrm{T}}b = c^{\mathrm{T}}x^*$, which shows that x^* is optimal. A symmetric argument works for y^*.

The following fundamental theorem completes the relationship between a standard problem and its dual. It states that the hypotheses of Corollary 2 are always satisfied if one of the problems is bounded feasible.

The Duality Theorem: If a standard linear programming problem is bounded feasible, then so is its dual; their values are equal, and there exist optimal vectors for both problems.

As a corollary of the Duality Theorem we have the **Equilibrium Theorem**. Let x^* and y^* be feasible vectors for a standard maximum problem (9A.1) and its dual (9A.2), respectively. Then x^* and y^* are optimal if and only if

$$y_i^* = 0 \quad \text{for all } i \text{ for which } \sum_{j=1}^{n} a_{ij}x_j^* < b_i \tag{9A.5}$$

and

$$x_j^* = 0 \quad \text{for all } j \text{ for which } \sum_{i=1}^{m} y_i^* a_{ij} > c_j \tag{9A.6}$$

Proof: For first part "If"
If equation (9A.5) implies that $y_i^* = 0$ unless there is equality in $\sum_{j=1}^{n} a_{ij}x_j^* < b_i$, thus

$$\sum_{i=1}^{m} y_i^* b_i = \sum_{i=1}^{m} y_i^* \sum_{j=1}^{n} a_{ij}x_j^* = \sum_{i=1}^{m} \sum_{j=1}^{n} y_i^* a_{ij}x_j^* \tag{9A.7}$$

Similarly from equation (9A.6), we have

$$\sum_{i=1}^{m} \sum_{j=1}^{n} y_i^* a_{ij}x_j^* = \sum_{j=1}^{n} c_j x_j^* \tag{9A.8}$$

According to Corollary 2, the x^* and y^* are optimal.
For second part "Only If"
As in the first line of the proof of Theorem 1

$$\sum_{j=1}^{n} c_j x_j^* \le \sum_{i=1}^{m} \sum_{j=1}^{n} y_i^* a_{ij}x_j^* \le \sum_{i=1}^{m} y_i^* b_i \tag{9A.9}$$

By the duality theorem, if $x*$ and $y*$ are optimal, the left side is equal to the right side so we get equality throughout. The equality of the first and second terms may be written as

$$\sum_{j=1}^{n}\left(c_j - \sum_{i=1}^{m} y_i^* a_{ij}\right)x_j^* = 0 \qquad (9A.10)$$

Since $x*$ and $y*$ are feasible, each term in this sum is nonnegative. The sum can be zero only if each term is zero. Thus if $\sum_{i=1}^{m} y_i^* a_{ij} > c_j$, then $x_j^* = 0$. A symmetric argument shows that if $\sum_{j=1}^{n} a_{ij} x_j^* < b_i$, then $y_i^* = 0$.

Equations (9A.5) and (9A.6) are sometimes called the complementary slackness conditions. They require that a strict inequality (a slackness) in a constraint in a standard problem implies that the complementary constraint in the dual be satisfied with equality.

The Simplex Method

Before we present the simplex method for solving a linear programming problem, we look at the following example first to illustrate how the simplex method works.

Example A3

$$\text{maximize} \quad 5x_1 + 4x_2 + 3x_3$$
$$\text{subject to} \quad 2x_1 + 3x_2 + x_3 \le 5$$
$$4x_1 + x_2 + 2x_3 \le 11$$
$$3x_1 + 4x_2 + 2x_3 \le 8$$
$$x_1, x_2, x_3 \ge 0$$

We start by adding so-called **slack variables**. For each of the less-than inequalities in the above problem we introduce a new variable that represents the difference between the right-hand side and the left-hand side. For example, for the first inequality,

$$2x_1 + 3x_2 + x_3 \le 5$$

we introduce the slack variable w_1 defined by

$$w_1 = 5 - 2x_1 - 3x_2 - x_3$$

so that the inequality becomes equality, that is,

$$2x_1 + 3x_2 + x_3 + w_1 = 5$$

It is clear then that this definition of w_1, together with the stipulation that w_1 be nonnegative, is equivalent to the original constraint. We carry out this procedure for each of the less-than constraints to get an equivalent representation of the problem:

$$\text{maximize} \quad y = 5x_1 + 4x_2 + 3x_3 \qquad\qquad (9A.11)$$
$$\text{subject to} \quad w_1 = 5 - 2x_1 - 3x_2 - x_3$$
$$w_2 = 11 - 4x_1 - x_2 - 2x_3$$
$$w_3 = 8 - 3x_1 - 4x_2 - 2x_3$$
$$x_1, x_2, x_3, w_1, w_2, w_3 \geq 0$$

Note that we have included a notation, y, for the value of the objective function, $5x_1 + 4x_2 + 3x_3$.

The simplex method is an iterative process in which we start with a solution $x_1, x_2, x_3, w_1, w_2, w_3$ that satisfies the equations and nonnegativities in the above equivalent problem and then look for a new solution $x_1', x_2', x_3', w_1', w_2', w_3'$, which is better in the sense that it has a larger objective function value

$$5x_1' + 4x_2' + 3x_3' > 5x_1 + 4x_2 + 3x_3$$

We continue this process until we arrive at a solution that cannot be improved. This final solution is then an optimal solution.

To start the iterative process, we need an initial feasible solution $x_1, x_2, x_3,$ w_1, w_2, w_3. For our example, this is easy. We simply set all the original variables to zero and use the defining equations to determine the slack variables

$$x_1 = 0, \quad x_2 = 0, \quad x_3 = 0, \quad w_1 = 5, \quad w_2 = 11, \quad w_3 = 8$$

The objective function value associated with this solution is $y = 0$.

We now ask whether this solution can be improved. Since the coefficient of x_1 is positive, if we increase the value of x_1 from zero to some positive value, we will increase y. But as we change its value, the values of the slack variables will also change. We must make sure that we do not let any of them go negative. Since $x_2 = x_3 = 0$, we see that $w_1 = 5 - 2x_1$, and so keeping w_1 nonnegative imposes the restriction that x_1 must not exceed 5/2. Similarly, the nonnegativity of w_2 imposes the bound that $x_1 \leq 11/4$, and the nonnegativity of w_3 introduces the bound that $x_1 \leq 8/3$. Since all of these conditions must be met, we see that x_1 cannot be made larger than the smallest of these bounds: $x_1 \leq 5/2$. Our new, improved solution then is

$$x_1 = 5/2, \quad x_2 = 0, \quad x_3 = 0, \quad w_1 = 0, \quad w_2 = 1, \quad w_3 = 1/2$$

This first step was straightforward. It is less obvious how to proceed. What made the first step easy was the fact that we had one group of variables that were initially zero and we had the rest explicitly expressed in terms of these. This property can be arranged even for our new solution. Indeed, we simply must rewrite the equations in (9A.11) in such a way that x_1, w_2, w_3, and y are expressed as functions of w_1, x_2, and x_3. That is, the roles of x_1 and w_1 must be swapped. To this end, we use the equation for w_1 in (9A.11) to solve for x_1

$$x_1 = \frac{5}{2} - \frac{1}{2}w_1 - \frac{3}{2}x_2 - \frac{1}{2}x_3$$

The equations for w_2, w_3, and y must also be doctored so that x_1 does not appear on the right. The easiest way to accomplish this is to do so-called **row operations** on the equations in the equivalent problem. For example, if we take the equation for w_2 and subtract two times the equation for w_1 and then bring the w_1 term to the right-hand side, we get

$$w_2 = 1 + 2w_1 + 5x_2$$

Performing analogous row operations for w_3 and ζ, we can rewrite the equations in (9A.11) as

$$y = 12.5 - 2.5w_1 - 3.5x_2 + 0.5x_3$$
$$x_1 = 2.5 - 0.5w_1 - 1.5x_2 - 0.5x_3$$
$$w_2 = 1 + 2w_1 + 5x_2 \qquad (9A.12)$$
$$w_3 = 0.5 + 1.5w_1 + 0.5x_2 - 0.5x_3$$

Note that we can recover our current solution by setting the "independent" variables to zero and using the equations to read off the values for the "dependent" variables.

Now we see that increasing w_1 or x_2 will bring about a *decrease* in the objective function value, and so x_3, being the only variable with a positive coefficient, is the only independent variable that we can increase to obtain a further increase in the objective function. Again, we need to determine how much this variable can be increased without violating the requirement that all the dependent variables remain nonnegative. This time we see that the equation for w_2 is not affected by changes in x_3, but the equations for x_1 and w_3 do impose bounds, namely, $x_3 \leq 5$ and $x_3 \leq 1$, respectively. The latter is the tighter bound, and so the new solution is

$$x_1 = 2, \quad x_2 = 0, \quad x_3 = 1, \quad w_1 = 0, \quad w_2 = 1, \quad w_3 = 0.$$

The corresponding objective function value is $y = 13$.

Once again, we must determine whether it is possible to increase the objective function further and, if so, how. Therefore, we need to write our equations with y, x_1, w_2, and x_3 written as functions of w_1, x_2, and w_3. Solving the last equation in (9A.12) for x_3, we get

$$x_3 = 1 + 3w_1 + x_2 - 2w_3.$$

Also, performing the appropriate row operations, we can eliminate x_3 from the other equations. The result of these operations is

$$\zeta = 13 - w_1 - 3x_2 - w_3$$
$$x_1 = 2 - 2w_1 - 2x_2 + w_3$$
$$w_2 = 1 + 2w_1 + 5x_2$$
$$x_3 = 1 + 3w_1 + x_2 - 2w_3$$

(9A.13)

We are now ready to begin the third iteration. The first step is to identify an independent variable for which an increase in its value would produce a corresponding increase in y. But this time there is no such variable, since all the variables have negative coefficients in the expression for ζ. This fact not only brings the simplex method to a standstill but also proves that the current solution is optimal. The reason is quite simple. Since the equations in (9A.13) are completely equivalent to those in (9A.11) and since all the variables must be nonnegative, it follows that $y \leq 13$ for every feasible solution. Since our current solution attains the value of 13, we see that it is indeed optimal.

Now for the standard maximum problem, the simplex method is presented as below. First of all, we add the slack variables $w = b - Ax$. The problem becomes: Find x and w to maximize $c^T x$ subject to $x \geq 0$, $u \geq 0$, and $u = b - Ax$.

We may use the following tableau to solve this problem if we write the constraint $w = b - Ax$ as $-w = Ax - b$.

	x_1	x_2	$\cdots$	x_n	-1
$-w_1$	a_{11}	a_{12}	$\cdots$	a_{1n}	b_1
$-w_2$	a_{21}	a_{22}	$\cdots$	a_{2n}	b_2
$\vdots$	$\vdots$	$\vdots$	$\ddots$	$\vdots$	$\vdots$
$-w_m$	a_{m1}	a_{m2}	$\cdots$	a_{mn}	b_m
	$-c_1$	$-c_2$	$\cdots$	$-c_n$	0

(9A.14)

We note as before that if $-c \geq 0$ and $b \geq 0$, then the solution is obvious: $x = 0$, $w = b$, and value equal to zero (since the problem is equivalent to minimizing $-c^T x$).

Suppose we want to pivot to interchange w_1 and x_1 and suppose $a_{11} = 0$. The equations

$$-w_1 = a_{11}x_1 + a_{12}x_2 + \cdots + a_{1n}x_n - b_1$$

$$-w_2 = a_{21}x_1 + a_{22}x_2 + \cdots + a_{2n}x_n - b_2$$

$$\cdots$$

$$-w_m = a_{m1}x_1 + a_{m2}x_2 + \cdots + a_{mn}x_n - b_m$$

become

$$-x_1 = \frac{1}{a_{11}}w_1 + \frac{a_{12}}{a_{11}}x_2 + \frac{a_{1n}}{a_{11}}x_n - \frac{b_1}{a_{11}}$$

$$-w_2 = -\frac{a_{21}}{a_{11}}w_1 + \left(a_{22} - \frac{a_{21}a_{12}}{a_{11}}\right)x_2 + \cdots \text{etc.}$$

In other words, the same pivot rule applies

$$\begin{pmatrix} p & r \\ c & q \end{pmatrix} \Rightarrow \begin{pmatrix} 1/p & r/p \\ -c/p & q-(rc/p) \end{pmatrix}$$

If you pivot until the last row and column (exclusive of the corner) are nonnegative, you can find the solution to the dual problem and the primal problem at the same time.

Let $x_{n+i} = w_i$, then we have $n + m$ variables x. Initially, we have n nonbasic variables $N = \{1, 2, \ldots, n\}$ (i.e., $x_1, \ldots, x_n$) and m basic variables $B = \{n + 1, n + 2, \ldots, n + m\}$ (i.e., $x_{n+1}, \ldots, x_{n+m}$).

Within each iteration of the simplex method, exactly one variable goes from nonbasic to basic and exactly one variable goes from basic to nonbasic. The variable that goes from nonbasic to basic is called the **entering variable**. It is chosen with the aim of increasing y, that is, one whose coefficient is positive: pick k from $\{j \in N : c_j' > 0\}$, where N is the set of nonbasic variables. Note that if this set is empty, then the current solution is optimal. If the set consists of more than one element (as is normally the case), then we have a choice of which element to pick. There are several possible selection criteria. Generally, we pick an index k having the largest coefficient (which again could leave us with a choice).

The variable that goes from basic to nonbasic is called the **leaving variable**. It is chosen to preserve nonnegativity of the current basic variables. Once we have decided that x_k will be the entering variable, its value will be increased from zero to a positive value. This increase will change the values of the basic variables.

$$x_i = b_i' - a_{ik}' x_k, \quad i \in B$$

We must ensure that each of these variables remains nonnegative. Hence, we require that

$$b_i' - a_{ik}' x_k \geq 0, \quad i \in B$$

Of these expressions, the only ones that can go negative as x_k increases are those for which a_{ik}' is positive; the rest remain fixed or increase. Hence, we can restrict our attention to those i's for which a_{ik}' is positive. And for such an i, the value of x_k at which the expression becomes zero is

$$x_k = \frac{b_i'}{a_{ik}'}$$

Since we do not want any of these to go negative, we must raise x_k only to the smallest of all of these values

$$x_k = \min_i \left(\frac{b_i'}{a_{ik}'} \right), \quad i \in B, a_{ik}' > 0$$

Therefore, with a certain amount of latitude remaining, the rule for selecting the leaving variable is pick l from $\{ i \in B: a_{ik}' > 0$ and b_i'/a_{ik}' is minimal$\}$.

The rule just given for selecting a leaving variable describes exactly the process by which we use the rule in practice. That is, we look only at those variables for which a_{ik}' is positive and among those we select one with the smallest value of the ratio b_i'/a_{ik}'.

This same "method" may be used to solve the dual problem—the standard minimum problem: Find y to minimize $y^T b$ subject to $y \geq 0$ and $y^T A \geq c^T$.

Similarly, we convert the inequalities into equalities by adding slack variables $s^T = y^T A - c^T \geq 0$. The problem can be restated: Find y and s to minimize $y^T b$ subject to $y \geq 0$, $s \geq 0$ and $s^T = y^T A - c^T$.

We write this problem in a tableau to represent the linear equations $s^T = y^T A - c^T$.

	s_1	s_2	$\cdots$	s_n	
y_1	a_{11}	a_{12}	$\ldots$	a_{1n}	b_1
y_2	a_{21}	a_{22}	$\ldots$	a_{2n}	b_2
$\vdots$	$\vdots$	$\vdots$	$\ddots$	$\vdots$	$\vdots$
y_m	a_{m1}	a_{m2}	$\ldots$	a_{mn}	b_m
1	$-c_1$	$-c_2$	$\cdots$	$-c_n$	0

(9A.15)

The last column represents the vector whose inner product with y we are trying to minimize.

If $-c \geq 0$ and $b \geq 0$, there is an obvious solution to the problem: namely, the minimum occurs at $y = 0$ and $s = -c$, and the minimum value is $y^T b = 0$. This is feasible since $y \geq 0$, $s \geq 0$, and $s^T = y^T A - c$, and yet $\Sigma y_i b_i$ cannot be made any smaller than 0, since $y \geq 0$, and $b \geq 0$.

Suppose then we cannot solve this problem so easily because there is at least one negative entry in the last column or last row. (exclusive of the corner). Let us pivot about a_{11} (suppose $a_{11} \neq 0$), including the last column and last row in our pivot operations, we get:

$$
\begin{array}{c|cccc|c}
 & y_1 & s_2 & \cdots & s_n & \\
\hline
y_1 & a'_{11} & a'_{12} & \ldots & a'_{1n} & b'_1 \\
y_2 & a'_{21} & a'_{22} & \ldots & a'_{2n} & b'_2 \\
\vdots & \vdots & \vdots & \ddots & \vdots & \vdots \\
y_m & a'_{m1} & a'_{m2} & \ldots & a'_{mn} & b'_m \\
\hline
1 & -c'_1 & -c'_2 & \cdots & -c'_n & v'
\end{array}
\tag{9A.16}
$$

Let $r = (r_1, \ldots, r_n) = (y_1, s_2, \ldots, s_n)$ denote the variables on top, and let $t = (t_1, \ldots, t_m) = (s_1, y_2, \ldots, y_m)^T$ denote the variables on the left. The set of equations are represented by the new tableau. Moreover, the objective function $y^T b$ may be written (replacing y_1 by its value in terms of s_1)

$$
\begin{aligned}
\sum_{i=1}^{m} y_i b_i &= \frac{b_1}{a_{11}} s_1 + \left(b_2 - \frac{a_{21} b_1}{a_{11}} \right) y_2 + \cdots + \left(b_m - \frac{a_{m1} b_1}{a_{11}} \right) y_2 + \frac{c_1 b_1}{a_{11}} \\
&= t^T b' + v'
\end{aligned}
\tag{9A.17}
$$

This is represented by the last column in the new tableau. We have transformed our problem into the following: Find vectors y and s, to minimize $t^T b'$ subject to $y \geq 0$, $s \geq 0$, and $r = t^T A' - c'$ (where t^T represents the vector $s_1, y_2, \ldots, y_m$, and r represents the vector $y_1, s_2, \ldots, s_n$).

Again, if $-c' \geq 0$ and $b' \geq 0$, we have the obvious solution: $t = 0$ and $r = -c'$ with value v'.

Similar to the standard maximum problem solved by the simplex method, this process will be continued until the optimal solution is obtained.

REFERENCES

[1] E. Hnyilicza, S.T.Y. Lee, and F.C. Schweppe, "Steady-State Security Regions: Set-Theoretic Approach," Proc., PICA Conference, pp. 347–355, 1975.

[2] R. Fischl, G.C. Ejebe, and J.A. DeMaio, "Identification of Power System Steady-State Security Regions under Load Uncertainty," IEEE Summer Power Meeting, Paper A76 495-2. *IEEE Trans on PAS* Vol. 95, No. 6, p. 1767, 1976.

[3] J.A. DeMaio and R. Fischl, "Fast Identification of the Steady-State Security Regions for Power System Security Enhancement," IEEE Winter Power Meeting, A.76076-0. *IEEE Trans. on PAS*, Vol. 95, No. 3, p. 758, 1976.

[4] F.D. Galiana and M.H. Banakar, "Approximation formula for dependent load flow variables," Paper F80 200-6, IEEE Winter Conference, New York, Feb. 1980.

[5] M.H. Banakar and F.D. Galiana, "Power System Security Corridors Concept and Computation," *IEEE Trans., PAS*, Vol. 100, pp. 4524–4532, 1981.

[6] F.F. Wu and S. Kumagai, "Steady-State Security regions of Power System," *IEEE Trans., CAS*, Vol. 29, pp. 703–711, 1982.

[7] C.C. Liu, "A New Method for Construction of Maximal Steady-State Regions of Power Systems," *IEEE Trans. PWRS*. Vol. 4, pp. 19–27, 1986.

[8] J.Z. Zhu, "A new expanding method to real power steady-state security regions of power system," Proceedings of Chinese Youth Excellent Science & Technology Papers, 1994, pp. 664–668, Science Press.

[9] J.Z. Zhu and G.Y. Xu, "Application of network theory with fuzzy to real power steady-state security regions," *Power Systems & Automation*, Vol. 5, No. 3, pp. 23–32, 1994.

[10] R.Q. Fan, J.Z. Zhu, and G.Y. Xu, "Power steady-state security regions with loads change," *Power Systems & Automation*, Vol. 5, No. 4, pp. 39–46, 1994.

[11] Y. Li, J.Z. Zhu, and G.Y. Xu, "Study of power system steady-state regions," *Proceedings of Chinese Society of Electrical Engineering*, Vol. 13, No. 2, 1993, pp. 15–22.

[12] J.Z. Zhu and C.S. Chang, "A new approach to steady-state security regions with N and N − 1 security," 1997 Intern. Power Eng. Conf., IPEC 97, Singapore, May, 1997.

[13] J.Z. Zhu, R.Q. Fan, G.Y. Xu, and C.S. Chang, "Construction of maximal steady-state security regions of power systems using optimization method," *Electric Power Systems Research*, Vol. 44, 1998, pp. 101–105.

[14] J.Z. Zhu, "Optimal power systems steady-state security regions with fuzzy constraints." Proceedings of IEEE Winter Meeting, New York, Jan. 27–30, 2002, Paper No. 02WM033.

[15] B. Stott and J.C. Marinho, "Linear Programming for Power System Network Security Applications," *IEEE Trans., PAS*, Vol. 98, pp. 837–848, 1979.

[16] E. Hobson, D.L. Fletcher, and W.O. Stadlin, "Network flow linear programming techniques and their application to fuel scheduling and contingency analysis," *IEEE Trans., PAS*, 1984, Vol. 103, pp. 1684–1691.

[17] A.J. Elacqua and S.L. Corey, "Security constrained dispatch at the New York power pool," *IEEE Trans., PAS*, 1982, Vol. 101, pp. 2876–2884.

[18] J.Z. Zhu and G.Y. Xu, "A New Economic Power Dispatch Method with Security," *Electric Power Systems Research*, Vol. 25, pp. 9–15, 1992.

[19] J.Z. Zhu and M.R. Irving, "Combined Active and Reactive Dispatch with Multiple Objectives using an Analytic Hierarchical Process," *IEE Proceedings, Part C*, Vol. 143, pp. 344–352, 1996.

[20] J.Z. Zhu and G.Y. Xu, "A Unified Model and Automatic Contingency Selection Algorithm for the P and Q Subproblems, *Electric Power Systems Research*," Vol. 32, pp. 101–105, 1995.

[21] J.Z. Zhu and G.Y. Xu, "Approach to Automatic Contingency Selection by Reactive Type Performance Index," *IEE Proceedings, Part C*, Vol. 138, pp. 65–68, 1991.

[22] T.S. Ferguson, *Linear Programming*, Academic Press, 1967.

[23] G.B. Dantzig, *Linear Programming and Extensions*, Princeton University Press, 1963.

[24] R.J. Vanderbei, *Linear Programming: Foundations and Extensions*, Kluwer, Boston, 1996.

[25] D.G. Luenberger, *Introduction to Linear and Nonlinear Programming*, Addison-Wesley Publishing Company, Inc. USA, 1973.

[26] G. Hadley, *Linear Programming*, Addison–Wesley, Reading, MA, 1962.

[27] J.K. Strayer, *Linear Programming and Applications*, Springer-Verlag, 1989.

[28] M. Bazaraa, J. Jarvis, and H. Sherali, *Linear Programming and Network Flows*, 2 edn, Wiley, New York. 1977.

10

REACTIVE POWER OPTIMIZATION

This chapter first introduces the concept of reactive power optimization and the classic method for reactive power dispatch. Then it addresses improved interior points, optimization neural network, evolutionary algorithm, and particle swarm optimization and their practical application in reactive power optimization. The analysis and calculation of reactive power pricing are also introduced in this chapter.

10.1   INTRODUCTION

The objectives of reactive power (VAR) optimization are to improve the voltage profile, to minimize system active power losses, and to determine optimal VAR compensation placement under various operating conditions. To achieve these objectives, power system operators utilize control options such as adjusting generator excitation, transformer tap changing, shunt capacitors, and SVC. However, the size of power systems and prevailing constraints produce strenuous circumstances for system operators to correct voltage problems at any given time. In such cases, there is certainly a need for decision-making tools in predominantly fluctuating and uncertain computational environments. There has been a growing interest in VAR optimization problems over the last decade [1–31]. Most conventional methods used in VAR optimization are based on linear programming and nonlinear programming. Some simplified treatments in these methods may induce local minima.

Recently, new methods based on artificial intelligence have been used in VAR optimization and VAR planning [17–29] such as an artificial neural network (ANN), expert system, genetic algorithms (GAs), and evolutionary programming (EP). EP and GAs are good methods to obtain global optimal optimizations. However, the excessive time consumption of EP and GAs will limit their applications in power systems, especially during real-time operation.

10.2 CLASSIC METHOD FOR REACTIVE POWER DISPATCH

10.2.1 Reactive Power Balance

The voltage profile of power system operation is determined by reactive power balance in the system. That is,

$$\sum_{i=1}^{NG} Q_{Gi} + \sum_{j=1}^{NC} Q_{Cj} = \sum_{k=1}^{ND} Q_{dk} + Q_{L} \tag{10.1}$$

where

Q_{Gi}: The reactive power generation of generator i

Q_{Cj}: The reactive power generation of the VAR compensation device j such as capacitor, SVC, etc.

Q_{dk}: The reactive power load at load bus k

Q_{L}: System reactive power loss. It includes the reactive power loss of transformer and transmission lines.

According to the experience of practical operations, the reactive power loss of transformer can be computed with the following approximated formula [30].

$$Q_{LT} = \frac{I_0\%}{100} S_N + \frac{V_S\%S^2}{100S_N} \left(\frac{V_N}{V}\right)^2 \tag{10.2}$$

where

Q_{LT}: The reactive power loss of the transformer

S_N: The rated MVA power of the transformer

V_N: The rated voltage of the transformer

$V_S\%$: The short-circuit voltage of the transformer

$I_0\%$: The no-load current of the transformer

V: The operation voltage of the transformer

The reactive power loss of transmission line ij can be computed as below:

$$Q_{LI} = \frac{P_i^2 + Q_i^2}{V_i^2} X - \frac{V_i^2 + V_j^2}{2} B \tag{10.3}$$

where

Q_{LI}: The reactive power loss of the transmission line
P_i: The real power at end i of the line
Q_i: The reactive power at end i of the line
V_i: The voltage at end i of transmission line ij
V_j: The voltage at end j of transmission line ij
X: The reactance of the line
B: The equivalent susceptance of the line (to ground)

10.2.2   Reactive Power Economic Dispatch

The purpose of the reactive power economic dispatch is to make the system real power loss minimal through determining the reactive power output of each reactive power source under the constraint condition of the system load demands.

The system real power loss can be represented as below:

$$P_L = P_L(P_1, P_2, \dots, P_n, Q_1, Q_2, \dots, Q_n) \tag{10.4}$$

For the classic reactive power dispatch problem, the real power outputs of the generators are already known, and the constraint is reactive power balance equation, that is,

$$\sum_{i=1}^{M} Q_{Gi} = Q_D + Q_L \tag{10.5}$$

For simplification, Q_G in equation (10.5) includes all reactive power sources such as generator, capacitor, SVC, etc.

Construct the Lagrange function for equations (10.4) and (10.5):

$$L = P_L - \lambda \left(\sum_{i=1}^{M} Q_{Gi} - Q_D - Q_L \right) \tag{10.6}$$

The necessary conditions for the extreme value of the Lagrange function are to set the first derivative of the Lagrange function with respect to each of the independent variables (Q_G and λ) equal to zero.

$$\frac{\partial L}{\partial Q_{Gi}} = \frac{\partial P_L}{\partial Q_{Gi}} - \lambda\left(1 - \frac{\partial Q_L}{\partial Q_{Gi}}\right) = 0 \quad i = 1, 2, \ldots, M$$

$$\frac{\partial L}{\partial \lambda} = -\left(\sum_{i=1}^{M} Q_{Gi} - Q_D - Q_L\right) = 0$$

(10.7)

From equation (10.7), we get

$$\frac{\partial P_L}{\partial Q_{Gi}} \times \frac{1}{\left(1 - \dfrac{\partial Q_L}{\partial Q_{Gi}}\right)} = \frac{\partial P_L}{\partial Q_{Gi}}\beta_i = \lambda \quad i = 1, 2, \ldots, N$$

$$\beta_i = \frac{1}{\left(1 - \dfrac{\partial Q_L}{\partial Q_{Gi}}\right)}$$

(10.8)

where

$\dfrac{\partial P_L}{\partial Q_{Gi}}$: The incremental rate of the system real power loss with respect to the reactive power source i

$\dfrac{\partial Q_L}{\partial Q_{Gi}}$: The incremental rate of the system reactive power loss with respect to the reactive power source i

Equation (10.8) is the formula of reactive power economic dispatch. It has the same form as equation (4.61) in Chapter 4.

The incremental loss rate $\dfrac{\partial P_L}{\partial Q_{Gi}}$ and $\dfrac{\partial Q_L}{\partial Q_{Gi}}$ can be computed by the impedance matrix method, which is shown below.

The system loss can be expressed as:

$$P_L + jQ_L = V^{T}\hat{I} = (ZI)^{T}\,\hat{I} = I^{T}Z^{T}\hat{I}$$

(10.9)

$$I = I_P + jI_Q$$

(10.10)

$$Z = R + jX$$

(10.11)

where

I: The current vector
$\hat{I}$: The conjugate current vector
V: The voltage vector
Z: The impedance matrix

Substituting equations (10.10) and (10.11) into equation (10.9), we get

$$P_{\mathrm{L}} = \sum_{i=1}^{n}\sum_{k=1}^{n} R_{jk}(I_{\mathrm{P}j}I_{\mathrm{P}k} + I_{\mathrm{Q}j}I_{\mathrm{Q}k}) \tag{10.12}$$

$$Q_{\mathrm{L}} = \sum_{i=1}^{n}\sum_{k=1}^{n} X_{jk}(I_{\mathrm{P}j}I_{\mathrm{P}k} + I_{\mathrm{Q}j}I_{\mathrm{Q}k}) \tag{10.13}$$

The relationship between injection power and current is

$$P_i + jQ_i = (V_i\cos\theta_i + jV_i\sin\theta_i)(I_{\mathrm{P}i} - jI_{\mathrm{Q}i}) \tag{10.14}$$

Then we get

$$I_{\mathrm{P}i} = (P_i\cos\theta_i + jQ_i\sin\theta_i)/V_i \tag{10.15}$$

$$I_{\mathrm{Q}i} = (P_i\sin\theta_i - jQ_i\cos\theta_i)/V_i \tag{10.16}$$

Substituting equations (10.15) and (10.16) into equations (10.12) and (10.13), we get

$$P_{\mathrm{L}} = \sum_{i=1}^{n}\sum_{k=1}^{n}[\alpha_{jk}(P_jP_k + Q_jQ_k) + \beta_{jk}(Q_jP_k - P_jQ_k)] \tag{10.17}$$

$$Q_{\mathrm{L}} = \sum_{i=1}^{n}\sum_{k=1}^{n}[\delta_{jk}(P_jP_k + Q_jQ_k) + \gamma_{jk}(Q_jP_k - P_jQ_k)] \tag{10.18}$$

where

$$\alpha_{jk} = \frac{R_{jk}}{V_jV_k}\cos(\theta_j - \theta_k) \tag{10.19}$$

$$\beta_{jk} = \frac{R_{jk}}{V_jV_k}\sin(\theta_j - \theta_k) \tag{10.20}$$

$$\delta_{jk} = \frac{X_{jk}}{V_jV_k}\cos(\theta_j - \theta_k) \tag{10.21}$$

$$\delta_{jk} = \frac{X_{jk}}{V_jV_k}\sin(\theta_j - \theta_k) \tag{10.22}$$

From equation (10.17), we get

$$\frac{\partial P_{\rm L}}{\partial P_i} = \sum_{i=1}^{n}\sum_{k=1}^{n}\frac{\partial}{\partial P_i}[\alpha_{jk}(P_jP_k + Q_jQ_k) + \beta_{jk}(Q_jP_k - P_jQ_k)]$$

$$= 2\sum_{k=1}^{n}(P_k\alpha_{ik} - Q_k\beta_{ik}) + \sum_{i=1}^{n}\sum_{k=1}^{n}\left[(P_jP_k + Q_jQ_k)\frac{\partial\alpha_{jk}}{\partial P_i} + \beta_{jk}(Q_jP_k - P_jQ_k)\frac{\beta_{jk}}{\partial P_i}\right]$$

$$(10.23)$$

The second term in equation (10.23) is very small, so it can be neglected. We get

$$\frac{\partial P_{\rm L}}{\partial P_i} \approx 2\sum_{k=1}^{n}(P_k\alpha_{ik} - Q_k\beta_{ik}) \tag{10.24}$$

In the high-voltage network, the angle difference of $\theta_j - \theta_k$ is very small. This means that $\sin(\theta_j - \theta_k) \approx 0$. Thus β_{jk} can be neglected. Then we have

$$\frac{\partial P_{\rm L}}{\partial P_i} \approx 2\sum_{k=1}^{n}P_k\alpha_{ik} \tag{10.25}$$

Similarly, we get

$$\frac{\partial P_{\rm L}}{\partial Q_i} \approx 2\sum_{k=1}^{n}Q_k\alpha_{ik} \tag{10.26}$$

$$\frac{\partial Q_{\rm L}}{\partial P_i} \approx 2\sum_{k=1}^{n}P_k\delta_{ik} \tag{10.27}$$

$$\frac{\partial Q_{\rm L}}{\partial Q_i} \approx 2\sum_{k=1}^{n}Q_k\delta_{ik} \tag{10.28}$$

Considering real power load and reactive power load are constant, we have

$$dP_i = d(P_{{\rm G}i} - P_{{\rm D}i}) = dP_{{\rm G}i} \tag{10.29}$$

$$dQ_i = d(Q_{{\rm G}i} - Q_{{\rm D}i}) = dQ_{{\rm G}i} \tag{10.30}$$

Thus equations (10.25)–(10.28) can be written as

$$\frac{\partial P_{\rm L}}{\partial P_{{\rm G}i}} \approx 2\sum_{k=1}^{n}P_k\alpha_{ik} \tag{10.31}$$

$$\frac{\partial P_{\rm L}}{\partial Q_{{\rm G}i}} \approx 2\sum_{k=1}^{n}Q_k\alpha_{ik} \tag{10.32}$$

$$\frac{\partial Q_{\rm L}}{\partial P_{{\rm G}i}} \approx 2\sum_{k=1}^{n}P_k\delta_{ik} \tag{10.33}$$

$$\frac{\partial Q_L}{\partial Q_{Gi}} \approx 2\sum_{k=1}^{n} Q_k \delta_{ik} \qquad (10.34)$$

If the system has enough reactive power sources, the steps of reactive power economic dispatch are [30]:

(1) Perform the calculation of power flow, using the results of real power economic dispatch. Thus the real power outputs of generators are fixed except for the reference unit.
(2) Compute λ for each reactive power source, using the above results as well as equations (10.32) and (10.34). If $\lambda < 0$, it means that system loss can be reduced by increasing this reactive power source. If $\lambda > 0$, it means that system loss will be increased if increasing this reactive power source. Thus, in order to reduce the system loss, we must increase the reactive power outputs for the reactive power resources with $\lambda < 0$ and reduce the reactive power outputs for the reactive power resources with $\lambda > 0$. Each time, select a source with minimum λ to increase output if $\lambda < 0$, and select a source with maximum λ to reduce the output if $\lambda < 0$, and then recompute power flow.
(3) Through the calculation of power flow, we get system loss. According to step (1), the change of real power loss is reflected in the power change of the reference unit. The reactive power dispatch will be continued until the power of the reference unit cannot be reduced.

It is noted that the following reactive power generation limits are not considered in the above calculation:

$$Q_{Gi\min} \leq Q_{Gi} \leq Q_{Gi\max} \qquad (10.35)$$

If they are considered, we need to check the constraints in equation (10.9). If the reactive power source has violation, set the reactive power output of this source to its corresponding limit. Then this source will not be considered in the rest of reactive power dispatch.

This is just a simple method for reactive power economic dispatch. A more complex reactive power optimization problem that contains network constraints is introduced in the following sections.

10.3   LINEAR PROGRAMMING METHOD OF VAR OPTIMIZATION

Reactive power optimization is a nonlinear optimization problem. If we consider network security constraints and bus voltage constraints, VAR optimization becomes a complex optimization problem. The linearization of the VAR optimization model is frequently adopted in conventional methods.

10.3.1   VAR Optimization Model

From Chapter 3, the optimal VAR control model M-1 that is to determine the optimum VAR support or compensation can be represented as:

$$\min P_L(Q_S, V_G, T) \qquad (10.36)$$

such that

$$Q(Q_S, V_G, T, V_D) = 0 \qquad (10.37)$$

$$Q_{Gmin} \le Q_G(Q_S, V_G, T) \le Q_{Gmax} \qquad (10.38)$$

$$V_{Dmin} \le V_D(Q_S, V_G, T) \le V_{Dmax} \qquad (10.39)$$

$$Q_{Smin} \le Q_S \le Q_{Smax} \qquad (10.40)$$

$$V_{Gmin} \le V_G \le V_{Gmax} \qquad (10.41)$$

$$T_{min} \le T \le T_{max} \qquad (10.42)$$

where

P_L: The system real power loss
V_G: The voltage magnitude at generator buses
Q_S: The VAR support in the system
Q_G: The VAR generation in the system
T: The tap position of the transformer
V_D: The voltage magnitude at load buses

The subscripts "min" and "max" in model M-1 represent the lower and upper limits of the constraint, respectively.

As in the classical reactive power dispatch method in Section 10.2, it is assumed that the real power dispatch (economic dispatch) is performed separately and real power generation (except at the slack bus) is regarded as constant in optimal VAR control. So the decoupled optimal constraints are considered in the above model M-1, in which equation (10.37) is the reactive power flow balance equation and equations (10.38) and (10.39) are the constraints of state variables Q_G and V_D. Equations (10.40)–(10.42) are the constraints of control variables.

The nonlinear VAR control problem M-1 can be successively linearized and rewritten as the following incremental model M-2, which is represented by a sensitivity matrix:

$$\min \Delta P_L = S_{LQ}^T \Delta Q_S + S_{LV}^T \Delta V_G + S_{LT}^T \Delta T \qquad (10.43)$$

such that

$$Q(\Delta Q_S, \Delta V_G, \Delta T, \Delta V_D) = 0 \tag{10.44}$$

$$\Delta Q_{Gmin} \le S_{QQ}\Delta Q_S + S_{QV}\Delta V_G + S_{QT}\Delta T \le Q_{Gmax} \tag{10.45}$$

$$\Delta V_{Dmin} \le S_{VQ}\Delta Q_S + S_{VV}\Delta V_G + S_{VT}\Delta T \le \Delta V_{Dmax} \tag{10.46}$$

$$\Delta Q_{Smin} \le \Delta Q_S \le Q_{Smax} \tag{10.47}$$

$$\Delta V_{Gmin} \le \Delta V_G \le \Delta V_{Gmax} \tag{10.48}$$

$$\Delta T_{min} \le \Delta T \le \Delta T_{max} \tag{10.49}$$

where S_{LQ}, S_{LV}, S_{LT} are the sensitivity matrices of real transmission losses to VAR compensation, voltage magnitude at generator buses, and transformer tap position, respectively. S_{QQ}, S_{QV}, S_{QT} are the sensitivity matrices of reactive power at generator buses to VAR compensation, voltage magnitude at generator buses, and transformer tap position, respectively. S_{VQ}, S_{VV}, S_{VT} are the sensitivity matrices of voltage magnitude at load buses to VAR compensation, voltage magnitude at generator buses, and transformer tap position, respectively.

The incremental variables in equations (10.43)–(10.49) can be obtained by iterative calculation as below:

$$\Delta Q_S = Q_S^{k+1} - Q_S^k \tag{10.50}$$

$$\Delta V_G = V_G^{k+1} - V_G^k \tag{10.51}$$

$$\Delta T = T^{k+1} - T^k \tag{10.52}$$

$$\Delta Q_{Gmax} = Q_{Gmax} - Q_G^k \tag{10.53}$$

$$\Delta Q_{Gmin} = Q_{Gmin} - Q_G^k \tag{10.54}$$

$$\Delta Q_{Smax} = Q_{Smax} - Q_S^k \tag{10.55}$$

$$\Delta Q_{Smin} = Q_{Smin} - Q_S^k \tag{10.56}$$

$$\Delta V_{Gmax} = V_{Gmax} - V_G^k \tag{10.57}$$

$$\Delta V_{Gmin} = V_{Gmin} - V_G^k \tag{10.58}$$

$$\Delta V_{Dmax} = V_{Dmax} - V_D^k \tag{10.59}$$

$$\Delta V_{Dmin} = V_{Dmin} - V_D^k \tag{10.60}$$

$$\Delta T_{max} = T_{max} - T^k \tag{10.61}$$

$$\Delta T_{min} = T_{min} - T^k \tag{10.62}$$

10.3.2 Linear Programming Method Based on Sensitivity

We first compute the sensitivity matrix mentioned in Section 10.3.1 before we solve VAR optimization model M-2. Reactive power generation and load can be represented as functions of bus voltage and transformer tap, respectively. That is.

$$Q_G = Q_G(V_D, V_G, T) = 0 \tag{10.63}$$

$$Q_D = Q_D(V_D, V_G, T) = 0 \tag{10.64}$$

From the above two equations, we get the following sensitivity matrices:

$$S_{VQ} = \left[\frac{\partial Q_D}{\partial V_D}\right]^{-1} \tag{10.65}$$

$$S_{VV} = \left[\frac{\partial V_D}{\partial V_G}\right] = -\left[\frac{\partial Q_D}{\partial V_D}\right]^{-1}\left[\frac{\partial Q_D}{\partial V_G}\right] = -[S_{VQ}]\left[\frac{\partial Q_D}{\partial V_G}\right] \tag{10.66}$$

$$S_{VT} = \left[\frac{\partial V_D}{\partial T}\right] = -\left[\frac{\partial Q_D}{\partial V_D}\right]^{-1}\left[\frac{\partial Q_D}{\partial T}\right] = -[S_{VQ}]\left[\frac{\partial Q_D}{\partial T}\right] \tag{10.67}$$

$$S_{QQ} = \left[\frac{\partial Q_G}{\partial V_D}\right]\left[\frac{\partial Q_D}{\partial V_D}\right]^{-1} = \left[\frac{\partial Q_G}{\partial V_D}\right][S_{VT}] \tag{10.68}$$

$$S_{QV} = \left[\frac{\partial Q_G}{\partial V_G}\right] + \left[\frac{\partial Q_G}{\partial V_D}\right]\left[\frac{\partial V_D}{\partial V_G}\right] = \left[\frac{\partial Q_G}{\partial V_G}\right] + \left[\frac{\partial Q_G}{\partial V_D}\right][S_{VV}] \tag{10.69}$$

$$S_{QT} = \left[\frac{\partial Q_G}{\partial T}\right] + \left[\frac{\partial Q_G}{\partial V_D}\right]\left[\frac{\partial V_D}{\partial T}\right] = \left[\frac{\partial Q_G}{\partial T}\right] + \left[\frac{\partial Q_G}{\partial V_D}\right][S_{VT}] \tag{10.70}$$

Linear VAR optimization model M-2 can be solved by linear programming (LP). The details of LP algorithm can be found in the Appendix of Chapter 9. The solution steps of VAR optimization solved by LP are summarized as below.

(1) Select the initial feasible points.
(2) Compute incremental variables and the limits based on the operation points according to equations (10.50)–(10.62).
(3) Compute the sensitivity matrices based on equations (10.65)–(10.70).
(4) Form the successive linear programming model based on the operation points and sensitivity matrices.
(5) Solve the linear programming problem, using the LP algorithm. Obtain the incremental control variables ΔQ_S, ΔV_G, ΔT.
(6) Compute the new control variables with equations (10.50)–(10.52) and perform P-Q decoupled power flow calculation to get the new state variables.

(7) Check the convergence:

$$|P_L^{k+1} - P_L^k| < \xi \qquad (10.71)$$

Stop iteration if equation (10.71) is satisfied. Otherwise, go back to step (2).

Example 10.1

The above-mentioned approach is used to solve the VAR optimization problem of a 6-bus system. The data of generation and load are listed in Table 10.1, and the data of lines are listed in Table 10.2. The results are shown in Table 10.3.

Table 10.1   The data of generation and load of 6-bus system

Bus Number	Bus Type	P_i (p.u.)	Q_i (p.u.)
1	Slack bus	/	/
2	PV	0.5	/
3	PQ	−0.55	−0.13
4	PQ	/	/
5	PQ	−0.30	−0.18
6	PQ	−0.50	−0.05

The symbol "−" in the Table stands for load.

Table 10.2   The data of lines of 6-bus system

Line Number	Bus Pair	R (p.u.)	X (p.u.)	Ratio for Transformer
1	1-6	0.123	0.518	/
2	1-4	0.080	0.370	/
3	4-6	0.097	0.407	/
4	6-5	0.000	0.300	1.025
5	5-2	0.282	0.640	/
6	2-3	0.723	1.050	/
7	4-3	0.000	0.133	1.100

Table 10.3   VAR optimization results for 6-bus system

	Variables	Initial Value	Optimum	Upper Limit	Lower Limit
VAR support	Q_{S4}	0.000	0.050	0.050	0.000
	Q_{S6}	0.000	0.055	0.055	0.000
Generator voltage	V_{G1}	1.050	1.100	1.100	1.000
	V_{G2}	1.100	1.150	1.150	1.100
Transformer ratio	T_{56}	1.025	0.973	1.100	0.900
	T_{43}	1.100	0.986	1.100	0.900

10.4   INTERIOR POINT METHOD FOR VAR OPTIMIZATION PROBLEM

10.4.1   Introduction

This section presents the analytic hierarchical process (AHP) and sensitivity analysis methods to select the optimal locations of VAR support service. The method is based on the observation that VAR support is important for weak buses/nodes where the voltage is low. We analyze the sensitivity values—voltage benefit factor (VBF) and loss benefit factor (LBF)—in Chapter 3. The AHP provides a useful means to consider these factors comprehensively in the selection and ranking of VAR support locations.

On the basis of the optimal selection of VAR support sites, the model of optimal VAR control is constructed, in which the objective is to minimize system real power losses and voltage variations at generator buses. Transformer tap positions and VAR compensation are chosen as control variables. The solution algorithm of the optimal VAR control model is the interior point method.

10.4.2   Optimal VAR Control Model

According to the previous section, the nonlinear VAR control problem can be linearized. If we introduce the penalty to the VAR support in model M-2 in Section 10.3, the incremental VAR optimization model M-3 can be represented as below.

$$\min \Delta P_{\mathrm{L}} = MS_{\mathrm{LQ}}^{\mathrm{T}}(H_{\mathrm{S}}\Delta Q_{\mathrm{S}}) + S_{\mathrm{LV}}^{\mathrm{T}}\Delta V_{\mathrm{G}} + S_{\mathrm{LT}}^{\mathrm{T}}\Delta T \qquad (10.72)$$

subject to constraints in equations (10.44)–(10.49)

M is the corresponding penalty coefficient in the objective function, which should be greater than the other coefficients in the objective function by 10–100. H_{S} is the weight of VAR support or compensation, which can be obtained according to the unified ranking weight coefficients in the next section, i.e.,

$$H_{\mathrm{S}} = 1/W_i \qquad (10.73)$$

This means that a bus with the smallest H_{S} is firstly selected to as the optimal VAR support site. Equation (10.72) means that the number of VAR support sites and total compensation amount are required to be as small as possible.

10.4.3   Calculation of Weighting Factors by AHP

From Chapter 3, the voltage benefit factors (VBF) and loss benefit factors (LBF) are expressed as follows:

$$\mathrm{LBF}_i = \frac{\sum\limits_{i}(P_{\mathrm{L0}} - P_{\mathrm{L}}(Q_{si}))}{Q_{si}} \times 100\% \quad i \in ND \qquad (10.74)$$

Table 10.4 Judgment matrix *A-PI*

A	PI_L	PI_V	PI_S
PI_L	1	2	3
PI_V	1/2	1	3
PI_S	1/3	1/3	1

$$\text{VBF}_i = \frac{\sum_i (V_i(Q_{si}) - V_{i0})}{Q_{si}} \times 100\% \quad i \in ND \tag{10.75}$$

To obtain a unified rank of VAR support locations, the AHP method is used, which is described in Chapter 7. Here, the hierarchy model consists of three sections. The first section is the unified ranking of VAR support locations. The second section is the performance indices, in which the PI_S reflects the relative importance of the load buses. PI_P and PI_V are defined as follows:

$$PI_L = \text{LBF}_i \tag{10.76}$$

$$PI_V = \text{VBF}_i \tag{10.77}$$

Obviously, eigenvectors of PI_L and PI_V can be obtained through normalization. However, it is very difficulty to obtain exactly PI_S and the corresponding eigenvector. But we can obtain them through forming and computing the judgment matrix of PI_S, according to the position of load buses in the power network. In addition, the judgment matrix $A\text{-}PI$, which is shown in Table 10.4 as an example, can also be obtained according to the 9-scale method for practical operating cases in power systems. Therefore, the unified ranking weight coefficients W_i can be computed as follows:

$$\begin{aligned} W_i = &W(A - PI_L) * W(PI_L - S_i) + W(A - PI_V) * W(PI_V - S_i) \\ &+ W(A - PI_S) * W(PI_S - S_i) \end{aligned} \tag{10.78}$$

10.4.4 Homogeneous Self-Dual Interior Point Method

The above-mentioned optimal VAR control model has the format of linear programming. We use the homogeneous self-dual interior point method to solve it.

A linear programming problem is given in standard form

$$\max c^T x$$
$$\text{subject to} \quad Ax \leq b$$
$$x \geq 0$$

and its dual

$$\min b^{\mathrm{T}} y$$
$$\text{subject to} \quad A^{\mathrm{T}} y \geq c$$
$$y \geq 0$$

These two problems can be solved by solving the following problem, which essentially combines the primal and dual problems into one problem:

$$\text{MAX } 0$$

Subject to

$$-A^{\mathrm{T}} y + c\varphi \leq 0$$
$$A^{\mathrm{T}} x - b\varphi \leq 0$$
$$-c^{\mathrm{T}} x + b^{\mathrm{T}} y \leq 0$$
$$x, y, \varphi \geq 0$$

Note that, beyond combining the primal and dual into one big problem, one new variable (φ) and one new constraint have been added. Hence, the total number of variables in primal-dual problem is $n + m + 1$ and the total number of constraints is $n + m + 1$. Furthermore, the objective function vanishes. Problems with such right-hand sides are called **homogeneous**. Also, the constraint matrix for the primal-dual problem is skew symmetric. That is, it is equal to the negative of its transpose. Homogeneous linear programming problems having a skew symmetric constraint matrix are called **self-dual**.

Let $z, w,$ and ψ denote the slack variables for the constraints in primal-dual problem:

$$\text{MAX } 0$$

Subject to

$$-A^{\mathrm{T}} y + c\varphi + z = 0$$
$$A^{\mathrm{T}} x - b\varphi + w = 0$$
$$-c^{\mathrm{T}} x + b^{\mathrm{T}} y + \psi = 0$$
$$x, y, \varphi, z, w, \psi \geq 0$$

If we introduce the error vector $\varepsilon, \rho, \gamma$, the above constraints can be written in matrix form as below:

$$\begin{bmatrix} \varepsilon \\ \rho \\ \gamma \end{bmatrix} = \begin{bmatrix} & -A^{\mathrm{T}} & c \\ A & & -b \\ -c^{\mathrm{T}} & b^{\mathrm{T}} & \end{bmatrix} \begin{bmatrix} x \\ y \\ \phi \end{bmatrix} + \begin{bmatrix} z \\ w \\ \phi \end{bmatrix} = \begin{bmatrix} -A^{\mathrm{T}} y + c\phi + z \\ Ax - b\phi + w \\ -c^{\mathrm{T}} x + b^{\mathrm{T}} y + \phi \end{bmatrix} \qquad (10.79)$$

The reduced KKT system for the primal-dual problem is given by [33–35]

$$\begin{bmatrix} -X^{\mathrm{T}}Z & -A^{\mathrm{T}} & c \\ A & -Y^{\mathrm{T}}W & -b \\ -c^{\mathrm{T}} & b^{\mathrm{T}} & -\varphi/\phi \end{bmatrix} \begin{bmatrix} \Delta x \\ \Delta y \\ \Delta\phi \end{bmatrix} = \begin{bmatrix} \varepsilon' \\ \rho' \\ \gamma' \end{bmatrix} \qquad (10.80)$$

where

$$\begin{bmatrix} \varepsilon' \\ \rho' \\ \gamma' \end{bmatrix} = \begin{bmatrix} -(1-\delta)\varepsilon + z - \delta\mu X^{-1} \\ -(1-\delta)\rho + w - \delta\mu Y^{-1} \\ -(1-\delta)\gamma + \varphi - \delta\mu/\phi \end{bmatrix} \qquad (10.81)$$

μ is a positive real parameter. For each $\mu > 0$, we define the associated central path in primal-dual space as the unique point that simultaneously satisfies the conditions of primal feasibility, dual feasibility, and μ-complementarity. In addition, $0 \le \delta \le 1$.

The system in equation (10.80) is not symmetric. One could use a general-purpose equation solver to solve it, but its special structure would be mostly ignored by such a solver. To exploit the structure, we solve this system in two stages. We start by using the first two equations to solve simultaneously for Δx and Δy in terms of $\Delta\varphi$:

$$\begin{bmatrix} \Delta x \\ \Delta y \end{bmatrix} = \begin{bmatrix} -X^{\mathrm{T}}Z & -A^{\mathrm{T}} \\ A & -Y^{\mathrm{T}}W \end{bmatrix}^{-1} \left(\begin{bmatrix} \varepsilon' \\ \rho' \end{bmatrix} - \begin{bmatrix} c \\ -b \end{bmatrix} \Delta\phi \right) \qquad (10.82)$$

or

$$\begin{bmatrix} \Delta x \\ \Delta y \end{bmatrix} = \begin{bmatrix} f_x \\ f_y \end{bmatrix} - \begin{bmatrix} g_x \\ g_y \end{bmatrix} \Delta\phi \qquad (10.83)$$

where f and g can be obtained by solving the following two equations:

$$\begin{bmatrix} -X^{\mathrm{T}}Z & -A^{\mathrm{T}} \\ A & -Y^{\mathrm{T}}W \end{bmatrix} \begin{bmatrix} f_x \\ f_y \end{bmatrix} = \begin{bmatrix} \varepsilon' \\ \rho' \end{bmatrix} \qquad (10.84)$$

$$\begin{bmatrix} -X^{\mathrm{T}}Z & -A^{\mathrm{T}} \\ A & -Y^{\mathrm{T}}W \end{bmatrix} \begin{bmatrix} g_x \\ g_y \end{bmatrix} = \begin{bmatrix} c \\ -b \end{bmatrix} \qquad (10.85)$$

Then we use equation (10.82) to eliminate Δx and Δy from the last equation in equation (10.80)

$$\begin{bmatrix} c^{\mathrm{T}} & b^{\mathrm{T}} \end{bmatrix} \left(\begin{bmatrix} f_x \\ f_y \end{bmatrix} - \begin{bmatrix} g_x \\ g_y \end{bmatrix} \Delta\phi \right) - \frac{\varphi}{\phi} \Delta\phi = \gamma' \qquad (10.86)$$

From equation (10.86), we get

$$\Delta\phi = \frac{c^T f_x - b^T f_y + \gamma'}{c^T g_x - b^T g_y - \phi/\phi} \tag{10.87}$$

Substituting equation (10.87) into equation (10.82), we get Δx and Δy. Therefore, both optimal solutions of primal and dual are obtained.

Example 10.2

The IEEE 14-bus system is used to test the presented approach. The IEEE 14-bus system has 5 generators, 8 loads, and 20 branches, in which 4-14, 4-18, 5-6 and 7-14 are transformation branches. The value of penalty coefficient M in equation (10.72) is taken arbitrarily in the range 10–100. The judgment matrix PI_S-S for the IEEE 14-bus system is given in Table 10.5, whose values reflect the relative importance in the power system between every pair of VAR support sites. These values were selected according to the engineer's knowledge and experience, using the 9-ratio scale method. For example, the element is chosen to be "2" if the users think the importance of site bus S8 is slightly higher than that of site S4. If both VAR sites are thought to be equally important (such as bus S8 and S10), the corresponding elements are set to be "1."

Single-hierarchy ranking is defined as that ranking is obtained by using only one index for all elements in one hierarchical structure. Table 10.6

Table 10.5 Judgment matrix PI_S-S for IEEE 14-bus system

PI_S	S4	S5	S8	S9	S10	S11	S12	S13
S4	1	1	1/2	1/7	1/3	1/5	1/3	1/5
S5	1	1	1/2	1/7	1/3	1/4	1/3	1/5
S8	2	2	1	1/6	1	1/3	1/2	1/4
S9	7	7	6	1	6	3	5	3
S10	3	3	1	1/6	1	1/4	1/2	1/5
S11	5	4	3	1/3	4	1	2	1/2
S12	3	3	2	1/5	2	1/2	1	1/3
S13	5	5	4	1/3	5	2	3	1

Table 10.6 Single hierarchy ranking of VAR support sites for IEEE 14-bus system

Bus	LBF_i	Rank	VBF_i	Rank
4	0.000376	7	0.000855	8
5	0.000337	8	0.000884	7
8	0.002309	6	0.001775	6
9	0.007674	2	0.001989	5
10	0.002618	5	0.002097	4
11	0.007407	3	0.002175	2
12	0.006757	4	0.002268	1
13	0.008840	1	0.002122	3

shows the single-hierarchy rank of VAR support sites of the IEEE 14-bus system. It can be observed from Table 10.6 that the major VAR support sites selected by the benefit factors LBF and VBF are the same, but different in ranking.

Table 10.7 provides the unified ranking results of VAR support sites, which coordinates PI_L, PI_V, and PI_S indices by use of AHP. The weighting coefficients W_i in Table 10.7 are computed through the calculation of equation (10.78). Obviously, the unified ranking list in Table 10.7 has considered the relative importance of VAR support sites in the power system.

With the use of the top three sites in the IEEE 14-bus system (buses S9, S13, and S11 in Table 10.7) for placing the VAR compensation or support, the corresponding VAR support values are obtained through the optimal VAR control model, which is solved by the interior point (IP) method. Table 10.8 provides the optimal VAR control results. The effectiveness of the IP

Table 10.7   Unified VAR compensation buses ranking list for IEEE 14-bus system

Bus No.	PI_L 0.528	PI_V 0.333	PI_S 0.140	Weighting Coefficient W_i	Rank No.
S4	0.01036	0.06033	0.03231	0.03008	8
S5	0.00928	0.06242	0.03322	0.03034	7
S8	0.06359	0.12529	0.05491	0.08321	6
S9	0.21135	0.14043	0.36790	0.20986	1
S10	0.07210	0.14803	0.06002	0.09577	5
S11	0.20400	0.15354	0.15165	0.18007	3
S12	0.18610	0.16012	0.08870	0.16400	4
S13	0.24347	0.14984	0.21128	0.20803	2

Table 10.8   Optimal VAR control results and comparison for IEEE 14-bus system (p.u.)

	Variable X_{min}	Variable X_{max}	Results by IP	Results by LP
T_{4-14}	0.900	1.100	0.975	0.975
T_{4-18}	0.900	1.100	1.100	1.100
T_{5-6}	0.900	1.100	1.100	1.100
T_{7-14}	0.900	1.100	0.950	0.950
Q_{S9}	0.000	0.200	0.200	0.200
Q_{S11}	0.000	0.200	0.050	0.059
Q_{S13}	0.000	0.200	0.161	0.170
V_{G1}	1.000	1.1000	1.100	1.100
V_{G2}	1.000	1.1000	1.091	1.092
V_{G3}	1.000	1.1000	1.086	1.084
V_{G6}	1.000	1.1000	1.071	1.068
V_{G7}	1.000	1.1000	1.100	1.100
Initial Loss	/	/	0.11646	0.11646
Final Loss	/	/	0.11004	0.11108
Loss Reduction (%)	/	/	5.513%	4.619%
CPU (s)	/	/	18.2	61.5

method is also evaluated by comparing it against the LP method. In view of loss reduction, load voltage modification, and convergence speed, the IP method appears superior to the LP method.

10.5   NLONN APPROACH

Chapter 6 presents a new nonlinear optimization neural network (NLONN) to solve the security-constrained economic dispatch problem. Since reactive power optimization is also a nonlinear optimization problem, we apply NLONN to the reactive power optimization problem in this section.

10.5.1   Placement of VAR Compensation

10.5.1.1   Sensitivity Method   For simplification, we use the perturbation method to compute the sensitivity of the bus voltage. The magnitude of the bus voltage sensitivity can be expressed by the total incremental bus voltage $\sum \Delta V_i$, which is obtained by increasing a small reactive power demand at a given load bus. The total incremental bus voltage may only include the voltage changes on several monitored buses. The bigger the value of $\sum \Delta V_i$, the more sensitive will be the voltage at a given bus to a change of reactive demand. This means that a load bus with the large value of $\sum \Delta V_i$ is a good candidate to be selected as a VAR compensation bus. If the maximal number of VAR compensation sites is m, we can obtain m VAR compensation sites according to the values of $\sum \Delta V_i$. Thus the corresponding sensitivity index can be expressed as

$$S_{VQ}^k = \frac{\sum\limits_{i \in NM} \Delta V_i}{\Delta Q_k}, \quad k = 1, \ldots, ND \tag{10.88}$$

where

NM: The set of the monitored buses
ND: The total number of load buses

10.5.1.2   Voltage Stability Margin Method   The method is demonstrated with a simple system as shown in Figure 10.1.

In Figure 10.1, $\underline{V}_1 = V_1 \angle 0$ is the voltage at the slack bus, which is the voltage source. P_2 and Q_2 are the active and reactive load demands, respectively. The load power factor is $\cos\phi$. The load-bus voltage is $\underline{V}_2 = V_2 \angle \alpha$. The line impedance is $\underline{Z}_1 = Z_1 \angle \theta$.

From Figure 10.1, we can obtain the following equations:
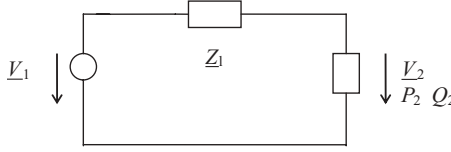
FIGURE 10.1   A simple system diagram

$$P_2 = \frac{V_1 * V_2}{Z_1}\cos(\theta + \alpha) - \frac{V_2^2}{Z_1}\cos\theta \qquad (10.89)$$

$$Q_2 = \frac{V_1 * V_2}{Z_1}\sin(\theta + \alpha) - \frac{V_2^2}{Z_1}\sin\theta \qquad (10.90)$$

According to equations (10.89) and (10.90), we get

$$(P_2^2 + Q_2^2)Z_1^2 + 2Z_1(P_2\cos\theta + Q_2\sin\theta)V_2^2 - V_1^2V_2^2 + V_2^4 = 0 \qquad (10.91)$$

The roots of equation (10.91) are

$$V_2(\pm) = \sqrt{\frac{1}{2}[V_1^2 - 2Z_1(P_2\cos\theta + Q_2\sin\theta) \pm \Delta]} \qquad (10.92)$$

where

$$\Delta = [V_1^2 - 2Z_1(P_2\cos\theta + Q_2\sin\theta)]^2 - 4(P_2^2 + Q_2^2)Z_1^2 \qquad (10.93)$$

When $\Delta = 0$, the two roots of equation (10.92) are the same, i.e.,

$$V_{cr} = V_2^+ = V_2^- = \sqrt{\frac{1}{2}[V_1^2 - 2Z_1(P_2\cos\theta + Q_2\sin\theta)]} \qquad (10.94)$$

where V_{cr} is the critical voltage of the load bus.
   Since $\Delta = 0$, from equation (10.93) we get

$$\frac{1}{2}[V_1^2 - 2Z_1(P_2\cos\theta + Q_2\sin\theta)] = Z_1\sqrt{P_2^2 + Q_2^2} \qquad (10.95)$$

According to equations (10.94) and (10.95), we have

$$V_{cr} = \sqrt{Z_1\sqrt{P_2^2 + Q_2^2}} \qquad (10.96)$$

due to

$$Q_2 = P_2 tg\phi \tag{10.97}$$

Substituting equation (10.97) into equation (10.96), we have

$$V_{cr} = \sqrt{Z_1 P_2 \sec\phi} \tag{10.98}$$

Substituting equation (10.97) into equation (10.93) with $\Delta = 0$, we have

$$\left[V_1^2 - 2Z_1(P_2\cos\theta + Q_2\sin\theta)\right]^2 = 4P_2^2\sec^2\phi Z_1^2 \tag{10.99}$$

$$P_2 = \frac{V_1^2}{2Z_1(\cos\theta + tg\phi\sin\theta + \sec\phi)} \tag{10.100}$$

Substituting equation (10.100) into equation (10.98), we get

$$V_{cr} = \frac{V_1}{\sqrt{2[1+\cos(\theta-\phi)]}} \tag{10.101}$$

According to equations (10.100) and (10.101), we get the critical power of load P_{cr}, i.e.,

$$P_{cr} = P_2 = \frac{V_1^2\cos\phi}{2Z_1[1+\cos(\theta-\phi)]} = \frac{V_{cr}^2\cos\phi}{Z_1} \tag{10.102}$$

From equations (10.101) and (10.102), we obtain the static voltage stability deposit coefficients, i.e., the real power margin index $K(P)$ and the voltage margin index $K(V)$.

$$K(P)_i = \frac{P_{cr} - P_{i0}}{P_{i0}} \cdot 100\% \quad i \in ND \tag{10.103}$$

$$K(V)_i = \frac{V_{cr} - V_{i0}}{V_{i0}} \cdot 100\% \quad i \in ND \tag{10.104}$$

where P_{i0} is the initial real power value of load bus i, V_{i0} is the initial voltage at load bus i, and ND is the number of load buses.

The real power margin index, which adequately reflects the stability deposit degree of system operation state, is used to represent the static stability degree of system voltage. Obviously, the load bus with a smaller value of $K(P)$ should be selected as a VAR compensation bus. Similarly, if the maximal number of VAR compensation sites is m, we can obtain m VAR compensation sites according to the values of $K(P)$.

To obtain a unified VAR compensation location ranking, a similar hierarchy model is set up as in Section 10.4, but two difference performance indices are used here. PI_P and PI_V are defined as follows.

$$PI_V = S_{VQ}^i \quad i \in ND \tag{10.105}$$

$$PI_P = 1/K(P)_i \quad i \in ND \tag{10.106}$$

Thus the unified ranking weight coefficients W_i for the VAR support sites can be computed by AHP. The details of AHP algorithm can be found in Chapter 7 and reference [32].

10.5.2 VAR Control Optimization

After VAR support locations are determined, VAR variables are optimized to improve voltage profiles and to minimize system real power losses as in model M-4:

$$\min F = \sum_{i \in N}(V_{i\max} - V_i) \tag{10.107}$$

such that

$$Q_i - D_i = \varphi_i(V, \theta, T) \quad i \in N \tag{10.108}$$

$$Q_{i\min} \leq Q_i \leq Q_{i\max} \quad i \in NG \cup NC \tag{10.109}$$

$$V_{i\min} \leq V_i \leq V_{i\max} \quad i \in N \tag{10.110}$$

$$T_{l\min} \leq T_l \leq T_{l\max} \quad l \in NT \tag{10.111}$$

where

V_i: The voltage magnitude at bus i
θ: The voltage angle at bus i
Q_i: The VAR compensation or VAR generation in the system
T: The transformer tap position
N: The set of buses in the system
NG: The set of generation buses
NC: The set of VAR compensation buses
NT: The set of transformer branches

In the above model M-4, equation (10.108) is a VAR power flow equation.

In contrast to most formulations that minimize real power losses, model M-4 aims to achieve VAR optimization by dealing with voltage profiles. Obviously, good voltage profiles lead to small real power losses. The advantage of model M-4 is that it also ensures sound system stability by controlling voltages. We may also consider both loss minimization and voltage modification as objective functions, which are discussed in the next section.

In addition to optimal placement of VAR compensation (Section 10.5.1), an additional term is added into model M-4 to penalize any further commitment of VAR compensation. As a result, model M-5 is formed to contribute further to the overall objective of VAR optimization:

$$\min F = \sum_{i \in N}(V_{i\max} - V_i) + M\sum_{i \in NC}(\beta_i C_i) \qquad (10.112)$$

such that

$$Q_i + C_i - D_i - \varphi_i(V, \delta, T) = 0 \quad i \in N \qquad (10.113)$$

$$-C_i + C_{i\max} \geq 0 \quad i \in NC \qquad (10.114)$$

$$C_i - C_{i\min} \geq 0 \quad i \in NC \qquad (10.115)$$

$$-Q_i + Q_{i\max} \geq 0 \quad i \in NG \cup NC \qquad (10.116)$$

$$Q_i - Q_{i\min} \geq 0 \quad i \in NG \cup NC \qquad (10.117)$$

$$-V_i + V_{i\max} \geq 0 \quad i \in N \qquad (10.118)$$

$$V_i - V_{i\min} \geq 0 \quad i \in N \qquad (10.119)$$

$$-T_l + T_{l\max} \geq 0 \quad l \in NT \qquad (10.120)$$

$$T_l - TC_{l\min} \geq 0 \quad i \in NT \qquad (10.121)$$

where C is the new increased VAR compensation. M is the corresponding penalty coefficient in the objective function, which should be greater than the other coefficients in the objective function by a factor of 10–100. β_i is the weight on VAR compensation, which can be obtained according to the unified ranking weight coefficients as in Section 10.5.1:

$$\beta_i = 1/W_i \qquad (10.122)$$

A large W_i corresponds to a small β_i. This means that VAR compensation at a bus with the smallest β_i is preferred to the others as the optimal VAR compensation site.

10.5.3   Solution Method

The VAR optimization model in equations (10.112)–(10.121) can be rewritten into a general form as constrained optimization problem.

$$\min f(x) \qquad (10.123)$$

such that

$$h_j(x) = 0 \quad j = 1, \ldots, m \tag{10.124}$$

$$g_i(x) \geq 0 \quad i = 1, \ldots, k \tag{10.125}$$

To change inequality constraints of equation (10.125) into equality constraints, new variables $y_1, \ldots \ldots, y_m$ (i.e., relaxation variables) are introduced into equation (10.125), In this way, equations (10.123)–(10.125) can be written as.

$$\min f(x) \tag{10.126}$$

such that

$$h_j(x) = 0 \quad j = 1, \ldots, m \tag{10.127}$$

$$g_i(x) - y_i^2 = 0 \quad i = 1, \ldots, k \tag{10.128}$$

The optimization neural network is applied to solve equations (10.126)–(10.128). The NLONN approach is described in Chapter 6.

10.5.4 Numerical Simulations

The characteristics of the proposed approach are examined with the IEEE 30-bus system. Data and parameters of the system are shown in Chapter 5. The IEEE 30-bus system has 6 generators, 21 loads, and 41 branches, in which 6-9, 6-10, 9-10, 4-12, 12-13, and 27-28 are branches with under-load-tap-setting transformers.

The judgment matrix PI_C-C for the IEEE 30-bus system is given in Table 10.9, whose values reflect the relative importance in the power system between every pair of VAR compensation buses.

Table 10.9 Judgment matrix PI_C-C for IEEE 30-bus system

PI_C	C10	C18	C19	C20	C21	C23	C24	C26	C29	C30
C10	1	1/2	1/2	1	1/2	1/7	1/2	1/3	1/7	1/3
C18	2	1	2	3	1	1/7	1/2	1/3	1/7	1/3
C19	2	1/2	1	2	1/2	1/7	1/3	1/3	1/7	1/3
C20	1	1/3	1/2	1	1	1/5	1/2	1/4	1/6	1/4
C21	2	1	2	1	1	1/7	1	1/3	1/5	1/3
C23	7	7	7	5	7	1	5	4	1	4
C24	2	2	3	2	1	1/5	1	1/2	1/5	1/2
C26	3	3	3	4	3	1/4	2	1	1/4	2
C29	7	7	7	6	5	1	5	4	1	4
C30	3	3	3	4	3	1/4	2	1/2	1/4	1

Single-hierarchy ranking is defined as that ranking as obtained by using only one method for all elements in one hierarchical structure. Table 10.10 shows the single-hierarchy VAR compensation sites ranking of the IEEE 30-bus system.

Two parallel methods, namely: the sensitivity method (SM) and the voltage stability margin method (VSMM), have been used to determine optimal placement of VAR compensation. Table 10.11 provides the unified VAR compensation ranking results, which coordinates SM and VSMM methods by using AHP for the IEEE 30-bus system.

Using the top four sites in the IEEE 30-bus system (buses C23, C26, C29, C30 in Table 10.11) for placing the VAR compensation, the corresponding VAR compensation utilization or settings are obtained with VAR optimization model M-5. Table 10.12 provides the VAR optimization results for the IEEE 30-bus system. Corresponding limits of the variables in Table 10.12 are $T_{max} = 1.1$, $T_{min} = 0.9$; $C_{max} = 0.3$, $C_{min} = 0.0$; $V_{Gmax} = 1.1$, $V_{Gmin} = 1.0$; $V_{Dmax} = 1.0$,

Table 10.10 Single hierarchy ranking of VAR compensation buses for IEEE 30-bus system

Bus	K_P	PI_P	Rank	PI_V	Rank
10	3.101	0.322	7	/	/
18	2.000	0.500	5	1.610	8
19	/	/	/	1.660	5
20	/	/	/	1.640	7
21	2.46	0.407	6	/	/
23	1.910	0.524	4	1.642	6
24	3.430	0.292	8	1.855	4
26	0.882	1.134	1	1.882	3
29	1.090	0.917	2	2.011	1
30	1.531	0.653	3	1.984	2

Table 10.11 Unified VAR compensation buses ranking list for IEEE 30-bus system

Bus No.	PI_P 0.528	PI_V 0.333	PI_C 0.140	Total Rank	Rank No.
C10	0.06780	0.00000	0.02857	0.03980	10
C18	0.10529	0.11271	0.04650	0.09964	5
C19	0.00000	0.11621	0.03492	0.04359	8
C20	0.00000	0.11481	0.03049	0.04250	9
C21	0.08570	0.0000	0.04505	0.05156	7
C23	0.11034	0.11495	0.27770	0.13542	3
C24	0.06147	0.12987	0.06050	0.08417	6
C26	0.23879	0.13176	0.10930	0.16113	2
C29	0.19309	0.14079	0.27196	0.17291	1
C30	0.13750	0.13890	0.09504	0.13216	4

Table 10.12   Results of optimal VAR control for IEEE 30-bus system

Branch	6-9	6-10	10-9	4-12	12-13	28-27		
T	1.00	1.05	0.90	1.075	1.10	1.05		
Bus	C23	C26	C29	C30				
Q_C	0.043	0.031	0.059	0.019				
Bus	NG1	NG2	NG5	NG8	NG11	NG13		
V_G	1.068	1.049	1.030	1.006	1.052	1.100		
Bus	C3	C4	C6	C7	C9	C10	C12	C14
V_D	1.000	0.991	0.996	1.000	1.000	1.000	1.000	0.978
Bus	C15	C16	C17	C18	C19	C20	C21	C22
V_D	0.967	0.992	0.992	0.942	0.951	0.963	0.984	0.983
Bus	C23	C24	C25	C26	C27	C28	C29	C30
V_D	0.947	0.958	0.972	0.930	1.000	0.987	0.967	0.962

Table 10.13   Comparison of results for IEEE 30-bus system

Method	Number of Var Compensations	Amount of Var Compensation	Lowest Load Voltage	Average Load Voltage
LP	4	0.1950	0.92178	0.97013
NNLONN	4	0.1520	0.93000	0.97758

$V_{Dmin} = 0.9$ (where T is the tap transformer position, C is the VAR compensation capacity, V_G is the voltage magnitude at generator buses, and V_D is the voltage magnitude at load buses).

Linear programming, which is the most conventional method used in reactive power optimization, is used to validate the results from the NLONN method. Results from both methods are given in Table 10.13 for the IEEE 30-bus system. If the same initial conditions are adopted for both methods, the NLONN method produce results with higher voltage profile with less VAR compensation capacity than its counterpart.

10.6   VAR OPTIMIZATION BY EVOLUTIONARY ALGORITHM

10.6.1   Mathematical Model

In the previous section, we deduced the voltage margin index $K(V)$, that is,

$$K(V)_i = \frac{V_{cr} - V_{i0}}{V_{i0}} \cdot 100\% \tag{10.129}$$

This means that voltage stability enhancement can be achieved through minimizing the voltage margin index values at every bus of the system and consequently the global power system K-index. Let

$$K_{\max} = \max\{K(V)_i\}, \quad i = 1, \dots, N \tag{10.130}$$

where N is the total number of buses of the system.

The objective is to minimize the $K_{\max}$, that is,

$$\min F_1 = \min K_{\max} \tag{10.131a}$$

Another objective for VAR optimization is system loss minimization, that is,

$$\min F_2 = \min P_L \tag{10.131b}$$

The constraints of VAR optimization are described in previous sections. Thus the problem can be mathematically formulated as a nonlinear constrained multiobjective optimization problem as follows:

$$\text{Minimize}[F_1, F_2] \tag{10.132}$$

Subject to

$$g(x, u) = 0 \tag{10.133}$$

$$h(x, u) \le 0 \tag{10.134}$$

where

x: The vector of dependent variables consisting of load bus voltages V_L, generator reactive power outputs Q_G, and transmission line loadings. Hence, x can be expressed as

$$x^T = [V_{L1}, \dots V_{LND}, Q_{G1}, \dots Q_{GNG}] \tag{10.135}$$

u: The vector of control variables consisting of generator voltages V_G, transformer tap settings T, and VAR compensations Q_c. Hence, u can be expressed as

$$u^T = [V_{G1}, \dots V_{GNG}, T_1, \dots T_{NT}, Q_{C1}, \dots Q_{CNC}] \tag{10.136}$$

g: The equality constraints
h: The inequality constraints

10.6.2 Evolutionary Algorithm of Multiobjective Optimization

Generally, the two functions, loss minimization and voltage stability index, are noncommensurable and often competing objectives. Multiobjective optimization with such objective functions gives rise to a set of optimal solutions,

instead of one optimal solution. The reason for the optimality of many solutions is that no one can be considered to be better than any other with respect to all objective functions. These optimal solutions are known as **Pareto-optimal** solutions.

A general multiobjective optimization problem consists of a number of objectives to be optimized simultaneously and is associated with a number of equality and inequality constraints. It can be formulated as follows:

$$\text{Minimize } f_i(x) \quad i = 1, \dots, N_{obj} \tag{10.137}$$

subject to

$$g_j(x, u) = 0 \quad j = 1, \dots, M \tag{10.138}$$

$$h_k(x, u) \leq 0 \quad k = 1, \dots, K \tag{10.139}$$

where f_i is the ith objective function, x is a decision vector that represents a solution, and N_{obj} is the number of objectives.

For a multiobjective optimization problem, any two solutions x^1 and x^2 can have one of two possibilities: One covers or dominates the other, or none dominates the other. In a minimization problem, without loss of generality, a solution x^1 dominates x^2 if the following two conditions are satisfied [23]:

1. $\forall i \in \{1, 2, \dots, N_{obj}\}: f_i(x^1) \leq f_i(x^2)$
2. $\exists j \in \{1, 2, \dots, N_{obj}\}: f_j(x^1) \leq f_j(x^2)$

If any of the above conditions is violated, solution x^1 does not dominate solution x^2. The solutions that are nondominated within the entire search space are denoted as Pareto-optimal and constitute the **Pareto-optimal set** or **Pareto-optimal front**.

There are some difficulties for the classic methods to solve such multiobjectives optimization problems:

- An algorithm has to be applied many times to find multiple Pareto-optimal solutions.
- Most algorithms demand some knowledge about the problem being solved.
- Some algorithms are sensitive to the shape of the Pareto-optimal front.
- The spread of Pareto-optimal solutions depends on efficiency of the single objective optimizer.

As we have analyzed in this book, AHP can be used to solve the mentioned multiobjective optimization problem. Here, we use another method, the strength Pareto evolutionary algorithm (SPEA), to solve it.

The SPEA-based approach has the following features [36]:

- It stores externally those individuals that represent a nondominated front among all solutions considered so far.
- It uses the concept of Pareto dominance in order to assign scalar fitness values to individuals.
- It performs clustering to reduce the number of individuals externally stored without destroying the characteristics of the trade-off front.

Generally, the algorithm can be described in the following steps.

Step (1) (Initialization): Generate an initial population and create an empty external Pareto-optimal set.

Step (2) (External set updating): The external Pareto-optimal set is updated as follows.

  (a) Search the population for the nondominated individuals and copy them to the external Pareto set.

  (b) Search the external Pareto set for the nondominated individuals and remove all dominated solutions from the set.

  (c) If the number of the individuals externally stored in the Pareto set exceeds the prespecified maximum size, reduce the set by clustering.

Step (3) (Fitness assignment): Calculate the fitness values of individuals in both external Pareto set and the population as follows.

  (a) Assign a real value $r \in [0, 1)$ called strength for each individual in the Pareto optimal set. The strength of an individual is proportional to the number of individuals covered by it. The strength of a Pareto solution is at the same time its fitness.

  (b) The fitness of each individual in the population is the sum of the strengths of all external Pareto solutions by which it is covered. To guarantee that Pareto solutions are most likely to be produced, a small positive number is added to the resulting value.

Step (4) (Selection): Combine the population and the external set individuals. Select two individuals at random and compare their fitness. Select the better one and copy it to the mating pool.

Step (5) (Crossover and Mutation): Perform the crossover and mutation operations according to their probabilities to generate the new population.

Step (6) (Termination): Check for stopping criteria. If any one is satisfied, then stop; otherwise copy new population to old population and go to Step 2. In this study, the search will be stopped if the generation counter exceeds its maximum number.

In some problems, the Pareto optimal set can be extremely large. In this case, reducing the set of nondominated solutions without destroying the char-

acteristics of the trade-off front is desirable from the decision maker's point of view. An average linkage-based hierarchical clustering algorithm [37] is employed to reduce the Pareto set to manageable size. It works iteratively by joining the adjacent clusters until the required number of groups is obtained. It can be described as: given a set P in which its size exceeds the maximum allowable size N, it is required to form a subset P^* with the size N. The algorithm is illustrated in the following steps.

Step (1): Initialize cluster set C; each individual $i \in P$ constitutes a distinct cluster.

Step (2): If number of clusters $\leq N$, then go to Step 5, else go to Step 3.

Step (3): Calculate the distance of all possible pairs of clusters.

The distance d_c of two clusters c_1 and $c_2 \in C$ is given as the average distance between pairs of individuals across the two clusters

$$d_c = \frac{1}{n_1 n_2} \sum_{i_1 \in c_1, i_2 \in c_2} d(i_1, i_2) \tag{10.140}$$

where n_1 and n_2 are the number of individuals in clusters c_1 and c_2, respectively. The function d reflects the distance in the objective space between individuals i_1 and i_2.

Step (4): Determine two clusters with minimal distance d_c. Combine them into a larger one. Go to Step 2.

Step (5): Find the centroid of each cluster. Select the nearest individual in this cluster to the centroid as a representative individual and remove all other individuals from the cluster.

Step (6): Compute the reduced nondominated set P^* by uniting the representatives of the clusters.

Upon having the Pareto-optimal set of nondominated solution, we can obtain one solution for the decision maker as the best compromise solution. Because of the imprecise nature of the decision maker's judgment, the ith objective function F_i is represented by a membership function μ_i defined as

$$\mu_i = \begin{cases} 1 & F_i \leq F_i^{\min} \\ \dfrac{F_i^{\max} - F_i}{F_i^{\max} - F_i^{\min}} & F_i^{\min} < F_i < F_i^{\max} \\ 0 & F_i \geq F_i^{\max} \end{cases} \tag{10.141}$$

where $F_i^{\min}$ and $F_i^{\max}$ are the minimum and maximum value of the ith objective function among all nondominated solutions, respectively.

For each nondominated solution k, the normalized membership function μ^k is calculated as

$$\mu^k = \frac{\sum_{i=1}^{N_{obj}} \mu_i^k}{\sum_{k=1}^{M} \sum_{i=1}^{N_{obj}} \mu_i^k} \tag{10.142}$$

where M is the number of nondominated solutions. The best compromise solution is that having the maximum value of μ^k.

The following modifications have been incorporated in the basic SPEA algorithm [23].

(a) A procedure is imposed to check the feasibility of the initial population individuals and the generated children through GA operations. This ensures the feasibility of Pareto-optimal nondominated solutions.

(b) In every generation, the nondominated solutions in the first front are combined with the existing Pareto-optimal set. The augmented set is processed to extract its nondominated solutions that represent the updated Pareto-optimal set.

(c) A fuzzy-based mechanism is employed to extract the best compromise solution over the trade-off curve and assist the decision maker to adjust the VAR sources efficiently.

10.7 VAR OPTIMIZATION BY PARTICLE SWARM OPTIMIZATION ALGORITHM

Similar to Section 10.6, two objectives, loss minimization and voltage modification, are used for VAR optimization problem. They are:

$$\min F_1 = \sum_i (V_i - V_{i0})^2 \quad i \in ND \tag{10.143}$$

$$\min F_2 = P_L(Q_S, V_G, T) \tag{10.144}$$

where V_{i0} is the feasible value of voltage on a load bus in the normal state.

The constraints of VAR optimization were described in previous sections. In this section, we use particle swarm optimization (PSO) to solve the VAR optimization problem.

According to Chapter 8, the velocity and position update equations of PSO are given by

$$V_{ij}^t = wV_{ij}^{t-1} + C_1 \times r_1 \times (P_{ij}^{t-1} - X_{ij}^{t-1}) + C_2 \times r_2 \times (P_{gbi}^{t-1} - X_{ij}^{t-1}) \tag{10.145}$$

$$X_{ij}^t = X_{ij}^{t-1} + V_{ij}^t \quad i = 1, \dots, N_D, \quad j = 1, \dots, N_{par} \tag{10.146}$$

where

w: The inertia weight

C_1, C_2: The acceleration coefficients

N_D: The dimension of the optimization problem (number of decision variables)

N_{par}: The number of particles in the swarm

r_1, r_2: Two separately generated uniformly distributed random numbers in the range [0, 1].

The inertia weighting factor for the velocity of particle is defined by the inertial weight approach

$$w(t) = w_{max} - \frac{w_{max} - w_{min}}{t_{max}} \times t \tag{10.147}$$

where t_{max} is the maximum number of iterations and t is the current number of iterations. w_{max} and w_{min} are the upper and lower limits of the inertia weighting factor, respectively.

Here, we use a modified PSO to solve the VAR optimization problem. The method is a variation of the classical PSO by splitting the cognitive component of the classical PSO into two different components. The first component can be called the good experience component. That is, the bird has a memory about its previously visited best position. This component is exactly the same as the cognitive component of the basic PSO. The second component is given the name of bad experience component. The bad experience component helps the particle to remember its previously visited worst position. To calculate the new velocity, the bad experience of the particle is also taken into consideration. This gives the new model of the PSO as below.

The new velocity update equation is given by [38]

$$V_{ij}^t = wV_{ij}^{t-1} + C_{1g} \times r_1 \times \left(P_{ij}^{t-1} - X_{ij}^{t-1} \right) + C_{1b} \times r_2 \times \left(X_{ij}^{t-1} - P_{wij}^{t-1} \right) + C_3 \times r_3 \times \left(P_{gbi}^{t-1} - X_{ij}^{t-1} \right) \tag{10.148}$$

where

C_{1g}: The acceleration coefficients, which accelerate the particle toward its best position

C_{1b}: The acceleration coefficients

P_{wi} : The worst position of the particle, which accelerates the particle away from its worst position

The positions are updated with the same equation (10.146). The inclusion of the worst experience component in the behavior of the particle gives additional exploration capacity to the swarm. By using the bad experience

Table 10.14   VAR optimization results and comparison for 30-bus system

	Conventional PSO	MPSO	CAPSO	IP-OPF
V_{G1}	1.10755	1.02367	1.02282	1.10000
V_{G2}	1.02458	0.99985	1.09093	1.05414
V_{G5}	1.02466	1.00202	1.03008	1.10000
V_{G8}	1.01421	1.01253	0.95000	1.03348
V_{G11}	1.01717	1.02636	1.04289	1.10000
V_{G13}	0.99613	1.03602	1.03291	1.01497
T_{6-9}	1.09699	1.04352	1.07894	0.99334
T_{6-10}	0.92509	0.99419	0.94376	1.05938
T_{4-12}	1.00048	1.00063	1.00064	1.00879
T_{27-28}	1.00714	1.00694	1.00693	0.99712
Q_{10}	0.15365	0.17739	0.15232	0.15253
Q_{24}	0.06220	0.06178	0.06249	0.08926
P_L (p.u.)	0.050922	0.050921	0.050921	0.051009

component, the bird (particle) can bypass its previous worst position and always try to occupy a better position.

Example 10.3

The VAR optimization solved by the MPSO (modified PSO) algorithm is tested on the IEEE 30-bus system. The system consists of 6 generators, 41 lines, 4 transformers, and 2 capacitor banks. In the transformer tests, tap settings are considered within the interval [0.9, 1.1]. The available reactive powers of capacitor banks are within the interval [0, 30] MVAr, and they are connected to buses 10 and 24. Voltages are considered within the range of [0.95, 1.1]. In this case, the decision space has 12 dimensions, namely, the 6 generator voltages, 4 transformer taps, and 2 capacitor banks. The values of the parameters of MPSO are determined as below.

The upper and lower limits of the inertia weight w_{max} and w_{min} are selected as 0.92 and 0.4, respectively. C_2 is selected as 2. C_{1g} is increased from 1.0 to 1.9 in steps 0.05, and C_{1b} is decreased from 1.0 to 0.1 in steps 0.05.

The test results are listed in Table 10.14. For the purpose of comparison, the several different results given by conventional PSO [25, 26], coordinated aggregation PSO [29], and interior point-based OPF algorithm [27] are also listed in Table 10.14. All PSO algorithms have similar results.

10.8   REACTIVE POWER PRICING CALCULATION

10.8.1   Introduction

In the power system, generation investments and fuel costs are the main system costs. However, these costs are expensive. There are other less expen-

sive generation services that should be provided in order to maintain system reliability and to meet the required security levels. Among these ancillary services are those associated with reactive power support and voltage control in the transmission network [39–43]. Especially in the competitive power markets, there is a need for procedures to incentivize the participants in the market to provide reactive services and ensure an adequate payment that guarantees the economic feasibility of this business. In addition, reactive power pricing addresses the important issue of providing information to the utilities, generating plants, and consumers about the true burden on the system. It can also reflect the embedded costs incurred by the utilities for wholesale transactions.

In Chapter 6, we discuss the real power pricing issue. There are some differences between the reactive power market and the real power market:

(a) The local geographic character of the reactive power market versus the systemwide character of the active power market

(b) The relatively smaller investments in new equipment needed to supply reactive power as compared to those associated with active power generation.

Investments in the reactive power market ease competition, as more agents can participate in the market (for instance, investing in SVCs). On the other hand, the local character of the reactive flows can mean that, in some moments, just one (or a few) generator can provide the required reactive energy, leading to monopolistic behavior. One way to avoid this possibility is by requiring longer-term bids than in active power markets. In this way, generators cannot bid, in any case, their reactive energy higher than the cost of alternative reactive power generation means. Actually, the market size grows because it is "enlarged" in the temporal direction, trying to compensate for the loss of competition among agents through the space.

The reactive energy market would be based on long-term bids provided by generators and other control elements to the system operator. The bid format includes the margin of the reactive power variation (generation and absorption) and the loss curve, which relates the internal equipment losses to the reactive power produced or absorbed by the control element. These loss curves will be priced at the marginal price of the hourly active energy market. The system operator should dispatch the system including the loss as an additional cost to be minimized. Both generator injections and reactive power demands would be remunerated or charged by multiplying the reactive power amount by the corresponding loss minimization spot price. Distribution utilities or large customers would adjust their reactive power demands, taking into account the current reactive power spot prices.

The reactive capacity market would be also based on long-term capacity bids provided by generators and SVCs to the system operator to ensure system voltage security. For selected bids there is a long-term obligation for voltage

regulation in their connection buses. The control element will receive a capacity payment for this service. To avoid the undesirable effects of the high volatility of security reactive spot prices, this regulating service would be remunerated by a capacity payment. The total equipment remuneration should be proportional to the impact of the equipment on the expected nonsupplied energy, and it should take into account the amount of the reactive power capacity provided and its type of control.

10.8.2   Reactive Power Pricing

Assume that the power system is working in its steady-state optimal operation point. This operation point is found by solving the VAR optimization problems, which are analyzed in the previous sections. If a load increases its reactive power demand in a small amount, the rest of the system will change in order to supply the additional demand keeping optimality conditions. It can be shown that the increase of the profit of the load must be equal to the increase of the cost of the rest of the system. This incremental cost is known as the reactive power spot price [40].

Two kind of incremental system costs can be separated: One is related to system losses and another is related to voltage security. Thus the reactive spot price can be also decomposed into two components: a losses component and a security component. The reactive spot pricing can be computed as below [39].

10.8.2.1 *Computation of Reactive Spot Prices at Generator Buses*
Consider first a bus in which is connected a reactive power source, generator, or SVC with enough reactive margin. Usually, any reactive load increment at that bus will be almost totally provided by the reactive source equipment connected to the same bus, and therefore the reactive spot price is the derivative of the equipment operating cost curve. In general, the operating reactive costs are due to the internal losses associated with the generation or absorption of reactive power. For a given injected power, these costs can be written as $c_j(Q_j, V_j)$. The reactive marginal price is:

$$\sigma_j = \frac{\partial c_j(Q_j, V_j)}{\partial Q_j} + \frac{\partial c_j(Q_j, V_j)}{\partial V_j} \frac{\partial V_j}{\partial Q_j} \qquad (10.149)$$

where

σ_j: The reactive power price at generator bus j

$\dfrac{\partial V_j}{\partial Q_j}$: The variation in the generator voltage when the injected reactive power changes

Generally, the second term in equation (10.149) is smaller than the first one.

10.8.2.2 *Computation of Reactive Spot Prices at Load Buses*   Consider now a load bus *i* where no reactive generation equipment is connected. Then, when increasing the reactive power load, assuming that the rest of the loads remain constant, the system cost is going to increase. The reasons are:

(a) The increment of reactive power generation
(b) The increment of the system active power losses produced for the increment of reactive power flows
(c) The possible redispatch caused by some system constraints

The reactive power spot price at the load bus can be decomposed as:

$$\sigma_i = \sum_{j \in NG} W_{ij}\sigma_j + \lambda\frac{\partial P_{\mathrm{L}}}{\partial Q_i} + \sum_{Nk} \sigma_{Nk,i} \tag{10.150}$$

where

W_{ij}: The weight factors that indicate in which amount each reactive power generation equipment responds to the assumed reactive demand increment in the absence of system constraints

$\dfrac{\partial P_{\mathrm{L}}}{\partial Q_i}$: The network active power losses increment caused by the assumed reactive load increment

λ: The system marginal active power price (This price is assumed to be almost equal to the active power spot price.)

$\sigma_{Nk,i}$: Represents the marginal contribution of the system constraint *Nk* to the system operation costs.

In equation (10.150), the reactive power spot price consists of a losses component and a security component. Therefore, the reactive price losses component $\sigma_{\mathrm{L}i}$ and the security component $\sigma_{\mathrm{S}i}$ can be expressed as

$$\sigma_{\mathrm{L}i} = \sum W_{ij}\sigma_j + \lambda\frac{\partial P_{\mathrm{L}}}{\partial Q_i} \tag{10.151}$$

$$\sigma_{\mathrm{S}i} = \sum_{Nk} \sigma_{Nk,i} \tag{10.152}$$

The security component of the reactive spot price can be obtained from the solution of the optimal reactive dispatch problem. The dual variable of the constraint obtained through the solution of the dispatch optimization problem will be used to compute the value of the security component.

According to the reactive spot price, the practical remuneration and charging procedures for reactive supply and voltage control services are summarized as below:

(a) Remuneration for the reactive energy provision, which is paid to generators and other voltage control equipment. The amount of the remuneration is set by the losses component of the reactive spot prices ($/MVAr-h) times the injected reactive power. The spot prices are computed by using the internal losses curves declared by the reactive sources in their long-term bids and the marginal price of the active energy hourly market.

(b) Remuneration for the regulating reactive power capacity, which is paid to generators and other voltage control equipment. The amount of the remuneration is associated with the available reactive capacity (in MVAR) and the control (time constant, integration in a secondary voltage control, etc.). Local or regional capacity payments should be calculated. To receive this capacity payment a long-term obligation to provide the regulating service should be agreed upon by the supplier agents and the system operator.

(c) The payments made by large customers and distribution utilities shall be associated with their reactive energy consumption times the corresponding losses component of the reactive spot prices. Usually distribution utilities can influence the required level of service by making contracts with embedded generators, by capacitor bank switching, etc.

(d) The difference between the total remuneration (a and b) and the reactive energy payments made by large customers and distribution utilities (c) is the bundled part of the service. This part could be dealt as a charge to all pool participants proportional to the sold or bought active energy amount, or included as an uplift in the pool market price.

10.8.3   Multiarea VAR Pricing Problem

The VAR pricing in the previous section concentrates on the single-area system. Since the multiarea power system is connected via inter-ties typically overburdened with local and global demands in the presence of uncertainty and violation, the presence of local area VAR provides control source to prevent voltage instability and power flow infeasible. Therefore, the values and benefit of VAR support service in the multiarea environment are very useful to the restructured power system [43, 44].

This section focuses on the multiarea system and computes the VAR optimization and pricing in a multiarea environment based on cost-benefit analysis (CBA) and nonlinear convex network flow programming (NLCNFP). The cost of reactive power support service is determined based on capability and contribution to improvement of system performance including factors such as security, reliability, and economics. CBA is used to select and rank the sites of VAR support. Only the selected optimal VAR support sites are considered in the calculation of VAR optimization.

10.8.3.1 *Optimal Model in Multiareas* Generally, the most economical arrangement of the pool is that the power transfers among areas are free to vary until the total generating cost within the pool is minimized. However, sometimes this practice is not adopted because utilities may want to retain some of their autonomy. A possible arrangement is that each area submits buy/sell quotations hourly to the central dispatcher or independent system operator (ISO) based on its marginal cost curve. The quotations are based on each potential seller's incremental cost of generating power and each potential buyer's decremental cost. As soon as an area has cheap generating cost, it always wants to sell (or deliver) MW power to other systems (or areas) as much as possible depending on the transfer capacity of tie-lines. In this case, reactive power support service in the area has two important roles:

(i) It can reduce costs and system loss and modify voltage profile.
(ii) It can increase the transfer capacity and thus increase the MW power delivery of tie lines.

Therefore, the following optimal model, in which the reactive power support service is provided in the selected area, is proposed for the multiarea power system [43].

Objective function:

(a) Power delivery maximization

$$\text{Max } F_{\text{Tie}} = \sum_{K=1}^{NTK} (P_{\text{Tie}-Ka}(q_{ci}) - P_{\text{Tie}-Ka}(0)) \quad \text{for optimization area} \quad (10.153)$$

(b) Loss minimization

$$\text{Min } F_{\text{L}} = P_{\text{L}a} \quad a \in NA \quad \text{for optimization area} \quad (10.154)$$

Constraints:

$$P_{\text{g}a} = P_{\text{d}a} + P_{\text{L}a} + \sum_{k=1}^{NTK} P_{\text{tie}-ka}(q_{ci}) \quad a \in NA \quad (10.155)$$

$$\sum_{a=1}^{NA} \sum_{i=1}^{NG(a)} P_{gia} - \sum_{a=1}^{NA} \sum_{i=1}^{ND(a)} P_{dia} - P_{\text{L}} = 0 \quad (10.156)$$

$$P_{gia\min} \leq P_{gia} \leq P_{gia\max} \quad (10.157)$$

$$-P_{ij\max} \leq P_{ij} \leq P_{ij\max} \quad ij = 1,\ldots, NL \quad (10.158)$$

$$-P_{\text{Tie}-\text{KaM}} \leq P_{\text{Tie}-Ka}(q_{ci}) \leq P_{\text{Tie}-\text{KaM}}, \quad k \in NTK, \quad a \in NA \quad (10.159)$$

$$Q(q_c, V_g, T, V_d) = 0 \qquad (10.160)$$

$$Q_{gi\min} \leq Q_{gi} \leq Q_{gi\max} \qquad (10.161)$$

$$V_{gi\min} \leq V_{gi} \leq V_{gi\max}, \quad i \in NG(a) \qquad (10.162)$$

$$V_{di\min} \leq V_{di} \leq V_{di\max}, \quad i \in ND(a) \qquad (10.163)$$

$$T_{i\min} \leq T_i \leq T_{i\max}, \quad i \in NT(a) \qquad (10.164)$$

$$q_{ci\min} \leq q_{ci} \leq q_{ci\max}, \quad i \in NC(a) \qquad (10.165)$$

where

F_{tie}: The net increase of MW power of tie lines related to area a after VAR support is provided

$P_{tie\text{-}ka}(q_{ci})$: The MW power of tie-line related to area a after VAR support is provided

$P_{tie\text{-}ka}(0)$: The real power of tie-line related to area a before VAR support is provided

$P_{tie\text{-}kaM}$: The limit of real power of tie-line related to area a

q_{ci}: The reactive power of capacitor at bus i

P_{di}: The real power load at load bus i

Q_{di}: The reactive power load at load bus i

V_{gi}: The voltage magnitude at generator bus i

V_{di}: The voltage magnitude at load bus i

P_{gi}: The real generation of generator i

Q_{gi}: The VAR generation of generator i

T: The transformer tap position

P_{ga}: The real power generation in area a

P_{da}: The real power load in area a

P_{La}: The real power loss in area a

$NG(a)$: The number of generation buses in area a

$NT(a)$: The number of transformer branches in area a

$ND(a)$: The number of the load buses in area a

NA: The number of areas

$NC(a)$: The number of VAR support sites in area a

NTK: The total number of tie-lines related to area a

P_{ij}: The real power flow through transmission line ij

NL: The number of transmission lines

Equation (10.155) is the real power balance for area a. For MW power of the tie-lines, a positive direction is taken when the power flow leaves the area

and a negative direction when the power flow enters the area. Equation (10.156) is the real power balance for overall system.

Two steps are used to solve the problem of VAR optimization and pricing. Step one is to solve the objective in equation (10.153) and satisfy the constraints. In this step, the increases of the power delivery on the tie-lines from the VAR support are computed. The loss and voltage benefit indices are also calculated based on cost-benefit analysis (CBA), which are used to select the optimal locations of VAR supports. Step two is to solve the objective in equation (10.154) and the constraints, where only the selected optimal VAR supports obtained in step one are considered.

The solution method of the above-mentioned optimization model is the nonlinear convex network flow programming (NLCNFP). The details of NLCNFP are described in Chapter 5.

10.8.3.2   *Calculation of VAR Pricing in Multiareas*   The reactive power pricing of each VAR support bus is generally divided into two parts [41]. One is the fixed part, and another is the variable part, i.e.,

$$C_{P(i)}(t) = C_{f(i)}(t) + C_{V(i)}(t) \qquad (10.166)$$

The investment cost (including installation cost) of the VAR source is the fixed part of VAR pricing at this VAR source bus, i.e.,

$$C_{f(i)} = C_{ci}q_{ci} \qquad (10.167)$$

where

$C_{f(i)}$: The fixed part of reactive power pricing at VAR source bus i

C_{ci}: The unit investment cost due to allocation of capacitors at load bus i ($/MVAR)

The variable cost of reactive power support service is determined based on capability and contribution to improvement of system performance for the given area, including factors such as security, reliability, and economics. In the single-area system, the contribution of VAR support is mainly evaluated by the reduction of system power loss, or the saving of generation cost. For the multiarea system, however, these benefits (loss reduction and generation cost saving) are smaller than the benefit of increasing power delivery on tie-lines. Therefore, the contribution or value of VAR support to the system in the multiareas is evaluated by calculating sensitivity of the objective function (net increase of power delivery on tie-lines) with respect to VAR support service in the optimization area. This sensitivity reflects dollar benefits from applying VAR support service. Therefore, the variable part of reactive power pricing at this VAR source bus can be written as follows:

$$C_{V(i)}(t) = \lambda \left. \frac{\partial F_{\text{Tie}}}{\partial Q_i} \right|_t \times q_{Ci}(t) \tag{10.168}$$

where

$C_{V(i)}(t)$: The variable part of reactive power pricing at VAR source bus i at time t

q_{ci}: The reactive power of capacitor at bus i at time t

λ: The pricing of electricity (\$/MWhr)

$\partial F_{\text{Tie}}/\partial Q_i$: The sensitivity of the objective function of increasing tie-line power delivery with respect to reactive power support (capacitor)

10.8.3.3 Cost-Benefit Analysis   In theory, all buses (locations) in a system can be selected as the VAR support sources. However, this is not a good approach. One hand, some locations are not effective and/or efficient as the VAR support sources, and on the other hand, it is expensive and time-consuming to consider all locations as the VAR sources. Thus we apply the CBA method to compute the benefit indices for each VAR source. Three benefit-to-cost ratio (BCR) indices are introduced. They are loss BCR, voltage BCR, and power delivery BCR.

$$\text{BCR}_{Li} = \frac{\sum\limits_{t=1}^{24} \lambda \left(P_{La}^t(0) - P_{La}^t(q_{ci}) \right)}{C(q_{Ci})} \tag{10.169}$$

$$\text{BCR}_{Pi} = \frac{\sum\limits_{t=1}^{24} \lambda \left(P_{\text{Tie}-k}^t(q_{ci}) - P_{\text{Tie}-k}^t(0) \right)}{C(q_{Ci})} \tag{10.170}$$

$$\text{BCR}_{Vi} = \frac{\sum\limits_{t=1}^{24} \lambda_V \left(\sum\limits_k V_k^t(q_{ci}) - \sum\limits_k V_k^t(0) \right)}{C(q_{Ci})} \tag{10.171}$$

or

$$\text{BCR}_{Li}^t = \frac{\lambda \left(P_{La}^t(0) - P_{La}^t(q_{ci}) \right)}{C(q_{Ci})/24} \tag{10.172}$$

$$\text{BCR}_{Pi}^t = \frac{\lambda \left(P_{\text{Tie}-K}^t(q_{ci}) - P_{\text{Tie}-K}^t(0) \right)}{C(q_{Ci})/24} \tag{10.173}$$

$$\text{BCR}_{Vi}^t = \frac{\lambda_V \left(\sum\limits_k V_k^t(q_{ci}) - \sum\limits_k V_k^t(0) \right)}{C(q_{Ci})/24} \tag{10.174}$$

$$C(q_{Ci}) = \frac{\alpha C_{Ci} q_{Ci}}{365} \tag{10.175}$$

where

$P_{La}^t(0)$: The real power loss in area a at time t before VAR source (e.g. capacitor) at bus i is provided

$P_{La}^t(q_{ci})$: The real power loss in area a at time t after VAR source at bus i is provided

$P_{Tie-K}^t(0)$: The tie-line power related to the optimization area at time t before capacitor at bus i is provided

$P_{Tie-K}^t(q_{ci})$: The tie-line power related to the optimization area at time t after capacitor at bus i is provided

$V_k^t(0)$: The voltage magnitude at bus k at time t before VAR source at bus i is provided

$V_k^t(q_{ci})$: The voltage magnitude at bus k at time t after VAR source at bus i is provided

$C(q_{Ci})$: The equivalent daily investment cost of capacitor at load bus i (\$/day)

BCR^t: hourly based benefit-to-cost ratio

α: The capital recovery factor (CRF), which is an important factor in economic analysis

A unified weighting coefficient that combines three BCR indices is presented as follows. It affects the comprehensive benefits from the each VAR support source. Thus it can be used to select the best VAR support sites.

$$W_i^t = \frac{BCR_{Li}^t}{\sum_i BCR_{Li}^t} + \frac{BCR_{Pi}^t}{\sum_i BCR_{Pi}^t} + \frac{BCR_{Vi}^t}{\sum_i BCR_{Vi}^t} \tag{10.176}$$

where W_i^t is the comprehensive benefit index for VAR support i.

It is noted that we assume that three benefit indices are equal important in the above. If the relative importance of three benefit indices is uncertain, and some other nontechnical factors are also considered, the AHP method introduced earlier should be adopted.

The presented VAR pricing and optimization scheme is tested with the IEEE 118-bus system. The 118-bus system consists of three areas, as shown in Figure 10.2. The system partition is shown in Table 10.15. Area 2 is selected as the optimization area. The tie-lines relating to area 2 are: L33-15, L34-19, L38-30, L68-81, L69-70, L69-75, L69-77. The direction of power on the tie-line is positive if the power is delivered from area 2 to the other areas; otherwise, it is negative if the power is transmitted from an other area to area 2.
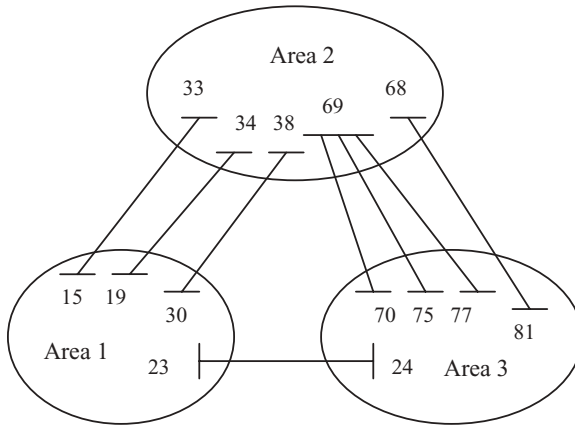
FIGURE 10.2 118-bus network with three areas

Table 10.15 The partitioned 118-bus system

Area	Area 1	Area 2	Area 3
Gen. buses	1, 4, 8, 10, 12, 20, 25, 26, 27, 31, 113	36, 40, 42, 43, 46, 49, 54, 59, 61, 65, 66, 69, 116	24, 72–74, 80, 87, 89–92, 97, 99, 100, 103, 107, 111, 112
Load buses	2, 3, 5–7, 9 11, 13–19, 21–23, 28–30, 32, 114, 115, 117	33–35, 37–39, 41, 44, 45, 47, 48, 50–53, 55–58, 60, 62–64, 67, 68	70, 71, 75, 76, 77, 79, 81–86, 88, 93–96, 98, 101, 102, 104–106, 108–110

It is assumed that the pricing of electricity λ is \$30/MWhr, and the investment cost of the VAR source-capacitor is \$100.0/kVAR. The capital recovery factor is 0.149. The total increase of power delivery on tie-lines in area 2 from VAR support service is given as column 2 in Table 10.16. The variable cost of VAR pricing for each reactive power support bus is computed and listed in column 3 in Table 10.16.

Because of network topology, VAR support at different load sites may produce different benefits. Cost-benefit analysis is used to calculate and compare these benefits. The results are shown in Table 10.17. Set the threshold of the unified weighting coefficient to 0.20 for selecting the best VAR support sites. Then the optimal VAR support sites will be B-39, B-45, B-52, and B-34. Based on these selected VAR support sources, the VAR optimal control results in area 2 are obtained and shown in Table 10.18.

Table 10.16   Results of VAR pricing for area 2 in IEEE 118-bus system

VAR Support Site	Power Delivery Increase (MW)	VAR Pricing ($/MVAr hr)
B-33	0.64100	3.84600
B-34	2.12000	12.7200
B-35	1.09000	6.54000
B-39	3.81000	22.8600
B-41	1.19000	7.14000
B-44	1.52000	9.12000
B-45	2.25000	13.5000
B-48	1.09000	6.54000
B-50	1.10000	6.60000
B-51	1.58000	9.48000
B-52	2.27000	13.6200
B-53	1.17000	7.02000
B-55	0.91000	5.46000
B-56	1.15000	6.90000
B-57	1.85000	11.1000
B-58	1.16000	6.96000
B-60	1.01000	6.06000
B-62	1.07000	6.42000
B-67	1.18000	7.08000

Table 10.17   Optimal ranking of VAR support sites in area 2

VAR Sites	BCR_{Li}^{t}	BCR_{Pi}^{t}	BCR_{Vi}^{t}	W_i^t	Rank
B-33	0.8660	2.2680	0.7980	0.10634	19
B-34	1.7700	7.6670	0.9600	0.21011	4
B-35	0.7900	3.8580	0.8360	0.12098	16
B-39	2.1200	13.487	1.5600	0.31774	1
B-41	0.9600	4.2120	0.9100	0.13631	10
B-44	0.8500	5.3810	0.8800	0.14139	8
B-45	1.8900	7.9650	1.1530	0.22930	2
B-48	0.8200	3.8580	0.7900	0.11975	17
B-50	0.8800	3.8940	0.8200	0.12449	13
B-51	1.0900	5.5930	0.9100	0.15600	6
B-52	1.6200	8.0350	1.2200	0.22162	3
B-53	1.0500	4.1420	0.8900	0.13850	9
B-55	0.9100	3.2210	0.8230	0.11926	18
B-56	0.9500	4.0710	0.8710	0.13226	12
B-57	1.5700	6.5490	1.0600	0.19553	5
B-58	1.3600	4.1060	0.9100	0.15322	7
B-60	0.9100	3.5750	0.8320	0.12331	14
B-62	0.8700	3.7880	0.7900	0.12129	15
B-67	0.9800	4.1770	0.8340	0.13260	11

Table 10.18   Results of VAR optimal controls in area 2 (p.u.)

Generator	V_{gi}	V_{gimax}	V_{gimin}	P_{gi}
G36	0.98530	1.05000	0.95000	1.73620
G40	1.05000	1.05000	0.95000	2.31446
G42	1.05000	1.05000	0.95000	2.15689
G46	1.04998	1.05000	0.95000	0.00006
G49	1.05000	1.05000	0.95000	1.95897
G54	0.97334	1.05000	0.95000	1.68445
G59	0.98891	1.05000	0.95000	1.77805
G61	0.96054	1.05000	0.95000	1.85933
G65	1.04821	1.05000	0.95000	1.06144
G66	1.05000	1.05000	0.95000	5.52085
G69 (slack)	1.05000	1.05000	0.95000	15.9408
G116	1.04669	1.05000	0.95000	0.27674

Transformer From	To	T_{imax}	T_{imin}	Tap T
38	37	1.10000	0.90000	1.02689
63	59	1.10000	0.90000	1.07930
64	61	1.10000	0.90000	1.09835
66	65	1.10000	0.90000	1.10000
68	69	1.10000	0.90000	1.05742

REFERENCES

[1] O. Alsac and B. Stott, "Optimal power flow with steady-state security," *IEEE Trans. Power System*, Vol. 93, 1974, pp. 745–751.

[2] D.I. Sun, B. Ashley, A. Hughes, and W.F. Tinney, "Optimal power flow by Newton approach," *IEEE Trans. Power System*, Vol. 103, No. 10, 1984, pp. 2864–2880.

[3] D. Pudjianto, S. Ahmed, and G. Strbac, "Allocation of VAR support using LP and NLP based optimal power flows," *IEE Proc. Generation, Transmission, and Distribution*, vol. 149, no. 4, pp. 377–383, 2002.

[4] K. Aoki, M. Fan, and A. Nishikori, "Optimal Var planning by approximation method for recursive mixed-integer linear programming," *IEEE Trans. Power Syst.*, vol. 3, no. 4, pp. 1741–1747, Nov. 1988.

[5] L.G. Dias and M.E. El-Hawary, "Security-constrained OPF: Influence of fixed tap transformer fed loads," *IEEE Trans. Power Syst.*, vol. 6, no. 4, pp. 1366–1372, Nov. 1991.

[6] N. Deeb and S.M. Shahidehpour, "Linear Reactive Power Optimization in a Large Power Network Using the Decomposition Approach," *IEEE Transactions on Power Systems*, Vol. 5, 1990, pp. 428–438.

[7] K. Mamandur and R. Chenoweth, "Optimal Control of Reactive Power Flow for Improvements in Voltage Profiles and for Real Power Loss Minimization," *IEEE Transactions PAS*, Vol. 100, 1981, pp. 3185–3194.

[8] M.O. Mansour and T.M. Abdel-Rahman, "Non-linear VAR Optimization Using Decomposition and Coordination," *IEEE Transactions PAS*, Vol. 103, 1984, pp. 246–255.

 [9] M.R. Irving and M.J.H. Sterling, "Efficient Newton-Raphson algorithm for load flow calculation in transmission and distribution networks," *IEE Proc. C*, Vol. 134, 1987.

[10] J.R.S. Mantovani and A.V. Garcia, "A heuristic method for reactive power planning," *IEEE Trans. Power Syst.*, vol. 11, no. 1, pp. 68–74, Feb. 1996.

[11] M. Delfanti, G. Granelli, P. Marannino, and M. Montagna, "Optimal capacitor placement using deterministic and genetic algorithms," *IEEE Trans. Power Syst.*, vol. 15, no. 3, pp. 1041–1046, Aug. 2000.

[12] K. Iba, H. Suzuki, K.I. Suzuki, and K. Suzuki, "Practical reactive power allocation/ operation planning using successive linear programming," *IEEE Trans. Power Syst.*, vol. 3, no. 2, pp. 558–566, May 1988.

[13] J.Z. Zhu and M.R. Irving, "Combined Active and Reactive Dispatch with Multiple Objectives Using Analytic Hierarchical Process," *IEE Proceedings Part C*, Vol. 143, 1996, pp. 344–352.

[14] J.Z. Zhu and C.S. Chang, "Power system optimal var planning with security and economic constraints," 1997 *Intern. Power Eng. Conf., IPEC'97, Singapore, May, 1997*, pp. 42–46.

[15] J.A. Momoh and J.Z. Zhu, "Improved interior point method for OPF problems," *IEEE Transactions on Power Systems*, Vol. 14, No. 3, Aug. 1999, pp. 1114–1120.

[16] J.Z. Zhu and X.F. Xiong, "Optimal Reactive Power Control using Modified Interior Point Method," *Electric Power Systems Research*, Volume 66, 2003, pp. 187–192.

[17] L.L. Lai and J.T. Ma, "Application of evolutionary programming to reactive power planning-comparison with nonlinear programming approach," *IEEE Trans. Power Syst.*, vol. 12, no. 1, pp. 198–206, Feb. 1997.

[18] J.Z. Zhu, C.S. Chang, W. Yan, and G.Y. Xu, "Reactive power optimization using an analytic hierarchical process and a nonlinear optimization neural network approach," *IEE Proc. Generation, Transmission, and Distribution*, vol. 145, no. 1, pp. 89–97, Jan. 1998.

[19] W.S. Jwo, C.W. Liu, C.C. Liu, and Y.T. Hsiao, "Hybrid expert system and simulated annealing approach to optimal reactive power planning," *IEE Proc. Generation, Transmission and Distribution*, vol. 142, no. 4, pp. 381–385, Jul. 1995.

[20] V.C. Ramesh and X. Li, "A fuzzy multiobjective approach to contingency constrained OPF," *IEEE Trans. Power Syst.*, vol. 12, no. 3, pp. 1348–1354, Aug. 1997.

[21] K.P. Wong, A. Li, and T.M.Y. Law, "Advanced constrained genetic algorithm load flow method," *IEE Proc. C*, Vol. 146, No. 6, 1999, pp. 609–618.

[22] K.H. Abdul-Rahman and S.M. Shahidehpour, "Application of fuzzy sets to optimal reactive power planning with security constraints," *IEEE Trans. Power System*, vol. 9, no. 2, pp. 589–597, May 1994.

[23] M.A. Abido, "Multiobjective Optimal VAR Dispatch Using Strength Pareto Evolutionary Algorithm," 2006 *IEEE Congress on Evolutionary Computation, Sheraton Vancouver, Wall Centre Hotel, Vancouver, BC, Canada, July 16–21, 2006*.

[24] F.C. Schweppe, M.C. Caramanis, R.D. Tabors, and R.E. Bohn, *Spot Pricing of Electricity*, Kluwer Academic Publishers, New York, 1988.

[25] S. Naka, T. Genji, T. Yura, and Y. Fukuyama, "A hybrid particle swarm optimization for distribution state estimation," *IEEE Trans. Power Syst.*, vol. 18, no. 1, pp. 60–68, Feb. 2003.

[26] A.A.A. Esmin, G. Lambert-Torres, and A.C.Z. de Souza, "A hybrid particle swarm optimization applied to loss power minimization," *IEEE Trans. Power Syst.*, vol. 20, no. 2, pp. 859–866, May 2005.

[27] C.Z. de Souza, L.M. Honorio, G.L. Torres, and G. Lambert-Torres, "Increasing the loadability of power systems through optimal-local-control actions," *IEEE Trans. Power Syst.*, vol. 19, no. 1, pp. 188–194, Feb. 2004.

[28] M.A. Abido and J.M. Bakhashwain, "Optimal VAR dispatch using a multiobjective evolutionary algorithm," *Int. J. Elect. Power Energy Syst.*, vol. 27, no. 1, pp. 13–20, 2005.

[29] G. Vlachogiannis and K.Y. Lee, "A Comparative Study on Particle Swarm Optimization for Optimal Steady-State Performance of Power Systems," *IEEE Trans. Power Syst.*, vol. 21, no. 4, pp. 1718–1728, 2006.

[30] Y. He, Z.Y. Wen, F.Y. Wang, and Q.H. Zhou, *Power Systems Analysis*, Huazhong Polytechnic University Press, 1985.

[31] W.Y. Li, *Secure Economic Operation of Power Systems*, Chongqing University Press, 1989.

[32] T.L. Saaty, *The Analytic Hierarchy Process*, McGraw Hill, Inc., New York. 1980.

[33] R.J. Vanderbei, *Linear Programming: Foundations and Extensions*.

[34] J.K. Strayer, *Linear Programming and Applications*, Springer-Verlag, 1989.

[35] D.W. Tank and J.J. Hopfield, "Simple Neural Optimization Networks: An A/D Converter, Signal Decision Network and A Linear Programming Circuit," *IEEE Transaction on Circuits and Systems*, Vol. 33, 1986, pp. 533–541.

[36] E. Zitzler and L. Thiele, "An Evolutionary Algorithm for Multiobjective optimization: The Strength Pareto Approach," Swiss Federal Institute of Technology, TIK-Report, No. 43, 1998.

[37] N. Morse, "Reducing the Size of Nondominated Set: Pruning by Clustering," *Computers and Operations Research*, Vol. 7, No. 1–2, 1980, pp. 55–66.

[38] A.I. Selvakumar and K. Thanushkodi, "A New Particle Swarm Optimization Solution to Nonconvex Economic Dispatch Problems," *IEEE Trans. Power Syst.*, vol. 22, no. 1, pp. 42–51, 2007.

[39] J.B. Gil, T.G. San Román, J.J. Alba Ríos, and P.S. Martín, "Reactive Power Pricing: A Conceptual Framework for Remuneration and Charging Procedures," *IEEE Trans. Power Syst.*, vol. 15, no. 2, pp. 483–489, 2000.

[40] M.L. Baughman and R. Siddiqi, "Real time pricing of reactive power: theory and case study results," *IEEE Transactions on Power Systems*, vol. 6, no. 1, Feb. 1991.

[41] J.Z. Zhu and J.A. Momoh, "Optimal VAR pricing and VAR placement using analytic hierarchy process," *Electric Power Systems Research*, Vol. 48, No. 1, 1998, pp. 11–17.

[42] J.A. Momoh and J.Z. Zhu, "Multiple indices for optimal VAR pricing and control," *International Journal of Decision Support Systems*, Vol. 24, No. 1, 1999, pp. 223–232.

[43] J.Z. Zhu, "VAR pricing computation in multi-areas by nonlinear convex network flow programming," *Electric Power Systems Research*, Vol. 65, No. 2, 2003, pp. 129–134.

[44] J.Z. Zhu and X.F. Xiong, "VAR optimization and pricing in multi-areas power system," *Proc. of IEEE General Meeting*, 2003.

11

OPTIMAL LOAD SHEDDING

When all available controls are unable to maintain the security of system operation during a disturbance or contingency, optimal load shedding will be used as the last resort to make the loss of blackout minimum. This chapter first introduces the traditional load-shedding methods such as underfrequency or undervoltage load shedding and then studies optimal power system load-shedding methods. These include intelligent load shedding, distributed interruptible load shedding, Everett optimization, analytic hierarchical process (AHP), and network flow programming (NFP). The related topic of congestion management is also introduced in this chapter.

11.1 INTRODUCTION

The security and stability of electrical power systems have always been one of the central and fundamental issues of concern in network planning and operation. Serving users of electricity is the duty of power systems that generate, transmit, and distribute electrical energy. Therefore, system operation, network growth and expansion are highly user dependent and the system should be able to satisfy their needs and requirements. Central requirements include reliability, quality of energy, and continued load capacity. Network designers and operation managers should continuously pay attention to these requirements and take the necessary steps to fulfill them and maintain the desired qualities. Especially, the US electric marketplace is in the midst of major

changes designed to promote competition. There is no longer vertical integration with guaranteed customers and suppliers. Electric generators and distributors will have to compete to sell and buy electricity. The stable utilities of the past will find themselves in a highly competitive environment [1–3]. In this new competitive power environment, buy/sell decision support systems are needed to find economical ways to serve critical loads with limited sources under various uncertainties. Decision-making is significantly affected by limited energy sources, generation cost, and network available transfer capacity. Generally, a congested system or system overloading can be reduced through some control strategy such as a generation rescheduling scheme, obtaining power support from a neighboring utility as well as optimal load shedding. In the particular case of power shortage, load shedding cannot be avoided. This, in turn, requires that the load demand be as determinate as possible so that each watt can be allocated.

In general, load shedding can be defined as the amount of load that must almost instantly be removed from a power system to keep the remaining portion of the system operational. This load reduction is in response to a system disturbance (and consequent possible additional disturbances) that results in a generation deficiency condition or network overloading situation. Common disturbances that can cause these conditions to occur include transmission line or transformer faults, loss of generation, switching errors, and lightning strikes. When a power system is exposed to a disturbance, its dynamics and transient responses are mainly controlled through two major dynamic loops. One is the excitation (including AVR) loop that will control the generator reactive power and system voltage. Another is the prime-mover loop, which will control the generator active power and system frequency.

11.2   CONVENTIONAL LOAD SHEDDING

Load shedding by frequency relays is the most commonly used method for controlling the frequency of power networks within set limits and maintaining network stability under critical conditions. In the conventional load-shedding methods, when frequency drops below the operational plan's set point, the frequency relays of the system issue commands to disconnect parts of the electrical power load in a stepwise manner, thereby preventing further frequency drop and its consequential effects [8].

The reason that frequency is the main criterion of system quality and security is as follows:

- A global variable of interconnected networks that has the same value in all parts of the network
- An indicator of the balance between supply and demand
- A critically important factor for the smooth operation of all users and particularly manufacturing and industries
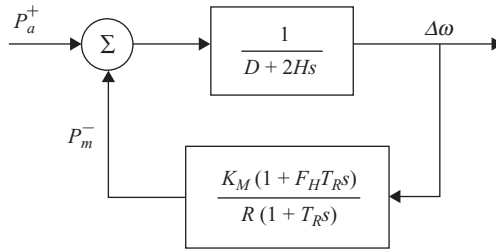
FIGURE 11.1   Steady-state frequency-response model

One of the main problems of all interconnected networks is a total blackout because of frequency drop as a consequence of some power station failure or transmission line breakage. Presently, in the power generation and transmission systems of the world, the most appropriate way of preventing a total or partial blackout that is triggered by frequency drop is quick and automatic load shedding.

To study situations of imbalance between power supply and demand, and the resulting frequency variations under the circumstances of severe and major disorders, a simplified model of the steady state for systems that consist mainly of thermal units is used [8–10], which is shown in Figure 11.1.

The expression of the model is as follows:

$$\Delta\omega = \frac{P_a}{D}\left(1 - e^{-\frac{D}{2H}t}\right)$$

(11.1)

where

H: System's inertial constant

D: Load damping coefficient

K_m: Frequency control loop gain

F_H: High-pressure re-warmed turbines' power portion

T_R: Rewarming time constant

P_m: Mechanical power of the turbine (per unit)

P_a: Accelerator's power

$\Delta\omega$: Speed change (per unit)

Equation (11.1) models the system at the initial conditions of major disorders when the governor's effect is lifted off because during the first seconds of the disorder, due to governor's response delay and its operating time constant, it cannot play a role in prevention of the frequency drop [9].

According to equation (11.1), the main factors and parameters that control the behavior of frequency and overloading are the amount of overloading

and the D and H parameters. The effect of these two parameters should be definitely considered in any load-shedding scheme.

The load damping coefficient (D) is an effective parameter that represents the relation between the load and the frequency. It cannot be ignored in planning for load-shedding schemes. In planning for load shedding, the load damping coefficient is normally expressed per unit as shown in the following formula:

$$D = \frac{F}{P} \frac{\Delta P}{\Delta F} \qquad (11.2)$$

The value of D varies from 0 to 7 and is to be determined once for each system and used in all cases of planning. The latest studies have shown $D = 3.3$ for the sample network [8].

The effect of D on the frequency drop gradient is quite visible as an increase in D causes a decrease in the frequency drop gradient. For any specified overloading, systems with a higher value of D will have a higher stability and the final system frequency will be stabilized at a higher level. Figure 11.2 clearly shows the effect of D on the frequency drop curve.

In commonly used stepwise methods, the load-shedding scheme has little relation to the degree of overload. Any overload triggers the same strategy of load shedding, as the degree of overload does not determine the number or quantity of the load shedding.

This kind of scheme greatly simplifies the task of harmonizing the relays and the steps of load shedding, as simple calculations and a process of trial
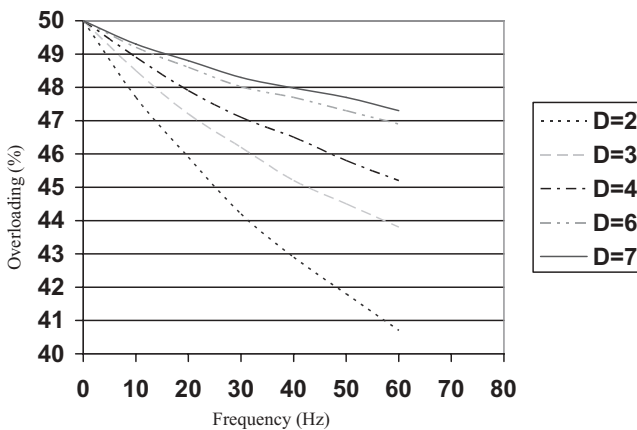
FIGURE 11.2   The effect of load damping coefficient on the frequency drop curve (system stability curves for various overloading)

and error would suffice. It is one of the obvious advantages of this kind of scheme. Once the steps of load shedding are specified, if at any step the frequency continues to drop (with regard to the specified delay times), then the next step will be automatically activated until the frequency stops dropping. In such strategies, increasing the number of steps can increase the costs and allow a more precise harmony and a minimized blackout area. Nevertheless, in almost all countries, only three to five steps are planned, with rare cases of more steps.

In such strategies or plans, the first step of load shedding is regulated in such a way that with any frequency drop below the set point, this step is activated to operate within its specific time delay. The time duration for frequency to drop from normal to below the set point is not taken into consideration, despite the fact that we know that the gradient of frequency drop is directly proportional to the amount of overload and severity of the case; therefore, it can be a basis to decide on whether only one step is adequate.

11.3   INTELLIGENT LOAD SHEDDING

11.3.1   Description of Intelligent Load Shedding

Conventional load shedding systems that rely solely on frequency measuring systems cannot be programmed with the knowledge gained by the power system designers. The system engineer must perform numerous system studies that include all of the conceivable system operating conditions and configurations to correctly design the power system. Unfortunately, the engineer's knowledge of the system that is gained through the studies is not utilized fully. Additionally, most data and study results are simply lost. This unavailability of information for future changes and enhancement of the system will significantly reduce the protection system performance.

The state-of-the-art load-shedding system uses real-time systemwide data acquisition that continually updates a computer-based real-time system model. This system produces the optimum solution for system preservation by shedding only the necessary amount of load and is called intelligent load shedding (ILS) [11].

This system must have the following capabilities:

- Able to map a very complex and nonlinear power system with a limited number of data collection points to a finite space.
- Automatically remember the system configuration, operation conditions as load is added or removed, and the system response to disturbances with all of the system configurations.
- Recognize different system patterns in order to predict system response for different disturbances.

- Utilize a built-in knowledge base trainable by user-defined cases.
- Adaptive self-learning and automatic training of system knowledge base due to system changes.
- Make fast, correct, and reliable decisions on load shedding priority based on the actual loading status of each breaker.
- Shed the minimum amount of load to maintain system stability and nominal frequency.
- Shed the optimal combinations of load breakers with complete knowledge of system dependencies.

In addition to having the above list of capabilities, the ILS system must have a dynamic knowledge base. For the knowledge base to be effective, it must be able to capture the key system parameters that have a direct impact on the system frequency response following disturbances. These parameters include:

- Power exchanged between the system and the grid both before and after disturbance
- Generation available before and after disturbances
- On-site generator dynamics
- Updated status and actual loading of each sheddable load
- The dynamic characteristics of the system loads. This includes rotating machines, constant impedance loads, constant current loads, constant power loads, frequency-dependent loads, or other types of loads.

Some additional requirements must be met during the designing and tuning of an ILS scheme:

- Carefully selected and configured knowledge base cases
- Ability to prepare and generate sufficient training cases for the system knowledge base to ensure accuracy and completeness
- Ability to ensure that the system knowledge base is complete, correct, and tested
- Ability to add user-defined logics
- Ability to add system dependencies
- To have an online monitoring system that is able to coherently acquire real-time system data
- The ability to run in a preventive and predictive mode so that it can generate a dynamic load shedding table that corresponds to the system configuration changes and prespecified disturbances (triggering)
- A centralized distributed local control system for the power system that the ILS system supervises
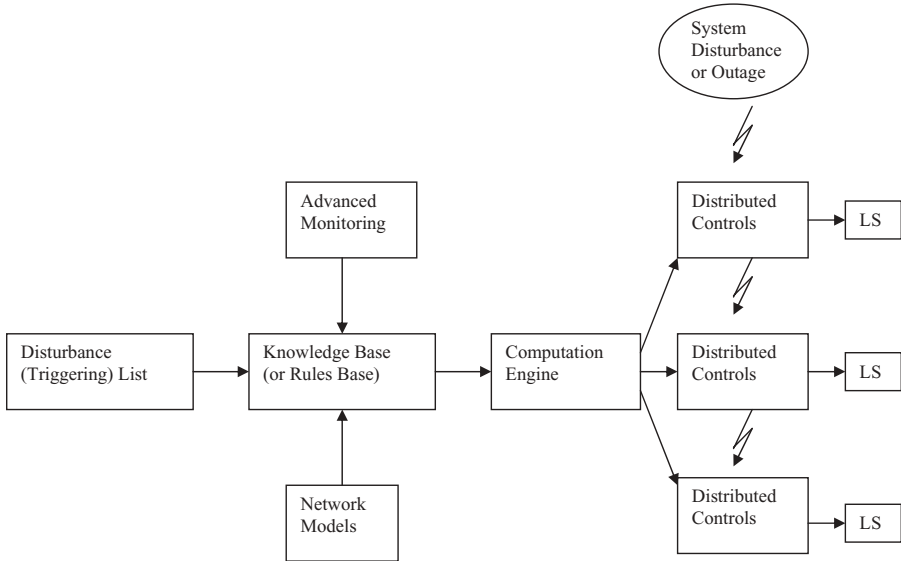
FIGURE 11.3   Function block diagram of the ILS scheme

11.3.2   Function Block Diagram of the ILS

In Figure 11.3, the system knowledge base is pretrained by using carefully selected input and output databases from offline system studies and simulations. System dynamic responses, including frequency variation, are among the outputs of the knowledge base.

The trained knowledge base runs in the background of an advanced monitoring system, which constantly monitors all of the system operating conditions. The network models and the knowledge base provide power system topology, connection information, and electric properties of the system component for ILS. The disturbance list is prepared for all prespecified system disturbances (triggers). Based on the input data and system updates, the knowledge base periodically sends requests to the ILS computation engine to update the load shedding tables, thus ensuring that the optimum load will be shed when a disturbance occur. The load shedding tables in turn are downloaded to the distributed controls that are located close to each sheddable load. When a disturbance occurs, fast load-shedding action can be taken.

11.4   FORMULATION OF OPTIMAL LOAD SHEDDING

In a competitive resource allocation environment, buy/sell decision support systems are needed to find economical ways to serve critical loads with limited sources under different uncertainties. Therefore, a value-driven load-shedding

approach is proposed for this purpose. The mathematical model of load shedding is expressed as follows.

11.4.1 Objective Function—Maximization of Benefit Function

$$\text{Max } H_i = \sum_{j=1}^{ND(K)} w_{ij} v_{ij} x_{ij}$$

$$or \quad \text{Min}(-H_i)$$

(11.3)

where

x_{ij}: Decision variable (it equals 0 or 1) on load bus j at the ith time stage

$ND(k)$: Total number of load sites in load center k

w_{ij}: Load priority to indicate the importance of the jth load site of the ith time stage

v_{ij}: Independent load values (or costs) in a specific load bus j at the ith time stage ($\$/kW$ or $\$/MW$)

H: Benefit function

In objective function (11.3), decision variable x_{ij} equals 1 if load demand P_{ij} is satisfied; otherwise, it equals 0 if the load demand is not satisfied, i.e., load shed appeared on the jth load site at the ith time stage. There are several different kinds of loads in a power system, such as critical load, important load and unimportant load, etc., and w_{ij} can reflect the relative importance of the different kind of loads. The more important the load site is (e.g., first important load), the larger the w_{ij} of the load site will be. In addition, each specific load has its independent load value (cost) v_{ij}, which is the value / cost per kW load at this location. Therefore, the unit of v_{ij} is $\$/kW$.

11.4.2 Constraints of Load Curtailment

The constraints of load curtailment reflect the system congestion case. These constraints include limited capacity in each load center and the whole system, as well as available transfer capacity of the key line (e.g., tie-line connecting different load center or source), which can be expressed as follows:

$$\sum_{j \in K} P_{ij} x_{ij} \le P_{iK}$$

(11.4)

$$\sum_{j=1}^{ND} P_{ij} x_{ij} \le P_{D}$$

(11.5)

$$\sum_{j \in K} P_{ij} x_{ij} = P_{SK} \le P_{SKATC}$$

(11.6)

where

P_{ij}: Load demand of the jth load site of the ith time stage
P_{iK}: Total amount of load center k available at the ith time stage
P_D: Total amount of system load available at the ith time stage
P_{SK}: Transmission power on the line connecting load center k
P_{SKATC}: Available transfer capacity of the line connecting load center k

It is noted that the power flow equation or Kirchhoff's current law must be satisfied during the load shedding, i.e.,

$$\sum_{G \to \omega} P_{iG} + \sum_{T \to \omega} P_{iT} + \sum_{j \to \omega} x_{ij} P_{ij} = 0 \quad \omega \in n \tag{11.7}$$

$$-P_{iT\,max} \le P_{iT} \le P_{iT\,max} \tag{11.8}$$

where n is the total node number in the system; $G \to \omega$ represents that generator G is adjacent to node ω; $T \to \omega$ represents that transmission line T is adjacent to node ω; and $j \to \omega$ represents that load j is adjacent to node ω.

The direction of power flow is specified when the power enters into the node, while the negative when it leaves from the node. Equation (11.8) gives the system network security constraints.

11.5 OPTIMAL LOAD SHEDDING WITH NETWORK CONSTRAINTS

11.5.1 Calculation of Weighting Factors by AHP

It is very difficult to compute exactly the weighting factor of each load in (11.3). The reason is that the relative importance of these loads is not the same, which is related to the power market operation conditions. According to the principle of AHP described in Chapter 7, the weighting factors of the loads can be determined through the ranking computation of a judgment matrix, which reflects the judgment and comparison of a series of pair of factors. The hierarchical model for computing the load weighting factors is shown in Figure 11.4, in which PI is the performance index of load center k.

The judgment matrix A-LD of the load shedding problem can be written as follows:

$$A - LD = \begin{bmatrix} w_{D1}/w_{D1} & w_{D1}/w_{D2} & \cdots\cdots & w_{D1}/w_{Dn} \\ w_{D2}/w_{D1} & w_{D2}/w_{D2} & \cdots\cdots & w_{D2}/w_{Dn} \\ \vdots & & \vdots & \\ w_{Dn}/w_{D1} & w_{Dn}/w_{D2} & \cdots\cdots & w_{Dn}/w_{Dn} \end{bmatrix} \tag{11.9}$$
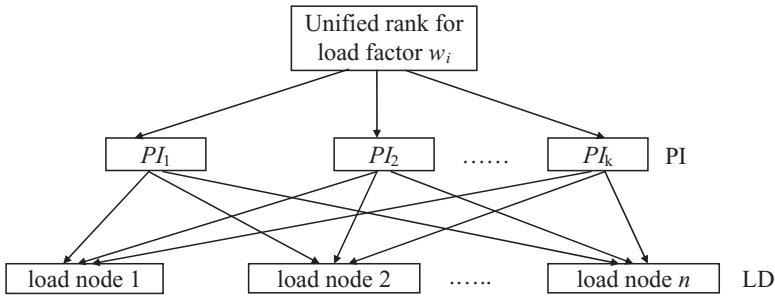
FIGURE 11.4   Hierarchy model of load weighting factor rank

where, w_{Di}, which is just what we need, is unknown. w_{Di}/w_{Dj}, which is the element of the judgment matrix $A\text{-}LD$, represents the relative importance of the ith load compared with the jth load. The value of w_{Di}/w_{Dj} can be obtained according to the experience of electrical engineers or system operators using some ratio scale methods. For example, a "1–9" scale method from Chapter 7 can be used.

Similarly, the judgment matrix $A\text{-}PI$ can be written as follows:

$$A - PI = \begin{bmatrix} w_{K1}/w_{K1} & w_{K1}/w_{K2} & \cdots\cdots & w_{K1}/w_{Kn} \\ w_{K2}/w_{K1} & w_{K2}/w_{K2} & \cdots\cdots & w_{K2}/w_{Kn} \\ \vdots & & \vdots & \\ w_{Kn}/w_{K1} & w_{Kn}/w_{K2} & \cdots\cdots & w_{Kn}/w_{Kn} \end{bmatrix} \quad (11.10)$$

where w_{Ki} is unknown. w_{Ki}/w_{Kj}, which is the element of judgment matrix $A\text{-}PI$, represents the relative importance of the ith load center compared with the jth load center. The value of w_{Ki}/w_{Kj} can also be obtained according to the experience of electrical engineers or system operators using some ratio scale methods.

Therefore, the unified weighting factor of the load w_I can be obtained from the following equation:

$$w_i = w_{Kj} \times w_{Di} \quad Di \in Kj \quad (11.11)$$

where $Di \in Kj$ means load Di is located in load center Kj.

11.5.2   Network Flow Model

After the weighting factors are computed by AHP, the above optimization model of load shedding corresponds to a network flow problem and can be solved by network flow programming (NFP). According to Chapter 5, the general NFP model can be written as

$$\text{Min } F = \sum C_{ij} f_{ij} \tag{11.12}$$

such that

$$\sum (f_{ij} - f_{ji}) = r \tag{11.13}$$

$$0 \le f_{ij} \le U_{ij} \tag{11.14}$$

However, there exist three disadvantages in the general NFP algorithm [14], i.e.,

(a) The initial arc flows must be feasible.
(b) The lower bound of flows should be zero.
(c) All flow variables must be nonnegative.

Because of these disadvantages, it is difficult to solve the optimal load shedding problem effectively by using the general NFP algorithm. A special NFP algorithm, "the out-of-kilter algorithm" (OKA), which is analyzed in Chapter 5, is adopted. The mathematical representation of the OKA network can be written as follows:

$$\text{Min } F = \sum C_{ij} f_{ij} \tag{11.15}$$

such that

$$\sum (f_{ij} - f_{ji}) = 0 \tag{11.16}$$

$$L_{ij} \le f_{ij} \le U_{ij} \tag{11.17}$$

Obviously, the optimal load-shedding model that is mentioned in Section 11.4 can be transformed into the OKA model shown in equations (11.15)–(11.17) and solved by the OKA. The details on the OKA model and algorithm can be found in Chapter 5.

11.5.3 Implementation and Simulation

The simulation system for load shedding is the IEEE 30-bus system. The capacity of the generator is given in Table 11.1. The daily load data including the independent load value/cost at each load site are listed in Table 11.2, in which the loads are divided into three load centers. Suppose generator G1 is out of service. The total source power is only 225.0 MW. This, in turn, leads to a power shortage for IEEE 30-bus system, i.e., the power supply is limited at some time stages. The total system generation resources and load demands are shown in Figure 11.5.

Table 11.1   Capacity of generators for IEEE 30-bus system

Gen.	PG1	PG2	PG5	PG8	PG11	PG13
P_{Gmax} (MW)	200.00	80.00	50.00	35.00	30.00	30.00
P_{Gmin} (MW	50.00	12.00	10.00	10.00	10.00	10.00

Table 11.2   Load data for IEEE 30-bus system

Load Center	Load Node	v_{ij} ($/kW)	Load t1 0.00–4.00 (MW)	Load t2 4.01– 8.00 (MW)	Load t3 8.01– 12.00 (MW)	Load t4 12.01– 16.00 (MW)	Load t5 16.01– 20.00 (MW)	Load t6 20.01– 24.00 (MW)
CK1	PD2	300.0	15.15	19.53	21.7	19.62	19.53	17.36
CK1	PD3	300.0	1.89	2.43	2.7	2.57	2.43	2.16
CK1	PD4	300.0	5.46	6.86	7.8	7.41	6.86	6.24
CK1	PD6	280.0	65.94	84.78	94.2	85.49	84.78	75.36
CK1	PD7	280.0	15.96	20.52	22.8	21.66	20.52	18.24
CK1	PD8	300.0	21.00	27.00	30.0	27.50	27.00	24.00
CK1	PD10	300.0	4.06	5.22	5.8	5.51	5.22	4.64
CK1	PD12	280.0	7.84	10.08	11.2	10.64	10.08	8.96
CK1	PD14	280.0	4.34	5.58	6.2	5.89	5.58	4.96
CK2	PD15	245.0	5.74	7.38	8.2	7.79	7.38	6.56
CK2	PD16	220.0	2.45	3.15	3.5	3.33	3.15	2.80
CK2	PD17	280.0	6.30	8.10	9.0	8.55	8.10	7.20
CK2	PD18	220.0	2.24	2.82	3.2	3.04	2.82	2.56
CK2	PD19	245.0	6.65	8.65	9.5	9.03	8.65	7.60
CK3	PD20	280.0	1.54	1.98	2.2	2.09	1.98	1.76
CK3	PD21	280.0	12.25	15.75	17.5	16.63	15.75	14.00
CK3	PD23	220.0	2.24	2.82	3.2	3.04	2.82	2.56
CK3	PD24	220.0	6.09	7.83	8.7	8.27	7.83	6.96
CK3	PD26	300.0	2.45	3.15	3.5	3.33	3.15	2.80
CK3	PD29	220.0	1.68	2.16	2.4	2.28	2.16	1.92
CK3	PD30	245.0	7.42	9.54	10.6	10.07	9.54	8.48

The judgment matrices *A-LD* and *A-PI* are provided in Tables 11.3 and 11.4, respectively. The weighting factors that reflect the relative importance of each load or each load center are computed by AHP. The results of the weighting factors are listed in Table 11.5. The optimal load shedding schemes are computed and obtained by the proposed approach. The calculation results are shown in Tables 11.6 and 11.7.

In Table 11.6, the decision variable $x = 1$ means that this load is committed, and $x = 0$ means that this load is curtailed. It can be known from Tables 11.6 and 11.7 that load curtailment appeared at time stage t2 ~ t6. Loads 15, 16, 18, 19, 29, and 30 are curtailed at time stage t2 ~ t5. Load 24 is curtailed at time

Power (MW)
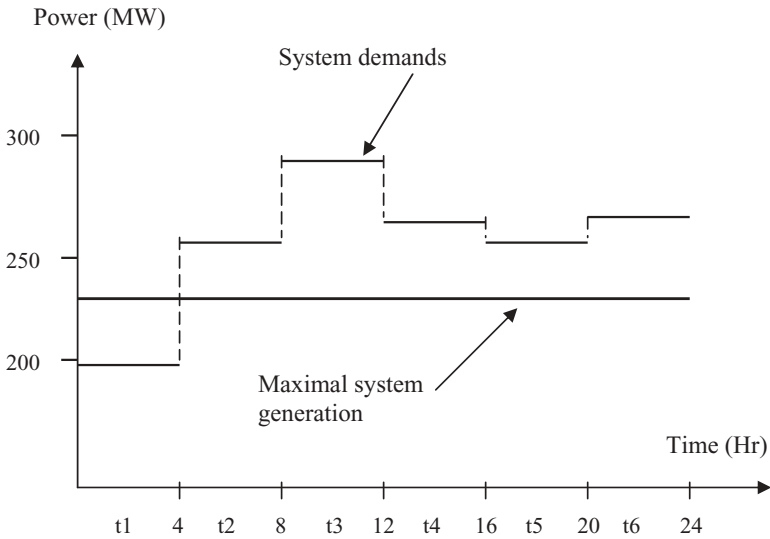
FIGURE 11.5 Total system generation and load demands

Table 11.3 Judgment matrix *A-PI*

PI	CK1	CK2	CK3
CK1	1	2	5
CK2	1/2	1	1/2
CK3	1/5	2	1

Table 11.4 Judgment matrix A-LD (1)

LD	2	3	4	6	7	8	10	12	14	15
2	1	2	2	1/3	1/5	2	1/2	2	2	3
3	1/2	1	1/2	1/4	2	1/2	1	2	2	3
4	1/2	2	1	1/2	2	1/3	2	2	3	2
6	3	4	2	1	4	2	3	3	3	3
7	5	1/2	1/2	1/4	1	1/2	2	2	2	3
8	1/2	2	3	1/2	2	1	3	2	2	4
10	2	1	1/2	1/3	1/2	1/3	1	2	3	3
12	1/2	1/2	1/2	1/3	1/2	1/2	1/2	1	1	2
14	1/2	1/2	1/3	1/3	1/2	1/2	1/3	1	1	2
15	1/3	1/3	1/2	1/3	1/3	1/4	1/3	1/2	1/2	1
16	1/3	1/2	1/3	1/4	1/3	1/4	1/3	1/2	1/3	1/2
17	1/2	2	1/2	1/2	1/3	1/2	2	1/2	1/2	3
18	1/3	1	1/2	1/3	1/3	1/3	1/2	1/2	1/3	1/2
19	1/3	1/2	1/2	1/3	1/3	1/3	1/3	1/2	1/3	1/2
20	1/3	1/2	1/3	1/3	1/3	1/3	1/2	1/3	1/2	5
21	1/3	1/3	1/2	1/3	1/4	1/4	1/3	1/3	1/2	5
23	2	3	1/2	1/2	1/2	1/2	1/2	1/2	1/3	3
24	1/3	1/3	1/2	1/3	1/3	1/2	1/3	1/3	1/3	1/3
26	1/3	1/3	1/2	1/3	1/2	1/3	1/3	1/2	1/2	3
29	1/3	1/3	1/3	1/3	1/3	1/2	1/3	1/3	1/3	1/2
30	1/3	1/3	1/2	1/3	1/3	1/3	1/2	1/3	1/3	2

Table 11.4 Judgment matrix A-LD (2)

LD	16	17	18	19	20	21	23	24	26	29	30
2	3	2	3	3	3	3	1/2	3	3	3	3
3	2	1/2	1	2	2	3	1/3	3	3	3	3
4	3	2	2	2	3	2	2	2	2	3	2
6	4	2	3	3	3	3	2	3	3	3	3
7	3	3	3	3	3	4	2	3	2	3	3
8	4	2	3	3	3	4	2	2	3	2	3
10	3	1/2	2	3	2	3	2	3	3	3	2
12	2	2	2	2	3	3	2	3	2	3	3
14	3	2	3	3	2	2	3	3	2	3	3
15	2	1/3	2	2	1/5	1/5	1/3	3	1/3	2	1/2
16	1	1/3	2	3	1/2	1/2	1/3	3	1/2	2	1/2
17	3	1	2	2	3	3	2	2	2	3	3
18	1/2	1/2	1	1/2	2	2	1/2	3	1/3	2	1/2
19	1/3	1/2	2	1	2	3	1/3	2	1/2	3	1/2
20	2	1/3	1/2	1/2	1	3	1/2	2	1/3	2	4
21	2	1/3	1/2	1/3	1/3	1	1/3	2	1/2	3	4
23	3	1/2	2	3	2	3	1	3	2	3	3
24	1/3	1/2	1/3	1/2	1/2	1/2	1/3	1	1/2	1/2	1/3
26	2	1/2	3	2	3	2	1/2	2	1	4	3
29	1/2	1/3	1/2	1/3	1/2	1/3	1/3	2	1/4	1	1/2
30	2	1/3	2	2	1/4	1/4	1/3	3	1/3	2	1

Table 11.5 Weighting factors computed by AHP

Load Center	Weighting Factor w_{Kj}	Load Node	v_{ij} ($/kW)	Weighting Factor w_{Di}	Unified Weighting Factor w_i
CK1	0.61185	PD2	300.0	0.07007	0.042872
CK1	0.61185	PD3	300.0	0.05425	0.033193
CK1	0.61185	PD4	300.0	0.06824	0.041753
CK1	0.61185	PD6	280.0	0.11115	0.068007
CK1	0.61185	PD7	280.0	0.08006	0.048985
CK1	0.61185	PD8	300.0	0.08616	0.052717
CK1	0.61185	PD10	300.0	0.06148	0.037617
CK1	0.61185	PD12	280.0	0.04999	0.030586
CK1	0.61185	PD14	280.0	0.05201	0.031822
CK2	0.17891	PD15	245.0	0.02356	0.004215
CK2	0.17891	PD16	220.0	0.02340	0.004186
CK2	0.17891	PD17	280.0	0.05430	0.009715
CK2	0.17891	PD18	220.0	0.02601	0.004653
CK2	0.17891	PD19	245.0	0.02701	0.004832
CK3	0.20925	PD20	280.0	0.03219	0.006736
CK3	0.20925	PD21	280.0	0.02843	0.005949
CK3	0.20925	PD23	220.0	0.05438	0.011379
CK3	0.20925	PD24	220.0	0.01677	0.003509
CK3	0.20925	PD26	300.0	0.03848	0.008052
CK3	0.20925	PD29	220.0	0.01686	0.003528
CK3	0.20925	PD30	245.0	0.02521	0.005275

Table 11.6   Optimal load shedding schemes and comparison for IEEE 30-bus system

Methods	AHP	LP	AHP	LP	AHP	LP	AHP	LP	AHP	LP	AHP	LP
Time stage	t1	t1	t2	t2	t3	t3	t4	t4	t5	t5	t6	t6
X2	1	1	1	1	1	1	1	1	1	1	1	1
X3	1	1	1	1	1	1	1	1	1	1	1	1
X4	1	1	1	1	1	1	1	1	1	1	1	1
X6	1	1	1	1	1	1	1	1	1	1	1	1
X7	1	1	1	1	1	1	1	1	1	1	1	1
X8	1	1	1	1	1	1	1	1	1	1	1	1
X10	1	1	1	1	1	1	1	1	1	1	1	1
X12	1	1	1	1	1	1	1	1	1	1	1	1
X14	1	1	1	1	1	0	1	1	1	1	1	1
X15	1	1	0	0	0	0	0	0	0	0	1	1
X16	1	1	0	0	0	0	0	0	0	0	1	1
X17	1	1	1	1	1	0	1	1	1	1	1	1
X18	1	1	0	0	0	0	0	0	0	0	1	0
X19	1	1	0	0	0	0	0	0	0	0	1	1
X20	1	1	1	1	0	0	1	0	1	1	1	1
X21	1	1	1	1	0	1	1	1	1	1	1	1
X23	1	1	1	0	1	0	1	0	1	0	1	0
X24	1	1	0	0	0	0	0	0	0	0	0	1
X26	1	1	1	1	1	1	1	1	1	1	1	1
X29	1	1	0	0	0	0	0	0	0	0	1	0
X30	1	1	0	0	0	0	0	0	0	0	1	1

stage t2 ~ t6. Load 21 is curtailed at time stages t3 and t4, and Load 20 is curtailed at time stage t3. The total load curtailments at each time stage are summarized in Table 11.7. It is noted that network security constraints are satisfied at any time period through the use of the proposed approach.

To further verify the AHP-based NFP approach, linear programming (LP) is used to solve the same load shedding problem without load priority factor w_{ij} that is determined by AHP. The corresponding results are compared with those obtained by the AHP-based NFP method and also listed in Tables 11.6 and 11.7 (Figs. 11.6 and 11.7). In the LP method, the loads with small MW demands and small costs are first considered for curtailment. The LP method also cannot handle or consider the relative importance of the load locations. The result comparison shows that the AHP-based NFP approach is truly optimal. It not only has maximal load benefits but also considers the relative importance of the load sites. For example, load site 23, which is always curtailed in the LP method when system generation is limited, is not curtailed in the AHP-based NFP method although it has a minimal load cost (220$/kW) and small MW load demands.

Table 11.7 Summary and comparison of optimal load shedding for IEEE 30-bus system

Methods	t1 AHP	t1 LP	t2 AHP	T2 LP	t3 AHP	t3 LP	t4 AHP	t4 LP	t5 AHP	t5 LP	t6 AHP	t6 LP
Time stage	t1		t2		t3		t4		t5		t6	
Max. system gen. (MW)	225.0	225.0	225.0	225.0	225.0	225.0	225.0	225.0	225.0	225.0	225.0	225.0
System demands (MW)	198.38	198.38	255.06	255.06	283.4	283.4	263.23	263.23	255.06	255.06	266.72	226.72
Committed loads (MW)	198.38	198.38	213.53	210.71	217.6	216.7	219.42	216.38	213.53	210.71	219.76	219.68
Total load shedding (MW)	0.0	0.0	41.53	44.35	65.80	66.7	43.81	46.85	41.53	44.35	6.96	7.04
Objective H_i	130.87	/	123.87	/	120.32	/	120.32	/	120.32	/	130.10	/
Benefit $\sum v_{ij} P_{ij}$ (×10³)$	55058	55058	60979	60358	62306	62246	62717	61463	60979	60358	61406	61388
Network security satisfied	Yes	Yes	Yes	Yes	Yes	Yes	Yes	Yes	Yes	Yes	Yes	Yes

FIGURE 11.6   Comparison of optimal load shedding results
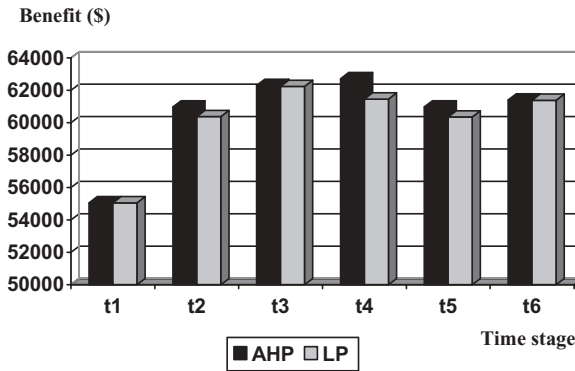
FIGURE 11.7   Comparison of the benefits from load shedding

11.6   OPTIMAL LOAD SHEDDING WITHOUT NETWORK CONSTRAINTS

11.6.1   Everett Method

If the network constraints are neglected, the load shedding problem in equations (11.3)–(11.6) can be easily solved by the Everett optimization technique, a generalized Lagrange multiplier [15–17]. The problem of load shedding can be represented as follows:

$$\text{Max } H_i = \sum_{i=1}^{m} H_i(x_i) \quad x_i \in s \tag{11.18}$$

such that

$$\sum_{i=1}^{m} C_i^k(x_i) \le c^k \quad \text{for all } k \tag{11.19}$$

where

x_i: A zero-one integer variable
S: Set that is interpreted as the set of possible strategies or actions
H(x): Benefit that accrues from employing the strategies $x \in S$
C^k: resource function

This load shedding model is a zero-one integer optimization problem. It is possible to solve problem (11.18)–(11.19) with integer-based optimization techniques. But this will have variable dimension problems in the large-scale power systems. Everett [14] showed that the Lagrange multiplier can be used to solve the maximization problem with many variables without any restrictions on continue or differentiability of the function being maximized. The aim of the generalized Lagrange multiplier is maximization rather than the location of stationary points as with the traditional Lagrange multipliers. This technique is discussed below.

The main theorem of the generalized Lagrange multiplier is as follows.

Theorem 1 [15]:

If (1) λ^k ($k = 1, 2, …, n$) are nonnegative real numbers,
(2) $x^* \in S$ maximizes the function

$$H(x) - \sum_{k=1}^{n} \lambda^k C^k(x) \quad x \in S \tag{11.20}$$

Then (3) x^* maximizes $H(x)$ over all of those $x \in S$ such that $C^k \le C^k(x^*)$ for all k.

Proof:

By assumptions 1 and 2 of Theorem 1, λ^k ($k = 1, 2, …, n$) are nonnegative real numbers, and $x^* \in S$ maximizes

$$H(x) - \sum_{k=1}^{n} \lambda^k C^k(x) \tag{11.21}$$

Over all $x \in S$. This means that, for all $x \in S$,

$$H(x^*) - \sum_{k=1}^{n} \lambda^k C^k(x^*) \ge H(x) - \sum_{k=1}^{n} \lambda^k C^k(x) \tag{11.22}$$

and hence that

$$H(x^*) \geq H(x) + \sum_{k=1}^{n} \lambda^k [C^k(x^*) - C^k(x)] \tag{11.23}$$

for all $x \in S$. However, if the latter inequality is true for all $x \in S$, it is necessarily true for any subset of S and hence true on that subset S^* of S for which the resources never exceed the resources $C^k(x^*)$, that is, $C^k \leq C^k(x^*)$, $x \in S^*$ for all k. Thus on the subset S^* the term

$$\sum_{k=1}^{n} \lambda^k [C^k(x^*) - C^k(x)] \tag{11.24}$$

is nonnegative by definition of the subset and the nonnegative of λ^k. Consequently, the inequality equation (11.23) reduces to

$$H(x^*) \geq H(x) \tag{11.25}$$

for all $x \in S^*$, and the theorem is proved.

In accordance with Theorem 1, for any choice of nonnegative λ^k ($k = 1$, 2, …, n), if an unconstrained maximum of the new Lagrange function [eq. (11.20)] can be found (where x^*, for example, is a strategy that produces the maximization), then this solution is a solution to that constrained maximization problem whose constraints are, in fact, the amount of each resource expended in achieving the unconstrained solution. Therefore, if x^* produces the unconstrained maximum and the required resources $C^k(x^*)$, then x^* itself produces the greatest benefit that can be achieved without using additional resource allocation.

With the Everett method, the problem of load shedding is changed into an unconstrained maximization. The key to solving this problem is choosing the Lagrange multipliers that correspond to the trial prices in the new competitive power market. In general, different choices of the trial prices λ^k lead to different schemes to resources provided and demands of customers to achieve the maximal benefit.

11.6.2 Calculation of Independent Load Values

Suppose v_i is the independent load value in a specific load bus. It reflects the value of supplement unit capacity generator for eliminating the load curtailment at node i ($/kW). However, load shedding is time dependent. A different time stage corresponds to a different level. Thus the load shedding study should be performed based on hourly load and the corresponding independent load values converted into hourly values.

The annual equipment value method, which is a dynamic assessment method, converts the cost of the operational lifetime to an annual cost. According to this method, the value v_i^t per hour can be calculated as follows:

$$v_i^t = \frac{\beta v_i \times 10^3}{365 \times 24} (\$/MW/hr) \qquad (11.26)$$

$$\beta = \frac{r(1+r)^n}{(1+r)^n - 1} \qquad (11.27)$$

where

v_i: The independent load value in a specific load bus ($/kW)

v_i^t: The per hour independent load value in a specific load bus ($/MW/hr)

r: The interest rate

n: The capital recovery years

β: The capital recovery factor (CRF), which is an important factor in economic analysis

It was assumed that 1 year = 365 days in equation (11.26).

Example

The testing system is shown in Figure 11.8, which is taken from reference [16], but with modified data. It consists of two generators and five loads at buses 3, 4, 5, 8, and 9, where loads 3, 4, and 5 are located in load center 1, and the others are located in load center 2. The weight factors reflecting the relative values of load centers are $w_1 = 0.58$, and $w_2 = 0.42$. The independent load values v in a specific load bus, the absolute load priority α to indicate
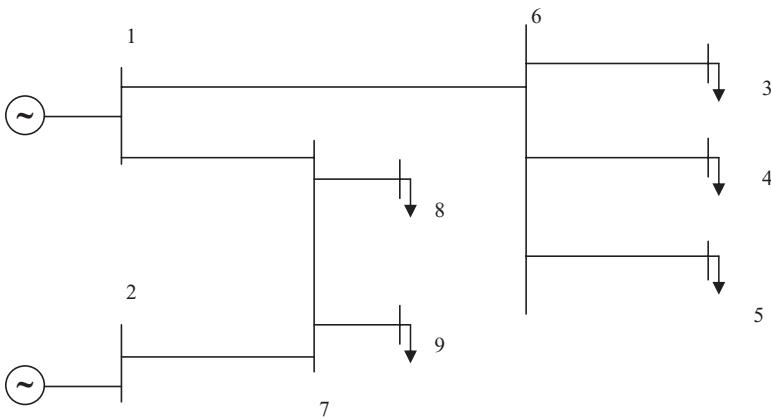
FIGURE 11.8 A simple network

Table 11.8   The values of load buses

Values	Load 3	Load 4	Load 5	Load 8	Load 9
v_i (S/kW)	150	200	180	190	220
α_i	1.14	1.25	1.30	1.10	1.22
Demand P_D (p.u.)	.270	.280	.260	.305	.310

Table 11.9   The hourly independent values of load buses

Values	Load 3	Load 4	Load 5	Load 8	Load 9
v_i (S/kW)	150	200	180	190	220
v_i (S/MW/hr)	23.26	31.02	27.92	29.47	34.12
v_i (S/p.u.MW/hr)	2326	3102	2792	2947	3412

the importance of each load bus, and the load demand for each load bus are given in Table 11.8. The capacity of generator 1 and generator 2 is $P_{G1} = 0.90$ and $P_{G2} = 0.6$ p.u., respectively. The available transfer capacity of key lines is $P_{1-6max} = 0.60$ p.u., $P_{2-7max} = 0.58$ p.u., $P_{1-7max} = 0.5$ p.u., respectively.

There are two test cases:

Case 1: Two generators are in operation, tie-line 1–7 is in outage.

Case 2: Generator 2 is in outage. No line outage.

First of all, we assume that the capital recovery years of investing generator n is 10 years, and that the interest rate is 6%. According to equation (11.27), we get the capital recovery factor (CRF) $\beta = 1.3587$. Then according to equation (11.26), we get the hourly independent load values, which are shown in Table 11.9.

For case 1, we can get the following objective function and constraints:

$$H = \sum_i \alpha_i v_i x_i$$

and constraints

$$P_{D3}x_3 + P_{D4}x_4 + P_{D5}x_5 \leq P_{G1}$$

$$P_{D3}x_3 + P_{D4}x_4 + P_{D5}x_5 \leq P_{1-6max}$$

$$P_{D8}x_8 + P_{D9}x_9 \leq P_{G2}$$

$$P_{D8}x_8 + P_{D9}x_9 \leq P_{2-7max}$$

Since tie-line 1–7 is in outage, the system becomes two subsystems, each of them has one generator. Thus we can solve two subproblems separately.

For subproblem 1:
Objective

$$H_1 = \sum_i \alpha_i v_i x_i = \alpha_3 v_3 x_3 + \alpha_4 v_4 x_4 + \alpha_5 v_5 x_5$$
$$= 1.14 \times 2326 x_3 + 1.25 \times 3120 x_4 + 1.30 \times 2792 x_5$$
$$= 2651.64 x_3 + 3900 x_4 + 3629.6 x_5$$

Subject to

$$P_{D3} x_3 + P_{D4} x_4 + P_{D5} x_5 \leq \min\{P_{G1}, P_{1-6\max}\}$$

i.e., $0.27 x_3 + 0.28 x_4 + 0.26 x_5 \leq \min\{0.90, 0.60\} = 0.60$
Compared with equations (11.18) and (11.19), the above load shedding problem is a linear model, i.e.,

$$\max H(x) = \sum_i H_i x_i \tag{11.28}$$

Such that

$$\sum_i P_i x_i \leq C \tag{11.29}$$

According to the generalized Lagrange multiplier technique, the Everett model for the load shedding problem can be written as follows.

$$\text{Max } L = H(x) - \sum_{k=1}^{n} \lambda^k C^k(x)$$
$$= \sum_i \{H_i x_i - \lambda[P_i x_i - C]\} = \sum_i \delta_i x_i + \lambda C \tag{11.30}$$

where

$$\delta_i = H_i - \lambda P_i \tag{11.31}$$

Thus, we have

$$L = 2651.64 x_3 + 3900 x_4 + 3629.6 x_5 - \lambda(0.20 x_3 + 0.22 x_4 + 0.28 x_5 - 0.60)$$
$$= (2651.64 - 0.27\lambda) x_3 + (3900 - 0.28\lambda) x_4 + (3629.6 - 0.26\lambda) x_5 + 0.60\lambda$$

If all $x_i = 1$, $\sum_i P_i x_i = 0.81 > C$, which equals 0.60. Thus some load should be curtailed.

It can be observed from the above Lagrange function that shedding load 3 will have the maximum benefit no matter what the value of the trial price λ is.

For subproblem 2:

Objective

$$H_2 = \sum_i \alpha_i v_i x_i = \alpha_8 v_8 x_8 + \alpha_9 v_9 x_9$$

$$= 1.1 \times 2947 x_8 + 1.22 \times 3412 x_9$$

$$= 3241.7 x_8 + 4162.64 x_9$$

subject to

$$P_{D8} x_8 + P_{D9} x_9 \leq \min \{P_{G2}, P_{2-7\max}\}$$

i.e., $\qquad 0.305 x_8 + 0.310 x_9 \leq \min \{0.70, 0.58\} = 0.58$

Then we have

$$L = 3241.7 x_8 + 4162.64 x_9 - \lambda (0.305 x_8 + 0.310 x_9 - 0.58)$$

$$= (3241.7 - 0.305\lambda) x_8 + (4162.64 - 0.310\lambda) x_9 + 0.58\lambda$$

If all $x_i = 1$, $\sum_i P_i x_i = 0.61 > C$, which equals 0.58. Thus some load should be curtailed.

It can be observed from the above Lagrange function that shedding load 8 will have the maximum benefit no matter what the value of the trial price λ is.

For case 2, one generator will supply two load centers since generator 2 is in outage. We have the following objective function and constraints.

Objective

$$h = w_1 H_1 + w_2 H_2 = w_1 (\alpha_3 v_3 x_3 + \alpha_4 v_4 x_4 + \alpha_5 v_5 x_5) + w_2 (\alpha_8 v_8 x_8 + \alpha_9 v_9 x_9)$$

$$= 0.58 (1.14 \times 2326 x_3 + 1.25 \times 3120 x_4 + 1.30 \times 2792 x_5)$$

$$+ 0.42 (1.1 \times 2947 x_8 + 1.22 \times 3412 x_9)$$

$$= 1537.95 x_3 + 2262 x_4 + 2105.17 x_5 + 1361.51 x_8 + 1748.31 x_9$$

subject to

(1) $0.27 x_3 + 0.28 x_4 + 0.26 x_5 \leq P_{1-6\max} = 0.60$

(2) $0.305 x_8 + 0.31 x_9 \leq P_{1-7\max} = 0.50$

(3) $0.27 x_3 + 0.28 x_4 + 0.26 x_5 + 0.305 x_8 + 0.31 x_9 \leq P_{G1} = 0.90$

Then we have the following Lagrange function for case 2:

$$L = 1537.95x_3 + 2262x_4 + 2105.17x_5 + 1361.51x_8 + 1748.31x_9$$
$$\quad - \lambda_1(0.27x_3 + 0.28x_4 + 0.26x_5 - 0.60) - \lambda_2(0.305x_8 + 0.310x_9 - 0.50)$$
$$\quad - \lambda_3(0.27x_3 + 0.28x_4 + 0.26x_5 + 0.305x_8 + 0.310x_9 - 0.90)$$
$$= (1537.95 - 0.27\lambda_1 - 0.27\lambda_3)x_3 + (2262 - 0.28\lambda_1 - 0.28\lambda_3)x_4$$
$$\quad + (2105.17 - 0.26\lambda_1 - 0.26\lambda_3)x_5 + (1361.51 - 0.305\lambda_2 - 0.305\lambda_3)x_8$$
$$\quad + (1748.31 - 0.31\lambda_2 - 0.31\lambda_3)x_9 + 0.60\lambda_1 + 0.50\lambda_2 + 0.90\lambda_3$$

If $\lambda_1 = \lambda_2 = \lambda_3 = 2000$ \$/p.u.MW/hr, and we assume there is no load shedding, we get the following results according to equations (11.28)–(11.31):

Load i	δ_i	x_i	$H_i x_i$	$P_i x_i$	$\delta_i x_i$	Rank (x_i)
Load 3	457.50	1	1537.95	0.27	457.50	4
Load 4	1142.00	1	2262.00	0.26	1142.00	1
Load 5	1065.70	1	2105.17	0.28	1065.70	2
Load 8	141.51	1	1361.51	0.305	141.51	5
Load 9	508.31	1	1748.31	0.31	508.31	3

However, constraints (1)–(3) are not satisfied. According to the above table, the optimal load shedding scheme is that load 8 and load 3 are curtailed, and the maximum benefit for this case is $H = 6115.27$.

If $\lambda_1 = \lambda_2 = \lambda_3 = 2500$ \$/p.u.MW/hr, we get the following results:

Load i	δ_i	x_i	$H_i x_i$	$P_i x_i$	$\delta_i x_i$	Rank (x_i)
Load 3	187.95	1	1537.95	0.27	187.95	4
Load 4	862.00	1	2262.00	0.26	862.00	1
Load 5	805.70	1	2105.17	0.28	805.70	2
Load 8	−138.49	1	1361.51	0.305	−138.49	5
Load 9	198.31	1	1748.31	0.31	198.31	3

According to the above table, the same optimal load shedding scheme is obtained, that is, load 8 and load 3 are curtailed, and the maximum benefit for this case is $H = 6115.27$.

However, if $\lambda_1 = \lambda_2 = \lambda_3 = 2700$ \$/p.u.MW/hr, we get the following results:

Load i	δ_i	x_i	$H_i x_i$	$P_i x_i$	$\delta_i x_i$	Rank (x_i)
Load 3	79.95	1	1537.95	0.27	79.95	3
Load 4	750.00	1	2262.00	0.26	750.00	1
Load 5	701.17	1	2105.17	0.28	701.17	2
Load 8	−285.49	1	1361.51	0.305	−285.49	5
Load 9	74.31	1	1748.31	0.31	74.31	4

According to the above table, a different load shedding scheme is obtained, that is, load 8 and load 9 are curtailed, and the maximum benefit for this case is $H = 5905.12$.

Obviously, the trial price λ_i affects the results of load shedding. Further calculations show that the optimal load-shedding scheme will be that load 8 and 3 are curtailed if $\lambda_1 = \lambda_2 = \lambda_3 \leq 2629.52700$ \$/p.u.MW/hr, and the optimal load shedding scheme will be that load 8 and 9 are curtailed if $\lambda_1 = \lambda_2 = \lambda_3 > 2629.52700$ \$/p.u.MW/hr.

11.7   DISTRIBUTED INTERRUPTIBLE LOAD SHEDDING

11.7.1   Introduction

Blackouts are becoming more frequent in industrial countries because of network deficiencies and continuous load growing. One possible solution to prevent blackouts is load curtailment. Both ***demand side management*** (*DSM*) and ***load shedding*** (*LS*) have been used to provide reliable power system operation under normal and emergency conditions. *DSM* is specifically devoted to peak demand shaving [18] and to encouraging efficient use of energy. *LS* is still a methodology used worldwide to prevent power system degradation to blackouts [19–21], and it acts in a repressive way.

To perform the *LS* program, it could be necessary to increase the number of interruptible customers and distribute them over all the system. Considering such small percentage values of load shedding, if the number of interruptible customers increased the impact on users would be negligible. Instead of detaching all the interruptible loads, only a part of the load could be disconnected from the network, in particular the part that can be interrupted or controlled (such as the lighting system, air conditioning, devices under UPS, pumps dedicated to tanks filling, etc.). This method is called a ***distributed interruptible load shedding*** (*DILS*) program [18].

Generally speaking, at least the following three levels of action should be assumed so that a customer can participate in the *DILS*, allowing the network manager to control the peak power withdrawal or to act during periods of network dysfunction:

- The financing of technologies that enable the implementation of *DILS* (electronic power meters, domestic and similar appliances, etc.)
- Incentives aimed at changing the behavior of some categories of end users
- Definition of *ad hoc* instruments for particular classes of consumers such as Public Administration, Data Centers, etc.

In addition, the customers could find it convenient to participate in the day-ahead market. Users with reducible power above a minimal threshold could present offers in the previous day market that, if accepted because competitive, could take part in the dispatch services market.

This way, the load curtailment would be paid according to the actual recorded interruption. Moreover, there would be more market efficiency,

created by the competition both between the interruptible services themselves and between these and the generation.

11.7.2 DILS Methods

To participate in the *DILS* program with interest, a user must have an economic profit and/or be less sensitive to dysfunctions. There are two different *DILS* techniques that can be adopted in automation sceneries only, for obtaining the desired load relief during criticalities [18]:

1. The first technique increases the cost of electric energy for all the users [8]. One can assume to know the response of the users statistically, in particular as to the way they change the subdivision between interruptible loads (which would become disconnectable) and uninterruptible loads depending on the cost of energy. In this case, the transmission of a price signal via the electronic power meter could be sufficient to avoid the loss.

2. The second technique is based on the transmission of an interruptible load percentage reduction signal *p* to every customer participating in the *DILS* program. The duration of the reduction might be contractually determined. Because of the uncertainty of how much power each single interruptible customer is actually drawing, the value of *p* will be larger than the fraction of the expected interruptible load, giving the wanted load relief.

Since it is more easily adoptable in practice by the distributor and the end user, the second *DILS* technique is analyzed here.

11.7.2.1 Analysis of Interruptible Load
The interruptible load of a customer can be considered as an essentially continuous random variable. This ensures that every percentage *p* of load reduction is actually achievable (possibly with low probability for some values of *p*). We denote by $Y_{I,k}(t)$ the random value of the interruptible load power of the single customer *k* of a given sector at time *t* and build its probability distribution at a fixed time, so that we omit the time argument temporarily and write $Y_{I,k}$ only.

The load $Y_{I,k}$ is composed of various combinations of continuous-adjustable and step-adjustable interruptible loads, which we write as

$$Y_{I,k} = Y_{CAI,k} + Y_{SAI,k} \tag{11.32}$$

where

$Y_{CAI,k}$: The interruptible continuous-adjustable loads
$Y_{SAI,k}$: The interruptible step-adjustable loads

The combinations of step-adjustable loads give rise to, say, m possible well-separated load levels of $Y_{\text{SAI},k}$, denoted by $l_1, \ldots, l_m$. Each level is taken with a different probability, so we introduce the probabilities $w(1), \ldots, w(m)$, which sum up to one, giving the probability distribution $w(\bullet)$ of $Y_{\text{SAI},k}$. On the other hand, $Y_{\text{CAI},k}$ has an absolutely continuous probability distribution with density $f_{\text{CAI}}(\bullet)$ on the range $(0, L_{\text{CAI}})$, where L_{CAI} is the maximum power of the interruptible continuous adjustable load.

Assuming $Y_{\text{SAI},k}$ and $Y_{\text{CAI},k}$ are independent, the distribution of $Y_{\text{I},k}$ is the mixture density resulting from the convolution of $w(\bullet)$ and $f_{\text{CAI}}(\bullet)$, that is,

$$f_Y(y) = \sum_{i=1}^{m} f_{\text{CAI}}(y - l_i) \bullet w(i) \tag{11.33}$$

where

Y: A random variable

y: A particular value that Y can take with ranging in $(0, l_m + L_{\text{CAI}})$

Since $f_{\text{CAI}}(\bullet)$ is a density, the mixture density $f_Y(\bullet)$ is never zero in $(0, l_m + L_{\text{CAI}})$ provided L_{CAI} is greater than the largest difference between consecutive step-adjustable load levels. This makes every load level within this interval actually achievable.

The argument we are making here ensures a smooth transition to lower load levels following reduction signals sent to customers. This is important if DILS is applied to few customers, but it becomes less and less important as the number of customers increases. Suppose a load point has N users connected to it. We now analyze the effect of a load shedding signal p sent to a given number of customers at time t to be carried out at time $(t + u)$. Let n, the number of customers participating in the DILS program, be less than N. If we know the probabilistic characterization of the load of a typical customer at any time t, and its subdivision into interruptible and uninterruptible, which will be the tool to assess the probability of reaching the desired load relief. For expository purposes, we take all N users belonging to the same class (e.g., all residential).

The total load of a single user can be written as

$$Y_k(t) = Y_{\text{I},k}(t) + Y_{\text{U},k}(t) \tag{11.34}$$

Where $Y_{\text{I},k}(t)$ and $Y_{\text{U},k}(t)$ are the interruptible and uninterruptible parts of the load respectively. Obviously $Y_{\text{I},k}(t)$ is zero for uninterruptible customers. Let us consider NA appliances (such as refrigerators, washing machines, dishwashers, etc.), and let the percentages of customers who possess each appliance be given by $P_1, \ldots, P_{\text{NA}}$. Finally, the indicator function $I(i \text{ has } j)$, takes a value of 1 if customer has the appliance j and zero otherwise. Then we can write

$$Y_k(t) = \sum_{j=1}^{NA} I(i \text{ has } j) \cdot w_j(t) \qquad (11.35)$$

where $w_j(t)$ is the (random) power absorbed by appliance j at time t. $I(\bullet)$ is the indicator function of a statement.

Let

$$\mu_j(t) = E(w_j(t)) \qquad (11.36)$$

$$\sigma_j^2(t) = \text{Var}(w_j(t)) \qquad (11.37)$$

We can derive the expected value and the variance of the load absorbed by a customer picked at random, under the hypothesis that the appliances are used independently of each other:

$$\mu_T(t) = \sum_{j=1}^{NA} p_j \mu_j(t) \qquad (11.38)$$

$$\sigma_T^2(t) = \sum_{j=1}^{NA} p_j[\sigma_j^2(t) + (1 - p_j \mu_j^2(t))] \qquad (11.39)$$

If the appliances are not independent, equation (11.38) is unchanged, whereas equation (11.39) is modified by adding twice the sum of all the covariances between pairs of products of random variables I (i has j) $w_j(t)$ and I (i has j') $w_{j'}(t)$.

The mean and variance in equations (11.38) and (11.39) are sufficient to approximate the probability distribution of the load with a Gaussian by the central limit theorem, provided the total number N of customers connected to a given load point is large enough, so that we can state that the total power $S(t)$ absorbed at time t has a Gaussian distribution, with mean $N\mu_T(t)$ and variance $N\sigma_T^2(t)$, as follows.

$$S(t) = S_I(t) + S_U(t) = \sum_{k=1}^{N} Y_{I,k}(t) + \sum_{k=1}^{N} Y_{U,k}(t)$$

$$= \sum_{k=1}^{N} Y_k(t) \sim N(N\mu_T(t), N\sigma_T^2(t)) \qquad (11.40)$$

By indexing from 1 to n those customers who take part in the *DILS* program, we can write the share of the total load actually available for curtailment as

$$S_{I,n}(t) = \sum_{k=1}^{n} Y_{I,k}(t) \qquad (11.41)$$

Suppose now that we possess a load forecasting method, which is precise enough to consider $s(t + u)$ as known when data are available up to time t. Certainly, $S_{I,n}(t)$ remains unobserved (we can only measure the total power taken by all the N customers), but the precisely forecasted $s(t + u)$ gives us some information about $S_{I,n}(t + u)$. This information is summarized by the conditional distribution $P(S_{I,n}(t + u) \mid S(t + u) = s(t + u))$. Let $\mu_I(t)$ and $\sigma_I^2(t)$ be the mean and variance of the load drawn by the interruptible appliances of a customer picked at random. By normal approximation, this conditional distribution is still Gaussian with mean

$$n\left\{\mu_I(t+u) + \frac{1}{N}\frac{\sigma_I^2(t+u)}{\sigma_T^2(t+u)}[s(t+u) - N\mu_T(t+u)]\right\} = n\mu \qquad (11.42)$$

And variance

$$n\left[\sigma_I^2(t+u)\left(1 - \frac{n}{N}\frac{\sigma_I^2(t+u)}{\sigma_T^2(t+u)}\right)\right] = n\sigma^2 \qquad (11.43)$$

This conditional Gaussian distribution will be the main ingredient for the determination of the optimal value of p.

If the customers connected to the same load point are not homogeneous, they can be split into homogeneous groups. If these groups are large enough, then the Gaussian approximation still applies for each group so that $S(t)$ will be Gaussian distributed and the conditional distribution of the interruptible load can be found in a similar way as above.

The effectiveness of the central limit theorem depends on both the shape of the individual load probability distribution and the degree of statistical correlation among customers' loads. A recent study [22] on the probability distribution of the aggregated residential load for extra-urban areas, based on a bottom-up approach, shows that the Gamma distribution exhibits the best goodness of fit among a set of candidate distributions, but that the Gaussian approximation still passes the test for a reasonably large number of users. If strong stochastic dependence among customers persists, due for example to spatial autocorrelation (the means $\mu_T(t)$ depend on time only), the Gaussian distribution could be inappropriate, and further study would be necessary to model the specific situation correctly.

11.7.2.2 Load Shedding Via the Probability of Failure

A load shedding request p, sent to customer k, implies a load relief of $pY_{I,k}$ kW. The customer can attain the new load level $(1 - p)Y_{I,k} + Y_{U,k}$. Overall, the load relief obtained when p is applied to n customers is

$$p\sum_{k=1}^{n} Y_{I,k} = pS_{I,n} \qquad (11.44)$$

Then we must set up a decision criterion to set p in such a way that we are confident that the requested load relief of r kW is achieved. We can formalize this by stating that p must be such that:

$$P(pS_{I,n} < r) \leq \alpha \tag{11.45}$$

where α is an acceptable probability that the desired load relief is not attained. In principle α can be zero, if the interruptible load is greater than (r/p) with probability one for some p. In some situations, when the absorbed load is very high and a small load relief is requested, this condition can be met.

Let F denote the cumulative conditional distribution function of $S_{I,n}$. Then the decision criterion for p is written as:

$$F\left(\frac{r}{p}\right) \leq \alpha \tag{11.46}$$

and is satisfied if

$$\frac{r}{p} = F^{-1}(\alpha) = q_\alpha \Rightarrow p = \frac{r}{q_\alpha} \tag{11.47}$$

The condition $r < q_\alpha$ is required for this to have an admissible solution.

In general there will be no closed-form expression for F. But we may employ the central limit theorem approximation introduced above with the appropriate conditional mean and variance of the single customer's load indicated by μ and σ^2. Then

$$F\left(\frac{r}{p}\right) \cong \Phi\left(\frac{\dfrac{r}{np} - \mu}{\dfrac{\sigma}{\sqrt{n}}}\right) \tag{11.48}$$

where Φ is the standard Gaussian cumulative density function, and the solution to equation (11.46) is

$$p = \frac{\dfrac{r}{n}}{\mu + z_\alpha \dfrac{\sigma}{\sqrt{n}}} \tag{11.49}$$

where z_α is the α-level percentage of the standard Gaussian distribution.

The probability level α can be chosen if a measure of the cost of not achieving the desired load relief is available, say c_0. Then the expected cost of not

attaining the load relief is given by αc_0 and α can be increased from zero up to a value of c_A / c_0, where c_A is the maximum acceptable cost (which would be lower than c_0).

11.7.2.3 Load Shedding Via the General Cost Function   A more sophisticated decision criterion of load shedding can be based on a cost function that increases with the actual load relief distance from the target, such as

$$c(p, S_{\mathrm{I},n}) = c_1 p S_{\mathrm{I},n} I(p S_{\mathrm{I},n} > r) + c_2 S_{\mathrm{I},n} I(p S_{\mathrm{I},n} < r) \qquad (11.50)$$

As mentioned before, $I(\bullet)$ is the indicator function of a statement and s is the total load at the time of the shedding. The two addenda account for the cost of an overshooting and an undershooting, respectively. The cost constants c_1 and c_2 can include per-kWh costs on the distributor's (energy not sold) and on the customer's (energy not available) side, because of a blackout or an excessive curtailment (since we are talking about energy and the cost function depends on power, we are implying a fixed duration of the shedding intervention). One should note that for the network operator, which manages the shedding action, it will be difficult to give a fair assessment of costs not incurred by itself. Considering the costs of the energy not sold only, given c_2, the order of magnitude of c_1 should be c_2, one possible choice being $c_1 = c_2$.

The load shedding problem becomes a search for the minimization of the expected value of the following cost function:

$$c(p) = E(c(p, S_{\mathrm{I},n})) = c_1 p \int_{r/p}^{\infty} s' f(s') \, ds' + c_2 s F\left(\frac{r}{p}\right) \qquad (11.51)$$

where f is the density function associated to F.

By using the Gaussian approximation, we get

$$c(p) \cong c_1 p \left\{ n\mu \left[1 - \Phi\left(\frac{\frac{r}{p} - n\mu}{\sqrt{n}\sigma} \right) \right] + \sqrt{n}\sigma\varphi\left(\frac{\frac{r}{p} - n\mu}{\sqrt{n}\sigma} \right) \right\} + c_2 s \Phi\left(\frac{\frac{r}{p} - n\mu}{\sqrt{n}\sigma} \right) \qquad (11.52)$$

where φ is the standard Gaussian density function.

This decision criterion based on the conditional Gaussian is an instance of Bayesian expected loss minimization [23]. The loss is represented by $c(p, S_{\mathrm{I},n})$ and the expectation is taken with respect to the posterior distribution of an unobservable quantity ($S_{\mathrm{I},n}$) conditionally on another observed quantity (s), through which the prior information on the former is updated.

11.8 UNDERVOLTAGE LOAD SHEDDING

11.8.1 Introduction

We discuss the load shedding problem from the view of voltage stability in this section. Load shedding is the ultimate countermeasure to save a voltage-unstable system, when there is no other alternative to stop an approaching collapse [24–29]. This countermeasure is cost effective in the sense that it can stop voltage instability triggered by large disturbances, against which preventive actions would not be economically justified (if at all possible) in view of the low probability of occurrence [26]. Load shedding is also needed when the system undergoes an initial voltage drop that is too pronounced to be corrected by generators (because of their limited range of allowed voltages) or load tap changers (because of their relatively slow movements and also limited control range).

In the practical system, this kind of load shedding belongs to the family of system protection schemes (also referred to as special protections scheme) (SPS) against long-term voltage instability. An SPS is a protection designed to detect abnormal system conditions and take predetermined corrective actions (other than the isolation of the faulted elements) to preserve as far as possible system integrity and regain acceptable performances [27].

The following SPS design has been chosen [29]:

- *Response-based*: Load shedding will rely on voltage measurements that reflect the initiating disturbance (without identifying it) and the actions taken so far by the SPS and by other controllers. On the contrary, an event-based SPS would react to the occurrence of specific events [28];

- *Rule-based*: Load shedding will rely on a combination of rules of the type:

$$\text{If } V < V_{\text{threshold}} \text{ during } t \text{ seconds, shed } \Delta P \text{ MW} \qquad (11.53)$$

  where V is measured voltage and $V_{threshold}$ is the corresponding threshold value.

- *Closed-loop operation*: An essential feature of the scheme considered here is the ability to activate the rule equation (11.53) several times, based on the measured result of the previous activations. This closed-loop feature allows the load shedding controllers to adapt their actions to the severity of the disturbance. Furthermore, it increases the robustness with respect to operation failures as well as system behavior uncertainties [30]. This is particularly important in voltage instability, where load plays a central role but its composition varies with time and its behavior under large voltage drops may not be known accurately;

- A *distributed* scheme is proposed for its ability to adjust to the disturbance location.

It is well known that time, location, and amount are three important and closely related aspects of load shedding against voltage instability [31]. The time available for shedding is limited by the necessity to avoid [25]:

- Reaching the collapse point corresponding to generator loss of synchronism or motor stalling
- Further system degradation due to undervoltage tripping of field current-limited generators, or line tripping by protections;
- The nuisance for customers of sustained low voltages. This requires fast, action even in the case of long-term voltage instability, if the disturbance has a strong initial impact [30].

As far as long-term voltage instability is concerned, if none of the above factors is limiting, one can show that there is a maximum delay beyond which shedding later requires shedding more [25]. On the other hand, it may be appropriate to activate other emergency controls first so that the amount of load shedding is reduced [30].

The shedding location matters a lot when dealing with voltage instability: Shedding at a less appropriate place requires shedding more. In practice, the region prone to voltage instability is well known beforehand. However, within this region, the best location for load shedding may vary significantly with the disturbance and system topology.

11.8.2   Undervoltage Load Shedding using Distributed Controllers

This undervoltage load shedding scheme relies on a set of controllers distributed over the region prone to voltage instability [30]. Each controller monitors the voltage V at a transmission bus and acts on a set of loads located at distribution level and having influence on V. Each controller operates as follows:

- It acts when its monitored voltage V falls below some threshold $V_{threshold}$.
- It can act repeatedly, until V recovers above $V_{threshold}$. This yields the already mentioned closed-loop behavior.
- It waits in between two sheddings, in order to assess the effect of the actions taken both by itself and by the other controllers.
- The delay between successive sheddings varies with the severity of the situation.
- The same holds true for the amount shed.

11.8.2.1   Individual Controller Design   As long as V remains above the specified threshold the controller is idle, while it is started as soon as a (severe) disturbance causes V to drop below $V_{threshold}$. Let t_0 be the time when this change takes place. The controller remains started until either the voltage

recovers, or a time τ is elapsed since t_0. In the latter case, the controller sheds a power ΔP^{sh} and returns to either idle (if V recovers above $V_{threshold}$) or started state (if V remains smaller than $V_{threshold}$). In the second case, the current time t is taken as the new value and the controller is ready to act again (provided of course that there remains load to shed).

The delay τ depends on the time evolution of τ as follows. A block of load is shed at a time such that:

$$\int_{t_0}^{t_0+\tau} (V_{threshold} - V(t))\, dt = C \tag{11.54}$$

where C is a constant to be adjusted. This control law yields an inverse-time characteristic: The deeper the voltage drops, the less time it takes to reach the value C and, hence, the faster the shedding. The larger C, the more time it takes for the integral to reach this value and hence, the slower the action.

Furthermore, the delay τ is lower bounded:

$$\tau_{min} \leq \tau \tag{11.55}$$

to prevent the controller from reacting on a nearby fault. Indeed, in normal situations time must be left for the protections to clear the fault and the voltage to recover to normal values.

The amount of load shedding depends on the voltage drop at the time period, that is,

$$\Delta P^{sh} = K \Delta V^d \tag{11.56}$$

where K is another constant to be adjusted and ΔV^d is the average voltage drop over the time period τ, that is,

$$\Delta V^d = \frac{1}{\tau} \int_{t_0}^{t_0+\tau} (V_{threshold} - V(t))\, dt \tag{11.57}$$

The controller acts by opening distribution circuit breakers and may disconnect interruptible loads only. Hence, the minimum load shedding corresponds to the smallest load whose breaker can be opened, while the maximum shedding corresponds to opening all the maneuverable breakers. Furthermore, to prevent unacceptable transients, it may be appropriate to limit the power disconnected in a single step to some value ΔP_{tr}^{sh}, which can be written as.

$$\min_k P_k \leq \Delta P^{sh} \leq \Delta P_{max}^{sh} \tag{11.58}$$

with

$$\Delta P_{\text{max}}^{\text{sh}} = \min\left(\sum_k P_k, P_{\text{tr}}^{\text{sh}}\right) \tag{11.59}$$

where P_k denotes the individual load power behind the kth circuit breaker under control, and the minimum in equation (11.58) and the sum in equation (11.59) extend over all maneuverable breakers.

The control logic focuses on active power, but load reactive power is obviously reduced together with active power. In the absence of more detailed information, we assume that both powers vary in the same proportion.

11.8.2.2 Cooperation Between Controllers

In this section we discuss the interaction of the various controllers used in load shedding.

Let us consider two close controllers: C_i monitoring bus i and C_j monitoring bus j. Let us assume that both controllers are started by a disturbance. When C_i sheds some load, it causes the voltages to increase not only at bus i but also at neighboring buses including the monitoring bus, j. Since V_i increases, the integral $\int(V_{\text{threshold}} - V_j(t))dt$ decreases. It can be observed from equations (11.56) and (11.57) that the ΔV^{d} decreases; consequently, the amount of load shedding will be reduced for the controller j. If the V_i is increased and larger than the $V_{\text{threshold}}$, the controller j will return to idle. Thus, when one controller sheds load, it slows down or inhibits the other controllers to restore voltages in the same area. This cooperation avoids excessive load shedding.

Obviously, the whole system will tend to automatically trigger the controller to shed the load first where voltages drop the most at the location of the controller. This means operating the controllers in a fully distributed way, each controller using local information and taking local actions, as underfrequency load shedding controllers do, which we discussed in Section 11.2.

Another way to implement the load shedding scheme in a centralized way is by collecting all voltage measurements at a central point, running the computations involved in equations (11.54)–(11.59) in a single processor, and sending back load shedding orders (with some communication delays to be taken into account). In this case, additional information exchanges and interactions between controllers may be envisaged without further penalizing the scheme. To protect the SPS against erroneous measurements, it is desirable for each controller to rely on several voltage measurements, taken at closely located buses. Some filtering can remove outliers from the measurements, and the average value of the valid ones can be used as V in equations (11.54) and (11.57). If all data are dubious, the controller should not be started; other controllers will take over.

11.8.2.3 Tuning the Parameters of the Controller

Obviously, the parameters of the controller affect the response of the controller as well as the scheme of load shedding. The tuning of the controllers should rely on a set of

scenarios combining different operating conditions and disturbances, as typically considered when planning SPS [30, 31].

The basic requirements are:

(1) Protection security: The SPS does not act in a scenario with acceptable postdisturbance system response. This is normally the case after any contingency.
(2) Protection dependability: All unacceptable postdisturbance system responses are saved by the SPS, possibly in conjunction with other available controls.
(3) Protection selectivity: In the latter case, as little load power as possible is interrupted.

The tuning mainly consists of choosing the best values for $V_{\text{threshold}}$, C, K, $\Delta P_{\text{tr}}^{\text{sh}}$, and τ_{min}. It is noted that the voltage threshold should be set high enough to avoid excessive shedding delays, which in turn would require shedding more and/or cause low load voltages. On the other hand, it should be low enough to obey requirement (1) above. It should thus be set a little below the lowest voltage value reached during any of the acceptable postdisturbance evolutions.

As for C and K, they should be selected so that, for all scenarios:

· The protection sheds as little load as possible and
· Some security margin is left with respect to values causing protection failure

Certainly, using the same C and K values for all controllers makes the design definitely simpler.

11.8.3   Optimal Location of Installing Controller

We know that the location of the controller affects not only the improvement of the voltage profile but also the economy of the system operation. Thus the location of installing the controller or SPS is very important. The optimal location of installing controller should be where:

(1) Voltage at that location has high improvement.
(2) Probability of the outage at that location is high.
(3) System loss has big reduction.
(4) Load at that location is less important.
(5) Load center where the load is located is less important.

For item (1), the performance index to evaluate the voltage improvement by load shedding can be computed as below:

$$PI_{LSV}^{j} = \frac{V_j\left(\Delta P_j^{sh}\right) - V_j(0)}{\Delta P_j^{sh}} \tag{11.60}$$

where

$V_j(0)$: The voltage at bus j before the load shedding

$V_j\left(\Delta P_j^{sh}\right)$: The voltage at bus j after the load shedding

ΔP_j^{sh}: The amount of the load shedding at bus j

PI_{LSV}^{j}: The performance index to assess the voltage improvement at bus j

The probability of the outage for each location can be obtained according to analysis of the historical outage or disturbance data in the system.

For item (3), the performance index to evaluate the loss reduction by load shedding can be computed as below:

$$PI_{LSPL}^{j} = \frac{P_L\left(\Delta P_j^{sh}\right) - P_L(0)}{\Delta P_j^{sh}} \tag{11.61}$$

where

$P_L(0)$: The system loss before the load shedding at bus j

$P_L\left(\Delta P_j^{sh}\right)$: The system loss after the load shedding at bus j

PI_{LSPL}^{j}: The performance index to assess the loss reduction at bus j

Actually, the performance index to evaluate the loss reduction by load shedding can also be obtained using loss sensitivity of load, which is discussed in Chapter 3.

Items (4) and (5) are related to the less important of the loads; we can use one performance PI_{LSKEY}^{j} to express them. In Section 11.5, we computed the unified weighting factors w_i of the loads that are based on the important loads. Obviously, the less important performance index PI_{LSKEY}^{j} will be

$$PI_{LSKEY}^{j} = \frac{1}{w_i} \tag{11.62}$$

Therefore, the hierarchical model for computing the optimal location of installing controller can be constructed as in Figure 11.9.

For the lower layers in the hierarchy model (Fig. 11.9), the performance indices for evaluating the individual load location can be computed based on equations (11.60)–(11.62). But for the upper layer in the hierarchy model, the relationship among all kinds of performance indices cannot be computed exactly. It can be only obtained based on system operation cases and the judgment of the engineer or operators. According to AHP, the judgment matrix *A-PI* can be written as follows.
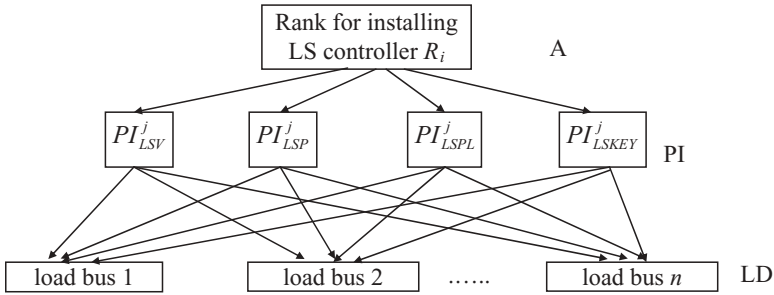
FIGURE 11.9   Hierarchy model of optimal location for installing LS controller

$$A - PI = \begin{bmatrix} w_{PI1}/w_{PI1} & w_{PI1}/w_{PI2} & \cdots\cdots & w_{PI1}/w_{PIn} \\ w_{PI2}/w_{PI1} & w_{PI2}/w_{PI2} & \cdots\cdots & w_{PI2}/w_{PIn} \\ \vdots & & & \vdots \\ w_{PIn}/w_{PI1} & w_{PIn}/w_{PI2} & \cdots\cdots & w_{PIn}/w_{PIn} \end{bmatrix} \qquad (11.63)$$

where, w_{PIi} is unknown. w_{PIi}/w_{PIj}, which is the element of judgment matrix A-PI, represents the relative importance of the ith performance index compared with the jth performance index. Here, there are only four performance indices for selecting the location of the controller. Thus, $n = 4$ in equation (11.63).

According to the hierarchy model in Figure 11.9 and the AHP approach, we can get the unified rank for all the locations of installing the LS controller. The number one in the rank list of locations will be first selected to install the LS controller. If there are K controllers, they will be installed in the system where the locations are the top K in the rank list.

11.9   CONGESTION MANAGEMENT

11.9.1   Introduction

Transmission congestion occurs when there is insufficient transmission capacity to meet the demands of all customers.

Congestion can be reduced by the following methods [32]:

(1) Generation redispatch
(2) Load shedding
(3) Using VAR support
(4) Expansion of transmission lines

Obviously, expansion of transmission lines involves lots of factors such as finances, time, environment, etc., and it is not realistic to solve the current

congestion problem. VAR support is discussed in Chapter 10. Several previous chapters analyzed the generation dispatch and redispatch issues. Congestion may be reduced by modification of generating schedules, but not for every situation. In heavily congested conditions, transmission congestion can only be relieved by curtailing a portion of nonfirm transactions. Thus we focus on the load shedding method for analyzing congestion management in this section.

11.9.2 Congestion Management in U.S. Power Industry

In the United States, congestion management is implemented in the various ISOs such as Pennsylvania-New Jersey-Maryland Interconnection (PJM), Electric Reliability Council of Texas (ERCOT), and NewYork Independent System Operator (NYISO).

11.9.2.1 PJM PJM Interconnection is a regional transmission organization that ensures the reliability of the electric power supply system in 13 states. PJM operates the wholesale electricity market and manages regional electric transmission planning to maintain the reliability of the power system.

The different methods to mitigate transmission emergencies due to overloads and excess transfers in transmission lines are adopted in PJM [33]. They are:

- Generator active power adjustment—raise/lower MW
- Phase angle regulator adjustment—increase/decrease phase angle
- Interchange schedule adjustment—import/export MW
- Transmission line switching—selected line switching
- Circuit breaker switching—change network topology
- Customer load shedding—internal procedure and NERC transmission loading relief procedure

Load shedding is the last option when the congestion cannot be alleviated through the remaining transmission emergency methods. Flow limits are further distinguished into normal limits, short-term emergency (STE) limits, and load dump (115% of STE). Violations may occur under actual (precontingency) or contingency (postcontingency) conditions.

PJM curtails loads that contribute to the overload before redispatching the generators if the transmission customers have indicated that they are not willing to pay transmission congestion charges. If overload persists even after redispatching the system, PJM will implement the NERC Transmission Loading Relief Procedure (TLR) [34]. The steps of TLR are:

(1) Notification of reliability coordinator
(2) Hold interchange transactions

    (3) Reallocate firm transmission service

    (4) Reallocate nonfirm transmission service

    (5) Curtail nonfirm

    (6) Redispatch generation

    (7) Curtail firm

    (8) Implement emergency procedures

11.9.2.2 ERCOT   ERCOT directs and ensures the reliable and cost-effective operation of its electric grid and enables fair and efficient market-driven solutions to meet customers' electric needs [35]. The following issues are addressed:

    (1) Ensures the grid can accommodate the scheduled energy transfers.

    (2) Ensures grid reliability.

    (3) Oversees retail transactions.

ERCOT develops four types of action plans to respond to electric system congestions.

- Precontingency action plan—used ahead of the contingency because not feasible once the contingency occurs
- Remedial action plan—used after contingency occurs
- Mitigation plan—similar to remedial action plan but only used after all available generation redispatch is exhausted. After the precontingency and remedial action plans are executed if relief is still needed, this method is appropriate
- Special protection plan—automatic actions using special protection systems

The Emergency Electric Curtailment Plan (EECP) [36, 37] was developed to respond to short supply situations and restore responsive reserve to required levels. This procedure will direct the system operator to declare an emergency notice for frequency restoration purposes.

11.9.2.3 NYISO   The NYISO manages New York's electricity transmission grid, a network of high-voltage lines that carries electricity throughout the state, and oversees the wholesale electricity market. NYISO addresses the following issues:

    (1) Maintains and enhances regional reliabilit.

    (2) Promotes and operates a fair and competitive electric wholesale market.

    (3) Provides quality customer service.

    (4) Tries to achieve these objectives in a cost-effective manner.

Severe system disturbances generally result in critically loaded transmission facilities, critical frequency deviations, high- or low-voltage conditions, or stability problems. The following operating states are defined for the state of New York [38]:

(1) Warning
(2) Alert
(3) Major emergency
(4) Restoration

The NYISO schedule coordinator, or the NYISO shift supervisor, forecasts the likelihood of the occurrence of states other than the Normal State in advance. If it is predicted that load relief either by voltage reduction or load shedding may be necessary during a future period, then the NYISO shift supervisor notifies all transmission owners and arranges corrective measures including:

• Curtailment of interruptible load
• Manual voltage reduction
• Curtailment of nonessential market participant load
• Voluntary curtailment of large load serving entities (LSE)
• Public appeals

NYISO reduces transmission flows that may cause thermal, voltage, and stability violations to properly allocate the reduction of transmission flows to relieve violations. When there are security violations that require reductions in transmission flow, NYISO takes action in the following sequence and to the extent possible, when system conditions and time permit:

1. Implement all routine actions using phase angle regulator tap positions, where possible.
2. Request all overgeneration suppliers that are contributing to the problem to adjust their generation to match their schedules.
3. Request voluntary shifts on generation either below minimum dispatchable levels or above normal maximum levels to help relieve the violation.
4. Request reduction or cancellation of all transactions that contribute to the violation. Applicable transactions shall be curtailed in accordance with curtailment procedures described in the *New York ISO Transmission and Dispatching Operations Manual* [39].

11.9.3 Congestion Management Method

The previous sections presented several approaches for optimal load shedding, which can be used for congestion management. Here, we present simple load shedding or load management methods for congestion management. They are:

- TLR Sensitivities-Based Load Curtailment
- Economic Load Management for Congestion Relief

11.9.3.1 *TLR Sensitivities-Based Load Curtailment*   We discuss power transfer distribution Factors (PTDF) in Chapter 3. The transmission line relief (TLR) sensitivities can be considered as the inverse of the PTDF. Both TLR and PTDF can measure the sensitivity of the flow on a line to load curtailment. PTDFs determine the sensitivity of the flow on an element such as transmission line to a single power transfer. TLR sensitivities determine the sensitivity of the flow on the single monitored element such as a transmission line to many different transactions in the system. In other words, TLR sensitivities gauge the sensitivity of a single monitored element to many different power transfers.

The TLR sensitivity values at all the load buses for the most overloaded line are considered and used for calculating the necessary load curtailment for alleviation of transmission congestion. The TLR sensitivity at a bus k for a congested line ij is S_{ij}^k, and is calculated by [32]

$$S_{ij}^k = \frac{\overline{\Delta P_{ij}}}{\Delta P_K} \tag{11.64}$$

The excess power flow on transmission line ij is given by

$$\overline{\Delta P_{ij}} = P_{ij} - P_{ij\,\text{max}} \tag{11.65}$$

where

P_{ij}: Actual power flow through transmission line ij
$P_{ij\text{max}}$: Flow limit of transmission line ij

The new load P_k^{new} at bus k can be calculated by

$$P_k^{\text{new}} = P_k - \frac{S_{ij}^k}{\sum\limits_{l=1}^{ND} S_{ij}^l} \overline{\Delta P_{ij}} \tag{11.66}$$

where

P_k^{new} : Load after curtailment at bus k
P_k: Load before curtailment at bus k
S_{ij}^l : Sensitivity of power flow on line ij due to load change at bus k
ND: Total number of load buses

The higher the TLR sensitivity, the more the effect of a single MW power transfer at any bus. So, based on the TLR sensitivity values the loads are

curtailed in required amounts at the load buses in order to eliminate the transmission congestion on the congested line *ij*.

This method can be implemented for systems where load curtailment is a necessary option for obtaining $(N-1)$ secure configurations.

It is noted that the sensitivity computed here is based on the perturbation, which is discussed in Chapter 3—Sensitivity Analysis. A limitation exists for this approach, that is, the sensitivity results are not stable. They are affected by power flow solution, including the selection of initial operation points. The more precise method for sensitivity calculation is based on matrix operation, which is purely related to network topology and will not be affected by the solution of power flow. The details are described in Chapter 3.

11.9.3.2 *Economic Load Management for Congestion Relief* Another possible solution for congestion management is to find customers who will volunteer to lower their consumption when transmission congestion occurs. By lowering the consumption, the congestion will "disappear," resulting in a significant reduction in bus marginal costs. A strategy to decide how much load should be curtailed for what customer is discussed here.

The anticipated effect of this congestion relief solution is to encourage consumers to be elastic against high prices of electricity. Hence, this congestion relief procedure could eventually protect all customers from high electricity prices in a deregulated environment [40].

The following three factors can be considered for the analysis of load management:

(1) Power flow effect through sensitivity index
(2) Economic factor for LMP index
(3) Load reduction preference for customer load curtailment index

The possible methods for these load management factors are presented below.

11.9.3.2.1 *Sensitivity Index* In Chapter 3, we discuss the load distributed sensitivity, which can be used to rank load sensitivity. The sensitivity of the congested line *ij* with respect to load bus k is S_{ij}^k. We can convert it to the new sensitivity with load distribution reference

$$S_{ij}^{k\text{new}} = S_{ij}^k - S_{\text{ldref}}^k \quad k = 1, \ldots, ND \tag{11.67}$$

where

S_{ldref}^k: The sensitivity of load distribution reference for the constraint *ij*, that is,

$$S_{\text{ldref}}^k = \frac{\sum\limits_{k=1}^{ND}(S_{ij}^k * P_{\text{d}k})}{\sum\limits_{k=1}^{ND}P_{\text{d}k}} \tag{11.68}$$

Load shedding can be performed based on the ranking of the distributed load reference based sensitivity $S_{ij}^{k\text{new}}$. The load with a high $S_{ij}^{k\text{new}}$ value will be curtailed first since it is more efficient to relieve the congestion than the load with low $S_{ij}^{k\text{new}}$ value.

11.9.3.2.2 LMP Index   High electricity price (LMP) is an incentive to reduce load. The following index measures the level of customer incentive to cut down on electricity consumption:

$$\text{LMP}^{k\text{new}} = \text{LMP}^k - \text{LMP}_{\text{ldref}}^k \quad k = 1, \ldots\ldots, ND \tag{11.69}$$

where

LMP^k: The electricity price of load bus k without considering load factor

$\text{LMP}^{k\text{new}}$: The electricity price of load bus k considering load factor

$\text{LMP}_{\text{ldref}}^k$: The electricity price of load bus k based on load distribution reference, that is,

$$\text{LMP}_{\text{ldref}}^k = \frac{\sum\limits_{k=1}^{ND}(\text{LMP}^k * P_{\text{d}k})}{\sum\limits_{k=1}^{ND}P_{\text{d}k}} \tag{11.70}$$

Load shedding can be performed based on the ranking of the distributed load reference based electricity price $\text{LMP}^{k\text{new}}$. The load with a high $\text{LMP}^{k\text{new}}$ value will be curtailed first since it is more of an incentive for customer to cut down on electricity consumption than the load with low $\text{LMP}^{k\text{new}}$ value. This is especially for the customer with a big load amount.

11.9.3.2.3 Customer Load Curtailment Index   If the required reduction of the power flow on the congested branch is given by ΔP_{ijc}, the required amount of adjustment ΔP_k at bus k will be given by

$$\Delta P_K = \frac{\Delta P_{ijc}}{S_{ij}^k} \tag{11.71}$$

Generally, the higher the sensitivity, the smaller the amount of curtailment needed. The customer is supposed to express the acceptable range of curtail-

ment by $\Delta P^{\max}$ and $\Delta P^{\min}$ at bus k, and the curtailment acceptance level is measured by

$$\mu_{Lk} = \frac{\Delta P^{\max} - \Delta P_k}{\Delta P^{\max} - \Delta P^{\min}} \tag{11.72}$$

If the index μ_{Lk} is between 0 and 1, then the required amount of load reduction is in the acceptable range of the customer, and if μ_{Lk} is less than 0 or greater than 1, then the required amount of load curtailment is more than the acceptable range.

11.9.3.2.4 Comprehensive Index for Congestion Relief We can comprehensively consider the three indices mentioned above. First of all, we normalize each of them as follows:

$$\mathrm{CR}_{\mathrm{SI}}^k = \frac{S_{ij}^{knew}}{\sum\limits_{k=1}^{ND} S_{ij}^{knew}} \quad k = 1, \ldots, ND \tag{11.73}$$

$$\mathrm{CR}_{\mathrm{LMP}}^k = \frac{\mathrm{LMP}^{knew}}{\sum\limits_{k=1}^{ND} \mathrm{LMP}^{knew}} \quad k = 1, \ldots, ND \tag{11.74}$$

$$\mathrm{CR}_{\mathrm{LCI}}^k = \frac{\mu_{Lk}}{\sum\limits_{k=1}^{ND} \mu_{Lk}} \quad k = 1, \ldots, ND \tag{11.75}$$

where

  $\mathrm{CR}_{\mathrm{SI}}^k$: The normalized sensitivity index
  $\mathrm{CR}_{\mathrm{LMP}}^k$: The normalized LMP index
  $\mathrm{CR}_{\mathrm{LCI}}^k$: The normalized customer load curtailment index

Then we compute the comprehensive index for congestion relief (CICR), using the following expression:

$$\mathrm{CICR}^k = W_{\mathrm{SI}}\mathrm{CR}_{\mathrm{SI}}^k + W_{\mathrm{LMP}}\mathrm{CR}_{\mathrm{LMP}}^k + W_{\mathrm{LCI}}\mathrm{CR}_{\mathrm{LCI}}^k, k = 1, \ldots, ND \tag{11.76}$$

where

  W_{SI}: The weight for the normalized sensitivity index
  W_{LMP}: The weight for the normalized LMP index
  W_{LCI}: The weight for the normalized customer load curtailment index
  $CICR^k$: The comprehensive index for congestion relief.

The weight factors can be determined according to the practical system operation status. If they cannot be easily obtained, the AHP method can be used. The sum of the factors should be 1.0. That is,

$$W_{\text{SI}} + W_{\text{LMP}} + W_{\text{LCI}} = 1 \qquad (11.77)$$

REFERENCES

[1] C.W. Richter and G.B. Sheble, "A profit-based unit commitment GA for the competitive environment," *IEEE Trans. On Power Systems*, *15*(2), 2000, 715–721.

[2] B. Tenenbaum, R. Lock, and J. Barker, "Electricity Privatization: Structural, Competitive and Regulatory Options," *Energy Policy*, *12*(12), 1992, 1134–1160.

[3] H. Rudnick, R. Palma, and J.E. Fernandez, "Marginal Pricing and Supplement Cost Allocation in Transmission Open Access," *IEEE Trans. On Power Systems*, *10*(2), 1995, 1125–1142.

[4] J.Z. Zhu, "Optimal Load Shedding Using AHP and OKA," *International Journal of Power and Energy Systems*, Vol. 25, No. 1, 2005, 40–49.

[5] T.H. Lee, D.H. Thorne, and E.F. Hill, "A Transportation Method for Economic Dispatching—Application and Comparison," *IEEE Trans. on Power Systems*, *99*(5), 1980, 2372–2385.

[6] E. Hobson, D.L. Fletcher, and W.O. Stadlin, "Network flow linear programming techniques and their application to fuel scheduling and contingency analysis," *IEEE Trans. On Power Systems*, *103*(4), 1984, 1684–1691.

[7] J.Z. Zhu and G.Y. Xu, "Application of Out-of-Kilter Algorithm to Automatic Contingency Selection and Ranking," *Proceedings of Intern. Symposium on Eng. Mathematics & Application, ISEMA-88*, 1988, 301–305.

[8] M.T. Ameli, S. Moslehpour, and H. Rahimikhoshmakani, "The Role of Effective Parameters in Automatic Load-Shedding Regarding Deficit of Active Power in a Power System," *The International Journal of Modern Engineering*, Vol. 7, No. 1, 2006.

[9] P. Anderson and M. Mirheydar, "A Low Order System Frequency Response Model," *IEEE Transaction on Power System*, Vol. 5, No. 3, August 1990.

[10] S. Chelgardee and M. Doozbakhshian, "The Designs For Under—Frequency Relays Used in Load–Shedding Dispatching Department," G 2162, 1990.

[11] F. Shokooh, J.J. Dai, S. Shokooh, J. Tastet, H. Castro, T. Khandelwal, and G. Donner, "An Intelligent Load Shedding (ILS) System Application in a Large Industrial Facility," *Industry Applications Conference*, Vol. 1, 2005, pp. 417–425.

[12] T.L. Saaty, *The Analytic Hierarchy Process*, McGraw Hill, Inc., New York, 1980.

[13] J.Z. Zhu, M.R. Irving, and G.Y. Xu, Automatic Contingency Selection and Ranking using an Analytic Hierarchical Process, *Electrical Machines & Power Systems*, Vol. 16, No. 4, 1998, pp. 389–398.

[14] D.K. Smith, *Network Optimization Practice*, Ellis Horwood, Chichester, UK, 1982.

[15] H. Everett, *Operations Research*, Vol. 11, 1963, pp. 399–417.

[16] J.A. Momoh, J.Z. Zhu, and J.L. Dolce, "Optimal allocation with network limitation for autonomous space power system," *AIAA Journal—Journal of Propulsion and Power*, Vol. 16, No. 6, Nov.–Dec., 2000, pp. 1112–1117.

[17] J.A. Momoh, J.Z. Zhu, and J.L. Dolce, "Aerospace power system automation—using Everett method," *AIP Conference Proceedings—January 22*, 1999, Volume 458, pp. 1653–1658.

[18] R. Faranda, A. Pievatolo, and E. Tironi, "Load Shedding: A New Proposal," *IEEE Trans. On Power Systems*, Vol. 22, No. 4, 2007, pp. 2086–2093.

[19] C. Concordia, L.H. Fink, and G. Poullikkas, "Load shedding on an isolated system," *IEEE Trans. Power Syst.*, vol. 10, no. 3, pp. 1467–1472, Aug. 1995.

[20] B. Delfino, S. Massucco, A. Morini, P. Scalera, and F. Silvestro, "Implementation and comparison of different under frequency load- shedding schemes," presented at the *IEEE Summer Meeting 2001, Vancouver, BC, Canada, Jul. 15–19*, 2001.

[21] D. Xu and A.A. Girgis, "Optimal load shedding strategy in power systems with distributed generation," presented at the *IEEE Power Engineering Society Winter Meeting, Columbus, OH, Feb.* 2001.

[22] E. Carpaneto and G. Chicco, "Probability distributions of the aggregated residential loads," presented at the *9th Int. Conf. Probabilistic Methods Applied to Power Systems, Stockholm, Sweden, Jun. 11–15*, 2006.

[23] J.O. Berger, *Statistical Decision Theory and Bayesian Analysis*, 2nd ed. New York: Springer-Verlag, 1985.

[24] C.W. Taylor, *Power System Voltage Stability*. New York: McGraw-Hill, 1994, EPRI Power Engineering Series.

[25] T. Van Cutsem and C. Vournas, *Voltage Stability of Electric Power Systems*. Boston, MA: Kluwer, 1998.

[26] C.W. Taylor, "Concepts of undervoltage load shedding for voltage stability," *IEEE Trans. Power Delivery*, vol. 7, no. 2, pp. 480–488, Apr. 1992.

[27] D.H. Karlsson, "System protection schemes in power networks," final report of CIGRE Task Force 38.02.19.

[28] V.C. Nikolaidis, C.D. Vournas, G.A. Fotopoulos, G.P. Christoforidis, E. Kalfaoglou, and A. Koronides, "Automatic load shedding schemes against voltage stability in the Hellenic system," *IEEE PES General Meeting, Tampa, FL, Jun.* 2007.

[29] B. Otomega and T.V. Cutsem, "Undervoltage load shedding using distributed controllers," *IEEE Trans. On Power Systems*, Vol. 22, No. 4, 2007, 1898–1907.

[30] D. Lefebvre, C. Moors, and T. Van Cutsem, "Design of an undervoltage load shedding scheme for the Hydro-Québec system," *IEEE PES General Meeting, Toronto, ON, Canada, Jul.* 2003.

[31] S. Arnborg, G. Andersson, D.J. Hill, and I.A. Hiskens, "On under-voltage load shedding in power systems," *Int. J. Electr. Power Energy Syst.*, vol. 19, pp. 141–149, 1997.

[32] S. Parnandi, Power Market Analysis Tool for Congestion Management, Master Thesis, West Virginia University, 2007.

[33] PJM Transmission and Voltage Emergicies, Online: http://www.pjm.com/services/ training/downloads/ops101-transemer.pdf.

[34] NERC Reliability Coordination Transmission Loading Relief, ftp://www.nerc. com/pub/sys/all updl/standards/rs/IRO-006-1.pdf.

[35] ERCOT, Online: http://www.ercot.com/about/index.html.

[36] ERCOT Emergency Electric Curtailment Plan, Online: http://nodal.ercot.com/protocols/nprr/040/keydocs/040NPRR-01 Synchronization of Emergency Electric Curtailment.doc.

[37] ERCOT Mitigation, Online: http://www.ercot.com/meetings/tac/keydocs/2004/1202/TAC12022004-19.doc.

[38] NewYork ISO Emergency Operations, Online: http://www.nyiso.com/public/webdocs/documents/manuals/operations/emopmnl.pdf.

[39] *New York ISO Transmission and Dispatching Manual*. Online: http://www.nyiso.com/public/webdocs/documents/manuals/operations/transdisp.pdf.

[40] T. Niimura and Y. Niu, "Transmission congestion relief by economic load management," *IEEE Power Engineering Society Summer Meeting*, Vol. 3, pp. 1645–1649, July 2002.

12

OPTIMAL RECONFIGURATION OF ELECTRICAL DISTRIBUTION NETWORK

The reconfiguration of the distribution network is also part of power system operation. This chapter sums up several major methods used to date in optimal reconfiguration of an electric distribution network. These are the simple branch exchange method, the optimal flow pattern, the rule-based comprehensive approach, mixed-integer linear programming, the genetic algorithm (GA) with matroid theory, and multiobjective evolution programming.

12.1 INTRODUCTION

The distribution networks are the most extensive part of the electrical power system. They produce a large number of power losses because of the low voltage level of the distribution system. The goal of reconfiguration of the distribution network is to find a radial operating structure that minimizes the power losses of the distribution system under the normal operation conditions. Generally, distribution networks are built as interconnected networks, while in operation they are arranged into a radial tree structure. This means that distribution systems are divided into subsystems of radial feeders, which contain a number of normally closed switches and a number of normally open switches. According to the graph theory, a distribution network can be represented with a graph of $G(N, B)$ that contains a set of nodes N and a set of branches B. Every node represents either a source node (supply transformer) or a sink node (customer load point), while a branch represents a feeder

section that can either be loaded (switch closed) or unloaded (switch open). The network is radial, so that the feeder sections form a set of trees where each sink node is supplied from exactly one source node. Therefore, the distribution network reconfiguration (DNRC) problem is to find a radial operating structure that minimizes the system power loss while satisfying operating constraints [1]. In fact, the distribution network reconfiguration can be viewed as a problem of determining an optimal tree of the given graph. Many algorithms have been used to solve the reconfiguration problem: heuristic methods [2–10], expert system, combinatorial optimization with discrete branch and bound methods [11–17], and evolution programming or genetic algorithm [1, 18–21].

Merlin and Back first proposed the discrete branch and bound method to reduce losses in a distribution network [3]. Because of the combinatorial nature of the problem, it requires checking a great number of configurations for a real-sized system. Shirmohammadi and Hong [8] used the same heuristic procedure mentioned by Merlin and Back [3]. Castro et al. [4] proposed search heuristic techniques to restore the service and load balance of the feeders. Castro and Franca [6] proposed modified heuristic algorithms to restore the service and load balance. The operation constraints are checked through a load flow solved by means of modified fast decoupled Newton–Raphson. Baran and Wu [5] presented a heuristic reconfiguration methodology based on the method of branch exchange to reduce losses and balance loads in the feeders. To assist in the search, two approximated load flows for radial networks with different degrees of accuracy are used. Also, they propose an algebraic expression that allows estimation of the loss reduction for a given topological change. Liu et al. [14] proposed an expert system to solve the problem of restoration and loss reduction in distribution systems. The model for the reconfiguration problem is a combinatorial nonlinear optimization problem. To find the optimal solution, it is necessary to consider all the possible trees generated due to the opening and closing of the switches existing in the network.

Nahman and Strbac presented another heuristic approach in reference [10]. The algorithm starts from a completely empty network, with all switches open and all loads disconnected. Load points are connected one by one by switching branches onto the current subtree. The search technique also does not necessarily guarantee global optima.

Zhu et al. [22] proposed a rule-based comprehensive approach to study distribution network reconfiguration (DNRC). The DNRC model with line power constraints is set up, in which the objective is to minimize the system power loss. Unlike the traditional branch exchange-based heuristic method, the switching branches are divided into three types. The rules that are used to select the optimal reconfiguration of the distribution network are formed based on system operation experiences and the types of the switching branches [23].

Recently, new methods based on genetic algorithm (GA) have been used in DNRC [1, 18–20]. GA-based methods are better than traditional heuristic algorithms in obtaining the global optima.

12.2   MATHEMATICAL MODEL OF DNRC

The mathematical model of DNRC can be expressed by either branch current or branch power.

(1) Use Current Variable

$$\text{Min } f = \sum_{l=1}^{NL} k_l R_l I_l^2 \quad l \in NL \tag{12.1}$$

such that

$$k_l |I_l| \leq I_{l\max} \qquad l \in NL \tag{12.2}$$

$$V_{i\min} \leq V_i \leq V_{i\max} \quad i \in N \tag{12.3}$$

$$g_i(I, k) = 0 \tag{12.4}$$

$$g_i(V, k) = 0 \tag{12.5}$$

$$\varphi(k) = 0 \tag{12.6}$$

where

I_l: The plural current in branch l

R_l: The resistance of branch l

V_i: The node voltage at node i

K_l: Represents the topological status of the branches. $k_l = 1$ if branch l is closed, and $k_l = 0$ if branch l is open.

N: The set of nodes

NL: The set of branches

In the above model, equation (12.2) stands for the branch current constraints. Equation (12.3) stands for the node voltage constraints. Equation (12.4) represents Kirchhoff's first law (KCL), and equation (12.5) represents Kirchhoff's second law (KVL). Equation (12.6) stands for topological constraints that ensure radial structure of each candidate topology. It consists of two structural constraints:

(a) Feasibility: All nodes in the network must be connected by some branches, i.e., there is no isolated node.

(b) Radiality: The number of branches in the network must be smaller than the number of nodes by one unit ($k_l * NL = N - 1$)

Therefore, the final network configuration must be radial and all loads must remain connected.

(2) Use Power Variable

$$\text{Min } f = \sum_{l=1}^{NL} k_l R_l \left(\frac{P_l^2 + Q_l^2}{V_l^2} \right) \quad l \in NL \tag{12.7}$$

such that

$$k_l |P_l| \leq P_{l\max} \qquad l \in NL \tag{12.8}$$

$$k_l |Q_l| \leq Q_{l\max} \qquad l \in NL \tag{12.9}$$

$$V_{i\min} \leq V_i \leq V_{i\max} \quad i \in N \tag{12.3}$$

$$g_i(P, k) = 0 \tag{12.10}$$

$$g_i(Q, k) = 0 \tag{12.11}$$

$$g_i(V, k) = 0 \tag{12.5}$$

$$\varphi(k) = 0 \tag{12.6}$$

where,

P_l: the real power in branch l

Q_l: the reactive power in branch l

The objective function in equation (12.7) is power losses. If voltage magnitudes are assumed to be 1.0 p.u. and reactive power losses are ignored in the objective function, equation (12.7) may be simplified as

$$\text{Min } f = \sum_{l=1}^{NL} k_l R_l P_l^2 \quad l \in NL \tag{12.12}$$

In the above model, equations (12.8) and (12.9) stand for the branch real power and reactive power constraints. Equations (12.10) and (12.11) represent Kirchhoff's first law.

Obviously, both DNRC models, whether with branch current expression or power expression, have the same function.

12.3   HEURISTIC METHODS

12.3.1   Simple Branch Exchange Method

The basic idea of the heuristic branch exchange method is to compute the change of power losses by operating a pair of switches (close one and open another one at the same time). The goal is to reduce power losses. The advantage of this method is simple and easily understood. The disadvantages are:

(1) The final configuration depends on the initial network configuration.
(2) The solution is a local optima, rather than global optima.
(3) It is time consuming for selecting and operating each pair of switches as well as computing the corresponding radial network load flow.

12.3.2   Optimal Flow Pattern

If the impedances of all branches in the loop network are replaced by the corresponding branch resistances, the load flow distribution that satisfies the KCL and KVL is called an optimal flow pattern. When the load flow distribution in a loop is an optimal flow, the corresponding network power losses will be minimal. Thus the basic idea of the optimal flow pattern is to open the switch of the branch that has a minimal current value in the loop [8]. The steps of the heuristic algorithm based an optimal flow pattern are:

(1) Compute load flow of initial radial network.
(2) Close all normal open switches to produce loop networks.
(3) Compute the equivalent injection current at all nodes in loops through injecting current method.
(4) Replace branch impedance by the corresponding branch resistance in the loop and then compute the optimal flow.
(5) Open a switch of the branch that has a minimal current value in the loop. Recompute the load flow for the remained network.
(6) Open next branch switch, and repeat step (5) until the network becomes a radial.

The advantages of this method are that (a) the final network configuration will not depend on the initial network topology; (b) the computing speed is much quicker than that in the simple branch exchange method; and (c) the complicated combination problem of switch operation becomes a heuristic problem by opening one switch each time.

However, there are some disadvantages since all normal open switches are closed in the initial network, i.e.,

(1) If there are many normal open switches in a network, it means that the calculation of optimal flow involves lots of loops. The final solution may not be optimal because of the mutual effects among the loops.

(2) When load flow is solved by the equivalent injection current method, it needs to compute the impedance matrix of Thevenin equivalent network with multiports. This will increase the calculation burden.

(3) It needs to compute loop network load flow twice for each single switch operation (before and after opening one switch).

12.3.3 Enhanced Optimal Flow Pattern

The enhanced optimal flow pattern combines the advantages of two heuristic algorithms mentioned in Sections 12.3.1 and 12.3.2, that is, the approach is based on optimal flow pattern but it does not close all normal open switches (only closing one switch and opening one other switch each time). In addition, this method does not care about the accuracy of network losses. It only focuses on the change of losses that are caused by switch operation. The calculation steps of the enhanced optimal flow pattern are as below:

(1) Open all normal open switches in a network so that the initial network is a tree structure.

(2) Close any one switch. In this way, there is only one loop in network.

(3) Compute the load flow for the single-loop network and get the equivalent injection current for all nodes in the loop.

(4) Change the single-loop network into a pure resistance network, and compute the optimal flow to find the branch that with the minimal current value. Open the switch on this branch.

(5) Compute the load flow for this new radial network, and proceed the calculation of next switch operation as steps (2)–(4).

(6) The algorithm will be stopped after going through all open switches.

The enhanced optimal flow pattern has eliminated the effect among multiple loops. Although the convergence process is related to the initial network, the final solution is stable and not related to the order of the switch operation [9]. The disadvantages of this method are:

(a) It needs twice the load flow calculations for operation of each pair of switches.

(b) The convergence process and speed are affected by the order of the switch operation.

12.4   RULE-BASED COMPREHENSIVE APPROACH

This section uses a rule-based comprehensive approach to study distribution network reconfiguration. The algorithm consists of a modified heuristic solution methodology and the rules base. It determines the switching actions based on a search by branch exchange to reduce the network's losses as well as to balance the load of the system.

12.4.1   Radial Distribution Network Load Flow

To get the precise expression of system power loss, the branch power will be computed through a radial distribution network load flow (RDNLF) method in the study. It is well known that in the distribution network the ratio of R/X (resistance/reactance) is relatively big, even bigger than 1.0 for some transmission lines. In this case, P-Q decoupled load flow is invalid for distribution network load flow calculation. It will also be complicated and time-consuming to use the Newton–Raphson load flow because the distribution network is only a simple radial tree structure. Therefore, the power summation-based radial distribution network load flow method (PSRDNLF) is presented in this section. The PSRDNLF calculation consists of three parts:

(1) Conduct optimal node order calculation for the whole radial network based on graph theory. Consequently, the branches are divided into different layers according to the distance between the ordered node and the "root of a tree" node. Figure 12.1 is an example of how to make an optimal node order.
The rules of node order are:
(a) Start from the root node.
(b) The nodes that connect to the root belong to the first layer.
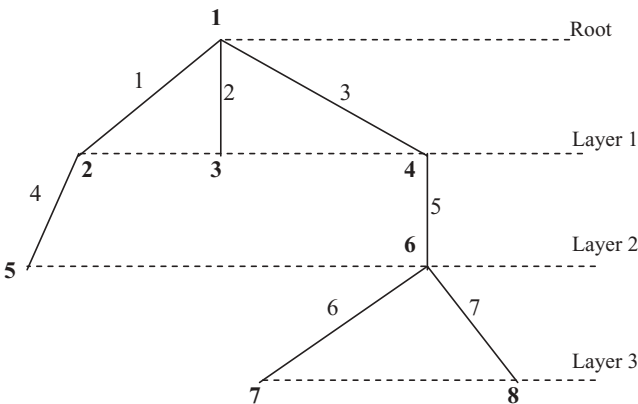
FIGURE 12.1   Example of optimal node order

    (c) The nodes that connect to the nodes in the first layer become the second layer, and so on.

    (d) The node number in layer n must be greater than the node number in layer $(n - 1)$. The node numbers in the same layer may be arbitrary.

    (e) For the branch number, for example, connecting to layer n and layer $n - 1$, the start node of the branch is the node in layer $n - 1$ and the end node is the node in layer n.

(2) Calculate the branch real power and reactive power from the "top of a tree" node to the "root of a tree" node, i.e., from last layer to first layer.

(3) Compute the node voltage from the "root of a tree" node to the "top of a tree node," i.e., from first layer to last layer.

The initial conditions are the given voltage vectors at root nodes as well as real and reactive power at load nodes. In final, the deviation of injection power at all nodes can be computed. The iteration calculation will be stopped if the deviation is less than the given permissive error.

If there are multiple generation sources in the distribution network, one source will be selected as a reference/slack source and others can be handled as negative loads.

12.4.2   Description of Rule-Based Comprehensive Method

Unlike the traditional branch exchange-based heuristic method, the rule-based comprehensive method combines the traditional branch exchange approach and a set of rules. The rules that are used to select the optimal reconfiguration of the distribution network are formed based on system operation experience.

In the rule-based comprehensive method, the switching branches are divided into three types.

(1) Type I: The switching branches are planned for maintenance in a short period according to the equipment maintenance schedule.

(2) Type II: The power flows of the switching branches almost reach their maximal power limits (e.g., 90%).

(3) Type III: The other switching branches that have enough available transfer capacity under the system operation conditions.

Thus the following rules will be used for the modified heuristic approach according to the practical system operation experience of the engineers.

(a) If the switching branches lead to system power losses increase, do not switch them.

(b) If the switching branches lead to system power losses reduce but cause the system to be overloaded, do not switch them.

(c) If the switching branches belong to type I mentioned above and also can lead to reduction of system power losses, select one that makes maximal power loss reduction, ΔPL_{I}.

(d) If the switching branches belong to type II mentioned above, and also can lead to reduction of system power losses, select one that makes maximal power loss reduction, ΔPL_{II}.

(e) If the switching branches belong to type III mentioned above, and also can lead to reduction of system power losses, select one that makes maximal power loss reduction, ΔPL_{III}.

(f) From (c) to (e), use the following formula to determine the branch that will be switched:

$$PI_{\mathrm{SW}i} = \frac{W_i \Delta PL_i}{W_{\mathrm{I}}\Delta PL_{\mathrm{I}} + W_{\mathrm{II}}\Delta PL_{\mathrm{II}} + W_{\mathrm{III}}\Delta PL_{\mathrm{III}}} \quad i = \mathrm{I, II, III} \qquad (12.13)$$

where

ΔPL_i: The change of system power losses before and after the branch switch.

W: The weighting coefficient of the different type of switching branches. According to the experiences of the engineers, the weighting factors of the three types of switches may be 1.0, 0.6, and 0.3, respectively. They may also be adjusted according to practical system operation situations.

$PI_{\mathrm{SW}i}$: The performance index of the switching branch i. The largest $PI_{\mathrm{SW}i}$ of each switching loop will be switched.

12.4.3 Numerical Examples

The rule-based comprehensive approach for distribution network reconfiguration is tested on 14-bus and 33-bus distribution systems as shown in Figures 12.2 and 12.3, respectively. The system data and parameters of the 14-bus system are listed in Tables 12.1 and 12.2.

The 14-bus test system contains 2 source transformers and 12 load nodes. The 3 initially open switches are "4 − 9," "14 − 11," and "6 − 3." The initial system power loss is 0.0086463 MW.

The results of the optimal configuration for the 14-bus distribution network are shown in Tables 12.3–12.5. Table 12.3 is the node voltage results comparison between the initial network and final configuration. Table 12.4 is the load flow results of the optimal configuration for the 14-bus system. Table 12.5 is the optimal open switches of the final network and the corresponding system losses, from which we know that the system losses reduction is 0.0003765 MW, i.e., 4.354%.
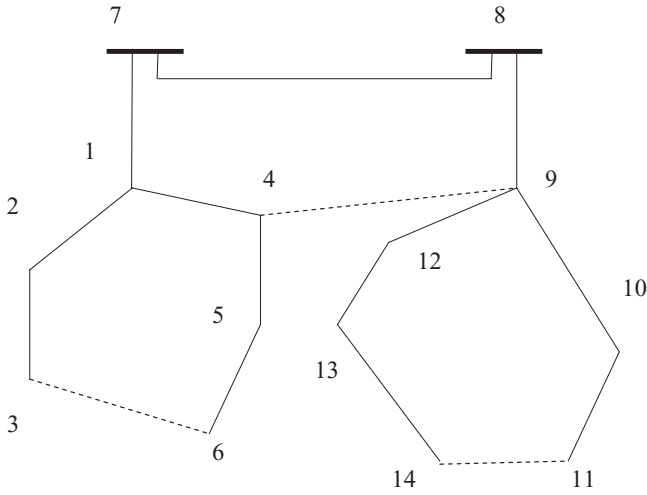
FIGURE 12.2   A 14-bus distribution system

Table 12.1   System load demand for 14-bus system

Node	Load P(MW)	Load Q(MVAR)
1	0.0000	0.0000
2	0.9000	0.7000
3	0.7000	0.5500
4	0.0000	0.0000
5	0.9000	0.7600
6	0.4000	0.3000
7	0.0000	0.0000
8	−2.2000	−1.0800
9	0.3000	0.2000
10	0.6000	0.4500
11	0.9000	0.7500
12	0.0000	0.0000
13	0.8000	0.6500
14	0.3000	0.2200

The system data and parameters of the 33-bus system are listed in Tables 12.6 and 12.7. The 33-bus test system consists of 1 source transformer and 32 load nodes. The 5 initially open switches are "33," "34," "35," "36," and "37." The total system load is 3.715 MW, while the initial system power loss is 0.202674 MW. The system base is $V = 12.66 \text{ kV}$ and $S = 10 \text{ MVA}$.

The calculation results of the final configuration of the 33-bus system are shown in Table 12.8. It can be observed that the same results are obtained as in reference [8].
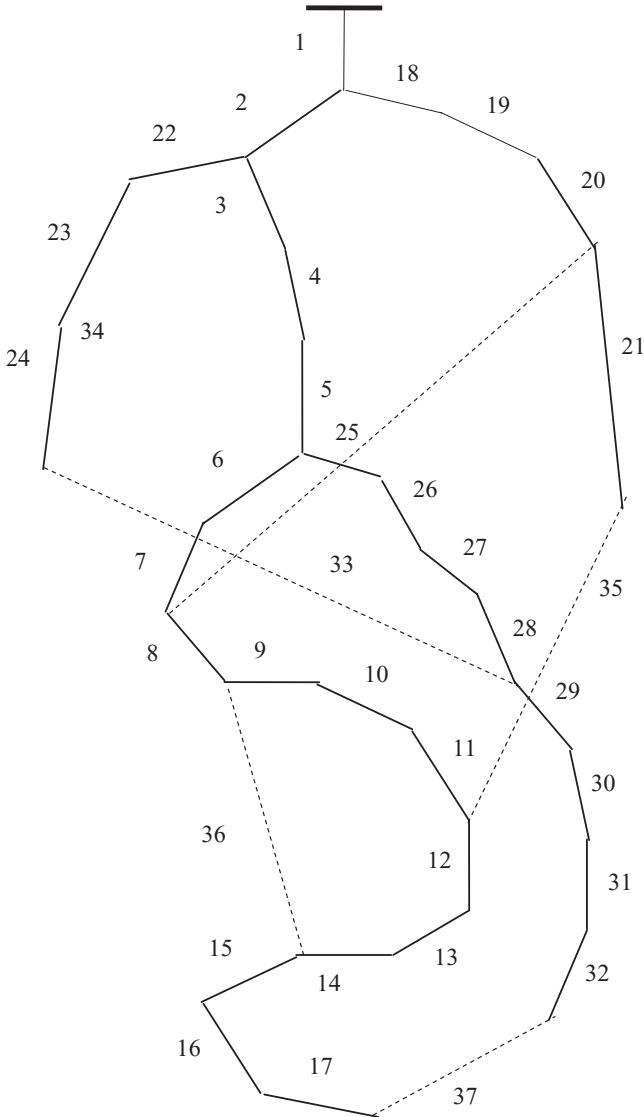
FIGURE 12.3   A 33-bus distribution system

12.5   MIXED-INTEGER LINEAR PROGRAMMING APPROACH

Because of the magnitude of the DNRC problem and its non linearnature, the use of a blend of optimization and heuristic techniques is one choice as in Section 12.4. The linearization of DNRC is another choice. Through performing a linearization of both the objective function and constraints, the DNRC is changed to a mixed-integer linear optimization problem [17].

Table 12.2   System branch parameters for 14-bus distribution network

Line No.	From Node i	To Node j	Resistance R (Ω)	Reactance X(Ω)
1	7	1	0.00575	0.00893
2	1	2	0.02076	0.03567
3	2	3	0.01284	0.01663
4	1	4	0.01023	0.01567
5	9	12	0.01023	0.01976
6	4	5	0.09385	0.11457
7	5	6	0.03220	0.04985
8	8	9	0.00575	0.00793
9	9	10	0.03076	0.04567
10	10	11	0.02284	0.03163
11	12	13	0.09385	0.11457
12	13	14	0.02810	0.04085
13	7	8	0.02420	0.42985
14	14	11	0.02500	0.04885
15	4	9	0.02300	0.04158
16	6	3	0.02105	0.04885

Table 12.3   Initial and final node voltages for 14-bus distribution network

Node	Initial V(p.u.)	Initial θ	Final V(p.u.)	Final θ
1	1.04964	−0.00656	1.04951	−0.00625
2	1.04890	−0.02275	1.04858	−0.02664
3	1.04873	−0.02514	1.04831	−0.03048
4	1.04936	−0.01157	1.04906	−0.00899
5	1.04704	−0.03738	1.04742	−0.02557
6	1.04678	−0.04275	1.04809	−0.03738
7	1.05000	0.00000	1.05000	0.00000
8	1.04927	−0.00317	1.04863	−0.00405
9	1.04894	−0.00834	1.04843	−0.00990
10	1.04798	−0.02480	1.04729	−0.02999
11	1.04756	−0.03072	1.04673	−0.03824
12	1.04867	−0.01503	1.04823	−0.01467
13	1.04674	−0.03819	1.04681	−0.03067
14	1.04657	−0.04136	1.04656	−0.04302

12.5.1   Selection of Candidate Subnetworks

The simplest way of modeling the topology of an electrical network is by means of the branch-to-node incidence matrix A, in which as many rows as connected components are omitted to ensure linear independence of the remaining rows. Given a single-component meshed network with $N + 1$ buses,

Table 12.4   Load flow of optimal configuration for 14-bus distribution network

Line No.	From Node i	To Node j	Real Power P (MW)	Reactive Power Q(MVAR)
1	7	1	4.30930	1.92709
2	1	2	3.10318	1.40266
3	1	4	1.20496	0.52344
4	2	3	2.20100	1.00101
5	4	5	0.90083	0.40074
6	4	9	0.30398	0.12245
7	3	6	1.00032	0.30039
8	9	12	0.80069	0.30062
9	9	8	−3.19940	−1.07969
10	9	10	2.40266	0.80148
11	12	13	0.80062	0.30056
12	10	11	1.80087	0.60057
13	11	14	0.70013	0.20020

Table 12.5   Optimal configuration results for 14-bus distribution network

Radial network	Initial network	Optimal configuration
Open switches	switch 4 − 9	switch 7 − 8
	switch 14 − 11	switch 13 − 14
	switch 6 − 3	switch 5 − 6
Power loss (MW)	0.0086463	0.0082699

a well-known theorem states that a set of N branches is a spanning tree if and only if the respective columns of constitute a full rank submatrix [27]. Thus graph-based algorithms are usually adopted to select the candidate subnetworks. Given the undirected graph of a single-component network, determining whether a candidate set of N branches constitutes a spanning tree reduces to checking whether they form a single connected component. Alternatively, instead of checking for radiality, on a posteriori, straightforward algorithm is available to generate radial subnetworks, either from scratch or by performing branch exchanges on existing radial networks.

For a meshed network, there are in general several alternative paths connecting a given bus to the substation, whereas in a radial network each bus is connected to the substation by a single unique path. Furthermore, the union of all node paths gives rise to the entire system. The connectivity of a meshed network, as well as that of its radial subnetworks, can then be represented by means of paths. Let π_n^i be the set of paths associated to bus i

$$\Pi_n^i = \left\{ \pi_l^i, \ldots, \pi_p^i, \ldots, \pi_n^i \right\} \tag{12.14}$$

where each path is a set of branches connecting bus to the substation. As noted above, any radial network is characterized by only one of those paths being

Table 12.6   System data and parameters for 33-bus distribution network

Line No.	Node i	Node j	Resistance R (Ω)	Reactance X (Ω)
1	1	2	0.0922	0.0470
2	2	3	0.4930	0.2512
3	3	4	0.3661	0.1864
4	4	5	0.3811	0.1941
5	5	6	0.8190	0.7070
6	6	7	0.1872	0.6188
7	7	8	0.7115	0.2351
8	8	9	1.0299	0.7400
9	9	10	1.0440	0.7400
10	10	11	0.1967	0.0651
11	11	12	0.3744	0.1298
12	12	13	1.4680	1.1549
13	13	14	0.5416	0.7129
14	14	15	0.5909	0.5260
15	15	16	0.7462	0.5449
16	16	17	1.2889	1.7210
17	17	18	0.7320	0.5739
18	2	19	0.1640	0.1565
19	19	20	1.5042	1.3555
20	20	21	0.4095	0.4784
21	21	22	0.7089	0.9373
22	3	23	0.4512	0.3084
23	23	24	0.8980	0.7091
24	24	25	0.8959	0.7071
25	6	26	0.2031	0.1034
26	26	27	0.2842	0.1447
27	27	28	1.0589	0.9338
28	28	29	0.8043	0.7006
29	29	30	0.5074	0.2585
30	30	31	0.9745	0.9629
31	31	32	0.3105	0.3619
32	32	33	0.3411	0.5302
34	8	21	2.0000	2.0000
36	9	15	2.0000	2.0000
35	12	22	2.0000	2.0000
37	18	33	0.5000	0.5000
33	25	29	0.5000	0.5000

active for each bus. Therefore, there is a need to represent the status of each path, for which the following binary variable is defined:

$$K_p^i = \begin{cases} 1, \text{ if } \pi_p^i \text{ is the active path for bus } i \\ 0, \text{ otherwise} \end{cases} \qquad (12.15)$$

Table 12.7   System load demand for 33-bus distribution network

Node No.	Real Power Load P (MW)	Reactive Power Load Q (MVAr)
2	100.0	60.0
3	90.0	40.0
4	120.0	80.0
5	60.0	30.0
6	60.0	20.0
7	200.0	100.0
8	200.0	100.0
9	60.0	20.0
10	60.0	20.0
11	45.0	30.0
12	60.0	35.0
13	60.0	35.0
14	120.0	80.0
15	60.0	10.0
16	60.0	20.0
17	60.0	20.0
18	90.0	40.0
19	90.0	40.0
20	90.0	40.0
21	90.0	40.0
22	90.0	40.0
23	90.0	50.0
24	420.0	200.0
25	420.0	200.0
26	60.0	25.0
27	60.0	25.0
28	60.0	20.0
29	120.0	70.0
30	200.0	100.0
31	150.0	70.0
32	210.0	100.0
33	60.0	40.0

A candidate subnetwork is both connected and radial if the following constraints are satisfied:

(1) Every node has at most one active path, i.e.,

$$\sum_{p \in \Pi_n^i} K_p^i = 1, \quad \forall \text{ node } i \tag{12.16}$$

(2) If π_p^i is active, then any path contained in π_p^i must be also active, which can be written as follows:

Table 12.8 Optimal configuration results for 33-bus distribution network

Radial network	Initial network	Final configuration	Results in Ref. [8]
Open switches	switch 33	switch 7	switch 7
	switch 34	switch 10	switch 10
	switch 35	switch 14	switch 14
	switch 36	switch 33	switch 33
	switch 37	switch 37	switch 37
Power loss (MW)	0.202674	0.141541	0.141541
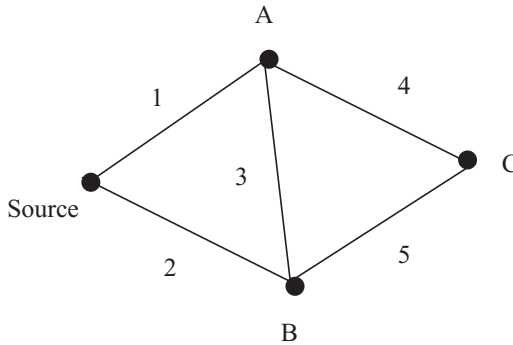
FIGURE 12.4 Simple electrical network with one source

Table 12.9 Node paths for the example of Figure 12.4

Node	Path	Path Branches
A	π_1^A	1
	π_2^A	2, 3
	π_3^A	2, 4, 5
B	π_1^B	2
	π_2^B	1, 3
	π_3^B	1, 4, 5
C	π_1^C	1, 4
	π_2^C	2, 5
	π_3^C	1, 3, 5
	π_4^C	2, 3, 4

$$K_p^i \le K_l^i, \quad \forall \pi_l^i \subset \pi_p^i \tag{12.17}$$

Figure 12.4 is a simple electrical network with one source node and three load nodes. Table 12.9 presents all possible paths for this network [17].

It is worth noting that, for computational efficiency, not all of the possible paths shown in Table 12.9 should be considered in practice. For example,

assuming the branch lengths represented in Figure 12.4 are proportional to their resistance, it is clear that paths π_3^A and π_3^B can be discarded, as they involve much more electrical distance than that of alternative paths for nodes A and B, respectively. Hence, for each node, only those paths whose total resistance does not exceed a previously defined threshold times the lowest node path resistance are considered. This significantly reduces the number of relevant candidate paths for realistic networks.

The inequality constraint in equation (12.17) can be better understood with the help of this example. We can easily check that the following inequalities hold (paths π_3^A, π_3^B are discarded).

$$\left.\begin{array}{c} W_3^C \le W_2^B \le W_1^A \\ W_1^C \le W_1^A \\ W_4^C \le W_2^A \le W_1^B \\ W_2^C \le W_1^B \end{array}\right\}$$

Although the concepts and variables presented above suffice for modeling the network radial structure, in order to handle other branch-related electrical constraints a second set of paths is introduced:

$$\Pi_b^j = \{\text{set of node paths sharing branch } j\}$$

Table 12.10 shows the set Π_b^j for every branch in the sample system of Figure 12.4. A graph-based effective procedure is as below.

Before describing the graph-based procedure, we assume that the meshed network connectivity is conveniently represented by a sparse structure allowing fast access to the set of buses adjacent to a given bus. The main idea consists of building an auxiliary tree, named the **mother tree**, by a breadth-first search, which contains all the feasible paths for the network under study. The system shown in Figure 12.4, whose mother tree is presented in Figure 12.5, will be used to illustrate this concept.

Table 12.10   Sets 5_b^j for the example of Figure 12.4

Branch j	Π_b^j
1	$\Pi_b^1 = \{\pi_1^A, \pi_2^B, \pi_3^B, \pi_1^C, \pi_3^C\}$
2	$\Pi_b^2 = \{\pi_2^A, \pi_3^A, \pi_1^B, \pi_2^C, \pi_4^C\}$
3	$\Pi_b^3 = \{\pi_2^A, \pi_2^B, \pi_3^C, \pi_4^C\}$
4	$\Pi_b^4 = \{\pi_3^A, \pi_3^B, \pi_1^C, \pi_4^C\}$
5	$\Pi_b^5 = \{\pi_3^A, \pi_3^B, \pi_2^C, \pi_3^C\}$
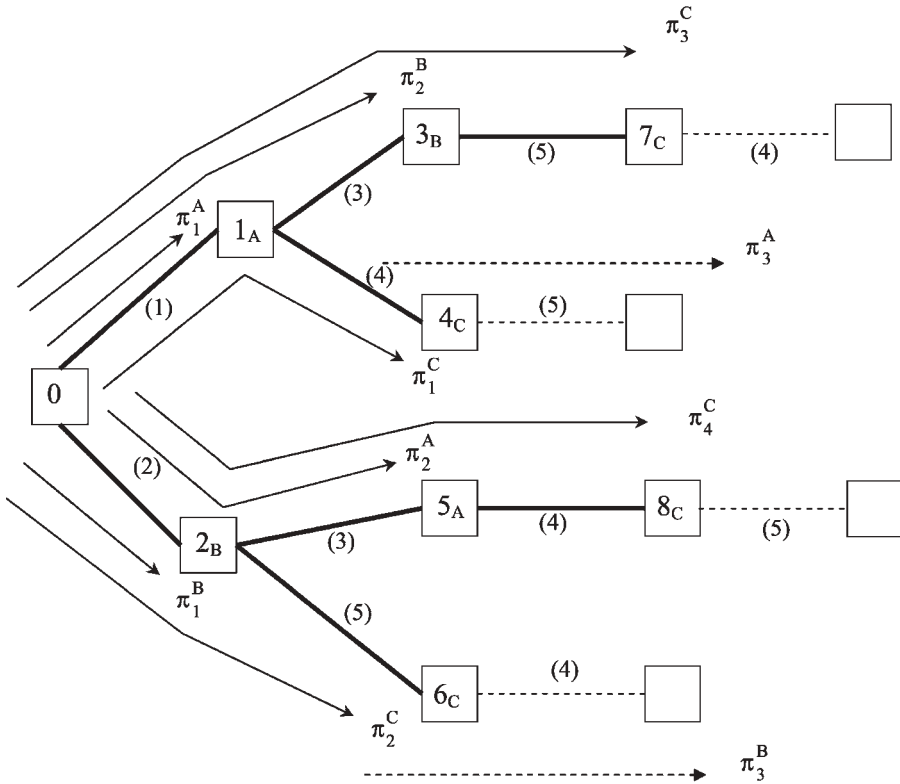
FIGURE 12.5   Mother tree for the example of Fig. 12.4

Every node N_L in the mother tree corresponds to a possible path for the related bus L. In this case, according to Table 12.9, the four-bus system will be translated into a mother tree with 8 nodes, assuming paths π_3^A and π_3^B are discarded. For example, bus A is associated to nodes I_A and 5_A in the mother tree, corresponding to paths π_1^A and π_2^A (see Table 12.9).

When building the mother tree the following rules are taken into account:

(A) Before a new node N_L is added to the mother tree, two conditions are checked:

  (1) A node N_L, associated to the same bus L, is not located upstream in the tree. Returning to the example, a new node, say 9_A, is not appended to node 7_C through branch (4) because bus A already appears upstream in the tree (node 1_A). These dead ends are shown in Figure 12.5 by dashed lines.

  (2) The impedance of the total path from the substation to the new node N_L does not exceed a threshold times the impedance of the electrically shortest path for bus L. In Figure 12.5, paths π_3^A and

π_3^B of Table 12.9 are not considered for this reason. These cases are represented in Figure 12.5 by dashed arrows.

(B) The mother tree is only swept two times, first downstream and then upstream. During the downstream sweep, both the mother tree and associated paths are obtained simultaneously. When the two rules described above preclude the addition of new nodes, the resulting mother tree is swept upstream in order to define the inequality constraints among paths, represented by (2), as well as the minimum and maximum power flows through every branch in the system.

For the radiality and electrical constraints to be easily expressed in the standard matrix-vector form, sets Π_n^i and Π_b^j are stored as sparse linked lists.

12.5.2 Simplified Mathematical Model

The mathematical model of DNRC can be written as below:

$$\text{Min } f = \sum_{l=1}^{NL} R_l \left(\frac{P_l^2 + Q_l^2}{V_l^2} \right) \quad l \in NL \tag{12.18}$$

s.t.

$$\sum_{j \to i} P_{\text{G}j} + \sum_{l \to i} P_l + \sum_{k \to i} P_{\text{D}k} = 0 \tag{12.19}$$

$$\sum_{j \to i} Q_{\text{G}j} + \sum_{l \to i} Q_l + \sum_{k \to i} Q_{\text{D}k} = 0 \tag{12.20}$$

$$P_l^2 + Q_l^2 \leq S_{l\max}^2 \tag{12.21}$$

$$\Delta V_l \leq \Delta V_{l\max} \tag{12.22}$$

$$\sum_{p \in \Pi_n^i} K_p^i = 1, \quad \forall \text{ node } i \tag{12.23}$$

$$K_p^i \leq K_l^i, \quad \forall \pi_l^i \subset \pi_p^i \tag{12.24}$$

If voltage magnitudes are assumed to be 1.0 p.u. the objective function becomes

$$\text{Min } f = \sum_{l=1}^{NL} R_l \left(P_l^2 + Q_l^2 \right) \quad l \in NL \tag{12.25}$$

The power flow P_l and Q_l comprise the total real and reactive load demanded downstream from node j plus the real and reactive losses of the respective branches. For simplification, the latter components of P_l and Q_l are omitted

as system losses are much smaller than power loads. Therefore, the real and reactive power flows equal to the sum of real and reactive power loads located downstream from node, that is,

$$P_l = \sum_{p \in \Pi_{NL}^l} K_p^i P_{Di} \tag{12.26}$$

$$Q_l = \sum_{p \in \Pi_{NL}^l} K_p^i Q_{Di} \tag{12.27}$$

These are equivalent to the node real and reactive balance equations without considering the branch loss.

Substituting them into the objective function, we get

$$\text{Min } f = \sum_{l=1}^{NL} R_l \left[\left(\sum_{p \in \Pi_{NL}^l} K_p^i P_{Di} \right)^2 + \left(\sum_{p \in \Pi_{NL}^l} K_p^i Q_{Di} \right)^2 \right] \quad l \in NL \tag{12.28}$$

The network connectivity is incorporated through the binary variables K_p^i. Since the simplification above, the computed power losses will be smaller than the actual losses.

Substituting equations (12.26) and (12.27) into equation (12.21), we get

$$\left(\sum_{p \in \Pi_{NL}^l} K_p^i P_{Di} \right)^2 + \left(\sum_{p \in \Pi_{NL}^l} K_p^i Q_{Di} \right)^2 \le S_{l\max}^2 \quad l \in NL \tag{12.29}$$

According to [5, 20], the voltage drop without considering power losses can be expressed as

$$V_i^2 - V_l^2 \approx 2(R_l P_l + X_l Q_l) \tag{12.30}$$

Then the total quadratic voltage drop through a path π_p^i reaching bus i is approximated by

$$V_s^2 - V_i^2 \approx 2 \sum_{l \in \Pi_p^i} (R_l P_l + X_l Q_l) \tag{12.31}$$

The voltage constraint can be expressed as

$$2 \sum_{l \in \Pi_p^i} \left[R_l \left(\sum_{p \in \Pi_{NL}^l} K_p^i P_{Di} \right) + X_l \left(\sum_{p \in \Pi_{NL}^l} K_p^i Q_{Di} \right) \right] \le \Delta V_{\max} \tag{12.32}$$

12.5.3 Mixed-Integer Linear Model

In Section 12.5.2, the DNRC model is simplified, in which the branch losses are ignored and bus complex voltages are removed from the model. Thus load

flow calculation is not required during the solution process. However, the resulting optimization problem is still quadratic in the binary variables K_p^i (path statuses). A piecewise linear function is used to replace approximately the quadratic branch power flows. In this way, the DNRC model is converted into a standard mixed-integer linear model:

$$\text{Min } f = \sum_{l=1}^{NL} R_l \left[\left(\sum_{t \in tp} C_p^{p(t)} \sum_{p \in \Pi_{NL}^l} K_p^i P_{Di} \right) + \left(\sum_{t \in tq} C_p^{q(t)} \sum_{p \in \Pi_{NL}^l} K_p^i Q_{Di} \right) \right] \quad l \in NL \quad (12.33)$$

such that

$$P_l^{(t)} = \sum_{p \in \Pi_{NL}^l} K_p^i P_{Di}, \quad t \in tp \tag{12.34}$$

$$Q_l^{(t)} = \sum_{p \in \Pi_{NL}^l} K_p^i Q_{Di}, \quad t \in tp \tag{12.35}$$

$$\left(\sum_{t \in tp} C_p^{p(t)} \sum_{p \in \Pi_{NL}^l} K_p^i P_{Di} \right) + \left(\sum_{t \in tq} C_p^{q(t)} \sum_{p \in \Pi_{NL}^l} K_p^i Q_{Di} \right) \leq S_{l\max}^2 \tag{12.36}$$

$$\begin{cases} 0 \leq P_l^{(1)} \leq \bar{P}_l^{(1)} \\ 0 \leq P_l^{(2)} \leq \left(\bar{P}_l^{(2)} - \bar{P}_l^{(1)} \right) \\ \quad \cdots\cdots \\ 0 \leq P_l^{(tp)} \leq \left(\bar{P}_l^{(tp)} - \bar{P}_l^{(tp-1)} \right) \end{cases} \quad l \in NL \tag{12.37}$$

$$\begin{cases} 0 \leq Q_l^{(1)} \leq \bar{Q}_l^{(1)} \\ 0 \leq Q_l^{(2)} \leq \left(\bar{Q}_l^{(2)} - \bar{Q}_l^{(1)} \right) \\ \quad \cdots\cdots \\ 0 \leq Q_l^{(tq)} \leq \left(\bar{Q}_l^{(tq)} - \bar{Q}_l^{(tq-1)} \right) \end{cases} \quad l \in NL \tag{12.38}$$

To reduce the problem size and to speed up the calculation, some additional features are considered.

- As noted above, those paths whose electrical length exceeds a certain threshold times the shortest distance to the substation for that node are discarded.
- If the set of paths Π_b^j associated with branch j comprises a single element π_l^i; then the respective flow P_j is constant and equal to P_{Li}, provided $W_l^i = 1$.
- If the set of paths Π_n^j associated with bus i comprises a single element π_l^i, then $W_l^i = 1$.

After the final reconfiguration is obtained by solving the mixed-integer linear model of DNRC, the exact losses as well as node voltage and branch flow may be computed by solving the radial load flow.

12.6   APPLICATION OF GA TO DNRC

12.6.1   Introduction

Chapter 4 discusses the application of genetic algorithms (GAs) to economic dispatch problem. GAs are considered when conventional techniques have not achieved the desired speed, accuracy, or efficiency [24–26].

The basic steps of general GA are as follows.

(1) Initialization: For the given control variables X, randomly select a variable population $\{X_0^1, X_0^2, \ldots, X_0^p\}$, where each individual X_0^i is represented by a binary code string. Each string consists of some binary codes, and each code is either 0 or 1. Then each individual corresponds to a fitness $f(X_0^i)$, and the population corresponds to a set of fitness $\{f(X_0^1), f(X_0^2), \ldots, f(X_0^p)\}$. Let generation be $k = 0$, go to next step.

(2) Selection: Select a pair of individuals from the population as a parent. Generally, the individual with bigger fitness has a bigger probability to be selected.

(3) Crossover: Crossover is an important operation in genetic algorithm. The purpose of the crossover is to exchange information fully among individuals. There are many crossover methods such as one-point crossover and multipoints crossover.

   (a) One-point crossover. Select randomly a truncation point in the parent strings and divide them into two parts. Then exchange the tail parts of the parent strings. An example of one-point crossover is below.

Parent generation   Child generation

100110 ⋮ 01101   One-point crossover   100110 ⋮ 10000
111011 ⋮ 10000   ⟶   111011 ⋮ 01101
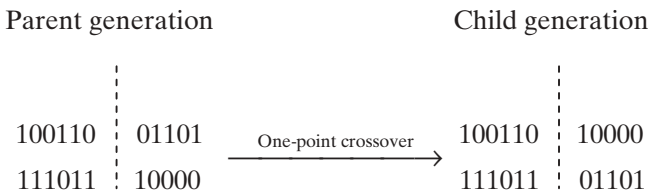
   (b) Multipoints crossover. Select randomly several truncation points in the parent strings and divide them into several parts. Then exchange some parts of the parent strings. Examples of two and three points crossovers are below:

Parent generation   Child generation

100 ┊ 11001 ┊ 101   →Two-points crossover→   100 ┊ 01110 ┊ 101
111 ┊ 01110 ┊ 000   111 ┊ 11001 ┊ 000

Parent generation   Child generation

100 ┊ 110 ┊ 01 ┊ 101   →Three-points crossover→   100 ┊ 011 ┊ 01 ┊ 000
111 ┊ 011 ┊ 10 ┊ 000   111 ┊ 110 ┊ 10 ┊ 101
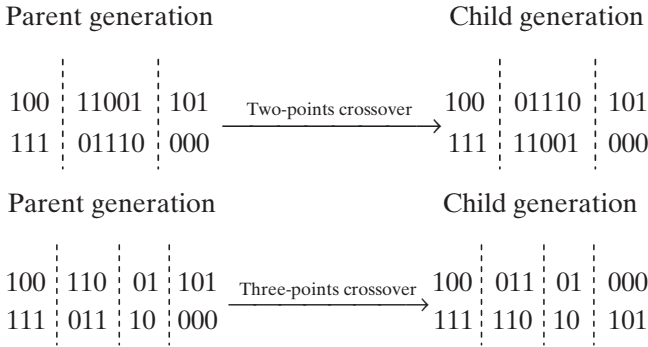
(4) Mutation: Mutation is another important operation in genetic algorithm. The good mutation will be kept, and the bad mutation will be discarded. Generally, the individual with smaller fitness has a bigger mutation probability. Similar to crossover, there are one-point mutation and multipoints mutation.

   (a) One-point mutation. Select randomly a binary code in the parent string and reverse the value of the binary code. An example of one point mutation is below:

   Parent generation   Child generation

   1101000001   →One-point mutation→   1101001001
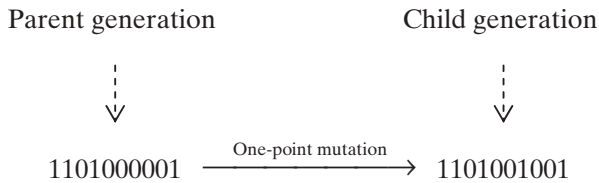
   (b) Multipoints mutation. Select randomly several truncation points in the parent strings and divide them into several parts. Then reverse the value of the binary code in some parts. Examples of two- and three-points mutations are below:

   Parent generation   Child generation

   111 ┊ 01110 ┊ 000   →Two-points mutation→   111 ┊ 10001 ┊ 000

   Parent generation   Child generation

   111 ┊ 01 ┊ 110 ┊ 000   →Three-points mutation→   111 ┊ 10 ┊ 110 ┊ 111
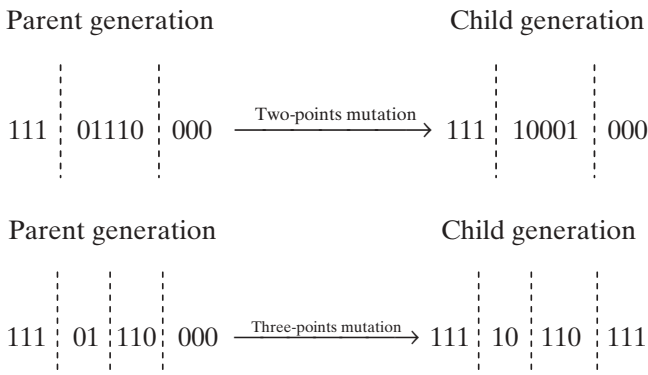
(5) Through steps (2)–(4), a new generation population is produced. Replace the parent generation with the new population and discard some bad individuals. In this way, a new parent population is formed. The calculation will be stopped if the convergence condition is satisfied. Otherwise, go back to step (2).

12.6.2 Refined GA Approach to DNRC Problem

GAs has shown to be an effective and useful approach for the DNRC problem [1, 18]. Some refinements of the approach are described in this section.

12.6.2.1 Genetic String In the early application of GA to DNRC, the string structure is expressed by "Arc No.(i)" and "SW. No.(i)" for each switch i. "Arc No.(i)" identifies the arc (branch) number that contains the ith open switch, and "SW. No.(i)" identifies the switch that is normally open on Arc No.(i). For large distribution networks, it is not efficient to represent every arc in the string, since its length will be very long. In fact, the number of open switch positions is identical to keep the system radial once the topology of the distribution networks is fixed, even if the open switch positions are changed. Therefore, to memorize the radial configuration, it is enough to number only the open switch positions. Figure 12.6 shows a simple distribution network with 5 switches that are normally open.

(a)   (b)
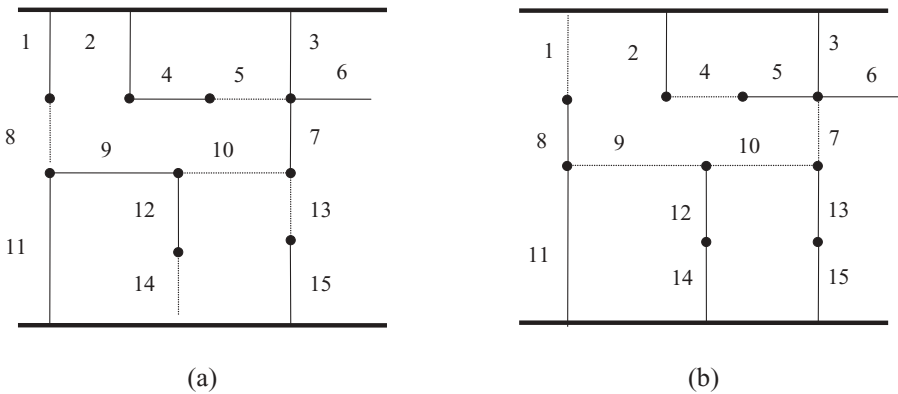
Source transformer busbars   ▬

Closed switches   ─────

Open switches   ┄┄┄┄┄

Sink nodes (load nodes)   ●

FIGURE 12.6 A simple distribution network

In Figure 12.6 (a), positions of 5 initially open switches 5, 8, 10, 13, and 14 determine a radial topology. In Figure 12.6 (b), positions of 5 initially open switches 1, 4, 7, 9, and 10 determine another radial topology. Therefore, to represent a network topology, only positions of the open switches in the distribution network need to be known. Suppose the number of normally open switches is N_o; the length of a genetic string depends on the number of open switches N_o. Genetic strings for Figure 12.6 (a) and (b) are represented as follows, respectively.

0 1 0 1	1 0 0 0	1 0 1 0	1 1 0 1	1 1 1 0

switch 5;   switch 8;   switch 10;   switch 13;   switch 14

Genetic string for Figure 12.6 (a)

0 0 0 1	0 1 0 0	0 1 1 1	1 0 0 1	1 0 1 0

switch1;   switch 4;   switch 7;   switch 9;   switch 10

Genetic string for Figure 12.6 (b)

12.6.2.2 *Fitness Function*

GAs are essentially unconstrained search procedures within a given represented space. Therefore, it is very important to construct an accurate fitness function as its value is the only information available to guide the search. In this section, the fitness function is formed by combining the object function and the penalty function, i.e.,

$$\text{Max } f = 1/L \tag{12.39}$$

where

$$
\begin{aligned}
L = & \Sigma_i |I_i|^2 k_i R_i + \beta_1 \max\left\{0, (|I_i| - I_{i\max})^2\right\} \\
& + \beta_2 \max\left\{0, (V_{i\min} - V_i)^2\right\} \\
& + \beta_3 \max\left\{0, (V_i - V_{i\max})^2\right\}
\end{aligned} \tag{12.40}
$$

where β_i ($i = 1, 2, 3$) is a large constant.

Suppose m is the population size; the values of the maximum fitness, the minimum fitness, sum of fitness, and average fitness of a generation are calculated as follows.

$$f_{\max} = \{f_i / f_i \geq f_j \; \forall \; f_j, j = 1, \ldots\ldots, m\} \tag{12.41}$$

$$f_{\min} = \{f_i / f_i \leq f_j \; \forall \; f_j, j = 1, \ldots\ldots, m\} \tag{12.42}$$

$$f_\Sigma = \Sigma_i f_i, \quad i = 1, \ldots\ldots, m \tag{12.43}$$

$$f_{av} = f_\Sigma / m \tag{12.44}$$

The strings are sorted according to their fitness and are then ranked accordingly.

12.6.2.3 Selection To obtain and maintain good performance of the fittest individuals, it is important to keep the selection competitive enough. There is no doubt that the fittest individuals have higher chances to be selected. In this chapter, the "roulette wheel selection" scheme is used, in which each string occupies an area of the wheel that is equal to the string's share of the total fitness, i.e., f_i/f_Σ.

12.6.2.4 Crossover and Mutation Crossover takes random pairs from the mating pool and produces two new strings, each being made of one part of the parent string. Mutation provides a way to introduce new information into the knowledge base. With this operator, individual genetic representations are changed according to some probabilistic rules. In general, the GA mutation probability is fixed throughout the whole search process. However, in practical application of DNRC, a small fixed mutation probability can only result in a premature convergence. Here, an adaptive mutation process is used to change the mutation probability, i.e.,

$$p(k+1) = \begin{cases} p(k) - p_{step}, & if\ f_{min}(k) \text{unchanged} \\ p(k) - p_{step}, & if\ f_{min}(k) \text{decreased} \\ p_{final}, & if\ p(k) - p_{step} < p_{final} \end{cases} \tag{12.45}$$

$$p(0) = p_{init} = 1.0 \tag{12.46}$$

$$p_{step} = 0.001 \tag{12.47}$$

$$p_{final} = 0.05 \tag{12.48}$$

where k is the generation number and p is the mutation probability.

The mutation scale will decrease as the process continues. The minimum mutation probability in this study is given as 0.05. This adaptive mutation not only prevents premature convergence, but also leads to a smooth convergence.

12.6.3 Numerical Examples

The modified GA approach for distribution network reconfiguration is tested on the 16-bus and 33-bus distribution systems. System data and parameters of the 16-bus system are listed in Table 12.11. The 16-bus test system, which is shown in Figure 12.7, contains 3 source transformers and 13 load nodes. The

Table 12.11 System data and parameters for 16-bus distribution network

Line No.	Node i	Node j	Resistance R (Ω)	Reactance X (Ω)	Receiving Node j		Receiving Node j Voltage (p.u.)
					P (MW)	Q (MVAr)	
1	1	4	0.0750	0.1000	2.0	1.6	0.9907 $\angle$ −.3968
3	4	5	0.0800	0.1100	3.0	0.4	0.9878 $\angle$ −.5443
2	4	6	0.0900	0.1800	2.0	−0.4	0.9860 $\angle$ −.6972
5	6	7	0.0400	0.0400	1.5	1.2	0.9849 $\angle$ −.7043
7	2	8	0.1100	0.1100	4.0	2.7	0.9791 $\angle$ −.7635
8	8	9	0.0800	0.1100	5.0	1.8	0.9711 $\angle$ −1.452
9	8	10	0.1100	0.1100	1.0	0.9	0.9769 $\angle$ −.7701
6	9	11	0.1100	0.1100	0.6	−0.5	0.9710 $\angle$ −1.526
10	9	12	0.0800	0.1100	4.5	−1.7	0.9693 $\angle$ −1.837
15	3	13	0.1100	0.1100	1.0	0.9	0.9944 $\angle$ −.3293
14	13	14	0.0900	0.1200	1.0	−1.1	0.9948 $\angle$ −.4562
16	13	15	0.0800	0.1100	1.0	0.9	0.9918 $\angle$ −.5228
12	15	16	0.0400	0.0400	2.1	−0.8	0.9913 $\angle$ −.5904
4	5	11	0.0400	0.0400			
13	10	14	0.0400	0.0400			
11	7	16	0.0900	0.1200			
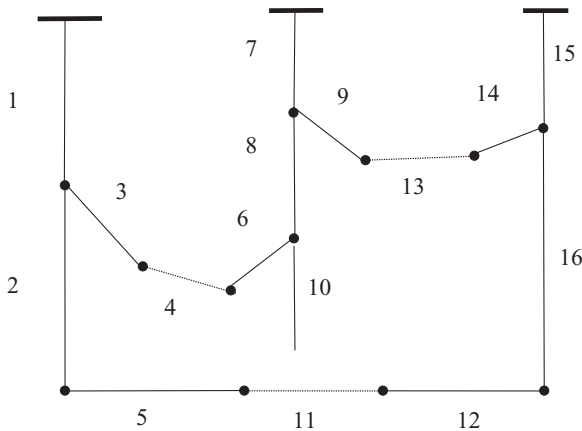
FIGURE 12.7 A 16-bus distribution system

3 initially open switches are "4," "11," and "13." The total system load is 23.7 MW, while the initial system power loss is 0.5114 MW. The 33-bus test system consists of 1 source transformer and 32 load points. The 5 initially open switches are "33," "34," "35," "36," and "37." The total system load is 3.715 MW, while the initial system power loss is 0.202674 MW. The system base is $V = 12.66$ kV and $S = 10$ MVA.

Table 12.12   DNRC results for 16-bus test system

Radial network	Initial network	Refined GA method
Open Switches	Switch 4	Switch 6
	Switch 11	Switch 9
	Switch 13	Switch 11
Power loss (MW)	0.5114	0.4661

Table 12.13   Comparison of DNRC results for 33-bus test system

Radial network	Initial network	Method in ref. [8]	Refined GA method
Open switches	Switch 33	Switch 7	Switch 7
	Switch 34	Switch 10	Switch 9
	Switch 35	Switch 14	Switch 14
	Switch 36	Switch 33	Switch 32
	Switch 37	Switch 37	Switch 33
Power loss (MW)	0.202674	0.141541	0.139532

Results on the two systems are listed in Tables 12.12 and 12.13. By comparing the results with reference [8], it can be seen that global optima have been found by the refined genetic algorithm.

12.7   MULTIOBJECTIVE EVOLUTION PROGRAMMING TO DNRC

Reducing the real power loss is the primary aim of network reconfiguration. Thus power loss is generally selected as the objective function of DNRC. If we handle some power and voltage constraints as objective functions, the DNRC will become a constrained multiobjective optimization problem.

12.7.1   Multiobjective Optimization Model

Three objective functions are considered here, they are minimization of power losses, minimizing the deviation of node voltage, and maximizing the branch capacity margin, which are expressed as follows.

(1) Minimization of power losses

$$\text{Min } f_1 = \sum_{l=1}^{NL} k_l R_l \left(\frac{P_l^2 + Q_l^2}{V_l^2} \right) \quad l \in NL \tag{12.49}$$

(2) Minimizing the deviation of node voltages

$$\text{Min } f_2 = \max |V_i - V_{i\text{rate}}| \quad i \in N \tag{12.50}$$

where

V_{irate}: The rated voltage at node i

f_2: The maximal deviation of node voltage in the network

Obviously, lower f_2 values indicate a higher-quality voltage profile and better security of the considered network configuration.

(3) Branch capacity margin

$$\text{Min } f_3 = 1 - \min_l \left[\frac{S_{l\max} - S_l}{S_{l\max}} \right] \quad l \in NL \tag{12.51}$$

where

$S_{l\max}$: The megavolt amperes (MVA) capacity of the branch l

S_l: The actual megavolt amperes (MVA) loading of the branch l

f_3: The relative value of the margin between the capacity and the actual megavolt amperes (MVA) loading of the branch

Obviously, a lower f_3 indicates a greater MVA reserve in the branches, implying that the considered network configuration is more secure.

Since the node voltages and branch flows are reflected in the objective functions, the corresponding constraints are omitted. The remaining constraints will be KCL and KVL laws, as well as network topological constraints equation (12.6).

12.7.2 EP-Based Multiobjective Optimization Approach

12.7.2.1 Multiobjective Optimization Algorithm [28–29] The above-mentioned multiobjective DNRC problem can be expressed in the following form:

$$\text{Min } f_l(x), \quad i \in N_o \tag{12.52}$$

subject to

$$g(x) = 0 \tag{12.53}$$

$$h(x) \leq 0 \tag{12.54}$$

where N_o is number of objective functions, and x is the decision vector.

These three objective functions are competing with each other; no point X simultaneously minimizes all of the objective functions. This multiobjective optimization problem can be solved by using the concept of noninferiority.

Definition The **feasible region of the constraints**, Ω, in the decision vector space X is the set of all decision vectors x that satisfy the constraints, such that

$$\Omega = \{x | g(x) = 0, h \leq (x) = 0\} \qquad (12.55)$$

The **feasible region of objective functions**, ψ, in the objective function space F is the image of f of the feasible region Ω in the decision vector space

$$\Psi = \{f | f = f(x), x \in \Omega\} \qquad (12.56)$$

A point $\hat{x} \in \Omega$ is a **local noninferior point** if and only if for some neighborhood of $\hat{x}$, there does not exist a Δx such that

$$\hat{x} + \Delta x \in \Omega \qquad (12.57)$$

and

$$f_i(x + \Delta x) \leq f_i(\hat{x}), \quad i = 1, 2, \ldots, N_o \qquad (12.58)$$

$$f_j(x + \Delta x) < f_j(\hat{x}), \quad \text{for some } j \in N_o \qquad (12.59)$$

A point $\hat{x} \in \Omega$ is a **global noninferior point** if and only if no other point $x \in \Omega$ exists there such that

$$f_i(x) \leq f_i(\hat{x}), \quad i = 1, 2, \ldots, N_o \qquad (12.60)$$

$$f_j(x) < f_j(\hat{x}), \quad \text{for some } j \in N_o \qquad (12.61)$$

Thus a global noninferior solution of the multiobjective problem is one in which any improvement of one objective function can be achieved only at the expense of at least one of the other objectives. Typically, an infinite number of noninferior points exist in a given multiobjective problem. A noninferior point is the same as the intuitive notion of an optimum trade-off solution, since a design is noninferior if improving an objective requires degradation in at least one of the other objectives. Clearly, if a decision-maker were able, he or she would not want to choose an inferior design. Thus the decision-maker attempts to generate noninferior solutions to a multiobjective problem when trying to obtain a final design.

The decision-maker combines subjective judgment with quantitative analysis, since the noninferior optimal solutions generally consist of an infinite number of points. This section introduces the interactive fuzzy satisfying algorithm based on evolution programming (EP) to determine the optimal noninferior solution for the decision-maker.

12.7.2.2 *EP Algorithm with Fuzzy Objective Functions*

12.7.2.2.1 Fuzzy Objective Function   A fuzzy set is typically represented by a membership function. A higher membership function implies greater satisfaction with the solution. One of the typical membership functions is the triangle, which is shown in Figure 12.8.

Here, we use the triangle model for representing fuzzy objective functions. The triangle membership function consists of lower and upper boundaries, together with a strictly monotonically decreasing membership function, which can be expressed as below.

$$\mu_{f_i(\overline{x})} = \begin{cases} 1, & \text{if } f_i \leq f_{i\min} \\ \dfrac{f_{i\max} - f_i}{f_{i\max} - f_{i\min}} & \text{if } f_{i\min} \leq f_i \leq f_{i\max} \\ 0, & \text{if } f_i \geq f_{i\max} \end{cases} \tag{12.62}$$

12.7.2.2.2 Evolution Programming [21]   The state variable $\overline{X}$ represents a chromosome of which each gene represents an opened switch to the network reconfiguration problem. The fitness function of $\overline{X}$ can be defined as

$$C(\overline{X}) = \frac{1}{1 + F(\overline{X})} \tag{12.63}$$

where

$$F(\overline{X}) = \underset{x \in \Omega}{\text{Min}} \left\{ \underset{i=1,2,\ldots,N_O}{\text{Max}} \left[\overline{\mu_{f_i}} - \mu_{f_i(\overline{X})} \right] \right\} \tag{12.64}$$

where

$\overline{\mu_{f_i}}$: The expected values of the objective function
$\mu_{f_i(\overline{x})}$: The actual values of the objective function
$C(\overline{X})$: The fitness function
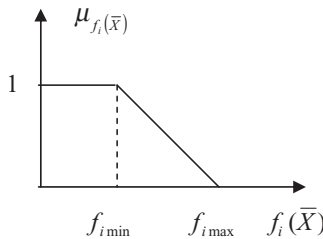
FIGURE 12.8 Fuzzy membership model

The function $F(\bar{X})$ is to minimize the objective with a maximum distance away from its expected value among the multiple objectives function. For a given μ_{f_i}, the solution reaches the optimum as the fitness value increases.

The steps of EP are detailed as follows.

Step (1): Input parameters.

Input the parameters of EP, such as the length of the individual and the population size N_P.

Step (2): Initialization.

The initial population is determined by selecting P_j from the set of the original switches and their derivatives according to the mutation rules. P_j is an individual, $j = 1, 2, \ldots, N_P$, with N_S dimensions, where N_S is the total number of switches.

Step (3): Scoring

Calculate the fitness value of an individual by equations (12.63) and (12.64).

Step (4): Mutation

In the network reconfiguration problem, the radial structure must be retained for each new structure and power must be supplied to each loading demand. Consequently, each P_j is mutated and assigned to P_{j+N_P}. The number of offspring n_j for each individual P_j is given by

$$n_j = G\left(N_P \times \frac{C_j}{\sum\limits_{j=1}^{N} C_j} \right) \tag{12.65}$$

where $G(x)$ is a function that rounds the element of x to the nearest integer number. More offspring are generated from the individual with a greater fitness. A combined population is formed from the old generation, and the new generation is mutated from the old generation.

Step (5): Competition.

Each individual P_j in the combined population has to compete with some other individuals to have the opportunity to be transcribed to the next generation. All individuals of the combined population are ranked in descending order of their corresponding fitness values. Then the first N_P individuals are transcribed to the next generation.

Step (6): Stop criterion.

Convergence is achieved when either the number of generations reaches the maximum number of generations or the sampled mean fitness function values do not change noticeably throughout several consecutive generations. The process will stop if one of these conditions is met; otherwise, it returns to the mutation step.

12.7.2.3 Optimization Approach For using the fuzzy objective function, the values of expected membership functions will be selected to generate a candidate solution of the multiobjective problem. The expected value is a real number in $[0, 1]$ and represents the importance of each objective function. The above-mentioned min-max problem is solved to generate the optimal solution. The optimization technique can now be described as follows.

Step (1): Input the data and set the interactive pointer $p = 0$

Step (2): Determine the upper and lower bounds for every objective function $f_{i\max}$ and $f_{i\min}$, as well as fuzzy membership $\mu_{f_i(X)}$.

Step (3): Set the initial expected value of each objective function $\overline{\mu_{f_i(0)}}$ for $i = 1, 2, \ldots, N_o$

Step (4): Apply EP to solve the min-max problem (64).

Step (5): Calculate the values of $\overline{X}, f_i(\overline{X})$, and $\mu_{f_i(\overline{X})}$. Go to the next step if they are satisfactory. Otherwise, set the interactive pointer $p = p + 1$ and choose a new expected value $\overline{\mu_{f_i(p)}}, i = 1, 2, \ldots, N_o$. Then go to step (4).

Step (6): Output the most satisfactory feasible solution $X^*, f_i(X^*)$, and $\mu_{f_i(X^*)}$

12.8 GENETIC ALGORITHM BASED ON MATROID THEORY

Section 12.5 analyzed the application of GAs to solve the DNRC problem in equations (12.1)–(12.6). To accelerate the GA convergence, a GA based on network matroid theory [30] is used to solve the same DNRC problem in this section.

12.8.1 Network Topology Coding Method

The distribution network topology coding method is fundamental for the GA convergence. On the one hand, a complex strategy could increase considerably the convergence time. On the other hand, a simple strategy does not allow an effective exploration of the research field. Various coding strategies are detailed in this section, and the GA operator's mechanisms are explained. Finally, their advantages and drawbacks are discussed.

12.8.1.1 Different Topology Coding Strategies The most simple topology representation for the GA is to consider a topology string formed by the binary status (closed/open) of each network branch [31] or at least each network switch. In [18] the arc (a branch or a series of branches) number and the switch position in each branch are considered for the radial topology representation. In [1, 32], only the opened switches positions are stored in the topology string.

Reference [17] proposes an efficient modeling method for distribution network connectivity. The path (a set of branches to the source) is determined
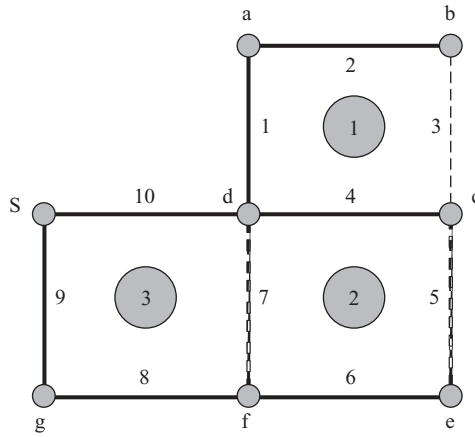
FIGURE 12.9   A simple meshed topology

for each node of the network. For a radial configuration, only a path to the source S is considered for each node. This method is discussed in Section 12.5. For example, in the simple topology in Figure 12.9, paths from each node to the source S are

a: $\pi_1^a = [1, 10], \pi_2^a = [2, 3, 4, 10], \pi_3^a = [7, 8, 9]$

$\pi_4^a = [2, 3, 5, 6, 8, 9], \pi_5^a = [2, 3, 5, 6, 7, 10], \pi_6^a = [2, 3, 4, 7, 8, 9]$

b: $\pi_1^b = [3, 4, 10], \pi_2^b = [2, 1, 10], \pi_3^b = [3, 4, 6, 8, 9]$

$\pi_4^b = [3, 5, 6, 7, 10], \pi_5^b = [2, 1, 7, 8, 9], \pi_6^b = [3, 4, 7, 8, 9]$

g: $\pi_1^g = [8, 7, 10], \pi_2^g = [9], \pi_3^g = [8, 6, 5, 4, 10], \pi_4^g = [8, 6, 5, 3, 2, 1, 10]$

As mentioned in Section 12.5, π_i^j is the path number i between node j and source S.

The general structure of the topology string for the simple topology in Figure 12.9 can be handled like this: For node a, only one of four paths is represented by bit 1, the rest are represented by bit 0. The same procedure is used for the other nodes.

12.8.1.2   The GA Operators   As we discussed above, the GA operators are mutation, selection, and crossover. The crossover is the most important operator of the GA. The traditional crossover process randomly selects two parents (chromosomes) for a gene exchange with a given crossover rate. This operator aims at mixing up genetic information coming from the two parents, to create new individuals.

The coding diagram is very important for the success of the crossover operation. A binary coding method cannot allow a high efficiency of the cross-

over process. Furthermore, **mesh checks** must be performed in order to validate each resulting topology (to detect any loop in the network or any not energized node).

The mutation operator can allow GA to avoid local optima. This operator randomly changes one gene in the string, and is applied with a probability that has been set in the initial phase. As in the crossover process, the topology coding strategy is very important for a fast and effective mutation operation.

12.8.2 GA with Matroid Theory

The reconfiguration problem tries to find out the optimal spanning tree among all the spanning trees of the DN graph for a given objective. In the first part of this section, an interesting property of the graph spanning trees is discussed. In the second part, it is shown that this can be generalized by using some properties proved for the matroid theory. The GA operators are then explained based on this new theoretical approach.

12.8.2.1 The Kruskal Lemma for the Graph Spanning Trees   For the graphs, the spanning trees exchange property has been proved by Kruskal [33]:

Let U and T be two spanning trees of the graph G, let $a \in U, a \notin T$; then there exists $b \in T$, such that $U - a + b$ is also a spanning tree in the graph G.

For the graph represented in Figure 12.9, two spanning trees are drawn in Figure 12.10. Consider $a = 6(a \notin T)$, edge in the U spanning tree. One edge b that replaces $a = 6$ in T in order to form another spanning tree can be found. Edge b can be selected in the loop formed by $T \cup a(=6)$. In Figure 12.10, this loop is formed by branches 4, 5, 6, and 7 (dotted arrow). Only edges 5 and 7 can replace edge 6 in U. Finally, edge 5 is chosen to replace edge 6 in U, and a new spanning tree is obtained (see the resulting tree in Fig. 12.10).

The matroid theory abstracts the important characteristics of matrix theory and graph theory. A matroid is defined by axioms of independent sets [34].

A pair (S, T) is called a matroid if S is a finite set and T is a nonempty collection of subsets of S:

$$\text{if} \quad I \in T \quad \text{and} \quad J \subseteq I, \quad \text{then} \quad J \in T$$

$$\text{if} \quad I, J \in T \quad \text{and} \quad I \leq J, \quad \text{then} \quad I + z \in T \quad \text{for some } z \in J \setminus I$$

The "**base**" concept has to be introduced. For $U \subseteq S$, a subset B of U is called a base of U if B is an inclusionwise maximal independent subset of U [34]. That is, $B \in T$, and there is no $Z \in T$ with $B \subset Z \subseteq U$. A subset of S is called **spanning** if it contains a base like a subset, so bases are just the inclusionwise minimal and independent spanning sets.
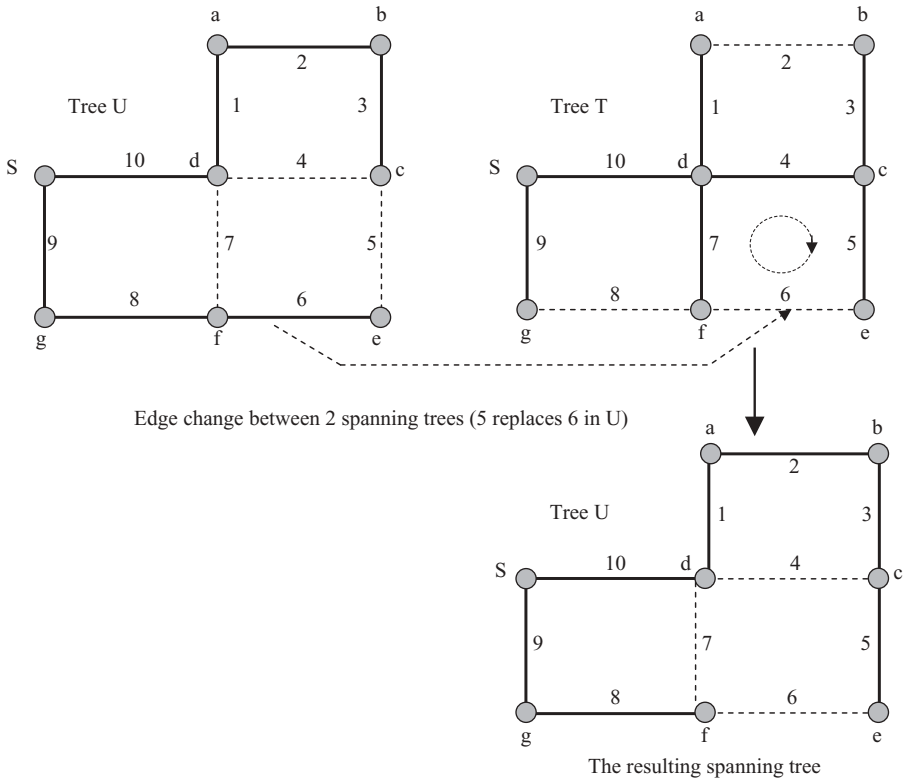
FIGURE 12.10   Branch exchange between 2 spanning trees

One of the matroid classes is the **graphic matroids**. Let $G = (V, E)$ be a graph (with V the vertices set and E the edges set). Let T be the collection of all subsets of E that form a **forest** (a graph in which any 2 vertices are connected by only 1 path); then $M = (E, T)$ is a matroid. The matroid M is called the **cycle matroid** of graph G, denoted $M(G)$. The bases of $M(G)$ are exactly the inclusionwise maximal forests of G. So if graph G is connected, the bases are spanning trees (the forest equivalent for a connected graph or radial configurations for a DN).

To link these theoretical aspects with the problem of spanning trees (radial topologies), the exchange property of bases, given in reference [34], is considered.

Let $M = (S, T)$ be a matroid. Let B_1 and B_2 be bases and let $x \in B_1 \backslash B_2$. Then there exists an element $y \in B_2 \backslash B_1$ such that both $B_1 - x + y$ and $B_2 - y + x$ are bases.

12.8.2.2   *Application to the DN Topology Modeling for GA*   According to graph theory, the group (the set of graph edges, the collection of all span-

ning trees) is a matroid. The spanning tree of a graph is a base. A branch exchange between two spanning trees of the same graph is always possible. New spanning trees for the same graph are obtained.

Furthermore, based on the matroid theory approach, not only one spanning tree is obtained (as shown in Fig. 12.10), but two spanning trees are obtained. Moreover, in order to find easily which edge in a spanning tree can replace another in the other spanning tree, the loop formed by adding the edge the other spanning tree must be determined.

From an electrical point of view, the branch exchange between two spanning trees can be seen as a load transfer between two supply points or between two paths to the same supply point.

The matroid approach allows the use of GA operators without checking the DN graph planarity. Besides, based on this approach, the GA operator success is always guaranteed, without a supplementary mesh check and extra computation time. An example is given in the next subsection.

12.8.2.3   *GA Operators Based on the Matroid Approach*   Examples for the mutation and crossover operators and initial population are given using the matroid approach [30] and applied to the graph illustrated in Figure 12.9.

12.8.2.3.1 Crossover   The crossover operator represents a gene exchange between two chromosomes. One or multiple crossover points can be randomly chosen. For the reconfiguration problem, this operation means one or several edges are exchanged between two spanning trees for a given DN graph.

In Figure 12.11, the first step for a crossover operation is shown between two chromosomes. Each chromosome represents two spanning trees for the graph illustrated in Figure 12.9. Only the open branches are considered here. In the graph theory this is called the **co-tree** concept (the branches missing from the tree). The theoretical approach given in the previous paragraph can be reformulated for the co-trees: A bidirectional branch exchange can be performed in order to obtain new co-trees. A crossover point is randomly chosen between the first and the second gene of the upper co-tree (see Fig. 12.11). In the corresponding co-tree represented by [30], the genes (branches) 7 and 5 have to be exchanged with branches in the second co-tree.

First, branch 7 is replaced. To identify rapidly what branches of the second co-tree could replace branch 7, the loop formed by closing branch 7 in the upper tree is determined (see the dotted arrow in Fig. 12.11). For this purpose, a **depth-first graph search** algorithm was used [34]. This loop is formed by branches 7, 8, 9, and 10. Only branch 8 is in the lower co-tree; it can then replace branch 7. The same procedure is employed in the second step.

12.8.2.3.2 Mutation   The mutation process is shown in Figure 12.12. After random selection of one (or multiple) branches in the chosen co-tree to be mutated, the corresponding loop is determined with a depth-first graph search algorithm (see the interrupted arrow in Fig. 12.12).
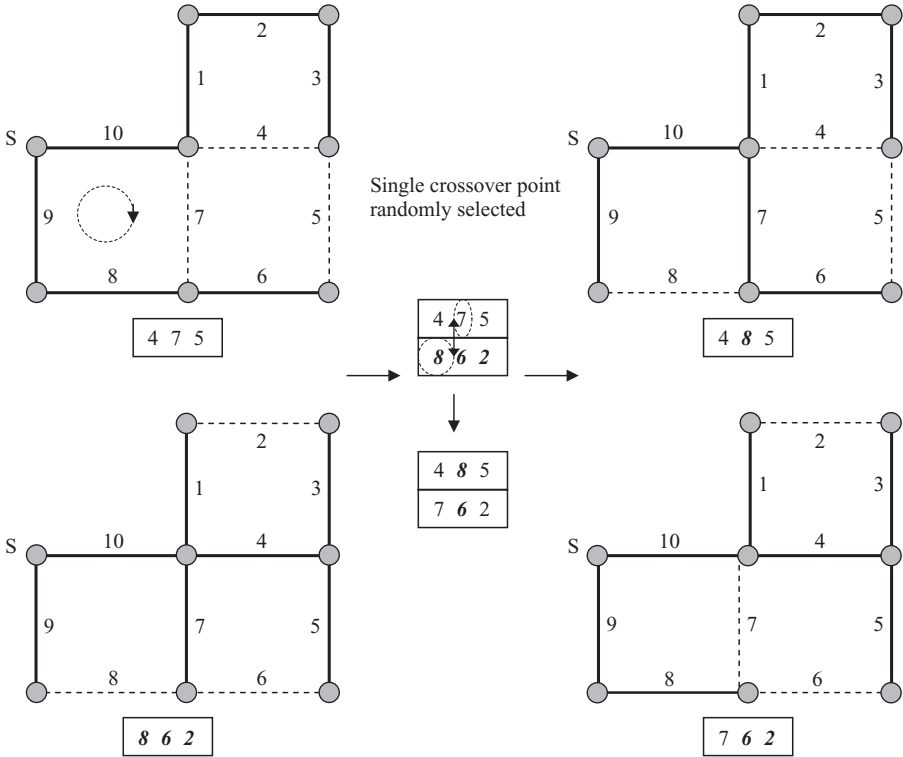
FIGURE 12.11 Crossover process based on the matroid approach (step 1)
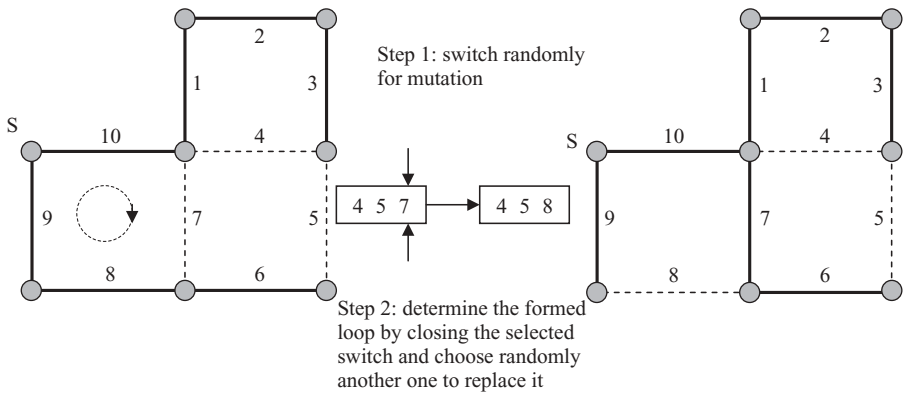
FIGURE 12.12 Mutation process based on the matroid approach

Table 12.14 DNRC results by GA based on matroid theory and comparison for 33-bus test system

Radial network	Initial network	Branch exchange method	Refined GA method	GA based on matroid theory
Open switches	switch 33	switch 7	switch 7	switch 7
	switch 34	switch 10	switch 9	switch 9
	switch 35	switch 14	switch 14	switch 14
	switch 36	switch 33	switch 32	switch 32
	switch 37	switch 37	switch 33	switch 37
Power loss (MW)	0.202674	0.141541	0.139532	0.13642

A new branch is randomly chosen in this loop, in order to replace the first selected. Any other test is not necessary to validate the new radial configuration.

12.8.2.3.3 Initial Population Generation Even if this step is performed once in the GA process, the randomly creation of the initial population can be time consuming. The initial population is generated by using the mutation process shown in Fig. 12.12. An initial feasible chromosome (co-tree) is randomly generated. The mutation process is used to randomly change each initial co-tree branch. The new chromosome feasibility is also implicitly guaranteed. The process is progressively repeated in order to create the initial population.

The same 33-bus system used in Section 12.4 is adopted for the DNRC test. The results and comparison are listed in Table 12.14, where the results based on refined GA and matroid theory-based GA are better than those based on the branch exchange method.

REFERENCES

[1] J.Z. Zhu, "Optimal reconfiguration of electrical distribution network using the refined genetic algorithm," *Electric Power Systems Research*, Vol. 62, No. 1, 2002, pp. 37–42.

[2] J.M. Wojciechowski, "An Approach Formula for Counting Trees in a Graph," *IEEE Trans. Circuit and Systems*, Vol. 32, No. 4, 1985, pp. 382–385.

[3] A. Merlin and H. Back, "Search for minimum-Loss Operating Spanning Tree Configuration in an Urban Power Distribution System," Proc. 5th Power System Computation Conference, Cambridge, 1975 Paper 1.2/6.

[4] C.H. Castro, J.B. Bunchand, and T.M. Topka, "Generalized Algorithms for distribution feeder deployment and sectionalizing", *IEEE Transaction on Power Apparatus and Systems*, Vol. 99. No. 2. March/April 1980, pp. 549–557.

[5] M.E. Baran and F. Wu, "Network Reconfiguration in distribution systems for loss reduction and load balancing." *IEEE Transactions on Power Delivery*, Vol. 4, No. 2, April 1989, pp. 1401–1407.

[6] C.H. Castro and A.L.M. Franca, "Automatic power distribution reconfiguration algorithm including operating constraints." IFAC Symposium on Planning and Operation of Electric Energy Systems, Rio de Janeiro 1985. pp. 181–186.

[7] S. Civanlar, et al., "Distribution Feeder Reconfiguration for Loss Reduction," *IEEE Trans. on Power Delivery*, Vol. 13, No. 3, July, 1988, pp. 1217–1223.

[8] D. Shirmohammadi and H.W. Hong, "Reconfiguration of Electric Distribution Networks for Resistive Line Losses Reduction," *IEEE Trans. PWRD*, Vol. 4, No. 2, 1989, pp. 1492–1498.

[9] S.K. Goswami, "A New Algorithm for the Reconfiguration of Distribution Feeders for Loss Minimization," *IEEE Trans. on Power Delivery*, Vol. 17, No. 3, July, 1992, pp. 1484–1491.

[10] J. Nahman and G. Strbac, "A New Algorithm for Service Restoration in Large-scale Urban Distribution Systems," *Electric Power Systems Research*, Vol. 29, 1994, pp. 181–192.

[11] V. Glamocanin, "Optimal Loss Reduction of Distribution Networks," *IEEE Trans. Power Systems*, Vol. 5, No. 3, 1990, pp. 774–782.

[12] D.W. Ross, J. Patton, A.I. Cohen, and M. Carson, "New Methods for Evaluating Distribution Automation and Control System Benefits," *IEEE Trans. PAS*, Vol. 100, June 1981, pp. 2978–2986.

[13] G. Strbac and J. Nahman, "Reliability Aspects in Structuring of Large Scale Urban Distribution Systems," IEE Conf. on Reliability of Transmission and Distribution Equipment, March 1995, pp. 151–156.

[14] C.C. Liu, S.J. Lee, and S.S. Venkata, "An expert system operational aid for restoration and loss reduction of distribution systems", *IEEE Transaction on Power Systems*, Vol. 3, No. 2, May 1988, pp. 619–626.

[15] T.J. Kendrew and J.A. Marks, "Automated Distribution Comes of Age." *IEEE Computer Applications in Power*, Vol. 2, No. 1, January 1989, pp. 07–10.

[16] H.D. Chiang and R.J. Jumeau, "Optimal Network Reconfiguration in Distribution Systems, Part 1: A New Formulation and A Solution Methodology," *IEEE Trans. Power Delivery*, Vol. 5, No. 4, 1990, pp. 1902–1909.

[17] E.R. Ramos, A.G. Expósito, J.R. Santos, and F.L. Iborra, "Path-Based Distribution Network Modeling: Application to Reconfiguration for Loss Reduction," *IEEE Trans on Power Systems*, Vol. 20, No. 2, May 2005, pp. 556–564.

[18] K. Nara, A. Shiose, M. Kitagawa, and T. Ishihara, "Implementation of Genetic Algorithm for Distribution System Loss Minimum Reconfiguration," *IEEE Trans. Power Systems*, Vol. 7, No. 3, 1992, pp. 1044–1051.

[19] B.A. Souza, H.D.M. Braz, and H.N. Alves, "Genetic Algorithm for Optimal Feeders Configuration" in Proceedings of the Brazilian Symposium of Intelligent Automation—SBAI, Bauru, Brazil, 2003.

[20] B.A. Souza, H.N. Alves, and H.A. Ferreira, "Microgenetic Algorithms and Fuzzy logic applied to the Optimal Placement of Capacitor Banks in Distribution Networks," *IEEE Trans. Power Systems*, Vol. 19, No. 2, 2004, pp. 942–947.

[21] Y.T. Hsiao, "Multiobjective Evolution Programming Method for Feeder Reconfiguration," *IEEE Trans. on Power Systems*, Vol. 19, No. 1, Feb. 2004, pp. 594–599.

[22] J.Z. Zhu, X.F. Xiong, D. Hwang, and A. Sadjadpour, "A comprehensive method for reconfiguration of electrical distribution network," IEEE/PES 2007 General Meeting, Tampa, USA, June 24–28, 2007.

[23] J.Z. Zhu, *Application of Network Flow Techniques to Power Systems*. First Edition, WA: Tianya Press, Technology, Dec. 2005.

[24] J.Z. Zhu, C.S. Chang, G.Y. Xu, and X.F. Xiong, "Optimal Load Frequency Control Using Genetic Algorithm," Proceedings of 1996 International Conference on Electrical Engineering, ICEE'96, Beijing, China, August 12–15, 1996, pp. 1103–1107.

[25] J.H. Holland, Adaptation in Nature and Artificial Systems, The University of Michigan Press, 1975.

[26] D.E. Goldberg, Genetic Algorithms in Search, Optimization and Machine Learning, Addision-Wesley, Reading, 1989.

[27] L.O. Chua, C.A. Desoer, and E.S. Kuh, Linear and Nonlinear Circuits. New York: McGraw-Hill, 1987.

[28] J.B.C. Chen and Z.J. Zhang, "The interactive step trade-off method for multi-objective optimization," *IEEE Trans. Syst., Man, Cybern.*, vol. SMC-20, May/June 1990, pp. 688–694.

[29] J.G. Lin, "Multiple-objective problems: pareto-optimal solutions by method of proper equality constraints," *IEEE Trans. Automat. Contr.*, vol. AC-21, pp. 641–650, Oct. 1976.

[30] B. Enacheanu, B. Raison, R. Caire, O. Devaux, W. Bienia, and N. HadjSaid, "Radial Network Reconfiguration Using Genetic Algorithm Based on the Matroid Theory," *IEEE Trans. on Power Systems*, Vol. 22, 2007.

[31] Y.T. Hsiao and C.Y. Chien, "Implementation of genetic algorithm for distribution systems loss minimum re-configuration," *IEEE Trans. Power Syst.*, Vol. 15, No. 4, Nov. 2000, pp. 1394–1400.

[32] J.Z. Zhu and C.S. Chang, "Refined genetic algorithm for minimum-loss reconfiguration of electrical distribution network", 1998 Intern. Conf. On EMPD, Singapore, 1998.

[33] J.B. Kruskal Jr., "On the Shortest Spanning Subtree of a Graph and the Traveling Salesman Problem," *Proceedings of the American Mathematical Society*, Vol. 7, No. 1, pp. 48–50, Feb. 1956.

[34] A. Schrijver, Combinatorial Optimization—Polyhedra and Efficiency. Springer-Verlag, Berlin, 2003, pp. 651–671.

13

UNCERTAINTY ANALYSIS IN POWER SYSTEMS

In most cases for the first 12 chapters, the variables and parameters have been deterministic. Actual power systems exhibit numerous parameters and phenomena that are either nondeterministic or so complex and dependent on so many diverse process that they may readily be regarded as nondeterministic or uncertain. This chapter comprehensively deals with various uncertain problems in power system operation such as uncertainty load analysis, probabilistic power flow, fuzzy power flow, economic dispatch with uncertainties, fuzzy economic dispatch, hydrothermal system operation with uncertainty, unit commitment with uncertainties, VAR optimization with uncertain reactive load, and probabilistic optimal power flow.

13.1 INTRODUCTION

The planning process of the regulated utilities does not capture the uncertainties in the operation and planning of power systems. In particular, the factors of uncertainty are increasing as the utility industry undergoes restructuring. Because of the restructuring under the pressure of various driving forces, we can foresee that those changes will become even wider in the near future. This is mainly because of the impact of many uncertainty factors and external factors related to the environment of this industry. Therefore, modern power systems are facing many new challenges, owing to environment and market pressures, as well as more uncertainties and/or inaccuracies [1–11].

Environmental pressure implies more loaded networks, market pressure increases competition, while uncertainty and inaccuracy increase the complexity of operation and planning. Consequently, these new challenges have huge, direct impacts on the operation and planning of modern power systems. They also raise some high requirements for modern power systems operation, i.e.,

(a) A stronger expectation from customers for higher reliability and quality of supply owing to the uncertainty factors as well as the increase of the share of electrical power in their overall energy consumption

(b) More electricity exchanges across large geographical areas resulting from a greater cooperation in the electricity market and greater competition in the energy market. There also exist lots of uncertainties in both the electricity market and the energy markets.

(c) Low production fuel cost and low price of electricity are needed in order to achieve the competitive strength in the energy market.

Furthermore, we can guarantee or say only one thing with absolute certainty in the modern electrical power industry: We are living and working with many unknowns [2]. Especially in modern power system operation, several inaccuracies and uncertainties will lead to deviation from operation and planning. These are mainly on the one hand the inaccuracies and uncertainties in input information, which is needed by operation and planning, and on the other hand modeling and solution inaccuracies. Therefore, it is very important to analyze the uncertainty in modern power system operation and to use the available controls to ensure the security and reliability of power systems.

13.2   DEFINITION OF UNCERTAINTY

Generally speaking, there are two kinds of uncertainties in power systems operation and planning [4]:

(1) Uncertainty in a mathematical sense, which means difference between measured, estimated values and true values; includes errors in observation or calculation

(2) Sources of uncertainty, including transmission capacity, generation availability, load requirements, unplanned outages, market rules, fuel price, energy price, market forces, weather and other interruptions, etc.

These uncertainties will affect power systems planning and operation in the following aspects:

• Entry of new energy producing/trading participants
• Increases in regional and intraregional power transactions

- Increasingly sensitive loads
- New types and numbers of generation resources

13.3   UNCERTAINTY LOAD ANALYSIS

Power loads, especially residential loads, are variable and uncertainty data. For example, the variability of the electricity consumption of a single residential customer generally depends on the presence at home of the family members and on the time of use of a few high-power appliances with relatively short duration of use during the day, and is subject to very high uncertainty. Probabilistic analysis and fuzzy theory can be used to analyze the uncertainty load.

13.3.1   Probability Representation of Uncertainty Load

Different probability distribution functions may be selected for the different kinds of uncertainty load. The following probability distribution functions are often used [12].

13.3.1.1   Normal Distribution   The general formula for the probability density function of the normal distribution for uncertain load P_D is

$$f(P_D) = \frac{e^{\frac{(P_D - \mu)^2}{2\sigma^2}}}{\sigma\sqrt{2\pi}} \tag{13.1}$$

$$\begin{array}{l} -\infty \leq P_D \leq \infty \\ \sigma > 0 \end{array} \tag{13.2}$$

where

P_D: The uncertain load

μ: The mean value of the uncertain load. It is also called the location parameter.

σ: The standard deviation of the uncertain load. It is also called the scale parameter.

The shape of the plot of the normal probability density function is shown in Figure 13.1.

13.3.1.2   Lognormal Distribution   Many probability distributions are not a single distribution, but are in fact a family of distributions. This is due to the distribution having one or more shape parameters.

Shape parameters allow a distribution to take on a variety of shapes, depending on the value of the shape parameter. These distributions are
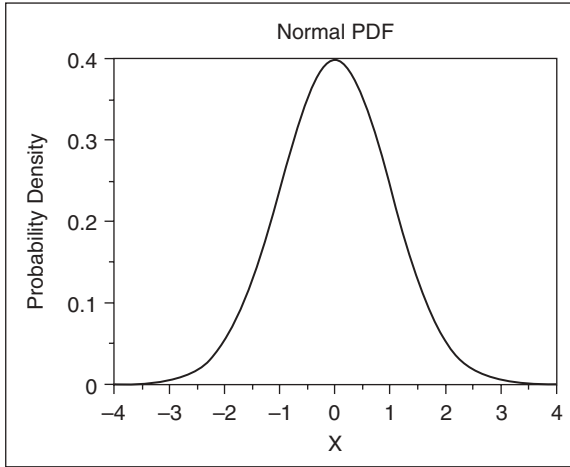
FIGURE 13.1   The plot of the normal probability density function

particularly useful in modeling applications since they are flexible enough to model a variety of uncertainty load data sets. The following is the equation of the lognormal distribution for uncertain load P_D.

$$f(P_D) = \frac{e^{-\frac{(\ln((P_D-\mu)/m))^2}{2a^2}}}{\sigma(P_D-\mu)\sqrt{2\pi}} \tag{13.3}$$

$$\begin{aligned} P_D &\geq \mu \\ \sigma &> 0 \end{aligned} \tag{13.4}$$

where

    m: The scale parameter
    ln: The natural logarithm

Figure 13.2 is an example of the shape for the plot of the lognormal probability density function for four values of σ.

13.3.1.3   *Exponential Distribution*   The formula for the probability density function of the exponential distribution for uncertain load P_D is

$$f(P_D) = \frac{e^{-\frac{P_D-\mu}{b}}}{b} \tag{13.5}$$

$$\begin{aligned} P_D &\geq \mu \\ b &> 0 \end{aligned} \tag{13.6}$$
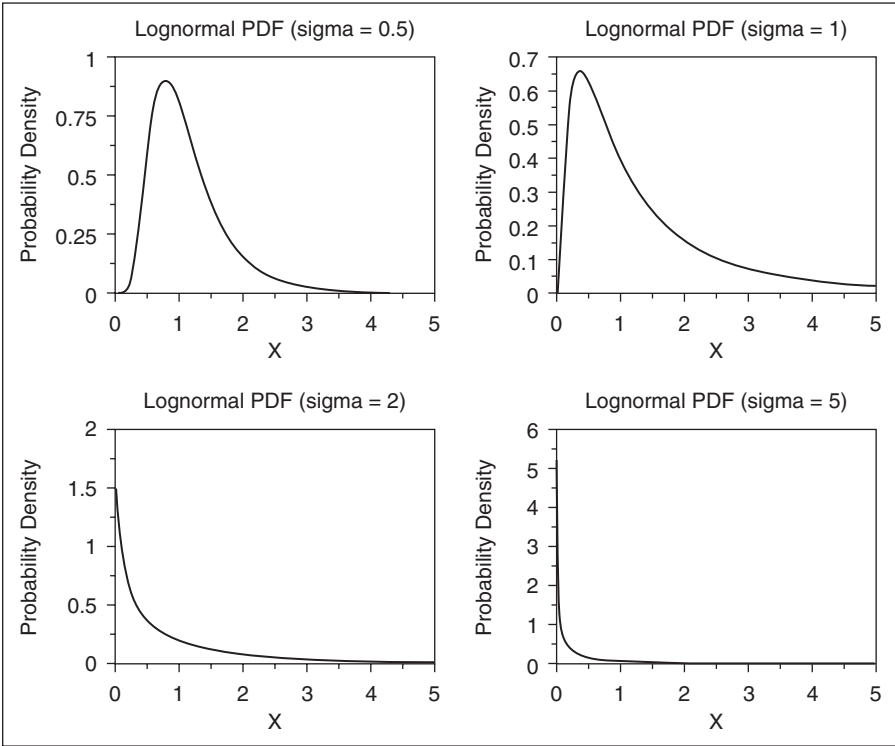
FIGURE 13.2   The plot of the lognormal probability density function

where

  b: The scale parameter

Figure 13.3 is an example of the shape for the plot of the exponential probability density function.

13.3.1.4   Beta Distribution   The general formula for the probability density function of the beta distribution for uncertain load P_D is

$$f(P_D) = \frac{(P_D - d)^{a-1}(c - P_D)^{b-1}}{B(a, b)(c - d)^{a+b-1}} = \frac{\Gamma(a+b)(P_D - d)^{a-1}(c - P_D)^{b-1}}{\Gamma(a)\Gamma(b)(c - d)^{a+b-1}} \quad (13.7)$$

$$d \leq P_D \leq c$$
$$a > 0 \quad\quad\quad\quad (13.8)$$
$$b > 0$$
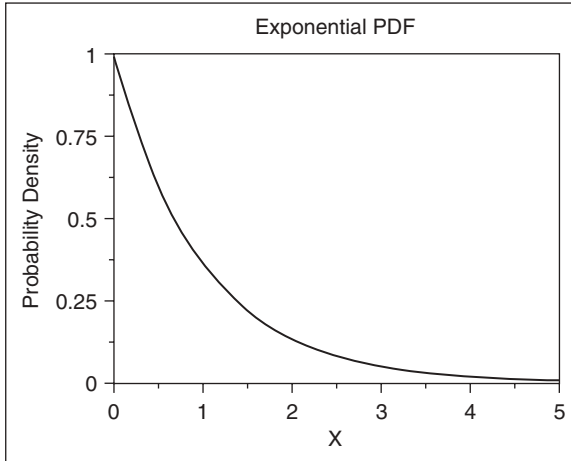
FIGURE 13.3 The plot of the exponential probability density function

where

a, b: The shape parameters
c: The upper bound
d: The lower bound
B(a,b): The beta function

Typically we define the general form of a distribution in terms of location and scale parameters. The beta is different in that we define the general distribution in terms of the lower and upper bounds. However, the location and scale parameters can be defined in terms of the lower and upper limits as follows:

location = *d*
scale = *c* − *d*

Figure 13.4 is an example of the shape for the plot of the beta probability density function for four different values of the shape parameters.

13.3.1.5 Gamma Distribution The general formula for the probability density function of the gamma distribution for uncertain load P_D is

$$f(P_D) = \frac{(P_D - \mu)^{a-1}}{b^a \Gamma(a)} e^{-\left(\frac{P_D - \mu}{b}\right)} \tag{13.9}$$
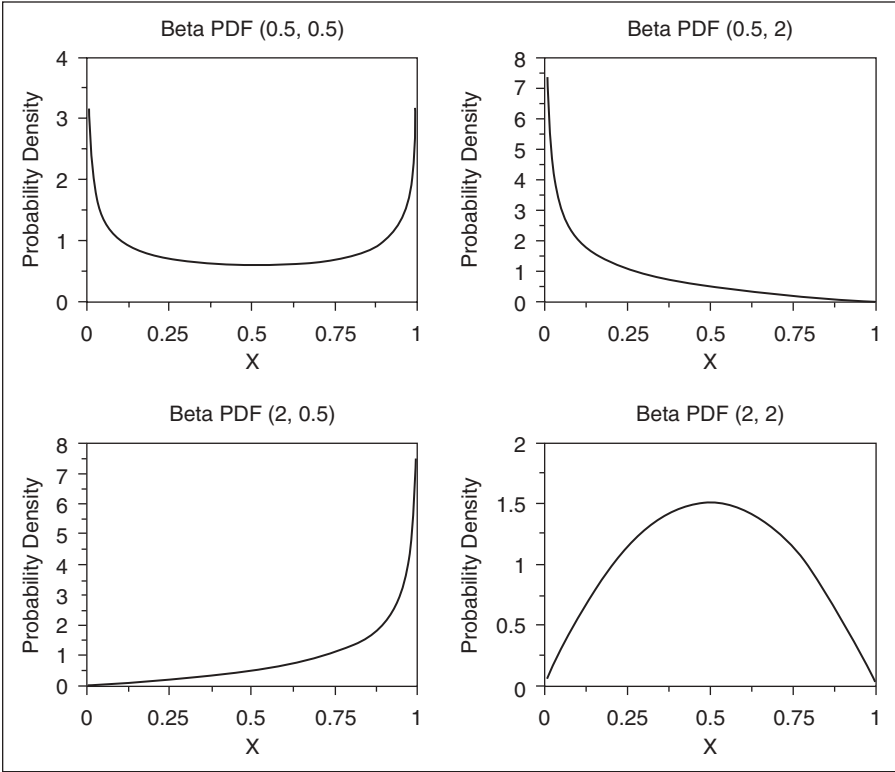
FIGURE 13.4   The plot of the beta probability density function

$$P_D \geq \mu$$
$$a > 0 \tag{13.10}$$
$$b > 0$$

where a is the shape parameter, μ is the location parameter, b is the scale parameter, and Γ is the gamma function, which has the formula

$$\Gamma(a) = \int_0^\infty t^{a-1} e^{-t} dt \tag{13.11}$$

Figure 13.5 is an example of the shape for the plot of the gamma probability density function.
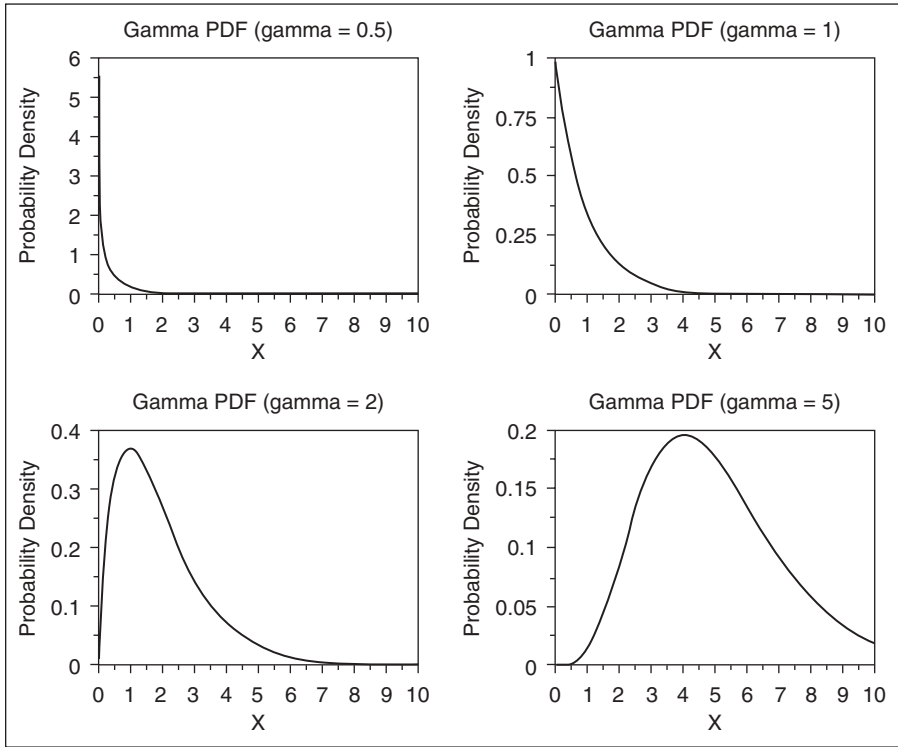
FIGURE 13.5   The plot of the gamma probability density function

13.3.1.6 Gumbel Distribution   The Gumbel distribution is also referred to as the extreme value type I distribution. The extreme value type I distribution has two forms. One is based on the smallest extreme, and the other is based on the largest extreme. We call these the minimum and maximum cases, respectively. Formulas and plots for both cases are given.

The general formula for the probability density function of the Gumbel (maximum) distribution for uncertain load P_D is

$$f(P_D) = \frac{1}{b} e^{\left(\frac{\mu - P_D}{b}\right)} e^{-e^{\left(\frac{\mu - P_D}{b}\right)}} \tag{13.12}$$

$$\begin{aligned} -\infty \le P_D \le \infty \\ b > 0 \end{aligned} \tag{13.13}$$

where μ is the location parameter and b is the scale parameter.

Figure 13.6 is an example of the shape for the plot of the Gumbel probability density function for the maximum case.
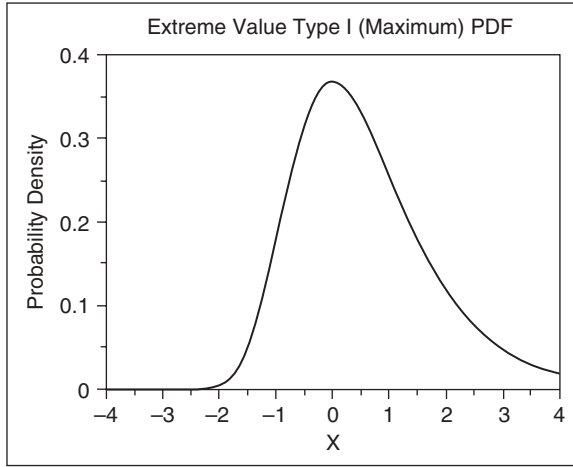
FIGURE 13.6 The plot of the Gumbel probability density function

13.3.1.7 *Chi-Square Distribution* The chi-square distribution results when v independent variables with standard normal distributions are squared and summed. The formula for the probability density function of the chi-square distribution for uncertain load P_D is

$$f(P_D) = \frac{P_D^{\frac{v}{2}-1}}{2^{\frac{v}{2}}\Gamma\left(\frac{v}{2}\right)} e^{-\left(\frac{P_D}{2}\right)} \tag{13.14}$$

$$P_D \geq 0 \tag{13.15}$$

where v is the shape parameter and Γ is the gamma function.

Figure 13.7 is an example of the shape for the plot of the chi-square probability density function for four different values of the shape parameter.

13.3.1.8 *Weibull Distribution* The formula for the probability density function of the Weibull distribution for uncertain load P_D is

$$f(P_D) = \frac{a(P_D - \mu)^{a-1}}{b^a} e^{-\left(\frac{P_D - \mu}{b}\right)^a} \tag{13.16}$$

$$P_D \geq \mu$$
$$a > 0 \tag{13.17}$$
$$b > 0$$

where a is the shape parameter, μ is the location parameter, and b is the scale parameter.
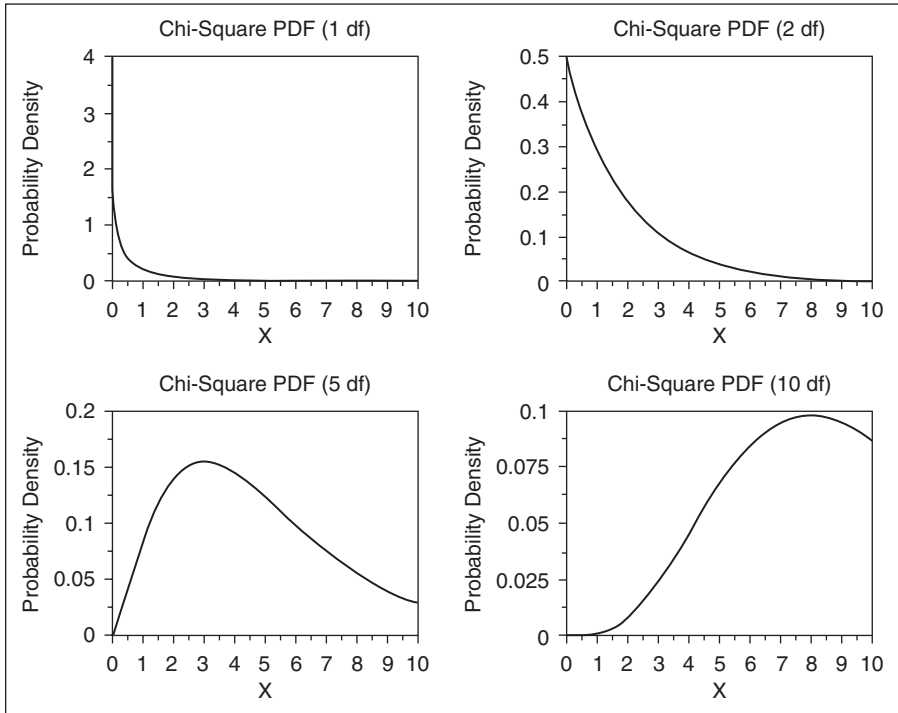
FIGURE 13.7   The plot of the chi-square probability density function

Figure 13.8 is an example of the shape for the plot of the Weibull probability density function.

13.3.2 Fuzzy Set Representation of Uncertainty Load

The uncertainty load P_D can also be represented by fuzzy sets, which are defined in the numbers set R and satisfy the normality and boundary conditions that are designed by fuzzy numbers. The membership function of a fuzzy number for the uncertainty load P_D corresponds to:

$$\mu_{P_D(x)} : R \in [0, 1] \tag{13.18}$$

The easiest way to express the fuzzy number is the LR fuzzy number. The uncertainty load P_D is said to be an LR type fuzzy number if

$$\mu_{P_D(x)} = \begin{cases} L\left(\dfrac{m-x}{a}\right), & x \le m, a > 0 \\ R\left(\dfrac{m-x}{b}\right), & x \ge m, b > 0 \end{cases} \tag{13.19}$$
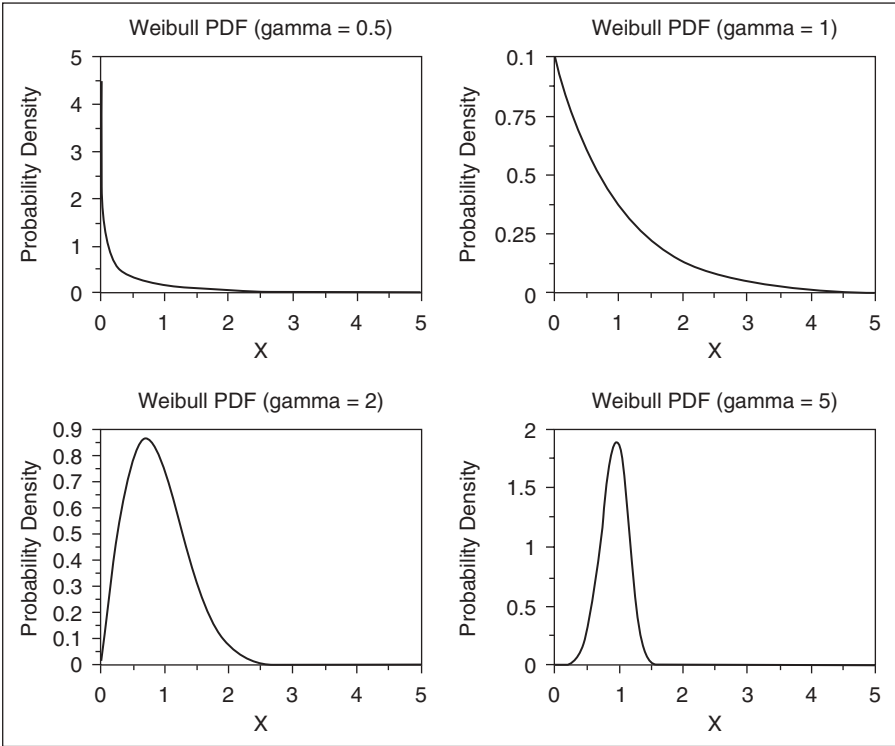
FIGURE 13.8 The plot of the Weibull probability density function

where m is the mean value of load P_D.

The LR type fuzzy number of the uncertainty load P_D can be written as

$$P_D = (m, a, b)_{LR} \tag{13.20}$$

One of the common LR fuzzy numbers is the triangular fuzzy number, which is shown in Figure 13.9.

The membership function of the fuzzy load in Figure 13.9 can be expressed as:

$$\mu_{P_D(x)} = \begin{cases} \dfrac{x-(d-\alpha)}{\alpha}, & \text{if } x \in [(d-\alpha), d] \\[2mm] \dfrac{(d+\beta)-x}{\beta}, & \text{if } x \in [d, (d+\beta)] \\[2mm] 0, & \text{otherwise} \end{cases} \tag{13.21}$$

where
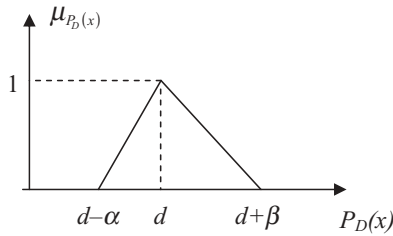
FIGURE 13.9   Uncertainty load with triangular fuzzy number

d: The model value of uncertainty load

α: The inferior dispersion of uncertainty load

β: The superior dispersion of uncertainty load

The principle of fuzzy number can be used to handle the uncertainty load. For example, for getting the sum of two uncertainty loads with positive triangular fuzzy number, the following fuzzy operation is used:

Let uncertainty load 1 be

$$P_{D1} = (d1, \alpha1, \beta1)_{LR} \tag{13.22}$$

and uncertainty load 2

$$P_{D2} = (d2, \alpha2, \beta2)_{LR} \tag{13.23}$$

The sum of the two uncertainty loads will be

$$(d1, \alpha1, \beta1)_{LR} \oplus (d2, \alpha2, \beta2)_{LR} = (d1 + d2, \alpha1 + \alpha2, \beta1 + \beta2)_{LR} \tag{13.24}$$

Sometimes, a simple way to represent the uncertainty load is by using an interval format of fuzzy numbers, which is based on γ-cuts of fuzzy numbers. The values of γ are within between 0 and 1. Applying the γ-cuts, the uncertainty load P_D can be represented as:

$$P_D^\gamma = [\gamma\alpha + (d - \alpha), (d + \beta) - \gamma\beta] \tag{13.25}$$

or

$$P_D^\gamma = \left[P_{D\min}^\gamma, P_{D\max}^\gamma \right] \tag{13.26}$$

$$P_{D\min}^\gamma = \gamma\alpha + (d - \alpha) \tag{13.27}$$

$$P_{D\max}^\gamma = (d + \beta) - \gamma\beta \tag{13.28}$$

For two different γ-cuts ($\gamma1 < \gamma2$), the relationship of two interval values of uncertainty load P_D is:

$$\left[P_{D\min}^{\gamma2}, P_{D\max}^{\gamma2}\right] \subset \left[P_{D\min}^{\gamma1}, P_{D\max}^{\gamma1}\right] \tag{13.29}$$

If there are two uncertainty loads P_{D1} and P_{D2},

$$P_{D1} = [P_{D1\min}, P_{D1\max}] \tag{13.30}$$

$$P_{D2} = [P_{D2\min}, P_{D2\max}] \tag{13.31}$$

Addition, subtraction, multiplication, and division of two uncertainty loads are defined as

$$\begin{aligned} P_{D1} + P_{D2} &= [P_{D1\min}, P_{D1\max}] + [P_{D2\min}, P_{D2\max}] \\ &= [P_{D1\min} + P_{D2\min}, P_{D1\max} + P_{D2\max}] \end{aligned} \tag{13.32}$$

$$\begin{aligned} P_{D1} - P_{D2} &= [P_{D1\min}, P_{D1\max}] - [P_{D2\min}, P_{D2\max}] \\ &= [P_{D1\min} - P_{D2\max}, P_{D1\max} - P_{D2\min}] \end{aligned} \tag{13.33}$$

$$\begin{aligned} P_{D1} \times P_{D2} &= [P_{D1\min}, P_{D1\max}] \times [P_{D2\min}, P_{D2\max}] \\ &= [\min(P_{D1\min} \times P_{D2\min}, P_{D1\min} \times P_{D2\min}, P_{D1\max} \times P_{D2\min}, P_{D1\max} \times P_{D2\max}), \\ &\quad \max(P_{D1\min} \times P_{D2\mathbf{min}}, P_{D1\min} \times P_{D2\min}, P_{D1\max} \times P_{D2\min}, P_{D1\max} \times P_{D2\max})] \end{aligned} \tag{13.34}$$

$$\begin{aligned} P_{D1}/P_{D2} &= [P_{D1\min}, P_{D1\max}]/[P_{D2\min}, P_{D2\max}] \\ &= [P_{D1\min}, P_{D1\max}][1/P_{D2\max}, 1/P_{D2\max}] \quad \text{if } 0 \notin [P_{D2\min}, P_{D2\max}] \end{aligned} \tag{13.35}$$

Some of the algebraic laws valid for real numbers remain valid for intervals of fuzzy numbers. Interval addition and multiplication are associative and commutative:

(a) Commutative:

$$P_{D1} + P_{D2} = P_{D2} + P_{D1} \tag{13.36}$$

$$P_{D1} \times P_{D2} = P_{D2} \times P_{D1} \tag{13.37}$$

(b) Associative:

$$(P_{D1} + P_{D2}) \pm P_{D3} = P_{D1} + (P_{D2} + P_{D3}) \tag{13.38}$$

$$(P_{D1} \times P_{D2})P_{D3} = P_{D1}(P_{D2} \times P_{D3}) \tag{13.39}$$

(c) Neutral element:

$$P_{D1} + 0 = 0 + P_{D1} = P_{D1} \tag{13.40}$$

$$1 \times P_{D1} = P_{D1} \times 1 = P_{D1} \tag{13.41}$$
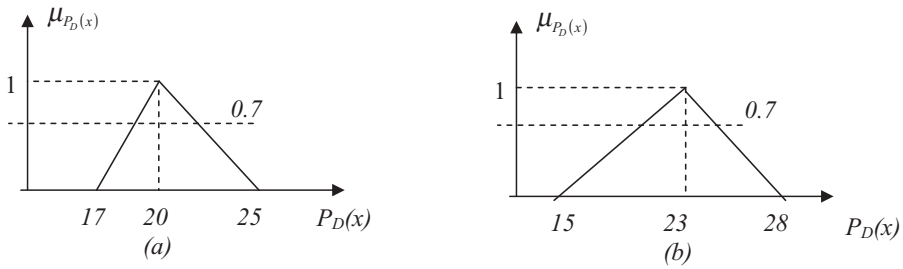
FIGURE 13.10   Two uncertainty loads with triangular fuzzy number

Example 13.1

There are two uncertainty loads, $P_{D1} = (20,3,5)_{LR}$ and $P_{D2} = (23,8,5)_{LR}$, which are shown in Figure 13.10.

The corresponding fuzzy membership functions can be presented as below:

$$\mu_{P_{D1}(x)} = \begin{cases} \dfrac{x-17}{3}, & \text{if } x \in [17,\,20] \\[2mm] \dfrac{25-x}{5}, & \text{if } x \in [20,25] \\[2mm] 0, & \text{otherwise} \end{cases}$$

$$\mu_{P_{D2}(x)} = \begin{cases} \dfrac{x-15}{8}, & \text{if } x \in [15,23] \\[2mm] \dfrac{28-x}{5}, & \text{if } x \in [23,28] \\[2mm] 0, & \text{otherwise} \end{cases}$$

The sum of two uncertainty loads will be

$$(20,3,5)_{LR} \oplus (23,8,5)_{LR} = (43,11,10)_{LR}$$

If we represent two uncertainty loads by using an interval format of fuzzy numbers and a 0.7-cut of fuzzy numbers, the uncertainty loads P_{D1} and P_{D2} can be represented as:

$$P_{D1}^{0.7} = [0.7 \times 3 + (20-3),\, (20+5) - 0.7 \times 5] = [19.1,\, 21.5]$$
$$P_{D2}^{0.7} = [0.7 \times 8 + (23-8),\, (23+5) - 0.7 \times 5] = [20.6,\, 24.5]$$

The sum of two uncertainty loads with interval format is computed as:

$$
\begin{aligned}
P_{D1}^{0.7} + P_{D2}^{0.7} &= \left[P_{D1\min}^{0.7}, P_{D1\max}^{0.7} \right] + \left[P_{D2\min}^{0.7}, P_{D2\max}^{0.7} \right] \\
&= \left[P_{D1\min}^{0.7} + P_{D2\min}^{0.7}, P_{D1\max}^{0.7} + P_{D2\max}^{0.7} \right] \\
&= [19.1 + 20.6, 21.5 + 24.5] \\
&= [39.7, 46]
\end{aligned}
$$

The same result can be obtained by using the sum of two uncertainty loads $P_{Dsum} = (43,11,10)_{LR}$ and a 0.7-cut of fuzzy numbers, that is,

$$
P_{Dsum}^{0.7} = [0.7 \times 11 + (43 - 11), (43 + 10) - 0.7 \times 10] = [39.7, 46]
$$

13.4   UNCERTAINTY POWER FLOW ANALYSIS

In the general power flow analysis, the input variables to the power flow problem are assumed to be deterministically known. The practical operation conditions with uncertainty factors are not considered. Consequently, the power flow results may not reflect the real status of system operation. This limitation will be overcome if a probabilistic approach or a fuzzy approach is applied.

13.4.1   Probabilistic Power Flow

From Chapter 2, the standard form of the load flow equations in rectangular form is:

$$
P_i = P_{Gi} - P_{Di} = \sum_j Y_{ij} V_i V_j \cos(\theta_i - \theta_j - \delta_{ij}) \tag{13.42}
$$

$$
Q_i = Q_{Gi} - Q_{Di} = \sum_j Y_{ij} V_i V_j \sin(\theta_i - \theta_j - \delta_{ij}) \tag{13.43}
$$

where

i, j: The bus number
P_i: The net real power injection
Q_i: The net reactive power injection
V: The magnitude of the bus voltage
θ: The phase angle of the bus voltage
Y_{ij}: The magnitude of the i-jth element of the admittance matrix
δ_{ij}: The angle of the i-jth element of the admittance matrix

The power flow problem can be expressed as two sets of nonlinear equations as below:

$$\mathbf{Y} = g(\mathbf{X}) \tag{13.44}$$

$$\mathbf{Z} = h(\mathbf{X}) \tag{13.45}$$

where $\mathbf{X}$ is the vector of unknown state variables (voltage magnitudes and angles at PQ buses and voltage angles and reactive power outputs at PV buses); $\mathbf{Y}$ is the vector of predefined input variables (real and reactive power at PQ buses and voltage magnitudes and real power at PV buses); $\mathbf{Z}$ is the vector of unknown output variables (real and reactive flows in the network elements); and g and h are the power flow functions.

As we mentioned in Section 13.3, the input variables such as power loads are uncertain and can be expressed with probabilistic distributions. Probabilistic power flow models input data (generation and loads) in a probabilistic way and calculate the probability distribution functions of line flows.

We assume that the input data have the nature of normal distribution, and the mean values and variances of input variables Y are $\bar{Y}$ and σ_Y^2, respectively. With the mean values $\bar{Y}$, the mean values of the state variables and output variables can be computed with conventional power flow methods. Then the variances of state variables and branch power flows can be computed with the following formulas.

$$\sigma_X^2 = \text{diag}\left(J^t \Lambda^{-1} J\right)^{-1} \tag{13.46}$$

$$\sigma_Z^2 = \text{diag}\left(D\left(J^t \Lambda^{-1} J\right)^{-1} D^t\right) \tag{13.47}$$

where

σ_X^2: The variances of state variables $\mathbf{X}$

σ_Z^2: The variances of branch power flows $\mathbf{Z}$

J: The Jacobian matrix of the power flow equations

Λ: The diagonal matrix of variances of the injected power σ_Y^2

D: The first-order matrix from the Taylor series expansion of $g(x)$

With mean values and variances of the state variables and output variables, the probabilistic distribution of power flow is obtained.

Probabilistic power flow provides the complete spectrum of all probable values of output variables, like bus voltages and flows, with their respective probabilities, taking into account generation unit unavailability, load uncertainty, dispatching criteria effects, and topological variations.

13.4.2 Fuzzy Power Flow

Fuzzy power flow analysis is needed if the input data such as load and generation power are given as fuzzy numbers.

Section 13.3.2 analyzes the uncertain load by using fuzzy numbers. The other input data with uncertainty in power flow calculation can be handled as the same way. If we use an interval format of fuzzy numbers to deal with the uncertain input data, the fuzzy power flow can be computed with the interval arithmetic method.

Power flow problems are nonlinear equations $F(x)$. One of the iteration operators for the solution of interval nonlinear equations is the Newton operator [13–16]:

$$N(x, \tilde{x}) := \tilde{x} - F'(x)^{-1} F(\tilde{x}) \tag{13.48}$$

Where

$F'(x)$: The interval Jacobian matrix

$N(x, \tilde{x})$: The Newton operator

$\tilde{x}$: The midpoint of the interval $[x_{\min}, x_{\max}]$, defined as:

$$\tilde{x} := \frac{(x_{\min} + x_{\max})}{2} \tag{13.49}$$

For each iteration, we need to solve the following interval linear equations for Δ_x:

$$F'(x)\Delta x = F(\tilde{x}) \tag{13.50}$$

Therefore, the solution of interval nonlinear equations reduces to the solutions of linear equation, but using interval arithmetic. It is noted that the solution of interval linear equations, which is at the heart of the nonlinear iterative solution, is a different proposition from the solution of ordinary linear equations. The solution set of the interval linear equations has a very complex nonconvex structure. The hull of the solution set is used, which is defined as the smallest interval vector that contains the solution set. Generally, the hull contains, in addition to the entire solution set, many nonsolutions. In this way, solving interval linear equations means obtaining the hull of the solution set. There are several methods to solve interval linear equations, such as:

(1) Krawczyk's method [11]
(2) Interval Gauss–Seidel iteration [14]
(3) LDU decomposition

The most widely used method to solve interval linear equations is the Gauss–Seidel iteration. The purpose of Gauss–Seidel iterations here is not to solve the power flow problems, but to solve the linear equations that result from Newton's method.

In a word, the fuzzy power flow problem can be solved by using interval arithmetic through linearizing the problem. However, the resulting linear equations must be solved by a Gauss–Seidel iterative process instead of by direct LDU factorization. The solution obtained is conservative, in that it contains all solution points and may also contain many nonsolutions.

13.5   ECONOMIC DISPATCH WITH UNCERTAINTIES

13.5.1   Min-Max Optimal Method

Chapters 4 and 5 discuss the economic dispatch problem, where the uncertain factors are not included. However, the economy of short-term operation of thermal power systems is influenced by approximations in operation planning methods and by the inaccuracies and uncertainties of input data. There are two major uncertain factors in economic dispatch, as discussed below.

13.5.1.1   Uncertain Loads   The forecast loads are important input information, which is characterized by uncertainty and inaccuracy because of the stochastic nature of the load, which is discussed in Section 13.3.

Let the load duration curve $P_D(t)$ be given in the form of intervals

$$P_{D\min}(t) \leq P_D(t) \leq P_{D\max}(t), \quad 0 \leq t \leq T \tag{13.51}$$

where T is time period.

13.5.1.2   Inaccuracy Fuel Cost Function

- Inaccuracy in the process of measuring or forecasting of input data
- Change of unit performance during the period between measuring and operation

The inaccuracies in the cost functions for steady-state operation are caused by the limited accuracy of the determination of the thermal dynamic performance, changing cooling water temperatures, changing calorific values and contamination, erosion, and attrition in boiler and turbine. These deviations lead to inaccurate values for heat inputs and fuel prices.

Similar to the uncertain load, the cost functions of generating units are also expressed in the form of intervals.

$$F_{\min}(P_{Gi}) \leq F(P_{Gi}) \leq F_{\max}(P_{Gi}), \quad i \in NG \tag{13.52}$$

where

$$P_{Gi\min} \leq P_{Gi} \leq P_{Gi\max}, \quad i \in NG \tag{13.53}$$

The most well-founded criterion for optimal scheduling of real power in power system under uncertainty is the criterion of min-max risk [17, 18] or possible losses caused by uncertainty of information. The risk function can be written as

$$R(\bar{P}_{Gi}(t), \tilde{U}(t)) = F_{\Sigma} - F_{\Sigma \min} \tag{13.54}$$

where

F_{Σ}: The actual total fuel cost of the generators, which is expressed as

$$F_{\Sigma} = \sum_{i=1}^{NG} F_i(\bar{P}_{Gi}(t), \tilde{U}(t)) \tag{13.55}$$

$F_{\Sigma \min}$: The minimal total fuel cost of the generators if we could obtain the deterministic information about the uncertainty factors, which is expressed as

$$F_{\Sigma \min} = \min \sum_{i=1}^{NG} F_i(\bar{P}_{Gi}(t), \tilde{U}(t)) \tag{13.56}$$

$\tilde{U}(t)$: The uncertain factors
$\bar{P}_{Gi}(t)$: The planned or expected power duration curve of units for the time period T

Operator min max R means the minimization of maximum risk caused by uncertainty factors, that is,

$$\min_{P_{Gi}(t)} \max_{\tilde{U}(t)} \int_0^T R(\bar{P}_{Gi}(t), \tilde{U}(t)) dt \tag{13.57}$$

The optimality conditions of the min-max problem arise from the main theorem of the game theory and can be expressed as follows:
If the $\bar{P}_{Gi}^0(t)$ is the optimal plan for the min max R criterion, then

$$R(\bar{P}_{Gi}^0(t), U^-(t)) = R(\bar{P}_{Gi}^0(t), U^+(t)) \tag{13.58}$$

Let E be the expected value of risk R and Ω be a set of mixed strategy of uncertain factors. The minimal-maximal problem can be expressed as below.

$$\min_{P_{Gi}(t)} \max_{\Omega} \int_0^T E(R(\bar{P}_{Gi}(t), \tilde{U}(t))) dt \tag{13.59}$$

It is possible to compose the deterministic equivalent of the min-max problem on the base of given above conditions. This requires the finding of the min-max load demand curves and cost functions of generating units. If we replace the deterministic curves by the min-max curves, we can use the initial deterministic model for calculating the min-max optimal results.

13.5.2 Stochastic Model Method

In this section, we present another approach to handle the uncertainty of the fuel cost of the generator units by use of the stochastic model.

A method of obtaining a stochastic model is to take a deterministic model and transform it into a stochastic model by (1) introducing random variables as inputs, as coefficients, or as both; and (2) introducing equation errors as disturbances. Since this type of model is only an approximation, it is important in this approach to make the randomness reflect a real situation.

From Chapter 4, the economic dispatch model can be expressed as below:

$$\min F = \sum_{i=1}^{N} F_i(P_{Gi}) \tag{13.60}$$

s.t.

$$\sum_{i=1}^{N} P_{Gi} = P_D + P_L \tag{13.61}$$

$$P_{Gi\min} \leq P_{Gi} \leq P_{Gi\max} \tag{13.62}$$

Suppose the fuel cost is a quadratic function, i.e.,

$$F_i = a_i P_{Gi}^2 + b_i P_{Gi} + c_i \tag{13.63}$$

A stochastic model of function F is formulated by taking the deterministic fuel cost coefficients a, b, c and the generator real power P_{Gi} as random variables. Any possible deviation of operating cost coefficient from their expected values is manipulated through the randomness of generator power output P_{Gi}. The randomness of P_{Gi} implies that power balance equation (13.61) is not a rigid constraint to be satisfied.

A simple way of converting a stochastic model to a deterministic model is to take its expected value [19]; therefore, the expected value of operating cost becomes

$$\bar{F} = E\left[\sum_{i=1}^{N}\left(a_i P_{Gi}^2 + b_i P_{Gi} + c_i\right)\right]$$

$$= \sum_{i=1}^{N}\left[E(a_i)E(P_{Gi}^2) + E(b_i)E(P_{Gi}) + E(c_i)\right]$$

$$= \sum_{i=1}^{N}\left[\bar{a}_i\left(\text{var } P_{Gi} + \bar{P}_{Gi}^2\right) + \bar{b}_i\bar{P}_{Gi} + \bar{c}_i\right]$$

$$= \sum_{i=1}^{N}\left[\bar{a}_i\, v\bar{P}_{Gi}^2 + \bar{a}\bar{P}_{Gi}^2 + \bar{b}_i\bar{P}_{Gi} + \bar{c}_i\right]$$

$$= \sum_{i=1}^{N}\left[\bar{a}_i\bar{P}_{Gi}^2\,(v+1) + \bar{b}_i\bar{P}_{Gi} + \bar{c}_i\right] \tag{13.64}$$

where v is the coefficient of variation random variable P_{Gi}. It is the ratio of standard deviation to the mean and is a measure of relative dispersion or uncertainty in the random variable. If $v = 0$, it implies no randomness or, in other words, complete certainty about the value of random variable.

If we use the B coefficient to compute the system network losses, we get

$$P_L = \sum_i \sum_j P_{Gi} B_{ij} P_{Gj} \tag{13.65}$$

Then the expected value of the network power losses is

$$\bar{P}_L = E\left[\sum_i \sum_j P_{Gi} B_{ij} P_{Gj}\right] = \sum_i \sum_j \bar{P}_{Gi} B_{ij} \bar{P}_{Gj} + \sum_i B_{ii}\, \text{var } P_{Gi}$$

$$\approx \sum_i \sum_j \bar{P}_{Gi} B_{ij} \bar{P}_{Gj} \tag{13.66}$$

where the variance of network loss has been neglected, since it is usually small.

In addition, the expected value of the load can be expressed as

$$\bar{P}_D = E[P_D] = \bar{P}_D \tag{13.67}$$

The stochastic model of economic dispatch can be written as below:

$$\min \bar{F} = \sum_{i=1}^{N}\left[\bar{a}_i\bar{P}_{Gi}^2\,(v+1) + \bar{b}_i\bar{P}_{Gi} + \bar{c}_i\right] \tag{13.68}$$

s.t.

$$\sum_{i=1}^{N} \bar{P}_{Gi} = \bar{P}_{D} + \bar{P}_{L} \tag{13.69}$$

$$\bar{P}_{Gi\min} \leq \bar{P}_{Gi} \leq \bar{P}_{Gi\max} \tag{13.70}$$

Since there is the stochastic error for the stochastic model, the expected value associated with deficit or surplus of generation can be treated as deviation proportional to the expectation of the square of power mismatch.

$$\delta = E\left[\left(\bar{P}_{D} + \bar{P}_{L} - \sum_{i=1}^{N} P_{Gi}\right)^2\right] = \sum_{i=1}^{N} E[\bar{P}_{Gi} - P_{Gi}]^2 = \sum_{i=1}^{N} \text{var} \, P_{Gi} \tag{13.71}$$

Using the Lagrange multiplier method to solve the above model, we get

$$L = \sum_{i=1}^{N} \left[\bar{a}_i \bar{P}_{Gi}^2 (v+1) + \bar{b}_i \bar{P}_{Gi} + \bar{c}_i\right] + \lambda\left(\bar{P}_{D} + \bar{P}_{L} - \sum_{i=1}^{N} P_{Gi}\right) + \mu \sum_{i=1}^{N} \text{var} \, P_{Gi} \tag{13.72}$$

According to optimality condition

$$\frac{\partial L}{\partial P_{Gi}} = 0$$

we have

$$2\bar{a}_i \bar{P}_{Gi} + \bar{b}_i + \lambda\left(\sum_{j} 2B_{ij} \bar{P}_{Gj}\right) + 2(\bar{a}_i + \mu)v\bar{P}_{Gi} = 0 \tag{13.73}$$

Solving the above equation, the stochastic optimal results of the economic dispatch can be obtained.

13.5.3 Fuzzy ED Algorithm

13.5.3.1 Fuzzy ED Model   Section 13.3 discusses how the real load can be modeled as fuzzy. Assume the load is a trapezoidal possibility distribution, which is shown in Figure 13.11. There are four break points: $P_{D}^{(1)}$, $P_{D}^{(2)}$, $P_{D}^{(3)}$ and $P_{D}^{(4)}$. The possibility distribution of each load refers to the mapping of a fuzzy variable on the [0, 1] interval, which is expected to be between p $P_{D}^{(1)}$ and $P_{D}^{(4)}$; however, it is more likely to be between $P_{D}^{(2)}$ and $P_{D}^{(3)}$.

Similarly, the corresponding real power generation can also be modeled as fuzzy. Therefore, the economic dispatch with fuzzy loads can be expressed as follows:
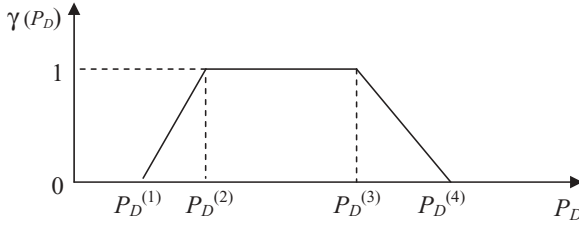
FIGURE 13.11   Uncertain load with trapezoidal possibility distribution

$$\min F = \sum_{i=1}^{NG} F_i\left(\tilde{P}_{Gi}\right) \tag{13.74}$$

s.t.

$$\sum_{i=1}^{NG} \tilde{P}_{Gi} = \sum_{j=1}^{ND} \tilde{P}_{Dj} + \tilde{P}_L \tag{13.75}$$

$$P_{Gi\min} \leq \tilde{P}_{Gi} \leq P_{Gi\max} \tag{13.76}$$

where

$\tilde{P}_{Gi}$: The fuzzy real power generation

$\tilde{P}_{Dj}$: The fuzzy real power load demand

$\tilde{P}_L$: The fuzzy real power losses

For simplifying the fuzzy economic dispatch problem, neglecting the network losses, and assuming the fuel cost is a linear function, i.e.,

$$F_i = c_i \tilde{P}_{Gi} \tag{13.77}$$

Then the minimization of cost function is equivalent to the minimization of fuzzy variable $\tilde{P}_{Gi}$, which can be translated to the minimization of its distance from the $\gamma\left(P_G\right)$ axis.

According to Figure 13.12, the distance of fuzzy variable $\tilde{P}_{Gi}$ is given as [20, 21]:

$$d = \frac{A_1 + (A_1 + A_2)}{2} \tag{13.78}$$

where A_1 and A_2 are areas shown in Figure 13.12. They can be computed as below:
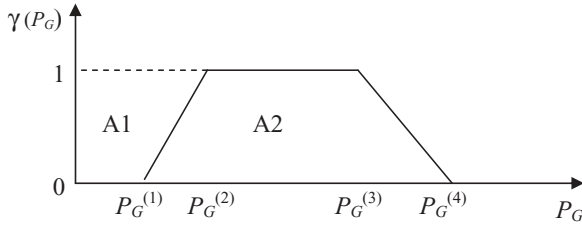
FIGURE 13.12 Uncertain generation with trapezoidal possibility distribution

$$A_1 = \frac{P_{Gi}^{(1)} + P_{Gi}^{(2)}}{2} \tag{13.79}$$

$$A_2 = \frac{\left(P_{Gi}^{(3)} - P_{Gi}^{(2)}\right) + \left(P_{Gi}^{(4)} - P_{Gi}^{(1)}\right)}{2} \tag{13.80}$$

Substituting equations (13.80) and (13.81) into equation (13.79), we get

$$d = \frac{P_{Gi}^{(1)} + P_{Gi}^{(2)} + P_{Gi}^{(3)} + P_{Gi}^{(4)}}{4} = \sum_{k=1}^{4} \frac{P_{Gi}^{(k)}}{4} \tag{13.81}$$

Thus the above-mentioned fuzzy economic dispatch problem can be written as follows:

$$\min F = \sum_{i=1}^{NG} \sum_{k=1}^{4} c_i \frac{P_{Gi}^{(k)}}{4} \tag{13.82}$$

s.t.

$$\sum_{i=1}^{NG} P_{Gi}^{(k)} = \sum_{j=1}^{ND} P_{Di}^{(k)}, \quad k = 1, \dots, 4 \tag{13.83}$$

$$P_{Gi\min} \le P_{Gi}^{(1)} \le P_{Gi}^{(2)} \le P_{Gi}^{(3)} \le P_{Gi}^{(4)} \le P_{Gi\max} \quad i = 1, \dots\dots, NG \tag{13.84}$$

13.5.3.2 Fuzzy Line Constraint The above fuzzy representation of real loads will result in fuzzy line flows with trapezoidal possibility distributions. Since DC flow is considered in fuzzy ED analysis, the fuzzy line flow can be expressed as below:

$$\tilde{P}_l = \sum_{m=1}^{NB} S_{lm} \tilde{P}_m, \quad l = 1, \dots, NL \tag{13.85}$$

where

$\tilde{P}_m$: The fuzzy bus real power injection
$\tilde{P}_l$: The fuzzy line real power flow
S: The DC-based sensitivity matrix

A contingency analysis is used to detect most severe outages, and contingency constraints are augmented to the base case to ensure a preventive control. According to Chapter 5, the contingency constraints are represented similar to equation (13.85) except that the sensitivity coefficients are adjusted for the contingency under consideration, i.e.,

$$\tilde{P}'_l = \sum_{m=1}^{NB} S'_{lm} \tilde{P}_m, \quad l = 1, \dots, NL \tag{13.86}$$

where

$\tilde{P}'_l$: The fuzzy line real power flow under the contingency situation
S': The DC-based sensitivity matrix under the contingency situation

If the phase shifter is considered, we represent phase shifters in terms of equivalent injected power. If a phase shifter is located on line t that connects buses i and j, the equivalent injected power at buses i and j and phase shifter angle can be simplified as

$$P_{\phi i} = b_t \phi_t = -\frac{\phi_t}{x_t} \tag{13.87}$$

$$P_{\phi j} = -b_t \phi_t = \frac{\phi_t}{x_t} \tag{13.88}$$

where

$P_{\phi i}$: The bus real power injection due to a phase shifter
ϕ_t: The phase shifter angle located on line t
x_t: The reactance of line t
b_t: The susceptance of line t

Thus the constraint related to the phase shifter angle in the fuzzy case can be written as

$$\phi_{i\min} \le x_t \tilde{P}_{\phi i} \le \phi_{i\max} \tag{13.89}$$

The fuzzy line flow with phase shifter can be expressed as below:

$$\tilde{P}_l = \sum_{m=1}^{NB} S_{lm} \left(\tilde{P}_m + \tilde{P}_{\phi m} \right), \quad l = 1, \ldots, NL \tag{13.90}$$

$$\tilde{P}_l' = \sum_{m=1}^{NB} S_{lm}' \left(\tilde{P}_m + \tilde{P}_{\phi m} \right), \quad l = 1, \ldots, NL \tag{13.91}$$

Therefore, the fuzzy economic dispatch model with the line constraints is written as

$$\min F = \sum_{i=1}^{NG} \sum_{k=1}^{4} c_i \frac{P_{Gi}^{(k)}}{4} \tag{13.92}$$

s.t.

$$\sum_{i=1}^{NG} P_{Gi}^{(k)} = \sum_{j=1}^{ND} P_{Di}^{(k)}, \quad k = 1, \ldots, 4 \tag{13.93}$$

$$P_{l\min} \le \sum_{m=1}^{NB} S_{lm} \left(\tilde{P}_m - \tilde{P}_{\phi m} \right) \le P_{l\max}, \quad l = 1, \ldots, NL \tag{13.94}$$

$$P_{l\min} \le \sum_{m=1}^{NB} S_{lm}' \left(\tilde{P}_m + \tilde{P}_{\phi m} \right) \le P_{l\max}, \quad l = 1, \ldots, NL \tag{13.95}$$

$$P_{Gi\min} \le P_{Gi}^{(1)} \le P_{Gi}^{(2)} \le P_{Gi}^{(3)} \le P_{Gi}^{(4)} \le P_{Gi\max} \quad i = 1, \ldots\ldots, NG \tag{13.96}$$

$$\frac{\phi_{i\min}}{x_t} \le P_{\phi i}^{(1)} \le P_{\phi i}^{(2)} \le P_{\phi i}^{(3)} \le P_{\phi i}^{(4)} \le \frac{\phi_{i\max}}{x_t} \quad t = 1, \ldots\ldots, NP \tag{13.97}$$

where

NP: The number of phase shifters
NB: The number of buses
NL: The number of lines

Since we use four sets of variables each describing one break point of the possibility distributions, Dantzig–Wolf decomposition (DWD) is applied to decompose the problem into four subproblems coupled by the constraints in equations (13.96) and (13.97). The dimension of the master problem is equal to the number of coupling constraints plus the number of subproblems, while each subproblem has a dimension equal to the number of constraints corresponding to each break point. The solution of the master problem generates new simplex multipliers (dual solution) that will adjust the cost function of the subproblems. The solution of the subproblems with the adjusted objective

function will provide the master problem with new columns to enter the
master basis matrix.

Example 13.2

The simulation example used here is from reference [20]. The fuzzy eco-
nomic dispatch method is tested on the modified IEEE 30-bus system. The
system has 6 generators, 41 lines, and 3 phase shifters. All phase shifters
have turns ratios equal to 1. Trapezoidal possibility distributions are used
to represent the system fuzzy real power loads. The break points of the load
possibility distribution are given in Table 13.1. The generator data are given
in Table 13.2, in which each generator cost function is approximated by
piecewise linear approximation.

Test Case 1

In this case, no line flow constraints are introduced in the problem and the
optimal power generation that corresponds to the system fuzzy load is
found. The break points of the generation possibility distributions are given
in Table 13.3. For the sake of comparison, in Table 13.3 we have included
the power generation corresponding to the fixed range of load values $P_D^{(1)}$
and $P_D^{(4)}$. This extreme range of loads provides a wider range of line flows
than that of the proposed fuzzy model, indicating that the fixed load interval
leads to an overestimate of the system behavior in an uncertain
environment.

Table 13.1   Possibility distributions for loads (p.u.)

Load Bus	$P_D^{(1)}$	$P_D^{(2)}$	$P_D^{(3)}$	$P_D^{(4)}$
3	0.000	0.020	0.030	0.050
4	0.020	0.040	0.070	0.100
7	0.100	0.150	0.220	0.270
10	0.020	0.030	0.060	0.080
12	0.050	0.080	0.110	0.150
14	0.030	0.050	0.080	0.100
15	0.040	0.070	0.100	0.130
16	0.010	0.030	0.050	0.060
17	0.030	0.070	0.100	0.140
18	0.000	0.020	0.040	0.070
19	0.040	0.060	0.090	0.130
20	0.000	0.010	0.020	0.040
21	0.100	0.150	0.200	0.230
23	0.000	0.020	0.030	0.050
24	0.050	0.070	0.100	0.120
26	0.010	0.030	0.050	0.060
29	0.000	0.010	0.020	0.030
30	0.060	0.090	0.110	0.140

Table 13.2   Generator data (p.u.)

Gen. Bus	Piecewise Section	P_{Gmin}	P_{Gmax}	Cost Coefficient ($/MWh)
G1	1	0.30	0.90	25.0
	2	0.00	0.35	37.5
	3	0.00	0.75	42.0
G2	1	0.20	0.50	28.0
	2	0.00	0.30	37.0
G5	1	0.15	0.25	30.0
	2	0.00	0.25	36.5
G8	1	0.10	0.15	27.0
	2	0.00	0.20	38.0
G11	1	0.10	0.20	27.5
	2	0.00	0.10	37.0
G13	1	0.12	0.20	36.0
	2	0.00	0.20	39.0

Table 13.3   Results of fuzzy economic dispatch

Gen. Bus	$P_G^{(1)}$	$P_G^{(2)}$	$P_G^{(3)}$	$P_G^{(4)}$	Power Gen. Range for Min and Max Load	
G1	0.900	0.900	0.968	1.217	0.900	1.250
G2	0.478	0.500	0.800	0.800	0.466	0.800
G5	0.150	0.488	0.500	0.500	0.150	0.500
G8	0.150	0.150	0.150	0.150	0.150	0.272
G11	0.200	0.200	0.300	0.300	0.200	0.300
G13	0.120	0.200	0.200	0.200	0.120	0.200

Test Case 2

The fuzzy power generations, given in Table 13.3, are used to compute the corresponding line flow possibility distributions. The break points of line 2–6 are 0.2252, 0.2808, 0.4333, and 0.5238 p.u. as compared to 0.2248 and 0.5430 p.u. for the fixed load interval, which indicates once again the overestimated results by the fixed interval. Line 2–6 has an overflow, as its flow limit is 0.5 p.u. Therefore, the optimal power generation is computed again by considering line 2–6 flow limit. In this case, the phase shifter on line 4–6 alleviates the overflow without any adjustment to the optimal power generation given in Table 13.2. The corresponding break points for the phase shifter on line 4–6 are 0.0, 0.0, 0.0, 0.56°, whereas the phase shifter range for the fixed load interval is between 0.00 and 1.02°. Thus a smaller range for the phase shifter angle is obtained by utilizing a possibility distribution for loads.

13.6   HYDROTHERMAL SYSTEM OPERATION WITH UNCERTAINTY

There are several complex and interrelated problems associated with the optimization of hydrothermal systems.

- Long-term regulation problem (1- to 2-year optimization period)
- Intermediate-term hydrothermal control (1- to 6-month planning period)
- Short-term hydrothermal dispatch (optimization period is from 1 day to 1 week)

For the short-term optimization problem, the applications of deterministic methods to hydrothermal system operation have been established, in which the water inflows and loads were considered to be deterministic. For the long-term regulation problem, it is necessary to use a stochastic representation for the load and river inflow [22, 23]. Since there are uncertainty factors in the short-term hydrothermal dispatch, the existing methods do not provide the system operators with a convincing answer on how to use the water in each separate reservoir. The following uncertainties should be taken into account in a large hydrothermal system operation:

- Uncertainty of the load
- Uncertainty of the unit availability
- Uncertainty of the river inflow

The uncertainty of the river inflows, loads, and unit availability can be dealt with in a stochastic representation. The methods to solve ED with uncertainty in the previous section can also be used to solve the uncertainty problem for the hydrothermal system operation.

13.7   UNIT COMMITMENT WITH UNCERTAINTIES

13.7.1   Introduction

The economy of unit commitment of power systems is influenced by approximations in the operation planning methods and by the inaccuracies and uncertainties of input data. However, most of the early work on the unit commitment problem uses a deterministic formulation neglecting the uncertainties, which are discussed in Chapter 7.

As we analyzed before, the uncertain load can be expressed as normal distribution with a specific correlation structure. Thus we use a chance-constrained optimization (CCO) formulation for the UCP assuming that the hourly loads follow a multivariate normal distribution [24]. The CCO formulation falls into a class of optimization procedures known as stochastic programming in which the solution methods take into consideration the randomness

in input parameters. The advantages of using stochastic programming over the corresponding expected value solution have been demonstrated over a wide spectrum of applications. In chance-constrained programming, the constraints can be violated with a preassigned (usually very small) level of probability. These probabilistic constraints can often be converted to certain deterministic equivalents, and the resulting program can be solved with general deterministic techniques.

In the stochastic model of UC, the equal constraint of real power balance is expressed by a "chance constraint," which requires that this condition be satisfied at a predetermined level of probability. The reserve constraint is considered in the UC because utilities are required to carry a reserve for many different contingencies such as load peaks, generator failures, scheduled outages, regulation, and local area protection. The reserve is usually referred to as operating reserve, which consists of two parts: spinning reserve (SR) and nonspinning reserve. The additional electricity available (synchronized) to serve load immediately is defined as the SR. In other words, the difference between the total amount of electricity ready to serve the customers and the current demand for electricity is the SR. Generally, the magnitude of the required amount of SR is predetermined and used as an operating constraint in the UC calculation. For example, it is taken to be 1.5 to 2 times the capacity of the largest generator or a percentage of the peak load. Instead of using the SR as a predetermined constraint, the stochastic method yields as an output the sets of generating units that need to be turned on such that the load is met with a high probability over the entire time horizon. The level of SR can be determined by fuzzy methods, which are similar to SR handling in the chance-constrained optimization.

13.7.2   Chance-Constrained Optimization Model

13.7.2.1   Deterministic UC Model   The mathematical model for the unit commitment is a mixed-integer nonlinear program. The basic deterministic formulation can be written as below:

$$\min F = \sum_{i=1}^{N} \sum_{t=1}^{T} [F_{i,t}(P_{i,t}, x_{i,t}) + S_{i,t}(P_{i,t}, x_{i,t})] \tag{13.98}$$

s.t.

$$\sum_{i=1}^{N} x_{i,t} P_{i,t} = P_{Dt} \quad t = 1, 2, \ldots, T \tag{13.99}$$

$$P_{i\min} \leq x_{i,t} P_{i,t} \leq P_{i\max} \tag{13.100}$$

$$\sum_{i=1}^{N} x_{i,t} P_{i\max} \geq (1+\alpha)P_{\mathrm{D}t} \quad t = 1, 2, \dots, T \tag{13.101}$$

$$x_{i,t} - x_{i,t-1} \leq x_{i,\gamma} \quad \gamma = t+1, \dots, \min\{t+t_{\mathrm{up}}-1, T\}, i = 1, 2, \dots, N, t = 1, 2, \dots, T \tag{13.102}$$

$$x_{i,t-1} - x_{i,t} \leq 1 - x_{i,\beta} \quad \beta = t+1, \dots, \min\{t+t_{\mathrm{down}}-1, T\}, i = 1, 2, \dots, N, t = 1, 2, \dots, T \tag{13.103}$$

$$x_{i,t} \in \{0, 1\} \quad t = 1, 2, \dots, T, i = 1, 2, \dots, N \tag{13.104}$$

where

$F_{i,t}$: The fuel cost of the generator unit i at time t

$S_{i,t}$: The cost of starting up unit i at time t

$P_{\mathrm{D}t}$: The load demand at time t

$P_{i,t}$: The power output of unit i at time t

T: The time period

$x_{i,t}$: The 0–1 variable; 1 if the unit i on at time t, 0 otherwise

$1 - \alpha$: The prescribed probability level for meeting load over the entire time horizon

t_{up}: The minimum number of hours required for a generator to stay up once it is on

t_{down}: The minimum number of hours required for a generator to stay down once it is off

The objective function consists of the total fuel cost and the starting up cost of the generators. Constraints in equations (13.102) and (13.103) are the uptime/downtime constraints that force the generators to stay up for at least a specified amount of time, t_{up}, once they are turned on and stay down for at least a specified time period, t_{down}, once they are shut down. Constraint (13.100) ensures that the power generated matches the minimum and maximum capacity requirements of the corresponding generators for all time periods. The spinning reserve constraint (13.101) attempts to ensure that there is enough power available to meet the demand in the event of an unusual contingency. The power balance constraint (13.99) is the linking constraints that link the decision variables of different generators and time periods. These constraints ensure that the estimated load is satisfied in all time periods. They cause difficulties in solving the problem because adding them to the constraint set makes the problem inseparable, thus requiring sophisticated techniques for finding a solution.

13.7.2.2 *Stochastic Model*   Let P_D, a random variable, denote the load at hour t. It can be expressed as a multivariate normal distribution with a specific correlation structure: $P_D \sim N(\mu, \Sigma)$ with mean vector μ and covariance matrix Σ where μ_t and σ_t are the corresponding mean and standard deviation for time period t. Changing the equal constraint of the real power balance equation into an inequality constraint, and replacing it by the following probabilistic constraint for each hour, gives a probability level for satisfying the linking constraint over all time periods.

$$P\left[\sum_{i=1}^{N} x_{i,t} P_{i,t} \geq P_D \quad t = 1, 2, \ldots, T\right] \geq 1 - \alpha \qquad (13.105)$$

We replace the probability constraint (13.105) by a set of T separate probability constraints each of which could be inverted to obtain a set of T equivalent deterministic linear inequalities. Initially we chose the T constraints in a manner such that together they were more stringent than constraint (13.105). The initial set of T individual linear constraints (13.110) replacing equation (13.105) were obtained by the following argument.

First we denote the event $\sum_{i=1}^{N} x_{i,t} P_{i,t} \geq P_D$ by A_t and its complement event $\sum_{i=1}^{N} x_{i,t} P_{i,t} < P_D$ by A_t^c. From Boole's inequality of probability theory, it is well known that:

$$P\left[\bigcup_{t=1}^{T} A_t\right] \leq \sum_{t=1}^{T} P[A_t] \qquad (13.106)$$

If

$$P[A_t^c] \leq \frac{\alpha}{T}, \quad t = 1, 2, \ldots, T \qquad (13.107)$$

then

$$P\left[\bigcap_{t=1}^{T} A_t\right] = 1 - P\left[\bigcup_{t=1}^{T} A_t^c\right] \geq 1 - \sum_{t=1}^{T} P[A_t^c] \geq 1 - \alpha \qquad (13.108)$$

Because P_D is normally distributed with mean μ_t and standard deviation σ_t, $P[A_t^c] \leq \frac{\alpha}{T}$ is equivalent to

$$P\left[\sum_{i=1}^{N} x_{i,t} P_{i,t} < P_{D}\right] \leq \frac{\alpha}{T} \tag{13.109}$$

which is equivalent to

$$\sum_{i=1}^{N} x_{i,t} P_{i,t} \geq \mu_t + (z_\alpha/T)\sigma_t \qquad t = 1, 2, \dots, T \tag{13.110}$$

where (z_α/T) is the $100(1 - \alpha/T)$th percentile of the standard normal distribution. Setting the initial value of z be $z = z_\alpha/T$, we get

$$\sum_{i=1}^{N} x_{i,t} P_{i,t} \geq \mu_t + z\sigma_t \qquad t = 1, 2, \dots, T \tag{13.111}$$

13.7.3 Chance-Constrained Optimization Algorithm

The deterministic form of the stochastic constraint is used in solving the UCP iteratively by using a different value for at each iteration. The steps of the CCO algorithm are below.

Step (1): Choose an initial value in equation (13.111).

Step (2): Choose a starting set of λ multipliers.

Step (3): For each unit i solve a dynamic program with $4T$ states and T stages; obtain $q^*(\lambda^k)$, which is the objective function value of the optimal solution to the Lagrange dual problem.

Step (4): Solve the economic dispatch problem for each hour, using the scheduled units, and obtain J^*, which is the objective function value of the optimal solution to the primal problem.

Step (5): Check the relative duality gap.

Step (6): Update λ, using

$$\lambda^{k+1} = \lambda^k + s^k g^k \tag{13.112}$$

where

$$s^k = \frac{\eta^k \left(J^* - q^*(\lambda^k)\right)}{\|g^k\|^2} \tag{13.113}$$

$$\eta^k = \frac{1+m}{k+m} \tag{13.114}$$

and g^k is the subgradient and m is a constant. If the gap is not small enough, then go back to step (3). Otherwise, continue.

Table 13.4   Values Used in Checking Convergence of z-Update Algorithm

p_{target}	0.8	0.9	0.95	0.99	0.999	0.9999
ε	0.005	0.005	0.005	0.005	0.0005	0.00005

Step (7): If the final solution is feasible, go to step (8). Otherwise, use the heuristic algorithm to derive a feasible solution.

Step (8): Evaluate the multivariate normal probability, using model (13.105); if it differs from the prescribed probability level by more than a preassigned small quantity (see Table 13.4) then update z and go back to step (2); otherwise, STOP.

The algorithm starts by choosing a high value for the initial z value as in equation (13.110), which makes the corresponding solution satisfy the load with a probability level higher than $p_{target} = 1 - \alpha$. At step (2), all λ multipliers are set to 0.0. Then at step (3) the dual problem is solved with dynamic programming and $q^*(\lambda^k)$, the objective function value for the solution to the Lagrange dual problem, is obtained. At this step the scheduling problem for each generator is solved separately to decide which generators should be turned on at each time period.

At step (4) an economic dispatch problem is solved for each time period separately. In solving the economic dispatch problem the algorithm obtains the operating levels for all of the scheduled generators determined at step (3); J^*, the objective function value of the solution to the primal problem, is calculated with the operating levels for the scheduled units at this step. At step (5) the duality gap is checked, and if it is less than δ then the algorithm proceeds to step (7); otherwise, the λ multipliers are updated with a subgradient method that determines the improving direction at step (6). The δ may be selected as 0.05%. Before proceeding to evaluate the multivariate normal probability one needs to check whether the final UC schedule is feasible, because Lagrange relaxation techniques frequently provide infeasible solutions. If the result is feasible, the algorithm continues to step (8); otherwise, a heuristic is used to derive a feasible solution and the algorithm proceeds to step (8) after this. The heuristic applied here is simply to turn on the cheapest generator available for the time periods that have a shortage of power. After modifying the schedule, the heuristic checks whether the duality gap is still less than δ.

At step (8) of the CCO algorithm one needs to calculate the multivariate normal probability. This is needed to ensure that the probabilistic constraint, equation (13.105), is satisfied with the prescribed joint probability over the entire time horizon. This calculation can become time consuming, especially when the dimension of the time horizon is large. A subregion adaptive algorithm for carrying out multivariate integration makes this calculation feasible. If the calculated probability level is in the ε neighborhood of p_{target} the algorithm terminates, since the goal of finding a schedule that satisfies the load

with a probability of p_{target} is accomplished; otherwise, the z-value is updated and the previous steps are repeated to obtain another schedule.

To update the z-value the following algorithm is used. The goal is to find a z-value in equation (13.111) that provides a schedule such that the load can be satisfied with a probability of $p_{target} = 1 - \alpha$ over the entire time horizon. This z-value needs to be obtained iteratively. The following iterative scheme may be used. First, start with two values that are known to be upper and lower bounds to the needed z-value. Then, run steps (2)–(7) of the CCO algorithm and then find the actual probabilities of meeting the load for these assumed z-values. They also indicate the direction and the magnitude by which we should change these z-values so that the probability target can be reached through successive iterations using interpolation. The correct z-value could be obtained in a few iterations.

The algorithm proceeds as follows. First we choose $z = z_\alpha$ in equation (13.111). Obviously, it yields a lower bound for the correct z-value; we call this z_{lower}. We now run steps (2)–(7) of the CCO algorithm for this lower bound and obtain an estimate of the probability with which the load is being met. We call this probability p_{lower}. Next we choose an arbitrary large value for z. We denote it by z_{upper}. In the next step we obtain the upper percentiles of the standard normal distribution for these probabilities p_{upper} and p_{lower} and denote them by z_1 and z_2, respectively. We also denote the corresponding percentile for the p_{target} value by z_{target}. Based on these values the updated z-value is obtained with the following linear interpolation formula:

$$z_{new} = z_{lower} + \frac{z_{target} - z_1}{z_2 - z_1}\left(z_{upper} - z_{lower}\right) \qquad (13.115)$$

If the z_{new} value is lower than z_2 and higher than z_{target}, then replace z_2 by z_{new}. If it is lower than z_{target} and higher than z_1, replace z_1 by z_{new}. Repeat this process, using equation (13.115) until p_{target} is reached.

13.8   VAR OPTIMIZATION WITH UNCERTAIN REACTIVE LOAD

13.8.1   Linearized VAR Optimization Model

As discussed in Chapter 10, the VAR optimization problem is concerned with minimizing real power transmission losses and improving the system voltage profile by dispatching available reactive power sources in the system. For the purpose of the simplification, the hypersurface of the nonlinear power loss function is approximated by its tangent hyperplane at the current operating point, and linear programming (LP) is adopted for the VAR control problem. This linear approximation is found to be valid over a small region that is formulated by imposing limits on the deviations of the control variables from their current values. Assume that the voltage phase angles will be fixed in each

optimization iteration to disregard the coupling between phase angles and reactive variables. Real power injections at various buses will be fixed except at the slack bus, which compensates for power losses. The deterministic operating points are found by executing an ac power flow after each LP iteration, which results in revised system voltage magnitudes and angles. The objective function and constraints are linearized around this new operating point assuming fixed active power-related variables.

The linearized objective function of VAR optimization can be written as [25, 26]:

$$\min \Delta P_L = \left[\frac{\partial P_L}{\partial V_1}, \frac{\partial P_L}{\partial V_2}, \ldots, \frac{\partial P_L}{\partial V_n}, \right] \begin{bmatrix} \Delta V_1 \\ \Delta V_2 \\ \vdots \\ \Delta V_n \end{bmatrix} \tag{13.116}$$

or

$$\min \Delta P_L = M \Delta V \tag{13.117}$$

where M is the row vector relating to real power loss increments to bus voltage increments.

There are $m + l + n$ constraints. The first m constraints are for reactive power sources and tap changing transformer terminals. We will refer to the matrix of reactive power injections at these buses as Q_1. The l equality constraints are for loads and junction buses that are not connected to transformer terminals, and we will refer to the matrix of reactive power injections at these buses as Q_2. The last n constraints are the limits on bus voltages. Therefore, the linearized form of the constraints is given as

$$\Delta Q_{1\min} \leq \Delta Q_1 = J_1^* \Delta V \leq \Delta Q_{1\max} \tag{13.118}$$

$$\Delta Q_2 = J_2^* \Delta V = 0 \tag{13.119}$$

$$\Delta V_{\min} \leq \Delta V \leq \Delta V_{\max} \tag{13.120}$$

where J_1^* and J_2^* are submatrices of J^*, which is the modified Jacobian matrix.

Similar to Section 13.5, the trapezoidal distribution is used to model the uncertainty of reactive power load. The possibility distribution will have a value of 1 for load values that are highly possible, and will drop for low possible loads. A zero possibility is assigned to load values that are rather impossible to occur.

As load changes, the magnitude of voltages at different buses will change accordingly. If the injected power at load bus i is changed by ΔQ_{ci} due to capacitor switching or load change, the corresponding change in load bus voltages is given as,

$$\Delta V_{Di} = D\Delta Q_{ci} \qquad (13.121)$$

where D is a nonnegative matrix, suggesting that if each ΔQ_{ci} is positive because of a load reduction, then ΔV_{Li} will be positive. On the other hand, if the injected power is decreased because of a load increase, then the load bus voltages will decrease.

For generator buses, it is obvious that an increase in the injected load power will cause the generator voltages to decrease and vice versa.

13.8.2 Formulation of Fuzzy VAR Optimization Problem

The minimization in the VAR optimization problem is subject to inequality and equality constraints, which are referred to as the operating constraints. The operating constraints will be a set of linking constraints imposed on bus voltages and four independent sets of constraints corresponding to the break points of the trapezoidal possibility distribution. With the same approach described in Section 13.5, the formulation of the fuzzy VAR optimization problem for determining the possibility distribution of transmission losses for a given possibility distribution of loads can be expressed as below:

$$\min \Delta P_L = \sum_{i=1}^{n} \sum_{k=1}^{4} \frac{M_i^{(k)} \Delta V_i^{(k)}}{4} \qquad (13.122)$$

s.t.

$$\Delta Q_{1\min} \le \Delta Q_1^{(k)} = J_1^{*(k)} \Delta V^{(k)} \le \Delta Q_{1\max} \qquad (13.123)$$

$$\Delta Q_2^{(k)} = J_2^{*(k)} \Delta V^{(k)} = 0 \qquad (13.124)$$

$$V_{\min} \le V^{(1)} + \Delta V^{(1)} \le V^{(2)} + \Delta V^{(2)} \le V^{(3)} + \Delta V^{(3)} \le V^{(4)} + \Delta V^{(4)} \le V_{\max} \qquad (13.125)$$

where, $k = 1, 2, 3, 4$ and equation (13.122) represents the minimization of fuzzy variables ΔP_L. The $J_1^{*(k)}$ and $J_2^{*(k)}$ are submatrices of matrices of $J^{*(k)}$, which is the modified Jacobian matrix of the kth break point of the possibility distribution. The dimension of the problem is very large, which will be reduced through the application of the DWD [27].

13.9 PROBABILISTIC OPTIMAL POWER FLOW

13.9.1 Introduction

We discuss the deterministic optimal power flow (OPF) problem in Chapter 8. If uncertain factors such as loads are considered as in the previous sections, we can transform the OPF problem into the **probabilistic optimal power flow (P-OPF)** problem [28, 29]. Probabilistic programming, or probabilistic

optimization, is concerned with the introduction of probabilistic randomness or uncertainty into conventional linear and nonlinear programs. However, the randomness introduced tends to have some structure to it, and this structure is generally represented with a **probability density function (PDF)**. The goal of the P-OPF problem is to determine the PDFs for all variables in the problem. These PDFs are the distributions of the optimal solutions. This section will introduce several P-OPF methods.

13.9.2 Two-Point Estimate Method for OPF

Generally, the OPF can be seen as a multivariate nonlinear function

$$Y = h(X) \tag{13.126}$$

where X is the input vector and Y is the output vector.

It must be noted that an uncertain input vector renders all output variables uncertain as well. To account for uncertainties in the P-OPF, a two-point estimate method (TPEM) [30], which is basically a variation of the original point estimate method (PEM), is used to decompose the problem (13.126) into several subproblems by taking only two deterministic values of each uncertain variable placed on both sides of the corresponding mean. The deterministic OPF is then run twice for each uncertain variable, once for the value below the mean, and once for the value above the mean, with other variables kept at their means. This method is described in detail below.

Suppose that $Y = h(X)$ is a general nonlinear multivariate function. The goal is to find the PDF $f_Y(y)$ of Y when the PDF $f_X(x)$ is known, where $x \in X$ and $y \in Y$. There are several approximate methods to address this problem. The PEM is a simple-to-use numerical method for calculating the moments of the underlying nonlinear function. The method was developed by Rosenblueth in the 1970s [31] and is used to calculate the moments of a random quantity that is a function of one or several random variables. Although the moments of the output variables are calculated, one has no information on the associated probability distribution (PD). Generally speaking, this PD can be any PD with the same first three moments; however, when the PD of the input variables is known, the output variables tend to have the same PD, as shown in the OPF problem, where both input and output variables are normally distributed. However, in some cases, the discrete behavior of the OPF results in PD of the output variables that is not normal anymore.

Let X denote a random variable with PDF $f_X(x)$; for $Y = h(X)$, the PEM uses two probability concentrations to replace $h(X)$ by matching the first three moments of $h(X)$. When Y is a function of n random variables, the PEM uses 2^n probability concentrations located at 2^n points to replace the original joint PDF of the random variables by matching up to the second- and third-order noncrossed moments. The moment of Y, i.e., $E(y^k)$, $k = 1,2$, where E is the exception, is then calculated by weighting the values of Y to the power of k

evaluated at each of the 2^n points. When n becomes large, the use of 2^n probability concentrations is not economical. Hence, a simplified method that makes use of only $2n$ estimates, which is referred to as a TPEM, is used in an OPF problem with uncertainty.

13.9.2.1 *Function of One Variable*

First, a fictitious distribution of X is chosen in such a way that the first three moments exactly match the first three moments of the given PDF of X. To estimate the first three moments of Y, one can choose a distribution of X having only two concentrations placed unsymmetrically around the X's expectation. If that is the case, one has enough parameters to take into account the first three moments of Y and to obtain a third-order approximation to the first three moments of Y. A particularly simple function satisfying these requirements consists in two concentrations, P_1 and P_2, of the probability density function $f_X(x)$, respectively, at $X = x_1$ and x_2

$$f_X(x) = P_1\delta(x - x_1) + P_2\delta(x - x_2) \tag{13.127}$$

where the lower case letters denote specific values of a random variable, and $\delta(\bullet)$ is Dirac's delta function.

Choosing

$$\eta_i = \frac{|x_i - \mu_X|}{\sigma_X}, \quad i = 1,2 \tag{13.128}$$

where μ_X and σ_X are the mean and the standard deviation of X, respectively, one can calculate the first three moments of $f_X(x)$. Thus, the jth moment is defined as

$$M_j(X) = \int_{-\infty}^{\infty} x^j f_X(x)dx \quad j = 1, 2, \dots \tag{13.129}$$

The central moments are

$$M_j'(X) = \int_{-\infty}^{\infty} (x - \mu_X)^j f_X(x)dx \quad j = 1, 2, \dots \tag{13.130}$$

The zeroth and the first moment always equal 1 and 0, respectively. The zeroth and the first three central moments of equation (13.127) are then

$$M_0' = 1 = P_1 + P_2 \tag{13.131}$$

$$M_1' = 0 = \eta_1 P_1 - \eta_2 P_2 \tag{13.132}$$

$$M_2' = \sigma_X^2 = \sigma_X^2 (\eta_1^2 P_1 + \eta_2^2 P_2) \tag{13.133}$$

$$M_3' = \nu_X \sigma_X^3 = \sigma_X^3 (\eta_1^3 P_1 - \eta_2^3 P_2) \tag{13.134}$$

where ν_X is the skewness of X.

Using the Taylor series expansion of $h(X)$ about μ_X yields

$$h(X) = h(\mu_X) + \sum_{j=1}^{\infty} \frac{1}{j!} g^{(j)}(\mu_X)(x - \mu_X)^j \tag{13.135}$$

where $g^{(j)}, j = 1,2, \dots$, stands for the jth derivative of h with respect to x. The mean value of Y can be calculated by taking the expectation of the above equation, resulting in

$$\mu_Y = E(h(X)) = \int_{-\infty}^{\infty} h(x) f_X(x) dx = h(\mu_X) + \sum_{j=1}^{\infty} \frac{1}{j!} g^{(j)}(\mu_X) M_j'(X) \tag{13.136}$$

Let

$$x_i = \mu_X + \eta_i \sigma_X, \quad i = 1, 2 \tag{13.137}$$

and P_i be the probability concentrations at location x_i, $i = 1,2$. Multiplying equation (13.135) by P_i, and summing them up, we get

$$P_1 h(x_1) + P_2 h(x_2) = h(\mu_X)(P_1 + P_2) + \sum_{j=1}^{\infty} \frac{1}{j!} g^{(j)}(\mu_X)(P_1 \eta_1^j + P_2 \eta_2^j) \sigma_X^j \tag{13.138}$$

From the first four terms of equations (13.136) and (13.138), we get

$$P_1 + P_2 = M_0'(X) = 1 \tag{13.139}$$

$$\eta_1 P_1 + \eta_2 P_2 = M_1'(X)/\sigma_X = \lambda_{X,1} \tag{13.140}$$

$$\eta_1^2 P_1 + \eta_2^2 P_2 = M_2'(X)/\sigma_X^2 = \lambda_{X,2} \tag{13.141}$$

$$\eta_1^3 P_1 + \eta_2^3 P_2 = M_3'(X)/\sigma_X^3 = \lambda_{X,3} \tag{13.142}$$

The above four equations have four unknowns, i.e., P_1, P_2, η_1 and η_2. Their solutions are

$$\eta_1 = \lambda_{X,3}/2 + \sqrt{1 + (\lambda_{X,3}/2)^2} \tag{13.143}$$

$$\eta_2 = \lambda_{X,3}/2 - \sqrt{1 + (\lambda_{X,3}/2)^2} \tag{13.144}$$

$$P_1 = -\eta_2/\varepsilon \tag{13.145}$$

$$P_2 = \eta_1/\varepsilon \tag{13.146}$$

where

$$\varepsilon = \eta_1 - \eta_2 = 2\sqrt{1 + (\lambda_{X,3}/2)^2} \tag{13.147}$$

For a normal distribution, $\lambda_{X,3} = 0$; then equations (13.143)–(13.146) can be simplified as

$$\eta_1 = 1 \tag{13.148}$$

$$\eta_2 = -1 \tag{13.149}$$

$$P_1 = P_2 = 1/2 \tag{13.150}$$

From equations (13.138)–(13.142) and equations (13.148)–(13.150), we get

$$h(\mu_X) + \sum_{j=1}^{3} \frac{1}{j!} g^{(j)}(\mu_X)\lambda_{X,j}\eta_X^j = P_1 h(x_1) + P_2 h(x_2)$$
$$-\sum_{j=4}^{\infty} \frac{1}{j!} g^{(j)}(\mu_X)\left(P_1\eta_1^j + P_2\eta_2^j\right)\sigma_X^j \tag{13.151}$$

Substituting equation (13.151) into equation (13.136)

$$\mu_Y = P_1 h(x_1) + P_2 h(x_2) + \sum_{j=4}^{\infty} \frac{1}{j!} g^{(j)}(\mu_X)\left(\lambda_{X,j} - P_1\eta_1^j - P_2\eta_2^j\right)\sigma_X^j \tag{13.152}$$

and neglecting the third term in equation (13.152), we get

$$\mu_Y \approx P_1 h(x_1) + P_2 h(x_2) \tag{13.153}$$

This is a third-order approximation if $h(X)$ is a third-order polynomial, meaning the derivatives of the order higher than three are zero. In this case, TPEM gives the exact solution to μ_Y.

Similarly, the second- and the third-order moment of Y can be approximated by

$$E(Y^2) \approx P_1 h(x_1)^2 + P_2 h(x_2)^2 \tag{13.154}$$

$$E(Y^3) \approx P_1 h(x_1)^3 + P_2 h(x_2)^3 \tag{13.155}$$

13.9.2.2 *Function of Several Variables* Let Y be a random quantity that is a function of n random variables, i.e.,

$$Y = h(X) = h(x_1, x_2, \ldots, x_n) \tag{13.156}$$

Let $\mu_{X,k}, \sigma_{X,k}, \nu_{X,k}$ stand for the mean, standard deviation, and skewness of X_k, respectively. Let $P_{k,i}$ stand for the concentrations (or weights) located at

$$X = [\mu_{X,1}, \mu_{X,2}, \ldots, \mu_{X,n}] \tag{13.157}$$

and

$$x_{k,i} = \mu_{X,k} + \eta_{k,i}\sigma_{X,k}, \quad i = 1, 2, \ldots, n \tag{13.158}$$

Expand equation (13.156) in a multivariable Taylor series about the mean value of X. Similar to the case of a function of one variable, the following three equations can be obtained by matching the first three moments of the probability density function of X_k.

$$\sum_{k=1}^{n} (P_{k,1} + P_{k,2}) = 1 \tag{13.159}$$

$$\eta_{k,1}P_{k,1} + \eta_{k,2}P_{k,2} = M_1'(X_k)/\sigma_{X,k} = \lambda_{X,k,1} \tag{13.160}$$

$$\eta_{k,1}^2 P_{k,1} + \eta_{k,2}^2 P_{k,2} = M_2'(X_k)/\sigma_{X,k}^2 = \lambda_{X,k,2} \tag{13.161}$$

$$\eta_{k,1}^3 P_{k,1} + \eta_{k,2}^3 P_{k,2} = M_3'(X_k)/\sigma_{X,k}^3 = \lambda_{X,k,3} \tag{13.162}$$

Equation (13.159) can also be expressed as

$$P_{k,1} + P_{k,2} = 1/n \tag{13.163}$$

We also can get the solution for the random variable X_k.

$$\eta_{k,1} = \lambda_{k,3}/2 + \sqrt{n + (\lambda_{k,3}/2)^2} \tag{13.164}$$

$$\eta_{k,2} = \lambda_{k,3}/2 - \sqrt{n + (\lambda_{k,3}/2)^2} \tag{13.165}$$

$$P_{k,1} = -\eta_{k,2}/(n\varepsilon_k) \tag{13.166}$$

$$P_{k,2} = \eta_{k,1}/(n\varepsilon_k) \tag{13.167}$$

where

$$\varepsilon_k = \eta_{k,1} - \eta_{k,2} = 2\sqrt{n + (\lambda_{k,3}/2)^2}, \quad k = 1, 2, \ldots, n \tag{13.168}$$

For symmetric probability distributions, $\lambda_{k,3} = 0$; then equations (13.164)–(13.167) can be simplified as below:

$$\eta_{k,1} = \sqrt{n} \tag{13.169}$$

$$\eta_{k,2} = -\sqrt{n} \tag{13.170}$$

$$P_{k,1} = P_{k,2} = 1/(2n) \tag{13.171}$$

Thus the first three moments can then be approximated by

$$E(Y) \approx \sum_{k=1}^{n} \sum_{i=1}^{2} (P_{k,i} h([\mu_{X,1}, \ldots, \mu_{k,i}, \ldots, \mu_{X,n}])) \tag{13.172}$$

$$E(Y^2) \approx \sum_{k=1}^{n} \sum_{i=1}^{2} \left(P_{k,i} h([\mu_{X,1}, \ldots, \mu_{k,i}, \ldots, \mu_{X,n}])^2\right) \tag{13.173}$$

$$E(Y^3) \approx \sum_{k=1}^{n} \sum_{i=1}^{2} \left(P_{k,i} h([\mu_{X,1}, \ldots, \mu_{k,i}, \ldots, \mu_{X,n}])^3\right) \tag{13.174}$$

13.9.2.3 Computational Procedure The procedure for computing the moments of the output variables for the OPF problem can be summarized in the following steps [29].

(1) Determine the number of uncertain variables.
(2) Set $E(Y) = 0$ and $E(Y^2) = 0$.
(3) Set $k = 1$.
(4) Determine the locations of concentrations $\eta_{k,1}$, $\eta_{k,2}$ and the probabilities of concentrations $P_{k,1}$, $P_{k,2}$ from equations (13.169)–(13.171).
(5) Determine the two concentrations $x_{k,1}$, $x_{k,2}$

$$x_{k,1} = \mu_{X,k} + \eta_{k,1} \sigma_{X,k} \tag{13.175}$$

$$x_{k,2} = \mu_{X,k} + \eta_{k,2} \sigma_{X,k} \tag{13.176}$$

where $\mu_{X,k}$, $\sigma_{X,k}$ are the mean and standard derivation of X_k, respectively.
(6) Run the deterministic OPF for both concentrations $x_{k,j}$, using

$$X = [\mu_{X,1}, \mu_{X,2}, \ldots, \mu_{X,n}]$$

(7) Update $E(Y)$ and $E(Y^2)$, using equations (13.172) and (13.173).
(8) Calculate the mean and the standard deviation

$$\mu_Y = E(Y) \tag{13.177}$$

$$\sigma_Y = \sqrt{E(Y)^2 - \mu_Y^2} \tag{13.178}$$

(9) Repeat steps (4) to (8) for $k = k + 1$ until the list of uncertain variables is exhausted.

13.9.2.4 Comparison TPEM with MCS   Since OPF is a deterministic tool, it would have to be run many times to encompass all, or at least the majority of, possible operating conditions. More accurate Monte Carlo simulations (MCS), which are able to handle "complex" random variables, are an option but are computationally more demanding and, as such, of limited use for online types of applications. Here, the mean and the standard deviation of the TPEM are compared with the corresponding values obtained with the MCS, which are calculated as

$$\mu_{MCS} = \frac{1}{N} \sum_{i=1}^{N} x_i \tag{13.179}$$

$$\sigma_{MCS} = \sqrt{\frac{1}{N} \sum_{i=1}^{N} (x_i - \mu_{MCS})^2} \tag{13.180}$$

where N is number of Monte Carlo samples, and x is the variable for which the mean μ_{MCS} and the standard deviation σ_{MCS} are calculated. The errors for the mean and standard deviation, respectively, are therefore defined as

$$\varepsilon_{\mu} = \frac{\mu_{MCS} - \mu_{TPEM}}{\mu_{MCS}} \times 100\% \tag{13.181}$$

$$\varepsilon_{\sigma} = \frac{\sigma_{MCS} - \sigma_{TPEM}}{\sigma_{MCS}} \times 100\% \tag{13.182}$$

The investigation and tests show that the output variables tend to have the same PD as the input variables, which is a normal distribution. Thus the corresponding mean and standard deviation of the TPEM and MCS work reasonably well in most cases, given the fact that output variables tend to be normally distributed.

It is noted that the TPEM approach is accurate provided that the OPF is "well behaved" and that the number of uncertain parameters is not "too large." In larger systems, the TPEM does not perform well if the number of uncertain variables is too large. With lower numbers of uncertain variables, the performance is adequate. The TPEM method is computationally significantly faster than using an MCS approach. This is especially true when the number of uncertain parameters is low, since the computational time is directly proportional to the number of uncertain variables. When the number of random variables is large, MCS is a better alternative, given its accuracy.

13.9.3 Cumulant-Based Probabilistic Optimal Power Flow [32]

13.9.3.1 Gram–Charlier A Series   The Gram–Charlier A Series allows many PDFs, including Gaussian and gamma distributions, to be expressed as

a series composed of a standard normal distribution and its derivatives. As a part of the proposed P-OPF method, distributions are reconstructed with the use of the Gram–Charlier A Series. The series can be stated as follows:

$$f(x) = \sum_{j=0}^{\infty} c_j He_j(x)\alpha(x) \tag{13.183}$$

where $f(x)$ is the PDF for the random variable X, c_j is the jth series coefficient, $He_j(x)$ is the jth Tchebycheff–Hermite, or Hermite, polynomial, and $\alpha(x)$ is the standard normal distribution function.

The Gram–Charlier form uses moments to compute series coefficients, while the Edgeworth form uses cumulants, which is discussed here.

Since the PDF for a normal distribution is an exponential term, taking derivatives successively returns the original function with a polynomial coefficient multiplier. These coefficients are referred to as Tchebycheff–Hermite, or Hermite, polynomials.

To illustrate how the Hermite polynomials are generated, the first four derivatives of the standard unit normal distribution are taken as follows:

$$D^0\alpha(x) = D^0 e^{-\frac{1}{2}x^2} = e^{-\frac{1}{2}x^2} \tag{13.184}$$

$$D^1\alpha(x) = D^1 e^{-\frac{1}{2}x^2} = -x e^{-\frac{1}{2}x^2} \tag{13.185}$$

$$D^2\alpha(x) = D^2 e^{-\frac{1}{2}x^2} = (x^2 - 1) e^{-\frac{1}{2}x^2} \tag{13.186}$$

$$D^3\alpha(x) = D^3 e^{-\frac{1}{2}x^2} = (3x - x^3) e^{-\frac{1}{2}x^2} \tag{13.187}$$

$$D^4\alpha(x) = D^4 e^{-\frac{1}{2}x^2} = (x^4 - 6x^2 + 3) e^{-\frac{1}{2}x^2} \tag{13.188}$$

where D^n is the nth derivative.

The Tchebycheff–Hermite polynomials are the polynomial coefficients in the derivatives. Using the results of the first four derivatives in equations (13.184)–(13.188), the first five Tchebycheff–Hermite polynomials are written as follows:

$$He_0(x) = 1 \tag{13.189}$$

$$He_1(x) = x \tag{13.190}$$

$$He_2(x) = x^2 - 1 \tag{13.191}$$

$$He_3(x) = x^3 - 3x \tag{13.192}$$

$$He_4(x) = x^4 - 6x^2 + 3 \tag{13.193}$$

Because of the structure of equations (13.184)–(13.188), the highest-power coefficients of the odd derivatives, i.e., the third, fifth, seventh, etc., are negative. Equations (13.189)–(13.193) have been formed following the convention

that the equations relating to the odd derivatives are multiplied by negative one, such that the coefficient of the highest power is positive [33].

Therefore, the nth Tchebycheff–Hermite polynomial can be symbolically written as

$$He_n(x)\alpha(x) = (-D)^n \alpha(x) \qquad (13.194)$$

In addition, a recursive relationship is available to determine third-order and higher polynomials

$$He_n(x) = xHe_{n-1}(x) - (n-1)He_{n-2} \qquad (13.195)$$

13.9.3.2 Edgeworth A Series Coefficients

Given the cumulants for a distribution in standard form, i.e., zero mean and unit variance, the coefficients for the Edgeworth form of the A series can be computed. To find the equations for the A series coefficients, an exponential representation of the PDF is broken into its series representation and equated with the Gram–Charlier A series in equation (13.183).

The PDF, as an exponential, is written in the following form using cumulants [9]:

$$f(x) = e^{\left(-\frac{K_3}{3!}D^3 + \frac{K_4}{4!}D^4 - \frac{K_5}{5!}D^5 + \cdots\right)}\alpha(x) \qquad (13.196)$$

where D^n is the nth derivative of the unit normal distribution, K_n is the nth cumulant, and $\alpha(x)$ is the standard unit normal PDF.

Expanding equation (13.196) as an exponential series yields

$$f(x) = \left[1 + \frac{\left(-\frac{K_3}{3!}D^3 + \frac{K_4}{4!}D^4 - \frac{K_5}{5!}D^5 + \cdots\right)}{1!} \right.$$
$$+ \frac{\left(-\frac{K_3}{3!}D^3 + \frac{K_4}{4!}D^4 - \frac{K_5}{5!}D^5 + \cdots\right)^2}{2!}$$
$$\left. + \frac{\left(-\frac{K_3}{3!}D^3 + \frac{K_4}{4!}D^4 - \frac{K_5}{5!}D^5 + \cdots\right)^3}{3!} + \cdots \right]\alpha(x) \qquad (13.196)$$

If each of the terms is expanded individually and grouped based on powers of D, the following result is obtained:

Table 13.5   A Series Coefficient Equation

Coefficient	Equation
0	1
1	0
2	0
3	$\dfrac{K_3}{6}$
4	$\dfrac{K_4}{24}$
5	$\dfrac{K_5}{120}$
6	$\dfrac{1}{720}(K_6 + 10K_3^2)$
7	$\dfrac{1}{5040}(K_7 + 35K_3K_4)$

$$f(x) = \left[1 - \frac{K_3}{3!}D^3 + \frac{K_4}{4!}D^4 - \frac{K_5}{5!}D^5 + \left(\frac{K_6}{6!} + \frac{K_3^2}{2!3!^2} \right)D^6 \right.$$
$$\left. + \left(\frac{K_7}{7!} + \frac{2K_3K_4}{2!3!4!} \right)D^7 + \cdots \right]\alpha(x) \qquad (13.197)$$

Returning to the definition for the Gram–Charlier A series in equation (13.183) and expanding the summation yields

$$f(x) = c_0 He_0(x)\alpha(x) + c_1 He_1(x)\alpha(x) + c_2 He_2(x)\alpha(x) + \cdots \qquad (13.198)$$

Comparing equations (13.197) and (13.198), the values for the coefficients can be determined. Based on the equations presented, the first seven terms of the Edgeworth form of the A series are presented in Table 13.5.

13.9.3.3 Adaptation of the Cumulant Method to the P-OPF Problem   The cumulant method relies on the behavior of random variables and their associated cumulants when they are combined in a linear fashion. This section discusses the formation of random variables from a linear combination of others and the role cumulants play in this combination.

Given a new random variable z, which is the linear combination of independent random variables, $c_1, c_1, \ldots, c_n$

$$z = a_1 c_1 + a_2 c_2 + \cdots + a_n c_n \qquad (13.199)$$

the moment generating function $\Phi_z(s)$ for the random variable z can be written as

$$\Phi_z(s) = E[e^{sz}] = E[e^{s(a_1c_1 + a_2c_2 + \cdots + a_nc_n)}]$$
$$= E[e^{s(a_1c_1)}e^{s(a_2c_2)} \ldots \ldots e^{s(a_nc_n)}] \tag{13.200a}$$

Since $c_1, c_2, \ldots, c_n$ are independent, the above equation can be written as

$$\Phi_z(s) = E[e^{s(a_1c_1)}]E[e^{s(a_2c_2)}] \ldots \ldots E[e^{s(a_nc_n)}]$$
$$= \Phi_{c_1}(a_1s)\Phi_{c_2}(a_2s) \ldots \ldots \Phi_{c_n}(a_ns) \tag{13.200b}$$

The cumulants for the variable z can be computed with the cumulant generating function, in terms of the component variables as follows:

$$\Psi_z(s) = \ln(\Phi_z(s)) = \ln(\Phi_{c_1}(a_1s)\Phi_{c_2}(a_2s) \cdots\cdots \Phi_{c_n}(a_ns))$$
$$= \ln(\Phi_{c_1}(a_1s)) + \ln(\Phi_{c_2}(a_2s)) + \cdots\cdots + \ln(\Phi_{c_n}(a_ns))$$
$$= \Psi_{c_1}(a_1s) + \Psi_{c_2}(a_2s) + \cdots\cdots + \Psi_{c_n}(a_ns) \tag{13.201}$$

To compute the second-order cumulant, the first- and second-order derivatives of the cumulant generating function for the random variable z are computed as

$$\Psi_z'(s) = a_1\Psi_{c_1}'(a_1s) + a_2\Psi_{c_2}'(a_2s) + \cdots\cdots + a_n\Psi_{c_n}'(a_ns) \tag{13.202}$$
$$\Psi_z''(s) = a_1^2\Psi_{c_1}''(a_1s) + a_2^2\Psi_{c_2}''(a_2s) + \cdots\cdots + a_n^2\Psi_{c_n}''(a_ns) \tag{13.203}$$

Evaluating equation (13.203) at $s = 0$ gives

$$\Psi_z''(0) = a_1^2\Psi_{c_1}''(0) + a_2^2\Psi_{c_2}''(0) + \cdots\cdots + a_n^2\Psi_{c_n}''(0) \tag{13.204}$$

Similarly, the nth-order cumulant for z, a linear combination of independent random variables, can be determined with the following equation:

$$\lambda_n = \Psi_z^{(n)}(0) = a_1^n\Psi_{c_1}^{(n)}(0) + a_2^n\Psi_{c_2}^{(n)}(0) + \cdots\cdots + a_n^n\Psi_{c_n}^{(n)}(0) \tag{13.205}$$

where the exponent (n) denotes the nth derivative with respect to s.

The cumulant method is adapted from the basic derivation above to accommodate the P-OPF problem when a logarithmic barrier interior point method (LBIPM)-type solution is used. The Hessian of the Lagrange function is necessary for the computation of the Newton step in the LBIPM. The inverse of the Hessian, however, can be used as the coefficients for the linear combination of random bus loading variables. The pure Newton step is computed at iteration k of the LBIPM with the following equation:

$$y_{k+1} = y_k - H^{-1}(y_k)G(y_k) \tag{13.206}$$

where y is the vector of variables. $G(y_k)$ is the gradient of the Lagrange function. $H^{-1}(y_k)$ is the inverse Hessian matrix, which contains the multipliers for a linear combination of PDFs for random bus loads.

It is necessary to introduce the cumulants related to the random loads into the system in such a way that the cumulants for all other system variables can be computed. Some characteristics of the gradient of the Lagrangian are used to accomplish this. When the gradient of the Lagrangian is taken, the power flow equations appear unmodified in this vector. Therefore, cumulant models in the bus loads map directly into the gradient of the Lagrangian. For the purposes of mapping, the mismatch vector, in equation (13.206), is replaced by a new vector containing the cumulants of the random loads in the rows corresponding to their associated power flow equations.

The linear mapping information contained in the inverse Hessian can be used to determine cumulants for other variables when bus loading is treated as a random variable. If $-H^{-1}(y_k)$ is written in the following form

$$-H^{-1} = \begin{bmatrix} a_{1,1} & a_{1,2} & \ldots a_{1,n} \\ a_{2,1} & a_{2,1} & \ldots a_{2,n} \\ \ldots & \ldots & \ldots & \ldots \\ a_{n,1} & a_{n,2} & \ldots a_{n,n} \end{bmatrix} \tag{13.207}$$

then the nth cumulant for the ith variables in y is computed with the following equation:

$$\lambda_{yi,n} = a_{i,1}^n \lambda_{x1,n} + a_{i,2}^n \lambda_{x2,n} +, \ldots, + a_{i,n}^n \lambda_{xn,n} \tag{13.208}$$

where y_i is the ith element in y, and $\lambda_{xj,n}$ is the nth cumulant for the jth component variable.

For the cumulant method used for P-OPF, the cumulants for unknown random variables are computed from known random variables, and PDFs are reconstructed with the Gram–Charlier/Edgeworth expansion theory.

13.10 COMPARISON OF DETERMINISTIC AND PROBABILISTIC METHODS

As we have analyzed in this chapter, it is impossible to obtain all available data in the real-time operation because of the above-mentioned uncertainties of power systems and competitive environment. Nevertheless, it is important to select an appropriate technique to handle these uncertainties. The existing deterministic methods and tools are not adequate to handle them. The probabilistic methods, gray mathematics, fuzzy theory, and analytic hierarchy process (AHP) [34–37] are very useful to compute the unavailable or uncertain data; so that power system operation problems such as the economic dispatch, optimal power flow, and state estimation can be solvable even some data are not available.

A comparison of the deterministic method and the probabilistic method is shown in Table 13.6.

Table 13.6   Deterministic vs. Probabilistic Methods

Methods Comparison	Deterministic Method	Probabilistic Method
Contingency selection	Typically a few probable and extreme contingencies	More exhaustive list of contingencies; Ranking based on Fuzzy/AHP methods
Contingency probabilistic	Based on judgment	Based on inadequate or uncertain data (ANN, Fuzzy and AHP methods)
Load levels (forecast)	Typically seasonal peaks and selected off-peak loads	Multiple levels with uncertain factors (Fuzzy, ANN)
Unit commitment	Traditional optimization technology	Optimization technology & AHP/Fuzzy/ANN
Security regions	Deterministic security region	Variable security regions
Criteria for decision	Well established	Need a suitable method/criteria to make decision (ANN, Fuzzy and AHP methods)

Through comparing the various approaches, the following methods to handle uncertainties are recommended:

- Characterization and probabilistic methods
- Probabilistic methods/tools for evaluating the contingencies
- Fuzzy/ANN/AHP methods to handle uncertainties (e.g., contingency ranking)
- Risk management tools to optimize energy utilization while maintaining the required levels of reliability
- Cost-benefit analysis (CBA) for quantifying the impact of uncertainty

REFERENCES

[1] A.S. Merlin, "Latest developments and future prospects of power system operation and control," *International Journal of Electrical Power and Energy System*, Vol. 16, No. 3, 1994, pp. 137–139.

[2] N. Rau, C.C. Fong, C.H. Grigg, and B. Silverstein, "Living with uncertainty," *IEEE Power Engineering Review*, November, 1994, pp. 24–26.

[3] K.H. Abdul-Rahman, S.M. Shahidehpour, and N.I. Deeb, "Effect of EMF on minimum cost power transmission," *IEEE Trans. On Power Systems*, Vol. 10, No. 1, 1995, pp. 347–353.

[4] M. Ivey, "Accommodating uncertainty in planning and operation," *Workshop on Electric Transmission Reliability*, Washington, DC, Sept. 17, 1999.

[5] A.M. Leite da Silva, V.L. Arienti, and R.N. Allan, "Probabilistic load flow considering dependence between input nodal powers," *IEEE Trans. on PAS*, Vol. 103, No. 6, 1984, pp. 1524–1530.

[6] M.E. El-Hawary and G.A.N. Mbamalu, "A comparison: probabilistic perturbation and deterministic based optimal power flow solutions," *IEEE Trans. On Power Systems*, Vol. 6, No. 3, 1991, pp. 1099–1105.

[7] P.W. Sauer and B. Hoveida, "Constrained stochastic power flow analysis," *Electric Power Systems Research*, Vol. 5, 1982, pp. 87–95.

[8] T.S. Karakatsanis and N.D. Hatziargyriou, "Probabilistic constrained load flow based on sensitivity analysis," *IEEE Trans. On Power Systems*, Vol. 9, No. 4, 1994, pp. 1853–1860.

[9] K.H. Abdul-Rahman, S.M. Shahidehpour, and N.I. Deeb, "AI approach to optimal VAR control with fuzzy reactive loads," *IEEE Trans. On Power Systems*, Vol. 10, No. 1, 1995, pp. 88–97.

[10] V. Miranda and J.T. Saraiva, "Fuzzy modeling of power system optimal load flow," *IEEE Trans. On Power Systems*, Vol. 7, No. 2, 1992, pp. 843–849.

[11] Z. Wang and F.L. Alvarado, "Interval arithmetic in power flow analysis," *IEEE Trans. On Power Systems*, Vol. 7, No. 3, 1992, pp. 1341–1349.

[12] NIST/SEMATECH e-Handbook of Statistical Methods, http://www.itl.nist.gov/div898/handbook.

[13] R.E. More, *Interval Analysis*, Prentice-Hall, Englewood Gliffs, NJ, 1996.

[14] F.N. Ris, *Interval Analysis and Applications to Linear Algebra*, D. Phil, Thesis, Oxford, 1972.

[15] E. Hansen and R. Smith, "Interval arithmetic in matrix computations, Part II," *SIAM Journal of Numerical Analysis*, Vol. 4, 1967, pp. 1–9.

[16] E. Hansen and S. Sengupta, "Bounding solutions of systems of equations using interval analysis," *BIT*, Vol. 21, 1981, pp. 203–211.

[17] M. Valdma, M. Keel, O. Liik, and H. Tammoja, "Method for Minimax Optimization of Power System Operation," Proc. of IEEE Bologna PowerTech 2003, 23–26 June 2003, Bologna, Italy. Paper 252: pp. 1–6.

[18] M. Valdma, M. Keel, and O. Liik, "Optimization of active power generation in electric power system under incomplete information," Proc. of Tenth Power Systems Computation Conference, 1990, Graz, Austria, pp. 1171–1176.

[19] K. Selvi, N. Ramaraj, and S.P. Umayal, "Genetic Algorithm Applications to Stochastic Thermal Power Dispatch," *IE(I) Journal EL*, Vol. 85, June 2004, pp. 43–48.

[20] K.H. Abdul-Rahman and S.M. Shahidehpour, "Static Security in Power System Operation with Fuzzy Real Load Constraints," *IEEE Trans. On Power Systems*, Vol. 10, No. 1, 1995, pp. 77–87.

[21] A. Kaufmann and M.M. Gupta, *Fuzzy Mathematical Models in Engineering and Management Science*, North-Holland Publishing Company, Amsterdam, 1988.

[22] T.S. Dillion and T. Tun, "Integration of the sub-problems involved in the optimal economic operation of hydro-thermal system," Proc. IFAC Symp. Contr. And Manag. of Integ. Indust. France, Sept. 1977, pp. 171–180.

[23] T. Tun and T.S. Dillion, "Sensitivity analysis of the problem of economic dispatch of hydro-thermal system," Proc. IFAC Symp. Autom. Contr. and Prot. of Elec. Power System, Melb. 1977.

[24] U.A. Ozturk, M. Mazumdar, and B.A. Norman, "A Solution to the Stochastic Unit Commitment Problem Using Chance Constrained Programming," *IEEE Trans. on Power Systems*, Vol. 19, No. 3, 2004, pp. 1589–1598.

[25] J. Qiu and S.M. Shahidehpour, "A New Approach for Mini- mizing Power Losses and Improving Voltage Profile," *IEEE Trans. on Power Systems*, Vol. 2, No. 2, pp. 287–295, May 1987.

[26] K.H. Abdul-Rahman and S.M. Shahidehpour, "Application of Fuzzy Sets to Optimal Reactive Power Planning with Security Constraints," *IEEE Trans. On Power Systems*, Vol. 9, No. 2, 1994, pp. 589–597.

[27] G.B. Dantzig and P. Wolfe, "The Decomposition Algorithm for Linear Programs," *Econometrica*, Vol. 29, No. 4, pp. 767–778, Oct. 1961.

[28] M. Madrigal, K. Ponnambalam, and V.H. Quintana, "Probabilistic optimal power flow," in Proc. IEEE Can. Conf. Electrical Computer Engineering, Waterloo, ON, Canada, May 1998, pp. 385–388.

[29] G. Verbič and C.A. Cañizares, "Probabilistic Optimal Power Flow in Electricity Markets Based on a Two-Point Estimate Method," *IEEE Trans. on Power Systems*, Vol. 21, No. 4, 2006, pp. 1883–1993.

[30] H.P. Hong, "An ef?cient point estimate method for probabilistic analysis," *Reliab. Eng. Syst. Saf.*, Vol. 59, pp. 261–267, 1998.

[31] E. Rosenblueth, "Point estimation for probability moments," *Proc. Nat. Acad. Sci. U S A.*, Vol. 72, No. 10, pp. 3812–3814, Oct. 1975.

[32] A. Schellenberg, W. Rosehart, and J. Aguado, "Cumulant based probabilistic optimal power flow (P-OPF)," *IEEE Trans. on Power Systems*, Vol. 20, No. 2, 2005, pp. 773–781.

[33] M.G. Kendall and A. Stuart, *The Advanced Theory of Statistics*, 4th ed. New York: Macmillan, 1977.

[34] T.L. Satty, *The Analytic Hierarchy Process*, McGraw Hill, Inc., New York, 1980.

[35] J.Z. Zhu and M.R. Irving, "Combined Active and Reactive Dispatch with Multiple Objectives using an Analytic Hierarchical Process," *IEE Proceedings, Part C*, Vol. 143, pp. 344–352, 1996.

[36] J.Z. Zhu, M.R. Irving, and G.Y. Xu, "Automatic contingency selection and ranking using an analytic hierarchical process," *Electrical Machines and Power Systems Journal*, No. 4, 1998.

[37] J.Z. Zhu and J.A. Momoh, "Optimal VAR pricing and VAR placement using analytic hierarchy process," *Electric Power Systems Research*, Vol. 48, No. 1, 1998, pp. 11–17.

AUTHOR BIOGRAPHY

Jizhong Zhu is currently working at AREVA T&D Inc. as a principal power systems engineer. He received his Ph.D. degree from Chongqing University, P.R. China, in Feb. 1990. Dr. Zhu was a full-time professor in Chongqing University. He won the "Science and Technology Progress Award of State Education Committee of China" in 1992 and 1995, respectively, "Sichuan Provincial Science and Technology Advancement Award" in 1992, 1993 and 1994, respectively, as well as the "Science and Technology Invention Prize of Sichuan Province Science & Technology Association" in 1992. Dr. Zhu was awarded as an Excellent Young Teacher by Chongqing City Government in 1992; selected as an Outstanding Science & Technology Researcher and won annual Science & Technology Medal of Sichuan Province in 1993. He was also selected as one of four outstanding young scientists working in China by The Royal Society of UK and China Science & Technology Association and awarded Royal Society Fellowship in 1994 and the national research prize "Fok Ying-Tong Young Teacher Research Medal" in 1996. He worked in a variety of places all over the world, including Chongqing University in China, Brunel University in the UK, the National University of Singapore, Howard University in the US, and AREVA T&D Inc. (since 2000). He is also an advisory professor at Chongqing University. His research interest is in the analysis, operation, planning and control of power systems. He has published four books as an author and coauthor, and has published over 100 papers in international journals and conferences.

INDEX